Fuzzy Techniques for Noise Removal in Image Sequences and Interval-valued Fuzzy Mathematical Morphology

Vaaglogische technieken voor ruisverwijdering in videobeelden en interval-waardige wiskundige vaagmorfologie

Tom Mélange

Proefschrift ingediend tot het behalen van de graad van
Doctor in de Wetenschappen: Wiskunde

Promotor: prof. dr. E. E. Kerre
Co-Promotor: prof. dr. M. Nachtegael

Vakgroep Toegepaste Wiskunde en Informatica
Voorzitter: prof. dr. G. Vanden Berghe
Faculteit Wetenschappen
Academiejaar 2009-2010

UNIVERSITEIT GENT

Acknowledgements

First of all, I want to show my gratitude to my promotor prof. dr. Etienne Kerre, who gave me the opportunity to do this research. It was a great honour to work with such a big name in the fuzzy community. But he is more than that. He takes care of his PhD students as a father, supports them and carefully follows up their work.

Additionally, I would like to thank prof. dr. Mike Nachtegael, the co-promotor of this thesis, for being a good office mate during my full 4 year period as a PhD student and for the advice he gave me during that time.

I am also greatly indebted to Stefan, Valérie, Jeroen, Koen and Klaas, who shared the office with me for one or more years and created a nice working atmosphere. Stefan and Valérie, that were both also active in the image processing domain, were very helpful to introduce me in the domain and became good friends.

Of course, also the other members of the Fuzziness and Uncertainty Modeling research group and the colleagues of the department of Applied Mathematics and Computer Science deserve a word of appreciation for the fine moments we shared at work and after work.

Next, I also owe the people at the Telecommunications and Information Processing (TELIN) department of our university, with which we cooperated on the FWO- and GOA-project, which brings me to acknowledge that this research was supported by the FWO-project $G.0667.06$ and the GOA-project $B/04138/01IV$ of Ghent University.

Further, this work could not have been accomplished without the help of my parents. I am grateful to them for letting me study and for supporting me whenever needed. Thanks also to my brothers, who showed a lot of interest in my work.

Last but not least, I thank my love Sofie. Knowing that you are there has always been a great support for me. Thank you for being there.

Tom Mélange
March 2010

Nederlandse Samenvatting

Beeldsequenties spelen een belangrijke rol in de hedendaagse wereld. Ze kunnen ons namelijk veel informatie verschaffen. Video's worden onder meer gebruikt voor verkeersobservaties, bewakingssystemen, autonome navigatie, ... Door een slechte beeldverwerving, -transmissie of -opname zijn de sequenties echter gewoonlijk onderhevig aan ruis. Hierdoor zal het resultaat van beeldverwerkingstechnieken soms sterk gereduceerd worden en is het vooraf filteren van de beelden dikwijls noodzakelijk. De meest voorkomende ruistypes zijn impulsruis, additieve ruis en multiplicatieve ruis. In het geval van impulsruis is een bepaald percentage van de pixels aangetast en is hun grijswaarde of één of meerdere van de kleurcomponenten vervangen door een ruiswaarde. Deze ruiswaarde kan één waarde uit een beperkte reeks vaste waarden zijn (meestal de minimaal of maximaal toegelaten waarde: zout-en-peper-ruis) of kan een willekeurige waarde uit een bepaalde verdeling zijn (gewoonlijk is dit een uniforme verdeling). Bij een beeld dat aangetast is door additieve ruis, is bij iedere grijswaarde of kleurcomponent van iedere pixel een ruiswaarde opgeteld die het resultaat is van een toevalsproces (bijvoorbeeld een willekeurige waarde uit een Gaussische verdeling). Multiplicatieve ruis tenslotte, wordt gekenmerkt door het feit dat de ruiswaarde die aan iedere grijswaarde of kleurcomponent wordt toegevoegd afhankelijk is van die grijswaarde of kleurcomponent zelf. Spikkelruis is een voorbeeld van dit laatste type.

Nadat in de twee hoofdstukken van het inleidende deel van de thesis de basisbegrippen betreffende vaagverzamelingleer en beeldverwerking behandeld zijn, worden in het tweede deel van de thesis verschillende videoruisfilters voorgesteld. In het ontwerp van deze filters zullen vaaglogica en vaagverzamelingenleer gebruikt worden. Vaagverzamelingenleer is een veralgemening van de klassieke scherpe verzamelingenleer. Terwijl scherpe verzamelingen in een universum X gemodelleerd worden als $X - \{0, 1\}$ afbeeldingen, worden vaagverzamelingen gekarakteriseerd als $X - [0, 1]$ afbeeldingen. In de klassieke verzamelingenleer behoort een element uit het universum dus steeds ofwel tot de verzameling ofwel niet. In de vaagverzamelingenleer zijn ook lidmaatschapsgraden tussen 0 en 1 mogelijk, wat een meer graduele overgang tussen behoren tot en niet behoren tot toelaat. Dergelijke graduele overgang maakt vaagverzamelingen zeer geschikt voor het verwerken van menselijke kennis waarin vaak linguïstische waarden (zoals groot, klein, ...) worden gebruikt. Door het gebruik van vaagverzamelingen is een verschil in grijswaarde tussen twee pixels niet noodzakelijk groot of niet groot, maar kan het ook in een bepaalde mate groot zijn. Vaagver-

zamelingenleer heeft zijn nut al meermaals bewezen in het beeldverwerkingsdomein zoals bijvoorbeeld geïllustreerd wordt in [54].

De eerste filter die we voorstellen, in hoofdstuk 3, is bedoeld voor grijswaardevideo's die onderhevig zijn aan additieve Gaussische ruis. De filter kan gezien worden als een vaaglogische verbetering van de filter gepresenteerd in [146, 149]. De ideeën achter deze filter werden vertaald in een vaaglogisch systeem gebaseerd op vaagregels. Eén van de voordelen van een vaagregel is dat nieuwe informatie eenvoudig kan toegevoegd worden, zoals bijvoorbeeld geïllustreerd wordt in de tweede kleuruitbreiding die beschreven wordt in het volgende hoofdstuk. Net zoals in [146, 149] wordt de filter ook uitgebreid van het pixeldomein naar het wavelet-domein. De wavelettransformatie transformeert een gegeven beeld in een beeld dat relatief weinig niet-verwaarloosbare coefficiënten bevat. Deze coefficiënten corresponderen met de details die aanwezig waren in het oorspronkelijke beeld, zodat het onderscheiden van ruis en details tijdens het ontruisingsproces eenvoudiger wordt. Experimentele resultaten tonen aan dat de voorgestelde pixel-domein methode de overige state-of-the-art pixel-domein methoden overtreft in performantie en dat de wavelet-domein methode kan concurreren met state-of-the-art wavelet-domein methoden van een gelijkaardige complexiteit en die zelfs overtreft op het gebied van PSNR (peak-signal-to-noise ratio) voor beeldsequenties bekomen met een stilstaande camera zonder zoom. De gepresenteerde wavelet filter wordt echter overtroffen door filters van een hogere complexiteit die bewegingsschatting en 3D-transformaties gebruiken.

In tegenstelling tot voor grijswaardevideo's, kunnen in de literatuur slechts weinig filters gevonden worden voor kleurenvideo's die aangetast werden door additieve Gaussische ruis. De reden hiervoor is dat grijswaardefilters op een rechtstreekse manier uitgebreid kunnen worden tot kleurensequenties. De grijswaardefilter kan namelijk toegepast worden op elk van de kleurbanden apart of op de helderheidscomponent Y van de YUV-transformatie van de beelden. In hoofdstuk 4 bieden we twee alternatieve kleuruitbreidingen voor de grijswaardefilter uit hoofdstuk 3. De eerste kleurenfilter is een vector-gebaseerde techniek die iedere kleurenpixel als één geheel beschouwt, waarvan de componenten niet afzonderlijk gebruikt mogen worden. De variabelen die gebruikt werden in het grijswaardefiltersysteem uit hoofdstuk 3 worden desgevallend uitgebreid van grijswaarden naar kleurvectors. In de tweede voorgestelde kleurenaanpak worden de verschillende kleurbanden afzonderlijk gefilterd met het grijswaardesysteem, dat echter uitgebreid wordt door het toevoegen van informatie uit de overige kleurbanden aan de vaagregels. Beide kleuruitbreidingen proberen dus zoveel mogelijk gebruik te maken van de correlatie tussen de verschillende kleurbanden om een zo optimaal mogelijk kleur- en detailbehoud te bekomen. De experimenten tonen aan dat de filters inderdaad beter in dit opzet slagen dan de gewoonlijk toegepaste YUV-aanpak.

Na de reductie van additieve Gaussische ruis in hoofdstuk 3 and 4, concentreren we ons in de volgende twee hoofdstukken op willekeurig verdeelde impulsruis. In hoofdstuk 5 ontwikkelen we twee grijswaardefilters voor dit ruistype. Om een zo goed mogelijk balans te vinden tussen ruisverwijdering en detailbehoud, wordt in beide filters de ruis in verschillende opeenvolgende filterstappen verwijderd. De details zullen gemakkelijker kunnen

behouden worden doordat niet alle ruis verwijderd moet worden in één drastische stap, wat onvermijdelijk gepaard zou gaan met detailverlies. Langs de andere kant zullen ook overgebleven ruispixels gemakkelijker gedetecteerd kunnen worden daar er, door het reeds gefilterd zijn van enkel buren in een vorige stap, meer betrouwbare buren zijn om de pixel mee te vergelijken. In de eerst beschreven methode wordt in elk van de filterstappen voor iedere pixel een graad berekend tot de welke hij als ruis wordt beschouwd. Iedere pixel die een niet-nul graad krijgt, wordt gefilterd. In de tweede voorgestelde ruisfilter wordt voor elke pixel nu zowel een graad tot de welke hij als ruis en tot de welke hij als ruisvrij gezien wordt. Pixels worden nu gefilterd als hun ruisgraad in die stap groter is dan hun ruisvrije graad. De filtering zelf gebeurt in beide algoritmes aan de hand van bewegingscompensatie. Deze techniek vindt zijn oorsprong in de compressie van video en werd reeds overgenomen in verschillende filters voor additieve Gaussische ruis. De techniek heeft echter nog niet echt zijn intrede gedaan bij impulsruisfilters. De gelijkenis van twee pixelblokken in twee opeenvolgende frames is gewoonlijk berekend aan de hand van een gemiddelde absolute afstand, een maat die nogal onderhevig is aan impulsen. Daarom stellen we een aanpassing van deze maat voor die rekening houdt met gedetecteerde ruis. Uit de experimenten kan men besluiten dat beide beschreven impulsruisfilters resulteren in een zeer goede balans tussen ontruiskracht en detailbehoud en alle andere vergeleken methoden overtreffen.

Als laatste filter, introduceren we ook een kleurenfilter voor het willekeurig verdeelde impulsruistype. Analoog als in het vorige hoofdstuk wordt de ruis opnieuw stap per stap verwijderd zodat een goede ruisverwijdering gecombineerd kan worden met een goed detailbehoud. De beschreven methode ontruist elk van de kleurbanden afzonderlijk, maar de vaagregels die de graad bepalen tot de welke een pixelcomponent als ruis of als ruisvrij beschouwd wordt, houden nu rekening met de extra informatie die beschikbaar is in de andere kleurbanden. Pixelcomponenten die een grotere ruisgraad dan ruisvrije graad hebben in een gegeven stap, worden opnieuw gefilterd. Hiertoe hebben we de bewegingsgecompenseerde techniek die toegepast werd in het vorige hoofdstuk verder uitgewerkt door de zoekruimte voor het vinden van een gelijkaardige pixelblok uit te breiden en ook blokken in het huidige frame te onderzoeken en zo naast de temporele informatie ook zoveel mogelijk de beschikbare spatiale informatie uit te buiten. Soms kan immers geen vergelijkbare blok gevonden worden in het vorige frame door bijvoorbeeld snelle beweging die groter is dan de zoekruimte. De experimenten tonen aan dat de voorgestelde kleurenfilter andere state-of-the-art methoden duidelijk overtreft zowel in termen van objectieve kwaliteitsmaten zoals de PSNR en het genormaliseerd kleurverschil (NCD) als visueel.

In tegenstelling tot het tweede deel van de thesis dat handelt over ruisverwijdering en eerder praktisch gericht is, is het derde deel van de thesis eerder theoretisch van aard. In dit derde deel bestuderen we de intervalwaardige wiskundige vaagmorfologie. Wiskundige morfologie is een theorie die ontwikkeld werd voor het analyseren van ruimtelijke structuren [127, 129] en die onder andere toegepast wordt in beeldverwerkingstechnieken zoals randdetectie, objectherkenning, patroonherkenning, beeldsegmentatie, beeldvergroting, ... De benaming ‘morfologie’ komt voort uit het feit dat de theorie tot doel heeft de vorm van objecten te analyseren. Het bijvoeglijk naamwoord ‘wiskundig’ is te wijten aan het ge-

bruik van onder andere verzamelingenleer, topologie en tralie-algebra tijdens deze analyse. De theorie werd geïntroduceerd in de jaren zestig door G. Matheron en J. Serra en spruit voort uit de studie naar de geometrie van poreuze media. Dergelijke media kunnen binair geïnterpreteerd worden in de zin dat een punt van een poreus medium ofwel tot een porie zal behoren ofwel tot de grondmassa rond de poriën. Daarom ontwikkelden G. Matheron en J. Serra een verzamelingenformalisme om binaire (zwart-wit) beelden te analyseren. De matrix rond de poriën kan dan gezien worden als de verzameling van voorwerppunten, terwijl de poriën zelf samen het complement van deze verzameling vormen. Beeldvoorwerpen kunnen dus verwerkt worden met behulp van eenvoudige verzamelingenbewerkingen zoals doorsnedes, unies, complementering en verschuivingen. Op basis van deze bewerkingen worden de morfologische basisoperatoren dilatatie en erosie en opening en sluiting als een combinatie van de eerste twee gedefiniëerd die een gegeven beeld omvormen met behulp van een structuurelement om op die manier meer informatie (grootte, vorm, ...) over de voorwerpen uit het beeld te verkrijgen. De binaire theorie werd in een later stadium uitgebreid naar grijswaardebeelden. Bekende aanpakken hiervoor zijn de umbrabenadering en de schijfjesbenadering, alsook een derde aanpak die steunt op het gegeven dat n-dimensionale grijswaardebeelden en vaagverzamelingen in $\mathbb{R}^n$ op eenzelfde manier gemodelleerd kunnen worden, namelijk als $\mathbb{R}^n - [0, 1]$ afbeeldingen. Bijgevolg kunnen vaagverzamelingenbewerkingen toegepast worden op grijsbeelden. Recent werd deze laatste aanpak nog verder uitgebreid op basis van uitbreidingen van de vaagverzamelingenleer. In deze thesis concentreren we ons op intervalwaardige vaagverzamelingen en de daarmee gepaard gaande intervalwaardige wiskundige vaagmorfologie. Zoals scherpe verzamelingen en vaagverzamelingen respectievelijk overeenstemmen met binaire en grijswaardebeelden, stemmen intervalwaardige vaagverzamelingen nu overeen met intervalwaardige beelden. Dit zijn beelden waarbij de beeldpunten niet langer op één specifieke grijswaarde worden afgebeeld, maar op een gesloten interval van grijswaarden, zodat onzekerheid omtrent de grijswaarde in rekening gebracht kan worden.

In hoofdstuk 7 geven we eerst een overzicht van de verschillende stappen in de evolutie van binaire wiskundige morfologie via de grijswaardemorfologiën naar intervalwaardige vaagmorfologie en bespreken we het intervalwaardige beeldmodel meer in detail. Vervolgens onderzoeken we de basiseigenschappen van de intervalwaardige vaagmorfologische operatoren.

Hoofdstuk 8 handelt over de decompositie van de intervalwaardige vaagmorfologische operatoren. Meer precies gaan we op zoek naar het verband tussen enerzijds de $[\alpha_1, \alpha_2]$-niveauverzameling van het resultaat van een morfologische operator op een intervalwaardig beeld voor een gegeven intervalwaardig structuurelement en anderzijds het resultaat van de corresponderende binaire operator op de $[\alpha_1, \alpha_2]$-niveauverzamelingen van het intervalwaardig beeld en structuurelement. In sommige gevallen vonden we een gelijkheid, in andere slechts een benadering. De bekomen resultaten zijn eerst en vooral interessant omdat ze ons een theoretisch verband verschaffen tussen intervalwaardige wiskundige vaagmorfologie en binaire wiskundige morfologie. Verder zal een omvorming in binaire operatoren ook de rekentijd die nodig is voor het berekenen van een dergelijke $[\alpha_1, \alpha_2]$-niveauverzameling

reduceren.

In hoofdstuk 9 tenslotte, wordt het omgekeerde vraagstuk onderzocht, namelijk de constructie van intervalwaardige morfologische operatoren uit de binaire morfologische operatoren. We vertrekken vanuit een meer algemeen standpunt en onderzoeken eerst de constructie van een intervalwaardige vaagverzameling uit een genestelde familie scherpe verzamelingen naar analogie met de constructie van een intervalwaardige vaagverzameling uit zijn $[\alpha_1, \alpha_2]$-niveauverzamelingen. Deze resultaten worden dan vervolgens gebruikt om stijgende binaire operatoren uit te breiden tot intervalwaardige vaagoperatoren door de uitkomst van deze laatste te definiëren als de intervalwaardige vaagverzameling die geconstrueerd wordt uit de familie die ontstaat door het toepassen van de binaire operator op de $[\alpha_1, \alpha_2]$-niveauverzamelingen van de argumenten. Wanneer we dit toepassen op de binaire dilatatie, vinden we de intervalwaardige vaagdilatatie gebaseerd op de infimumoperator. Dit geeft ons opnieuw een mooi theoretisch verband tussen intervalwaardige wiskundige vaagmorfologie en binaire wiskundige morfologie.

De resultaten in deze thesis werden gepubliceerd in internationale tijdschriften [73, 74, 79, 80, 81, 85] en werden gepresenteerd op internationale conferenties [75, 76, 77, 78, 82, 83, 84, 86]. Ook bijdragen tot andermans werk werden gepubliceerd in internationale tijdschriften [101, 106, 130], in een hoofdstuk in een boek [31] en in de proceedings van internationale conferenties [91, 97, 98, 99, 100, 102, 103, 104, 105, 107, 120, 131].

Contents

Preface

Image sequences play an important role in today's world. They provide us a lot of information. Videos are for example used for traffic observations, surveillance systems, autonomous navigation and so on. Due to bad acquisition, transmission or recording, the sequences are however usually corrupted by noise, which hampers the functioning of many image processing techniques. A preprocessing module to denoise the images often becomes necessary. The most common noise types that can be distinguished are impulse noise, additive noise and multiplicative noise. In the case of impulse noise, a certain percentage of the pixel grey values or colour components is replaced by noise values. Such noise value can be fixed (usually as the minimum or maximum allowed value: salt and pepper noise) or the result of a random process (usually with a uniform distribution). If an image is corrupted by additive noise, then a random value from a given distribution (e.g. a Gaussian distribution) has been added to each pixel. In the multiplicative noise type, finally, the intensity of the noise value added to a pixel depends on the intensity of the pixel grey value or colour component itself (e.g. speckle noise).

After a short overview of the basic concepts in fuzzy set theory and image processing, respectively given in the two chapters of the introductionary first part of this thesis, we introduce several algorithms for the denoising of image sequences in Part II. In those video filters, fuzzy logic and fuzzy set theory is used. Fuzzy set theory [142] is a generalisation of classical crisp set theory. Where crisp sets in a universe X can be modelled by $X - \{0, 1\}$ mappings, fuzzy sets are characterized as $X - [0, 1]$ mappings (membership functions). In classical set theory an element $x \in X$ belongs to a set or doesn't belong to it. In fuzzy set theory also membership degrees between zero and one and thus a more gradual transition between belonging to and not belonging to is allowed. This makes fuzzy sets very useful for the processing of human knowledge, where linguistic values (e.g. large, small, ...) are used. For example, a difference in grey level is not necessarily large or not large, but can be large to some degree. Fuzzy set theory has already shown to be very effective in the domain of image processing as illustrated e.g. in [54].

The first proposed filter, discussed in Chapter 3, is intended for greyscale image sequences corrupted by additive Gaussian noise. It can be seen as a fuzzy logic based improvement of the multiple class averaging filter (MCA) from [146, 149]. We took the ideas behind the MCA filter and translated those in a fuzzy logic framework containing fuzzy rules. One of the advantages of such fuzzy rule is that it is easy to include new infor-

mation as is e.g. illustrated in the second colour extension presented in the next chapter. Analogously to the MCA filter, the proposed filtering framework was first developed in the pixel domain and additionally extended to the wavelet domain. The wavelet transform of an image results in a sparse representation of its content. The transformed image contains relatively few non-negligible coefficients that correspond to the details in the image, which facilitates the denoising process.

Only few filters for colour videos corrupted by Gaussian noise can be found in literature. Greyscale methods can be extended to colour sequences in a straightforward way by applying them on each of the colour bands separately or by applying them on the Y-component of the YUV-transform of the frames. In Chapter 4, we present two alternative colour extensions of the greyscale method introduced in Chapter 3. The first alternative is a vector-based approach in which the colour vectors are treated as entities of which the different colour components are not used separately. The used variables in the filtering framework are accordingly extended from grey values to colour vectors. In the second alternative, each of the colour bands is filtered separately by the filtering framework from the previous chapter, in which the fuzzy rules are now extended by integrating colour information, i.e., information from the other colour bands. Both extensions thus try to exploit the correlation between the different colour bands.

In the next two chapters, we concentrate on image sequences corrupted by random impulse noise. In Chapter 5 two greyscale filters for this noise type are developed. To find a good trade-off between noise removal and detail preservation, in both filters the noise is removed step by step. Details are better preserved because not all noise needs to be filtered in one drastic denoising step and remaining noise pixels will be easier to detect if some of its neighbours have already been filtered and more reliable neighbours are available for comparison. In the first presented algorithm, in each of the successive steps, for each pixel a degree is calculate to which it is considered noisy. All pixels that are noisy to some degree will be filtered in this step. The second presented algorithm calculates in each step for each pixel both a degree to which it is considered noisy and noisefree. Pixels are now filtered if their noisy degree is larger than their noisefree degree in this step. For the filtering of the pixels, we apply motion compensation, a technique used in video compression, that is already adopted in video filters for additive Gaussian noise, but has not really found its way to impulse noise video filters yet. For the calculation of the correspondence between two pixel blocks in successive frames, we have made the commonly used mean absolute distance (MAD) adaptive to the impulse noise.

Next, in Chapter 6, an impulse noise filter for colour sequences is introduced. Analogously as in the previous chapter, the noise is again removed step by step to combine a good noise removal to a good detail preservation. The filter denoises each of the colour bands separately. However, the fuzzy rules that are used to determine the degrees to which a pixel component is considered noisy and noisefree now benefit from the extra information that is available from the other colour bands. Pixel components for which the noisy degree is larger than the noisefree degree are filtered in the considered step. For this filtering, we further develop the motion compensated technique from the previous chapter by searching

for a similar block not only in the previous frame, but also in the current frame. In the case that, e.g. due to motion, no similar block can be found in the previous frame, there is still a probability that a similar block can be found in the current frame.

Where Part II that introduces fuzzy techniques for the removal of noise in video is more practical, Part III of the thesis is more theoretical. In this part we study interval-valued fuzzy mathematical morphology. Mathematical morphology is a theory intended for the analysis of spatial structures [127, 129] that has found application in e.g. edge detection, object recognition, pattern recognition, image segmentation, image magnification, ... The term 'morphology' reflects to the fact that the theory aims at analysing the shape of objects. The adjective 'mathematical' results from the use of set theory, topology, lattice algebra and so on in this analysis. The theory was introduced in the sixties by G. Matheron and J. Serra and arises from the study of the geometry of porous media. Since a point of a porous medium either belongs to a pore or to the matrix surrounding the pores, porous media can be looked at in a binary way. Inspired by this study, G. Matheron and J. Serra introduced a set formalism to analyse binary (black-and-white) images. In the above, the matrix can be considered as the set of object points, while the pores constitute the complement of this set. Image objects can thus be processed by simple operations as unions, intersections, complementation and translations. Using these set operations, the basic morphological operators dilation and erosion and the opening and closing, as a combination of the former two, are defined to transform a given image by the help of a structuring element in order to obtain information (size, shape, ...) about the image objects. Binary mathematical morphology was later extended to greyscale images by the threshold and umbra approach as well as by a fuzzy approach that is based on the observation that fuzzy sets in the universe $\mathbb{R}^n$ and n-dimensional greyscale images can be modelled in the same way, i.e., as mapping from $\mathbb{R}^n$ into the unit interval $[0, 1]$. This allows us to apply fuzzy set operations on greyscale images. Recently, fuzzy mathematical morphology has been further extended based on extensions of fuzzy set theory. In this thesis we concentrate on the extension based on interval-valued fuzzy sets, called interval-valued fuzzy mathematical morphology. Where classical crisp sets and fuzzy sets respectively corresponded to binary and greyscale images, interval-valued fuzzy sets now correspond to interval-valued images, where an image element is not longer mapped onto one specific grey value, but onto an interval of grey values, such that uncertainty concerning the grey value is allowed.

In Chapter 7, we give an overview of the evolution from binary mathematical morphology over the different greyscale morphology theories to interval-valued fuzzy mathematical morphology and the interval-valued image model and we investigate the basic properties of the interval-valued fuzzy morphological operators.

Chapter 8 deals with the decomposition of the interval-valued fuzzy morphological operators. We investigate the relationship between the $[\alpha_1, \alpha_2]$-cut of the result of such operator applied on an interval-valued image and structuring element and the result of the corresponding binary operator applied on the $[\alpha_1, \alpha_2]$-cut of the image and structuring element. Sometimes an equality can be found and sometimes only an approximation can be found. These results are first of all interesting because they provide a link between interval-valued

fuzzy mathematical morphology and binary mathematical morphology, but such conversion into binary operators also reduces the computation time needed for the calculation of such $[\alpha_1, \alpha_2]$-cut.

In Chapter 9, the reverse problem is tackled, i.e., the construction of interval-valued morphological operators from the binary ones. We start from a more general perspective and investigate the construction of an interval-valued fuzzy set from a nested family of crisp sets in analogy to the construction of an interval-valued fuzzy set from its $[\alpha_1, \alpha_2]$-cuts. These results are then additionally used to extend increasing binary operators to interval-valued fuzzy operators by defining the result as the interval-valued fuzzy set that is constructed from the family that arises by applying the binary operator on the $[\alpha_1, \alpha_2]$-cuts of its arguments. Application on the binary dilation results in the interval-valued fuzzy dilation based on a specific t-norm (the infimum operator), which again provides us a nice theoretical link between interval-valued fuzzy and binary mathematical morphology.

The results in this thesis have been published in international journals [73, 74, 79, 80, 81, 85] and have been presented on international conferences [75, 76, 77, 78, 82, 83, 84, 86]. Also contributions to other people's work have been published in international journals [101, 106, 130], in a book chapter [31] and in the proceedings of international conferences [91, 97, 98, 99, 100, 102, 103, 104, 105, 107, 120, 131].

Part I

Introduction to Image Processing and Fuzzy Set Theory

1
Introduction to Fuzzy Set Theory

In this chapter, we introduce the basic concepts of fuzzy set theory, which will be needed for a good comprehension of the remainder of this thesis. For a more extensive study, we refer the interested reader to [53].

1.1 Fuzzy Sets

1.1.1 Characterization

In classical set theory, a set A in a universe X divides the universe into two parts: the elements that belong to A (and thus satisfy a given defining property) and the elements that do not belong to A (and do not satisfy the defining property). As a consequence, a classical set (or crisp set) A in a universe X can be represented by the function χ_A given by

$$\begin{aligned} \chi_A : \quad & X \to \{0,1\} \\ & x \to 1, \text{ if } x \in A, \\ & x \to 0, \text{ if } x \notin A, \end{aligned}$$

which we call the characteristic function of A. The class of all crisp sets in a universe X is denoted by $\mathcal{P}(X)$.

However, in real life situations, an object often satisfies a property to some degree, i.e., it does not completely satisfy the property, but also does not completely not satisfy the property. For example, when do we call a person *tall*? We can not say that a man of $1m80$ is not tall at all. However, there are still a lot of people that are taller. E.g., a man of $2m$ satisfies the property *tall* to a higher degree. It is clear that classical crisp sets are not able

to represent the property *tall*. In that case, we would have to choose one value, e.g. $1m80$, and all lengths greater or equal to this value are called tall and all other lengths are called not tall. So two persons of e.g. $1m60$ and $1m79$, that differ a considerable number of centimeters in length, are both called not tall. However, a person of $1m80$, who is only $1cm$ taller than a person of $1m79$, would suddenly be called tall. To overcome this problem, Zadeh introduced the concept of a fuzzy set [142] by extending the characteristic functions to membership functions and in this way allowing a gradual transition between satisfying a property (belonging to a set) or not. An element can now also have a membership degree between 0 and 1. The more an object belongs to the set (e.g. the taller a person), the higher its membership degree. Summarized, a fuzzy set A in a universe X is characterized by the function χ_A given by

$$\begin{aligned} \chi_A : \quad & X \to [0,1] \\ & x \to \chi_A(x), \end{aligned}$$

which we call the membership function of A. For the ease of notation, in the remainder of this thesis, we will use the name of the set for its membership function, i.e., we will write $A(x)$ instead of $\chi_A(x)$. Further, the class of all fuzzy sets in a universe X is denoted by $\mathcal{F}(X)$.

1.1.2 Basic Concepts

In this subsection, we give some basic concepts concerning fuzzy sets that will return in the remainder of this work.

Definition 1.1. *Let $A \in \mathcal{F}(X)$. The support d_A of A is defined as*[1]*:*

$$d_A = \{x \in X | A(x) > 0\}.$$

Definition 1.2. *Let $A \in \mathcal{F}(X)$. The kernel k_A of A is defined as*[2]*:*

$$k_A = \{x \in X | A(x) = 1\}.$$

Definition 1.3. *Let $A \in \mathcal{F}(X)$ and let $\alpha \in]0,1]$. The weak α-cut A_α of A is defined as:*

$$A_\alpha = \{x \in X | A(x) \geq \alpha\}.$$

Remark that the choice $\alpha = 0$ would not yield new information (because it would result in the universe X). Further, in a lot of properties this special case would need to be excluded. Therefore, this case is usually also excluded from the definition.

Definition 1.4. *Let $A \in \mathcal{F}(X)$ and let $\alpha \in [0,1[$. The strong α-cut $A_{\overline{\alpha}}$ of A is defined as:*

$$A_{\overline{\alpha}} = \{x \in X | A(x) > \alpha\}.$$

[1] Also the notation $supp\ A$ is often used.
[2] Also the notation $ker\ A$ is often used.

Remark that the choice $\alpha = 1$ would not yield new information (because it would result in the empty set $\emptyset$). Further, in a lot of properties this special case would need to be excluded. Therefore, this case is usually also excluded from the definition.

Definition 1.5. *Let $A \in \mathcal{F}(X)$. A is called normalized if*

$$(\exists x \in X)(A(x) = 1).$$

Definition 1.6. *Let $A \in \mathcal{F}(X)$. A is called pseudo-normalized if*

$$\sup_{x \in X} A(x) = 1.$$

Definition 1.7. *Let $A \in \mathcal{F}(X)$. The height $h(A)$ of A is defined as*[3]*:*

$$h(A) = \sup_{x \in X} A(x).$$

Definition 1.8. *Let $A \in \mathcal{F}(X)$. The plinth $p(A)$ of A is defined as*[4]*:*

$$p(A) = \inf_{x \in X} A(x).$$

1.2 Fuzzy Logical Operators

Analogous to the extension of a crisp set to a fuzzy set, the binary Boolean logic is extended to fuzzy logic by also allowing truth values between zero and one. The Boolean negation ($\neg$), conjunction ($\wedge$), disjunction ($\vee$) and implication ($\rightarrow$) on $\{0, 1\}$ are respectively generalized by negators, conjunctors, disjunctors and implicators on $[0, 1]$ [137].

1.2.1 Definitions

Definition 1.9.

- *A negator $\mathcal{N}$ on $[0, 1]$ is a decreasing $[0, 1] - [0, 1]$ mapping that coincides with the Boolean negation on $\{0, 1\}$, i.e., $\mathcal{N}(0) = 1$ and $\mathcal{N}(1) = 0$.*
- *A negator $\mathcal{N}$ is an involutive negator on $[0, 1]$ if $(\forall x \in [0, 1])(\mathcal{N}(\mathcal{N}(x)) = x)$.*

The best known involutive negator is Zadeh's standard negator $\mathcal{N}_s$, given by $\mathcal{N}_s(x) = 1 - x$ for all $x \in [0, 1]$.

Definition 1.10.

- *A conjunctor $\mathcal{C}$ on $[0, 1]$ is an increasing $[0, 1]^2 - [0, 1]$ mapping that coincides with the Boolean conjunction on $\{0, 1\}^2$, i.e., $\mathcal{C}(0, 0) = \mathcal{C}(0, 1) = \mathcal{C}(1, 0) = 0$ and $\mathcal{C}(1, 1) = 1$.*

[3] Also the notation $hgt\ A$ is often used.
[4] Also the notation $plt\ A$ is often used.

- *A conjunctor $\mathcal{C}$ is a semi-norm on* $[0,1]$ *if* $(\forall x \in [0,1])(\mathcal{C}(1,x) = \mathcal{C}(x,1) = x)$.
- *A semi-norm $\mathcal{C}$ is a triangular norm (t-norm) on* $[0,1]$ *if it is commutative and associative.*

Well-known triangular norms are e.g. the minimum operator $\mathcal{C}_M$, the product $\mathcal{C}_P$, the Łukasiewicz t-norm $\mathcal{C}_W$ and the drastic t-norm $\mathcal{C}_Z$:

$$\begin{aligned}
\mathcal{C}_M(x,y) &= \min(x,y),\\
\mathcal{C}_P(x,y) &= x \cdot y,\\
\mathcal{C}_W(x,y) &= \max(0, x+y-1),\\
\mathcal{C}_Z(x,y) &= \begin{cases} \min(x,y) & \text{if } \max(x,y) = 1\\ 0 & \text{else} \end{cases},
\end{aligned}$$

with $(x,y) \in [0,1]^2$.

Definition 1.11.

- *A disjunctor $\mathcal{D}$ on* $[0,1]$ *is an increasing* $[0,1]^2 - [0,1]$ *mapping that coincides with the Boolean disjunction on* $\{0,1\}^2$*, i.e.,* $\mathcal{D}(1,1) = \mathcal{D}(0,1) = \mathcal{D}(1,0) = 1$ *and* $\mathcal{D}(0,0) = 0$.
- *A disjunctor $\mathcal{D}$ is a semi-conorm on* $[0,1]$ *if* $(\forall x \in [0,1])(\mathcal{D}(0,x) = \mathcal{D}(x,0) = x)$.
- *A semi-conorm $\mathcal{D}$ is a triangular conorm (t-conorm) on* $[0,1]$ *if it is commutative and associative.*

Well-known triangular conorms are e.g. the maximum operator $\mathcal{D}_M$, the probabilistic sum $\mathcal{D}_P$, the Łukasiewicz t-conorm $\mathcal{D}_W$ and the drastic t-conorm $\mathcal{D}_Z$:

$$\begin{aligned}
\mathcal{D}_M(x,y) &= \max(x,y),\\
\mathcal{D}_P(x,y) &= x+y-x \cdot y,\\
\mathcal{D}_W(x,y) &= \min(1, x+y),\\
\mathcal{D}_Z(x,y) &= \begin{cases} \max(x,y) & \text{if } \min(x,y) = 0\\ 1 & \text{else} \end{cases},
\end{aligned}$$

with $(x,y) \in [0,1]^2$.

Definition 1.12.

- *An implicator $\mathcal{I}$ on* $[0,1]$ *is a hybrid monotonic* $[0,1]^2 - [0,1]$ *mapping (i.e., decreasing in the first argument and increasing in the second argument) that coincides with the Boolean implication on* $\{0,1\}^2$*, i.e.,* $\mathcal{I}(0,0) = \mathcal{I}(0,1) = \mathcal{I}(1,1) = 1$ *and* $\mathcal{I}(1,0) = 0$*. Every implicator $\mathcal{I}$ induces a negator $\mathcal{N}_\mathcal{I}$ defined by* $\mathcal{N}_\mathcal{I}(x) = \mathcal{I}(x,0),\ \forall x \in [0,1]$.
- *An implicator $\mathcal{I}$ is a border implicator on* $[0,1]$ *if* $(\forall x \in [0,1])(\mathcal{I}(1,x) = x)$.

- *A border implicator $\mathcal{I}$ is a model implicator on $[0,1]$ if it is contrapositive w.r.t. its induced negator, i.e., $(\forall(x,y) \in [0,1]^2)(\mathcal{I}(x,y) = \mathcal{I}(\mathcal{N}_{\mathcal{I}}(y), \mathcal{N}_{\mathcal{I}}(x)))$, and if it fulfills the exchange principle, i.e., $(\forall(x,y,z) \in [0,1]^3)(\mathcal{I}(x,\mathcal{I}(y,z)) = \mathcal{I}(y,\mathcal{I}(x,z)))$.*

Well-known model implicators are e.g. the Kleene-Dienes implicator $\mathcal{I}_{KD}$, the Reichenbach implicator $\mathcal{I}_R$ and the Łukasiewicz implicator $\mathcal{I}_W$:

$$\begin{aligned} \mathcal{I}_{KD}(x,y) &= \max(1-x, y), \\ \mathcal{I}_R(x,y) &= 1 - x + x \cdot y, \\ \mathcal{I}_W(x,y) &= \min(1, 1-x+y), \end{aligned}$$

with $(x,y) \in [0,1]^2$.

1.2.2 Fuzzy If-Then Rules

The fuzzy logical operators are e.g. used to calculate the activation degree of a fuzzy if-then rule. Such fuzzy rules will constitute the basis of the noise filters for video sequences developed in Part II of this thesis. Consider for example the following fuzzy rule:

Fuzzy Rule 1.1.
IF (a *is* A OR b *is* B) AND c *is* NOT C
THEN d *is* D.

In this rule $A \in \mathcal{F}(X_1)$, $a \in X_1$, $B \in \mathcal{F}(X_2)$, $b \in X_2$, $C \in \mathcal{F}(X_3)$, $c \in X_3$ and $D \in \mathcal{F}(X_4)$, $d \in X_4$ (where (some of) the universes X_1, X_2, X_3 and X_4 may coincide). The degree $D(d)$ to which d is D (belongs to D), i.e., the degree to which the consequent of the rule is true, equals the activation degree of the rule, i.e., the degree to which the antecedent of the rule is true. So, if we use a conjunctor $\mathcal{C}$, a disjunctor $\mathcal{D}$ and a negator $\mathcal{N}$ for the AND-, OR- and NOT-operator respectively, the degree $D(d)$ is then given by

$$D(d) = \mathcal{C}(\mathcal{D}(A(a), B(b)), \mathcal{N}(C(c))).$$

1.3 Fuzzy Set Operations

1.3.1 Complement, Intersection and Union of Fuzzy Sets

The definition of the complement, intersection and union of crisp sets is based on the Boolean logical operators. Indeed, let $A, B \in \mathcal{P}(X)$, then

$$\begin{aligned} co(A) &= \{x \in X | \neg(x \in A)\}, \\ A \cap B &= \{x \in X | (x \in A) \wedge (x \in B)\}, \\ A \cup B &= \{x \in X | (x \in A) \vee (x \in B)\}. \end{aligned}$$

So, to extend the crisp set operations to fuzzy sets, fuzzy logical operators are used.

Definition 1.13. *Let $A, B \in \mathcal{F}(X)$. If $\mathcal{N}$ is a negator on $[0,1]$, then the $\mathcal{N}$-complement $co_{\mathcal{N}}(A)$ of A is defined as the fuzzy set in X given by:*

$$(co_{\mathcal{N}}(A))(x) = \mathcal{N}(A(x)),\ \forall x \in X.$$

If $\mathcal{C}$ is a conjunctor on $[0,1]$, then the $\mathcal{C}$-intersection $A \cap_{\mathcal{C}} B$ of A and B is defined as the fuzzy set in X given by:

$$(A \cap_{\mathcal{C}} B)(x) = \mathcal{C}(A(x), B(x)),\ \forall x \in X.$$

If $\mathcal{D}$ is a disjunctor on $[0,1]$, then the $\mathcal{D}$-union $A \cup_{\mathcal{D}} B$ of A and B is defined as the fuzzy set in X given by:

$$(A \cup_{\mathcal{D}} B)(x) = \mathcal{D}(A(x), B(x)),\ \forall x \in X.$$

If $\mathcal{C}$ (respectively $\mathcal{D}$) is the operator $\mathcal{C}_M$ (respectively the operator $\mathcal{D}_M$), then the intersection (respectively union) is called the Zadeh-intersection (respectively Zadeh-union) and the notation $\cap_{\mathcal{C}}$ is simplified to $\cap$ (respectively $\cup_{\mathcal{D}}$ to $\cup$).

If $\mathcal{C}$ and $\mathcal{D}$ are commutative and associative (in particular if they are a t-norm and a t-conorm), then the above definitions can be extended to the intersection and union of an arbitrary finite family of fuzzy sets. If further the conjunctor $\mathcal{C}$ and the disjunctor $\mathcal{D}$ can also be extended to an infinite number of arguments, then also an extension to infinite families is possible. For the Zadeh-intersection and Zadeh-union and an arbitrary (infinite) family $(A_j)_{j \in J}$ in $\mathcal{F}(X)$, this becomes:

$$\begin{aligned} (\cap_{j \in J} A_j)(x) &= \inf_{j \in J} A_j(x),\ \forall x \in X, \\ (\cup_{j \in J} A_j)(x) &= \sup_{j \in J} A_j(x),\ \forall x \in X. \end{aligned}$$

1.3.2 Inclusion of Fuzzy Sets

The inclusion of two fuzzy sets is defined as follows:

Definition 1.14. *Let $A, B \in \mathcal{F}(X)$, then*

$$A \subseteq B \Leftrightarrow (\forall x \in X)(A(x) \leq B(x)).$$

1.4 $\mathcal{L}$-Fuzzy Sets

In some cases, the interval $[0,1]$ does not suffice as an evaluation space. Therefore, Goguen generalized the fuzzy sets introduced by Zadeh to $\mathcal{L}$-fuzzy sets [40], where $\mathcal{L}$ is a complete lattice.

1.4.1 Lattice Theory

To give the definition of a complete lattice [7], we have to start from that of a partially ordered set.

Definition 1.15. *A partially ordered set (poset) is a couple $(P, \leq_P)$, where P is a non-empty set and $\leq_P$ is a binary relation (ordering)*[5] *on P that satisfies:*

- $(\forall x \in P)(x \leq_P x)$ *(reflexivity),*
- $(\forall (x, y) \in P^2)(x \leq_P y$ *and* $y \leq_P x \Rightarrow x = y)$ *(anti-symmetry),*
- $(\forall (x, y, z) \in P^3)(x \leq_P y$ *and* $y \leq_P z \Rightarrow x \leq_P z)$ *(transitivity).*

If further also each two elements in the partially ordered set $(P, \leq_P)$ are comparable (i.e., $(\forall (x, y) \in P^2)(x \leq_P y$ or $y \leq_P x)$), then $(P, \leq_P)$ is called a totally ordered set or chain.

Some important concepts that are defined in a poset are the following:

Definition 1.16. *Let $(P, \leq_P)$ be a poset, $A \subseteq P$ and $b \in P$.*

- *b is an upper bound of $A \Leftrightarrow (\forall a \in A)(a \leq_P b)$,*
- *b is a lower bound of $A \Leftrightarrow (\forall a \in A)(b \leq_P a)$,*
- *A is bounded above in $(P, \leq_P) \Leftrightarrow (\exists b \in P)(b$ is an upper bound of $A)$,*
- *A is bounded below in $(P, \leq_P) \Leftrightarrow (\exists b \in P)(b$ is a lower bound of $A)$,*
- *A is bounded in $(P, \leq_P) \Leftrightarrow A$ is bounded above and A is bounded below,*
- *b is the greatest element of $A \Leftrightarrow b \in A$ and b is an upper bound of A,*
- *b is the least element of $A \Leftrightarrow b \in A$ and b is a lower bound of A,*
- *b is the supremum of A ($b = \sup A$) $\Leftrightarrow b$ is the least upper bound of A,*
- *b is the infimum of A ($b = \inf A$) $\Leftrightarrow b$ is the greatest lower bound of A.*

By the help of those concepts, the definition of a complete lattice can be given.

Definition 1.17. *A poset $(P, \leq_P)$ is called a lattice if every doubleton in P has a supremum and infimum.*

Definition 1.18. *A lattice $(L, \leq_L)$ is called bounded if L has a greatest and a least element. A lattice $(L, \leq_L)$ is called complete if every non-empty subset of L has a supremum and infimum.*

Remark that a complete lattice is also bounded. The greatest and least element of a bounded lattice $\mathcal{L} = (L, \leq_L)$ are unique and will be denoted by $1_\mathcal{L}$ and $0_\mathcal{L}$ respectively.

To end this subsection, we introduce the different lattice-morphisms.

Definition 1.19. *[7, 28] Let $\mathcal{L} = (L, \leq_L)$ be a complete lattice and f an $L - L$ mapping. If for all $(x, y) \in L^2$ it holds that*

[5] The binary relation $\leq_P$ puts an ordering on the elements of P and should be read as "is less than or equal to".

- $f(\inf(x,y)) = \inf(f(x), f(y))$, *then* f *is a meet-morphism,*
- $f(\sup(x,y)) = \sup(f(x), f(y))$, *then* f *is a join-morphism,*
- $f(\inf(x,y)) = \sup(f(x), f(y))$, *then* f *is a dual meet-morphism,*
- $f(\sup(x,y)) = \inf(f(x), f(y))$, *then* f *is a dual join-morphism.*

If for each family $(x_j)_{j\in J}$ *in* L*, where* J *is an arbitrary index family, it holds that*

- $f(\inf_{j\in J} x_j) = \inf_{j\in J} f(x_j)$, *then* f *is an inf-morphism,*
- $f(\sup_{j\in J} x_j) = \sup_{j\in J} f(x_j)$, *then* f *is a sup-morphism,*
- $f(\inf_{j\in J} x_j) = \sup_{j\in J} f(x_j)$, *then* f *is a dual inf-morphism,*
- $f(\sup_{j\in J} x_j) = \inf_{j\in J} f(x_j)$, *then* f *is a dual sup-morphism.*

1.4.2 Characterization

For a complete lattice $\mathcal{L} = (L, \leq_L)$, an $\mathcal{L}$-fuzzy set A in a universe X is characterised by its membership function χ_A:

$$\begin{aligned} \chi_A : \quad & X \to L \\ & x \to \chi_A(x). \end{aligned}$$

Analogously as for fuzzy sets, we will simplify the notation $\chi_A(x)$ to $A(x)$ for the membership degree of an element $x \in X$ in the $\mathcal{L}$-fuzzy set A. The higher this degree (w.r.t. $\leq_L$), the more the element belongs to the set. The class of all $\mathcal{L}$-fuzzy sets in a universe X is denoted by $\mathcal{F}_{\mathcal{L}}(X)$.

Remark that $([0,1], \leq)$ forms a complete lattice and that fuzzy sets as introduced by Zadeh are a special case of $\mathcal{L}$-fuzzy sets.

1.5 $\mathcal{L}$-Fuzzy Logical Operators

1.5.1 Definitions

The fuzzy logical operators on $[0,1]$ can be extended to operators on $\mathcal{L} = (L, \leq_L)$ as follows.

Definition 1.20.

- *A negator* $\mathcal{N}$ *on* $\mathcal{L}$ *is a decreasing* $L - L$ *mapping (w.r.t.* $\leq_L$*) that satisfies* $\mathcal{N}(0_{\mathcal{L}}) = 1_{\mathcal{L}}$ *and* $\mathcal{N}(1_{\mathcal{L}}) = 0_{\mathcal{L}}$.
- *A negator* $\mathcal{N}$ *is an involutive negator on* $\mathcal{L}$ *if* $(\forall x \in L)(\mathcal{N}(\mathcal{N}(x)) = x)$.

Definition 1.21.

- *A conjunctor $\mathcal{C}$ on $\mathcal{L}$ is an increasing $L^2 - L$ mapping (w.r.t. $\leq_L$) that satisfies $\mathcal{C}(0_\mathcal{L}, 0_\mathcal{L}) = \mathcal{C}(0_\mathcal{L}, 1_\mathcal{L}) = \mathcal{C}(1_\mathcal{L}, 0_\mathcal{L}) = 0_\mathcal{L}$ and $\mathcal{C}(1_\mathcal{L}, 1_\mathcal{L}) = 1_\mathcal{L}$.*
- *A conjunctor $\mathcal{C}$ is a semi-norm on $\mathcal{L}$ if it satisfies $(\forall x \in L)(\mathcal{C}(1_\mathcal{L}, x) = \mathcal{C}(x, 1_\mathcal{L}) = x)$.*
- *A semi-norm $\mathcal{C}$ is a t-norm on $\mathcal{L}$ if it is commutative and associative.*

Definition 1.22.

- *A disjunctor $\mathcal{D}$ on $\mathcal{L}$ is an increasing $L^2 - L$ mapping (w.r.t. $\leq_L$) that satisfies $\mathcal{D}(1_\mathcal{L}, 1_\mathcal{L}) = \mathcal{D}(0_\mathcal{L}, 1_\mathcal{L}) = \mathcal{D}(1_\mathcal{L}, 0_\mathcal{L}) = 1_\mathcal{L}$ and $\mathcal{D}(0_\mathcal{L}, 0_\mathcal{L}) = 0_\mathcal{L}$.*
- *A disjunctor $\mathcal{D}$ is a semi-conorm on $\mathcal{L}$ if it satisfies $(\forall x \in L)(\mathcal{D}(0_\mathcal{L}, x) = \mathcal{D}(x, 0_\mathcal{L}) = x)$.*
- *A semi-conorm $\mathcal{D}$ is a t-conorm on $\mathcal{L}$ if it is commutative and associative.*

Definition 1.23.

- *An implicator $\mathcal{I}$ on $\mathcal{L}$ is a hybrid monotonic $L^2 - L$ mapping (i.e., decreasing in the first argument (w.r.t. $\leq_L$) and increasing in the second argument (w.r.t. $\leq_L$)) that satisfies $\mathcal{I}(0_\mathcal{L}, 0_\mathcal{L}) = \mathcal{I}(0_\mathcal{L}, 1_\mathcal{L}) = \mathcal{I}(1_\mathcal{L}, 1_\mathcal{L}) = 1_\mathcal{L}$ and $\mathcal{I}(1_\mathcal{L}, 0_\mathcal{L}) = 0_\mathcal{L}$. Every implicator $\mathcal{I}$ induces a negator $\mathcal{N}_\mathcal{I}$ defined by $\mathcal{N}_\mathcal{I}(x) = \mathcal{I}(x, 0_\mathcal{L})$, $\forall x \in L$.*
- *An implicator $\mathcal{I}$ is a border implicator on $\mathcal{L}$ if it satisfies $(\forall x \in L)(\mathcal{I}(1_\mathcal{L}, x) = x)$.*
- *A border implicator $\mathcal{I}$ is a model implicator on $\mathcal{L}$ if it is contrapositive w.r.t. its induced negator, i.e., $(\forall (x, y) \in L^2)(\mathcal{I}(x, y) = \mathcal{I}(\mathcal{N}_\mathcal{I}(y), \mathcal{N}_\mathcal{I}(x)))$, and if it fulfills the exchange principle, i.e., $(\forall (x, y, z) \in L^3)(\mathcal{I}(x, \mathcal{I}(y, z)) = \mathcal{I}(y, \mathcal{I}(x, z)))$.*

In the above definition, it is already mentioned that every implicator $\mathcal{I}$ on $\mathcal{L}$ induces a negator $\mathcal{N}_\mathcal{I}$ on $\mathcal{L}$ given by $\mathcal{N}_\mathcal{I}(x) = \mathcal{I}(x, 0_\mathcal{L})$, $\forall x \in L$. Further, also conjunctors and implicators can be induced by other logical operators.

Let $\mathcal{N}$ and $\mathcal{C}$ be respectively a negator and a conjunctor on $\mathcal{L}$. Then the operator $\mathcal{D}_{\mathcal{C},\mathcal{N}}$ given by $\mathcal{D}_{\mathcal{C},\mathcal{N}}(x, y) = \mathcal{N}(\mathcal{C}(\mathcal{N}(x), \mathcal{N}(y)))$, $\forall (x, y) \in L^2$ is a disjunctor on $\mathcal{L}$. Analogously, if $\mathcal{N}$ and $\mathcal{D}$ are respectively a negator and a disjunctor on $\mathcal{L}$, then the operator $\mathcal{C}_{\mathcal{D},\mathcal{N}}$ given by $\mathcal{C}_{\mathcal{D},\mathcal{N}}(x, y) = \mathcal{N}(\mathcal{D}(\mathcal{N}(x), \mathcal{N}(y)))$, $\forall (x, y) \in L^2$ is a conjunctor on $\mathcal{L}$. If $\mathcal{N}$ is an involutive negator, then a conjunctor $\mathcal{C}$ and a disjunctor $\mathcal{D}$ are called dual with respect to $\mathcal{N}$ if and only if $\mathcal{C} = \mathcal{C}_{\mathcal{D},\mathcal{N}}$ and $\mathcal{D} = \mathcal{D}_{\mathcal{C},\mathcal{N}}$.

Let $\mathcal{N}$ and $\mathcal{I}$ be respectively a negator and an implicator on $\mathcal{L}$. Then the operator $\mathcal{C}_{\mathcal{I},\mathcal{N}}$ given by $\mathcal{C}_{\mathcal{I},\mathcal{N}}(x, y) = \mathcal{N}(\mathcal{I}(x, \mathcal{N}(y)))$, $\forall (x, y) \in L^2$ is a conjunctor on $\mathcal{L}$ and it is called the conjunctor induced by $\mathcal{I}$ and $\mathcal{N}$.

Let $\mathcal{N}$ and $\mathcal{C}$ be respectively a negator and a conjunctor on $\mathcal{L}$. Then the operator $\mathcal{I}_{\mathcal{C},\mathcal{N}}$ given by $\mathcal{I}_{\mathcal{C},\mathcal{N}}(x, y) = \mathcal{N}(\mathcal{C}(x, \mathcal{N}(y)))$, $\forall (x, y) \in L^2$ is an implicator on $\mathcal{L}$ and it is called the implicator induced by $\mathcal{C}$ and $\mathcal{N}$.

Let $\mathcal{N}$ and $\mathcal{D}$ be respectively a negator and a disjunctor on $\mathcal{L}$. Then the operator $\mathcal{I}_{\mathcal{D},\mathcal{N}}$ given by $\mathcal{I}_{\mathcal{D},\mathcal{N}}(x, y) = (\mathcal{D}(\mathcal{N}(x), y))$, $\forall (x, y) \in L^2$ is an implicator on $\mathcal{L}$ and it is called the implicator induced by $\mathcal{D}$ and $\mathcal{N}$.

Let $\mathcal{C}$ be a conjunctor on $\mathcal{L}$ that satisfies $(\forall x \in L)(\mathcal{C}(1_{\mathcal{L}}, x) = 0_{\mathcal{L}} \Rightarrow x = 0_{\mathcal{L}})$. Then the operator $\mathcal{I}_{\mathcal{C}}$ given by $\mathcal{I}_{\mathcal{C}}(x, y) = \sup\{z \in L | \mathcal{C}(x, z) \leq_L y\},\ \forall (x, y) \in L^2$ is an implicator on $\mathcal{L}$ and it is called the residual implicator of $\mathcal{C}$ [32].

Further, the order relation $\leq_L$ on the lattice $\mathcal{L}$ can be extended to the logical operators as follows:

Definition 1.24. *Let $\mathcal{N}_1$ and $\mathcal{N}_2$ be two negators on $\mathcal{L}$, then*

$$\mathcal{N}_1 \leq_L \mathcal{N}_2 \Leftrightarrow (\forall x \in L)(\mathcal{N}_1(x) \leq_L \mathcal{N}_2(x)).$$

Let $\mathcal{C}_1$ and $\mathcal{C}_2$ be two conjunctors on $\mathcal{L}$, then

$$\mathcal{C}_1 \leq_L \mathcal{C}_2 \Leftrightarrow (\forall (x, y) \in L^2)(\mathcal{C}_1(x, y) \leq_L \mathcal{C}_2(x, y)).$$

Let $\mathcal{D}_1$ and $\mathcal{D}_2$ be two disjunctors on $\mathcal{L}$, then

$$\mathcal{D}_1 \leq_L \mathcal{D}_2 \Leftrightarrow (\forall (x, y) \in L^2)(\mathcal{D}_1(x, y) \leq_L \mathcal{D}_2(x, y)).$$

Let $\mathcal{I}_1$ and $\mathcal{I}_2$ be two implicators on $\mathcal{L}$, then

$$\mathcal{I}_1 \leq_L \mathcal{I}_2 \Leftrightarrow (\forall (x, y) \in L^2)(\mathcal{I}_1(x, y) \leq_L \mathcal{I}_2(x, y)).$$

1.5.2 Some Properties

In this subsection, we will give some properties concerning the $\mathcal{L}$-fuzzy logical operators, that will be used in the remainder of this thesis.

Lemma 1.5.1. *Let $\mathcal{C}$ be a conjunctor on $\mathcal{L}$ and let $(a_j)_{j \in J}$ and $(b_j)_{j \in J}$ be families in L, with J an arbitrary index family. It holds that:*

(i) $\sup\limits_{j \in J} \mathcal{C}(a_j, b_j) \leq_L \mathcal{C}\left(\sup\limits_{j \in J} a_j, \sup\limits_{j \in J} b_j\right)$,

(ii) $\inf\limits_{j \in J} \mathcal{C}(a_j, b_j) \geq_L \mathcal{C}\left(\inf\limits_{j \in J} a_j, \inf\limits_{j \in J} b_j\right)$.

Proof. (i) Since the partial mappings of $\mathcal{C}$ are increasing it follows that

$$\mathcal{C}(a_i, b_i) \leq_L \mathcal{C}\left(\sup_{j \in J} a_j, \sup_{j \in J} b_j\right),$$

for all couples (a_i, b_i) (with $i \in J$). As a consequence, $\mathcal{C}\left(\sup\limits_{j \in J} a_j, \sup\limits_{j \in J} b_j\right)$ is an upper bound for the set $\{\mathcal{C}(a_i, b_i) | i \in J\}$, and thus

$$\sup_{j \in J} \mathcal{C}(a_j, b_j) \leq_L \mathcal{C}\left(\sup_{j \in J} a_j, \sup_{j \in J} b_j\right).$$

(ii) Analogous.

□

Lemma 1.5.2. *Let $\mathcal{D}$ be a disjunctor on $\mathcal{L}$, and let $(a_j)_{j\in J}$ and $(b_j)_{j\in J}$ be families in L, with J an arbitrary index family. It holds that:*

(i) $\sup_{j\in J} \mathcal{D}(a_j, b_j) \leq_L \mathcal{D}\left(\sup_{j\in J} a_j, \sup_{j\in J} b_j\right)$,

(ii) $\inf_{j\in J} \mathcal{D}(a_j, b_j) \geq_L \mathcal{D}\left(\inf_{j\in J} a_j, \inf_{j\in J} b_j\right)$.

Proof. Analogous to the proof of Lemma 1.5.1. □

Lemma 1.5.3. *[28] If $\mathcal{I} = \mathcal{I}_\mathcal{C}$ with $\mathcal{C}$ a conjunctor on $\mathcal{L}$ for which $(\forall x \in L)(\mathcal{C}(1_\mathcal{L}, x) = 0_\mathcal{L} \Rightarrow x = 0_\mathcal{L})$, then*

$$(\forall (a, b) \in L^2)(b \leq_L \mathcal{I}_\mathcal{C}(a, \mathcal{C}(a, b))).$$

Proof. For all $(a, b) \in L^2$:

$$\begin{array}{rcl} \mathcal{I}_\mathcal{C}(a, \mathcal{C}(a, b)) & = & \sup\{\delta \in L | \mathcal{C}(a, \delta) \leq_L \mathcal{C}(a, b)\} \\ & \geq_L & b. \end{array}$$

□

Lemma 1.5.4. *[28] If $\mathcal{I} = \mathcal{I}_\mathcal{C}$ with $\mathcal{C}$ t-norm on $\mathcal{L}$, of which the partial mappings are sup-morphisms, then*

$$(\forall (a, b) \in L^2)(\mathcal{C}(a, \mathcal{I}_\mathcal{C}(a, b)) \leq_L b).$$

Proof. For all $(a, b) \in L^2$:

$$\begin{array}{rcl} \mathcal{C}(a, \mathcal{I}_\mathcal{C}(a, b)) & = & \mathcal{C}(a, \sup\{\delta \in L | \mathcal{C}(a, \delta) \leq_L b\}) \\ & = & \sup\{\mathcal{C}(a, \delta) | \delta \in L \text{ and } \mathcal{C}(a, \delta) \leq_L b\} \\ & \leq_L & b. \end{array}$$

□

Lemma 1.5.5. *[93, 28]*

1. *If $\mathcal{I} = \mathcal{I}_{\mathcal{C},\mathcal{N}}$ with $\mathcal{C}$ an associative conjunctor on $\mathcal{L}$ and $\mathcal{N}$ an involutive negator on $\mathcal{L}$, then it holds that:*

$$(\forall (a, b, c) \in L^3)(\mathcal{I}(a, \mathcal{I}(b, c)) = \mathcal{I}(\mathcal{C}(a, b), c)).$$

2. *If $\mathcal{I} = \mathcal{I}_{\mathcal{C}}$ with $\mathcal{C}$ a t-norm on $\mathcal{L}$, then it holds that:*

$$(\forall (a,b,c) \in L^3)(\mathcal{I}(a,\mathcal{I}(b,c)) \leq_L \mathcal{I}(\mathcal{C}(a,b),c)).$$

If the partial mappings of $\mathcal{C}$ are sup-morphisms, then

$$(\forall (a,b,c) \in L^3)(\mathcal{I}(a,\mathcal{I}(b,c)) = \mathcal{I}(\mathcal{C}(a,b),c)).$$

Proof.

1. Suppose that $\mathcal{I} = \mathcal{I}_{\mathcal{C},\mathcal{N}}$ with $\mathcal{C}$ an associative conjunctor on $\mathcal{L}$ and $\mathcal{N}$ an involutive negator on L. For all $(a,b,c) \in L^3$:

$$\begin{array}{rcl} \mathcal{I}(a,\mathcal{I}(b,c)) & = & \mathcal{N}[\mathcal{C}(a,\mathcal{N}(\mathcal{I}(b,c)))] \\ & = & \mathcal{N}[\mathcal{C}(a,\mathcal{N}(\mathcal{N}[\mathcal{C}(b,\mathcal{N}(c))]))] \\ & = & \mathcal{N}[\mathcal{C}(a,\mathcal{C}(b,\mathcal{N}(c)))] \\ & = & \mathcal{N}[\mathcal{C}(\mathcal{C}(a,b),\mathcal{N}(c))] \\ & = & \mathcal{I}(\mathcal{C}(a,b),c) \end{array}$$

2. Suppose now that $\mathcal{I} = \mathcal{I}_{\mathcal{C}}$ with $\mathcal{C}$ a t-norm on $\mathcal{L}$. For all $(a,b,c,d) \in L^4$ it holds that

$$\mathcal{C}(b,\mathcal{C}(a,d)) \leq_L c \Rightarrow \mathcal{C}(a,d) \leq_L \mathcal{I}_{\mathcal{C}}(b,c).$$

Indeed, if $\mathcal{C}(b,\mathcal{C}(a,d)) \leq_L c$, then

$$\mathcal{C}(a,d) \in \{\epsilon \in L | \mathcal{C}(b,\epsilon) \leq_L c\}$$

and thus

$$\mathcal{C}(a,d) \leq_L \sup\{\epsilon \in L | \mathcal{C}(b,\epsilon) \leq_L c\} = \mathcal{I}_{\mathcal{C}}(b,c).$$

Due to the associativity and commutativity of $\mathcal{C}$, it follows that for all $(a,b,c) \in L^3$:

$$\begin{array}{rcl} \mathcal{I}_{\mathcal{C}}(a,\mathcal{I}_{\mathcal{C}}(b,c)) & = & \sup\{\delta \in L | \mathcal{C}(a,\delta) \leq_L \mathcal{I}_{\mathcal{C}}(b,c)\} \\ & \leq_L & \sup\{\delta \in L | \mathcal{C}(b,\mathcal{C}(a,\delta)) \leq_L c\} \\ & = & \sup\{\delta \in L | \mathcal{C}(\mathcal{C}(a,b),\delta) \leq_L c\} \\ & = & \mathcal{I}_{\mathcal{C}}(\mathcal{C}(a,b),c). \end{array}$$

If the partial mappings of $\mathcal{C}$ are sup-morphisms, then it also holds for all $(a,b,c,d) \in L^4$ that

$$\mathcal{C}(b,\mathcal{C}(a,d)) \leq_L c \Leftarrow \mathcal{C}(a,d) \leq_L \mathcal{I}_{\mathcal{C}}(b,c).$$

Indeed, since the partial mapping $\mathcal{C}(b,.)$ is increasing, it follows from $\mathcal{C}(a,d) \leq_L \mathcal{I}_{\mathcal{C}}(b,c)$ that

$$\mathcal{C}(b,\mathcal{C}(a,d)) \leq_L \mathcal{C}(b,\mathcal{I}_{\mathcal{C}}(b,c)).$$

Applying Lemma 1.5.4 results in $\mathcal{C}(b,\mathcal{C}(a,d)) \leq_L c$. As a consequence

$$\sup\{\delta \in L | \mathcal{C}(a,\delta) \leq_L \mathcal{I}_{\mathcal{C}}(b,c)\} = \sup\{\delta \in L | \mathcal{C}(b,\mathcal{C}(a,\delta)) \leq_L c\}.$$

□

1.6 $\mathcal{L}$-Fuzzy Set Operations

1.6.1 Complement, Intersection and Union of $\mathcal{L}$-Fuzzy Sets

The $\mathcal{L}$-fuzzy logical operators can be used to define the complement, intersection and union of $\mathcal{L}$-fuzzy sets:

Definition 1.25. *Let $A, B \in \mathcal{F}_{\mathcal{L}}(X)$. If $\mathcal{N}$ is a negator on $\mathcal{L}$, then the $\mathcal{N}$-complement $co_{\mathcal{N}}(A)$ of A is defined as the $\mathcal{L}$-fuzzy set in X given by:*

$$(co_{\mathcal{N}}(A))(x) = \mathcal{N}(A(x)),\ \forall x \in X.$$

If $\mathcal{C}$ is a conjunctor on $\mathcal{L}$, then the $\mathcal{C}$-intersection $A \cap_{\mathcal{C}} B$ of A and B is defined as the $\mathcal{L}$-fuzzy set in X given by:

$$(A \cap_{\mathcal{C}} B)(x) = \mathcal{C}(A(x), B(x)),\ \forall x \in X.$$

If $\mathcal{D}$ is a disjunctor on $\mathcal{L}$, then the $\mathcal{D}$-union $A \cup_{\mathcal{D}} B$ of A and B is defined as the $\mathcal{L}$-fuzzy set in X given by:

$$(A \cup_{\mathcal{D}} B)(x) = \mathcal{D}(A(x), B(x)),\ \forall x \in X.$$

If $\mathcal{C}$ (respectively $\mathcal{D}$) is the infimum operator (respectively the supremum operator), then the intersection (respectively union) is called the Zadeh-intersection (respectively Zadeh-union) and the notation $\cap_{\mathcal{C}}$ is simplified to $\cap$ (respectively $\cup_{\mathcal{D}}$ to $\cup$).

If $\mathcal{C}$ and $\mathcal{D}$ are commutative and associative (in particular if they are a t-norm and a t-conorm), then the above definitions can be extended to the intersection and union of an arbitrary finite family of $\mathcal{L}$-fuzzy sets. If further the conjunctor $\mathcal{C}$ and the disjunctor $\mathcal{D}$ can also be extended to an infinite number of arguments, then also an extension to infinite families is possible. For the Zadeh-intersection and Zadeh-union and an arbitrary (infinite) family $(A_j)_{j \in J}$ in $\mathcal{F}_{\mathcal{L}}(X)$, this becomes:

$$\begin{aligned} (\cap_{j \in J} A_j)(x) &= \inf_{j \in J} A_j(x),\ \forall x \in X, \\ (\cup_{j \in J} A_j)(x) &= \sup_{j \in J} A_j(x),\ \forall x \in X. \end{aligned}$$

1.6.2 Inclusion of $\mathcal{L}$-Fuzzy Sets

Definition 1.26. *Let $A, B \in \mathcal{F}_{\mathcal{L}}(X)$, then*

$$A \subseteq B \Leftrightarrow (\forall x \in X)(A(x) \leq_L B(x)).$$

1.7 Interval-valued Fuzzy Sets

In Part III, we will focus on a special case of $\mathcal{L}$-fuzzy sets, namely the interval-valued fuzzy sets.

1.7.1 Characterization

Interval-valued fuzzy sets [117] are $\mathcal{L}$-fuzzy sets where the complete lattice $\mathcal{L}$ is given by $\mathcal{L}^I = (L^I, \leq_{L^I})$. L^I here stands for the set of all closed subintervals of the unit interval $[0,1]$, i.e.

$$L^I = \{[x_1, x_2] | [x_1, x_2] \subseteq [0,1]\}.$$

We will denote the lower and upper bound of an element x of L^I by respectively x_1 and x_2: $x = [x_1, x_2]$ (Fig. 1.1). Further, the partial ordering $\leq_{L^I}$ on L^I is defined by

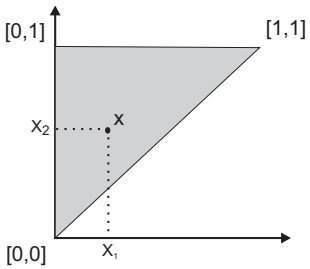

Figure 1.1: Graphical representation of L^I.

$$x \leq_{L^I} y \Leftrightarrow x_1 \leq y_1 \text{ and } x_2 \leq y_2,\ \forall x, y \in L^I.$$

The infimum and supremum of an arbitrary subset S of L^I are then respectively given by:

$$\begin{aligned} \inf S &= [\inf_{x \in S} x_1, \inf_{x \in S} x_2], \\ \sup S &= [\sup_{x \in S} x_1, \sup_{x \in S} x_2]. \end{aligned}$$

We use the notations $0_{\mathcal{L}^I}$ for $\inf L^I = [0,0]$ and $1_{\mathcal{L}^I}$ for $\sup L^I = [1,1]$.

Related orderings on L^I that we wil also use in this thesis are ($\forall x, y \in L^I$):

$$\begin{aligned} x <_{L^I} y &\Leftrightarrow x \leq_{L^I} y \text{ and } x \neq y, \\ x \ll_{L^I} y &\Leftrightarrow x_1 < y_1 \text{ and } x_2 < y_2, \\ x \geq_{L^I} y &\Leftrightarrow y \leq_{L^I} x, \\ x >_{L^I} y &\Leftrightarrow y <_{L^I} x, \\ x \gg_{L^I} y &\Leftrightarrow y \ll_{L^I} x. \end{aligned}$$

Summarized, an interval-valued fuzzy set A in a universe X is characterised by the mapping

$$\begin{aligned} A: \quad & X \to L^I \\ & x \to A(x) = [A_1(x), A_2(x)] \end{aligned}$$

So, an interval-valued fuzzy set can also be seen as an extension of a classical fuzzy set, where now uncertainty concerning the membership degree is allowed. Instead of mapping an element in the universe onto one specific membership value in $[0,1]$, it is now mapped onto a subinterval of $[0,1]$.

Finally, in the remainder, we will denote the class of all interval-valued sets in the universe X by $\mathcal{F}_{\mathcal{L}^I}(X)$.

1.7.2 Basic Concepts

The basic concepts concerning fuzzy sets as introduced in Subsection 1.1.2, can be extended to interval-valued fuzzy sets in a straightforward way. In particular, we give the definitions for the support and the $[\alpha_1, \alpha_2]$-cuts of interval-valued fuzzy sets.

Definition 1.27. *Let $A \in \mathcal{F}_{\mathcal{L}^I}(X)$. The support d_A of A is defined as:*

$$d_A = \{x \in X | A(x) \neq 0_{\mathcal{L}^I}\} = \{x \in X | A_2(x) > 0\}.$$

For the definitions of the different $[\alpha_1, \alpha_2]$-cuts of an interval-valued fuzzy set, we need to introduce the notation $U_{L^I} = \{[x_1, x_2] \in L^I | x_2 = 1\}$.

Definition 1.28. [135] *Let $A \in \mathcal{F}_{\mathcal{L}^I}(X)$.*
For $[\alpha_1, \alpha_2] \in L^I \backslash \{0_{\mathcal{L}^I}\}$, the weak $[\alpha_1, \alpha_2]$-cut $A^{\alpha_2}_{\alpha_1}$ of A is defined as:

$$\begin{aligned} A^{\alpha_2}_{\alpha_1} &= \{x | x \in X,\ A_1(x) \geq \alpha_1 \text{ and } A_2(x) \geq \alpha_2\} \\ &= \{x | x \in X \text{ and } A(x) \geq_{L^I} [\alpha_1, \alpha_2]\}. \end{aligned}$$

For $[\alpha_1, \alpha_2] \in L^I \backslash U_{L^I}$, the strict $[\alpha_1, \alpha_2]$-cut $A^{\overline{\alpha_2}}_{\overline{\alpha_1}}$ of A is defined as:

$$\begin{aligned} A^{\overline{\alpha_2}}_{\overline{\alpha_1}} &= \{x | x \in X,\ A_1(x) > \alpha_1 \text{ and } A_2(x) > \alpha_2\} \\ &= \{x | x \in X \text{ and } A(x) \gg_{L^I} [\alpha_1, \alpha_2]\}. \end{aligned}$$

The cases $[\alpha_1, \alpha_2] = 0_{\mathcal{L}^I}$ and $[\alpha_1, \alpha_2] \in U_{L^I}$ are excluded for respectively the weak and the strict $[\alpha_1, \alpha_2]$-cut. Since $\{x | x \in X,\ A_1(x) \geq 0 \text{ and } A_2(x) \geq 0\} = X$ and $\{x | x \in X \text{ and } A_2(x) > 1\} = \emptyset$, these cases don't yield new information.

Also cuts based only on the lower or upper bound can be defined.

Definition 1.29. *Let $A \in \mathcal{F}_{\mathcal{L}^I}(X)$.*
For $\alpha_1 \in]0,1]$, the weak α_1-subcut A_{α_1} of A is defined as:

$$A_{\alpha_1} = \{x | x \in X \text{ and } A_1(x) \geq \alpha_1\}.$$

For $\alpha_2 \in]0,1]$, the weak α_2-supercut A^{α_2} of A is defined as:

$$A^{\alpha_2} = \{x | x \in X \text{ and } A_2(x) \geq \alpha_2\}.$$

For $\alpha_1 \in [0,1[$, the strict α_1-subcut $A_{\overline{\alpha_1}}$ of A is defined as:

$$A_{\overline{\alpha_1}} = \{x | x \in X \text{ and } A_1(x) > \alpha_1\}.$$

For $\alpha_2 \in [0,1[$, the strict α_2-supercut $A^{\overline{\alpha_2}}$ of A is defined as:

$$A^{\overline{\alpha_2}} = \{x | x \in X \text{ and } A_2(x) > \alpha_2\}.$$

The cases $\alpha_1 = 0$ and $\alpha_1 = 1$ are excluded for respectively the weak and the strict α_1-subcut. Since $\{x | x \in X \text{ and } A_1(x) \geq 0\} = X$ and $\{x | x \in X \text{ and } A_1(x) > 1\} = \emptyset$, these cases don't yield new information. An analogous reasoning holds for the weak and strict α_2-supercut.

Finally, also a combination of weak and strong bounds is possible.

Definition 1.30. *Let $A \in \mathcal{F}_{\mathcal{L}^I}(X)$.*
For $[\alpha_1, \alpha_2] \in L^I \backslash U_{L^I}$, the weak-strict $[\alpha_1, \alpha_2]$-cut $A_{\alpha_1}^{\overline{\alpha_2}}$ of A is defined as:

$$A_{\alpha_1}^{\overline{\alpha_2}} = \{x | x \in X,\ A_1(x) \geq \alpha_1 \text{ and } A_2(x) > \alpha_2\}.$$

For $[\alpha_1, \alpha_2] \in L^I \backslash \{1_{\mathcal{L}^I}\}$, the strict-weak $[\alpha_1, \alpha_2]$-cut $A_{\overline{\alpha_1}}^{\alpha_2}$ of A is defined as:

$$A_{\overline{\alpha_1}}^{\alpha_2} = \{x | x \in X,\ A_1(x) > \alpha_1 \text{ and } A_2(x) \geq \alpha_2\}.$$

The cases $[\alpha_1, \alpha_2] \in U_{L^I}$ and $[\alpha_1, \alpha_2] = 1_{\mathcal{L}^I}$ are excluded for respectively the weak-strict and strict-weak $[\alpha_1, \alpha_2]$-cut. Since $\{x | x \in X \text{ and } A_2(x) > 1\} = \emptyset$ and $\{x | x \in X \text{ and } A_1(x) > 1\} = \emptyset$, these cases don't yield new information.

1.7.3 Construction of Interval-valued Fuzzy Logical Operators

Interval-valued fuzzy logical operators can be constructed using fuzzy logical operators defined on $[0,1]$ in a straighforward way.

Proposition 1.7.1. *Let $(x, y) \in (L^I)^2$.*

- *If $\mathcal{N}$ is a negator on $[0,1]$, then the operator $\tilde{\mathcal{N}}$, given by*

$$\tilde{\mathcal{N}}(x) = [\mathcal{N}(x_2), \mathcal{N}(x_1)],\ \forall x \in L^I,$$

  is a negator on $\mathcal{L}^I$.

- *If $\mathcal{C}$ is a conjunctor on $[0,1]$, then the operator $\tilde{\mathcal{C}}$, given by*

$$\tilde{\mathcal{C}}(x, y) = [\mathcal{C}(x_1, y_1), \mathcal{C}(x_2, y_2)],\ \forall (x, y) \in (L^I)^2,$$

  is a conjunctor on $\mathcal{L}^I$.

- *If $\mathcal{D}$ is a disjunctor on $[0,1]$, then the operator $\tilde{\mathcal{D}}$, given by*

$$\tilde{\mathcal{D}}(x,y) = [\mathcal{D}(x_1,y_1), \mathcal{D}(x_2,y_2)],\ \forall (x,y) \in (L^I)^2,$$

  is a disjunctor on $\mathcal{L}^I$.
- *If $\mathcal{I}$ is an implicator on $[0,1]$, then the operator $\tilde{\mathcal{I}}$, given by*

$$\tilde{\mathcal{I}}(x,y) = [\mathcal{I}(x_2,y_1), \mathcal{I}(x_1,y_2)],\ \forall (x,y) \in (L^I)^2,$$

  is an implicator on $\mathcal{L}^I$.

For example, the (extended) standard negator $\mathcal{N}_s$, given by

$$\mathcal{N}_s(x) = [1-x_2, 1-x_1],\ \forall x \in L^I,$$

is an involutive negator on $\mathcal{L}^I$.

The conjunctor $\mathcal{C}_{\min}$, based on the minimum t-norm $\mathcal{C}_M$, i.e.,

$$\mathcal{C}_{\min}(x,y) = [\min(x_1,y_1), \min(x_2,y_2)],\ \forall (x,y) \in (L^I)^2,$$

is a t-norm on $\mathcal{L}^I$.

The disjunctor $\mathcal{D}_{\max}$, that extends the maximum t-conorm $\mathcal{D}_M$, i.e.,

$$\mathcal{D}_{\max}(x,y) = [\max(x_1,y_1), \max(x_2,y_2)],\ \forall (x,y) \in (L^I)^2,$$

is a t-conorm on $\mathcal{L}^I$.

The extended Kleene-Dienes implicator $\mathcal{I}_{EKD}$, given by

$$\mathcal{I}_{EKD}(x,y) = [\max(1-x_2,y_1), \max(1-x_1,y_2)],\ \forall (x,y) \in (L^I)^2,$$

is a model implicator on $\mathcal{L}^I$. Remark that $\mathcal{I}_{EKD} = \mathcal{I}_{\mathcal{C}_{\min},\mathcal{N}_s} = \mathcal{I}_{\mathcal{D}_{\max},\mathcal{N}_s}$.

Also other ways of constructing interval-valued fuzzy logical operators from fuzzy ones exist. For a more thorough study, we refer the interested reader to [34].

1.8 Intuitionistic and Bipolar Fuzzy Sets

Although being different semantically, intuitionistic [2] and bipolar fuzzy sets [8, 9] are formally equivalent. They namely are $\mathcal{L}$-fuzzy sets where the complete lattice $\mathcal{L}$ is given by $\mathcal{L}^* = (L^*, \leq_{L^*})$, with

$$L^* = \{(x_1,x_2) | (x_1,x_2) \in [0,1]^2 \text{ and } x_1 + x_2 \leq 1\},$$

and

$$(x_1,x_2) \leq_{L^*} (y_1,y_2) \Leftrightarrow x_1 \leq y_1 \text{ and } x_2 \geq y_2,\ \forall (x_1,x_2),(y_1,y_2) \in L^*.$$

So, an intuitionistic (respectively bipolar) fuzzy set A in a universe X is characterised by the mapping

$$\begin{aligned} A: \quad & X \to L^* \\ & x \to A(x) = (A_1(x), A_2(x)). \end{aligned}$$

For an intuitionistic fuzzy set A in X, $A_1(x)$ defines for each element $x \in X$ the degree to which x belongs to A (membership degree) and $A_2(x)$ the degree to which x does not belong to A (non-membership degree). The degree of indetermination or hesitation is then given by $1 - A_1(x) - A_2(x)$. Bipolar fuzzy sets on their turn, are used to represent bipolar information. For a bipolar fuzzy set A in X, $A_1(x)$ denotes the degree to which x satisfies a given property (positive information) and $A_2(x)$ (negative information) denotes the degree to which x satisfies the opposite property. Bipolar information is e.g. 'to the left of-to the right of' and 'close to-far from'. Remark that such opposite relations don't need to be each others complement and some indetermination is possible. The main thing is that bipolar fuzzy sets don't need to represent one physical object, but rather more complex information, possibly coming from different sources.

The infimum and supremum of an arbitrary subset S of L^* are respectively given by:

$$\begin{aligned} \inf S &= (\inf_{x \in S} x_1, \sup_{x \in S} x_2), \\ \sup S &= (\sup_{x \in S} x_1, \inf_{x \in S} x_2). \end{aligned}$$

The notations $0_{\mathcal{L}^*}$ and $1_{\mathcal{L}^*}$ respectively stand for $\inf L^* = (0, 1)$ and $\sup L^* = (1, 0)$. Further, the class of all intuitionistic and bipolar fuzzy sets over the universe X are respectively denoted by $\mathcal{IFS}(X)$ and $\mathcal{BFS}(X)$.

Finally, intuitionistic and bipolar fuzzy set theory are isomorphic to interval-valued fuzzy set theory as shown in [35]. The isomorphism $\Phi : \mathcal{F}_{\mathcal{L}^I}(X) \to \mathcal{IFS}(X)$ is given as follows: for all $A \in \mathcal{F}_{\mathcal{L}^I}(X)$ and all $x \in X$ it holds that if A maps x onto $A(x) = [A_1(x), A_2(x)]$, then the intuitionistic fuzzy set $\Phi(A)$ maps x onto the couple $\Phi(A)(x) = (A_1(x), 1 - A_2(x))$ (and analogously for bipolar fuzzy sets). So all definitions and results in interval-valued fuzzy set theory can be translated to the intuitionistic or bipolar case. This holds in particular for the results concerning interval-valued mathematical morphology that are discussed in Part III of this thesis.

2
Introduction to Image Processing

In this chapter, we give a short overview of some basic image processing concepts that will be used in this thesis. Section 2.1 discusses the representation of images and videos (images sequences) and introduces the notations. Next, the different noise types by which images can be degraded are listed in Section 2.2. Section 2.3 presents some objective measures to determine the similarity between two images (e.g., a filtered image and the original image that the filtered one tries to approximate/restore). In Section 2.4 finally, the basic concepts of the discrete wavelet transform are given.

2.1 Representation of Images and Videos

2.1.1 Binary Images

An n-dimensional[1] binary (or black-and-white) image can be modelled by an $\mathbb{R}^n - \{0, 1\}$ mapping, that maps each image point onto black (0) or white (1). The set of all image points (that is a subset of $\mathbb{R}^n$), is called the image domain. If we agree to map the points that do not belong to the image onto 0 (i.e., black), the image domain can be generalised to $\mathbb{R}^n$. For the case of simplicity, some devices (such as fax machines) are restricted to binary images, i.e., the most simple kind of images. However, binary images can also arise as the output of a binary decision on the image points (e.g., segmentation into two classes, edge detection,...).

[1] $n \in \mathbb{N} \setminus \{0\}$.

Remark that an $\mathbb{R}^n - \{0,1\}$ mapping can also be seen as the characteristic function of a crisp set in $\mathbb{R}^n$. A binary image A can thus be seen as a crisp subset of $\mathbb{R}^n$. An element $x \in \mathbb{R}^n$ then belongs to the (foreground of) image A, if it corresponds to a white point in the image. If x corresponds to a black point, then x doesn't belong to the image (belongs to the background).

It is well known that the universe $\mathbb{R}^n$ contains an infinite number of elements. Therefore, it is technically impossible to store an image onto a computer or any other device without sampling the image domain. To do this, the image domain is divided by a raster of a finite number of n-dimensional regions (called image elements[2]) and the image can be stored as an n-dimensional matrix. Each image element is then assigned the value (0 or 1) that is the most prominent in that region. The image is thus modelled as an $\mathbb{Z}^n - \{0,1\}$ mapping then and we call it a digital image. For an image A, the colour (black or white) of the image element at location $x \in \mathbb{Z}^n$ in the raster, is denoted by $A(x)$. As an example, a (digital) binary Lena image (as the result of Canny edge detection on the greyscale Lena image in Fig. 2.2) is given in Fig. 2.1 (a). In the enlarged crop of the right eye in that image (Fig. 2.1 (b)) the pixels are clearly visible.

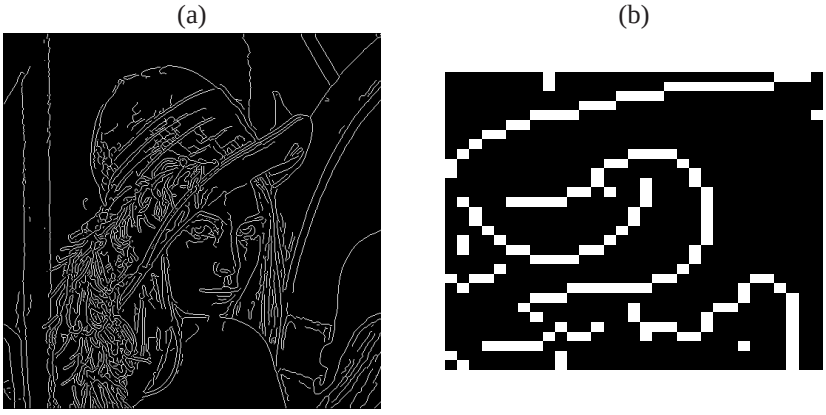

Figure 2.1: (a) The binary Lena image. (b) Enlarged crop of the right eye in the binary Lena image.

2.1.2 Greyscale Images

A n-dimensional greyscale (or monochrome) image is represented by an $\mathbb{R}^n - [0,1]$ mapping. Image points are not longer only mapped onto black (0) or white (1), but can also be mapped onto a grey value (or grey level) in between those two. The darker an image point, the lower its grey value.

[2]If $n = 2$, we call them picture elements (pixels); if $n = 3$ the term volume elements (voxels) is used.

Analogously to the remark that a binary image could be seen as a crisp set in $\mathbb{R}^n$, we can now remark that a greyscale image can also be considered as a fuzzy set in $\mathbb{R}^n$, where the $\mathbb{R}^n - [0,1]$ mapping corresponds to the membership function. The membership degree of an image point can then e.g. be seen as the degree to which it is bright.

Further, analogously to the storage of a binary image, also for the storage of a greyscale image the image domain needs to be sampled from $\mathbb{R}^n$ to $\mathbb{Z}^n$. However, since also the interval $[0,1]$ contains an infinite number of values, now also the set of allowed grey values needs to be sampled to a finite subchain $I_r = \{0, \frac{1}{r-1}, \ldots, \frac{r-2}{r-1}, 1\}$ ($r \in \mathbb{N} \setminus \{0,1\}$) of $[0,1]$. If m bits are used for the storage of a grey value, then 2^m grey values are possible. To work with integer values, the interval $[0,1]$ is then sometimes rescaled to the interval $[0, 2^m - 1]$. A greyscale image that is the result of such sampling, is called a digital greyscale image. For an image A, the grey value of the image element at location $x \in \mathbb{Z}^n$, is, analogously as for binary images, denoted by $A(x)$. As an example, a (digital) greyscale Lena image is given in Fig. 2.2 (a). In the enlarged crop of the right eye in that image (Fig. 2.2 (b)) the pixels are again clearly visible.

(a) (b)

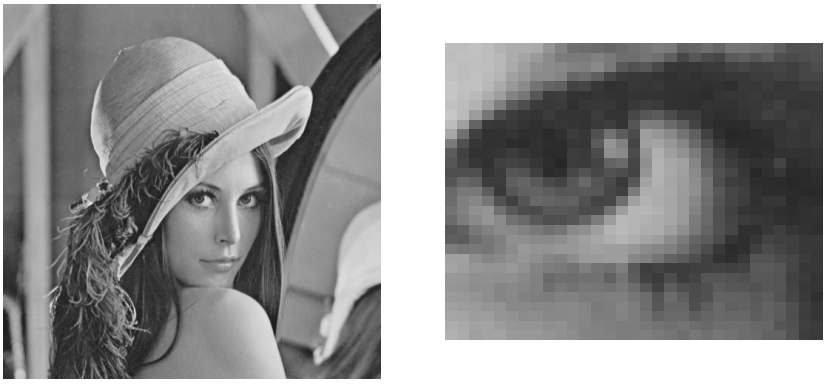

Figure 2.2: (a) The greyscale Lena image. (b) Enlarged crop of the right eye in the greyscale Lena image.

2.1.3 Colour Images

In a colour image, an element from the image domain is now not longer mapped onto a grey value, but onto a colour. The representation of a colour depends on the used colour model. A colour model is an abstract mathematical model to represent colours by tuples[3] of numbers. All colours that can be represented in this colour model then form the colour

[3] Usually 3- or 4-tuples are used.

space[4]. The best known colour model is the RGB model, in which colours are obtained by mixing the three primary colours red, green and blue together in different proportions[5]. Colours can then be represented by a 3-tuple, i.e., a vector containing three components, where the first component represents the amount of red, the second component the amount of green and the third component the amount of blue that is needed to obtain the colour. If these proportions are given by values in the interval $[0, 1]$, a colour image modelled in the RGB colour model, can then be represented by an $\mathbb{R}^n - [0, 1]^3$ mapping. The vectors $(1, 0, 0)$, $(0, 1, 0)$ and $(0, 0, 1)$ then respectively correspond to red, green and blue. Vectors for which the three components are equal, correspond to grey values. In particalur, $(0, 0, 0)$ corresponds to black and $(1, 1, 1)$ to white (Fig. 2.3). All red (respectively green and blue) component values of the images points together form the red (respectively green and blue) colour band. Such colour band can thus actually be modelled in the same way as a greyscale image, i.e., as an $\mathbb{R}^n - [0, 1]$ mapping. For an image A, we will denote the red (respectively green and blue) colour band by A^R (respectively A^G and A^B).

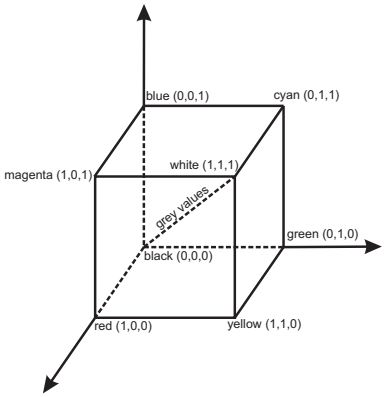

Figure 2.3: Graphical representation of the RGB colour model.

To obtain a digital colour image, i.e., a colour image that can be stored on a device, the image domain again needs to be sampled from $\mathbb{R}^n$ to $\mathbb{Z}^n$ and analogously to the grey values of a greyscale image, also the colour component values need to be sampled. If m bits are used for the storage of a colour component, i.e., 2^m values are possible, the interval $[0, 1]$ can again be rescaled to the interval $[0, 2^m - 1]$ to work with integers. Analogously to binary and greyscale images, for an image A, $A(x) = (A^R(x), A^G(x), A^B(x))$ now denotes the RGB colour vector at location $x \in \mathbb{Z}^n$. As an example, a (digital) colour Lena image is given in Fig. 2.4 (a). In the enlarged crop of the right eye in that image (Fig. 2.4 (b)) the pixels are again clearly visible.

[4]Remark that usually not all colours that can be seen by the human eye, can be represented in a given colour model.

[5]The colours red, green and blue can be explicitly defined by their wavelength.

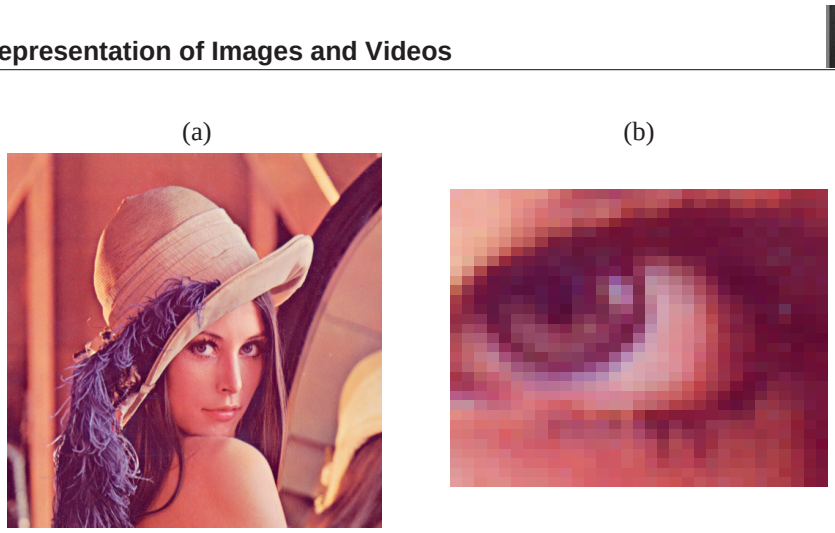

Figure 2.4: (a) The colour Lena image. (b) Enlarged crop of the right eye in the colour Lena image.

Apart from the RGB model, several other colour models exists (e.g., the YUV, YCbCr, YIQ, HSV, HSL, CMY, CMYK, XYZ, $L^*a^*b^*$, $L^*u^*v^*$ models). For more information on these models, we refer to [118, 128]. We will only give a few remarks here.

The YUV, YCbCr and YIQ colour models (used for colour television broadcasting) are based on the fact that the human eye is more sensitive to changes in brightness[6] than to changes in hue[7] and saturation[8]. The Y-component in these models (that is identical to the Y-component in the XYZ colour model) contains the information on the brightness of a colour. The other components contain the colour information (i.e., hue and saturation). As a consequence, by omitting the colour information and only using the Y-component, we can obtain a greyscale image from a colour image (e.g., the greyscale Lena image in Fig. 2.2 corresponds to the Y-component obtained from the colour Lena image in Fig. 2.4).

Further, the $L^*a^*b^*$ and $L^*u^*v^*$ colour models have been designed to obtain a linear colour model, i.e., a model in which equal geometric distances correspond to roughly equal perceived colour differences. In the RGB colour model for example, a small difference in one of the colour components might in some cases result in a visually very different colour and in other cases in a colour for which the difference to the original colour can hardly be detected by the human eye. The $L^*a^*b^*$ and $L^*u^*v^*$ colour models are consequently good models to determine the colour preservation after the processing of an image.

[6] Brightness is the human visual sensation to which an area appears to emit more or less light, to which an area seems to be more or less clear.

[7] Hue is the attribute of a visual sensation according to which an area appears to be similar to one or to the proportions of two of the perceived (opponent) colours red, yellow, green and blue. E.g., purple can be seen as lying somewhere between red and blue, orange between red and yellow, ...

[8] The saturation of a colour, sometimes called colour intensity, indicates how much white light is present in the colour. The lower the saturation, the more dull the colour. E.g., red and pink are two different saturations of the colour hue red.

2.1.4 Videos

A video (or image sequence) is a sequence of images (frames), that show the evolution of a scenery over time. The successive frames of a video are thus highly correlated (unless there is a scene switch between them). If the image sequence is denoted by I, then the notation $I(t)$ stands for the t-th frame of I. In this thesis we will only consider videos of which the frames are digital $2D$ images. If (x, y, t) denotes the pixel in the x-th row and the y-th column (where the counting starts from the upper left corner) of the t-th frame in the sequence, then for a greyscale video (respectively colour video) $I(x, y, t)$ denotes the grey value (respectively the colour vector $(I^R(x, y, t), I^G(x, y, t), I^B(x, y, t))$) at that location. In the remainder of this thesis, we will also sometimes combine the spatial coordinates of a pixel in a vector $\mathbf{r} = (x, y)$, i.e., $(\mathbf{r}, t) = (x, y, t)$.

2.1.5 Image Models Used in This Thesis

In Part II of this thesis, we will assume the greyscale and colour video frames to be digital images where we work with integer grey values and colour component values for which $m = 8$ bits are used to store them (i.e., grey values and colour component values belong to $[0, 255] \cap \mathbb{Z}$). Further, colour images are assumed to be modelled in the RGB colour model. In Part III of this thesis, grey values are assumed to belong to the interval $[0, 1]$, such that greyscale images can be seen as fuzzy sets, which allows us to apply techniques from fuzzy set theory on them. Further, in Part III, we will also consider both the theoretical continuous case (unsampled images and thus a continuous image domain $\mathbb{R}^n$ and grey values belonging to $[0, 1]$) and the practical discrete case (digital images and thus a discrete image domain $\mathbb{Z}^n$ and grey values belonging to the discrete subset I_r of $[0, 1]$).

2.2 Noise Types

Images contain a lot of information. However, they are usually degraded by noise that was introduced during the image capturing, the transmission or the recording [92]. This can e.g. be caused by dust sitting on the lense, by the detector itself that is not working as it should be, by the fact that the electronics convert radiant energy to an electrical signal or by electromagnetic distortions during transmission. The three main categories of noise that can be distinguished are impulse noise, additive noise and multiplicative noise. In their introduction below as well as in the remainder of this thesis, we will use the notations I_o and I_n for the original noisefree image sequence and the sequence corrupted by noise respectively. We will define the noise types for greyscale sequences. For colour images, the definitions remain valid by applying them on each of the colour bands separately. We will illustrate the different noise types on the 10-th frame of the greyscale and colour "Salesman" sequence (Fig. 2.5).

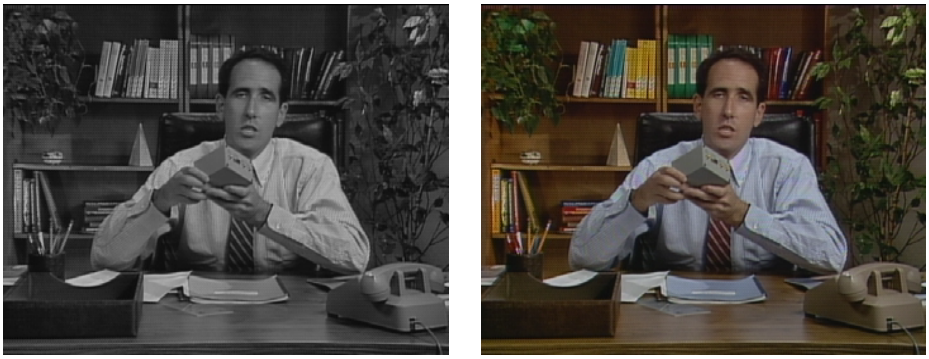

Figure 2.5: 10-th frame of the original noisefree greyscale (a) and colour (b) "Salesman" sequence.

2.2.1 Impulse Noise

Impulse noise is characterized by the fact that only part of the image pixels are affected, while the others remain unchanged. Further, a changed grey value of a noisy pixel, is not related the original noisefree value. Two types of impulse noise can be found in literature:

- *Fixed (valued) impulse noise*: the grey level of a corrupted pixel is always replaced by one of k fixed grey values $n_1 \dots n_k$:

$$I_n(x,y,t) = \begin{cases} n_1, & \text{with probability } pr_1, \\ n_2, & \text{with probability } pr_2, \\ \dots, & \\ n_k, & \text{with probability } pr_k, \\ I_o(x,y,t), & \text{with probability } 1 - \sum_{i=1}^{k} pr_i. \end{cases}$$

  The best known example of this type of noise is salt-and-pepper noise, where there are only two noise values n_1 and n_2, given by the minimum and maximum allowed grey level (i.e., $n_1 = 0$ (black) and $n_2 = 2^m - 1$ (white) if we work with integer grey values stored by m bits). As an example, Fig. 2.6 shows the 10-th frame of respectively the greyscale and colour "Salesman" sequence, corrupted by salt-and-pepper noise with $pr_1 = pr_2 = 2.5\%$.

- *Random (valued) impulse noise*: in contrary to the fixed valued impulse noise case, the grey level of an affected pixel is now replaced by a random grey value instead of one of a few fixed values:

$$I_n(x,y,t) = \begin{cases} I_o(x,y,t), & \text{with probability } 1 - pr, \\ \eta(x,y,t), & \text{with probability } pr, \end{cases}$$

(a) (b)

Figure 2.6: 10-th frame of the greyscale (a) and colour (b) "Salesman" sequence corrupted by salt-and-pepper noise ($pr_1 = pr_2 = 2.5\%$).

where $pr \in [0, 1]$ denotes the probability that a grey value is corrupted and replaced by a random grey value $\eta(x, y, t)$ coming from a given distribution. Corresponding to the literature [1, 17], we will consider the uniform distribution in this thesis. As an example, Fig. 2.7 shows the 10-th frame of respectively the greyscale and colour "Salesman" sequence, corrupted by random impulse noise with $pr = 5\%$.

(a) (b)

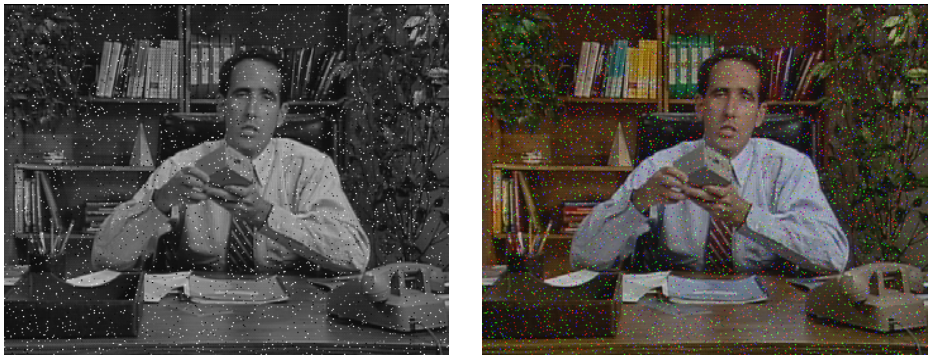

Figure 2.7: 10-th frame of the greyscale (a) and colour (b) "Salesman" sequence corrupted by random impulse noise ($pr = 5\%$).

2.2.2 Additive Noise

In the case of additive noise, a random noise value is added to the grey value of each pixel:

$$I_n(x, y, t) = I_o(x, y, t) + \eta(x, y, t),$$

where $\eta(x, y, t)$ is a random noise value coming from a given distribution. Several distributions can be found in literature such as a Gaussian distribution, a Poisson distribution, a Laplacian distribution, a Cauchy distribution, ... The most studied among them is the Gaussian distribution of which the probability density function is given by:

$$f_N(x; \mu, \sigma) = \frac{1}{\sigma\sqrt{2\pi}} e^{-\frac{1}{2}(\frac{x-\mu}{\sigma})^2},$$

for $x \in \mathbb{R}$ and where μ and σ respectively denote the mean and standard deviation of the noise. Usually $\mu = 0$, an assumption that we will adopt in this thesis.As an example, Fig. 2.8 shows the 10-th frame of respectively the greyscale and colour "Salesman" sequence, corrupted by Gaussian noise with $\sigma = 20$. The Gaussian noise model is a very good approx-

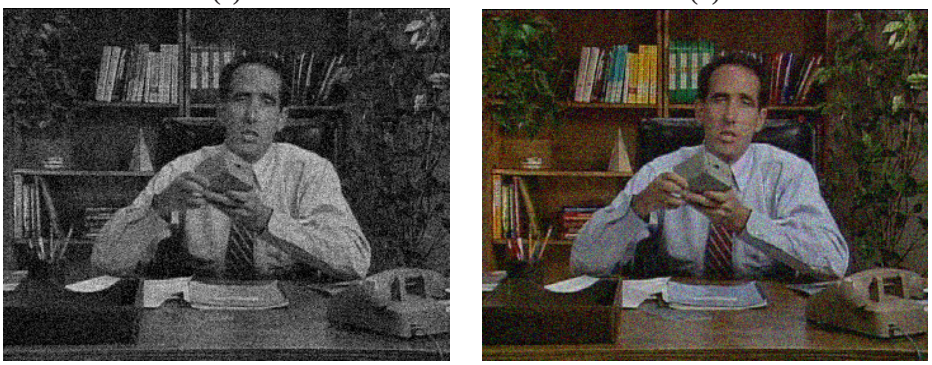

Figure 2.8: 10-th frame of the greyscale (a) and colour (b) "Salesman" sequence corrupted by Gaussian noise ($\sigma = 20$).

imation of the noise that is present in many imaging systems. However, to model noise with a more impulsive behavior, a distribution with heavier tails is needed. In this case, an α-stable distribution [39, 43, 88], that is a generalization of the Gaussian model, might result in a better approximation. For most α values, there is no closed-form expression for the probability density function of the α-stable distribution, but its characteristic function ϕ is given by

$$\phi(t) = \begin{cases} \exp(i\lambda t - \gamma|t|^\alpha(1 + i\beta sgn(t)\tan\frac{\alpha\pi}{2})) & \alpha \neq 1 \\ \exp(i\lambda t - \gamma|t|(1 + i\beta sgn(t)\frac{2}{\pi}\log|t|)) & \alpha = 1 \end{cases},$$

where $t \in \mathbb{R}$, $i = \sqrt{-1}$ is the complex unit,

$$sgn(t) = \begin{cases} 1 & t > 0 \\ 0 & t = 0 \\ -1 & t < 0 \end{cases},$$

the characteristic component $\alpha \in]0, 2]$ controls the heaviness of the tails (the lower α, the heavier the tails and the more impulsive the noise), the location parameter $\lambda \in \mathbb{R}$ corresponds to the mean ($\alpha \in]1, 2]$) or median ($\alpha \in]0, 1]$), the dispersion parameter γ determines the spread of the density around λ and the skewness parameter $\beta \in [-1, 1]$ is an index for the symmetry of the distribution ($\beta = 0$ means that the distribution is symmetric). The cases $\alpha = 2$, $\beta = 0$ and $\alpha = 1$, $\beta = 0$ respectively correspond to the Gaussian and Cauchy distribution.

2.2.3 Multiplicative Noise

If an image is corrupted by multiplicative noise, then to each grey value, a noise value is added that is a random multiple of the original grey value:

$$I_n(x, y, t) = I_o(x, y, t) + \eta(x, y, t) \cdot I_o(x, y, t),$$

where $\eta(x, y, t)$ is a random noise value coming from a given distribution. For example speckle noise, that e.g. occurs in satellite images (SAR images), medical images (ultrasound images) and in television environments, is usually modelled this way, with $\eta(x, y, t)$ coming from a uniform distribution, given by:

$$f_U(x; \sigma) = \begin{cases} \frac{1}{2\sigma\sqrt{3}} & |x| \leq \sqrt{3}\sigma \\ 0 & \text{else} \end{cases},$$

for $x \in \mathbb{R}$ and where σ denotes the standard deviation of the noise. The higher this standard deviation, the higher the noise level. As an example, Fig. 2.9 shows the 10-th frame of respectively the greyscale and colour "Salesman" sequence, corrupted by speckle noise with $\sigma = 25$.

2.3 Similarity Measures

To be able to judge the performance of image and video filtering methods, such as the ones developed in Part II of this thesis, objective measures of similarity and dissimilarity between a filtered frame (image) $I_f(t)$ and the original one $I_o(t)$ are needed. Some well-known measures are:

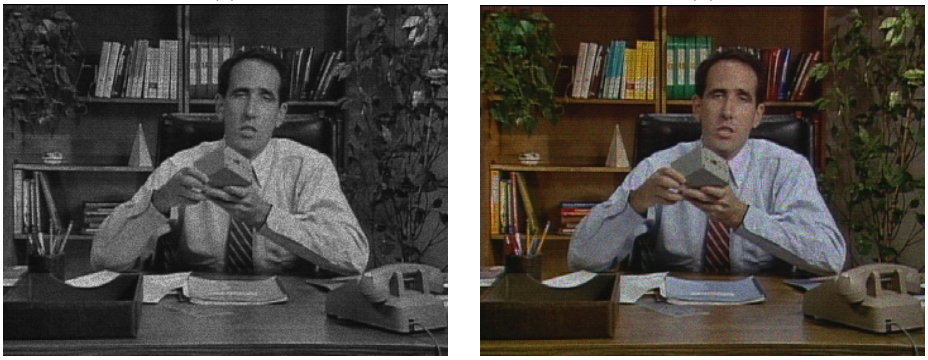

Figure 2.9: 10-th frame of the greyscale (a) and colour (b) "Salesman" sequence corrupted by speckle noise ($\sigma = 25$).

- The mean squared error (MSE), defined as

$$MSE(I_o(t), I_f(t)) = \frac{\sum_{x=1}^{M}\sum_{y=1}^{N}(I_o(x,y,t) - I_f(x,y,t))^2}{N \cdot M},$$

where $I_o(t)$ and $I_f(t)$ respectively denote an original and a filtered greyscale frame, each containing M rows and N columns of pixels. If $I_o(t)$ and $I_f(t)$ are colour frames, then the average is taken over the three colour bands:

$$MSE(I_o(t), I_f(t)) = \frac{\sum_{c\in\{R,G,B\}}\sum_{x=1}^{M}\sum_{y=1}^{N}(I_o^c(x,y,t) - I_f^c(x,y,y))^2}{3 \cdot M \cdot N}.$$

The higher the MSE, the more dissimilar (less similar) the frames $I_o(t)$ and $I_f(t)$. Remark however, that the interpretation of the MSE is highly dependent on the number of bits m that is used for the storage of a grey value or colour component value. The visual difference between two successive grey values or colour component values is larger if there are less allowed values, i.e., for a smaller m. So an average difference of 10 grey levels, i.e, an MSE equal to 100, will e.g. look better for $m = 10$ than for $m = 8$.

Finally, several variants on the MSE have been developed, such as the mean absolute difference (MAD), where the absolute difference between two values is used instead of the squared difference, and the root mean squared error (RMSE), that is given by the square root of the MSE.

- The peak signal to noise ratio (PSNR), defined as

$$PSNR(I_o(t), I_f(t)) = 10 \cdot \log_{10} \frac{(2^m - 1)^2}{MSE(I_o(t), I_f(t))},$$

where $I_o(t)$ and $I_f(t)$ respectively denote an original and a filtered (greyscale or colour) frame, each containing M rows and N columns of pixels and where m denotes the number of bits used for the storage of a grey value or colour component value. The higher the PSNR value, the more similar (less dissimilar) the images. Since the maximal possible grey value or colour component value ($2^m - 1$) is taken into account, the interpretation of the PSNR no longer depends on m. Further, the logarithmic decibel scale is used, because many signals (the PSNR/MSE does not need to be restricted to images) have a wide dynamic range.

- The normalized colour difference (NCD), defined as

$$NCD(I_o(t), I_f(t)) = \frac{\sum_{x=1}^{M} \sum_{y=1}^{N} \left\| I_o^{LAB}(x,y,t) - I_f^{LAB}(x,y,t) \right\|_2}{\sum_{x=1}^{M} \sum_{y=1}^{N} \left\| I_o^{LAB}(x,y,t) \right\|_2},$$

where $\|\cdot\|_2$ is the Euclidean norm and $I_o^{LAB}(x,y,t)$ and $I_f^{LAB}(x,y,t)$ respectively denote the $L^*a^*b^*$-transform of the original and the filtered colour frame $I_o(t)$ and $I_f(t)$, each containing M rows and N columns of pixels. The lower the NCD value, the more similar (less dissimilar) the images. Since the $L^*a^*b^*$ colour model is linear, i.e., approaches the human perception, the NCD is a good measure to evaluate the quality and colour preservation of processed images intended for human inspection.

2.4 The Discrete Wavelet Transform

In this section, the discrete wavelet transform is introduced. Since this transform is only used in Subsection 3.2.2 of this thesis, only a basic understanding of the transform is aimed here. For a broader background we e.g. refer to [24, 26, 72, 87, 134]. More recently, also other new wavelet-like decompositions with better orientation selectivity can be found in literature (e.g., complex wavelets [56], steerable pyramids [52], curvelets [15], contourlets [36], shearlets [60], ...).

The main idea behind the use of wavelets, is to analyze a signal at different scales, i.e., looking at it from various distances. At a coarser scale, the rude structure of the signal is unfolded, while at a finer scale, the finer details can be studied. A classical example in this context is that of a picture showing a forest. Coarse-scale, medium-scale and fine-scale approximations then respectively approximate the trees, the leaves and the lice that are eating those leaves.

2.4.1 Multiresolution Analysis

Multiresolution analysis [24] is a sequence of approximation subspaces $\{V_j\}_{j\in\mathbb{Z}}$ of $L_2(\mathbb{R})$ that satisfy: [9]

1. The V_j are generated by a scaling function $\phi \in L_2(\mathbb{R})$ (called the father wavelet) in the sense that for each fixed j, the family
$$\phi_{j,k}(t) = 2^{j/2}\phi(2^j t - k),\ k \in \mathbb{Z}$$
constitutes a Riesz basis for V_j.
2. The family $\{V_j\}_{j\in\mathbb{Z}}$ is increasing: $V_j \subset V_{j+1},\ \forall j \in \mathbb{Z}$.
3. For all $f \in L_2(\mathbb{R})$, the orthogonal projections $P_j f$ onto V_j satisfy $\lim_{j\to+\infty} P_j f = f$ and $\lim_{j\to-\infty} P_j f = 0$.

From the above, it follows that $f \in V_j$ is equivalent to the function $\tilde{f} \in V_{j+1}$ for which $(\forall x \in \mathbb{R})(\tilde{f}(x) = f(2x))$ and that V_j is invariant under translation over 2^{-j}. From $V_j \subset V_{j+1}$ it also follows that ϕ is the solution of a two-scale equation
$$\phi(t) = \sqrt{2}\sum_{n\in\mathbb{Z}} h[n]\phi(2t-n).$$
In the case where the integer translates of ϕ are orthonormal, the orthogonal projection corresponds to the best approximation $A_j f$ of f in the approximation space V_j (i.e., at the scale 2^j):
$$A_j f = \sum_{k\in\mathbb{Z}} \langle f, \phi_{j,k}\rangle\, \phi_{j,k}.$$
If the integer translates of ϕ only constitute a Riesz basis (but are not orthonormal), a dual scaling function $\tilde{\phi}$ can be constructed such that $\left\langle \tilde{\phi}, \phi_{0,k} \right\rangle = \delta_{0,k}$ and the best approximation becomes
$$A_j f = \sum_{k\in\mathbb{Z}} \left\langle f, \tilde{\phi}_{j,k} \right\rangle \phi_{j,k}.$$
The scalar products $\left\langle f, \tilde{\phi}_{j,k} \right\rangle$ are denoted by $s_{j,k}$ and are called the scaling coefficients. Also the dual scaling function $\tilde{\phi}$ satisfies a scaling equation[10]
$$\tilde{\phi}(t) = \sqrt{2}\sum_{n\in\mathbb{Z}} \tilde{h}[n]\tilde{\phi}(2t-n). \tag{2.1}$$

[9] $L_2(\mathbb{R})$ is the Hilbert space of square integrable functions, i.e., the $\mathbb{R}-\mathbb{R}$ functions f such that $\|f\|^2 = \int_{-\infty}^{+\infty} |f(t)|^2 dt < +\infty$, with the scalar product of two such functions f and g defined as $\langle f, g\rangle = \int_{-\infty}^{+\infty} f(t)g^*(t)dt$, where g^* denotes the complex conjugate of g.

[10] For the duality to hold it is necessary that $2\sum_{n\in\mathbb{Z}} \tilde{h}[n]h^*[n+2k] = \delta_{k,0}$, where h^* is the complex conjugate of h. Under some additional technical assumptions, this condition becomes sufficient [26, 23].

If we now define

$$\begin{aligned} g[n] &= (-1)^n \tilde{h}[1-n], \\ \tilde{g}[n] &= (-1)^n h[1-n], \end{aligned}$$

the wavelets ψ (called the mother wavelet) and $\tilde{\psi}$ are derived as

$$\psi(t) = \sqrt{2} \sum_{n \in \mathbb{Z}} g[n] \phi(2t-n), \; \tilde{\psi}(t) = \sqrt{2} \sum_{n \in \mathbb{Z}} \tilde{g}[n] \tilde{\phi}(2t-n). \tag{2.2}$$

As an example, the scaling function and corresponding wavelet function for the orthogonal Daubechies wavelet $db2$ is depicted in Fig. 2.10. Remark that in the orthonormal case,

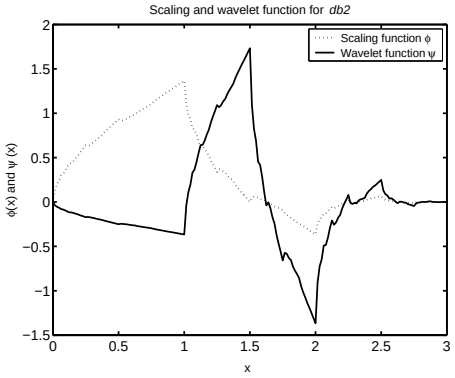

Figure 2.10: The scaling function and corresponding wavelet function for the orthogonal Daubechies wavelet $db2$.

$\phi = \tilde{\phi}$, $h[n] = \tilde{h}[n]$, $g[n] = \tilde{g}[n]$ and $\psi = \tilde{\psi}$. If we define $\psi_{j,k}$ ($j, k \in \mathbb{Z}$) as $\psi_{j,k}(t) = 2^{j/2}\psi(2^j t - k), \; \forall t \in \mathbb{R}$ (and analogously for $\tilde{\psi}$), then a direct computation now shows that [24]

$$A_{j+1} f - A_j f = \sum_{k \in \mathbb{Z}} \left\langle f, \tilde{\psi}_{j,k} \right\rangle \psi_{j,k}.$$

The scalar products $\left\langle f, \tilde{\psi}_{j,k} \right\rangle$ are denoted by $w_{j,k}$ and are called the wavelet coefficients. It holds that the family $\{\psi_{j,k}\}_{k \in \mathbb{Z}}$ constitutes a Riesz basis for a detail space W_j that is the complement of V_j in V_{j+1} (i.e., $V_{j+1} = V_j \oplus W_j$) and thus contains the detail information needed to go from an approximation at scale 2^j to an approximation at scale 2^{j+1}. Moreover, it holds that

$$\left\langle \psi_{j,k}, \tilde{\psi}_{j',k'} \right\rangle = \delta_{j,j'} \delta_{k,k'}$$

and $\{\psi_{j,k}\}_{j,k \in \mathbb{Z}}$ constitutes a Riesz basis of $L_2(\mathbb{R})$ [23]. For any j_1, it is thus possible to obtain $A_{j_1} f$ from a coarser approximation $A_{j_0} f$ ($j_0 < j_1$) by adding a combination of

wavelets at intermediate scales:

$$A_{j_1} f = A_{j_0} f + \sum_{j=j_0}^{j_1-1} \sum_{k\in\mathbb{Z}} w_{j,k}\psi_{j,k} = \sum_{k\in\mathbb{Z}} s_{j_0,k}\phi_{j_0,k} + \sum_{j=j_0}^{j_1-1} \sum_{k\in\mathbb{Z}} w_{j,k}\psi_{j,k}.$$

By taking limits $j_1 \to +\infty$ and $j_0 \to -\infty$, we obtain

$$f = \sum_{k\in\mathbb{Z}} s_{j_0,k}\phi_{j_0,k} + \sum_{j=j_0}^{+\infty} \sum_{k\in\mathbb{Z}} w_{j,k}\psi_{j,k} = \sum_{j,k\in\mathbb{Z}} w_{j,k}\psi_{j,k}.$$

2.4.2 The Discrete Wavelet Transform

For the computation of the wavelet coefficients in the wavelet representation Mallat has introduced a fast filter bank algorithm [71] that is in literature usually referred to as the discrete wavelet transform. This algorithm goes as follows. We assume that the multiresolution analysis axioms hold and we start with a function f in V_j. From formula (2.1) we derive

$$\begin{aligned}
\tilde{\phi}_{j,k}(t) &= 2^{j/2}\phi(2^j t - k) \\
&= 2^{(j+1)/2} \sum_{n\in\mathbb{Z}} \tilde{h}[n]\phi(2^{j+1}t - 2k - n) \\
&= \sum_{l\in\mathbb{Z}} \tilde{h}[l-2k]\tilde{\phi}_{j+1,k}(t).
\end{aligned}$$

As a consequence

$$s_{j,k} = \left\langle f, \tilde{\phi}_{j,k} \right\rangle = \left\langle f, \sum_{l\in\mathbb{Z}} \tilde{h}[l-2k]\tilde{\phi}_{j+1,k} \right\rangle = \sum_{l\in\mathbb{Z}} \widehat{h}[2k-l]s_{j+1,l},$$

where $\widehat{h}[k] = \tilde{h}[-k]$ for all $k \in \mathbb{Z}$. The scaling coefficients at the scale 2^j are thus computed by convolving[11] the scaling coefficients from the scale 2^{j+1} with the filter $\widehat{h}$ and downsampling by 2. The filter $\widehat{h}$ is a low-pass filter, i.e., only the lower frequencies of the signal (corresponding to the rude signal features) are passed, which results in a kind of averaging or blurring. Analogously, we find that

$$w_{j,k} = \left\langle f, \tilde{\psi}_{j,k} \right\rangle = \sum_{l\in\mathbb{Z}} \widehat{g}[2k-l]s_{j+1,l},$$

where $\widehat{g}[k] = \tilde{g}[-k]$ for all $k \in \mathbb{Z}$. The filter $\widehat{g}$ is a high-pass filter, that passes only the higher frequencies of the signal (corresponding to the finer signal features). The filter bank thus separates the signal into averages (smooth parts) and differences (rough parts). Fig. 2.11 illustrates the decomposition into three levels of a one-dimensional signal $f(x)$.

[11] The convolution $u * v$ of two discrete one-dimensional signals u and v is for all $k \in \mathbb{Z}$ defined as $(u*v)(k) = \sum_{l=-\infty}^{+\infty} u(l)v(k-l)$.

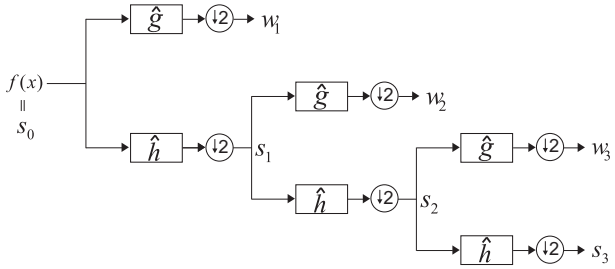

Figure 2.11: A three-level one-dimensional wavelet decomposition. The coefficient subscripts denote the decomposition level to which the coefficients belong.

For the reconstruction, it can be derived from expressions (2.1) and (2.2) that

$$s_{j+1,k} = \sum_{l \in \mathbb{Z}} h[k-2l] s_{j,l} + \sum_{l \in \mathbb{Z}} g[k-2l] w_{j,l}.$$

The scaling coefficients at the scale 2^j can thus be computed by taking the sum of the convolution of the upsampled (by inserting a zero between each two coefficients) scaling and wavelet coefficients from the scale 2^{j+1} with the filter h and g respectively. The reconstruction of the original signal $f(x)$ from the wavelet coefficients is illustrated in Fig. 2.12.

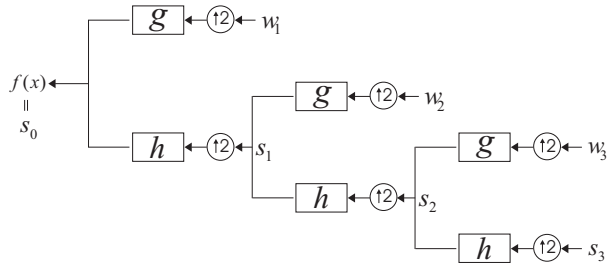

Figure 2.12: A three-level one-dimensional wavelet reconstruction. The coefficient subscripts denote the decomposition level to which the coefficients belong.

2.4.3 Extension to Images

The multiresolution analysis from Subsection 2.4.1 can be extended to images (i.e, to the 2D case[12]) in a separable and non-separable manner. In this thesis, we will only consider

[12] And more general to the n-dimensional case.

the separable case [71] in which the detail spaces are spanned by shifts and dilations of the wavelet functions $\Psi^{LH}(x,y) = \phi(x)\psi(y)$, $\Psi^{HL}(x,y) = \psi(x)\phi(y)$ and $\Psi^{HH}(x,y) = \psi(x)\psi(y)$ and the approximation spaces by shifts and dilations of $\Phi^{LL}(x,y) = \phi(x)\phi(y)$. The 2D discrete wavelet transform algorithm is then a straightforward extension of the 1-dimensional one. The scaling coefficients that serve as the input for the first decomposition step are approximated by the image grey levels. Each row of the image is then first filtered by the low-pass filter $\widehat{h}$ or the high-pass filter $\widehat{g}$ of the filter bank. For an $M \times N$ image, this results in 2 $M \times N/2$ images. Additionally each of the columns is again filtered by $\widehat{h}$ or $\widehat{g}$ resulting in 3 $M/2 \times N/2$ detail images (the rows or the columns have been filtered by $\widehat{g}$) and one $M/2 \times N/2$ approximation image (both the rows and columns were filtered by $\widehat{h}$). This 2-dimensional decomposition is shown in Fig. 2.13, in which the wavelet coefficients in the detail bands at scale 2^{j+1} are denoted by w_{j+1}^{LH}, w_{j+1}^{HL} and w_{j+1}^{HH} and respectively correspond to horizontal, vertical and diagonal oriented image structures. The scaling coefficients of the approximation band at scale 2^{j+1} are denoted by s_{j+1}. This band roughly corresponds to averaging the approximation band at the previous scale 2^{j+2} and can be further decomposed into the next scale 2^j. The usual representation of the obtained frequency subbands is given in Fig. 2.14 and illustrated for the Lena image in Fig. 2.15. From Fig. 2.15 it can be seen

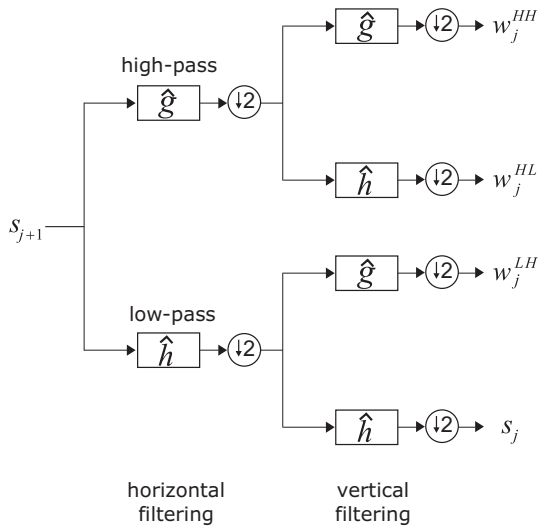

Figure 2.13: A decomposition level in the two-dimensional discrete wavelet transform.

that the discrete wavelet transform has an edge detection property, meaning that the large wavelet coefficients correspond to image edges. Further, it can also be noticed that only few large coefficients appear in the detail images. This sparsity makes the wavelet transform very useful for image coding and compression and usually also facilitates the denoising of

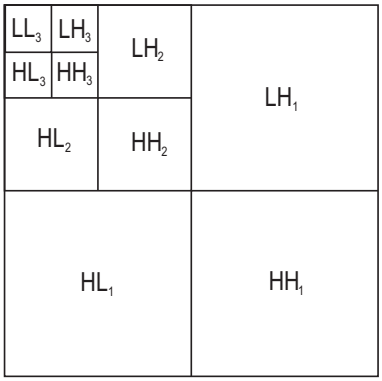

Figure 2.14: Usual representation of the frequency subbands in the two-dimensional discrete wavelet transform.

the image.

In an analogous way as for the decomposition, also the reconstruction algorithm can be extended from the 1-dimensional case.

2.4.4 The Non-decimated Discrete Wavelet Transform

A disadvantage of the discrete wavelet transfrom, is that it is not invariant under translation, which leads to numerous artefacts when an image is reconstructed after modification of its wavelet coefficients. Therefore, for denoising applications, usually a redundant non-decimated wavelet transform is used, that approaches translation invariance and is therefore called the stationary wavelet transform. In this transform, the representation of a signal has an equal number of wavelet coefficients in each scale. The signal is decomposed into a family of wavelets $\{\psi'_{j,k}\}_{j,k\in\mathbb{Z}}$, with $\psi'_{j,k}(x) = 2^{j/2}\psi(2^j(x-k))$, that are no longer linearly independent and thus don't constitute a basis anymore:

$$f = \sum_{j,k\in\mathbb{Z}} \left\langle f, \tilde{\psi}'_{j,k} \right\rangle \psi'_{j,k}.$$

The transform is computed as follows, where the filter that arises by inserting $2^j - 1$ zeros between each two coefficients of a filter h is denoted by h^j:

$$s_{j,k} = \sum_{l\in\mathbb{Z}} \widehat{h}^j[k-l]s_{j+1,l}, \qquad w_{j,k} = \sum_{l\in\mathbb{Z}} \widehat{g}^j[k-l]s_{j+1,l},$$

$$s_{j+1,k} = \frac{1}{2}\Big(\sum_{l\in\mathbb{Z}} h^j[k-l]s_{j,l} + \sum_{l\in\mathbb{Z}} g^j[k-l]w_{j,l}\Big).$$

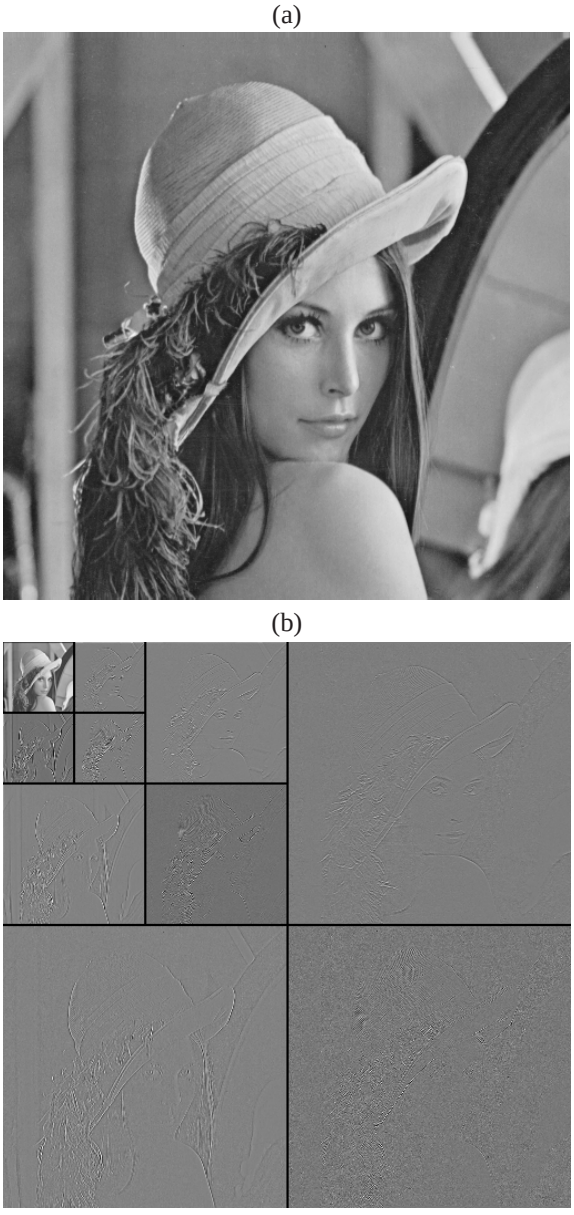

Figure 2.15: A three-level wavelet decomposition (b) of the Lena image (a) based on the ‘db2’ wavelet.

This algorithm is called the à trous algorithm [46, 72] and is illustrated on an example image in Fig. 2.16. For the non-decimated transform to be a consistent extension of the decimated discrete wavelet transform from Subsection 2.4.2, all the coefficients of the latter transform should reappear in the new transform. This will be the case, since by inserting the zeros between the filter coefficients, the extra coefficients in the redundant representation will be skipped before applying the convolution.

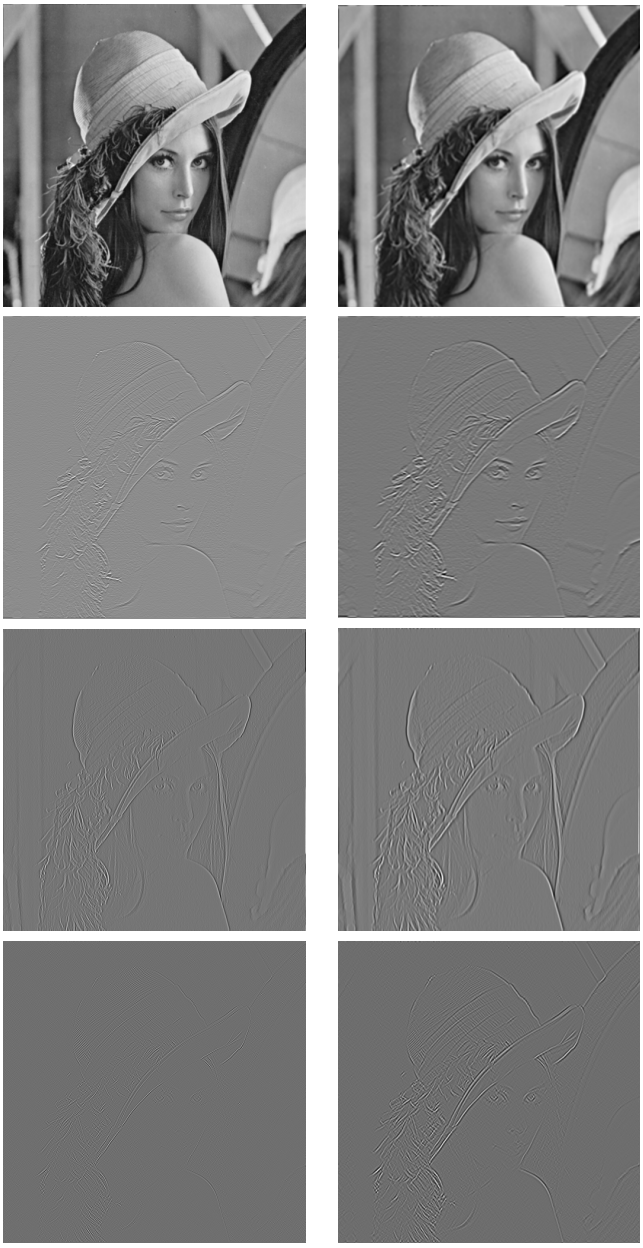

Figure 2.16: The LL, LH, HL and HH band (up to down) of the first (left) and second (right) undecimated wavelet decomposition level (based on the 'db2' wavelet) of the image in Fig. 2.15 (a).

Part II

Fuzzy Techniques for Noise Removal in Image Sequences

3
Additive Gaussian Noise in Greyscale Image Sequences

The first filters for video denoising were single resolution filters. These were often some well-known 2D filters extended to a spatio-temporal (3D) neighbourhood that also contains pixels from neighbouring frames. Some examples are the 3D KNN-filter [27, 89, 147] and the 3D threshold averaging filter [61, 147], which try to preserve the details by averaging only over the k nearest neighbours (KNN) and the neighbours lying within a certain distance (usually two times the standard deviation of the noise is chosen as threshold) from the given pixel value respectively. More recent extensions of these filters, that are made more adaptive to a local spatio-temporal neighbourhood are e.g. the motion and detail adaptive KNN-filter [148] and the multiple class averaging filter [146, 149]. Another well-known single resolution method is the 3D rational filter [22], where the filtered output for a pixel is determined as a rational function of the grey values in a spatio-temporal neighbourhood. Other recent single resolution filters can e.g. be found in [41, 141]. Both filters take into account pixels from neighbouring frames in the averaging, that are not necessarily the pixels at the same spatial position, but the estimated corresponding object pixels which possibly have been displaced due to motion between frames.

Later, the wavelet transform, which has proven very effective in still image denoising [3, 125], also found its way in the denoising of videos. In [114, 124] a 3D wavelet transform is applied and the resulting coefficients are denoised by adaptive thresholding. However, most wavelet domain filters use a less complex separable 2D transform applied on each frame separately [4, 21, 48, 50, 62, 70, 110, 146, 149, 150] and combine it with time-recursive filtering, either in the wavelet domain or in the pixel domain.

The most fundamental difference between video and image denoising is that in video applications also information from previous frames is available. When working with a

delay in time even information from future frames can be used. The main difficulty in exploiting this additional info is possible motion. Some filters simply take into account pixels at corresponding positions in the previous (and future) frames only when no motion between the successive frames is detected. Such motion detection filters are for example [110, 146, 148, 149]. Other more complex filters always take into account information from the previous frames, by filtering along an estimated motion trajectory and are called motion compensated filters [21, 48, 41, 141, 150]. In [21, 41, 141] the motion is estimated in the pixel domain, while in [48, 150] the motion vectors are computed in the wavelet domain. Most available motion estimation algorithms are designed for video coding applications [16, 133, 138]. In such applications, the accuracy of the motion vectors is less important than for denoising purposes. Recently, in [50, 51], an efficient video filtering scheme is proposed, which makes use of motion estimators from video codecs, but with additional filtering of the motion vectors and with appropriately defined reliabilities to estimated motion.

The filter in [41] only filters temporally. Usually however, the temporal filtering, which uses information from neighbouring frames, is combined with a spatial filtering. When the spatial and temporal filtering steps are performed separately, the one after the other or independently and subsequently combined, we speak of a separable filter [4, 21, 48, 50, 110, 150]. In [4] e.g., the authors combine their image denoising method from [3] with a selective wavelet shrinkage method which estimates the level of noise corruption as well as the amount of motion in the image sequence. Filters that integrate spatial and temporal filtering in one step, such as [22, 25, 62, 114, 124, 141, 146, 148, 149], are called non-separable.

The method proposed in this chapter [79, 86] is a fuzzy logic based improvement of the multiple class averaging filter (MCA) from [146, 149] for the denoising of greyscale image sequences corrupted with additive Gaussian noise. Fuzzy set theory and fuzzy logic offer us a powerful tool for representing and processing human knowledge. Binary decisions are replaced by a gradual transition, which is more appropriate when dealing with complex systems. The main differences between the proposed method and the filter from [146, 149] are: (i) pixels are not divided into discrete classes and dealt with based on their class index like in [146, 149], but they are treated individually, which leads to an increased performance; (ii) the complicated heuristic construction of exponential functions to tune the pixel weights in the method of [146, 149] to the class index and to the detected motion and detail is replaced by a fuzzy rule containing linguistic values, which represent human knowledge and which are more natural to work with and to understand. The use of fuzzy logic also provides a more theoretical base; (iii) in the wavelet-based extension of the method, we opt for an additional time-recursive averaging instead of a filtering of the low-frequency band ; and (iv) the fuzzy rule used in our method is easy to extend and to include new information in future work.

Experimental results show that our method outperforms other state-of-the-art filters of a comparable complexity. The chapter is structured as follows: Our algorithm for the denoising of greyscale image sequences is first explained in the pixel domain in Section 3.1 and extended to the wavelet domain in Section 3.2. Section 3.3 handles the choice of the

parameter values. Finally, experimental results and conclusions are presented in Section 3.4 and Section 3.5 respectively.

3.1 Pixel Based Spatio-temporal Filter for Greyscale Image Sequences

In this section, we improve the multiple class averaging filter (MCA) from [146, 149] in the pixel domain by incorporating fuzzy logic. The ideas behind the filter are the following: (i) to avoid spatio-temporal blur, one should only take into account neighbouring pixels from the current frame in case of detected motion; (ii) to preserve the details in the frame content, the filtering should be less strong when large spatial activity (e.g. a large variance) is detected in the current filtering window. As a consequence more noise will be left, but large spatial activity corresponds to high spatial frequencies and for these the eye is less sensitive [6]. In the case of homogeneous areas, strong filtering should be performed to remove as much noise as possible.

The general filtering framework used in the proposed method is presented in Subsection 3.1.1. Additionally the crucial weight determination step, which is the main novelty of our greyscale method compared to the MCA filter, is explained in Subsection 3.1.2. In the proposed method we determine the weights in the filtering window by the use of fuzzy sets and fuzzy logic instead of a heuristic construction with exponential functions as it is the case in the MCA filter. Subsection 3.1.3 finally, discusses some complexity notes.

3.1.1 The General Filtering Framework

In this subsection, the filtering framework used in both the MCA and the proposed filter is explained. In the following, the noisy input sequence and the corresponding filtered sequence are respectively denoted by I_n and I_f.

The filtering window used in the framework is a $3 \times 3 \times 2$ sliding window, consisting of 3×3 pixels in the current frame and 3×3 pixels in the previous frame. As introduced in [146, 149] we will use the terms *current window* and *previous window* for the window pixels contained in respectively the current and the previous frame (Fig. 3.1). This window is moved through each frame from top left to bottom right, each time filtering the central pixel by averaging the noise. The position of this central pixel in the filtering window is denoted by $(\mathbf{r}, t)$ where $\mathbf{r} = (x, y)$ stands for the spatial position and t for the temporal position. An arbitrary position in the $3 \times 3 \times 2$ window (this may also be the central pixel position) is denoted by $(\mathbf{r'}, t')$, with $\mathbf{r'} = (x + k, y + l)$ $(-1 \leq k, l \leq 1)$ and $t' = t$ or $t' = t - 1$.

The output of the proposed filter for the central pixel in the window is finally determined as a weighted average (with adaptive weights) of the pixel values in the $3 \times 3 \times 2$ window:

$$I_f(\mathbf{r}, t) = \frac{\sum_{\mathbf{r'}} \sum_{t'=t-1}^{t} W(\mathbf{r'}, t', \mathbf{r}, t) I_n(\mathbf{r'}, t')}{\sum_{\mathbf{r'}} \sum_{t'=t-1}^{t} W(\mathbf{r'}, t', \mathbf{r}, t)}. \tag{3.1}$$

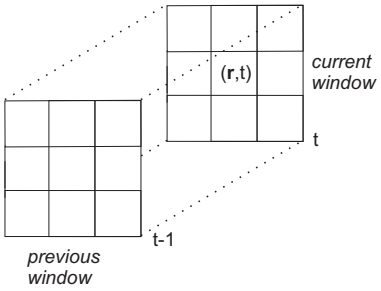

Figure 3.1: The $3 \times 3 \times 2$ filtering window consisting of the previous and the current window.

3.1.2 Weight Determination

In this subsection, we focus on the fundamental step in the filtering framework, namely the determination of the weights. To make the method motion and detail adaptive, we adopt the difference value $\Delta(\mathbf{r'}, t', \mathbf{r}, t)$, the detail value $d(\mathbf{r}, t)$ and the motion value $m(\mathbf{r}, t)$ from [146, 149]:

(i) The absolute difference in grey value between the two pixel positions $(\mathbf{r}, t)$ and $(\mathbf{r'}, t')$ is denoted by:

$$\Delta(\mathbf{r'}, t', \mathbf{r}, t) = |I_n(\mathbf{r'}, t') - I_n(\mathbf{r}, t)|. \tag{3.2}$$

(ii) The function $d(\mathbf{r}, t)$ indicating the local amount of detail is calculated as the standard deviation in the current window:

$$I_{av}(\mathbf{r}, t) = \frac{1}{9} \sum_{\mathbf{r'}} I_n(\mathbf{r'}, t) \ ,$$

$$d(\mathbf{r}, t) = \Big(\frac{1}{9} \sum_{\mathbf{r'}} \big(I_n(\mathbf{r'}, t) - I_{av}(\mathbf{r}, t) \big)^2 \Big)^{\frac{1}{2}} \ . \tag{3.3}$$

(iii) The motion indicator $m(\mathbf{r}, t)$ finally, is defined as the absolute difference between the average grey value in the current window and the average grey value in the previous window:

$$\begin{aligned} m(\mathbf{r}, t) &= |I_{av}(\mathbf{r}, t) - I_{av}(\mathbf{r}, t-1)| \\ &= \frac{1}{9} | \sum_{\mathbf{r'}} \big(I_n(\mathbf{r'}, t) - I_n(\mathbf{r'}, t-1) \big) |. \end{aligned} \tag{3.4}$$

MCA Filter

In the MCA filter [146, 149], the pixels are classified into four discrete index classes, depending on the $\Delta(\mathbf{r'}, t', \mathbf{r}, t)$ value:

$$i(\mathbf{r'}, t', \mathbf{r}, t) = \begin{cases} 0 & \Delta(\mathbf{r'}, t', \mathbf{r}, t) \leq k\sigma, \\ 1 & k\sigma < \Delta(\mathbf{r'}, t', \mathbf{r}, t) \leq 2k\sigma, \\ 2 & 2k\sigma < \Delta(\mathbf{r'}, t', \mathbf{r}, t) \leq 3k\sigma, \\ 3 & 3k\sigma < \Delta(\mathbf{r'}, t', \mathbf{r}, t), \end{cases} \tag{3.5}$$

where σ represents the standard deviation of the Gaussian noise and k is a parameter. When details are detected in a region, higher weights are assigned to pixels which are similar to the pixel being filtered (i.e., pixels from the lower index classes, which have smallest $\Delta(\mathbf{r'}, t', \mathbf{r}, t)$ values) to preserve these details. In homogeneous regions however, the difference in weight compared to pixels from the higher index classes will be smaller and strong filtering is performed. This is done by determining the weights by a heuristic composition of exponential functions that is inversely proportional to the amount of detail, motion and the class index. In [149] the weights for the pixels in the window are defined as:

$$W(\mathbf{r'}, t', \mathbf{r}, t) = \begin{cases} exp\left(\frac{-i(\mathbf{r'}, t', \mathbf{r}, t)}{\eta(d(\mathbf{r}, t))\sigma}\right)\beta(m(\mathbf{r}, t), t') & i(\mathbf{r'}, t', \mathbf{r}, t) = 0, 1, 2, \\ 0 & i(\mathbf{r'}, t', \mathbf{r}, t) = 3, \end{cases} \tag{3.6}$$

where the function

$$\eta(d) = K_1 exp(-K_2 d) + K_3 exp(-K_4 d),$$

is used to determine the slope of the exponential function in (3.6) and K_1, K_2, K_3 and K_4 are parameters. The function $\beta(m(\mathbf{r}, t), t')$ in (3.6) is chosen to restrict the contribution (decreasing the weight) of the pixels from the previous window in case of motion:

$$\beta(m(\mathbf{r}, t), t') = \begin{cases} 1 & t' = t, \\ exp(-\gamma m(\mathbf{r}, t)) & t' = t - 1. \end{cases}$$

In this equality, the parameter γ is used to control the sensitivity of the motion detector. In [146] the function $\eta(d)$ is omitted and the weights are then defined as:

$$W(\mathbf{r'}, t', \mathbf{r}, t) = \begin{cases} exp\left(\frac{-i(\mathbf{r'}, t', \mathbf{r}, t)d(\mathbf{r}, t)}{K_d\sigma}\right)\beta(m(\mathbf{r}, t), t') & i(\mathbf{r'}, t', \mathbf{r}, t) = 0, 1, 2, \\ 0 & i(\mathbf{r'}, t', \mathbf{r}, t) = 3, \end{cases} \tag{3.7}$$

where K_d is a parameter.

Proposed Filter

In our fuzzy motion and detail adaptive video filter, we use the above introduced filtering framework and the values $\Delta(\mathbf{r'}, t', \mathbf{r}, t)$, $m(\mathbf{r}, t)$ and $d(\mathbf{r}, t)$ (Fig. 3.2). In contrast to the

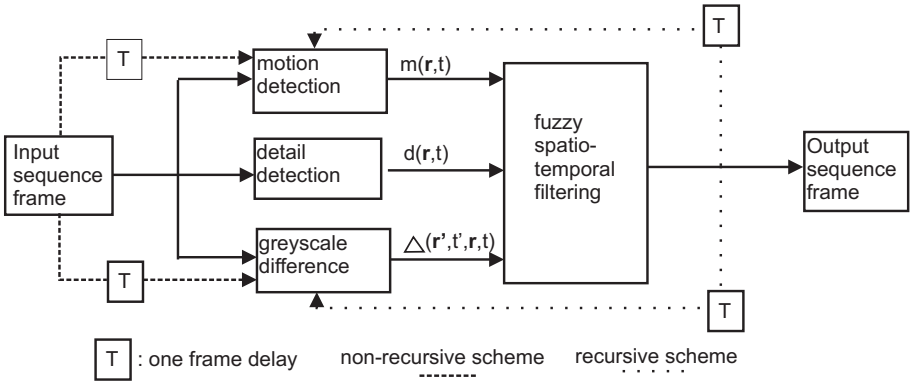

Figure 3.2: The general filtering scheme of the proposed filter.

MCA filter we no longer use discrete index classes to express the similarity of a pixel to the central window pixel. Also our determination of the weights in (3.1) differs from the strategy used in [146, 149]. The artificial construction of exponential functions in the MCA method is replaced by a more natural fuzzy logic framework with linguistic values.

The four index classes are replaced by one fuzzy set [142] "large difference" for the values $\Delta(\mathbf{r'}, t', \mathbf{r}, t)$. The membership degree of a difference in this set is an indication of whether the difference is large rather than small. So, a pixel $I_n(\mathbf{r'}, t')$ that would belong to a low index class in the MCA filter now corresponds to a small membership degree of the value $\Delta(\mathbf{r'}, t', \mathbf{r}, t)$ in the fuzzy set "large difference". We will use a linguistic value "large" not only for the difference $\Delta(\mathbf{r'}, t', \mathbf{r}, t)$, but also for the motion value $m(\mathbf{r}, t)$ and the detail value $d(\mathbf{r}, t)$ and introduce the fuzzy sets "large motion" and "large detail". We will further also use a linguistic value "reliable" to indicate whether a given neighbourhood pixel is reliable to be used in the filtering of the central window pixel, and represent it by the fuzzy set "reliable neighbourhood pixel".

In the following the notations μ_{Δ}, μ_d and μ_m are used to denote the membership functions characterizing respectively the fuzzy sets (i) large difference, (ii) large detail and (iii) large motion. For the sake of simplicity and computational reasons piecewise linear functions are used, as shown in Fig. 3.3. As can be seen in Fig. 3.3, the membership functions are completely determined by the parameters thr_1, T_1, T_2, t_1 and t_2.

Using the introduced fuzzy sets for the crucial weight determining step, we replace the heuristic combination of exponential functions in the original MCA method by a more natural fuzzy logic framework with linguistic values. The weight $W(\mathbf{r'}, t', \mathbf{r}, t)$ for the pixel at position (**r'**,t') is now defined as the degree to which it is reliable to be used in the filtering of the central window pixel, i.e., its membership degree in the fuzzy set "reliable neighbourhood pixel", which is the activation degree of Fuzzy Rule 3.1 or 3.2 depending on whether $t' = t$ or $t' = t - 1$.

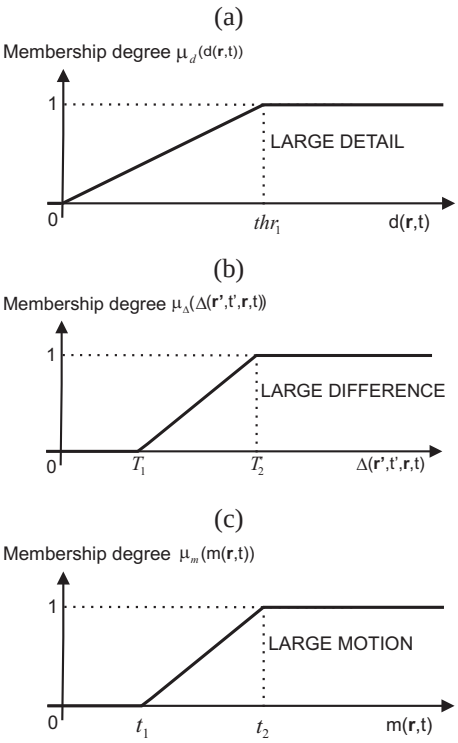

Figure 3.3: (a) The membership function μ_d for the fuzzy set "large detail", (b) The membership function μ_Δ for the fuzzy set "large difference" and (c) The membership function μ_m for the fuzzy set "large motion".

Fuzzy Rule 3.1. *Assigning the membership degree in the fuzzy set "reliable neighbourhood pixel" of the pixel at spatial position* **r'** *in the current frame ($t' = t$) of the window with central pixel position (***r***,t):*
IF(*the detail value $d(\mathbf{r}, t)$ is* LARGE AND *the difference $\Delta(\mathbf{r'}, t', \mathbf{r}, t)$ is*
NOT LARGE) OR (*the detail value $d(\mathbf{r}, t)$ is* NOT LARGE)
THEN *the pixel at position (***r'***,t') is a* RELIABLE *neighbourhood pixel for the filtering of the central window pixel.*

Fuzzy Rule 3.2. *Assigning the membership degree in the fuzzy set "reliable neighbourhood pixel" of the pixel at spatial position* **r'** *in the previous frame ($t' = t - 1$) of the window with central pixel position (***r***,t):*
IF((*the detail value $d(\mathbf{r}, t)$ is* LARGE AND *the difference $\Delta(\mathbf{r'}, t', \mathbf{r}, t)$ is*
NOT LARGE) OR (*the detail value $d(\mathbf{r}, t)$ is* NOT LARGE))
AND *the motion value $m(\mathbf{r}, t)$ is* NOT LARGE
THEN *the pixel at position (***r'***,t') is a* RELIABLE *neighbourhood pixel for the filtering of the central window pixel.*

For the AND-, OR- and NOT-operators in the above Fuzzy Rules 3.1 and 3.2, we have respectively used the algebraic product, the probabilistic sum and the standard negator as t-norm, t-conorm and negator. As demonstrated in Subsection 3.4.2, we however see a comparable performance when using other norms and conorms.

Take now for example Fuzzy Rule 3.1. This rule has an activation degree (corresponding to the membership degree in the fuzzy set "reliable neighbourhood pixel" and thus the weight $W(\mathbf{r'}, t', \mathbf{r}, t)$ in (3.1) for the pixel in the sliding window at position $(\mathbf{r'}, t')$) equal to:

$$\alpha_1 \cdot (1 - \alpha_2) + (1 - \alpha_1) - \alpha_1 \cdot (1 - \alpha_2) \cdot (1 - \alpha_1), \tag{3.8}$$

with $\alpha_1 = \mu_d(d(\mathbf{r}, t))$ and $\alpha_2 = \mu_\Delta(\Delta(\mathbf{r'}, t', \mathbf{r}, t))$. For the activation degree of Fuzzy Rule 3.2, an extra factor $(1 - \alpha_3)$ ($\alpha_3 = \mu_m(m(\mathbf{r}, t))$) needs to be added.

Notice that it is impossible that all weights in (3.1) are equal to zero. In the above expression (3.8) either α_1 or $1 - \alpha_1$ is always greater than zero ($\alpha_1 \in [0, 1]$), and for the central pixel position $\mathbf{r}$, we always have that $\alpha_2 = 0$ (see expression (3.2) and Fig. 3.3 (b)).

The proposed fuzzy rules are very natural to work with since they directly express the underlying ideas put in a formal framework: (i) When large spatial activity is detected, one should filter less to preserve the details. This means that the neighbouring pixels that are assigned a considerable weight in (3.1), should be similar to the central pixel in the filtering window ($d(\mathbf{r}, t)$ is large AND $\Delta(\mathbf{r'}, t', \mathbf{r}, t)$ is not large). In the opposite case (OR), i.e., in homogeneous areas ($d(\mathbf{r}, t)$ is not large) no extra conditions should be imposed on the neighbouring pixels. All pixels should get a considerable weight to perform strong smoothing. (ii) When motion is detected between the current and the previous window, only pixels from the current frame should be taken into account in the averaging. This

means that pixels from the previous frame only should get a considerable weight when the motion detector yields a low value ($m(\mathbf{r}, t)$ is not large) (corresponding to the second (AND) in Fuzzy Rule 3.2).

Apart from being a formal representation of the ideas, the fuzzy rules also produce the desired result. In the case of spatio-temporal structures, the detail and motion value will be large and only for neighbouring pixels with a small difference in grey value (relative to the central pixel in the filtering window), the Fuzzy Rules 3.1 and 3.2 will have a considerable activation degree. In this way fine spatio-temporal details are preserved at the expense of some noise remaining.

In a spatio-temporal uniform area, the detail and motion values will not be large. So even for neighbouring pixels with a large difference in grey value (relative to the central pixel), the Fuzzy Rules 3.1 and 3.2 will have a considerable activation degree. Hence, because of the many considerable weights in (3.1), strong filtering is performed.

Finally, we also propose a recursive scheme of the fuzzy motion and detail adaptive video filter. In this scheme, we always use the filtered value $I_f(\mathbf{r'}, t-1)$ for the neighbouring pixels in the already filtered previous frame. For pixels in the current frame, the noisy values $I_n(\mathbf{r'}, t-1)$ are used, except for the determination of $\Delta(\mathbf{r'}, t', \mathbf{r}, t)$, where the filtered value is used when already available (i.e., for pixels that have been filtered already in a previous step). In this way, we get a better estimate of whether the pixel at position (**r'**,t') belongs to the same object as the pixel at position $(\mathbf{r}, t)$ or not.

3.1.3 Some Notes on the Complexity

It is clear that the complexity of the proposed filter is linear in terms of the number of pixels in a frame. Every pixel is filtered by averaging a constant number of neighbourhood pixels, which are all assigned a weight using a constant number of operations. The calculation of the activation degree of the used fuzzy rules has a low complexity. The activation degree of Fuzzy Rule 3.1 is given in expression (3.8). For Fuzzy Rule 3.2, an extra multiplication with $(1 - \alpha_3)$ ($\alpha_3 = \mu_m(m(\mathbf{r}, t))$) is needed. To calculate the activation degree of Fuzzy Rule 3.1, 3 multiplications, 2 sums and 3 subtractions are performed. For the activation degree of Fuzzy Rule 3.2 an extra subtraction and multiplication are required. For the MCA filter, the calculation of the weight in expression (3.6) requires 7 multiplications, one division, and the calculation of 3 exponential functions and 4 opposites. The alternative in expression (3.7) can be computed by 4 multiplications, one division and the calculation of 2 exponential functions and 2 opposites. The use of fuzzy logic in the weight calculation is thus not more complex. The proposed individual treatment of the pixels, however, requires the weight calculation for each individual pixel. In the MCA filter, weights are only calculated for the different index classes, which results in a little lower complexity.

3.2 Wavelet Based Spatio-temporal Filter with Additional Pixel Based Time-recursive Averaging for Greyscale Image Sequences

In this section our method is extended to the wavelet domain. The procedure is the following: each processed frame is first decomposed using the 2D wavelet transform [72]. Next, an adapted version of the proposed method from Section 3.1 is applied on each of the resulting wavelet bands separately. Finally, the inverse wavelet transform is applied, followed by an additional time-recursive averaging in the pixel domain (see Fig. 3.4).

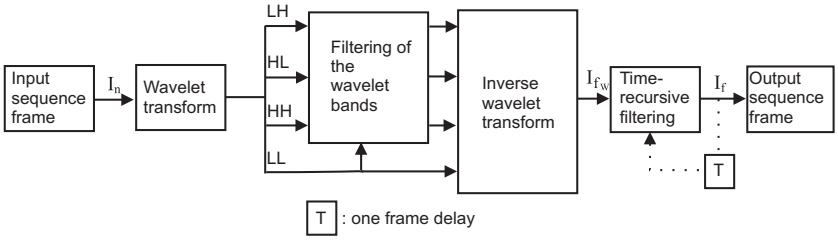

Figure 3.4: The filtering scheme for the proposed wavelet domain method.

3.2.1 Basic Notions

The wavelet transform of an image results in a representation that is very useful for image denoising. The transform compacts image details (such as edges and texture) into a small number of spatially clustered large coefficients, while small coefficients correspond to homogeneous regions in the original image.

We use the notation $y_{s,d}(\mathbf{r}, t)$ for the wavelet coefficient at resolution scale s, orientation d and spatial position $\mathbf{r}$ in the wavelet decomposition of the noisy frame with temporal position t. For the results in this chapter, we have opted for a non-decimated wavelet decomposition (which is known to give better denoising results than the decimated one) using the Haar-wavelet with three orientation subbands, leading to three detail images at each scale, characterized by horizontal ($d = LH$), vertical ($d = HL$) and diagonal ($d = HH$) directions and a low-frequency band (denoted by LL).

Due to the linearity of the wavelet transform, additive noise in the pixel domain remains additive after the transformation as well, resulting in:

$$y_{s,d}(\mathbf{r}, t) = \beta_{s,d}(\mathbf{r}, t) + \epsilon_{s,d}(\mathbf{r}, t),$$

where $y_{s,d}(\mathbf{r}, t)$ and $\beta_{s,d}(\mathbf{r}, t)$ are respectively the noisy and the noise-free wavelet coefficient and $\epsilon_{s,d}(\mathbf{r}, t)$ is the corresponding noise component.

3.2.2 Fuzzy Motion and Detail Adaptive Averaging in the Wavelet Domain

The proposed method is now extended to the wavelet domain. Large differences in grey value in the pixel domain indicate the occurrence of an edge. To preserve the edges, pixels with a large difference in grey value, relative to the pixel being filtered in the current step, should not be taken into account in the averaging. Only pixels from the same object, i.e., belonging to the same side of the edge, should be averaged and are expected to have a similar grey value. In the wavelet domain, edges result in large coefficients. So to preserve the edges, only the large coefficients, corresponding to these edges, should be averaged to filter out the noise. Small coefficients should get small weights in this case, and vice versa for homogeneous areas. This also holds for wavelet coefficients in the previous window. When there is no motion, the wavelet coefficients corresponding to the same edge in the previous frame are expected to be of a similar size. Hence, similar values should result in large weights and large differences in small weights.

Because the region of wavelet coefficients that are influenced by a given pixel value expands with increasing scale, an averaging scheme becomes less and less efficient for higher scales. Therefore we have used only two scales in the wavelet decomposition, which is insufficient to remove all the noise. To overcome this problem, in [146, 149], also the low-frequency band is filtered to obtain a better noise removal. In this chapter, we choose instead for an additional time-recursive filtering in the pixel domain as in [110], but in a more adaptive fuzzy logic based way.

Filtering of the Wavelet Bands

The filtering of the wavelet bands is adapted in an analogous way as in [146, 149]:

- We adopt the corresponding definition for the detail value $d(\mathbf{r}, t)$ from [146, 149]:

$$d(\mathbf{r}, t) = \Big(\sum_{\mathbf{r'}} y_{s,d}^2(\mathbf{r'}, t) \Big)^{\frac{1}{2}}. \tag{3.9}$$

- For all detail bands the same motion indicator value is used, which is computed on the low-frequency band. This motion value is defined as the absolute difference between the central coefficient value in the current window and in the previous window of the low-frequency band.
- The parameters that define the membership functions μ_Δ, μ_d and μ_m in Fig. 3.3 need to be adapted to the specific detail band.

Since $m(\mathbf{r}, t)$, $d(\mathbf{r}, t)$ and $\Delta(\mathbf{r'}, t', \mathbf{r}, t)$ are all three defined, Fuzzy Rules 3.1 and 3.2 can still be used to determine the weights in (3.1). The only difference is that we are now working with wavelet coefficients instead of grey values.

Additional Time-Recursive Filter in the Pixel Domain

Let I_{f_W} and I_f respectively denote the sequence after the filtering of the wavelet bands and the inverse wavelet transform and the sequence after the additional time-recursive filtering (see Fig. 3.4).

First, the absolute difference between the pixels in the current frame after the filtering of the wavelet bands and the pixel at the corresponding position in the previous frame, which has already been processed by the additional time-recursive filter, is computed:

$$TD(\mathbf{r},t) = |I_{f_W}(\mathbf{r},t) - I_f(\mathbf{r},t-1)|. \tag{3.10}$$

For each difference, its membership degree $\mu_{TD}(TD(\mathbf{r},t))$ in the fuzzy set "large temporal difference" is then calculated. The membership function μ_{TD} of this fuzzy set is depicted in Fig. 3.5.

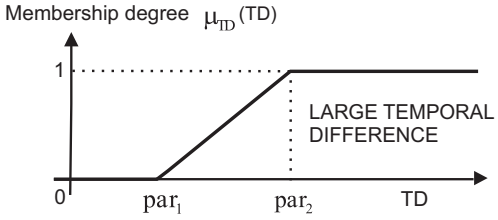

Figure 3.5: The membership function μ_{TD} for the fuzzy set "large temporal difference".

The final output of the additional time-recursive filter is given by

$$I_f(\mathbf{r},t) = \frac{1-\mu_{TD}(TD(\mathbf{r},t))}{2} I_f(\mathbf{r},t-1) + \frac{1+\mu_{TD}(TD(\mathbf{r},t))}{2} I_{f_W}(\mathbf{r},t), \tag{3.11}$$

where the contribution of $I_f(\mathbf{r},t-1)$ is limited to a maximum of $\frac{1}{2}$ to prevent noise propagation in time.

3.3 Parameter Selection

It is clear that the membership functions in Fig. 3.3 and 3.5 are completely determined by their respective parameters. These parameter values have been experimentally selected using the "Salesman", "Trevor", "Tennis" and "Flower Garden" sequences, which all have their own characteristics. The "Salesman" sequence represents a standard sequence with moderate detail (shelfs, books,...) and moderate motion (person). The "Trevor" sequence contains very fast motion (moving arms). In the "Tennis" sequence we deal with a zooming camera and a detailed background (wall). The "Flower garden" sequence finally, combines very detailed regions (flower field) with homogeneous regions (sky).

The parameters have been set in the following way. The proposed method was applied on each of the above sequences, for the different noise levels $\sigma = 5, 10, 15, 20, 25$ with parameters varying over a range of possible values. After plotting the optimal parameter values (in terms of PSNR) for the different sequences and noise levels, a linear relationship was found between these optimal parameter values and the noise level. Therefore the parameters have been determined by the best fit through the observations. As an illustration, the optimal values for the parameter T_2 of the proposed pixel domain method together with the best fitting line through these points are depicted in Fig. 3.6. The parameters are thus

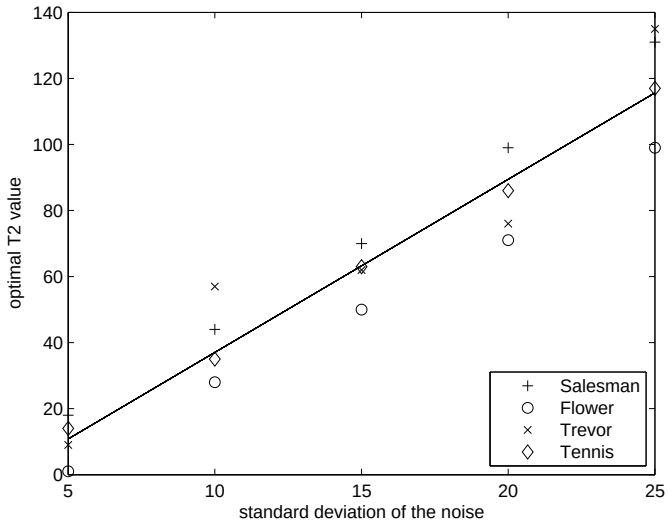

Figure 3.6: Optimal value for the parameter T_2 of the proposed pixel domain method.

linearly dependent of the noise level. For the results in this chapter, we assume a known standard deviation of the noise. In most practical cases however, the standard deviation σ is not known and should be estimated. A commonly used noise estimation method is the wavelet domain median absolute deviation (MAD) estimator of Donoho and Johnstone [37].

The selected parameter values that determine the membership functions used in the pixel domain method are given in Table 3.1.

Table 3.2 presents the selected thr_1, T_1 and T_2 values for the different waveletbands in the wavelet domain method. The parameters t_1 and t_2 for the membership function μ_m and the parameters par_1 and par_2 for the membership function μ_{TD} are determined as given in Table 3.3.

Table 3.1: Selected parameter values for the pixel domain method.

parameter	selected value
thr_1	$1.36\sigma + 1.2$
T_1	$0.79\sigma + 0.25$
T_2	$5.24\sigma - 15.35$
t_1	$0.465\sigma - 0.625$
t_2	$1.795\sigma + 3.275$

Table 3.2: Selected thr_1, T_1 and T_2 values for the different detail bands.

Band	thr_1	T_1	T_2
LH_1	$5.5733\sigma - 14.2667$	$0.8867\sigma - 1.9667$	$2.94\sigma + 2.9$
HL_1	$5.5733\sigma - 14.2667$	$0.8867\sigma - 1.9667$	$2.94\sigma + 2.9$
HH_1	$46.6267\sigma - 243.0667$	$0.8867\sigma - 1.9667$	$2.94\sigma + 2.9$
LH_2	$2.7533\sigma - 1.3$	$2.7067\sigma - 8.2667$	$2.8867\sigma + 0.8333$
HL_2	$2.7533\sigma - 1.3$	$2.7067\sigma - 8.2667$	$2.8867\sigma + 0.8333$
HH_2	$8.8267\sigma - 26.9333$	$2.7067\sigma - 8.2667$	$2.8867\sigma + 0.8333$

3.4 Experimental Results

In this section we will show some experimental results obtained from the test sequences “Salesman”, “Tennis”, “Deadline”, “Trevor”, “Flower garden” and “Miss America”. As mentioned in Subsection 3.2.1 and 3.2.2, for the experiments, our wavelet domain algorithm has been implemented with a non-decimated wavelet transform using the Haar-wavelet and only two decomposition levels have been used.

In Subsection 3.4.1 we compare our method with other state-of-the-art methods both in the pixel domain and the wavelet domain. Additionally, in Subsection 3.4.2, the use of different fuzzy aggregators is tested.

3.4.1 Comparison to Other State-Of-The-Art Methods

In this subsection, we compare our method to other state-of-the-art methods. We first compare our pixel domain method to other pixel domain methods and then do the comparison for the wavelet domain method.

Table 3.3: Selected t_1, t_2, par_1 and par_2 values for the wavelet domain method.

parameter	selected value
t_1	$3.22\sigma + 1.5667$
t_2	$36.7667\sigma + 16.5$
par_1	$0.555\sigma - 0.725$
par_2	$1.36\sigma + 5.1$

Pixel Domain

The non-recursive (FMDAF) and recursive (RFMDAF) scheme of our fuzzy motion and detail adaptive filter in the pixel domain have been compared to the following well-known filters that also operate in the pixel domain (all with parameter values as suggested in the respective papers):

- the rational filter (Rational) [22],
- the 3D-KNN filter (KNN) [147] as an extension of the 2D-KNN filter [27, 89],
- the threshold averaging filter (THR) [61, 147],
- the motion and detail adaptive KNN filter (MDA-KNN) [147, 148],
- the recursive scheme of the multiple class averaging filter (RMCA) [146] (which performs better than the non-recursive one as shown in [146]).

Fig. 3.7 and Fig. 3.8 give the PSNR results for six test sequences processed with the above mentioned methods and for the noise levels $\sigma = 10$ and $\sigma = 15$ respectively. It can be seen that in terms of PSNR the FMDAF and RFMDAF filters outperform the other pixel domain methods. The MDA-KNN filter gives comparable results on the "Salesman" and "Deadline" sequences. Further, we also note that comparable results are found on the "Flower garden" sequence for the RMCA and the THR filters. For a visual comparison, the original "Trevor" sequence, the sequence with added Gaussian noise ($\sigma = 10$), and the noisy sequence processed by the different filters can be found on `http://www.fuzzy.ugent.be/tmelange/results/greygauss/pixel`. From the tests we also found that our method adapts better to motion than the RMCA method. In Fig.3.9 a part of the 18th frame of the "Trevor" sequence with added Gaussian noise ($\sigma = 10$) processed by the FMDAF method, the RFMDAF method and the RMCA method is given. One clearly sees that our method has given a lower weight to those pixels from the previous frame situated in the fast moving arm.

Finally, we observed that the recursive scheme (RFMDAF) of the proposed filter removes slightly more noise than the non-recursive scheme (FMDAF), but this at the expense of little loss of spatial texture. Fig. 3.10 shows the 18th frame of the "Tennis" sequence with added Gaussian noise ($\sigma = 20$), processed by the FMDAF and by the RFMDAF. The texture on the wall is best preserved by the FMDAF method. But on the other hand, by

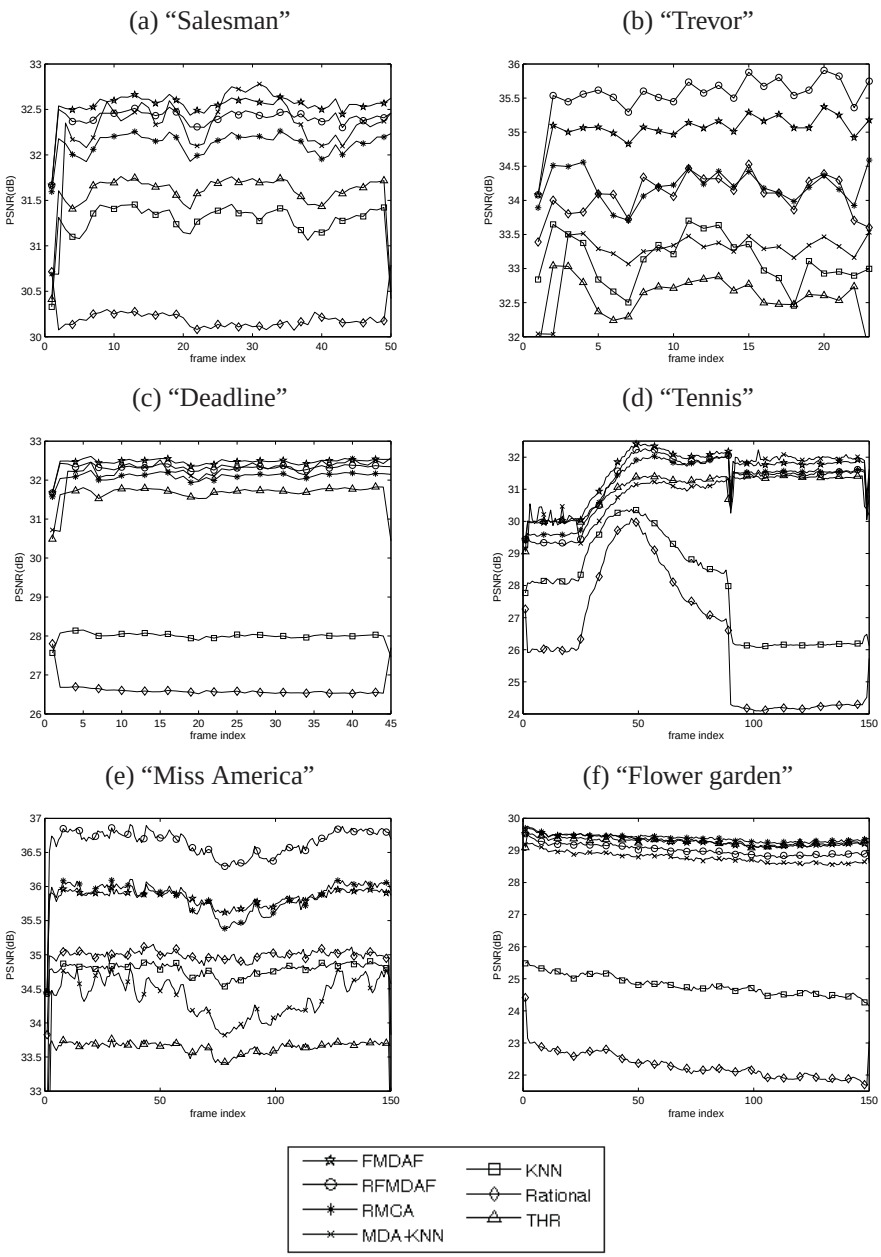

Figure 3.7: Performance comparison for the pixel domain methods applied to the different test sequences with added Gaussian noise ($\sigma = 10$).

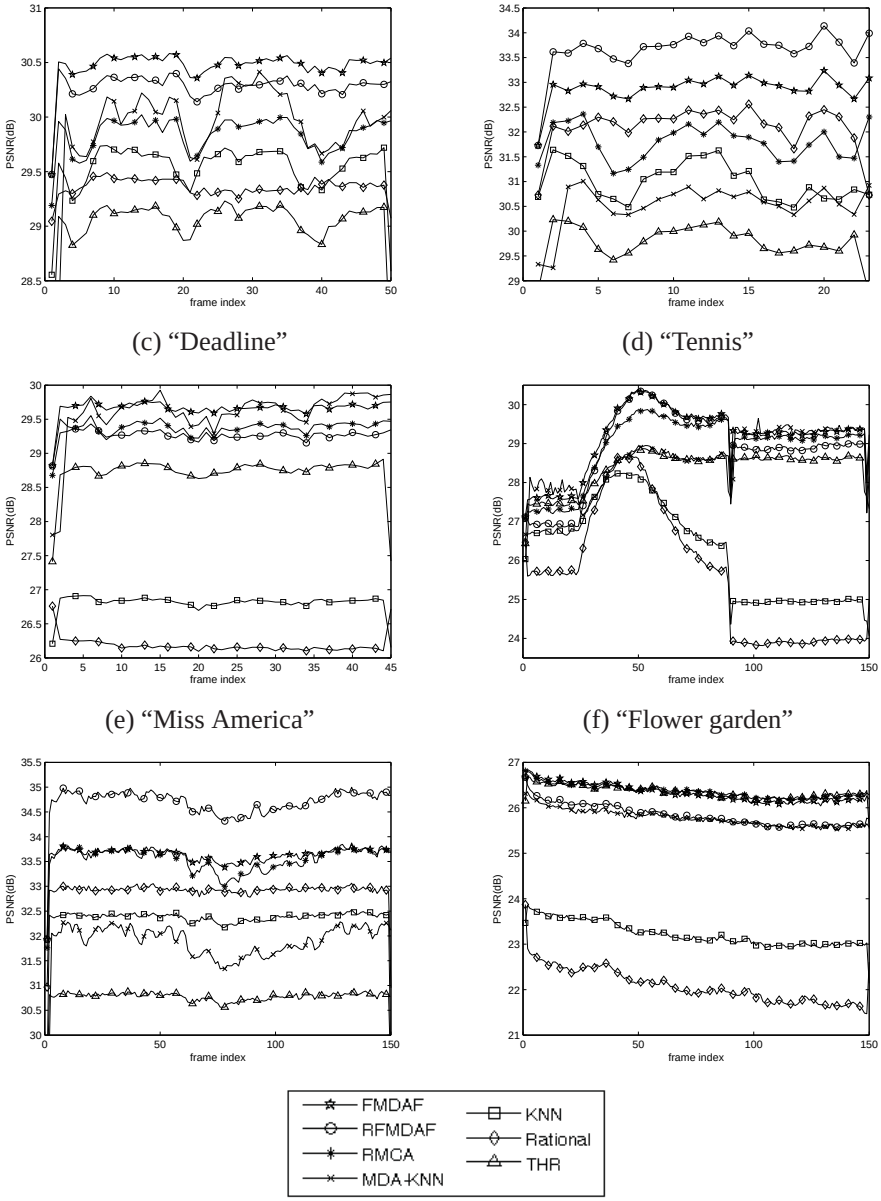

Figure 3.8: Performance comparison for the pixel domain methods applied to the different test sequences with added Gaussian noise ($\sigma = 15$).

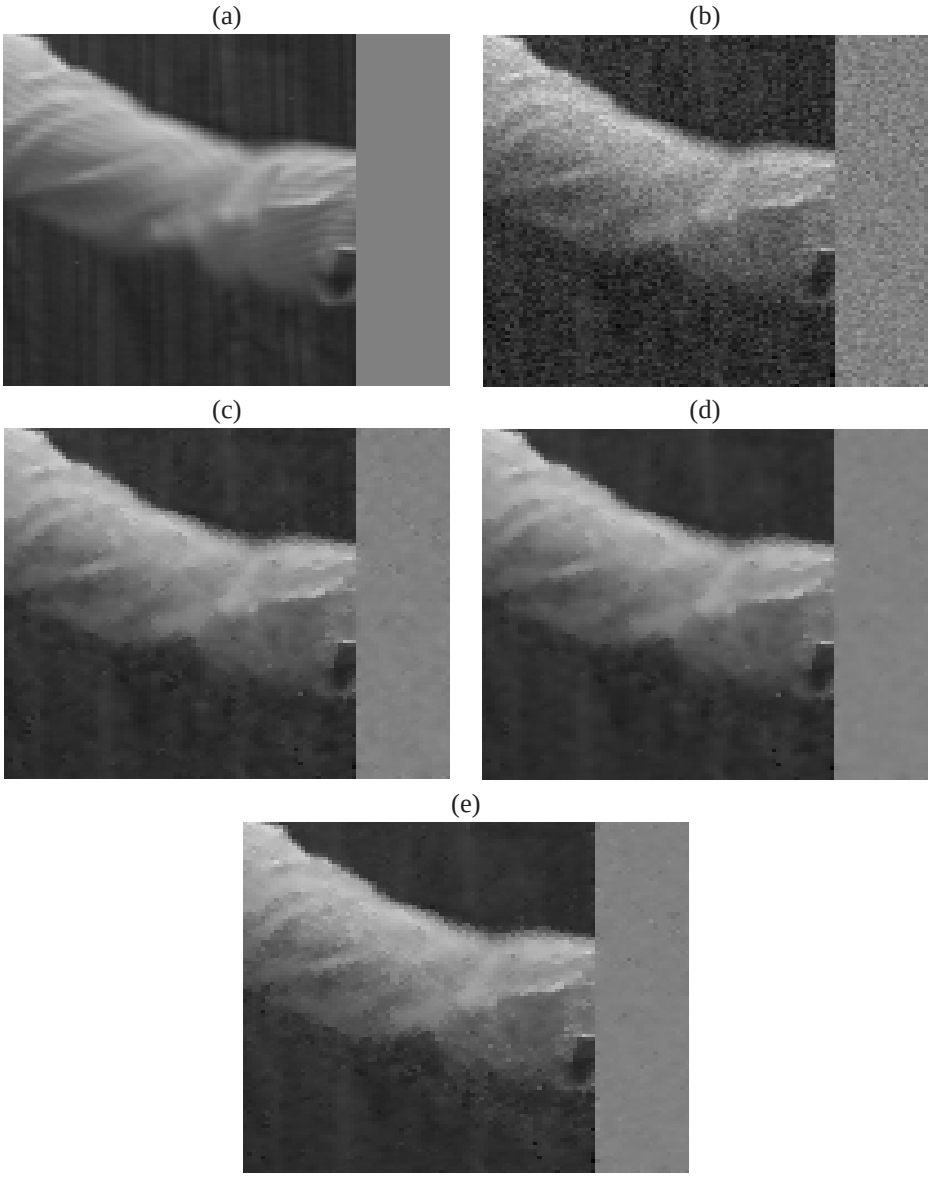

Figure 3.9: Part of the 18th frame of the "Trevor" sequence (a) original; (b) with added Gaussian noise ($\sigma = 10$); (c) processed by the FMDAF method; (d) processed by the RFMDAF method and (e) processed by the RMCA.

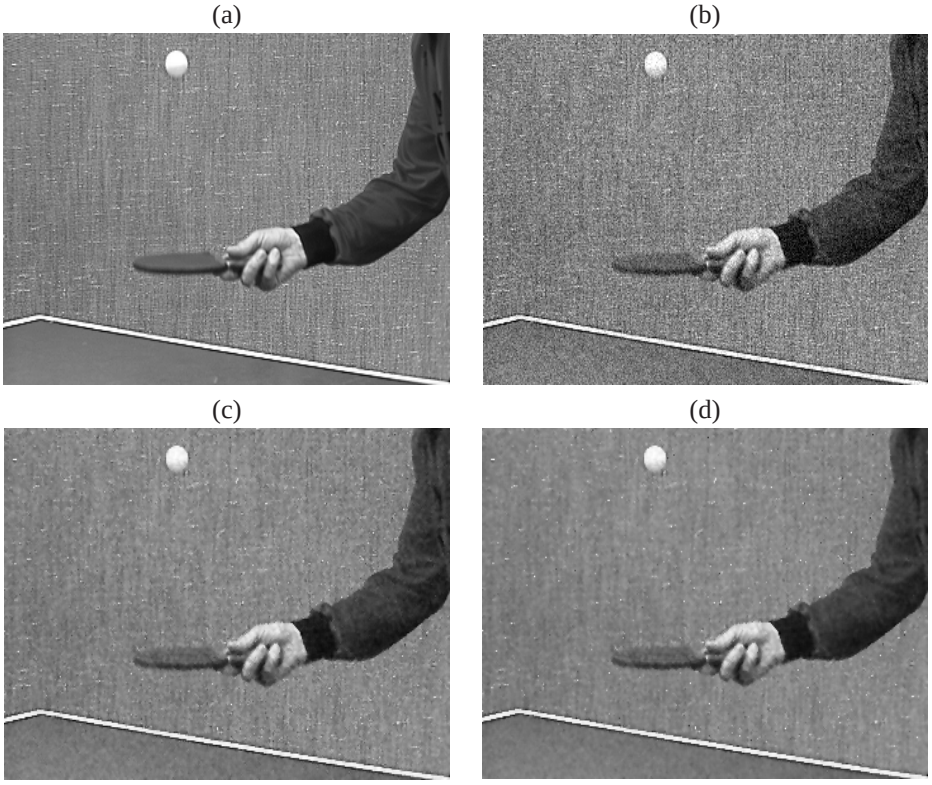

Figure 3.10: 18th frame of the "Tennis" sequence (a) original; (b) with added Gaussian noise ($\sigma = 20$); (c) processed by the FMDAF method and (d) processed by the RFMDAF method.

looking carefully at the table, one sees that more noise is removed by the RFMDAF than by the FMDAF.

Wavelet Domain

The recursive (WRFMDAF) scheme of our wavelet domain method (which outperforms the non-recursive one) has been compared to the following methods (all with parameter values as suggested in the respective papers):

- the recursive scheme of the wavelet domain multiple class averaging filter (WRMCA) [146] (non-decimated transform with the quadratic spline wavelet),
- the 3D wavelet transform filter (3DWF) [124] with the signal adaptive threshold from [125] (3-D dual-tree complex wavelet transform),
- the sequential wavelet domain and temporal filter (SEQWT) [110] (non-decimated transform with the symmlet-8 wavelet),
- the adaptive spatio-temporal filter (ASTF) [21] (64-tap Johnston filter [49]),
- the video filter based on inter-frame statistical modelling of the wavelet coefficients (FISMW) [70] (decimated transform with the orthogonal symmlet-8 wavelet),
- the sparse 3D transform-domain collaborative filter for video (VBM3D) [25] (the decimated biorthogonal wavelet bior1.5 for the 2D-transform of the blocks and the decimated Haar-wavelet for the third dimension in the first step and the dct-transform (2D) and the decimated Haar-wavelet (third dimension) in the second step).

Fig. 3.11 and 3.12 give the PSNR results for the processed “Salesman”, “Trevor”, “Deadline”, “Tennis”, “Miss America” and “Flower Garden” sequences. It can be seen that our method works best for a still camera filming possibly moving objects (“Salesman”, “Trevor”, “Deadline”, “Miss America”). On such sequences our proposed wavelet based recursive WRFMDAF method clearly outperforms the ASTF method. We also see a better performance for the WRFMDAF than for the RMCA filter and similar results to those of the SEQWT filter. Taking into account that the degradations that result from using a decimated transform instead of a non-decimated one can reach up to 1 dB [18, 110], we might also conclude a similar performance for the FISMW filter. Still, more sophisticated filters like the VBM3D filter, consisting of two steps in which blocks are grouped by spatio-temporal predictive block-matching and each 3D group is filtered by a 3D transform domain shrinkage, and the complex 3D wavelet transform method 3DWF show better results in terms of PSNR than our proposed filter. For the “Flower garden” sequence, the received results are worse, because the performance of the additional time-recursive filtering in pixels where no motion is detected, will be reduced for a moving camera.

For a visual comparison, the original “Deadline” sequence, the sequence with added Gaussian noise ($\sigma = 10$), and the filtering results obtained by the different compared wavelet domain filters are available on `http://www.fuzzy.ugent.be/tmelange/results/greygauss/wavelet`. We see that a little less noise is removed by the WRFMDAF and WRMCA filters than by the SEQWT and FISMW filters, but on the other

hand details are well preserved and less artefacts around the edges are introduced by the WRFMDAF filter.

It can be concluded that, for sequences obtained by a still camera, our method has a better performance in terms of PSNR than the other multiresolution filters of a similar complexity, but it is outperformed by some more sophisticated methods.

3.4.2 The Use of Other Fuzzy Aggregators

In this subsection, we compare the performance of the proposed method, implemented with different triangular norms and conorms. In Table 3.4 the results in terms of PSNR are given for different sequences processed with the RWFMDAF filter implemented with the suggested product norm and probabilistic sum conorm and other popular triangular norms and conorms. It can be seen that the performance of all aggregators are very comparable. Only the weak norm and strong conorm seem to perform less good on some of the sequences. Therefore, we have chosen for the simple intermediate algebraic product and probabilistic sum.

Table 3.4: Comparison of the different aggregators.

Sequence ($\sigma = 10$)	$PSNR_{av}$			
	algebraic product/ probabilistic sum	minimum/ maximum	weak/ strong	Łukasiewicz
"Salesman"	**34.37**	34.36	34.10	34.36
"Trevor"	36.41	**36.42**	35.55	36.29
"Deadline"	33.95	33.91	33.74	**33.98**
"Tennis"	31.44	31.37	31.47	**31.55**
"Miss America"	**37.48**	**37.48**	36.76	37.42
"Flower Garden"	28.27	28.13	**28.50**	28.44

3.5 Conclusion

In this chapter we have presented a new fuzzy motion and detail adaptive video filter intended for the reduction of additive Gaussian noise in digital image sequences. The proposed method is a fuzzy logic based improvement of the multiple class averaging filter (MCA) from [146, 149]. Pixels are no longer divided into discrete classes but are treated individually and the heuristic construction of exponential functions to assign the filtering weights to the neighbourhood pixels is replaced by a more theoretical underbuilt fuzzy logic framework in which fuzzy rules, that correspond to the ideas behind the MCA filter, are used.

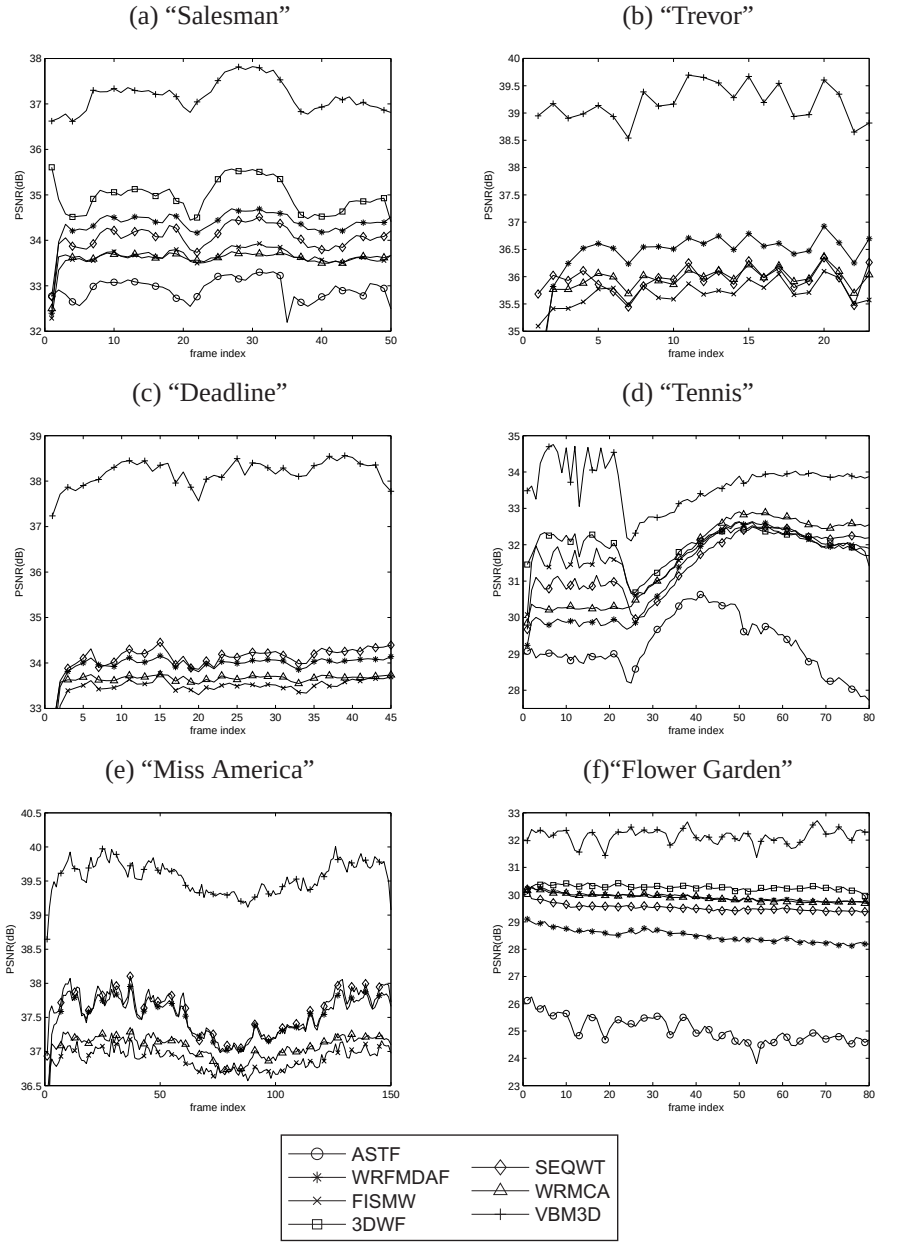

Figure 3.11: Performance comparison for the wavelet domain methods applied to the different test sequences with added Gaussian noise ($\sigma = 10$).

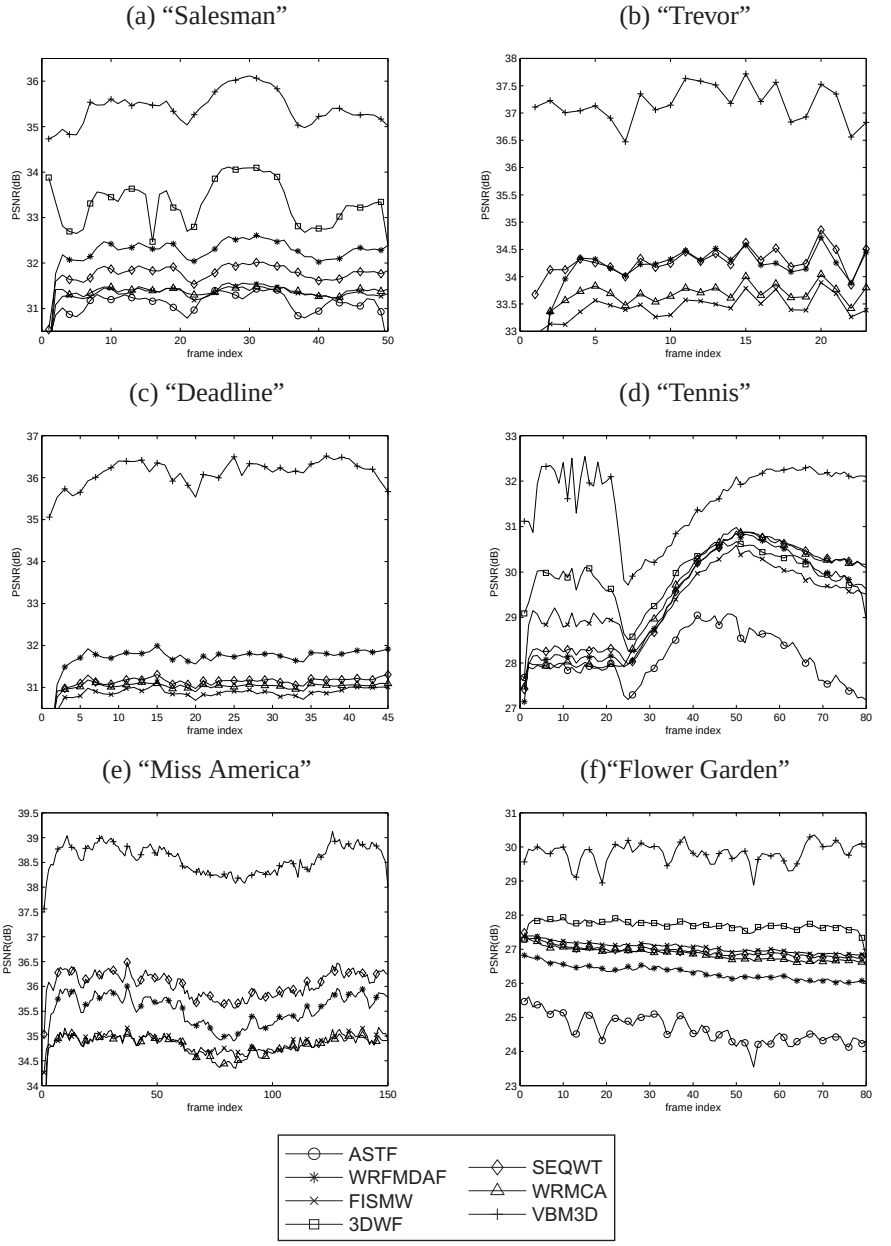

Figure 3.12: Performance comparison for the wavelet domain methods applied to the different test sequences with added Gaussian noise ($\sigma = 15$).

The proposed algorithm has first been defined in the pixel domain and was additionally extended to the wavelet domain.

Experimental results show that the introduction of fuzzy logic into the filtering framework improves the filtering results and that our pixel domain greyscale method and the wavelet domain extension outperform respectively other state-of-the-art pixel domain filters and other state-of-the-art wavelet domain filters of a comparable complexity in terms of PSNR.

4
Additive Gaussian Noise in Colour Image Sequences

Most video filters that exist in literature are designed for greyscale sequences corrupted by additive Gaussian noise, e.g. [4, 21, 50, 70, 79, 110, 124, 149]. Hardly no video filters for colour sequences can be found, since greyscale methods can straightforwardly be extended to colour video. For colour image sequences modelled in the RGB colour space, one can e.g. filter each of the colour bands R, G and B separately. This might however result in the introduction of colour artefacts since the correlation between the different colour bands is neglected. Therefore, the commonly used alternative is to filter only the luminance component Y of the YUV-transform with the given greyscale method, possibly with an additional averaging of the chrominance components U and V.

In this chapter, we introduce two other colour extensions [75, 76] for the greyscale method outlined in Chapter 3 of this thesis. Both colour extensions consist of two subfilters.

The first subfilter of the first proposed colour filtering framework [75] is a vector-based extension of the greyscale video filter in Chapter 3, that treats each pixel as a colour vector and that does not use the components separately. The used detail, difference and motion values used in the fuzzy rules are extended from grey values to colour vectors.

In the first subfilter of the second proposed colour filter [76], the greyscale method from Chapter 3 is extended by adding colour information to the fuzzy logic framework. Each of the colour bands is denoised separately by averaging the noise in an analogous way as in the greyscale method. However, the fuzzy rules that determine the weights assigned to the pixels considered in the averaging, now also require information from the other colour bands. Due to this increase in information, we can expect a more reliable estimation of the degree to which a neighbouring pixel is similar to the pixel that is filtered.

To further improve the results, the first subfilter of both colour extensions is combined

with a second subfilter. Especially around edges in the image, some colour artefacts might have appeared because sometimes not enough similar neighbours can be found to completely average the noise and it might also happen that a neighbouring pixel is wrongly considered as belonging to the same object (similar). In both proposed colour filters, for the second subfilter, we have used an extension of the second subfilter in [119]. This subfilter is based on the simplified assumption that for similar pixels the pixel value differences in the three different colour components should all three be approximately the same. The pixel being filtered is estimated from a neighbour by estimating the differences in each band equal to the average over the different colour bands.

The experimental results show that the proposed colour extensions perform very well in terms of PSNR and NCD and form a good alternative for the YUV-approach.

The structure of the chapter is as follows: The two proposed colour video filters are respectively explained in Section 4.1 and Section 4.2. Additionally, Section 4.3 presents a comparison between the different colour extensions. Finally, Section 4.4 concludes the chapter.

4.1 First Proposed Colour Filter

The first proposed filtering framework [75] consists of two subfilters which are defined in Subsection 4.1.1 and Subsection 4.1.2 respectively. In the first subfilter a $3 \times 3 \times 2$ sliding window is used, which is moved through the frame from top left to bottom right, each time filtering the central position in the window. This window consists of 3×3 pixels in the current frame and 3×3 pixels in the previous frame as shown in Fig. 4.1. The central position in the window is denoted by $(\mathbf{r}, t)$, where $\mathbf{r} = (x, y)$ and t respectively stand for the spatial and temporal position in the image sequence. An arbitrary pixel position in the sliding window (which may also be the central position) is denoted by $(\mathbf{r'}, t')$, with $\mathbf{r'} = (x + k, y + l)$, $(-1 \leq k, l \leq 1)$ and $t' = t$ or $t' = t - 1$. Further, the second subfilter uses a 3×3 window in the current frame for which similar notations will be used as for the $3 \times 3 \times 2$ window. Finally, the noisy input sequence and the output of the first and second fuzzy subfilter are respectively denoted by I_n, I_{f_1} and I_f.

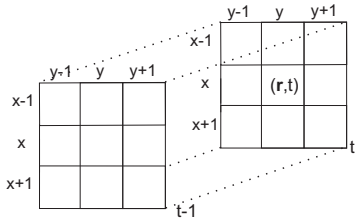

Figure 4.1: The $3 \times 3 \times 2$ filtering window consisting of 3×3 pixels in the current frame and 3×3 pixels in the previous frame.

4.1.1 First Subfilter

In this first subfilter, the fuzzy logic filtering framework introduced in Chapter 3 is extended from grey values to colour vectors. In this vector-based approach, the colours are handled as vectors and none of the colour components is used separately. Analogously to the greyscale method, the output of this first subfilter is for each pixel defined as a weighted average over the colour vectors in a $3 \times 3 \times 2$ filtering window surrounding the pixel. The filtered colour vector $I_{f_1}(\mathbf{r}, t)$ for the considered central pixel in the window is thus given by:

$$I_{f_1}(\mathbf{r}, t) = \frac{\sum_{\mathbf{r'}} W(\mathbf{r'}, t-1, \mathbf{r}, t) I_f(\mathbf{r'}, t-1) + \sum_{\mathbf{r'}} W(\mathbf{r'}, t, \mathbf{r}, t) I_n(\mathbf{r'}, t)}{\sum_{\mathbf{r'}} \sum_{t'=t-1}^{t} W(\mathbf{r'}, t', \mathbf{r}, t)}, \tag{4.1}$$

where the weights $W(\mathbf{r'}, t', \mathbf{r}, t)$ correspond to the activation degree of one of the Fuzzy Rules 4.1 and 4.2 given below. These fuzzy rules are again based on a detail value $d(\mathbf{r}, t)$, a difference value $\Delta(\mathbf{r'}, t', \mathbf{r}, t)$ and a motion value $m(\mathbf{r}, t)$, that are vector extensions of the values introduced in Chapter 3 and that were adopted from [149].

Detail, Difference and Motion Values

- The detail value $d(\mathbf{r}, t)$ is equal to the standard deviation of the 3×3 pixels of the sliding window belonging to the current frame:

$$I_{av}(\mathbf{r}, t) = \frac{1}{9} \sum_{\mathbf{r'}} I_n(\mathbf{r'}, t).$$

$$d(\mathbf{r}, t) = \Big(\frac{1}{9} \sum_{\mathbf{r'}} \|I_n(\mathbf{r'}, t) - I_{av}(\mathbf{r}, t)\|_2^2\Big)^{\frac{1}{2}}.$$

- The difference value $\Delta(\mathbf{r'}, t', \mathbf{r}, t)$ in the fuzzy rules is defined by

$$\Delta(\mathbf{r'}, t, \mathbf{r}, t) = \|I_n(\mathbf{r'}, t) - I_n(\mathbf{r}, t)\|_2,$$

  for pixels in the current frame ($t' = t$) and by

$$\Delta(\mathbf{r'}, t-1, \mathbf{r}, t) = \|I_f(\mathbf{r'}, t-1) - I_n(\mathbf{r}, t)\|_2,$$

  for pixels in the previous frame ($t' = t-1$).
- The motion value $m(\mathbf{r}, t)$ used for the filtering is finally determined as:

$$m(\mathbf{r}, t) = \|I_n(\mathbf{r}, t) - I_f(\mathbf{r}, t-1)\|_2.$$

To be able to express whether the above defined values are “large”, we introduce the fuzzy sets “large detail value”, “large difference” and “large motion value”. The membership functions of these three fuzzy sets are respectively denoted by μ_d, μ_Δ and μ_m and

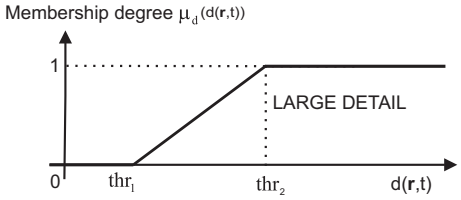

Figure 4.2: The membership function μ_d of the fuzzy set "large detail value".

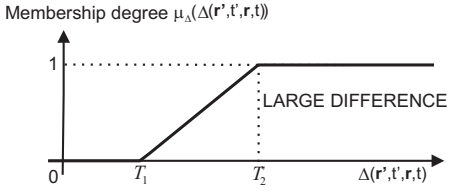

Figure 4.3: The membership function μ_Δ of the fuzzy set "large difference".

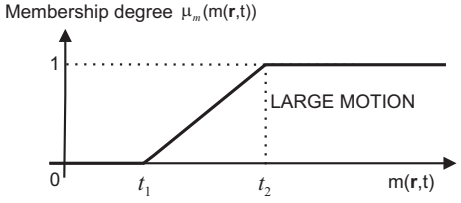

Figure 4.4: The membership function μ_m of the fuzzy set "large motion value".

are depicted in Fig. 4.2, 4.3 and 4.4. The parameters thr_1, thr_2, T_1, T_2, t_1 and t_2 that define the exact form of these functions have been experimentally determined as explained in Subsection 4.1.3.

Using the above introduced values and fuzzy sets, the weights $W(\mathbf{r'}, t', \mathbf{r}, t)$ in (4.1) can now be determined based on a fuzzy rule.

Weight Determination

Depending on whether the window pixel at position $(\mathbf{r'}, t')$ lies in the current ($t' = t$) or in the previous ($t' = t - 1$) frame, the weight $W(\mathbf{r'}, t', \mathbf{r}, t)$ in (4.1) is determined as the activation degree of one of the fuzzy rules given below. The rules remain the same as in Chapter 3, but with the adapted detail, difference and motion values and they are now used to assign weights to colour vectors instead of grey values.

Fuzzy Rule 4.1. *Determining the membership degree in the fuzzy set "large weight" of the weight $W(\mathbf{r'}, t', \mathbf{r}, t)$ for the pixel at position **r'** in the current frame ($t' = t$) of the window with central pixel position $(\mathbf{r}, t)$:*

IF (*the detail value $d(\mathbf{r}, t)$ is* LARGE AND *$\Delta(\mathbf{r'}, t', \mathbf{r}, t)$ is* NOT LARGE)

OR (*the detail value $d(\mathbf{r}, t)$ is* NOT LARGE)

THEN *the pixel at position **r'** is a* RELIABLE *neigbhourhood pixel for the filtering of $I_n(\mathbf{r}, t)$.*

Fuzzy Rule 4.2. *Determining the membership degree in the fuzzy set "large weight" of the weight $W(\mathbf{r'}, t', \mathbf{r}, t)$ for the pixel at position **r'** in the previous frame ($t' = t - 1$) of the window with central pixel position $(\mathbf{r}, t)$:*

IF ((*the detail value $d(\mathbf{r}, t)$ is* LARGE AND *$\Delta(\mathbf{r'}, t', \mathbf{r}, t)$ is* NOT LARGE)

OR (*the detail value $d(\mathbf{r}, t)$ is* NOT LARGE))

AND *the motion value $m(\mathbf{r}, t)$ is* NOT LARGE

THEN *the pixel at position **r'** is a* RELIABLE *neigbhourhood pixel for the filtering of $I_n(\mathbf{r}, t)$.*

For the results in this chapter, we have chosen to use the algebraic product, the probabilistic sum and the standard negator N_s for the AND-, OR- and NOT-operators in these rules. There is however no remarkable difference to the results obtained by using other t-norms and t-conorms. The weight $W(\mathbf{r'}, t', \mathbf{r}, t)$ (corresponding to the activation degree of one of the two rules or thus the degree to which $I_n(\mathbf{r'}, t')$ is reliable for the filtering of $I_n(\mathbf{r}, t)$) is thus more precisely given by

$$W(\mathbf{r'}, t', \mathbf{r}, t) = \omega \cdot (1 - \theta) + (1 - \omega) - \omega \cdot (1 - \theta) \cdot (1 - \omega),$$

for pixel positions in the window belonging to the current frame and by

$$W(\mathbf{r'}, t', \mathbf{r}, t) = \Big(\omega \cdot (1 - \theta) + (1 - \omega) - \omega \cdot (1 - \theta) \cdot (1 - \omega)\Big) \cdot (1 - \psi),$$

for pixel positions in the window belonging to the previous frame, where

$$\begin{aligned}\omega &= \mu_d(d(\mathbf{r},t)),\\ \theta &= \mu_\Delta(\Delta(\mathbf{r'},t',\mathbf{r},t)),\\ \psi &= \mu_m(m(\mathbf{r},t)).\end{aligned}$$

4.1.2 Second Subfilter

Because sometimes not enough similar neighbours can be found to completely average the noise in the first subfilter and because some pixels might have been wrongly considered similar in the first subfilter, some colour artefacts might still be present after applying the first subfilter. To further improve the result, the first subfilter is combined with an additional second subfilter, which is an extension of the second subfilter in [119]. Based on the simplified assumption that the difference between similar pixels is approximately the same in all three colour bands, a pixel is estimated from a neighbour by estimating a difference in a given colour component equal to the average over all three colour bands. So a difference that is larger than the average is made smaller and vice versa. The final output is a weighted average over the estimations obtained from the different neighbours, where the weight is the degree to which we believe that the neighbour belongs to the same object. The weights are introduced because for neighbours not belonging to the same object, the simplified assumption does not hold.

Local Differences and Correction Terms

As mentioned before, for this second subfilter, a 3×3 sliding window is used. In each step the central pixel in this window, at position $(\mathbf{r},t)$ in the image sequence, is filtered. For each pixel in the sliding window, local differences (gradients) in the three colour bands (each separately) are calculated. The differences in the red, green and blue neighbourhoods are respectively denoted by LD^R, LD^G and LD^B and they are calculated based on the output of the first subfilter:

$$\begin{aligned}LD^R(\mathbf{r'},\mathbf{r},t) &= I^R_{f_1}(\mathbf{r'},t) - I^R_{f_1}(\mathbf{r},t),\\ LD^G(\mathbf{r'},\mathbf{r},t) &= I^G_{f_1}(\mathbf{r'},t) - I^G_{f_1}(\mathbf{r},t),\\ LD^B(\mathbf{r'},\mathbf{r},t) &= I^B_{f_1}(\mathbf{r'},t) - I^B_{f_1}(\mathbf{r},t).\end{aligned} \tag{4.2}$$

Next, for each position in the window one correction term is determined using the calculated local differences. This correction term is defined as the average of the local difference in the red, green and blue component at the given position:

$$\epsilon(\mathbf{r'},\mathbf{r},t) = \frac{1}{3}\Big(LD^R(\mathbf{r'},\mathbf{r},t) + LD^G(\mathbf{r'},\mathbf{r},t) + LD^B(\mathbf{r'},\mathbf{r},t)\Big). \tag{4.3}$$

Output of the second subfilter

In [119], the output for each component of the central pixel is an average of the corresponding components of the neighbourhood pixels, corrected with the corresponding correction term:

$$\begin{aligned} I_f^R(\mathbf{r},t) &= \frac{1}{9}\sum_{\mathbf{r'}}\Big(I_{f_1}^R(\mathbf{r'},t)-\epsilon(\mathbf{r'},\mathbf{r},t)\Big),\\ I_f^G(\mathbf{r},t) &= \frac{1}{9}\sum_{\mathbf{r'}}\Big(I_{f_1}^G(\mathbf{r'},t)-\epsilon(\mathbf{r'},\mathbf{r},t)\Big),\\ I_f^B(\mathbf{r},t) &= \frac{1}{9}\sum_{\mathbf{r'}}\Big(I_{f_1}^B(\mathbf{r'},t)-\epsilon(\mathbf{r'},\mathbf{r},t)\Big). \end{aligned}$$

However, pixels that belong to another object and that have another colour, have a negative influence on the output. In homogeneous areas, neighbouring pixels are expected to be almost the same, and the local differences to be almost 0. So the method further averages the remaining differences caused by the noise. For a pixel belonging to another object however, the assumption that the local differences are expected to be equal in all components does not always hold. Therefore we assign weights $WT(\mathbf{r'},\mathbf{r},t)$ to the neighbouring pixels, based on whether they are expected to belong to the same object or not. To make this decision, we use the Euclidian distance between the central pixel and the considered neighbourhood pixel, given by

$$\delta(\mathbf{r'},\mathbf{r},t)=\big(LD^R(\mathbf{r'},\mathbf{r},t)^2+LD^G(\mathbf{r'},\mathbf{r},t)^2+LD^B(\mathbf{r'},\mathbf{r},t)^2\big)^{\frac{1}{2}}.$$

The weights themselves are then calculated using the following fuzzy rule that expresses that the value $\delta(\mathbf{r'},t,\mathbf{r},t)$ should not be large. Otherwise, the considered pixel is expected to belong to another object.

Fuzzy Rule 4.3. *Assigning the weight in the second subfilter for the pixel at position $(\mathbf{r'},t)$ in the filtering window:*

IF $\delta(\mathbf{r'},\mathbf{r},t)$ *is* NOT LARGE

THEN *the pixel at position $(\mathbf{r'},t)$ has a* LARGE WEIGHT $WT(\mathbf{r'},\mathbf{r},t)$ *in the second subfilter.*

The membership function μ_δ that determines the fuzzy set "large Euclidian distance" is depicted in Fig 4.5. The weights in the filtering are again chosen equal to their membership degree in the fuzzy set "large weight", i.e., $WT(\mathbf{r'},\mathbf{r},t)=1-\mu_\delta(\delta(\mathbf{r'},\mathbf{r},t))$.

Finally, if not $WT(\mathbf{r'},\mathbf{r},t)=0$ for all neighbouring pixels in the 3×3 window, the output of the second subfilter for the central pixel in the window is determined as follows:

$$I_f^R(\mathbf{r},t) = \frac{\sum_{\mathbf{r'}} WT(\mathbf{r'},\mathbf{r},t)\Big(I_{f_1}^R(\mathbf{r'},t)-\epsilon(\mathbf{r'},\mathbf{r},t)\Big)}{\sum_{\mathbf{r'}} WT(\mathbf{r'},\mathbf{r},t)},$$

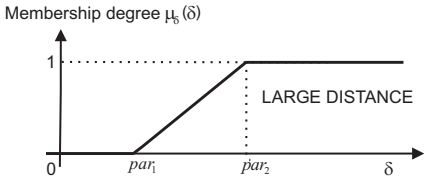

Figure 4.5: The membership function μ_δ of the fuzzy set "large Euclidian distance".

$$I_f^G(\mathbf{r},t) = \frac{\sum_{\mathbf{r'}} WT(\mathbf{r'},\mathbf{r},t)\Big(I_{f_1}^G(\mathbf{r'},t)-\epsilon(\mathbf{r'},\mathbf{r},t)\Big)}{\sum_{\mathbf{r'}} WT(\mathbf{r'},\mathbf{r},t)},$$
$$I_f^B(\mathbf{r},t) = \frac{\sum_{\mathbf{r'}} WT(\mathbf{r'},\mathbf{r},t)\Big(I_{f_1}^B(\mathbf{r'},t)-\epsilon(\mathbf{r'},\mathbf{r},t)\Big)}{\sum_{\mathbf{r'}} WT(\mathbf{r'},\mathbf{r},t)},$$

where $\epsilon(\mathbf{r'},\mathbf{r},t)$ is the correction term for the components of the neighbouring pixel at position $(\mathbf{r'},t)$. If the central pixel is so corrupt that all neighbouring pixels get a weight equal to zero, the output is calculated by giving all neigbhouring pixels in the window a weight equal to 1 and the corrupt central pixel the weight 0:

$$I_f^R(\mathbf{r},t) = \frac{1}{8}\sum_{\mathbf{r'}\neq\mathbf{r}}\Big(I_{f_1}^R(\mathbf{r'},t)-\epsilon(\mathbf{r'},\mathbf{r},t)\Big),$$
$$I_f^G(\mathbf{r},t) = \frac{1}{8}\sum_{\mathbf{r'}\neq\mathbf{r}}\Big(I_{f_1}^G(\mathbf{r'},t)-\epsilon(\mathbf{r'},\mathbf{r},t)\Big),$$
$$I_f^B(\mathbf{r},t) = \frac{1}{8}\sum_{\mathbf{r'}\neq\mathbf{r}}\Big(I_{f_1}^B(\mathbf{r'},t)-\epsilon(\mathbf{r'},\mathbf{r},t)\Big).$$

4.1.3 Parameter Selection

The parameters that determine the membership functions in the above described filtering framework have been set as follows. For the respective noise levels $\sigma = 5, 10, 15, 20$, the optimal parameters in terms of the mean PSNR values averaged over the sequences "Salesman", "Tennis", "Flowers" and "Chair" have been determined by letting them vary over a range of possible values. As illustrated for the parameters T_1 and par_2 in Fig. 4.6, this led to a linear relationship between these optimal values and the noise level. Hence, the parameters are set as the best fitting line through the observations, as shown in Fig. 4.6. The equations of those straight lines are given in Table 4.1, where σ stands for the standard deviation of the Gaussian noise. If this standard deviation is not known, it can be estimated e.g. by the wavelet domain median absolute deviation (MAD) estimator from [37].

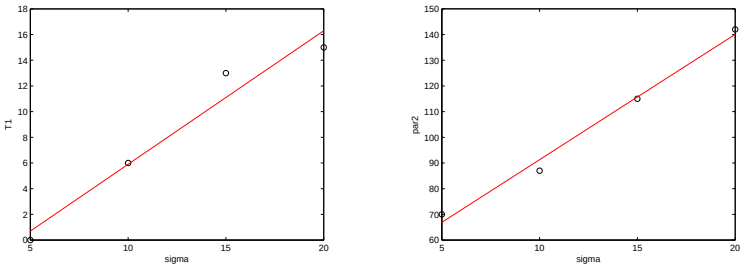

Figure 4.6: Selection of the parameter values.

Table 4.1: Selected parameter values for the membership functions.

parameter	optimal value
thr_1	0
thr_2	$0.64\sigma + 0.5$
T_1	$1.04\sigma - 4.5$
T_2	$4.06\sigma - 0.5$
t_1	$3.2\sigma - 18$
t_2	$11.46\sigma - 25.5$
par_1	0
par_2	$4.88\sigma + 42.5$

4.2 Second Proposed Colour Filter

In this section, the second proposed filtering framework for colour video [76] is outlined. The method is a superposition of two subfilters, presented in respectively Subsection 4.2.1 and Subsection 4.2.2.

Analogously to the first proposed filter, in the first subfilter a $3 \times 3 \times 2$ sliding window (Fig. 4.1) is used, while for the second subfilter the window is restricted to the 3×3 pixels in the current frame. The notations $(\mathbf{r}, t)$ and $(\mathbf{r'}, t')$ ($\mathbf{r'} = (x + k, y + l)$, $(-1 \leq k, l \leq 1)$ and $t' = t$ or $t' = t - 1$) again stand for the spatial and temporal position in the image sequence of respectively the central and an arbitrary pixel in the sliding window.

4.2.1 First Subfilter

The subfilter explained in this subsection, is a non-vector-based colour extension of the filtering framework introduced in Chapter 3.

The filtering is based on averaging the noise using the pixel component values in the neighbourhood that are similar to the given pixel component value and probably belong to the same object. Each colour band is filtered separately, but in the filtering of each colour band, the information from the other colour bands is used to confirm that a neighbouring pixel does indeed belong to the same object.

In the following the output of the first fuzzy subfilter is denoted by I_{f_1}, while the noisy input sequence is denoted by I_n. The output of the first subfilter for the central pixel in the window is determined as a weighted mean of the pixel values in the $3 \times 3 \times 2$ window:

$$I^R_{f_1}(\mathbf{r}, t) = \frac{\sum_{\mathbf{r'}} \sum_{t'=t-1}^{t} W^R(\mathbf{r'}, t', \mathbf{r}, t) I^R_n(\mathbf{r'}, t')}{\sum_{\mathbf{r'}} \sum_{t'=t-1}^{t} W^R(\mathbf{r'}, t', \mathbf{r}, t)}, \tag{4.4}$$

$$I^G_{f_1}(\mathbf{r}, t) = \frac{\sum_{\mathbf{r'}} \sum_{t'=t-1}^{t} W^G(\mathbf{r'}, t', \mathbf{r}, t) I^G_n(\mathbf{r'}, t')}{\sum_{\mathbf{r'}} \sum_{t'=t-1}^{t} W^G(\mathbf{r'}, t', \mathbf{r}, t)}, \tag{4.5}$$

$$I^B_{f_1}(\mathbf{r}, t) = \frac{\sum_{\mathbf{r'}} \sum_{t'=t-1}^{t} W^B(\mathbf{r'}, t', \mathbf{r}, t) I^B_n(\mathbf{r'}, t')}{\sum_{\mathbf{r'}} \sum_{t'=t-1}^{t} W^B(\mathbf{r'}, t', \mathbf{r}, t)}. \tag{4.6}$$

The weights $W^R(\mathbf{r'}, t', \mathbf{r}, t)$, $W^G(\mathbf{r'}, t', \mathbf{r}, t)$ and $W^B(\mathbf{r'}, t', \mathbf{r}, t)$ in the above weighted means are determined as the activation degree of Fuzzy Rule 4.6 or 4.7 (depending on whether $t' = t$ or $t' = t - 1$). In these fuzzy rules, a detail value $d(\mathbf{r}, t)$, three difference values $\Delta^R(\mathbf{r'}, t', \mathbf{r}, t)$, $\Delta^G(\mathbf{r'}, t', \mathbf{r}, t)$ and $\Delta^B(\mathbf{r'}, t', \mathbf{r}, t)$ (one for each colour band) and a motion value $m(\mathbf{r}, t)$ are used, which we will discuss first. For the AND-, OR- and NOT-operators, respectively the algebraic product, the probabilistic sum and the standard negator have been used for the results in this chapter. These operators yielded the best results, but the results obtained by other aggregation operators are comparable.

Detail, Difference and Motion Values

- In our proposed method, only one detail value $d(\mathbf{r},t)$ is used for all three colour bands. This detail value depends however on the three detail values computed on each colour band separately. These three detail values are equal to the standard deviation calculated in the respective colour bands on the 3×3 pixels of the filtering window belonging to the current frame. Therefore, for each colour band the average value in the current frame of the filtering window needs to be computed first:

$$\begin{aligned} I_{av}^{R}(\mathbf{r},t) &= \frac{1}{9}\sum_{\mathbf{r'}} I_{n}^{R}(\mathbf{r'},t), \\ I_{av}^{G}(\mathbf{r},t) &= \frac{1}{9}\sum_{\mathbf{r'}} I_{n}^{G}(\mathbf{r'},t), \\ I_{av}^{B}(\mathbf{r},t) &= \frac{1}{9}\sum_{\mathbf{r'}} I_{n}^{B}(\mathbf{r'},t). \end{aligned}$$

  The three single band detail values are then given by:

$$\begin{aligned} d^{R}(\mathbf{r},t) &= \Big(\frac{1}{9}\sum_{\mathbf{r'}} \big(I_{n}^{R}(\mathbf{r'},t) - I_{av}^{R}(\mathbf{r},t)\big)^{2}\Big)^{\frac{1}{2}}. \\ d^{G}(\mathbf{r},t) &= \Big(\frac{1}{9}\sum_{\mathbf{r'}} \big(I_{n}^{G}(\mathbf{r'},t) - I_{av}^{G}(\mathbf{r},t)\big)^{2}\Big)^{\frac{1}{2}}, \\ d^{B}(\mathbf{r},t) &= \Big(\frac{1}{9}\sum_{\mathbf{r'}} \big(I_{n}^{B}(\mathbf{r'},t) - I_{av}^{B}(\mathbf{r},t)\big)^{2}\Big)^{\frac{1}{2}}. \end{aligned}$$

  For the calculation of the activation degree of Fuzzy Rules 4.6 and 4.7, we will not need to know the exact value of $d(\mathbf{r},t)$. Only the membership degree $\mu_d\big(d(\mathbf{r},t)\big)$ of $d(\mathbf{r},t)$ in the fuzzy set "large detail value" will be needed. This membership degree is determined by the following fuzzy rule:

  Fuzzy Rule 4.4. *Assigning the membership degree in the fuzzy set "large detail value" of the detail value $d(\mathbf{r},t)$ for the pixel at the central position $(\mathbf{r},t)$ in the filtering window of the current step:*

  IF $d^{R}(\mathbf{r},t)$ *is* LARGE AND $d^{G}(\mathbf{r},t)$ *is* LARGE AND $d^{B}(\mathbf{r},t)$ *is* LARGE

  THEN $d(\mathbf{r},t)$ *is* LARGE.

  The membership function μ_{sbd} of the fuzzy set "large single band detail value" is given in Fig. 4.7, with the parameters thr_1 and thr_2 experimentally selected as explained in Subsection 4.2.3. The membership degree $\mu_d\big(d(\mathbf{r},t)\big)$ is thus given by:

$$\mu_d\big(d(\mathbf{r},t)\big) = \mu_{sbd}\big(d^{R}(\mathbf{r},t)\big) \cdot \mu_{sbd}\big(d^{G}(\mathbf{r},t)\big) \cdot \mu_{sbd}\big(d^{B}(\mathbf{r},t)\big).$$

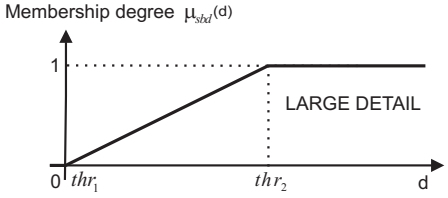

Figure 4.7: The membership function μ_{sbd} of the fuzzy set "large single band detail value".

- The three difference values $\Delta^R(\mathbf{r'}, t', \mathbf{r}, t)$, $\Delta^G(\mathbf{r'}, t', \mathbf{r}, t)$ and $\Delta^B(\mathbf{r'}, t', \mathbf{r}, t)$ that are used in the fuzzy rules to determine the weights in (4.4)-(4.5) are given by:

$$\begin{aligned}\Delta^R(\mathbf{r'}, t', \mathbf{r}, t) &= |I_n^R(\mathbf{r'}, t') - I_n^R(\mathbf{r}, t)|,\\ \Delta^G(\mathbf{r'}, t', \mathbf{r}, t) &= |I_n^G(\mathbf{r'}, t') - I_n^G(\mathbf{r}, t)|,\\ \Delta^B(\mathbf{r'}, t', \mathbf{r}, t) &= |I_n^B(\mathbf{r'}, t') - I_n^B(\mathbf{r}, t)|.\end{aligned}$$

The membership function μ_Δ of the fuzzy set "large difference" is given in Fig. 4.8,

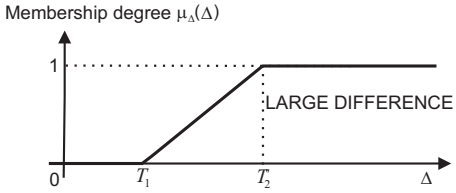

Figure 4.8: The membership function μ_Δ of the fuzzy set "large difference".

with the parameters T_1 and T_2 experimentally selected as explained in Subsection 4.2.3.

- Analogously to the detail value $d(\mathbf{r}, t)$ also only one motion value $m(\mathbf{r}, t)$ is used for the filtering of all three colour bands. This value depends however again on three values computed for each of the colour bands separately. These three single band motion values are:

$$\begin{aligned}m^R(\mathbf{r}, t) &= \Big|I_{av}^R(\mathbf{r}, t) - I_{av}^R(\mathbf{r}, t-1)\Big|\\ &= \Big|\frac{1}{9}\sum_{\mathbf{r'}} I_n^R(\mathbf{r'}, t) - \frac{1}{9}\sum_{\mathbf{r'}} I_f^R(\mathbf{r'}, t-1)\Big|,\\ m^G(\mathbf{r}, t) &= \Big|I_{av}^G(\mathbf{r}, t) - I_{av}^G(\mathbf{r}, t-1)\Big|\\ &= \Big|\frac{1}{9}\sum_{\mathbf{r'}} I_n^G(\mathbf{r'}, t) - \frac{1}{9}\sum_{\mathbf{r'}} I_f^G(\mathbf{r'}, t-1)\Big|,\end{aligned}$$

$$\begin{aligned} m^B(\mathbf{r},t) &= \Big| I^B_{av}(\mathbf{r},t) - I^B_{av}(\mathbf{r},t-1) \Big| \\ &= \Big| \frac{1}{9} \sum_{\mathbf{r'}} I^B_n(\mathbf{r'},t) - \frac{1}{9} \sum_{\mathbf{r'}} I^B_f(\mathbf{r'},t-1) \Big|. \end{aligned}$$

Just as it was the case for the detail value $d(\mathbf{r},t)$, we will also not need to know the exact value of $m(\mathbf{r},t)$ for the calculation of the activation degree of Fuzzy Rule 4.6 and 4.7. Only the membership degree $\mu_m\big(m(\mathbf{r},t)\big)$ of $m(\mathbf{r},t)$ in the fuzzy set "large motion value" will be needed. This membership degree is obtained from the following fuzzy rule:

Fuzzy Rule 4.5. *Assigning the membership degree in the fuzzy set "large motion value" of the motion value $m(\mathbf{r},t)$ for the pixel at the central position $(\mathbf{r},t)$ in the filtering window of the current step:*

IF ($m^R(\mathbf{r},t)$ *is* LARGE AND $m^G(\mathbf{r},t)$ *is* LARGE) OR
($m^R(\mathbf{r},t)$ *is* LARGE AND $m^B(\mathbf{r},t)$ *is* LARGE) OR
($m^G(\mathbf{r},t)$ *is* LARGE AND $m^B(\mathbf{r},t)$ *is* LARGE)
THEN $m(\mathbf{r},t)$ *is* LARGE.

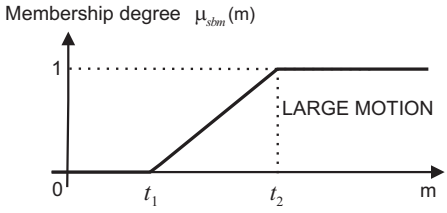

Figure 4.9: The membership function μ_{sbm} of the fuzzy set "large single band motion value".

The membership function μ_{sbm} of the fuzzy set "large single band motion value" is given in Fig 4.9, with the parameters t_1 and t_2 experimentally selected as explained in Subsection 4.2.3. The membership degree $\mu_m\big(m(\mathbf{r},t)\big)$ is thus given by:

$$\mu_m\big(m(\mathbf{r},t)\big) = \alpha + (\beta + \gamma - \beta \cdot \gamma) - \alpha \cdot (\beta + \gamma - \beta \cdot \gamma), \tag{4.7}$$

with

$$\begin{aligned} \alpha &= \mu_{sbm}\big(m^R(\mathbf{r},t)\big) \cdot \mu_{sbm}\big(m^G(\mathbf{r},t)\big), \\ \beta &= \mu_{sbm}\big(m^R(\mathbf{r},t)\big) \cdot \mu_{sbm}\big(m^B(\mathbf{r},t)\big), \\ \gamma &= \mu_{sbm}\big(m^G(\mathbf{r},t)\big) \cdot \mu_{sbm}\big(m^B(\mathbf{r},t)\big). \end{aligned}$$

Weight Determination

As mentioned above, the weights $W^R(\mathbf{r'}, t', \mathbf{r}, t)$, $W^G(\mathbf{r'}, t', \mathbf{r}, t)$ and $W^B(\mathbf{r'}, t', \mathbf{r}, t)$ in the weighted means (4.4)-(4.5) are determined as the activation degree of the Fuzzy Rules 4.6 and 4.7, that correspond to the ideas that were adopted from the multiple class averaging filter [149]. If large detail is detected, i.e., if a calculated detail value is large, then we should filter less by averaging only over pixels that are quite similar, i.e., for which there is no large difference in the considered colour component and also in at least one of the other components. On the other hand, if there is not much detail detected, i.e., in the case that the calculated detail value is not large, strong filtering should be performed, i.e., we don't put a condition on the difference between the considered and the filtered pixel in the considered colour band (the check in the other colour bands remains for the case that the calculated detail value was not completely reliable). Further, if the pixel for which the weight is calculated belongs to the previous frame, we only want to give it a large weight if there is no motion detected in the filtering window, i.e., if a calculated motion value is not large. In the filtering of the red colour band, this results in the following two fuzzy rules, depending on whether the pixel lies in the current or the previous frame:

Fuzzy Rule 4.6. *Assigning the membership degree in the fuzzy set "large weight" of the weight $W^R(\mathbf{r'}, t', \mathbf{r}, t)$ for the red component value at position **r'** in the current frame ($t' = t$) of the window with central pixel position $(\mathbf{r}, t)$:*

IF $\Big($(*the detail value $d(\mathbf{r}, t)$ is* LARGE AND *the difference $\Delta^R(\mathbf{r'}, t', \mathbf{r}, t)$ is* NOT LARGE AND (*the difference $\Delta^G(\mathbf{r'}, t', \mathbf{r}, t)$ is* NOT LARGE OR *the difference $\Delta^B(\mathbf{r'}, t', \mathbf{r}, t)$ is* NOT LARGE)$)$ OR $\big($(*the detail value $d(\mathbf{r}, t)$ is* NOT LARGE) AND (*the difference $\Delta^G(\mathbf{r'}, t', \mathbf{r}, t)$ is* NOT LARGE OR *the difference $\Delta^B(\mathbf{r'}, t', \mathbf{r}, t)$ is* NOT LARGE)$)\Big)$

THEN *the red component value at position **r'** is* RELIABLE *for the filtering of the red component value $I_n^R(\mathbf{r'}, t', \mathbf{r}, t)$.*

Fuzzy Rule 4.7. *Assigning the membership degree in the fuzzy set "large weight" of the weight $W^R(\mathbf{r'}, t', \mathbf{r}, t)$ for the red component value at position **r'** in the previous frame ($t' = t - 1$) of the window with central pixel position $(\mathbf{r}, t)$:*

IF $\Big($(*the detail value $d(\mathbf{r}, t)$ is* LARGE AND *the difference $\Delta^R(\mathbf{r'}, t', \mathbf{r}, t)$ is* NOT LARGE AND (*the difference $\Delta^G(\mathbf{r'}, t', \mathbf{r}, t)$ is* NOT LARGE OR *the difference $\Delta^B(\mathbf{r'}, t', \mathbf{r}, t)$ is* NOT LARGE)$)$ OR $\big($(*the detail value $d(\mathbf{r}, t)$ is* NOT LARGE) AND (*the difference $\Delta^G(\mathbf{r'}, t', \mathbf{r}, t)$ is* NOT LARGE OR *the difference $\Delta^B(\mathbf{r'}, t', \mathbf{r}, t)$ is* NOT LARGE)$)\Big)$

AND *the motion value $m(\mathbf{r}, t)$ is* NOT LARGE

THEN *the red component value at position **r'** is* RELIABLE *for the filtering of the red component value $I_n^R(\mathbf{r'}, t', \mathbf{r}, t)$.*

Similar fuzzy rules, switching the role of the red colour band and the colour band that needs to be filtered, are used to determine the weights $W^G(\mathbf{r'}, t', \mathbf{r}, t)$ and $W^B(\mathbf{r'}, t', \mathbf{r}, t)$ in expressions (4.5)-(4.6) to filter the green and blue colour band respectively.

Summarized, for pixel positions in the window belonging to the current frame ($t' = t$), the weight $W^R(\mathbf{r'}, t', \mathbf{r}, t)$ in (4.4) is thus given by

$$W^R(\mathbf{r'}, t', \mathbf{r}, t) = \omega \cdot \theta \cdot \phi + (1 - \omega) \cdot \phi - (\omega \cdot \theta \cdot \phi) \cdot ((1 - \omega) \cdot \phi),$$

where

$$\begin{aligned}
\omega &= \mu_d(d(\mathbf{r}, t)) \\
\theta &= (1 - \mu_\Delta(\Delta^R(\mathbf{r'}, t', \mathbf{r}, t))) \\
\phi &= (1 - \mu_\Delta(\Delta^G(\mathbf{r'}, t', \mathbf{r}, t))) + (1 - \mu_\Delta(\Delta^B(\mathbf{r'}, t', \mathbf{r}, t))) \\
&\quad - (1 - \mu_\Delta(\Delta^G(\mathbf{r'}, t', \mathbf{r}, t))) \cdot (1 - \mu_\Delta(\Delta^B(\mathbf{r'}, t', \mathbf{r}, t))).
\end{aligned}$$

For pixel positions in the window belonging to the previous frame ($t' = t - 1$), an extra factor $1 - \mu_m(m(\mathbf{r}, t))$ is needed.

4.2.2 Second Subfilter

Analogously as in the first proposed colour video filter, also the first subfilter of this second proposed filter is combined with a second subfilter. We have again used the extension of the second subfilter in [119] as described in Subsection 4.1.2.

4.2.3 Parameter Selection

Analogously as for the first proposed filter, the parameters that determine the membership functions used in the above described second proposed filter, have been set by determining the optimal values in terms of the mean PSNR values averaged over the sequences “Salesman”, “Tennis”, “Flowers” and “Chair” and this for the respective noise levels $\sigma = 5, 10, 15, 20$. This was done by letting the parameter values vary over a range of possible values. Again a linear relationship between these optimal values and the noise level was found, such that the final parameters have been selected as the best fitting line through the observations. The selection process is illustrated in Fig. 4.10 for the parameters thr_2 and T_2. The selected parameter values, as a function of the noise level, are given in Table 4.2.

4.3 Experimental Results

In this section we present the results of our experiments, in which we have used the test sequences “Salesman”, “Tennis”, “Deadline”, “Flower Garden”, “Foreman” and “Bus”, corrupted by additive Gaussian noise of zero mean and standard deviation $\sigma = 5, 10, 15, 20, 25$.

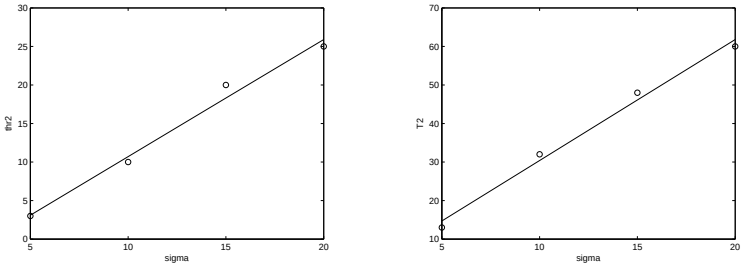

Figure 4.10: Optimal parameter values in terms of the PSNR.

Table 4.2: The used parameter values.

Parameter	Value
thr_1	0
thr_2	$1.52\sigma - 4.5$
T_1	0
T_2	$3.14\sigma - 1.0$
t_1	$0.72\sigma - 4.0$
t_2	$2.22\sigma - 4.5$
par_1	$1.1\sigma - 7.5$
par_2	$6\sigma + 35$

We have compared the two proposed colour filters to the filtering approach that denoises the Y component of the YUV transform with the recursive wavelet extension of the original greyscale method outlined in Chapter 3 (which outperforms other greyscale methods of a similar complexity as shown in Chapter 3) combined with an additional averaging (3×3 window) of the chrominance components U and V. The PSNR and NCD results of this comparison can be found in Fig. 4.11 and 4.12 respectively, where the vector-based first colour filter, the colour-rule-based second colour filter and the YUV approach are respectively denoted by FMDAF-RGB, FMDAF-CR and FMDAF-YUV. From those graphs, it can be concluded that, both in terms of PSNR and NCD, the two proposed filtering frameworks are a better alternative for the usually applied filtering of the Y-component.

For a visual comparison, we have made the original and noisy "Deadline" ($\sigma = 15$) and "Salesman" ($\sigma = 15$) sequence and the results after applying the respective filters available on `http://www.fuzzy.ugent.be/tmelange/results/colourgauss`. When looking carefully to e.g. the left side of the phone in the "Salesman" sequence (Fig. 4.13), we see that some red and green shine (colour artefacts) is visible in the result of the FMDAF-YUV method. This is much less the case in the result of the two proposed colour filters, which might explain the better PSNR and NCD values.

We see however also that the wavelet domain method has removed more noise and produces a smoother result. This smoother result can however be attributed to the use of a wavelet domain filter. If the original pixel domain greyscale method would have been used, we would also have had a little more noise remaining. Remark also that the smoother result also has as a result that the details have been smoothed a little more. For the "Salesman" sequence, see e.g. the eyes and face in Fig. 4.14. This trade-off between noise removal and detail preservation is one of the main challenges in the development of a noise filter.

Finally, remark also that the two proposed colour filters will have a smaller complexity, since in the YUV-approach, a wavelet transform is applied and six wavelet bands need to be filtered instead of three colour bands or one vector band.

4.4 Conclusion

In this chapter we have presented two new fuzzy video filters for the removal of Gaussian noise in colour image sequences. In the first proposed filter, the fuzzy logic framework from Chapter 3 was extended to colour videos through a vector-based approach, while in the second proposed filter, the framework was extended by filtering each of the colour bands separately, with information from the other colour bands added to the used fuzzy rules. Both extensions were additionally combined with a refinement of the colour restorating subfilter from [119] to remove possible colour artefacts.

Experimental results show that the proposed methods are a good alternative for the commonly used YUV-colour extension of the original greyscale method, both in terms of PSNR and NCD.

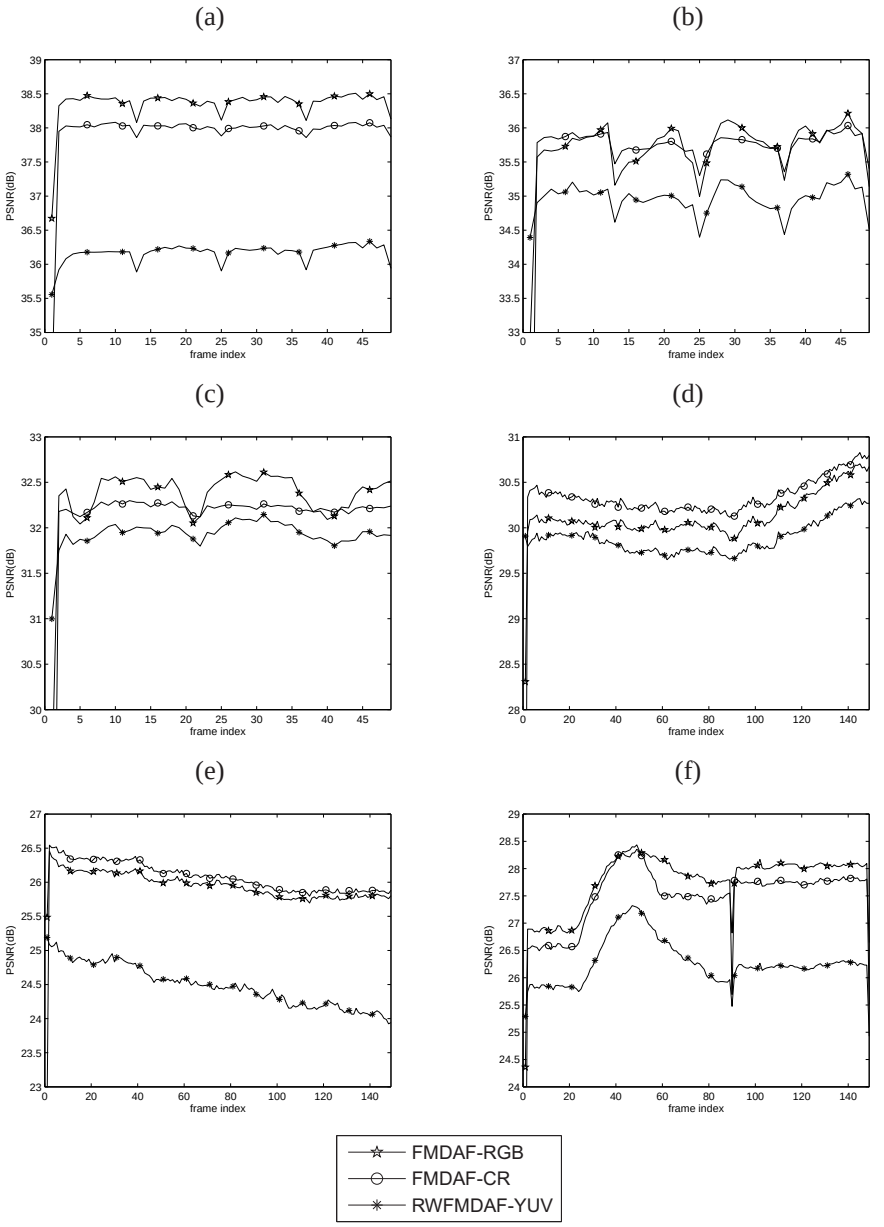

Figure 4.11: PSNR results for the different methods applied on the sequences (a) "Deadline" ($\sigma = 5\%$), (b) "Foreman" ($\sigma = 10\%$), (c) "Salesman" ($\sigma = 15\%$), (d) "Bus" ($\sigma = 15\%$), (e) "Flower Garden" ($\sigma = 20\%$) and (f) "Tennis" ($\sigma = 25\%$).

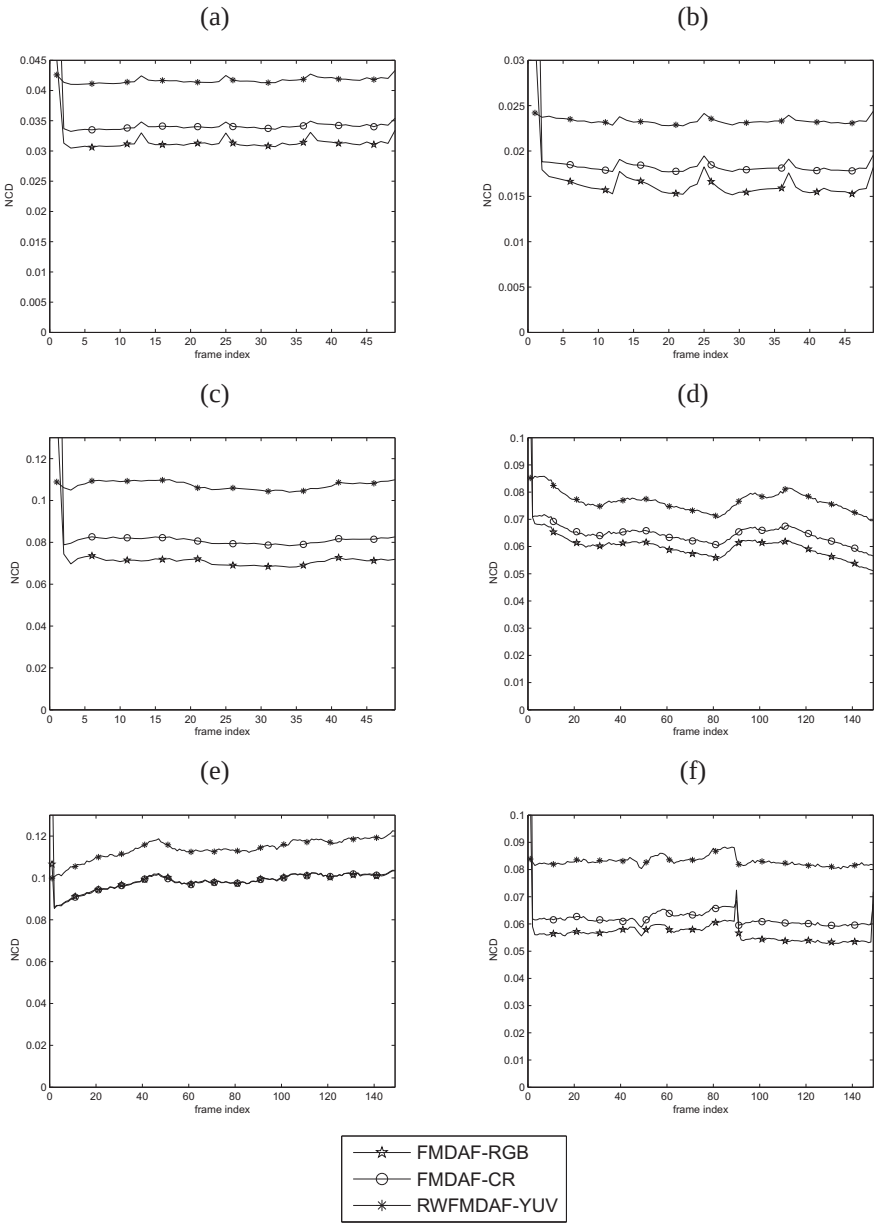

Figure 4.12: NCD results for the different methods applied on the sequences (a) "Deadline" ($\sigma = 5\%$), (b) "Foreman" ($\sigma = 10\%$), (c) "Salesman" ($\sigma = 15\%$), (d) "Bus" ($\sigma = 15\%$), (e) "Flower Garden" ($\sigma = 20\%$) and (f) "Tennis" ($\sigma = 25\%$).

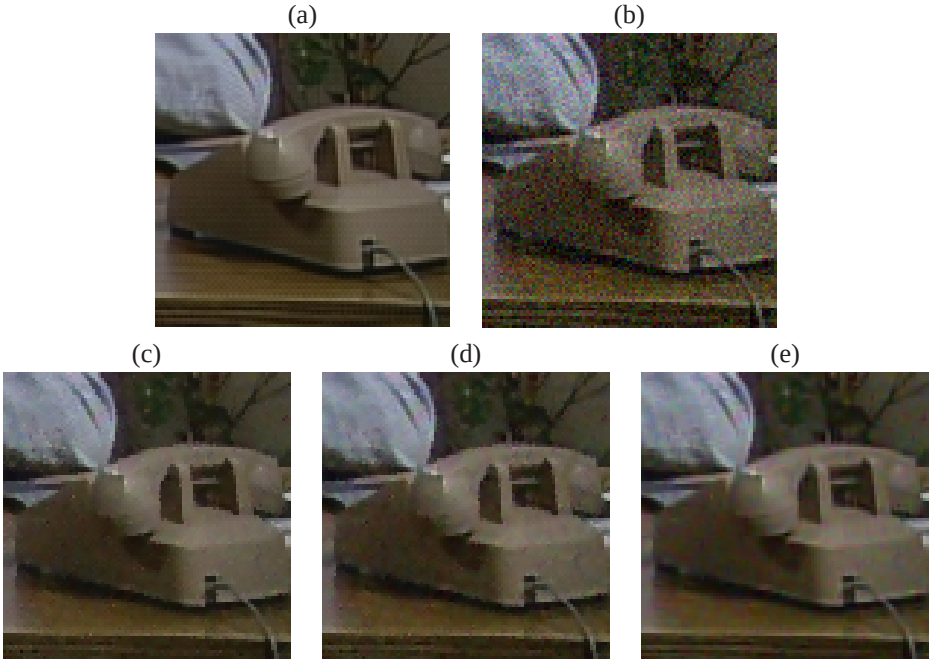

Figure 4.13: Enlarged part of the phone in the 20-th frame of the "Salesman" sequence: (a) original, (b) noisy ($\sigma = 15$), (c) $FMDAF - RGB$, (d) $FMDAF - CR$ and (e) $FMDAF - YUV$.

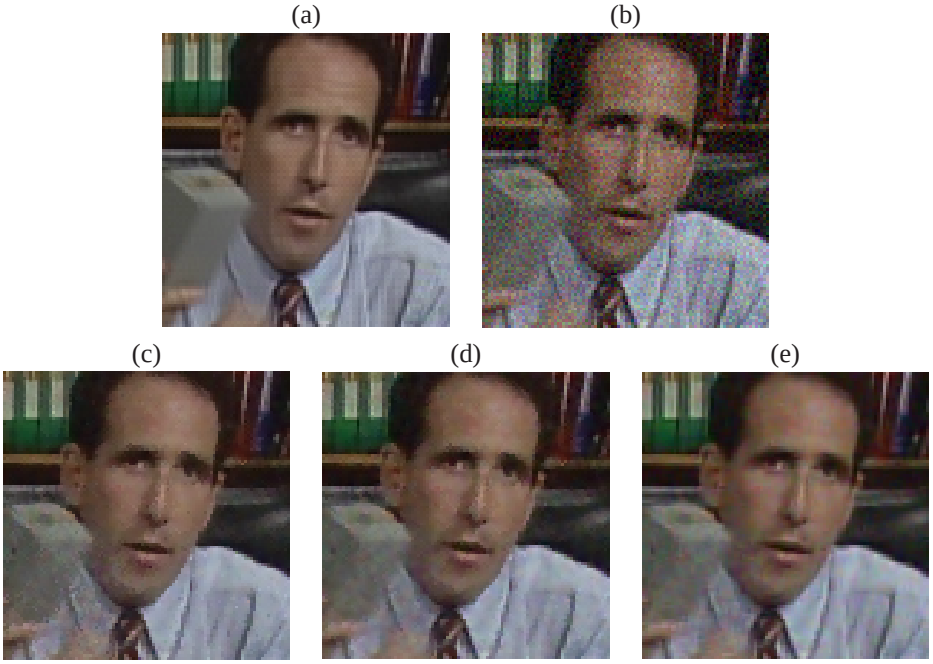

Figure 4.14: Enlarged part of the face in the 20-th frame of the "Salesman" sequence: (a) original, (b) noisy ($\sigma = 15$), (c) $FMDAF - RGB$, (d) $FMDAF - CR$ and (e) $FMDAF - YUV$.

5
Random Impulse Noise in Greyscale Image Sequences

Most video filters that can be found in literature are designed for sequences corrupted by additive Gaussian noise (e.g. [41, 50, 70, 79, 141]). Much less video filters exist for the removal of impulse noise. However, numerous 2D techniques have been developed for the denoising of still images and can be applied on each frame of the sequence consecutively. The best known among them are the median based rank-order filters (e.g., [20, 45, 58]), but also several fuzzy techniques (e.g., [42, 59, 115, 116, 121, 122, 135, 140]) have already turned up that performed very well compared to the rank-order ones. A huge drawback of applying 2D spatial filters on image sequences however is that the temporal correlation between successive frames is neglected. As a consequence, temporal inconsistencies will arise. Some examples of 3D impulse noise filtering schemes, that also take into account pixels from neighbouring frames, can e.g. be found in [22, 38, 55, 66, 139]. In the 3D rational filter [22], the filter output for a pixel is determined as a rational function of the grey values in a spatio-temporal neighbourhood. To avoid that in the presence of fast motion, pixels from the previous frame would be used wrongly, a movement detector is used. In the case of motion only a spatial filtering is performed, i.e., the output is a rational function of only the spatial neighbouring grey values. In [55], two variants on the classical median filter in a 3D neighbourhood are presented: the adaptive 3D median filter and the weighted 3D median filter. The adaptive 3D median filter first detects whether a pixel might be noisy and only the detected pixels are finally filtered. If the number of detected pixels in the previous frame are low, stronger conditions are used for this detection and vice versa. The filtered output for the detected pixels is determined as the median in the 3D neighbourhood of the considered pixel. The non-detected pixels remain unfiltered to preserve the details. The weighted 3D median filter assigns weights to the neighbouring pixels used in the calculation

of the median, i.e., each pixel is added a number of times (where the number is equal to the pixels weight) to the set of pixels of which the median is calculated to serve as the filter output. The closer a pixel lies to the centre of the neighbourhood, the higher its weight. The LUM (lower-upper-middle) smoother in [66] extends the standard LUM smoothers [45] by introducing an adaptive smoothing control. Using a fixed smoothing level for a whole image namely results in excessive smoothing in some given regions and insufficient smoothing in other regions. The peak-and-valley filter, presented in [139], is a generic n-dimensional filter. It is composed of two conditional rules, independently applied one after the other. The first rule detects pixels that are larger than their neighbourhood (peaks), the second one detects pixels that are smaller than their neighbourhood (valleys). Pixels that were detected are finally filtered as the most similar pixel in their neighbourhood. The filter proposed in [38] finally, is a motion compensated adaptive spatio-temporal least mean fourth (LMF) L-filter in which the filter weights are determined by minimizing the kurtosis.

The main drawback of the above filters is that in their aim to remove as much noise as possible, they also filter too many noisefree pixels, resulting in detail loss, or vice versa, by trying to preserve the details, too many noise pixels are not detected. In this chapter, we present two algorithms [74, 77, 80] in which the noise is removed step by step in order to have a good noise removal and a good detail preservation at the same time and thus to minimize the trade-off between noise removal and detail preservation. In the successive filtering steps, the noisy pixels are first detected and only the detected pixels are filtered in order to preserve the details. The filtering is performed in a motion compensated way such that the temporal information is exploited as much as possible. Further, the filtering steps make use of fuzzy set theory. In the first proposed filter [80], for each pixel a degree to which it is considered noisy is calculated. Pixels having a non-zero degree will be filtered. In the second proposed method [74, 77], for each pixel both a degree to which it is considered noisy and noisefree is calculated. The pixel will now be filtered if the noisy degree is larger than the noisefree degree.

From the experimental results it can be seen that the proposed filters combine a good noise removal with a good detail preservation. They are shown to outperform other state-of-the-art random impulse noise filters both in terms of PSNR and visually.

The chapter is structured as follows: The different filtering steps of the two proposed algorithm are discussed one by one in Section 5.1 and 5.2 respectively. Next, the two proposed filters are compared to other state-of-the-art filters in Section 5.3 and the chapter is concluded in Section 5.4.

5.1 First Proposed Algorithm

The proposed algorithm [80] consists of different separate noise detection and filtering steps, both spatial and temporal as illustrated in Fig. 5.1. For a lot of pixels, it is obvious that they will be noisefree because of the clear correspondence to their spatio-temporal neighbours. It would be a needless effort to investigate whether such pixels are noisy. Therefore, in a first detection (5.1.1) we investigate which pixels can be considered to be surely noisefree and

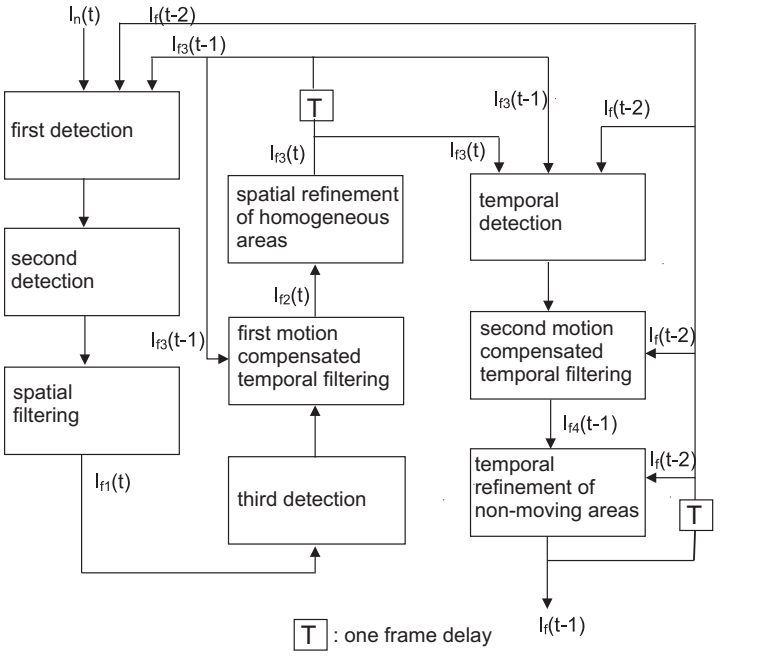

Figure 5.1: Overview of the different steps in the proposed algorithm.

should not be filtered. If a pixel and some of its neighbours and the corresponding pixels in the previous and preprevious frame are all similar, then we assume that these pixels belong to the same object and that they are noisefree. Such pixels will not be investigated or filtered any further in the algorithm. For other pixels, we start the investigation to determine whether they are noisy. In the second detection step (5.1.2), pixels are detected as noisy if there is a direction in which the two neighbours have a small difference in grey value (and probably belong to the same object), but are quite different from the pixel that is investigated. We however check that the considered pixel does not belong to a line, which might be the reason for this difference in grey value. Next, a first temporary filtering on a spatial basis is performed (5.1.3). The result of this filtering, denoted by I_{f_1}, facilitates the detection of the remaining noisy pixels. Now that a considerable part of the noise is removed, a next spatial detection step (5.1.4) is performed in which pixels are thought to be noisy if they have a considerably larger or smaller grey value than all its neighbouring pixels, except one (to allow a possible second noisy pixel). Additionally, we perform a motion compensated filtering (5.1.5) for all pixels that have been detected noisy up to now (I_{f_2}), followed by a refinement in homogeneous areas (5.1.6)(I_{f_3}). Some random impulses result in a small difference compared to their neighbours and will not have been detected. In homogeneous areas, small differences, that however are relatively large in such an area, will now also be considered as noisy. Up to now, all noise detection was performed spatially. Some noisy pixels are however too difficult to detect on a spatial base. Therefore, we use the temporal information available in sequences to perform a last noise detection (5.1.7). A frame delay is applied to be able to compare a pixel to its temporal neighbours in respectively the previous and next frame and to detect temporal impulses. Remark that the fact that the t-th frame is already filtered based on spatial information, makes the temporal detection for the $t-1$-th frame more reliable since the previous and next frame are both already filtered (the previous one completely and the next one already based on spatial information). Pixels that have been detected in this step, are then filtered (I_{f_4}), again by the help of motion compensation (5.1.8). Finally, in analogy to the spatial refinement, a temporal refinement is performed (I_f) to remove small impulses in non-moving areas (5.1.9). The result of the successive filtering steps is illustrated in Fig. 5.2 and 5.3 for the 20-th frame of the "Salesman" sequence.

5.1.1 First Detection

The first detection determines whether a pixel value $I_n(x, y, t)$ should be considered noisefree. We assume that this is the case when this pixel is similar to the pixels $I_{f_3}(x, y, t-1)$ and $I_f(x, y, t-2)$ at the corresponding position in respectively the previous and preprevious frame and when these pixels $I_{f_3}(x, y, t-1)$ and $I_f(x, y, t-2)$ are similar too. Two pixels are considered similar when their absolute difference in grey value is small to some non-zero degree, where the linguistic value "small" is represented by a fuzzy set of which the membership function μ_S is depicted in Fig. 5.4. The parameter p_1 is selected in Subsection 5.1.10. Further at least two neighbours $I_n(x+k, y+l, t)$ ($k, l \in \{-1, 0, 1\}, (k, l) \neq (0, 0)$) need to be found, that are similar to the central pixel and for which the same condition holds,

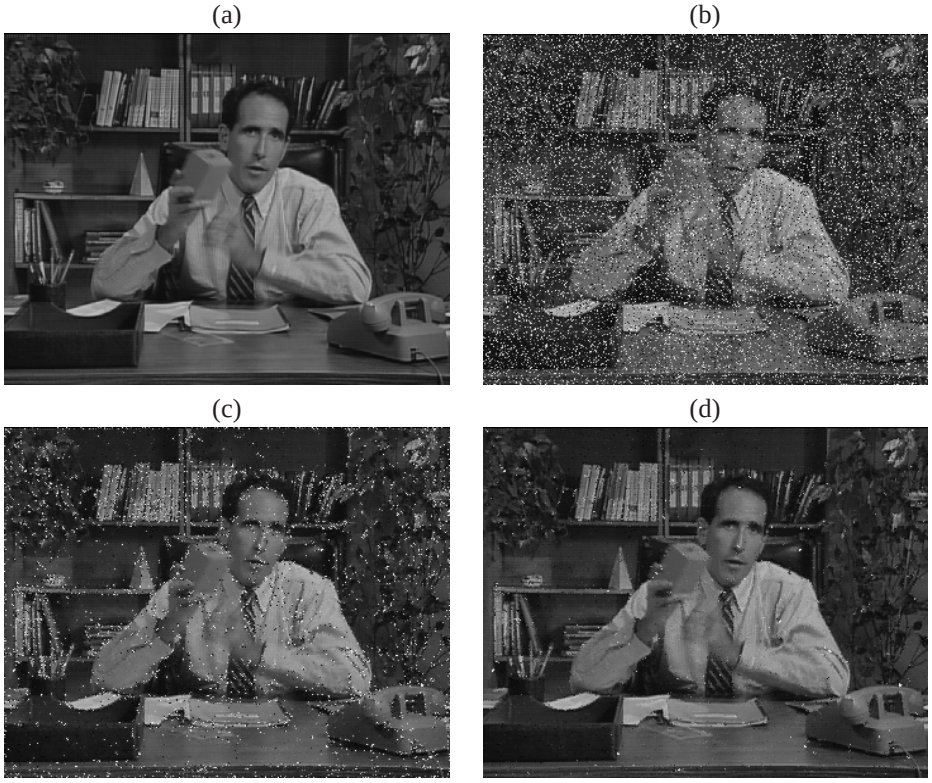

Figure 5.2: The original 20-th frame of the "Salesman" sequence: (a) the frame corrupted by 25% random impulse noise (b)($PSNR = 14.27dB$) and the result after (c) the first spatial filtering ($PSNR = 19.48dB$) and (d) the first motion compensated filtering ($PSNR = 27.58dB$)respectively.

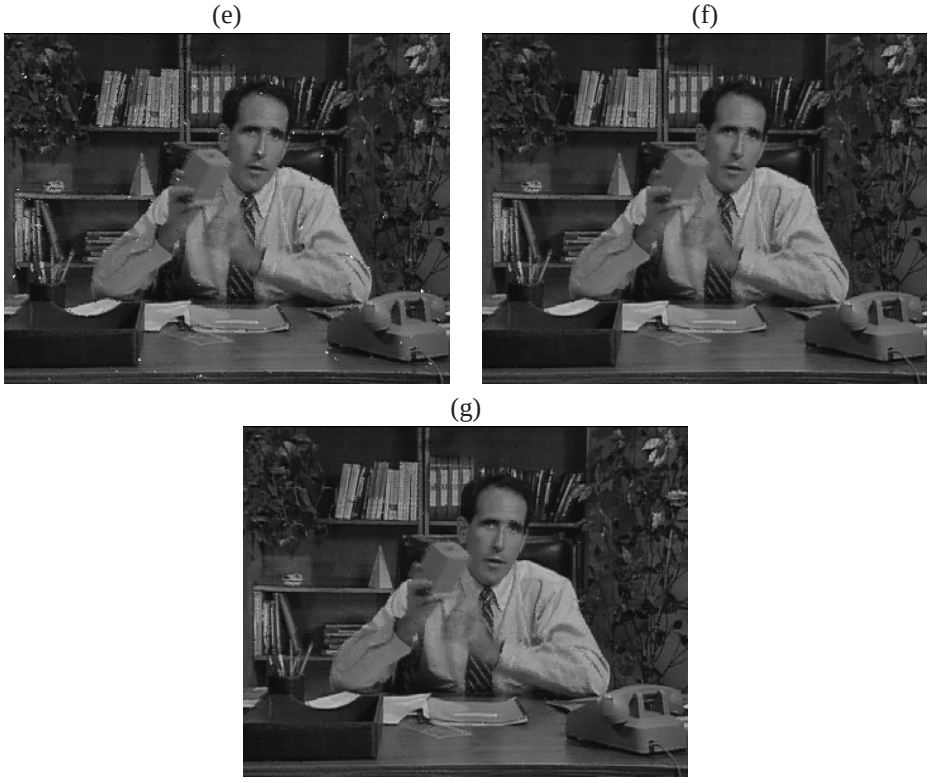

Figure 5.3: The original 20-th frame of the "Salesman" sequence: the result after (e) the spatial refinement ($PSNR = 28.45dB$), (f) the second motion compensated filtering ($PSNR = 31.99dB$) and (g) the temporal refinement ($PSNR = 32.74dB$) respectively.

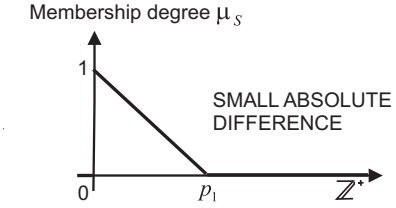

Figure 5.4: The membership function μ_S of the fuzzy set "small absolute difference".

i.e., these neighbours are also similar to the corresponding pixels $I_{f_3}(x+k, y+l, t-1)$ and $I_f(x+k, y+l, t-2)$ in the previous and the preprevious frame and these pixels $I_{f_3}(x+k, y+l, t-1)$ and $I_f(x+k, y+l, t-2)$ are also similar. If this is the case, the central pixel in the filtering window is assumed noisefree. The other pixels need to be investigated further to see whether they are noisy or not.

$$\mu_{noisefree}(x,y,t) = \begin{cases} 1 & \text{if } \mu_S(|I_n(x,y,t) - I_{f_3}(x,y,t-1)|) > 0 \text{ and} \\ & \mu_S(|I_n(x,y,t) - I_f(x,y,t-2)|) > 0 \text{ and} \\ & \mu_S(|I_{f_3}(x,y,t-1) - I_f(x,y,t-2)|) > 0 \text{ and} \\ & (\exists(x',y'),(x'',y''))((x',y') \neq (x'',y'') \text{ and} \\ & x-1 \leq x', x'' \leq x+1 \text{ and} \\ & y-1 \leq y', y'' \leq y+1 \text{ and} \\ & \mu_S(|I_n(x,y,t) - I_n(x',y',t)|) > 0 \text{ and} \\ & \mu_S(|I_n(x,y,t) - I_n(x'',y'',t)|) > 0 \text{ and} \\ & \mu_S(|I_n(x',y',t) - I_{f_3}(x',y',t-1)|) > 0 \text{ and} \\ & \mu_S(|I_n(x',y',t) - I_f(x',y',t-2)|) > 0 \text{ and} \\ & \mu_S(|I_{f_3}(x',y',t-1) - I_f(x',y',t-2)|) > 0 \text{ and} \\ & \mu_S(|I_n(x'',y'',t) - I_{f_3}(x'',y'',t-1)|) > 0 \text{ and} \\ & \mu_S(|I_n(x'',y'',t) - I_f(x'',y'',t-2)|) > 0 \text{ and} \\ & \mu_S(|I_{f_3}(x'',y'',t-1) - I_f(x'',y'',t-2)|) > 0), \\ 0 & \text{else.} \end{cases}$$

5.1.2 Second Detection

For those pixels that have not been detected as noisefree in the first step, it is needed to further investigate whether they are really noisy and need to be filtered.

The detection of noisy pixels in this step goes as follows. If in a given direction two opposite neighbours $I_n(x+k, y+l, t)$ and $I_n(x-k, y-l, t)$, (with $(k,l) \in \{(-1,-1),(-1,0),(-1,1),(0,1)\}$ corresponding to the directions $N-S$, $NE-SW$, $E-W$ and $SE-NW$), are similar ($\mu_S|I_n(x+k, y+l, t) - I_n(x-k, y-l, t)|) > 0$) and each of these two opposite neighbours has two similar neighbours (and can thus be considered reliable), then the central pixel is considered noisy for this direction i (with $i \in dir = \{N-S, NE-SW, E-W, SE-NW\}$) if the difference in grey value with respect to the central pixel is large positive or large negative for the two opposite neighbours. The membership functions μ_{LN} and μ_{LP} of the fuzzy sets that are used to represent the linguistic variables "large negative difference" and "large positive difference" are depicted in Fig. 5.5. Further, for the results in this chapter, the and- and or-operator are translated by the algebraic product and the probabilistic sum respectively. These aggregators are a good choice from a computational point of view and other aggregation operators resulted in similar results. The degree $D_i(x,y,t)$

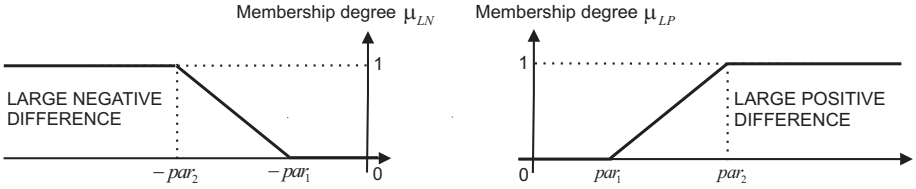

Figure 5.5: The respective membership functions μ_{LN} and μ_{LP} of the fuzzy sets "large negative difference" and "large positive difference".

to which $I_n(x, y, t)$ is considered noisy in the direction i then becomes:

$$D_i(x, y, t) = (lp_1 \cdot lp_2) + (ln_1 \cdot ln_2) - (lp_1 \cdot lp_2) \cdot (ln_1 \cdot ln_2),$$

with

$$\begin{aligned} lp_1 &= \mu_{LP}(I_n(x, y, t) - I_n(x + k, y + l, t)), \\ lp_2 &= \mu_{LP}(I_n(x, y, t) - I_n(x - k, y - l, t)), \\ ln_1 &= \mu_{LN}(I_n(x, y, t) - I_n(x + k, y + l, t)), \\ ln_2 &= \mu_{LN}(I_n(x, y, t) - I_n(x - k, y - l, t)), \end{aligned}$$

if the two opposite neighbours in this direction each also have two similar neighbours. If this is not the case, then $D_i(x, y, t) = 1$. However, we don't want the pixel to be detected if there is a direction in which the two opposite neighbours, or one of the three pixels in their prolongation, as illustrated in Fig. 5.6, are similar to the central pixel. In this case the central pixel might belong to a line and should not be considered noisy. The occurrence of a line is saved in a variable $L(x, y, t)$. The variable $L(x, y, t)$ receives the value *true* if a line is detected and the value *false* in the other case. Finally, the central pixel is assigned a

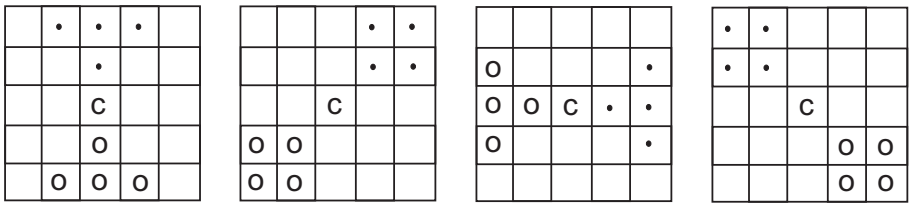

Figure 5.6: Illustration of the second detection step. The central window pixel ('c') might belong to a line if in one of the four directions, two opposite neighbours, or one of the three pixels in their prolongation, are similar to the central pixel. This is the case if in one of the four directions (corresponding to the four subfigures) one pixel indicated with '·' and one pixel indicated with 'o' are similar to the central pixel.

membership degree $\mu_{noise,1}(x, y, t) = min_{i \in dir}(D_i(x, y, t))$ in the fuzzy set "noisy" if it is not noisefree ($\mu_{noisefree}(x, y, t) = 0$, see Subsection 5.1.1) and no line is detected:

$$\mu_{noise,1}(x,y,t) = \begin{cases} 0 & \text{if } \mu_{noisefree}(x,y,t) = 1 \\ & \text{or } L(x,y,t) = true, \\ min_{i \in dir}(D_i(x,y,t)) & \text{else.} \end{cases}$$

5.1.3 Spatial Filtering

Based on $\mu_{noise,1}$ that was determined in the previous step, a first spatial filtering is performed to facilitate the remaining noise detection. For a general image (or frame) I, a general noise membership function μ and a general filtering window of size $(2 \cdot W + 1) \times (2 \cdot W + 1)$, the spatial filtering framework for the pixel at spatial location (x, y) in I is determined as a weighted sum of the neighbourhood grey values, where the weight of a grey value corresponds to the degree of belief that it is not noisy (where the noisy degree is given by a function μ and where the standard negator is used for the not-operator):

$$SF_{\mu}^{I}(x,y,W) = \frac{\sum_{k=-W}^{+W} \sum_{l=-W}^{+W} \big(1 - \mu(x+k, y+l)\big) \cdot I(x+k, y+l)}{\sum_{k=-W}^{+W} \sum_{l=-W}^{+W} \big(1 - \mu(x+k, y+l)\big)}$$

If $\sum_{k=-W}^{+W} \sum_{l=-W}^{+W} \big(1 - \mu(x+k, y+l)\big) = 0$, which is unlikely to happen in practical situations, then $SF_{\mu}^{I}(x,y,W) = \text{median}\{I(x+k, y+l) | -W \leq k, l \leq W\}$.

In our proposed filter, the current frame $I_n(t)$, the membership function $\mu_{noise,1}$ restricted to the current frame (denoted by $\mu_{noise,1}(t)$) and a window of size $(2 \cdot W_1 + 1) \times (2 \cdot W_1 + 1)$ (where the parameter W_1 is determined in subsection 5.1.10) are used. The result of the first spatial filtering is then given by

$$I_{f_1}(x,y,t) = SF_{\mu_{noise,1}(t)}^{I_n(t)}(x,y,W_1).$$

5.1.4 Third Detection

A considerable part of the noise is already removed by the previous steps, however, there is still noise left that has to be removed. Therefore, we continue the denoising based on this first estimate I_{f_1}. For the pixels that have not been considered noisefree in the first detection ($\mu_{noisefree}(x,y,t) = 0$), but that also have not been detected as noisy in the previous step ($\mu_{noise,1}(x,y,t) = 0$), we further investigate whether they might be noisy. If the difference in grey value is large positive or large negative compared to all eight neighbours, then the central pixel should be considered noisy. If there is only one neighbour for which the difference in grey value is not large positive and not large negative, then it is checked whether the opposite neighbour or one of the its neighbours or one of the pixels in their prolongation (as illustrated in Fig. 5.7) are similar to the central pixel or the neighbour for which the difference in grey value is not large positive or not large negative. If there exist such a pixel, then the central pixel might belong to a line and should not be detected as noise. The information about a possible line is stored in the variable $PL(x,y,t)$. $PL(x,y,t) =$

true indicates that a possible line is detected by the above described detection method; $PL(x, y, t) =$ *false* indicates there isn't such a line.

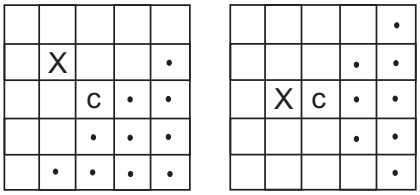

Figure 5.7: Illustration of the third detection step. If 'X' stands for the only neighbour for which the difference in grey value compared to the central pixel 'c' is not large positive and not large negative, then the central pixel is considered noisy, unless one of the opposite pixels indicated by '·' is similar to 'c' or to 'X'.

Summarized, we get the noise membership function $\mu_{noise,2}$ for this step, given by:

$$\mu_{noise,2}(x,y,t) = \begin{cases} 1 & \text{if } \mu_{noisefree}(x,y,t) = 0 \text{ and} \\ & ((NN(x,y,t) = 8 \text{ or } NP(x,y,t) = 8) \text{ or} \\ & (((NN(x,y,t) = 7 \text{ and } NP(x,y,t) = 0) \text{ or} \\ & (NP(x,y,t) = 7 \text{ and } NN(x,y,t) = 0)) \\ & \text{and } PL(x,y,t) = \textit{false}), \\ \mu_{noise,1}(x,y,t) & \text{else,} \end{cases}$$

where $NN(x, y, t)$ (respectively $NP(x, y, t)$) denotes the number of neighbours of the pixel at location (x, y, t) for which the difference in grey value compared to that pixel at location (x, y, t) is large negative (respectively large positive) to some non-zero degree.

5.1.5 First Motion Compensated Temporal Filtering

In this step, all pixels that have been detected as noise to some degree, i.e., the pixels belonging to the support of the fuzzy set "noisy" or thus for which $\mu_{noise,2}(x, y, t) > 0$, are filtered temporally based on motion compensation. This includes the pixels that have already been temporary filtered in 5.1.3. However, in that first spatial filtering, also pixels that have only just been detected as noise in the third detection could have been taken into account in the averaging, and thus a better filtering is needed. To compensate the motion between successive frames, we introduce a noise adaptive mean absolute difference (MAD) between two blocks of image pixels. In a general notation and for a general block size $(2 \cdot W + 1) \times (2 \cdot W + 1)$ it is given by:

$$MAD_{I_2}^{I_1,\mu}(x,y,r,s,W) = \frac{\sum_{k=-W}^{+W}\sum_{l=-W}^{+W}\Phi(\mu(x+k,y+l))|I_1(x+k,y+l) - I_2(x+k+r,y+l+s)|}{\sum_{k=-W}^{+W}\sum_{l=-W}^{+W}\Phi(\mu(x+k,y+l))},$$

where I_1 and I_2 are the two frames between which motion is estimated (usually the noisy current and filtered previous frame respectively), x and y indicate the spatial coordinates of the central pixel of the considered block in I_1 and r and s respectively stand for the vertical and horizontal coordinates of the displacement vector, which means that the central pixel of the block that is considered in I_2 has spatial coordinates $(x+r, y+s)$. Further, the function μ gives the degree $\mu(x,y)$ to which a pixel (x,y) is considered noisy. The function Φ makes it possible to consider only those pixels that have a membership degree equal to zero (or thus to do a reliable motion compensation by only taking into account noisefree pixels):

$$\Phi(\mu(x,y)) = \begin{cases} 1 & \text{if } \mu(x,y) = 0, \\ 0 & \text{else.} \end{cases}$$

If $\sum_{k=-W}^{+W} \sum_{l=-W}^{+W} \Phi(\mu(x+k, y+l)) = 0$ or if not for at least half of the noisefree pixels, the absolute difference $|I_1(x+k, y+l) - I_2(x+k+r, y+l+s)|$ is not large positive (i.e., $\mu_{LP}(|I_1(x+k, y+l) - I_2(x+k+r, y+l+s)|) = 0$), the noise adaptive MAD is not reliable and is assigned the value $+\infty$.

Using this above introduced MAD, the best matching $(2 \cdot W_1 + 1) \times (2 \cdot W_1 + 1)$ block in a search region of size $(2 \cdot W_2 + 1) \times (2 \cdot W_2 + 1)$ (where the parameter W_2 is determined in subsection 5.1.10) in the previous frame I_{f_3} (already processed up to step 5.1.6, since from then on a frame delay will be applied as will be seen later in 5.1.7) is determined by the following displacement vector (where in analogy to the notation $I(t)$ for the t-th frame in an image sequence I, the notation $\mu(t)$ stands for the restriction of a general function μ (e.g., noise membership function) to the pixels of the t-th frame of the sequence):

$$(u(x,y,t), v(x,y,t)) = \underset{-W_2 \leq r,s \leq W_2}{\arg\min} \; MAD_{I_{f_3}(t-1)}^{I_n(t), \mu_{noise,2}(t)}(x,y,r,s,W_1).$$

The minimum value itself is denoted by $minmad(x,y,t)$.

For noisy pixels, the output of the temporal filter is then the corresponding motion compensated pixel in the previous frame, if this motion compensated candidate pixel exists. Otherwise, the spatial filtering framework is used again:

$$I_{f_2}(x,y,t) = MCF_{I_{f_3}(t-1)}^{I_n(t), \mu_{noise,2}(t)}(x,y,u(x,y,t), v(x,y,t), minmad(x,y,t)),$$

with in a general notation

$$MCF_{I_2}^{I_1,\mu}(x,y,u,v,minmad) = \begin{cases} I_2(x+u, y+v) & \text{if } \mu(x,y) > 0 \text{ and } minmad \neq +\infty, \\ SF_{\mu}^{I_1}(x,y,W_1) & \text{if } \mu(x,y) > 0 \text{ and } minmad = +\infty, \\ I_1(x,y) & \text{else,} \end{cases}$$

where μ is again a function that determines the detected noise degree of a pixel and the variable $minmad$ determines whether the filtering of a pixel (x,y) in frame I_1 is performed temporally by the help of frame I_2 and the displacement vector (u,v) or by the spatial filtering framework.

5.1.6 Spatial Refinement of Homogeneous Areas

To cope with noisy pixels in homogeneous regions that are quite similar to their original value and that are not detected as noise, the following refinement is performed to smooth these regions. A pixel, that was not determined noisefree by the first detection method (i.e., $\mu_{noisefree}(x,y,t) = 0$), is adapted if the central pixel in an 3×3 neighbourhood is larger or smaller than all other pixel values in this neighbourhood and one of the following conditions holds (with $M(x,y,t) = \max\{I_{f_2}(x+k,y+l,t)| -1 \leq k,l \leq 1,\ (k,l) \neq (0,0)\}$ and $m(x,y,t) = \min\{I_{f_2}(x+k,y+l,t)| -1 \leq k,l \leq 1,\ (k,l) \neq (0,0)\}$):

- $\mu_S(M(x,y,t) - m(x,y,t)) > 0$ (i.e., the minimum and the maximum value in this neighbourhood are similar),
- $\mu_{LP}(I_{f_2}(x,y,t) - M(x,y,t)) > 0$ (i.e., the difference ($I_{f_2}(x,y,t) - M(x,y,t)$) is large positive),
- $\mu_{LN}(I_{f_2}(x,y,t) - m(x,y,t)) > 0$ (i.e., the difference ($I_{f_2}(x,y,t) - m(x,y,t)$) is large negative),
- $I_{f_2}(x,y,t) - M(x,y,t) > M(x,y,t) - m(x,y,t)$ (i.e., the difference ($I_{f_2}(x,y,t) - M(x,y,t)$) is relatively large),
- $m(x,y,t) - I_{f_2}(x,y,t) > M(x,y,t) - m(x,y,t)$ (i.e., the difference ($m(x,y,t) - I_{f_2}(x,y,t)$) is relatively large).

If this is the case, the pixel is filtered as $I_{f_3}(x,y,t) = (M(x,y,t) + m(x,y,t))/2$, otherwise the pixel remains unchanged, i.e., $I_{f_3}(x,y,t) = I_{f_2}(x,y,t)$.

5.1.7 Temporal Detection

Due to the aim to preserve possible lines and edges, still not all noisy pixels were detected. Until now, noise was detected based on spatial information (if we don't take into account the detection of noisefree pixels in 5.1.1). To remove the remaining noise, in this step, also the noise detection works temporally. To detect a noisy impulse pixel, we compare it to its temporal neighbours in the previous and next frame respectively. To have a good detection, it is needed that this previous and next frame are as noisefree as possible. To have a more or less noisefree next frame, we have to do the temporal detection with a one frame delay, so that the next frame is already processed up to step 5.1.6 at this point and most of the noise in that frame has already been removed. So the temporal noise detection is performed for the previous frame. The detection consists of two stages. In the first stage, each pixel (in the previous frame $I_{f_3}(t-1)$ as explained above) that is not considered noisefree by the first detection step, is compared to the corresponding pixels in the preprevious ($I_f(t-2)$,

already completely filtered) and current frame ($I_{f_3}(t)$) as follows:

$$\mu_{temp,1}(x,y,t-1) = \begin{cases} 1 & \text{if } \mu_{LP}(|I_{f_3}(x,y,t-1) - I_f(x,y,t-2)|) > 0 \\ & \text{and } \mu_{LP}(|I_{f_3}(x,y,t-1) - I_{f_3}(x,y,t)|) > 0 \\ & \text{and } \mu_{noisefree}(x,y,t-1) = 0, \\ 0 & \text{else.} \end{cases}$$

This comparison is used to determine in a second stage whether a pixel is considered noisy on a temporal basis. A pixel is called noisy when it differs from its temporal neighbours ($\mu_{temp,1}(x,y,t) = 1$) and also one of the following conditions holds:

(a) The number of pixels within a 5×5 neighbourhood (in the considered previous frame) for which $\mu_{temp,1}(x+k, y+l, t-1) = 1$ (with $-2 \leq k, l \leq 2$) is smaller than or equal to 2. This number is chosen small enough to avoid that a moving line would be detected.

(b) The number of pixels within a 7×7 neighbourhood such that $\mu_S(|I_{f_3}(x+k, y+l, t-1) - I_{f_3}(x,y,t-1)|) = 0$ is larger than or equal to $7 \times 7 - 6$ (The central pixel and possible some similar noisy neighbours (but not enough in number to form a line or object), which have not been detected by the spatial detection steps in order to preserve lines and details, differ from the neighbourhood). To summarize:

$$\mu_{noise,3}(x,y,t-1) = \begin{cases} 1 & \text{if } \mu_{temp,1}(x,y,t-1) = 1 \text{ and } \big(\text{(a) or (b)}\big) \text{ hold,} \\ 0 & \text{else.} \end{cases}$$

5.1.8 Second Motion Compensated Temporal Filtering

Based on the previous detection step, a second motion compensated filtering is performed. Again, all pixels belonging to the support of the fuzzy set "noisy", i.e., the pixels for which $\mu_{noise,3}(x,y,t-1) > 0$, are filtered (remember that we use a frame delay and that in this step, pixels from the previous frame are filtered). This might include pixels that have already been filtered temporary in one of the previous steps, but for which the filtering result was not yet sufficient e.g. due to not yet detected noisy neighbours taken into account in the filtering. The displacement vector that determines the best matching $(2 \cdot W_1 + 1) \times (2 \cdot W_1 + 1)$ block in a search region of size $(2 \cdot W_2 + 1) \times (2 \cdot W_2 + 1)$ in the filtered preprevious frame $I_f(t-2)$ to the considered block in the previous frame with central pixel given by the spatial coordinates (x, y), is given by:

$$(w(x,y,t-1), z(x,y,t-1)) = \underset{-W_2 \leq r,s \leq W_2}{\arg\min} \; MAD_{I_f(t-2)}^{I_{f_3}(t-1), \mu_{noise,3}(t-1)}(x,y,r,s,W_1).$$

The minimum value itself is denoted by $minmad_2(x,y,t-1)$. The noisy central pixel is then filtered as:

$$I_{f_4}(x,y,t-1) =$$
$$MCF_{I_f(t-2)}^{I_{f_3}(t-1),\mu_{noise,3}(t-1)}(x,y,w(x,y,t-1),z(x,y,t-1),minmad_2(x,y,t-1)).$$

5.1.9 Temporal Refinement of Non-moving Areas

In a non-moving area, pixel values in a frame correspond to the pixel values at the corresponding spatial position in a previous or next frame. This should make it possible to easily detect whether a noisy pixel remained noisy in such a non-moving area. Therefore a temporal detection as in Subsection 5.1.7 is performed:

$$\mu_{temp,2}(x,y,t-1) = \begin{cases} 1 & \text{if } \mu_{LP}(|I_{f_4}(x,y,t-1) - I_f(x,y,t-2)|) > 0 \\ & \text{and } \mu_{LP}(|I_{f_4}(x,y,t-1) - I_{f_3}(x,y,t)|) > 0 \\ & \text{and } \mu_{noisefree}(x,y,t-1) = 0, \\ 0 & \text{else.} \end{cases}$$

A $(2\cdot W_3+1)\times(2\cdot W_3+1)$ (where the parameter W_3 is determined in subsection 5.1.10) region centered around the spatial position (x,y) is determined as non-moving if

(a') $\mu_S(MAD_{I_f(t-2)}^{I_{f_4}(t-1),\mu_{temp,2}(t-1)}(x,y,0,0,W_3)) > 0$ and

(b') $\sum_{k=-W_3}^{+W_3}\sum_{l=-W_3}^{+W_3}\Phi(\mu_{temp,2}(x+k,y+l)) > 2\cdot W_3\cdot(2\cdot W_3+1)$.

A remaining noisy pixel in such a region is then filtered as the corresponding pixel in the previous frame:

$$I_f(x,y,t-1) = \begin{cases} I_f(x,y,t-2) & \text{if } \mu_{temp,2}(x,y,t-1) = 1 \text{ and (a') and (b') hold,} \\ I_{f_4}(x,y,t-1) & \text{else.} \end{cases}$$

5.1.10 Parameter Selection

To determine the parameters par_1, par_2 and p_1, and thus the membership functions introduced in Fig. 5.5, we have used a pixel neighbourhood of size 5×5 ($W_1 = 2$), a search window of 17×17 ($W_2 = 8$) pixels for the motion compensation and a window of size 7×7 ($W_3 = 3$) for the temporal refinement of non-moving areas. We have let the parameters run over a range of possible values and computed the arithmetic mean of the PSNR result of the nine sequences "Salesman", "Trevor" and "Tennis", each corrupted with respectively 5%, 15% and 25% random impulse noise. The higher the PSNR value, the better the result. The arithmetic mean over the nine test sequences reached its maximum for the parameter values $par_1 = 24$, $par_2 = 38$, $p_1 = 11$, that we will use for the remaining experiments.

For the determination of the window sizes W_1, W_2 and W_3, we performed the following experiments. First, for the selection of W_1, we have let this parameter run over the values 0 to 6 and have used the fixed values $W_2 = 8$ and $W_3 = 3$ for the other window sizes to process the "Salesman", "Trevor" and "Tennis" sequence, each corrupted with 15% random

Table 5.1: Determination of the parameter W_1. (Average PSNR (dB) values.)

	W_1						
Sequence	0	1	2	3	4	5	6
"Salesman"	30.17	34.98	**35.29**	35.10	34.84	34.73	34.57
"Trevor"	31.31	**37.86**	37.61	37.29	36.95	36.44	36.18
"Tennis"	25.62	25.14	25.84	**25.96**	25.93	25.83	25.70

impulse noise. The resulting average PSNR values are given in Table 5.1. From those results, we conclude that $W_1 = 2$ is a good choice, that we will use for the remaining experiments.

The used value for the parameter W_2 is determined analogously, by letting it run over the values 5 to 14, and processing the "Salesman", "Trevor" and "Tennis" sequence, each corrupted with 15% random impulse noise, for the fixed values $W_1 = 2$ and $W_3 = 3$. The average PSNR results can be found in Table 5.2. It can be seen that the value $W_2 = 8$ that we used up to now was a good choice, that we can continue to use for the remaining experiments.

Table 5.2: Determination of the parameter W_2. (Average PSNR (dB) values.)

	W_2									
Sequence	5	6	7	8	9	10	11	12	13	14
"Salesman"	35.26	**35.29**	**35.29**	**35.29**	35.28	35.26	35.26	35.23	35.20	35.14
"Trevor"	37.43	37.51	37.60	37.61	37.69	37.74	37.76	**37.79**	**37.79**	37.77
"Tennis"	**25.84**	25.82	25.82	**25.84**	**25.84**	25.83	25.82	25.82	25.81	25.78

Finally, also the window size W_3 is determined in an analogous way. For the fixed values $W_1 = 2$ and $W_2 = 8$, we let the parameter W_3 take on the values 1 to 9 and process the sequences "Salesman", "Trevor" and "Tennis", each corrupted with 15% random impulse noise. Table 5.3 gives the results of these experiments. For the experiments in the next subsection, we will use $W_3 = 3$.

Table 5.3: Determination of the parameter W_3. (Average PSNR (dB) values.)

	W_3								
Sequence	1	2	3	4	5	6	7	8	9
"Salesman"	35.20	35.27	**35.29**	35.28	35.25	35.24	35.20	35.19	35.17
"Trevor"	37.64	**37.67**	37.61	37.57	37.49	37.45	37.37	37.31	37.24
"Tennis"	25.77	25.80	25.84	**25.85**	**25.85**	25.84	25.84	25.83	25.83

5.2 Second Proposed Algorithm

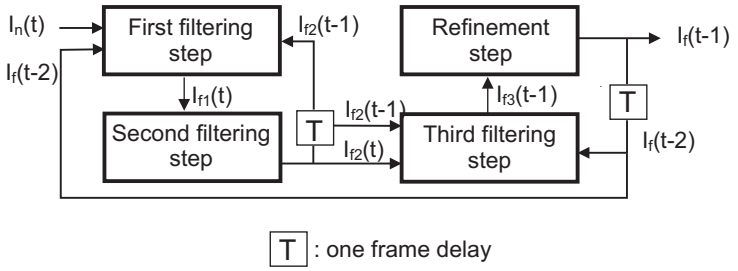

Figure 5.8: Overview of the different steps in the proposed algorithm.

To preserve as much details as possible, in the proposed method [74, 77], the noise is removed by successive filtering steps as illustrated in Fig. 5.8. It might be easier to distinguish noise from small details if a considerable part of the noise has already been removed in a previous step. The algorithm consists of three filtering steps and one refinement step. In the first step (5.2.1), both a degree to which a pixel is considered noisefree and to which it is considered noisy is calculated. If the noisy degree is larger than the noisefree degree, the pixel is filtered. A pixel is considered noisefree if its grey value corresponds to that of the corresponding pixels in the previous frames or to most of its spatial neighbours. The pixel is considered noisy if it differs from its temporal neighbour in the previous frame, and this does not hold for most of its neighbours (such that the difference is not caused by motion). The output sequence of this first step is denoted by I_{f_1}.The second step (5.2.2)(output I_{f_2}) filters pixels for which the difference in grey value to all its neighbours is large positive or large negative. If there is one neighbour for which the difference is not large positive and not large negative, it is checked whether the considered pixel and that neighbour might belong to a line. If not, the pixel will be filtered also. After this step, the remaining noise consists mostly of clustered noise pixels with a similar grey value. In the third step (5.2.3)(output I_{f_3}), these small clusters (similar spatial neighbours) are filtered based on temporal information. To be able to better detect impulses in time, a frame delay is applied such that pixels can be compared to both the corresponding pixel in the previous and next frame. The next frame will then have been processed up to the second step and most of the noise will have been removed already. Analogously to the first step, a noisefree degree and a noisy degree are calculated again in this third step. A pixel is considered noisefree if its grey value corresponds to that of its temporal neighbours or if there is a neighbour with similar grey value (that probably belongs to the same object) that corresponds to its temporal neighbours (the considered pixel might belong to the border of a slightly moving object). The pixel is considered noisy if its grey value does not correspond to that of its temporal neighbours and this does not hold for most of its neighbours (but possibly holds for a small cluster). The refinement step (5.2.4)(output I_f), finally, is intended to remove small impulses (noise

value similar to the original value) that may not have been detected up to now, but that are relatively large in a homogeneous (spatially) or non-moving (temporally) area. The result of the successive filtering steps is illustrated in Fig. 5.9 for the 20-th frame of the "Salesman" sequence.

5.2.1 First Filtering Step

Detection

In this first detection step, we determine by the help of fuzzy rules a degree to which a given pixel is considered noisefree and a degree to which that pixel is considered noisy. If the noisy degree is larger than the noisefree degree, then the pixel will be filtered, otherwise the pixel will remain unchanged.

A pixel can be considered noisefree if it is similar to the pixel at the same spatial location in the previous and preprevious frame and has also some similar neighbours. If the noisefree situation of the pixel is not confirmed in time, possibly due to motion, we will require more spatial confirmation (similar neighbours). The noisefree degree is determined as follows:

Fuzzy Rule 5.1.
IF (*the absolute differences* $|I_n(x,y,t) - I_{f_2}(x,y,t-1)|$ AND $|I_n(x,y,t) - I_f(x,y,t-2)|$ *are* NOT LARGE POSITIVE AND *there are two neighbours* $(x+k, y+l, t)$ *(*$-2 \leq k,l \leq 2$ *and* $(k,l) \neq (0,0)$*) for which* $|I_n(x,y,t) - I_n(x+k,y+l,t)|$ *is* NOT LARGE POSITIVE)
OR *there are four neighbours* $(x+k, y+l, t)$ *(*$-2 \leq k,l \leq 2$ *and* $(k,l) \neq (0,0)$*) for which* $|I_n(x,y,t) - I_n(x+k,y+l,t)|$ *is* NOT LARGE POSITIVE
THEN *the pixel at position* (x,y,t) *is considered* NOISEFREE.

The linguistic term "large positive" in this rule can be represented by a fuzzy set of which the membership function μ_{LP} is depicted in Fig. 5.10 (see Section 5.2.5 for the determination of the parameters). Further, for the conjunction (AND), disjunction (OR) and negation (NOT) in the fuzzy rules, in this chapter we will use the product, probabilistic sum and standard negator, because these yielded the best results. The difference compared to the results for another choice of operators is however neglectible. The degree to which the pixel at position (x,y,t) now belongs to the fuzzy set "noisefree" corresponds to the degree to which the antecedent in the fuzzy rule is true. This degree is calculated as follows. The degree to which there are two (respectively four) neighbours for which the absolute difference in grey value is not large positive, denoted by $max_2(x,y,t)$ (respectively $max_4(x,y,t)$), is determined as the second (respectively fourth) largest element in the set

$$\{1 - \mu_{LP}(|I_n(x,y,t) - I_n(x+k,y+l,t)|) \mid -2 \leq k,l \leq 2 \text{ and } (k,l) \neq (0,0)\}.$$

For the pixel at position (x,y,t) this results in a noisefree degree

$$\mu_{noisefree}(x,y,t) = \alpha_1(x,y,t) \cdot \alpha_2(x,y,t) \cdot max_2(x,y,t) + max_4(x,y,t) -$$

Figure 5.9: The original 20-th frame of the "Salesman" sequence (a), the frame corrupted by 25% random impulse noise (b)($PSNR = 14.27dB$) and the result after the first (c)($PSNR = 19.48dB$), second (d)($PSNR = 26.38dB$), third (e)($PSNR = 32.20dB$) and refinement step (f)($PSNR = 33.22dB$) respectively.

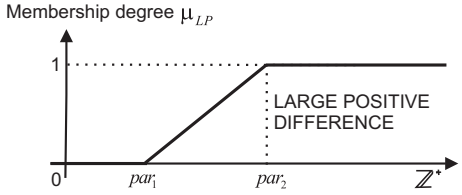

Figure 5.10: The membership function μ_{LP} of the fuzzy set "large positive difference".

$$\alpha_1(x,y,t) \cdot \alpha_2(x,y,t) \cdot max_2(x,y,t) \cdot max_4(x,y,t),$$

where

$$\begin{aligned} \alpha_1(x,y,t) &= (1-\mu_{LP}(|I_n(x,y,t) - I_{f_2}(x,y,t-1)|)), \\ \alpha_2(x,y,t) &= (1-\mu_{LP}(|I_n(x,y,t) - I_f(x,y,t-2)|)). \end{aligned}$$

A pixel is considered noisy if the difference in grey value compared to the pixel at the same spatial location in the previous frame is large positive or large negative and if this does not hold for its neighbours (the difference is thus not caused by motion). This should also be confirmed spatially by the fact that there is a direction in which the differences in grey level between the considered pixel and the two respective neighbours are both large positive or large negative and if the difference in grey value of those two neighbours is not large positive (and the pixel is thus an impulse between two pixels that are expected to belong to the same object).

Fuzzy Rule 5.2.
IF((*the difference* $I_n(x,y,t) - I_{f_2}(x,y,t-1)$ *is* LARGE POSITIVE AND NOT *for five neighbours* $(x+k,y+l,t)$ *(*$-2 \leq k,l \leq 2$ *and* $(k,l) \neq (0,0)$*) the difference* $I_n(x+k,y+l,t) - I_{f_2}(x+k,y+l,t-1)$ *is* LARGE POSITIVE)
OR (*the difference* $I_n(x,y,t) - I_{f_2}(x,y,t-1)$ *is* LARGE NEGATIVE AND NOT *for five neighbours* $(x+k,y+l,t)$ *(*$-2 \leq k,l \leq 2$ *and* $(k,l) \neq (0,0)$*) the difference* $I_n(x+k,y+l,t) - I_{f_2}(x+k,y+l,t-1)$ *is* LARGE NEGATIVE))

AND((*in one of the four directions the differences* $I_n(x,y,t) - I_n(x+k,y+l,t)$ *and* $I_n(x,y,t) - I_n(x-k,y-l,t)$ $((k,l) \in \{(-1,-1),(-1,0),(-1,1),(0,1)\})$ *are both* LARGE POSITIVE OR *both* LARGE NEGATIVE) AND *the absolute difference* $|I_n(x+k,y+l,t) - I_n(x-k,y-l,t)|$ *is* NOT LARGE \verb*POSITIVE?)?*

THEN *the pixel at position* (x,y,t) *is considered* NOISY.

Analogously to the linguistic term "large positive", also the term "large negative" can be represented by a fuzzy set with the membership function given in Fig. 5.11 (see Section 5.2.5 for the determination of the parameters). The degree to which for five neighbours the differences in grey value compared to the corresponding pixels in the previous frame are

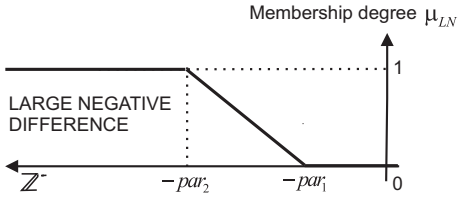

Figure 5.11: The membership function μ_{LN} of the fuzzy set "large negative difference".

large positive, denoted by $t_{pos}(x,y,t)$ is determined as the fifth largest value in the set

$$\{\mu_{LP}(I_n(x+k,y+l,t) - I_{f_2}(x+k,y+l,t-1))| - 2 \leq k,l \leq 2 \text{ and } (k,l) \neq (0,0)\}.$$

Analogously, $t_{neg}(x,y,t)$ corresponds to the fifth largest value in the set

$$\{\mu_{LN}(I_n(x+k,y+l,t) - I_{f_2}(x+k,y+l,t-1))| - 2 \leq k,l \leq 2 \text{ and } (k,l) \neq (0,0)\}.$$

The degree to which the difference between the pixel at position (x,y,t) and the corresponding pixel in the previous frame is large positive or large negative and this is not the case for five of its neigbhours is then given by

$$\begin{aligned} tempimp(x,y,t) = \\ (\gamma_1(x,y,t) \cdot (1 - t_{pos}(x,y,t))) + (\gamma_2(x,y,t) \cdot (1 - t_{neg}(x,y,t))) - \\ (\gamma_1(x,y,t) \cdot (1 - t_{pos}(x,y,t))) \cdot (\gamma_2(x,y,t) \cdot (1 - t_{neg}(x,y,t))), \end{aligned}$$

where

$$\begin{aligned} \gamma_1(x,y,t) &= \mu_{LP}(I_n(x,y,t) - I_{f_2}(x,y,t-1)), \\ \gamma_2(x,y,t) &= \mu_{LN}(I_n(x,y,t) - I_{f_2}(x,y,t-1)). \end{aligned}$$

The degree to which there is a direction in which the pixel at position (x,y,t) is an impulse, denoted by $spatimp(x,y,t)$, is determined as the maximum value in the set

$$\begin{aligned} \{(\epsilon^1_{(k,l)}(x,y,t) + \epsilon^2_{(k,l)}(x,y,t) - \epsilon^1_{(k,l)}(x,y,t) \cdot \epsilon^2_{(k,l)}(x,y,t)) \cdot \epsilon^3_{(k,l)}(x,y,t) \\ |(k,l) \in \{(-1,-1),(-1,0),(-1,1),(0,1)\}\}, \end{aligned}$$

where

$$\begin{aligned} \epsilon^1_{(k,l)}(x,y,t) &= \mu_{LP}(I_n(x,y,t) - I_n(x+k,y+l,t)) \cdot \\ &\qquad \mu_{LP}(I_n(x,y,t) - I_n(x-k,y-l,t)), \\ \epsilon^2_{(k,l)}(x,y,t) &= \mu_{LN}(I_n(x,y,t) - I_n(x+k,y+l,t)) \cdot \\ &\qquad \mu_{LN}(I_n(x,y,t) - I_n(x-k,y-l,t)), \\ \epsilon^3_{(k,l)}(x,y,t) &= 1 - \mu_L(|I_n(x+k,y+l,t) - I_n(x-k,y-l,t)|). \end{aligned}$$

Combining the above, we get

$$\mu_{noisy}(x,y,t) = tempimp(x,y,t) \cdot spatimp(x,y,t).$$

Filtering

All pixels (x,y,t) for which $\mu_{noisy}(x,y,t) > \mu_{noisefree}(x,y,t)$ are filtered (denoted by $\mu_{unch}(x,y,t) = 0$), the other pixels remain unchanged (denoted by $\mu_{unch}(x,y,t) = 1$):

$$\mu_{unch}(x,y,t) = \begin{cases} 0 & \mu_{noisy}(x,y,t) > \mu_{noisefree}(x,y,t), \\ 1 & \text{else.} \end{cases}$$

The filtering is performed in a motion compensated way. To calculate the correspondence between two blocks of image pixels of size $(2 \cdot W + 1) \times (2 \cdot W + 1)$ (where W is a general parameter), the following noise adaptive mean absolute difference (MAD) is introduced:

$$MAD_{I'}^{I,\mu}(x,y,r,s,W) = \frac{\sum_{k=-W}^{+W} \sum_{l=-W}^{+W} \mu(x+k,y+l)|I(x+k,y+l) - I'(x+k+r,y+l+s)|}{\sum_{k=-W}^{+W} \sum_{l=-W}^{+W} \mu(x+k,y+l)},$$

where I and I' are the two frames between which motion is estimated, x and y indicate the spatial coordinates of the central pixel of the considered block in I and r and s respectively stand for the vertical and horizontal coordinates of the displacement vector, i.e., the block that is considered in I' has $(x + r, y + s)$ as central pixel. μ is a binary function that indicates whether a pixel at spatial location (x,y) is reliable, i.e., to be used ($\mu(x,y) = 1$) or not ($\mu(x,y) = 0$). Using only reliable (noisefree) pixels will result in a better motion compensation. If $\sum_{k=-W}^{+W} \sum_{l=-W}^{+W} \mu(x+k,y+l) = 0$ or if not for at least half of the noisefree pixels, the absolute difference $|I(x+k,y+l) - I'(x+k+r,y+l+s)|$ is not large positive (i.e., $\mu_{LP}(|I(x+k,y+l) - I'(x+k+r,y+l+s)|) = 0$), the noise adaptive MAD is not reliable and is assigned the value $+\infty$.

For the filtering of a pixel (x,y,t) in this first step of our algorithm, we determine the displacement vector $(u(x,y,t), v(x,y,t))$ for the best matching $(2 \cdot W_1 + 1) \times (2 \cdot W_1 + 1)$ block in a search region of size $(2 \cdot W_2 + 1) \times (2 \cdot W_2 + 1)$ in the previous frame I_{f_2} (see Section 5.2.5 for the determination of the parameters W_1 and W_2) and by using the restriction of μ_{unch} to the current frame (denoted by $\mu_{unch}(t)$) as:

$$(u(x,y,t), v(x,y,t)) = \underset{-W_2 \leq r,s \leq W_2}{\arg\min} MAD_{I_{f_2}(t-1)}^{I_n(t),\mu_{unch}(t)}(x,y,r,s,W_1).$$

The previous frame has been processed up to step 5.2.2 at this moment. As will be seen later, a frame delay will be applied as from step 5.2.3. The minimum value itself is denoted by $minmad(x,y,t)$. The parameters W_1 and W_2 are determined in section 5.2.5.

A pixel (x,y,t) for which $\mu_{unch}(x,y,t) = 0$, is then filtered as the corresponding motion compensated pixel in the previous frame, if it exists ($minmad(x,y,t) \neq +\infty$).

Otherwise (if $minmad(x,y,t) = +\infty$), a spatial filtering is performed. If $\mu_{unch}(x,y,t) = 1$, the pixel remains unchanged in this step. Summarized, the output of this first step for a pixel (x,y,t) is given by:

$$I_{f_1}(x,y,t) \quad = \quad MCF^{I_n(t),\mu_{unch}(t)}_{I_{f_2}(t-1)}(x,y,u(x,y,t),v(x,y,t)),minmad(x,y,t)),$$

with (for general frames I and I', general binary function μ, displacement vector (u,v) and variable $minmad$)

$$MCF^{I,\mu}_{I'}(x,y,u,v,minmad) = \begin{cases} I'(x+u,y+v) & \text{if } \mu(x,y) = 0 \text{ and } minmad \neq +\infty \\ SF^I_\mu(x,y,W_1) & \text{if } \mu(x,y) = 0 \text{ and } minmad = +\infty \\ I(x,y) & \text{else} \end{cases},$$

where the spatial filtering framework is given by

$$SF^I_\mu(x,y,W) = \frac{\sum_{k=-W}^{+W}\sum_{l=-W}^{+W}\mu(x+k,y+l)\cdot I(x+k,y+l)}{\sum_{k=-W}^{+W}\sum_{l=-W}^{+W}\mu(x+k,y+l)}.$$

If $\sum_{k=-W}^{+W}\sum_{l=-W}^{+W}\mu(x+k,y+l) = 0$, which is unlikely to happen in practical situations, $SF^I_\mu(x,y,W) = \text{median}\{I(x+k,y+l)| -W \leq k,l \leq W\}$.

5.2.2 Second Filtering Step

In our aim to preserve the details as much as possible, the noise is removed in successive steps. In this step the noise is detected based on the output of the previous step (I_{f_1}).

If for all 8 neighbours $(x+k,y+l,t)$ ($-1 \leq k,l \leq 1$ and $(k,l) \neq (0,0)$) the difference $I_{f_1}(x,y,t) - I_{f_1}(x+k,y+l,t)$ is large positive to some degree (i.e., $\mu_{LP}(I_{f_1}(x,y,t) - I_{f_1}(x+k,y+l,t)) > 0$) or for all 8 neighbours this difference is large negative to some degree, then the pixel (x,y,t) is considered noisy and should be filtered ($\mu'_{unch}(x,y,t) = 0$).

If $\mu_{LP}(I_{f_1}(x,y,t) - I_{f_1}(x+k,y+l,t)) > 0$ for 7 neighbours or $\mu_{LN}(I_{f_1}(x,y,t) - I_{f_1}(x+k,y+l,t)) > 0$ for 7 neighbours and if for the remaining eighth neighbour both $\mu_{LP}(I_{f_1}(x,y,t) - I_{f_1}(x+k,y+l,t)) = 0$ and $\mu_{LN}(I_{f_1}(x,y,t) - I_{f_1}(x+k,y+l,t)) = 0$, then this neighbour and the central pixel (x,y,t) might belong to a corrupted line. It is then checked whether for the opposite neighbour or one of the neighbouring neighbours or one of the pixels in their prolongation (as illustrated in Fig. 5.12) the difference in grey level compared to the central pixel or the neighbour for which the difference in grey value was not large positive and not large negative, is also not large positive and not large negative (i.e., has degree zero). If this is the case, then we have detected a possible line which is stored as $PL(x,y,t) =$ *true* and the pixel will not be filtered ($\mu'_{unch}(x,y,t) = 1$). Otherwise no line is detected ($PL(x,y,t) =$ *false*) and $\mu'_{unch}(x,y,t) = 0$. In all other cases, the pixels are not detected as noise ($\mu'_{unch}(x,y,t) = 1$).

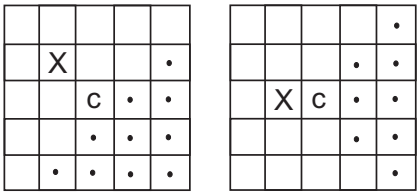

Figure 5.12: Illustration of the third detection step. If 'X' stands for the only neighbour for which the difference in grey value compared to the central pixel 'c' is not large positive and not large negative, then the central pixel is considered noisy, unless if for one of the opposite pixels indicated by '·' the difference in grey level compared to 'c' or to 'X' is not large positive and not large negative.

Analogously to the first step, the pixels for which $\mu'_{unch}(x,y,t) = 0$ are again filtered in a motion compensated way:

$$(u'(x,y,t), v'(x,y,t)) = \underset{-W_2 \leq r,s \leq W_2}{\arg\min} MAD_{I_{f_2}(t-1)}^{I_{f_1}(t),\mu'_{unch}(t)}(x,y,r,s,W_1),$$

with the minimum value itself denoted by $minmad'(x,y,t)$. The output of this step for the pixel at position (x,y,t) then becomes

$$I_{f_2}(x,y,t) \quad = \quad MCF_{I_{f_2}(t-1)}^{I_{f_1}(t),\mu'_{unch}(t)}(x,y,u'(x,y,t),v'(x,y,t),minmad'(x,y,t)).$$

5.2.3 Third Filtering Step

Up to now, most of the noise has been filtered. However, due to our aim to preserve details as much as possible, little clusters of similar noisy pixels are still present, which we will try to detect in this third detection step. Since the remaining noisy pixels are clustered, we will detect the impulses based on temporal information. To be able to detect such temporal impulses, we will compare a pixel to the corresponding pixels in the previous and the next frame. The detection will only work well if the next frame is also more or less noisefree. To achieve this, a frame delay is applied from this step on, such that the next frame is already processed up to step 5.2.2 and most of the noise has been removed.

For each pixel $(x,y,t-1)$ a noisefree degree and a noisy degree is calculated again analogously to the first step (5.2.1). If the noisy degree is larger than the noisefree degree, the pixel needs to be filtered.

We consider a pixel $(x,y,t-1)$ to be noisefree if its grey value is not very different from that of both its two temporal neighbours $(x,y,t-2)$ and (x,y,t) and if the pixel has a similar neighbour (not a large difference in grey value) for which the same holds.

Fuzzy Rule 5.3.
IF((*the absolute difference* $|I_{f_2}(x,y,t-1) - I_f(x,y,t-2)|$ *is* NOT LARGE POSITIVE)
OR (*the absolute difference* $|I_{f_2}(x,y,t-1) - I_{f_2}(x,y,t)|$ *is* NOT LARGE POSITIVE))

AND (*there is a neighbour* $(x+k, y+l, t)$ *(*$-1 \leq k, l \leq 1$ *and* $(k,l) \neq (0,0)$*) for which the absolute difference* $|I_{f_2}(x,y,t-1) - I_{f_2}(x+k, y+l, t-1)|$ *is* NOT LARGE POSITIVE AND *for which* (*the absolute difference* $|I_{f_2}(x+k, y+l, t-1) - I_f(x+k, y+l, t-2)|$ *is* NOT LARGE POSITIVE) OR (*the absolute difference* $|I_{f_2}(x+k, y+l, t-1) - I_{f_2}(x+k, y+l, t)|$ *is* NOT LARGE POSITIVE))

THEN *the pixel at position* $(x, y, t-1)$ *is considered* NOISEFREE.

The degree to which such a neighbour can be found, denoted by $neighbour(x, y, t-1)$, is determined as the maximum value in the set

$$\{\theta_{(k,l)}(x, y, t-1) \cdot \psi_{(k,l)}(x, y, t-1)| - 1 \leq k, l \leq 1 \text{ and } (k,l) \neq (0,0)\},$$

where

$$\begin{aligned}
\theta_{(k,l)}(x, y, t-1) &= 1 - \mu_{LP}(|I_{f_2}(x, y, t-1) - I_{f_2}(x+k, y+l, t-1)|), \\
\psi^1_{(k,l)}(x, y, t-1) &= (1 - \mu_{LP}(|I_{f_2}(x+k, y+l, t-1) - I_f(x+k, y+l, t-2)|)), \\
\psi^2_{(k,l)}(x, y, t-1) &= (1 - \mu_{LP}(|I_{f_2}(x+k, y+l, t-1) - I_{f_2}(x+k, y+l, t)|)), \\
\psi_{(k,l)}(x, y, t-1) &= \psi^1_{(k,l)}(x, y, t-1) + \psi^2_{(k,l)}(x, y, t-1) - \\
&\qquad \psi^1_{(k,l)}(x, y, t-1) \cdot \psi^2_{(k,l)}(x, y, t-1).
\end{aligned}$$

The noisefree degree for the pixel $(x, y, t-1)$ is then given by

$$\mu''_{noisefree}(x, y, t-1) = \psi_{(0,0)}(x, y, t-1) \cdot neighbour(x, y, t-1).$$

On the other hand, a pixel is considered to be noisy if it differs in grey value from both its temporal neighbours and if there are not 7 neighbours in a 7×7 neighbourhood that have a similar neighbour (and are thus more reliable) and that differ in grey value from both their temporal neighbours. If 7 such neighbours can be found, the pixel is expected to belong to a moving object. The number has been chosen small enough not to detect lines and large enough to detect the small noise clusters.

Fuzzy Rule 5.4.
IF((*the absolute difference* $|I_{f_2}(x,y,t-1) - I_f(x,y,t-2)|$ *is* LARGE POSITIVE) AND (*the absolute difference* $|I_{f_2}(x,y,t-1) - I_{f_2}(x,y,t)|$ *is* LARGE POSITIVE))

AND(*there are* NOT *seven neighbourhood pixels* $(x+k, y+l, t)$ *(*$-3 \leq k, l \leq 3$ *and* $(k,l) \neq (0,0)$*) that* (*have a neighbour* $(x+k+i, y+l+j, t)$ *(*$-1 \leq i, j \leq 1$ *and* $(i,j) \neq (0,0)$*) for which the absolute difference* $|I_{f_2}(x+k, y+l, t-1) - I_{f_2}(x+k+i, y+l+j, t-1)|$ *is* NOT LARGE POSITIVE) AND *for which* (*the absolute difference* $|I_{f_2}(x+k, y+l, t-1) - I_f(x+k, y+l, t-2)|$ *is* LARGE POSITIVE) AND(*the absolute difference* $|I_{f_2}(x+k, y+l, t-1) - I_{f_2}(x+k, y+l, t)|$ *is* LARGE POSITIVE))

THEN *the pixel at position* $(x, y, t-1)$ *is considered* NOISY.

The degree to which there exist 7 such neighbours is denoted by $max_7(x, y, t-1)$ and is determined as the seventh largest value in the set

$$\{(1 - \psi_{k,l}(x, y, t-1)) \cdot \phi_{(k,l)}(x, y, t-1)| - 3 \leq k, l \leq 3 \text{ and } (k,l) \neq (0,0)\},$$

where

$$\phi_{(k,l)}(x,y,t-1) = \max\{1-\mu_{LP}(|I_{f_2}(x+k,y+l,t-1)-I_{f_2}(x+k+i,y+l+j,t-1)| \\ |-1\le i,j\le 1 \text{ and } (i,j)\neq(0,0)\}.$$

The noisy degree for the pixel $(x,y,t-1)$ is then given by

$$\mu''_{noisy}(x,y,t-1) = (1-\psi_{(0,0)}(x,y,t-1))\cdot(1-max_7(x,y,t-1)).$$

Analogously to the first step, pixels for which $\mu''_{noisy}(x,y,t-1) > \mu''_{noisefree}(x,y,t-1)$ will be filtered. The others remain unchanged:

$$\mu''_{unch}(x,y,t-1) = \begin{cases} 0 & \mu''_{noisy}(x,y,t-1) > \mu''_{noisefree}(x,y,t-1) \\ 1 & \text{else} \end{cases}.$$

The pixels for which $\mu''_{unch}(x,y,t-1)=0$ are again filtered in a motion compensated way:

$$(u''(x,y,t-1),v''(x,y,t-1)) = \underset{-W_2\le r,s\le W_2}{\arg\min} MAD^{I_{f_2}(t-1),\mu''_{unch}(t)}_{I_f(t-2)}(x,y,r,s,W_1),$$

with the minimum value itself denoted by $minmad''(x,y,t-1)$. The output of this step for the pixel $(x,y,t-1)$ then becomes

$$I_{f_3}(x,y,t-1) = \\ MCF^{I_{f_2}(t-1),\mu''_{unch}(t-1)}_{I_f(t-2)}(x,y,u''(x,y,t-1),v''(x,y,t-1),minmad''(x,y,t-1)).$$

5.2.4 Refinement Steps

In these final refinement steps, the result from the previous step is further refined both temporally and spatially. Some very small impulses might not have been detected by the algorithm. However, such impulses might be relatively large in non-moving and homogeneous areas.

Since the pixels in non-moving areas will correspond to the pixels in a previous or next frame, remaining isolated noisy pixels can be detected more easily. We perform the following temporal detection:

$$\mu_{nonmov}(x,y,t-1) = \begin{cases} 0 & \text{if } \mu_{LP}(|I_{f_3}(x,y,t-1)-I_f(x,y,t-2)|)>0 \\ & \text{and } \mu_{LP}(|I_{f_3}(x,y,t-1)-I_{f_2}(x,y,t)|)>0, \\ 1 & \text{else.} \end{cases}$$

A 5×5 area centered around the spatial position (x,y) is determined as non-moving between frame $t-2$ and $t-1$ if

(NM) $\sum_{k=-2}^{2}\sum_{l=-2}^{2}\mu_{nonmov}(x+k,y+l,t-1) > 20$.

A detected noisy pixel in a non-moving area is then filtered as follows:

$$I_{f_4}(x,y,t-1) = \begin{cases} I_f(x,y,t-2) & \text{if } \mu_{nonmov}(x,y,t-1) = 0 \text{ and (NM) holds} \\ & \text{and } \mu_{LP}(|I_f(x,y,t-2) - I_{f_2}(x,y,t)|) = 0, \\ I_{f_3}(x,y,t-1) & \text{else.} \end{cases}$$

Additionally, also a spatial refinement is performed. A pixel $(x,y,t-1)$ will be filtered if it is larger or smaller than all its neighbours and one of the following conditions is fulfilled (where $M(x,y,t-1)$ and $m(x,y,t-1)$ respectively denote the maximum and minimum grey value of its neighbours (3×3 neighbourhood)):

- $\mu_{LP}(I_{f_4}(x,y,t-1) - M(x,y,t-1)) > 0$,
- $\mu_{LN}(I_{f_4}(x,y,t-1) - m(x,y,t-1)) > 0$,
- $I_{f_4}(x,y,t-1) - M(x,y,t-1) > M(x,y,t-1) - m(x,y,t-1)$,
- $m(x,y,t-1) - I_{f_4}(x,y,t-1) > M(x,y,t-1) - m(x,y,t-1)$.

If one of the conditions is fulfilled, the final filtering result for the pixel $(x,y,t-1)$ becomes $I_f(x,y,t-1) = (M(x,y,t-1)+m(x,y,t-1))/2$. Otherwise the pixel remains unchanged: $I_f(x,y,t-1) = I_{f_4}(x,y,t-1)$.

5.2.5 Parameter Selection

The parameters par_1 and par_2 that determine the membership functions μ_{LP} and μ_{LN} (Fig. 5.10 and 5.11) are selected as follows. We have fixed the size of the pixel neighbourhood and the search window in the motion compensated filtering as 5×5 ($W_1 = 2$) and 11×11 ($W_2 = 5$) respectively and have let the parameters par_1 and par_2 run over a range of possible values. For each pair of values for par_1 and par_2 the arithmetic mean of the PSNR result of the nine sequences "Salesman", "Trevor" and "Tennis", each corrupted with respectively 5%, 15% and 25% random impulse noise was computed. The parameter values were then selected as those for which this arithmetic mean over the nine test sequences reached its maximum: $par_1 = 11$, $par_2 = 43$. These values will be used in the remaining experiments.

Next, the window size W_1 was selected by fixing $W_2 = 5$ again and by letting W_1 run from 0 to 5. The arithmetic mean of the PSNR values over the nine test sequences, as discussed above, are given in Table 5.4. It can be concluded that $W_1 = 2$ is the best choice.

Table 5.4: Determination of the parameter W_1. (Arithmetic mean of the average PSNR (dB) values.)

	W_1					
	0	1	2	3	4	5
PSNR	25.01	33.57	33.69	33.57	33.43	33.27

So we will use that value from now on.

Finally, the value for W_2 is selected in an analogous way. We have let it run over the values 4 to 15 for the processing of the nine test sequences. The arithmetic mean of the PSNR values over the nine test sequences can be found in Table 5.5. It can be seen that from the value $W_2 = 8$ on the PSNR value hardly increases anymore. Therefore we will use the value $W_2 = 8$ in the remaining experiments.

Table 5.5: Determination of the parameter W_2. (Arithmetic mean of the average PSNR (dB) values.)

	W_2											
	4	5	6	7	8	9	10	11	12	13	14	15
PSNR	33.63	33.69	33.72	33.77	33.80	33.80	33.80	33.81	33.83	33.84	33.85	33.84

5.3 Experimental Results

The remainder of the section is structured as follows: in Subsection 5.3.1 the proposed method is compared to other state-of-the-art filters and additionally Subsection 5.3.2 discusses some complexity notes.

5.3.1 Comparison to Other State-of-the-Art Filters

In this subsection, the performance of the proposed method is compared to the following 3D filters: the 3D rational filter (RAT) [22], the adaptive 3D median filter (A3DM) and the weighted 3D median filter (W3DM) [55], the adaptive 3D LUM smoother (LUM) [66] and the peak-and-valley filter (PAV) [139]. Further, the proposed method is also compared to the 2D fuzzy random impulse noise reduction method (FRINRM) [122], as a representative of the 2D filters, to show that the proposed filter takes real advantage from the temporal information. In [122], it is shown that the FRINRM filter outperforms all other compared state-of-the-art 2D methods and is thus a good representative of the 2D impulse noise filters.

All methods have been processed on the “Salesman”, “Trevor”, “Tennis”, “Deadline”, “Miss America” and “Foreman” sequences, for random impulse noise levels ranging from 5% to 30%. The results of these experiments (in terms of PSNR) can be found in the graphs in Fig. 5.13. From these graphs, we see that the proposed method outperforms all other methods in terms of PSNR.

For a visual evaluation of the compared methods, the results of the different methods performed on the “Tennis”, “Deadline” and “Salesman” sequences, respectively corrupted with 5%, 15% and 25% random impulse noise, are made available on `http://www.fuzzy.ugent.be/tmelange/results/greyimpulse`. Further, Fig. 5.14 and 5.15 and Fig. 5.16 and 5.17 show the original frame, the noisy frame and the filtering result for all of the compared methods for respectively the 110-th frame of the “Tennis”

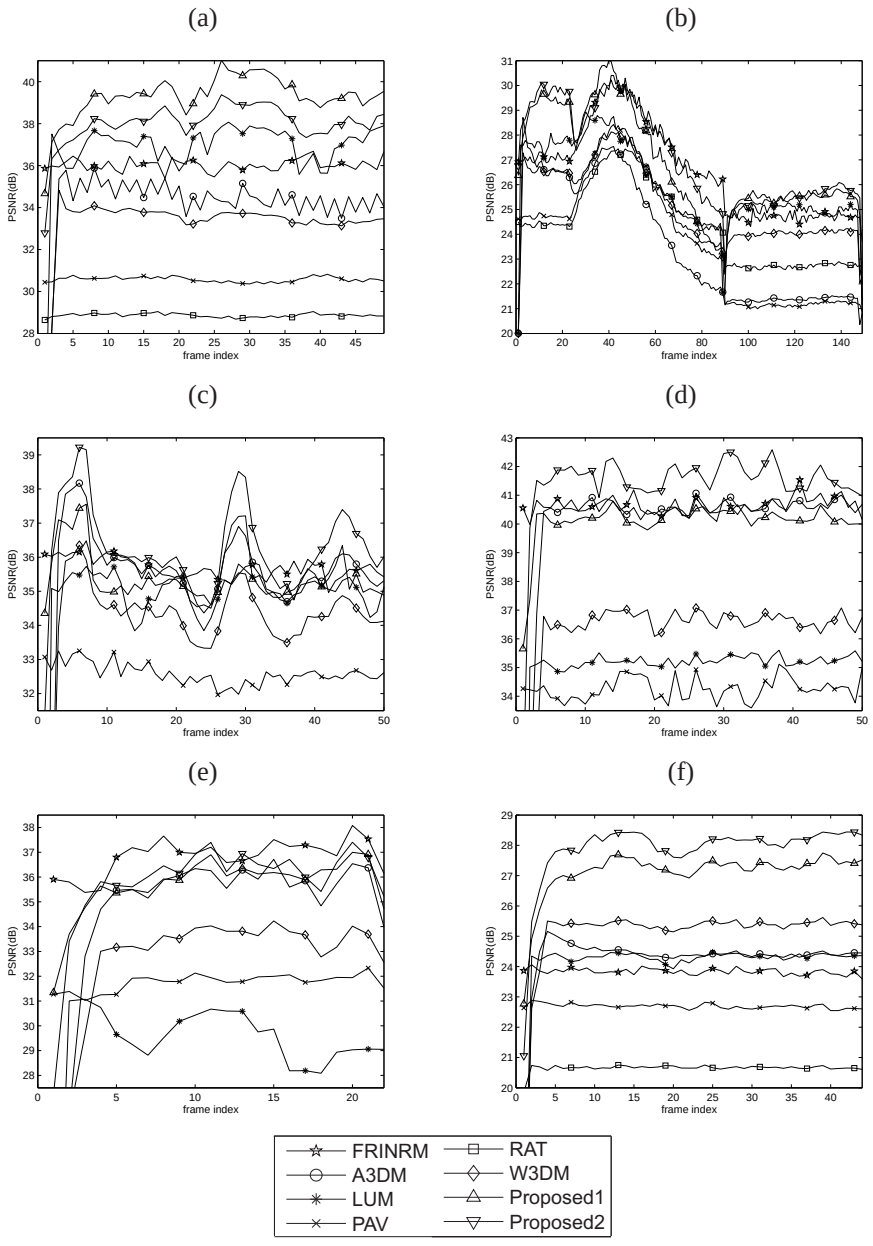

Figure 5.13: PSNR results for the different methods applied on the sequences (a) “Salesman” (5% noise), (b) “Tennis” (10% noise), (c) “Foreman” (15% noise), (d) “Miss America” (20% noise), (e) “Trevor” (25% noise) and (f) “Deadline” (30% noise)

sequence and the 20-th frame of the "Deadline" sequence. It can be seen that the rational filter results in a moderate detail preservation and also leaves a lot of noise. The peak-and-valley filter succeeds in removing the noise better, but for higher noise levels, little groups of impulse pixels remain present. Further, also some detail loss arises due to the filtering of too many noisefree pixels. This is also the case for both the adaptive and the weighted 3D median filter and can e.g. be seen at the side lines and the net in the "Tennis" sequence in Fig. 5.14. On the other hand, both filters have an acceptable denoising capacity. The LUM-smoother seems to preserve details quite well, but has problems with moving objects and fails to remove the noise adequately at higher noise levels. For the 2D FRINRM method, we see the expected drawbacks of only using spatial information. The filter has very good PSNR results frame per frame, but when watching the sequences, a lot of temporal inconsistencies can be noticed. Further, the filter also performs less for sequences with a detailed background (e.g., "Deadline", "Salesman"), where additional (temporal) information could improve the detail preservation and noise detection and again also avoid temporal artefacts. The two proposed filters, finally, combine the best detail preservation to the best noise removal and have a similar performance. Around the edges, however, we see a slightly better denoising and detail restoration by the second proposed method.

5.3.2 Some Notes on the Complexity

In the previous subsection, it was shown that the proposed methods yield the best filtering results. It should however be mentioned that in the development of the proposed methods, we have focused on the performance and not on the complexity, which was more the case in the compared methods. Because we did not focus on the complexity, only a few comments are given. It should be remarked that the largest computational cost of the methods comes from the motion compensated filtering. Also, the higher the noise level, the more pixels that need to be filtered and thus the higher the running time. As an illustration, Table 5.6 gives the running time for the processing of the "Salesman" sequence corrupted by different noise levels by the second proposed algorithm. The algorithm was implemented in matlab in combination with the mex-function and executed on an Intel(R) Xeon(R) CPU X3220 @ 2.40GHz. A faster motion compensation could be accomplished by using fast motion

Table 5.6: Average running time (seconds per frame) for the processing of the "Salesman" sequence.

	% random impulse noise							
	0	5	10	15	20	25	30	35
Running time	0.4792	0.9708	1.4306	1.8692	2.2832	2.6870	3.0697	3.4338

estimation techniques such as those presented in [111, 143, 144]. Remark further also that in each of the filtering steps, the detection (respectively filtering) of a pixel does not depend on the detection (respectively filtering) of the other pixels in the frame and could be performed in parallel.

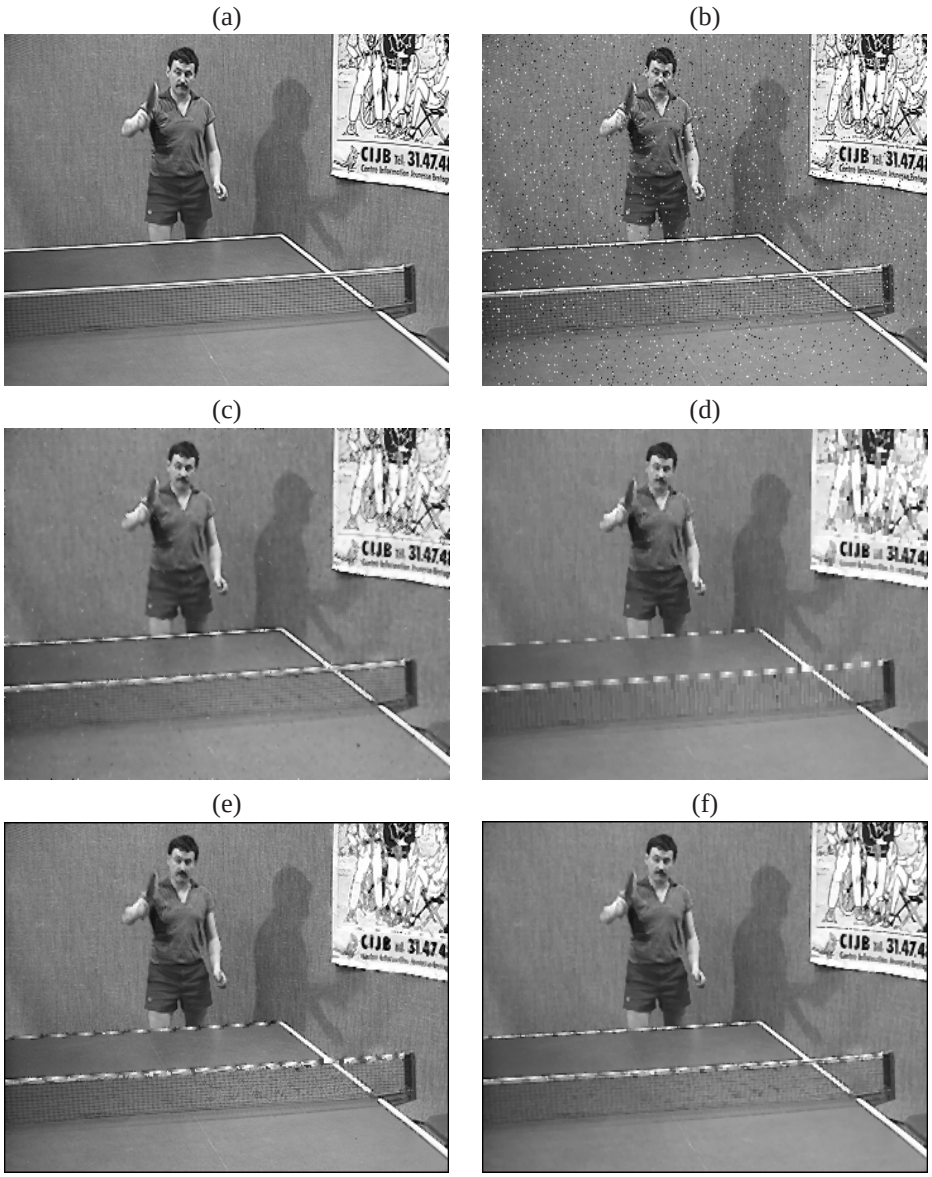

Figure 5.14: 110-th frame of the "Tennis" sequence: (a) original, (b) noisy (5%), (c) RAT, (d) PAV, (e) A3DM and (f) W3DM.

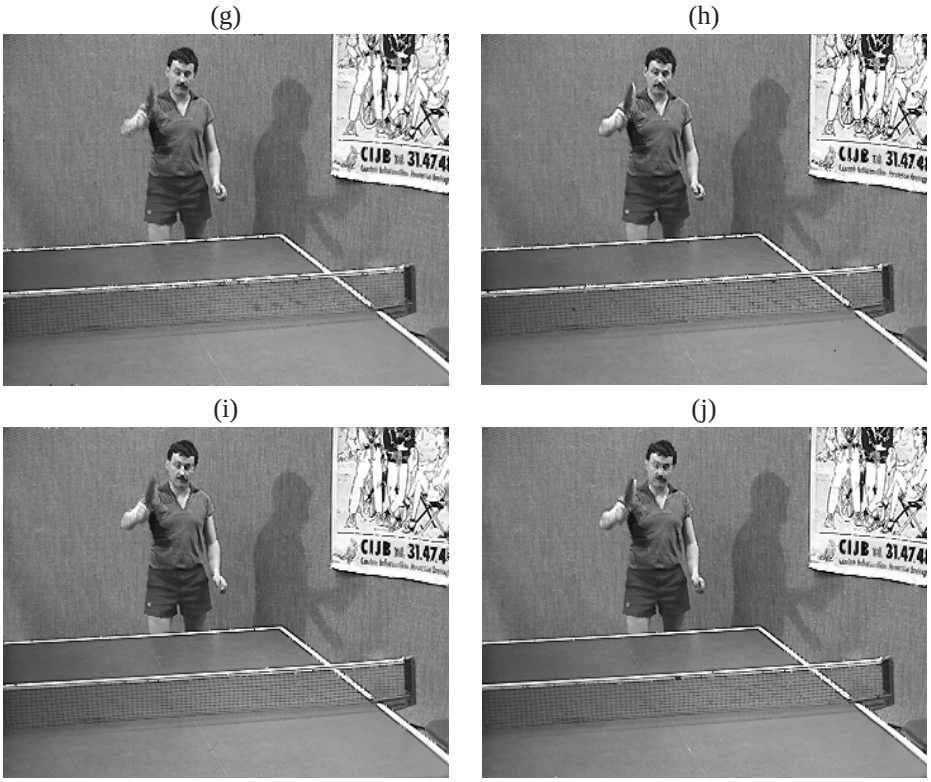

Figure 5.15: 110-th frame of the "Tennis" sequence: (g) LUM, (h) FRINRM, (i) the first proposed algorithm and (j) the second proposed algorithm.

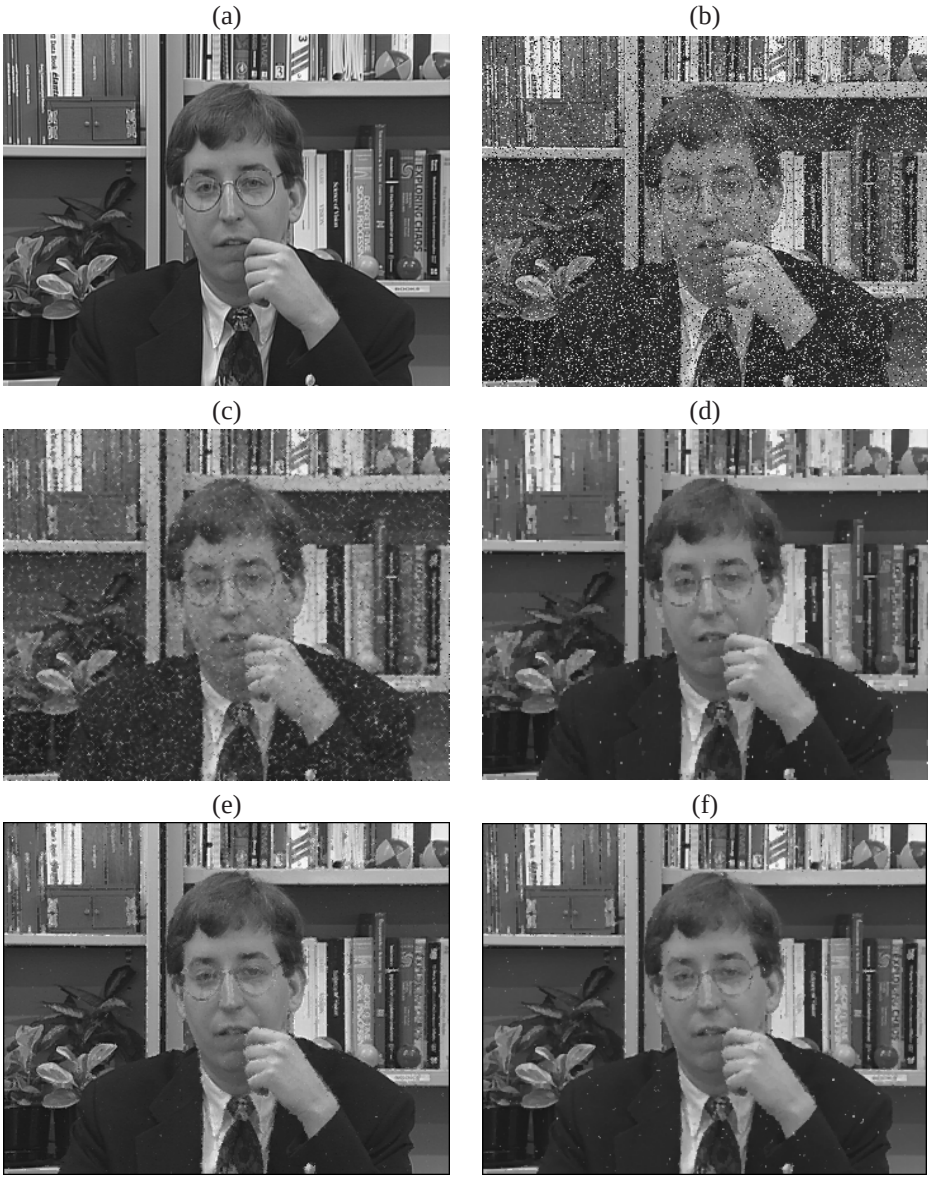

Figure 5.16: 20-th frame of the "Deadline" sequence: (a) original, (b) noisy (5%), (c) RAT, (d) PAV, (e) A3DM and (f) W3DM.

Figure 5.17: 20-th frame of the “Deadline” sequence: (g) LUM, (h) FRINRM, (i) the first proposed algorithm and (j) the second proposed algorithm.

5.4 Conclusion

In this chapter we have presented two new video filters for the removal of random valued impulse noise in digital greyscale image sequences. Both filters remove the noise step by step in order to preserve the details as much as possible.

The noise detection steps of the first proposed method have been developed in a fuzzy logic framework by assigning to each pixel a degree to which it is noisy, but it should be mentioned that e.g. by working with the support of a fuzzy set, many of the decisions in the framework are merely binary. The power of fuzzy set theory is however more exploited in the second proposed method. In the different filtering steps of the second proposed method, fuzzy rules containing linguistic values were used to determine the degree to which a pixel is considered noisy or noisefree. If the noisy degree is larger than the noisefree degree, the pixel will be filtered.

The filtering of the detected pixels in both methods is performed in a motion compensated way in order to exploit the temporal information as much as possible. The pixels that are considered noisefree remain unchanged.

From the experimental results it could be concluded that the proposed methods outperform other state-of-the-art methods both in terms of PSNR and visually. A good trade-off between noise removal and detail preservation was found.

6
Random Impulse Noise in Colour Image Sequences

Analogously as in the greyscale case, only few colour video filters for the impulse noise case can be found (e.g. [63, 112]). However, several impulse noise filters for both greyscale and colour still images exist. The median based rank-order filters are the most widely spread among them (e.g., [14, 19, 20, 45, 47, 55, 58, 64, 65, 67, 68, 69]), but also some fuzzy techniques can be found [42, 59, 90, 115, 116, 121, 122, 123, 136, 140]. As mentioned before, using a 2D filter on each of the frames of a video successively would however result in temporal inconsistencies due to the neglection of the temporal correlation between successive frames. A better alternative would be to use extended 3D filtering windows, in which also pixels from neighbouring frames are taken into account [22, 38, 55, 63, 66, 112, 139]. Further, using a greyscale filter on each of the colour bands of a colour image or video frame separately, will analogously introduce several colour artefacts, especially in textured areas, due to the neglection of the correlation between the different colour bands. To incorporate this correlation, vector-based methods were introduced. Most of these methods are based on ordering the vectors in a predefined filtering window. The output for a given colour pixel is then the pixel in the window around the given pixel, that has the smallest accumulated distance (Euclidean distance, angular distance,...) to all other vectors in the window [14, 19, 47, 63, 64, 65, 67, 68, 69, 112], or which is the most similar to all window pixels [90]. To avoid blurring due to the filtering of noisefree pixels, this filtering framework has been further refined by weighted filtering techniques [55, 58, 65] and switching schemes where the filter is only used for detected noisy pixels [63, 64, 68, 69, 90, 112]. The drawback of vector-based methods, however, is that their performance is highly reduced for higher noise levels. Consider for example a neighbourhood in which all pixels have one noisy component, and the other components are noisefree. So, although a lot of

the components are still noisefree, no noisefree vector will be found for the output of the vector-based methods. It would be better to filter the colour bands separately, but by using information from the other colour bands. However, not much alternatives for the vector-based approach can be found in literature. Some examples developed for still images are e.g. [121, 122, 123].

In this chapter, we present a filter [73, 78] for the removal of random impulse noise in colour image sequences, in which each of the colour components is filtered separately based on fuzzy rules in which information from the other colour bands is integrated. The filtering is divided into three successive filtering steps. To preserve the details as much as possible, the noise is removed step by step. Only pixels that have been detected to be noisy in the current step are filtered. This filtering is done by blockmatching, a technique used for video compression that has already been adopted in video filters for the removal of Gaussian noise (e.g. [41, 51, 141]), but that has not really found its way to impulse noise filters yet. The correspondence between blocks is usually calculated by a mean absolute distance (MAD), that is heavily subject to noisy impulses. Therefore, we introduce a MAD measure that is adaptive to detected noisy pixel components. To benefit as much as possible from the spatial and temporal information available in the sequence, the search region for corresponding blocks contains pixel blocks both from the previous and current frame. The experiments show that the proposed method outperforms other state-of-the-art filters both visually and in terms of objective quality measures such as the PSNR and NCD.

The chapter is structured as follows: The successive filtering steps of the proposed filter are discussed in Section 6.1. Values for the used parameters are determined in Section 6.2 and additionally a comparison to other state-of-the-art filters is carried out in Section 6.3. The chapter is finally concluded in Section 6.4.

6.1 The Proposed Algorithm

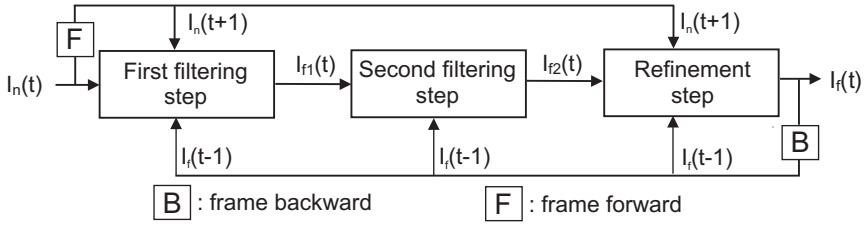

Figure 6.1: Overview of the different steps in the proposed algorithm.

The proposed filtering framework [73, 78] denoises a noisy sequence I_n in three successive filtering steps as depicted in Fig. 6.1. By removing the noise step by step, the details can be preserved as much as possible. Indeed, if a considerable part of the noise has already been removed in a previous step, and more noisefree neighbours to compare to are available,

it will be easier to distinguish noise from small details. In the first step (6.1.1) (with output denoted by I_{f_1}), we calculate for each pixel component a degree to which it is considered noisefree and a degree to which it is considered noisy. If the noisefree degree is smaller than the noisy degree, the pixel component remains unchanged, otherwise it is filtered. The determination of both degrees is mainly based on temporal information (comparison to the corresponding pixel component in the previous frame). Remark however that only in non-moving areas large differences can be assigned to noise. In areas where there is motion, such differences might also be caused by that motion. As a consequence, and as can be seen in Fig. 6.2, impulses in moving areas will not always be detected in this step. They can however be detected in the second step (6.1.2)(output I_{f_2}). Analogously as to the first step, again a noisefree degree and a noisy degree are calculated. However, the detection is now mainly based on colour information. A pixel component can be seen as noisy if there is no similarity to its (spatio-temporal) neighbours in the given colour, while there is in the other colour bands. The third step (6.1.3)(output I_f), finally, removes the remaining noise and refines the result by using as well temporal as spatial and colour information. For example, homogeneous areas can be refined by removing small impulses that are relatively large in that region, but are not large enough to be detected in detailed regions and that thus have not been detected yet by the previous general detection steps. The results of the different successive filtering steps is illustrated for the 20-th frame of the "Salesman" sequence in Fig. 6.2.

6.1.1 First Filtering Step

Detection

In this detection step, we calculate for each of the components of each pixel a degree to which it is considered noisefree and a degree to which it is thought to be noisy. A component for which the noisy degree is larger than the noisefree degree, i.e., that is more likely to be noisy than noisefree, will be filtered. Other pixel components will remain unchanged. The noisefree degree and noisy degree are determined by fuzzy rules as follows.

We consider a pixel component to be noisefree if it is similar to the corresponding component of the pixel at the same spatial location in the previous or next frame and to the corresponding component of two neighbouring pixels in the same frame. In the case of motion, the pixels in the previous frames can not be used to determine whether a pixel component in the current frame is noisefree. Therefore, more confirmation (more similar neighbours or also similar in the other colour components) is wanted instead. For the noisefree degree of the red component (and analogously for the other components), this is achieved by the following fuzzy rule:

Fuzzy Rule 6.1.
IF(*(*$|I_n^R(x,y,t)-I_f^R(x,y,t-1)|$ *is* NOT LARGE POSITIVE OR $|I_n^R(x,y,t)-I_n^R(x,y,t+1)|$ *is* NOT LARGE POSITIVE*)* AND *there are two neighbours* $(x+k,y+l,t)$ *(*$-2 \leq k,l \leq 2$ *and* $(k,l) \neq (0,0)$*) for which* $|I_n^R(x,y,t) - I_n^R(x+k,y+l,t)|$ *is* NOT LARGE

Figure 6.2: The original 20-th frame of the "Salesman" sequence (a), the frame corrupted by 20% random impulse noise (b)($PSNR = 15.05dB$) and the result after the first (c)($PSNR = 23.72dB$), second (d)($PSNR = 29.42dB$) and refinement step (e)($PSNR = 36.78dB$) respectively.

POSITIVE)

OR(*there are four neighbours* $(x+k, y+l, t)$ *(*$-2 \leq k, l \leq 2$ *and* $(k,l) \neq (0,0)$*) for which* $|I_n^R(x,y,t) - I_n^R(x+k, y+l, t)|$ *is* NOT LARGE POSITIVE OR *(there are two neighbours* $(x+k, y+l, t)$ *(*$-2 \leq k, l \leq 2$ *and* $(k,l) \neq (0,0)$*) for which* $|I_n^R(x,y,t) - I_n^R(x+k, y+l, t)|$ *is* NOT LARGE POSITIVE AND *(*$|I_n^G(x,y,t) - I_n^G(x+k, y+l, t)|$ OR $|I_n^B(x,y,t) - I_n^B(x+k, y+l, t)|$ *are* NOT LARGE POSITIVE*)))*

THEN *the red component* $I_n^R(x,y,t)$ *is considered* NOISEFREE.

To represent the linguistic value "large positive" in the above rule, a fuzzy set is used, with a membership function μ_{LP} as depicted in Fig. 6.3 (see Section 6.2 for the determination of the parameters). For the conjunction (AND), disjunction (OR) and negation (NOT), in this chapter, we will use the minimum operator, the maximum operator and the standard negator ($\mathcal{N}_s(x) = 1 - x, \forall x \in [0,1]$) respectively. Those operators are simple in use and yielded the best results, but the difference compared to the results for another choice of operators is neglectible. The outcome of the rule, i.e., the degree to which the red component

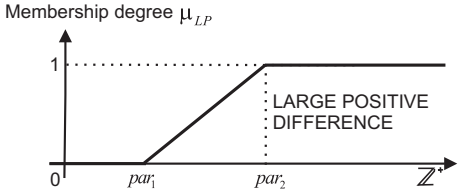

Figure 6.3: The membership function μ_{LP} of the fuzzy set *large positive*.

of the pixel at position (x,y,t) is considered noisefree, is determined as the degree to which the antecedent in the fuzzy rule is true:

$$\mu^R_{noisefree}(x,y,t) = \max(\min(\max(\alpha_1(x,y,t), \alpha_2(x,y,t)), M_2(x,y,t)), \max(M_4(x,y,t), M_{2b}(x,y,t))),$$

where

$$\begin{aligned} \alpha_1(x,y,t) &= (1 - \mu_{LP}(|I_n^R(x,y,t) - I_f^R(x,y,t-1)|)), \\ \alpha_2(x,y,t) &= (1 - \mu_{LP}(|I_n^R(x,y,t) - I_n^R(x,y,t+1)|)), \end{aligned}$$

and where $M_2(x,y,t)$ and $M_4(x,y,t)$ respectively denote the degree to which there are two (respectively four) neighbours for which the absolute difference in the red component value is not large positive, that is determined as the second (respectively fourth) largest element in the set

$$\{1 - \mu_{LP}(|I_n^R(x,y,t) - I_n^R(x+k, y+l, t)|) | -2 \leq k, l \leq 2 \text{ and } (k,l) \neq (0,0)\}$$

and $M_{2b}(x,y,t)$ denotes the degree to which there are two neighbours for which the absolute differences in the red component and one of the two colour components are not large positive, determined as the second largest element in the set

$$\{\min(1-\mu_{LP}(|I_n^R(x,y,t)-I_n^R(x+k,y+l,t)|),\\ \max(1-\mu_{LP}(|I_n^G(x,y,t)-I_n^G(x+k,y+l,t)|),\\ 1-\mu_{LP}(|I_n^B(x,y,t)-I_n^B(x+k,y+l,t)|)))\\ |-2\le k,l\le 2 \text{ and } (k,l)\neq(0,0)\}.$$

Analogously, a degree to which the component of a pixel is considered noisy is calculated. In this step, we consider a pixel component to be noisy if the absolute difference in that component is large positive compared to the pixel at the same spatial location in the previous frame and if not for five of its neighbours the absolute difference in this component and one of the other two colour bands is large positive compared to the pixel at the same spatial location in the previous frame (which means that the difference is not caused by motion). Further, we also want a confirmation either by the fact that in this colour band, there is a direction in which the differences between the considered pixel and the two respective neighbours in this direction are both large positive or large negative and if the absolute difference between those two neighbours is not large positive (i.e., there is an impulse between two pixels that are expected to belong to the same object) or by the fact that there is no large difference between the considered pixel and the pixel at the same spatial location in the previous frame in one of the other two colour bands. For the red component (and analogously for the other components) this leads to the following fuzzy rule.

Fuzzy Rule 6.2.
IF($|I_n^R(x,y,t)-I_f^R(x,y,t-1)|$ *is* LARGE POSITIVE AND NOT *(for five neighbours* $(x+k,y+l,t)$ *(*$-2\le k,l\le 2$ *and* $(k,l)\neq(0,0)$*)* $|I_n^R(x+k,y+l,t)-I_f^R(x+k,y+l,t-1)|$ *is* LARGE POSITIVE AND *(*$|I_n^G(x+k,y+l,t)-I_f^G(x+k,y+l,t-1)|$ OR $|I_n^B(x+k,y+l,t)-I_f^B(x+k,y+l,t-1)|$ *is* LARGE POSITIVE*)))*

AND (*(in one of the four directions (the differences* $I_n^R(x,y,t)-I_n^R(x+k,y+l,t)$ AND $I_n^R(x,y,t)-I_n^R(x-k,y-l,t)$ $((k,l)\in\{(-1,-1),(-1,0),(-1,1),(0,1)\})$ *are both* LARGE POSITIVE OR *both* LARGE NEGATIVE*)* AND *the absolute difference* $|I_n^R(x+k,y+l,t)-I_n^R(x-k,y-l,t)|$ *is* NOT LARGE POSITIVE*)* OR *(*$|I_n^G(x,y,t)-I_f^G(x,y,t-1)|$ *is* NOT LARGE POSITIVE OR $|I_n^B(x,y,t)-I_f^B(x,y,t-1)|$ *is* NOT LARGE POSITIVE*))*

THEN *the red component* $I_n^R(x,y,t)$ *is considered* NOISY.

Analogously to the linguistic term “large positive”, also “large negative” is represented by a fuzzy set, characterized by the membership function given in Fig. 6.4 (see Section 6.2 for the determination of the parameters). The degree to which for five neighbours the absolute differences in the red component and one of the other two components are large positive

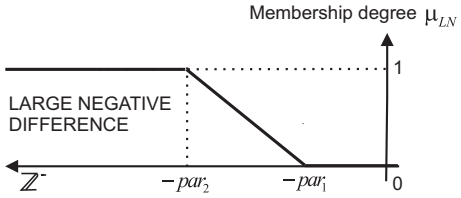

Figure 6.4: The membership function μ_{LN} of the fuzzy set *large negative*.

compared to the corresponding pixels in the previous frame, denoted by $t_{pos}(x, y, t)$, is determined as the fifth largest value in the set

$$\{\min(\mu_{LP}(|I_n^R(x+k, y+l, t) - I_f^R(x+k, y+l, t-1)|),$$
$$\max(\mu_{LP}(|I_n^G(x+k, y+l, t) - I_f^G(x+k, y+l, t-1)|),$$
$$\mu_{LP}(|I_n^B(x+k, y+l, t) - I_f^B(x+k, y+l, t-1)|)))$$
$$| -2 \leq k, l \leq 2 \text{ and } (k, l) \neq (0, 0)\}.$$

The degree to which the absolute difference between the pixel at position (x, y, t) and the corresponding pixel in the previous frame is large positive and five of its neighbours do not show motion is then given by

$$\beta(x, y, t) = \min(\mu_{LP}(|I_n^R(x, y, t) - I_f^R(x, y, t-1)|), 1 - t_{pos}(x, y, t)).$$

Further, the degree to which there is no large difference between the considered pixel and the pixel at the same spatial location in the previous frame in one of the other two colour bands is given by

$$\delta(x, y, t) =$$
$$\max(1 - \mu_{LP}(|I_n^G(x, y, t) - I_f^G(x, y, t-1)|), 1 - \mu_{LP}(|I_n^B(x, y, t) - I_f^B(x, y, t-1)|)).$$

Finally, the degree to which there is a direction in which the pixel at position (x, y, t) is an impulse, denoted by $\gamma(x, y, t)$, is determined as the maximum value in the set

$$\{\min(\max(\epsilon^1_{(k,l)}(x, y, t), \epsilon^2_{(k,l)}(x, y, t)), \epsilon^3_{(k,l)}(x, y, t))$$
$$|(k, l) \in \{(-1, -1), (-1, 0), (-1, 1), (0, 1)\}\},$$

where

$$\begin{aligned}
\epsilon^1_{(k,l)}(x, y, t) &= \min(\mu_{LP}(I_n^R(x, y, t) - I_n^R(x+k, y+l, t)), \\
&\qquad \mu_{LP}(I_n^R(x, y, t) - I_n^R(x-k, y-l, t))), \\
\epsilon^2_{(k,l)}(x, y, t) &= \min(\mu_{LN}(I_n^R(x, y, t) - I_n^R(x+k, y+l, t)), \\
&\qquad \mu_{LN}(I_n^R(x, y, t) - I_n^R(x-k, y-l, t))), \\
\epsilon^3_{(k,l)}(x, y, t) &= 1 - \mu_{LP}(|I_n^R(x+k, y+l, t) - I_n^R(x-k, y-l, t)|).
\end{aligned}$$

Combining the above, we get

$$\mu^R_{noisy}(x,y,t) = \min(\beta(x,y,t), \delta(x,y,t), \gamma(x,y,t)).$$

Filtering

In this subsection, we discuss the filtering for the red colour band. The filtering of the other colour bands is analogous. We decide to filter all red pixel components that are considered more likely to be noisy than noisefree, i.e., for which $\mu^R_{noisy}(x,y,t) > \mu^R_{noisefree}(x,y,t)$. The red components of the other pixels remain unchanged to avoid the filtering of noisefree pixels (that might have been uncorrectly assigned a low noisy degree, but for which the high noisefree degree assures us that it is noisefree) and thus detail loss. On the other hand, noisy pixel components might remain unfiltered due to an uncorrect high noisefree degree, but those pixels can still be detected in a next filtering step.

$$\mu^R_{unch}(x,y,t) = \begin{cases} 0 & \mu^R_{noisy}(x,y,t) > \mu^R_{noisefree}(x,y,t), \\ 1 & \text{else.} \end{cases}$$

So $\mu_{unch}(x,y,t) = (\mu^R_{unch}(x,y,t), \mu^G_{unch}(x,y,t), \mu^B_{unch}(x,y,t))$ is a vector that gives information whether the respective colour component of the colour pixel $I_n(x,y,t)$ should be filtered. Analogously as $I_n(t)$ denotes the t-th frame of I_n, $\mu_{unch}(t)$ denotes the 2D array of vectors that gives information about the pixel components of the t-th frame of the sequence I_n. To exploit the spatial and temporal information in the sequence as much as possible, the filtering is performed by blockmatching. To do this, a noise adaptive mean absolute difference (MAD) is used to calculate the correspondence between the colour components of two $(2 \cdot W + 1) \times (2 \cdot W + 1)$ blocks of image pixels (where W is a general parameter that determines the block size):

$${}^R MAD^{I,\mu}_{\widetilde{I},\widetilde{\mu}}(x,y,r,s,W) = \frac{\sum_{k=-W}^{+W} \sum_{l=-W}^{+W} P^{\mu^R,r}_{\widetilde{\mu}^R,s}(x+k,y+l) D^{I^R,r}_{\widetilde{I}^R,s}(x+k,y+l)}{\sum_{k=-W}^{+W} \sum_{l=-W}^{+W} P^{\mu^R,r}_{\widetilde{\mu}^R,s}(x+k,y+l)},$$

with

$$P^{\mu^R,r}_{\widetilde{\mu}^R,s}(x+k,y+l) = \mu^R(x+k,y+l) \cdot \widetilde{\mu}^R(x+k+r,y+l+s),$$

and

$$D^{I^R,r}_{\widetilde{I}^R,s}(x+k,y+l) = |I^R(x+k,y+l) - \widetilde{I}^R(x+k+r,y+l+s)|,$$

and where I and $\widetilde{I}$ are the two frames (2D colour images) to which the blocks belong, x and y indicate the spatial coordinates of the central pixel of the considered block in I and r and s respectively stand for the vertical and horizontal coordinates of the displacement vector, i.e., the block that is considered in $\widetilde{I}$ has $(x+r, y+s)$ as central pixel. The binary functions μ^c and $\widetilde{\mu}^c$ ($c \in \{R,G,B\}$) indicate whether the pixel components $I^c(x,y)$ and $\widetilde{I}^c(x,y)$ are reliable and should be used ($\mu^c(x,y) = 1$, respectively $\widetilde{\mu}^c(x,y) = 1$) or not

($\mu^c(x,y) = 0$, respectively $\widetilde{\mu}^c(x,y) = 0$). Using only noisefree pixel components allows us to calculate a more reliable measure to estimate whether two blocks would correspond in the red component if they were both noisefree. If $\sum_{k=-W}^{+W} \sum_{l=-W}^{+W} \mu^R(x+k, y+l) \cdot \widetilde{\mu}^R(x+k+r, y+l+s) = 0$, the noise adaptive MAD is assigned the value $+\infty$. Further, the noise adaptive MAD is not considered reliable if not for at least half of the positions in the $(2 \cdot W + 1) \times (2 \cdot W + 1)$ blocks, both compared values are reliable ($\mu^R(x+k, y+l) = 1$ and $\widetilde{\mu}^R(x+k+r, y+l+s) = 1$) or not for half of the reliable positions the absolute difference $|I^R(x+k, y+l) - \widetilde{I}^R(x+k+r, y+l+s)|$ is not large positive (i.e., $\mu_{LP}(|I^R(x+k, y+l) - \widetilde{I}^R(x+k+r, y+l+s)|) = 0$). It is also not considered reliable if both the green and blue component of the central pixels are reliable (i.e., $\mu^G(x,y) = 1$, $\mu^G(x+r, y+s) = 1$, $\mu^B(x,y) = 1$ and $\mu^B(x+r, y+s) = 1$) and their absolute difference is large positive (i.e., $\mu_{LP}(|I^G(x,y) - \widetilde{I}^G(x+r, y+s)|) = 1$ and $\mu_{LP}(|I^B(x,y) - \widetilde{I}^B(x+r, y+s)|) = 1$). In these cases, the noise adaptive MAD is changed to the value $+\infty$, such that the block will not be used for the filtering.

For the filtering of a red component $I_n^R(x,y,t)$ in this first step of our algorithm, we determine the displacement vectors $(\underline{u}(x,y,t), \underline{v}(x,y,t))$ and $(\overline{u}(x,y,t), \overline{v}(x,y,t))$ for the best matching $(2 \cdot W_1 + 1) \times (2 \cdot W_1 + 1)$ block in a search region of size $(2 \cdot W_2 + 1) \times (2 \cdot W_2 + 1)$ in respectively the previous frame $I_f(t-1)$ and the current frame $I_n(t)$ (due to large motion, sometimes no corresponding block might be found in the previous frame, but the region around the given pixel in the current frame might be similar) as follows (For the selection of the parameters W_1 and W_2, we refer to section 6.2):

$$(\underline{u}(x,y,t), \underline{v}(x,y,t)) = \underset{-W_2 \leq r,s \leq W_2}{\arg\min} {}^R MAD_{I_f(t-1), Id}^{I_n(t), \mu_{unch}(t)}(x,y,r,s,W_1).$$

The minimum value itself is denoted by $\underline{minmad}(x,y,t)$. We have used the identity function Id for the binary function corresponding to the previous frame, since this frame has already been filtered and should be noisefree.

$$(\overline{u}(x,y,t), \overline{v}(x,y,t)) = \underset{-W_2 \leq r,s \leq W_2, (r,s) \neq (0,0), \mu_{unch}(x+r,y+s,t)=1}{\arg\min} {}^R MAD_{I_n(t), \mu_{unch}}^{I_n(t), \mu_{unch}(t)}(x,y,r,s,W_1).$$

The minimum value itself is denoted by $\overline{minmad}(x,y,t)$. We have restricted ourselves here to pixels $(x+r, y+s, t)$, for which $\mu_{unch}^R(x+r, y+s, t) = 1$, since only noisefree pixels should be used to replace the noisy pixel component $I_n^R(x,y,t)$.

A pixel component $I_n^R(x,y,t)$ for which $\mu_{unch}^R(x,y,t) = 0$, is then filtered as the noisefree center of the best corresponding block in the search region, if it exists (i.e., if it holds that $min(\underline{minmad}(x,y,t), \overline{minmad}(x,y,t)) < +\infty$). Otherwise, a spatial filtering is performed. If $\mu_{unch}^R(x,y,t) = 1$, the pixel component remains unchanged in this step. Summarized, the output of this first step for the red component $I_n^R(x,y,t)$ is given as follows.

If $\mu_{unch}^R(x,y,t) = 1$, then

$$I_{f_1}^R(x,y,t) = I_n^R(x,y,t),$$

else if $\mu^R_{unch}(x,y,t) = 0$, then

$$I^R_{f_1}(x,y,t) = FILT^{I^R_n(t),\mu^R_{unch}(t)}_{I^R_f(t-1)}(x,y,\underline{u}(x,y,t),\underline{v}(x,y,t),\overline{u}(x,y,t),\overline{v}(x,y,t),$$
$$\underline{minmad}(x,y,t),\overline{minmad}(x,y,t)),$$

with (in a general notation)

$$FILT^{I,\mu}_{\widetilde{I}}(x,y,u,v,\widetilde{u},\widetilde{v},m,\widetilde{m}) = \begin{cases} I(x+u,y+v) & \text{if } m = min(m,\widetilde{m}) < +\infty \\ \widetilde{I}(x+\widetilde{u},y+\widetilde{v}) & \text{if } \widetilde{m} = min(m,\widetilde{m}) < +\infty \\ SF^I_\mu(x,y,W_1) & \text{if } m = \widetilde{m} = +\infty \end{cases},$$

where the spatial filtering framework is given by

$$SF^I_\mu(x,y,W) = \frac{\sum_{k=-W}^{+W}\sum_{l=-W}^{+W}\mu(x+k,y+l)\cdot I(x+k,y+l)}{\sum_{k=-W}^{+W}\sum_{l=-W}^{+W}\mu(x+k,y+l)}.$$

If $\sum_{k=-W}^{+W}\sum_{l=-W}^{+W}\mu(x+k,y+l) = 0$, which is unlikely to happen in practical situations, then $SF^I_\mu(x,y,W) = \text{median}\{I(x+k,y+l)|\ -W \le k,l \le W\}$.

6.1.2 Second Filtering Step

In our aim to preserve the details as much as possible, the noise is removed in successive steps. In this step the noise is detected based on the output of the previous step (I_{f_1}). Also in this second filtering step, a degree to which a pixel component is expected to be noisefree and a degree to which a pixel component is expected to be noisy, is calculated. In the calculation of those degrees, we now take into account information from the other colour bands.

A colour component of a pixel is considered noisefree if the difference between that pixel and the corresponding pixel in the previous frame, is not large in the given component and also not large in one of the other two colour components. It is also considered noisefree if there are two neighbours for which the difference in the given component and one of the other two components are not large. So the other colour bands are used here as a confirmation for the observations in the considered colour band to make those more reliable.

For the red component (and analogously for the other colour components), this gives the following fuzzy rule.

Fuzzy Rule 6.3.
IF($|I^R_{f_1}(x,y,t) - I^R_f(x,y,t-1)|$ AND ($|I^G_{f_1}(x,y,t) - I^G_f(x,y,t-1)|$ OR $|I^B_{f_1}(x,y,t) - I^B_f(x,y,t-1)|$) *are* NOT LARGE POSITIVE)

OR (*for two neighbours* $(x+k,y+l,t)$ $(-1 \le k,l \le 1$ *and* $(k,l) \neq (0,0))$ $|I^R_{f_1}(x,y,t) - I^R_{f_1}(x+k,y+l,t)|$ *is* NOT LARGE POSITIVE AND ($|I^G_{f_1}(x,y,t) - I^G_{f_1}(x+k,y+l,t)|$ *is*

NOT LARGE POSITIVE OR $|I^B_{f_1}(x,y,t)-I^B_{f_1}(x+k,y+l,t)|$ *is* NOT LARGE POSITIVE)) THEN *the red component* $I^R_{f_1}(x,y,t)$ *is considered* NOISEFREE.

The degree to which the red component of the pixel at position (x,y,t) is considered noisefree is then given by:

$$\mu^R_{2,noisefree}(x,y,t) = \max(\zeta(x,y,t), \eta(x,y,t)),$$

where

$$\begin{aligned}\zeta(x,y,t) = \min(&1-\mu_{LP}(|I^R_{f_1}(x,y,t) - I^R_f(x,y,t-1)|),\\ &\max(1-\mu_{LP}(|I^G_{f_1}(x,y,t) - I^G_f(x,y,t-1)|),\\ &\quad 1-\mu_{LP}(|I^B_{f_1}(x,y,t) - I^B_f(x,y,t-1)|)))\end{aligned}$$

and $\eta(x,y,t)$ is the second largest element in the set

$$\begin{aligned}\{\min(&1-\mu_{LP}(|I^R_{f_1}(x,y,t) - I^R_{f_1}(x+k,y+l,t)|),\\ &\max(1-\mu_{LP}(|I^G_{f_1}(x,y,t) - I^G_{f_1}(x+k,y+l,t)|),\\ &\quad 1-\mu_{LP}(|I^B_{f_1}(x,y,t) - I^B_{f_1}(x+k,y+l,t)|)))\\ &\quad | -1 \le k,l \le 1 \text{ and } (k,l) \neq (0,0)\}.\end{aligned}$$

A pixel component is considered noisy if there are three neighbours that differ largely in that component, but are similar (not a large difference) in the other two components. It is also considered noisy if in the considered colour band, its value is larger or smaller than the component values of all its neighbours and this is not the case in both other colour bands.

For the red component of a pixel (and analogously for the other components), this corresponds to the following fuzzy rule.

Fuzzy Rule 6.4.
IF(*for three neighbours* $(x+k,y+l,t)$ ($-1 \le k,l \le 1$ *and* $(k,l) \neq (0,0)$) $|I^R_{f_1}(x,y,t)-I^R_{f_1}(x+k,y+l,t)|$ *is* LARGE POSITIVE AND $|I^G_{f_1}(x,y,t) - I^G_{f_1}(x+k,y+l,t)|$ *is* NOT LARGE POSITIVE AND $|I^B_{f_1}(x,y,t) - I^B_{f_1}(x+k,y+l,t)|$ *is* NOT LARGE POSITIVE)
OR(((*for all neighbours* $(x+k,y+l,t)$ ($-1 \le k,l \le 1$ *and* $(k,l) \neq (0,0)$) $I^R_{f_1}(x,y,t)-I^R_{f_1}(x+k,y+l,t)$ *is* LARGE POSITIVE) OR (*for all neighbours* $(x+k,y+l,t)$ ($-1 \le k,l \le 1$ *and* $(k,l) \neq (0,0)$) $I^R_{f_1}(x,y,t) - I^R_{f_1}(x+k,y+l,t)$ *is* LARGE NEGATIVE)) AND NOT (((*for all neighbours* $(x+k,y+l,t)$ ($-1 \le k,l \le 1$ *and* $(k,l) \neq (0,0)$) $I^G_{f_1}(x,y,t)-I^G_{f_1}(x+k,y+l,t)$ *is* LARGE POSITIVE) OR (*for all neighbours* $(x+k,y+l,t)$ ($-1 \le k,l \le 1$ *and* $(k,l) \neq (0,0)$) $I^G_{f_1}(x,y,t) - I^G_{f_1}(x+k,y+l,t)$ *is* LARGE NEGATIVE)) AND ((*for all neighbours* $(x+k,y+l,t)$ ($-1 \le k,l \le 1$ *and* $(k,l) \neq (0,0)$) $I^B_{f_1}(x,y,t) - I^B_{f_1}(x+k,y+l,t)$ *is* LARGE POSITIVE) OR (*for all neighbours* $(x+k,y+l,t)$ ($-1 \le k,l \le 1$ *and* $(k,l) \neq (0,0)$) $I^B_{f_1}(x,y,t) - I^B_{f_1}(x+k,y+l,t)$ *is*

LARGE NEGATIVE)))) THEN *the red component* $I^R_{f_1}(x,y,t)$ *is considered* NOISY.

The noisy degree for the red component of the pixel at position (x,y,t) is then calculated as follows:

$$\mu^R_{2,noisy}(x,y,t) = \max(\theta(x,y,t), \kappa(x,y,t)),$$

where $\theta(x,y,t)$ is the third largest element in the set

$$\{\min(\mu_{LP}(|I^R_{f_1}(x,y,t) - I^R_{f_1}(x+k,y+l,t)|), \min(1-\mu_{LP}(|I^G_{f_1}(x,y,t) - I^G_{f_1}(x+k,y+l,t)|), 1-\mu_{LP}(|I^B_{f_1}(x,y,t) - I^B_{f_1}(x+k,y+l,t)|))) \mid -1 \le k,l \le 1 \text{ and } (k,l) \neq (0,0)\},$$

and

$$\kappa(x,y,t) = \min(\max(m^R_1(x,y,t), m^R_2(x,y,t)), 1 - \min(\max(m^G_1(x,y,t), m^G_2(x,y,t)), \max(m^B_1(x,y,t), m^B_2(x,y,t)))),$$

where

$$m^c_1(x,y,t) = \min\{\mu_{LP}(I^R_{f_1}(x,y,t) - I^R_{f_1}(x+k,y+l,t)) \mid -1 \le k,l \le 1 \text{ and } (k,l) \neq (0,0)\},$$

$$m^c_2(x,y,t) = \min\{\mu_{LN}(I^R_{f_1}(x,y,t) - I^R_{f_1}(x+k,y+l,t)) \mid -1 \le k,l \le 1 \text{ and } (k,l) \neq (0,0)\},$$

with $c \in \{R,G,B\}$.

All red components (and analogously all green and all blue components) for which $\mu^R_{2,noisy}(x,y,t) > \mu^R_{2,noisefree}(x,y,t)$ are filtered ($\mu^R_{2,unch}(x,y,t) = 0$), the other red components remain unchanged ($\mu^R_{2,unch}(x,y,t) = 1$):

$$\mu^R_{2,unch}(x,y,t) = \begin{cases} 0 & \mu^R_{2,noisy}(x,y,t) > \mu^R_{2,noisefree}(x,y,t), \\ 1 & \text{else.} \end{cases}$$

Analogously to the first step, for the filtering of the red components (and analogously the green and blue components) for which $\mu^R_{2,unch}(x,y,t) = 0$, we search for the noisefree center of the best corresponding block in the search region in the current and previous frame.

$$(\underline{u}'(x,y,t), \underline{v}'(x,y,t)) = \underset{-W_2 \le r,s \le W_2}{\arg\min} {}^R MAD^{I_{f_1}(t), \mu_{2,unch}(t)}_{I_f(t-1), Id}(x,y,r,s,W_1).$$

The minimum value itself is denoted by $\underline{minmad}'(x,y,t)$.

$(\overline{u}'(x,y,t), \overline{v}'(x,y,t)) =$

$$\underset{-W_2 \le r,s \le W_2,(r,s)\neq(0,0),\mu^R_{2,unch}(x+r,y+s,t)=1}{\arg\min} {}^{R}MAD^{I_{f_1}(t),\mu_{2,unch}(t)}_{I_{f_1}(t),\mu_{2,unch}(t)}(x,y,r,s,W_1).$$

The minimum value itself is denoted by $\overline{minmad}'(x,y,t)$.

If $\mu^R_{2,unch}(x,y,t)=0$, then $I^R_{f_1}(x,y,t)$ is filtered as

$$I^R_{f_2}(x,y,t) = FILT^{I^R_{f_1}(t),\mu^R_{2,unch}(t)}_{I^R_f(t-1)}(x,y,\underline{u}'(x,y,t),\underline{v}'(x,y,t),\overline{u}'(x,y,t),\overline{v}'(x,y,t),$$
$$\underline{minmad}'(x,y,t),\overline{minmad}'(x,y,t)).$$

Red pixel components that are considered noisefree ($\mu^R_{2,unch}(x,y,t)=1$) remain unchanged:

$$I_{f_2}(x,y,t) = I_{f_1}(x,y,t).$$

6.1.3 Third Filtering Step

The result from the previous steps is further refined based on temporal, spatial and colour information. Namely, the red component (and analogously the green and blue component) of a pixel is refined in the following cases:

- In non-moving areas, pixels will correspond to the pixels in the previous frame, which allows us to detect remaining isolated noisy pixels. If (x,y,t) lies in a non-moving 3×3 neighbourhood, i.e.,

$$\frac{\sum_{k=-1}^{1}\sum_{l=-1}^{1}\sum_{c\in\{R,G,B\}}|I^c_{f_2}(x+k,y+l,t)-I^c_f(x+k,y+l,t-1)|}{24} - \frac{\sum_{c\in\{R,G,B\}}|I^c_{f_2}(x,y,t)-I^c_f(x,y,t-1)|}{24} < par_1,$$

  and if $|I^R_{f_2}(x,y,t)-I^R_f(x,y,t-1)|>par_2$ and $|I^R_f(x,y,t-1)-I^R_n(x,y,t+1)|<par_1$, then the red component $I^R_{f_2}(x,y,t)$ is considered to be noisy ($\mu^R_{3,unch}(x,y,t)=0$). The last check is to prevent noise propagation in the case that the pixel in the previous frame would not have been filtered correctly.

- Very small impulses might not have been detected by the algorithm. In homogeneous areas however, such impulses might be relatively large and can be detected more easily. Let $L^R_2(x,y,t)$ and $S^R_2(x,y,t)$ respectively denote the second largest and second smallest red component value among the 8 neighbours in a 3×3 neighbourhood around $I^R_{f_2}(x,y,t)$. If $L^R_2(x,y,t)-S^R_2(x,y,t)<par_2$ (homogeneous neighbourhood) and further also $I^R_{f_2}(x,y,t)-L^R_2(x,y,t)>L^R_2(x,y,t)-S^R_2(x,y,t)$ or $S^R_2(x,y,t)-I^R_{f_2}(x,y,t)>L^R_2(x,y,t)-S^R_2(x,y,t)$ (the red component is clearly larger or smaller than the neighbourhood), then the red component $I^R_{f_2}(x,y,t)$ is considered to be noisy ($\mu^R_{3,unch}(x,y,t)=0$).

- Based on colour information, the red component $I^R_{f_2}(x,y,t)$ is considered to be noisy ($\mu^R_{3,unch}(x,y,t)=0$) if in a 3×3 neighbourhood two neighbours $I^R_{f_2}(x+k,y+l,t)$ ($-1\leq k,l\leq 1$, $(k,l)\neq(0,0)$) can be found for which $|I^R_{f_2}(x,y,t)-I^R_{f_2}(x+k,y+l,t)|>par_2$ and $|I^R_{f_2}(x,y,t)-I^R_{f_2}(x+k,y+l,t)|>|I^G_{f_2}(x,y,t)-I^G_{f_2}(x+k,y+l,t)|+|I^B_{f_2}(x,y,t)-I^B_{f_2}(x+k,y+l,t)|$.

In all other cases the red component value is considered to be noisefree and should not be adapted anymore ($\mu^R_{3,unch}(x,y,t)=1$).

Analogously as in the previous steps, for the filtering of the red components for which $\mu^R_{3,unch}(x,y,t)=0$, we search for the noisefree center of the best corresponding block in the search region in the current and previous frame.

$$(\underline{u}''(x,y,t),\underline{v}''(x,y,t))=\underset{-W_2\leq r,s\leq W_2}{\arg\min}\ {}^RMAD^{I_{f_2}(t),\mu_{3,unch}(t)}_{I_f(t-1),Id}(x,y,r,s,W_1).$$

The minimum value itself is denoted by $\underline{minmad}''(x,y,t)$.

$$(\overline{u}''(x,y,t),\overline{v}''(x,y,t))=\underset{-W_2\leq r,s\leq W_2,(r,s)\neq(0,0),\mu^R_{3,unch}(x+r,y+s,t)=1}{\arg\min}\ {}^RMAD^{I_{f_2}(t),\mu_{3,unch}(t)}_{I_{f_2}(t),\mu_{3,unch}(t)}(x,y,r,s,W_1).$$

The minimum value itself is denoted by $\overline{minmad}''(x,y,t)$.

A red component $I^R_{f_2}(x,y,t)$ for which $\mu^R_{3,unch}(x,y,t)=0$, is filtered as

$$I_f(x,y,t)=FILT^{I_{f_2}(t),\mu''_{unch}(t)}_{I_f(t-1)}(x,y,\underline{u}''(x,y,t),\underline{v}''(x,y,t),\overline{u}''(x,y,t),\overline{v}''(x,y,t),\underline{minmad}''(x,y,t),\overline{minmad}''(x,y,t)).$$

Otherwise ($\mu^R_{3,unch}(x,y,t)=1$), it remains unchanged:

$$I^R_f(x,y,t)=I^R_{f_2}(x,y,t).$$

6.2 Parameter Selection

In this section, the parameter values for the membership functions and the window sizes are determined.

We first select the parameters par_1 and par_2 that determine the membership functions μ_{LP} and μ_{LN} in Fig. 6.3 and 6.4. To do this, we have fixed the window sizes W_1 and W_2 of the pixel neighbourhood and the search region in the filtering as $W_1=2$ (5×5 neighbourhood) and $W_2=5$ (11×11 search region) and we have let the parameters par_1 and par_2 run over a range of possible values. The parameter values were then determined as the couple (par_1,par_2) for which the arithmetic mean of the PSNR result of the nine

sequences “Salesman”, “Bus” and “Tennis”, each corrupted with respectively 5%, 15% and 25% random impulse noise in each of the colour bands, reached its maximum. The obtained values, which we will also use in the remaining experiments, are $(par_1, par_2) = (20, 31)$ (Table 6.1).

Table 6.1: Determination of the parameters par_1 and par_2. (Arithmetic mean of the average PSNR (dB) values around the maximum.)

$par_1 \backslash par_2$	29	30	31	32	33
18	32.38	32.39	32.40	32.38	32.37
19	32.39	32.41	32.41	32.40	32.39
20	32.39	32.41	**32.42**	32.40	32.39
21	32.39	32.40	32.41	32.40	32.39
22	32.39	32.40	32.41	32.40	32.39

Next, the window sizes W_1 and W_2 are set. For the above selected parameter values for par_1 and par_2, we now let the parameters W_1 and W_2 run over a range of possible values. As can be seen in Table 6.2, from the couple $(W_1, W_2) = (2, 7)$ on, the arithmetic mean of the PSNR values of the nine test sequences hardly increases. Although we have focused in this chapter on the noise filtering capability of the filter and not on its complexity, it should be mentioned that most of the computation time needed by the method goes to the filtering of detected pixels, i.e., the search for the best matching block. The size of a block (the number of pixels that has to be handled for each block) and the size of the search region (the number of blocks to which a given block should be compared) increases quadratic with respect to respectively W_1 and W_2. Therefore, we have decided to use the couple $(W_1, W_2) = (2, 7)$ for the remaining experiments. With respect to the complexity, we also remark that the higher the noise level, the more noisy pixels, and thus the more pixels that need to be filtered, i.e., the more pixels for which the block matching is performed. A first possibility to reduce the computation time would be to use faster block matching techniques such as those presented in [111, 143, 144]. Further, it can also be remarked that the detection (respectively filtering) of a pixel is independent of the detection (respectively filtering) of the other pixels in the frame and could thus be performed in parallel.

6.3 Experimental Results

In this section, the performance of the proposed method is compared to that of the adaptive vector median filter (AVMF) from [63, 64], the video adaptive vector directional median filter (VAVDMF) with 3D filtering window from [112] and the 2D fuzzy impulse noise reduction method for colour images (INRC) from [123].

The adaptive vector median filter [63, 64] orders the pixels (colour vectors) in the 3D filtering window based on increasing accumulated (Euclidean) distance to the other pixels

Table 6.2: Determination of the parameters W_1 and W_2. (Arithmetic mean of the average PSNR (dB) values.)

$W_1 \backslash W_2$	5	6	7	8	9	10	11
1	31.42	31.42	31.41	31.38	31.33	31.31	31.27
2	32.42	32.49	32.57	32.57	32.55	32.55	32.54
3	32.45	32.54	32.63	32.64	32.64	32.64	32.64
4	32.46	32.56	32.65	32.67	32.67	32.67	32.67
5	32.35	32.45	32.55	32.57	32.57	32.58	32.58

in the window. If the Euclidean distance between the central pixel in the window and the mean of a given number of vectors that have the lowest accumulated distance, is greater than a given threshold, then the central pixel is filtered as the pixel with the lowest accumulated distance, otherwise, it remains unchanged.

In the video adaptive vector directional median filter [112], the vectors are first ordered based on increasing angular distance. If the absolute distance between the central pixel in the window and the mean of a given number K of vectors that have the lowest accumulated angular distance, is greater than a given threshold, then the central pixel is filtered as the pixel with the lowest accumulated absolute distance (magnitude), otherwise, it remains unchanged.

To show that the proposed filter takes real advantage from the temporal information, we have also compared the proposed filter to the 2D fuzzy impulse noise reduction method for colour images. As shown in [123], the INRC filter outperforms all other compared state-of-the-art 2D methods and can thus be accepted as a good representative for the 2D impulse noise filters. Further, this filter is also a representative of a non-vector-based filter, in which the colour bands are filtered separately. However, in the detection of noisy pixel components, also information from the other components is used.

All methods have been processed on the "Salesman", "Bus", "Tennis", "Deadline", "Chair" and "Foreman" sequences, for random impulse noise levels (in each colour band) ranging from $pr = 5\%$ to $pr = 30\%$. The results of these experiments, in terms of PSNR and in terms of NCD respectively, are presented in Fig. 6.5 and 6.6, from which it can be concluded that the proposed method outperforms all other methods. Since the objective measures do not always tell everything, we also did a visual comparison. The results of the different compared methods performed on the noisy "Tennis" ($pr = 5\%$), "Deadline" ($pr = 15\%$) and "Salesman" ($pr = 25\%$) sequences, can be found on `http://www.fuzzy.ugent.be/tmelange/results/colourimpulse`. Fig. 6.7 and 6.8 respectively show for the 110-th frame of the "Tennis" sequence and the 20-th frame of the "Deadline" sequence, the original frame, the noisy frame and the result obtained by the different compared methods.

We see that the VAVDMF removes the noise very well. However, also too many noise-free pixels are filtered, which results in both spatial and temporal inconsistencies, especially

around edges. Further, the filter also performs less well in the case of motion (e.g. “Salesman” (arms), “Tennis” (ball), “Chair”, “Bus”), due to the fact that the pixels in the filtering window from the previous and next frame, will then not always correspond to the same object.

The other vector-based method, i.e., the AVMF, preserves the details very well. However, it fails to remove the noise adequately. Even for lower noise levels, small impulses remain visible. Analogously as the VAVDMF, it also performs less well in the case of motion.

Next, the INRC results in a very good noise removal, even for high noise levels. At the cost of this, however, too much details get lost (e.g., side lines on the table in “Tennis”) and the images become a little blurry. Further, also several temporal inconsistencies in non-moving areas can be detected, especially when they are detailed (e.g., background “Deadline”, “Salesman”). This is no surprise, since the 2D filter does not benefit from the available extra temporal information in such non-moving area.

Finally, the proposed fuzzy filter combines a very good detail preservation to a very good noise removal and clearly outperforms all compared filters. The filter benefits very well from the extra information coming from similar regions in a spatio-temporal neighbourhood.

6.4 Conclusion

In this chapter, we have presented a new filtering framework for colour videos corrupted by random valued impulse noise. In order to preserve the details as much as possible, the noise is removed step by step. The detection of noisy colour components is based on fuzzy rules in which information from spatial and temporal neighbours as well as from the other colour bands is used. Detected noisy components are filtered based on blockmatching where a noise adaptive mean absolute difference is used and where the search region contains pixels blocks from both the previous and current frame.

The experiments showed that the proposed method outperforms other state-of-the-art methods both in terms of objective measures such as PSNR and NCD and visually.

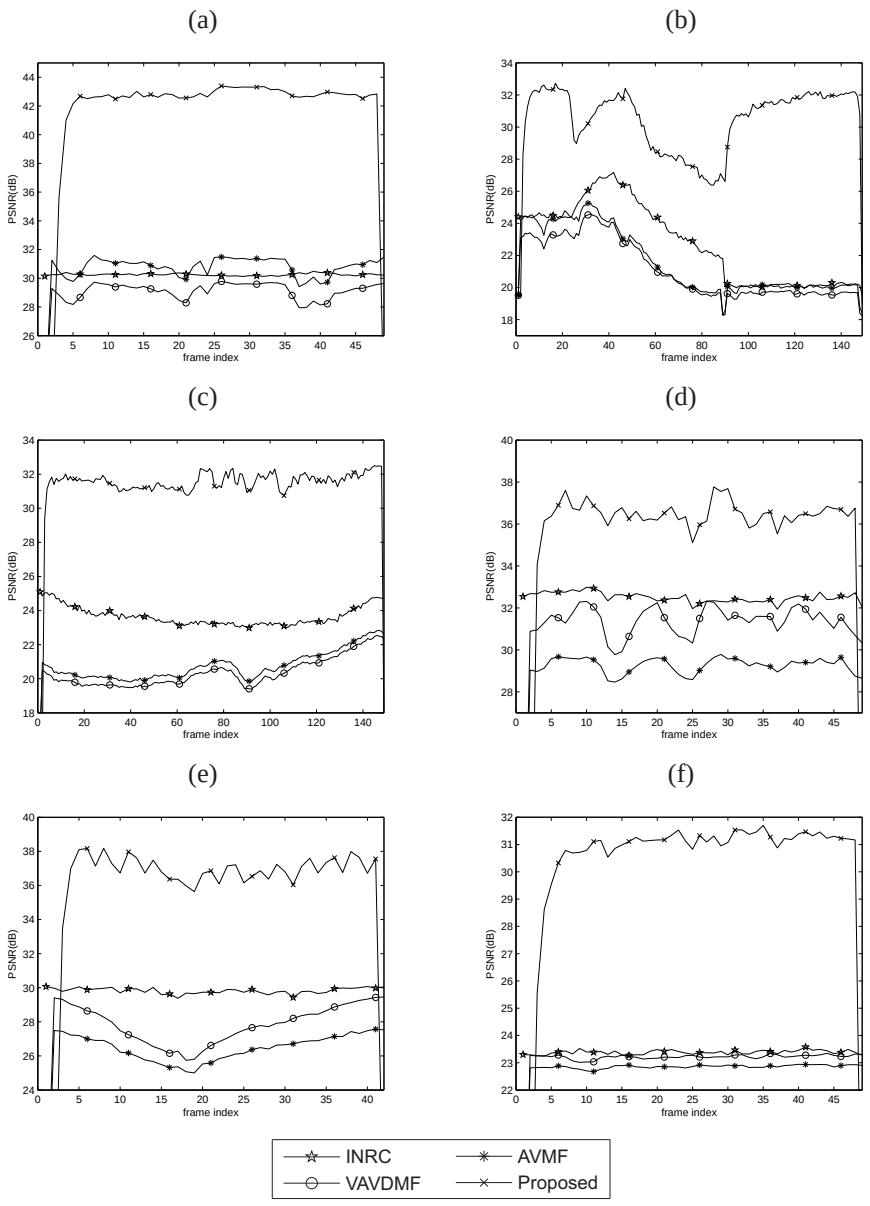

Figure 6.5: PSNR results for the different methods applied on the sequences (a) "Salesman" ($pr = 5\%$), (b) "Tennis" ($pr = 10\%$), (c) "Bus" ($pr = 15\%$), (d) "Foreman" ($pr = 20\%$), (e) "Chair" ($pr = 25\%$) and (f) "Deadline" ($pr = 30\%$).

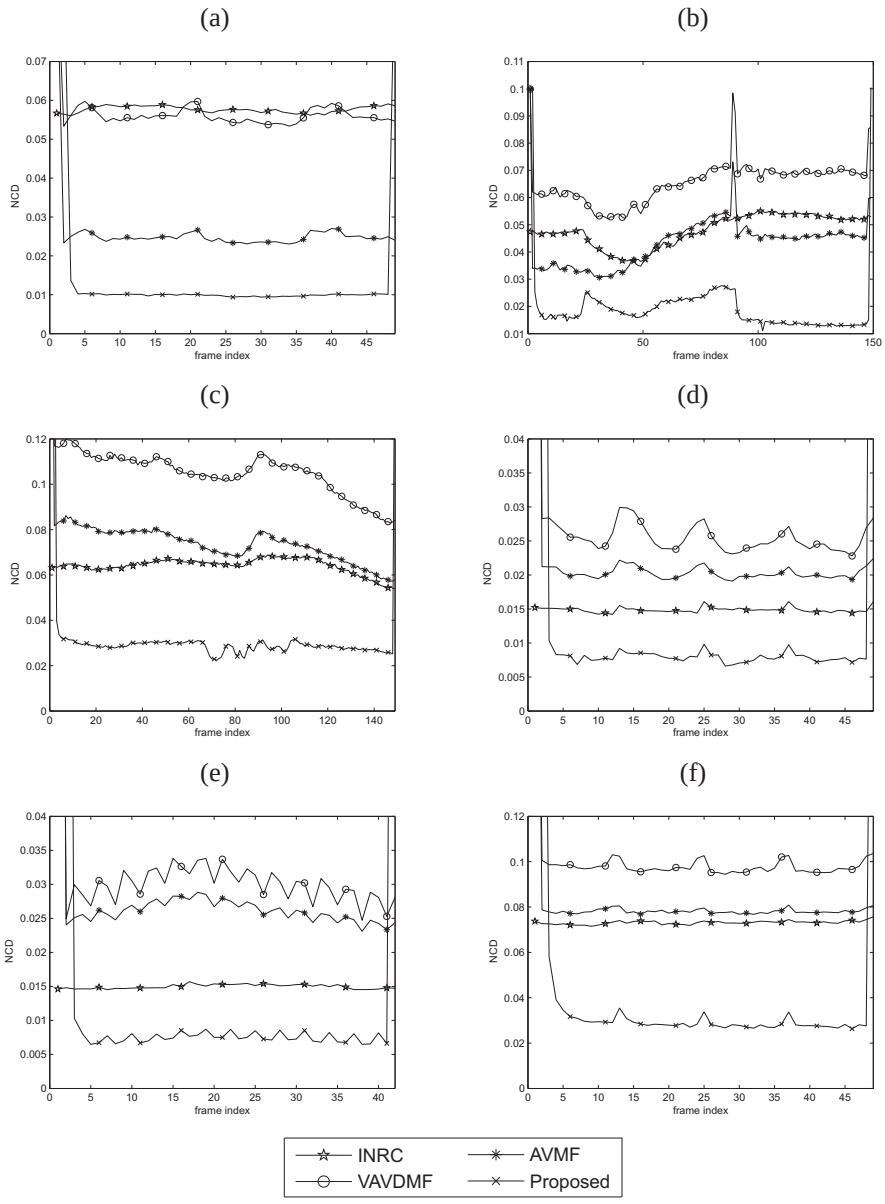

Figure 6.6: NCD results for the different methods applied on the sequences (a) "Salesman" ($pr = 5\%$), (b) "Tennis" ($pr = 10\%$), (c) "Bus" ($pr = 15\%$), (d) "Foreman" ($pr = 20\%$), (e) "Chair" ($pr = 25\%$) and (f) "Deadline" ($pr = 30\%$).

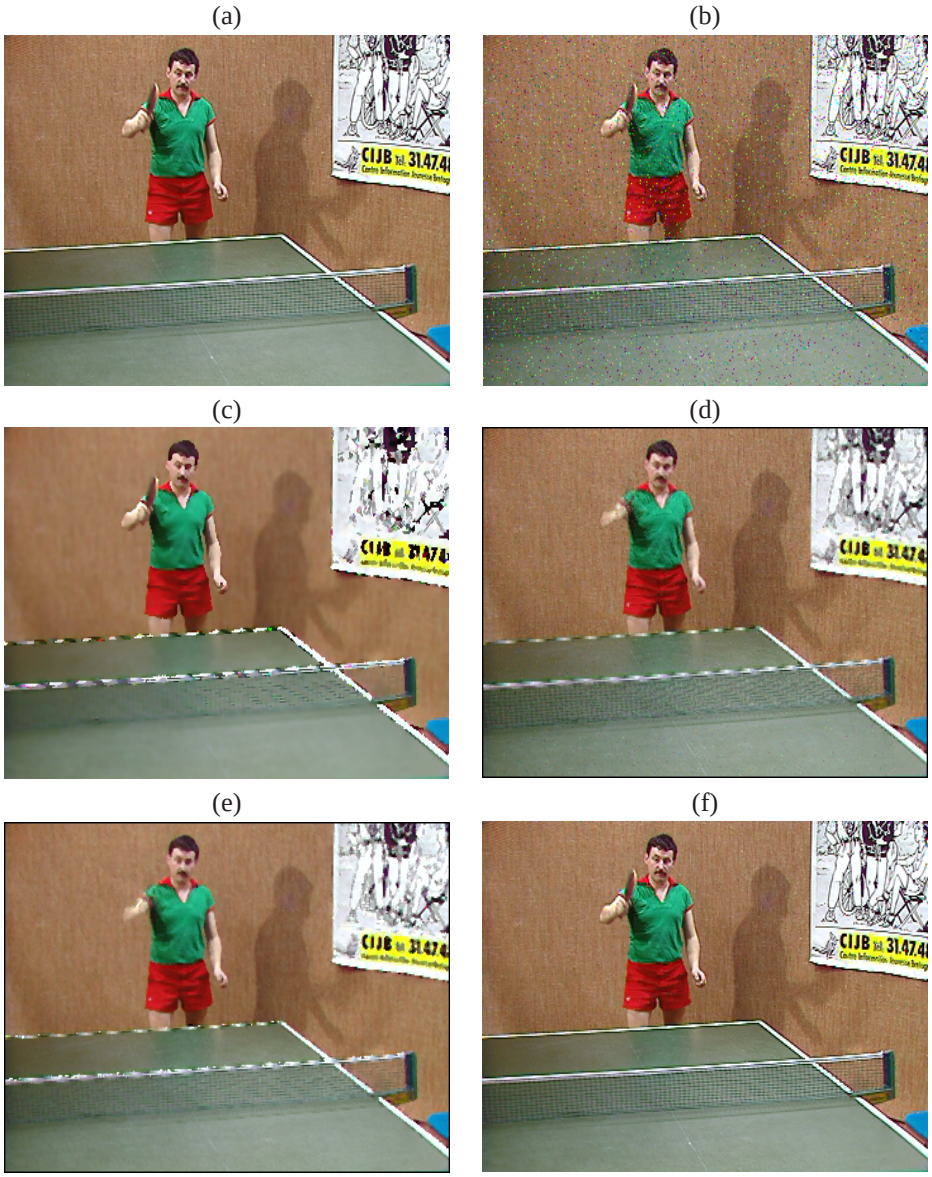

Figure 6.7: 110-th frame of the "Tennis" sequence: (a) original, (b) noisy ($pr = 5\%$), (c) INRC, (d) AVMF, (e) VAVDMF and (f) Proposed.

Figure 6.8: 20-th frame of the "Deadline" sequence: (a) original, (b) noisy ($pr = 25\%$), (c) INRC, (d) AVMF, (e) VAVDMF and (f) Proposed.

Part III

Interval-valued Fuzzy Mathematical Morphology

7
From Binary to Interval-valued Fuzzy Mathematical Morphology

Many theories have been developed in the domain of image processing to extract specific information from images such as edges, patterns, ... One of these theories is mathemathical morphology, in which an image is transformed into another image by a morphological operator, using a structuring element. The basic morphological operators used for such transformation are the dilation, erosion, opening and closing. Further, the structuring element is usually very small compared to the given image and can be chosen by the user in function of the desired goal. Mathematical morphology was originally developed for binary (black-white) images [126], and was later extended to greyscale images by two different approaches: (i) the threshold approach [126] and (ii) the umbra approach [44]. In the first approach, the structuring element still has to be binary; in the second approach, also greyscale structuring elements are allowed. Later, a third approach was introduced, inspired on the observation that greyscale images and fuzzy sets are modeled in the same way (i.e., as mappings from a universe $\mathcal{U}$ into the unit interval $[0, 1]$): fuzzy mathematical morphology [29, 113, 132]. Recently, also extensions of fuzzy mathematical morphology started to get attention [8, 9, 103, 104]. In this thesis, we concentrate on an extension based on interval-valued fuzzy set theory. A pixel is now mapped onto an interval of grey levels instead of onto one specific grey level, in this way allowing uncertainty regarding the measured grey levels.

The structure of this chapter is as follows: the different basic morphological operators for binary images and structuring elements are introduced in Section 7.1. These concepts are then extended to greyscale images and structuring elements in Section 7.2 by the thresh-

old approach (7.2.1), the umbra approach (7.2.2) and the fuzzy approach (7.2.3). Finally, fuzzy mathematical morphology is further extended to interval-valued fuzzy mathematical morphology in Section 7.3, where we will also discuss some basic properties of the morphological operators.

7.1 Binary Mathematical Morphology

The basic morphological operators are the dilation, erosion, opening and closing. For a binary image $A \subseteq \mathbb{R}^n$ and a binary structuring element $B \subseteq \mathbb{R}^n$, they are defined as follows [1]:

Definition 7.1. [126] *Let $A, B \subseteq \mathbb{R}^n$. The binary dilation $D(A,B)$, the binary erosion $E(A,B)$, the binary closing $C(A,B)$ and the binary opening $O(A,B)$ are the sets given by:*

$$\begin{aligned} D(A,B) &= \{y | y \in \mathbb{R}^n \text{ and } T_y(B) \cap A \neq \emptyset\}, \\ E(A,B) &= \{y | y \in \mathbb{R}^n \text{ and } T_y(B) \subseteq A\}, \\ C(A,B) &= E(D(A,B),-B), \\ O(A,B) &= D(E(A,B),-B), \end{aligned}$$

where the translation $T_y(B)$ of B by the vector $y \in \mathbb{R}^n$ is defined as $T_y(B) = \{x \in \mathbb{R}^n | x - y \in B\}$, and the reflection $-B$ of B is given by $-B = \{-b | b \in B\}$.

The definitions of the binary dilation and erosion are illustrated in Fig. 7.1.

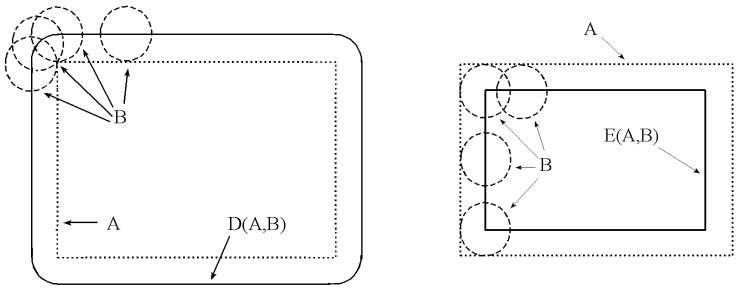

Figure 7.1: Geometrical interpretation of the binary dilation (left) and erosion (right). The centre of the structuring element B coincides with the origin of the coordinate system.

The binary closing and opening are combinations of the dilation and erosion. Explicit expressions for the closing and opening are given as follows:

$$C(A,B) = \{y | y \in \mathbb{R}^n \text{ and } T_y(-B) \subseteq D(A,B)\}$$

[1] Remark that also another definition for the dilation and closing is frequently used in literature (e.g. [44]). In those definitions $-B$ is used instead of B.

$$
\begin{aligned}
&= \{y | y \in \mathbb{R}^n \text{ and } (\forall z \in \mathbb{R}^n)(z \in T_y(-B) \Rightarrow T_z(B) \cap A \neq \emptyset)\} \\
&= \{y | y \in \mathbb{R}^n \text{ and } (\forall z \in \mathbb{R}^n)(y \in T_z(B) \Rightarrow T_z(B) \cap A \neq \emptyset)\}, \\
O(A,B) &= \{y | y \in \mathbb{R}^n \text{ and } T_y(-B) \cap E(A,B) \neq \emptyset\} \\
&= \{y | y \in \mathbb{R}^n \text{ and } (\exists z \in \mathbb{R}^n)(z \in T_y(-B) \text{ and } T_z(B) \subseteq A)\} \\
&= \{y | y \in \mathbb{R}^n \text{ and } (\exists z \in \mathbb{R}^n)(y \in T_z(B) \text{ and } T_z(B) \subseteq A)\}.
\end{aligned}
$$

Further, the dilation and erosion can also be written as:

$$
\begin{aligned}
D(A,B) &= \{y | y \in \mathbb{R}^n \text{ and } (\exists b \in B)(y + b \in A)\} \\
&= \bigcup_{b \in B} T_{-b}(A), \\
E(A,B) &= \{y | y \in \mathbb{R}^n \text{ and } (\forall b \in B)(y + b \in A)\} \\
&= \bigcap_{b \in B} T_{-b}(A).
\end{aligned}
$$

As an example, the binary dilation and erosion of a binary image by the structuring element $B = \begin{pmatrix} 1 & 1 & 1 \\ 1 & \underline{1} & 1 \\ 1 & 1 & 1 \end{pmatrix}$ (the underlined element corresponds to the origin in the coordinate system) are depicted in Fig. 7.2. It can be seen that a dilation enlarges objects in the image while the erosion reduces them.

For a list of basic properties of the binary morphological operators, we refer to [93, 126]. One of those properties, that can be deduced from the above is that it will always hold that $E(A,B) \subseteq D(A,B)$. As a consequence the image $D(A,B) \setminus E(A,B)$, that we call the (binary) morphological gradient $G^B(A)$, can serve as an edge image of A. This morphological gradient is illustrated in Fig. 7.3 for the original image and its dilation and erosion depicted in Fig. 7.2. More examples of practical applications of mathematical morphology can be found in [127, 129].

7.2 Greyscale Mathematical Morphology

Binary morphology was extended to greyscale images in different ways. The threshold approach [126] was a first effort, in which the structuring element still had to be binary. The umbra approach [44] also allowed greyscale structuring elements, but had as drawback that the result of a morphological operation on an $\mathbb{R}^n - [0,1]$ mapping (such as a greyscale image) is not always an $\mathbb{R}^n - [0,1]$ mapping. The third main approach is the fuzzy approach [29, 113, 132], in which none of the two above mentioned shortcomings form a problem anymore.

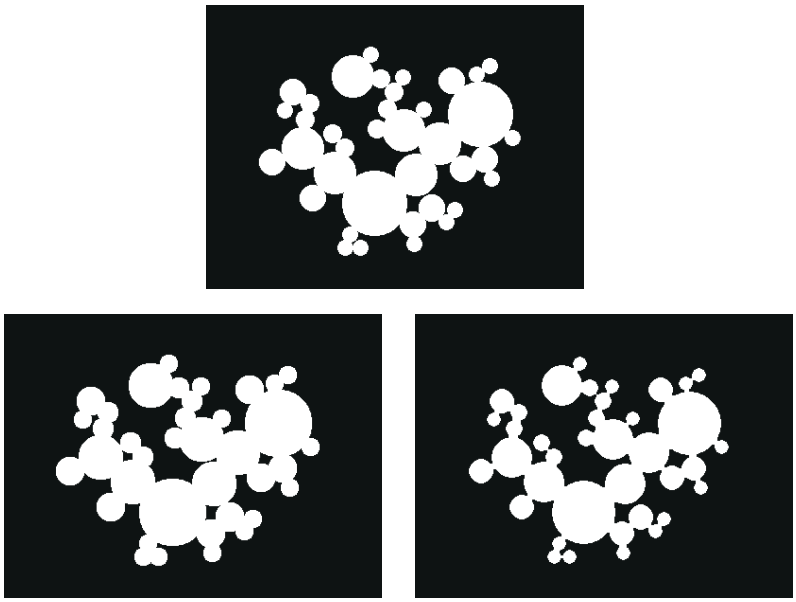

Figure 7.2: The original binary image (top), the binary dilation (bottom left) and the binary erosion (bottom right) for the given structuring element B.

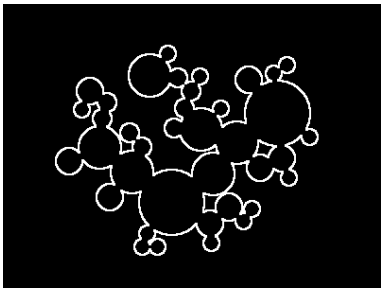

Figure 7.3: The binary morphological gradient image of the image in Fig. 7.2.

7.2.1 The Threshold Approach

The class of mappings from $\mathbb{R}^n$ onto $[0,1]$ coincides with the class of fuzzy sets on $\mathbb{R}^n$. So for an $\mathbb{R}^n - [0,1]$ mapping f, we can define a weak α-cut analogously as for fuzzy sets as $f_\alpha = \{x \in \mathbb{R}^n | f(x) \geq \alpha\}$. Then it will also hold that $f(x) = sup\{\alpha \in]0,1] | x \in f_\alpha\}$. Further, in analogy to the support of a fuzzy set, we write $d_f = \{x \in \mathbb{R}^n | f(x) > 0\}$.

The binary morphological operators are then extended to greyscale images by applying the binary operators on each weak α-cut ($\alpha \in]0,1]$) of the greyscale image (Fig. 7.4). For a greyscale image A and a binary structuring element B this becomes:

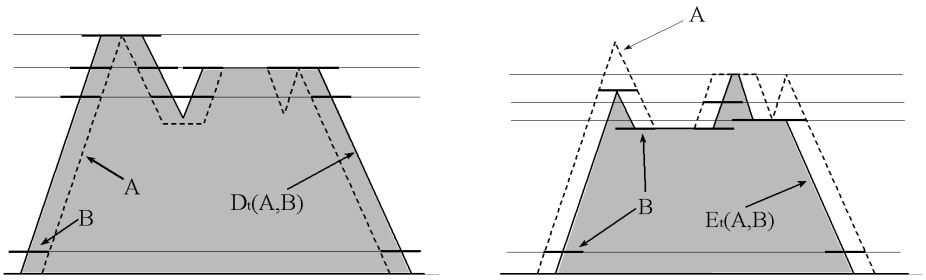

Figure 7.4: Example of the construction of the t-dilation (left) and the t-erosion (right) ($n = 1$).

$$\begin{aligned} D_t(A,B)(y) &= \sup\{\alpha \in]0,1] | y \in D(A_\alpha, B)\} \\ &= \sup\{\alpha \in]0,1] | (\exists x \in B)(y + x \in A_\alpha)\} \\ &= \sup\{\alpha \in]0,1] | (\exists x \in T_y(B))(x \in A_\alpha)\} \\ &= \sup\{\alpha \in]0,1] | (\exists x \in T_y(B) \cap d_A)(A(x) \geq \alpha)\} \\ &= \sup\{A(x) | x \in T_y(B) \cap d_A\}, \end{aligned}$$

$$\begin{aligned} E_t(A,B)(y) &= \sup\{\alpha \in]0,1] | y \in E(A_\alpha, B)\} \\ &= \sup\{\alpha \in]0,1] | (\forall x \in B)(y + x \in A_\alpha)\} \\ &= \sup\{\alpha \in]0,1] | (\forall x \in T_y(B))(x \in A_\alpha)\} \\ &= \sup\{\alpha \in]0,1] | (\forall x \in T_y(B))(A(x) \geq \alpha)\} \\ &= \inf\{A(x) | x \in T_y(B)\}, \end{aligned}$$

Definition 7.2. [126] *Let A be a greyscale image and B a binary structuring element. The t-dilation $D_t(A,B)$, the t-erosion $E_t(A,B)$, the t-closing $C_t(A,B)$ and the t-opening*

$O_t(A,B)$ are the greyscale images given for all $y \in \mathbb{R}^n$ by:

$$\begin{aligned} D_t(A,B)(y) &= \sup_{x \in T_y(B) \cap d_A} A(x) \\ E_t(A,B)(y) &= \inf_{x \in T_y(B)} A(x) \\ C_t(A,B)(y) &= E_t(D_t(A,B), -B)(y), \\ O_t(A,B)(y) &= D_t(E_t(A,B), -B)(y), \end{aligned}$$

where the translation $T_y(B)$ of B by the vector $y \in \mathbb{R}^n$ is defined as $T_y(B) = \{x \in \mathbb{R}^n | x - y \in B\}$, and the reflection $-B$ of B is given by $-B = \{-b | b \in B\}$.

As an example, the t-dilation and t-erosion of the greyscale camera image by the structuring element $B = \begin{pmatrix} 1 & 1 & 1 \\ 1 & \underline{1} & 1 \\ 1 & 1 & 1 \end{pmatrix}$ are depicted in Fig. 7.5. It can be seen that a dilation brightens objects in the image while the erosion makes them darker.

For a list of basic properties of the t-morphological operators, we refer to [93, 126].

7.2.2 The Umbra Approach

In this approach, the result of the morphological operators on $\mathbb{R}^n - [0,1]$ mappings is not necessarily an $\mathbb{R}^n - [0,1]$ mapping, but can also be e.g. an $\mathbb{R}^n - [-1,1]$ (as we will see for the erosion). Therefore, in the umbra-approach, greyscale images are modelled as $\mathbb{R}^n - \overline{\mathbb{R}}$ mappings [2] instead of $\mathbb{R}^n - [0,1]$ mappings as we usually do. By agreement, now $A(x) = -\infty$ (instead of $A(x) = 0$ (see Chapter 2)) for elements $x \in \mathbb{R}^n$ for which the image A is originally not defined. So, for the support we get $d_f = \{x \in \mathbb{R}^n | f(x) > -\infty\}$ for an $\mathbb{R}^n - \overline{\mathbb{R}}$ mapping f.

Remark that the points below or above the graph of an $\mathbb{R}^n - \overline{\mathbb{R}}$ mapping are crisp subsets of $\mathbb{R}^{n+1}$ (i.e., binary $n+1$-dimensional images). Such subsets are respectively called umbras (below) and dual umbras (above). For a greyscale image A and greyscale structuring element B, the u-dilation is now defined as the surface of the binary dilation of the umbra of A by the dual umbra of B. Analogously, the u-erosion is the surface of the binary erosion of the umbra of A by the umbra of B (Fig. 7.6). For more details, we refer to [44, 93]. The resulting explicit expressions are as follows:

Definition 7.3. [*44*] *Let A be a greyscale image and B a greyscale structuring element. The u-dilation $D_u(A,B)$, the u-erosion $E_u(A,B)$, the u-closing $C_u(A,B)$ and the u-opening $O_u(A,B)$ are the greyscale images given for all $y \in \mathbb{R}^n$ by:*

$$\begin{aligned} D_u(A,B)(y) &= \sup_{x \in T_y(d_B) \cap d_A} A(x) + B(x-y), \\ E_u(A,B)(y) &= \inf_{x \in T_y(d_B)} A(x) - B(x-y), \end{aligned}$$

[2] The notation $\overline{\mathbb{R}}$ here stands for $\overline{\mathbb{R}} = \mathbb{R} \cup \{-\infty, +\infty\}$.

Figure 7.5: The original camera image (top), the t-dilation (bottom left) and the t-erosion (bottom right) for the given structuring element B.

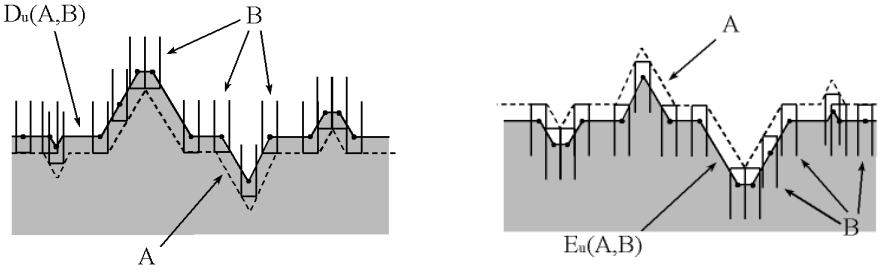

Figure 7.6: Example of the construction of the u-dilation (left) and the u-erosion (right) ($n = 1$).

$$\begin{aligned} C_u(A,B)(y) &= E_u(D_u(A,B),-B)(y), \\ O_u(A,B)(y) &= D_u(E_u(A,B),-B)(y), \end{aligned}$$

where the translation $T_y(d_B)$ of B by the vector $y \in \mathbb{R}^n$ is defined as $T_y(d_B) = \{x \in \mathbb{R}^n | x - y \in d_B\}$, and the reflection $-B$ of B is given by $(-B)(x) = B(-x),\ \forall x \in \mathbb{R}^n$.

It can be checked that if A and B are both $\mathbb{R}^n - [0,1]$ functions, then $D_u(A,B)$ and $E_u(A,B)$ are respectively $\mathbb{R}^n - [0,2]$ and $\mathbb{R}^n - [-1,1]$ functions.

As an example, the (rescaled) u-dilation and u-erosion of the original camera image (Fig. 7.5) by the structuring element $B = \begin{pmatrix} 0.86 & 0.86 & 0.86 \\ 0.86 & \underline{1} & 0.86 \\ 0.86 & 0.86 & 0.86 \end{pmatrix}$ are depicted in Fig. 7.7. It can be seen that a dilation brightens objects in the image while the erosion makes them darker.

Figure 7.7: The u-dilation (left) and the u-erosion (right) of the camera image for the given structuring element B.

For a list of basic properties of the u-morphological operators, we refer to [44, 93].

7.2.3 Fuzzy Mathematical Morphology

Since greyscale images are modelled by $\mathbb{R}^n - [0,1]$ mappings, they can be seen as fuzzy sets on $\mathbb{R}^n$. So, to extend the binary operators to greyscale images, the binary intersection and inclusion (that are clearly quite important in the definition of the binary operators) can be extended to a fuzzy intersection and inclusion measure. This is done by fuzzifying the underlying logical operators, i.e., the conjunction and the implication on $\{0,1\}$. As we have seen in Chapter 1, the fuzzification of these operators are respectively given by a conjunctor

and an implicator on the unit interval [3] [4]. For a conjunctor $\mathcal{C}$ and an implicator $\mathcal{I}$ on $[0,1]$, it can be checked that the measures $Inc_{\mathcal{I}}$ and $Int_{\mathcal{C}}$, given for all fuzzy sets A and B in a universe X by

$$\begin{aligned} Inc_{\mathcal{I}}(A,B) &= \inf_{x\in X} \mathcal{I}(A(x),B(x)), \\ Int_{\mathcal{C}}(A,B) &= \sup_{x\in X} \mathcal{C}(A(x),B(x)), \end{aligned}$$

respectively extend the binary inclusion and intersection (i.e., for crisp sets A and B, $Inc_{\mathcal{I}}(A,B) = 1$ if $A \subseteq B$ and $Inc_{\mathcal{I}}(A,B) = 0$ if $A \not\subseteq B$ and $Int_{\mathcal{C}}(A,B) = 1$ if $A \cap B \neq \emptyset$ and $Int_{\mathcal{C}}(A,B) = 0$ if $A \cap B = \emptyset$).

For $A, B \in \mathcal{F}(\mathbb{R}^n)$, we then get:

$$\begin{aligned} D_{\mathcal{C}}(A,B)(y) &= Int_{\mathcal{C}}(T_y(B),A) \\ &= \sup_{x\in\mathbb{R}^n} \mathcal{C}((T_y(B))(x),A(x)) \\ &= \sup_{x\in\mathbb{R}^n} \mathcal{C}(B(x-y),A(x)) \\ &= \sup_{x\in T_y(d_B)\cap d_A} \mathcal{C}(B(x-y),A(x)), \end{aligned}$$

and

$$\begin{aligned} E_{\mathcal{I}}(A,B)(y) &= Inc_{\mathcal{I}}(T_y(B),A) \\ &= \inf_{x\in\mathbb{R}^n} \mathcal{I}((T_y(B))(x),A(x)) \\ &= \inf_{x\in\mathbb{R}^n} \mathcal{I}(B(x-y),A(x)) \\ &= \inf_{x\in T_y(d_B)} \mathcal{I}(B(x-y),A(x)). \end{aligned}$$

Definition 7.4. [29] *Let $\mathcal{C}$ be a conjunctor on $[0,1]$, $\mathcal{I}$ an implicator on $[0,1]$, and $A, B \in \mathcal{F}(\mathbb{R}^n)$. The fuzzy dilation $D_{\mathcal{C}}(A,B)$ and erosion $E_{\mathcal{I}}(A,B)$ are the fuzzy sets in $\mathbb{R}^n$ defined for all $y \in \mathbb{R}^n$ by (where $T_y(d_B) = \{x \in \mathbb{R}^n | x - y \in d_B\}$ and $(-B)(x) = B(-x),\ \forall x \in \mathbb{R}^n$):*

$$D^I_{\mathcal{C}}(A,B)(y) = \sup_{x\in T_y(d_B)\cap d_A} \mathcal{C}(B(x-y),A(x)),$$

[3] Remark that this approach is very general and is only based on generalizing the underlying logical framework. The resulting dilations and erosions are thus not a priori connected. Some authors also require the dilation and erosion to be dual [11] or to form an adjunction as in the algebraic framework in [33, 94]. Such connection can be translated into a connection between the underlying logical operators, i.e., the used conjunctor and implicator. If further also stronger morphological properties such as the commutativity and the iterativity of the dilation are required, the conjunctors will need to be restricted to t-norms [10].

[4] In [96] it is shown that fuzzy mathematical morphology is compatible with binary morphology and that fuzzy mathematical morphology is compatible with greyscale morphology based on the threshold approach if we restrict ourselves to semi-norms and border implicators.

$$\begin{aligned} E^I_{\mathcal{I}}(A,B)(y) &= \inf_{x \in T_y(d_B)} \mathcal{I}(B(x-y), A(x)), \\ C_{\mathcal{C},\mathcal{I}}(A,B)(y) &= E_{\mathcal{I}}(D_{\mathcal{C}}(A,B), -B)(y), \\ O_{\mathcal{C},\mathcal{I}}(A,B)(y) &= D_{\mathcal{C}}(E_{\mathcal{I}}(A,B), -B)(y). \end{aligned}$$

Remark that if $y \notin D(d_A, d_B)$, then $D_{\mathcal{C}}(A,B)(y) = 0$.

As an example, the fuzzy dilation and erosion (where the minimum operator and the Kleene-Dienes operator were used as conjunctor and implicator respectively) of the original camera image (Fig. 7.5) by the structuring element $B = \begin{pmatrix} 0.86 & 0.86 & 0.86 \\ 0.86 & \underline{1} & 0.86 \\ 0.86 & 0.86 & 0.86 \end{pmatrix}$ are depicted in Fig. 7.8. It can be seen that a dilation brightens objects in the image while the erosion makes them darker.

Figure 7.8: The fuzzy dilation (left) and erosion (right) (where the minimum operator and the Kleene-Dienes operator were used as conjunctor and implicator respectively) of the camera image for the given structuring element B.

For the basic properties of the morphological operators in this approach, we refer to [29, 93].

7.3 Interval-valued Fuzzy Mathematical Morphology

Recently, fuzzy mathematical morphology has been further extended to extensions of fuzzy sets ($\mathcal{L}$-fuzzy sets) by extending the fuzzy logical operators on $([0,1], \leq)$ to $\mathcal{L} = (L, \leq_L)$. In this work, we will focus on the extension based on interval-valued fuzzy set theory. Before introducing the interval-valued fuzzy morphological operators and their basic properties, we first discuss the interpretation of images that correspond to interval-valued fuzzy sets [103].

7.3.1 Interval-valued Images

As discussed in Chapter 2, binary and greyscale images can respectively be seen as crisp sets and fuzzy sets in $\mathbb{R}^n$. Interval-valued images now have the same representation as interval-valued fuzzy sets, which allows us to apply techniques from interval-valued fuzzy set theory on them (e.g. to define the interval-valued fuzzy morphological operators). For such images, a pixel in the image domain is no longer mapped onto one specific grey value, but onto an interval of grey values to which the grey value is expected to belong (a closed subinterval of $[0, 1]$). The grey levels of the pixels in a greyscale image namely can be uncertain. Firstly, in any device, the captured grey levels are rounded up or down to an element of a finite set of allowed values. Further, uncertainty may also arise when several takes of an image result in different grey levels for some of the pixels. This is sometimes the case under identical recording circumstances and can certainly be expected under variable circumstances such as illumination changes due to clouds covering the sun, ... Also, the camera or an object in the scenery can slightly shift position in between takes, which might result in large differences (uncertainty) in the measured grey level of pixels. Especially pixels at the edge of an object will suffer from this. Finally, in the context of mathematical morphology, there might also exist uncertainty regarding the grey levels in the structuring element that is used. This structuring element can be chosen by the user, but in some cases he might not be completely sure how to estimate the importance or thus weight that is assigned to a pixel in this structuring element. In this case, the use of intervals to which the value is likely to belong instead of choosing one specific value, might offer a solution.

In Fig. 7.9, three different takes of the camera image scene are given: a cloudy, a sunny and a slightly shifted take. Due to different recording circumstances and a shift in position of the objects in the image, there is uncertainty concerning the grey values in the image. To take this uncertainty into account, an interval-valued image can be constructed as follows. The lower bound (respectively the upper bound) of the intervals to which the grey value of a pixel is expected to belong is chosen as the lowest (respectively the highest) grey level over the three takes. These lower bound and upper bound image are given in Fig. 7.10 together with a representation of the difference between the two. The larger this difference (more white in the difference image), the wider the corresponding interval and the larger the uncertainty at the considered pixel position.

Remark that also other interpretations are possible. The image does not need to represent a natural scene, but it can e.g. also represent a degree to which a certain property is satisfied at a certain location. If there is uncertainty concerning that degree, intervals can be used. Remark further that since interval-valued fuzzy set theory is equivalent to intuitionistic and bipolar fuzzy set theory, all results of interval-valued morphology can be translated to the equivalent morphologies. For an interpretation of bipolar fuzzy images, we refer to [8, 9].

As a side-note, we would like to mention that also in other image processing problems such as inverse halftoning [13], as well as in the context of wavelets [12], interval-valued representations occur in a natural way. They have also found to be useful in edge detection applications [5]. Further, imprecision in grey levels is also considered in [108].

Figure 7.9: Three different takes on the camera image: cloudy (upper), sunny (middle) and shifted (lower).

Figure 7.10: Lower bound image (upper), upper bound image (middle) and difference image (lower) of the interval-valued camera image.

7.3.2 The Interval-valued Fuzzy Morphological Operators

The fuzzy morphological operators can be further extended to interval-valued fuzzy sets by extending the logical operators from $[0,1]$ to $\mathcal{L}^I$.

Definition 7.5. [8] *Let $\mathcal{C}$ be a conjunctor on $\mathcal{L}^I$, let $\mathcal{I}$ be an implicator on $\mathcal{L}^I$, and let $A, B \in \mathcal{F}_{\mathcal{L}^I}(\mathbb{R}^n)$. The interval-valued fuzzy dilation $D^I_{\mathcal{C}}(A,B)$ and erosion $E^I_{\mathcal{I}}(A,B)$ are the interval-valued fuzzy sets in $\mathbb{R}^n$ defined by (where $T_y(d_B) = \{x \in \mathbb{R}^n | x - y \in d_B\}$)*

$$D^I_{\mathcal{C}}(A,B)(y) = \sup_{x \in T_y(d_B) \cap d_A} \mathcal{C}(B(x-y), A(x)), \forall y \in \mathbb{R}^n, \tag{7.1}$$

and

$$E^I_{\mathcal{I}}(A,B)(y) = \inf_{x \in T_y(d_B)} \mathcal{I}(B(x-y), A(x)), \forall y \in \mathbb{R}^n. \tag{7.2}$$

Remark that if $y \notin D(d_A, d_B)$, then $D^I_{\mathcal{C}}(A,B)(y) = 0_{\mathcal{L}^I}$.

With the reflection $-B$ of an interval-valued fuzzy set B in $\mathbb{R}^n$ defined as $(-B)(x) = B(-x), \forall x \in \mathbb{R}^n$, the definitions of the interval-valued fuzzy closing and fuzzy opening are then given by:

Definition 7.6. *Let $\mathcal{C}$ be a conjunctor on $\mathcal{L}^I$, let $\mathcal{I}$ be an implicator on $\mathcal{L}^I$, and let $A, B \in \mathcal{F}_{\mathcal{L}^I}(\mathbb{R}^n)$. The interval-valued fuzzy closing $C^I_{\mathcal{C},\mathcal{I}}(A,B)$ and interval-valued fuzzy opening $O^I_{\mathcal{C},\mathcal{I}}(A,B)$ are the interval-valued fuzzy sets in $\mathbb{R}^n$ given by:*

$$C^I_{\mathcal{C},\mathcal{I}}(A,B) = E^I_{\mathcal{I}}(D^I_{\mathcal{C}}(A,B), -B), \tag{7.3}$$

$$O^I_{\mathcal{C},\mathcal{I}}(A,B) = D^I_{\mathcal{C}}(E^I_{\mathcal{I}}(A,B), -B). \tag{7.4}$$

As discussed in Chapter 2, to process images on a computer or any other device, in practice a two-fold sampling of the images is needed: the image domain is sampled down from $\mathbb{R}^n$ to $\mathbb{Z}^n$ and the grey levels are sampled down from the unit interval $[0,1]$ to a finite subchain of it. As a consequence, the greyscale intervals used for interval-valued images, will in practice belong to the finite sublattice $\mathcal{L}^I_{r,s} = (L^I_{r,s}, \leq_{\mathcal{L}^I})$ of $\mathcal{L}^I$, with $L^I_{r,s} = \{[\frac{r-k}{r-1}, \frac{s-l}{s-1}] | k,l \in \mathbb{Z} \text{ and } 1 \leq k \leq r \text{ and } 1 \leq l \leq s\}$ for given integers r and s ($r, s \in \mathbb{N} \setminus \{0,1\}$)[5]. So, in practice interval-valued images can be seen as belonging to the class of all interval-valued fuzzy sets in $\mathbb{Z}^n$ with membership intervals in $L^I_{r,s}$, which we will denote by $\mathcal{F}_{\mathcal{L}^I_{r,s}}(\mathbb{Z}^n)$. If an interval-valued fuzzy set A belongs to $\mathcal{F}_{\mathcal{L}^I_{r,s}}(\mathbb{Z}^n)$, then, $\forall x \in \mathbb{Z}^n$, $A_1(x) \in I_r = \{\frac{r-k}{r-1} | k \in \mathbb{Z} \text{ and } 1 \leq k \leq r\}$. Analogously the upper bound $A_2(x) \in I_s = \{\frac{s-l}{s-1} | l \in \mathbb{Z} \text{ and } 1 \leq l \leq s\}$.

Due to the characterization of the supremum and the infimum, sometimes stronger properties will hold in the practical discrete framework than in the theoretical continuous framework. This will for example be the case for the decomposition and construction properties

[5] Remark that usually $r = s$, since the lower and upper bound of the intervals both represent allowed grey levels on the same device.

discussed in Chapters 8 and 9. Therefore we will here give the explicit discrete definitions of the interval-valued fuzzy morphological operators. Remark that the definitions of negators, conjunctors and implicators on the lattice $\mathcal{L}^I_{r,s} = (L^I_{r,s}, \leq_{L^I})$ are analogous to the corresponding definitions on $\mathcal{L}^I = (L^I, \leq_{L^I})$ (where now $L^I_{r,s}$ takes the role of L^I). However, not every operator on $\mathcal{L}^I$ has a corresponding operator on $\mathcal{L}^I_{r,s}$. The conjunctor $\mathcal{C}$, given by $\mathcal{C}(x, y) = [x_1 \cdot y_1, x_2 \cdot y_2]$ for all $x, y \in L^I$, for example, is not defined on $\mathcal{L}^I_{r,s}$ due to the fact that the interval with as lower and upper bound the product of respectively the lower and upper bounds of two elements of $L^I_{r,s}$ does not necessarily belong to $L^I_{r,s}$.

The definitions of the discrete interval-valued fuzzy dilation and erosion can now be written as follows:

Definition 7.7. *Let $\mathcal{C}$ be a conjunctor on $\mathcal{L}^I_{r,s}$, let $\mathcal{I}$ be an implicator on $\mathcal{L}^I_{r,s}$, and let $A, B \in \mathcal{F}_{\mathcal{L}^I_{r,s}}(\mathbb{Z}^n)$. The discrete interval-valued fuzzy dilation $D^I_{\mathcal{C}}(A, B) \in \mathcal{F}_{\mathcal{L}^I_{r,s}}(\mathbb{Z}^n)$ is for all $y \in \mathbb{Z}^n$ defined by:*

$$\begin{aligned} D^I_{\mathcal{C}}(A,B)(y) &= \sup_{x \in T_y(d_B) \cap d_A} \mathcal{C}(B(x-y), A(x)) \\ &= [\max_{x \in T_y(d_B) \cap d_A} \mathcal{C}(B(x-y), A(x))_1, \\ &\quad \max_{x \in T_y(d_B) \cap d_A} \mathcal{C}(B(x-y), A(x))_2]. \end{aligned}$$

(For $y \notin D(d_A, d_B)$, $D^I_{\mathcal{C}}(A, B)(y) = 0_{\mathcal{L}^I}$.)
The discrete interval-valued fuzzy erosion $E^I_{\mathcal{I}}(A, B) \in \mathcal{F}_{\mathcal{L}^I_{r,s}}(\mathbb{Z}^n)$ is for all $y \in \mathbb{Z}^n$ defined by:

$$\begin{aligned} E^I_{\mathcal{I}}(A,B)(y) &= \inf_{x \in T_y(d_B)} \mathcal{I}(B(x-y), A(x)) \\ &= [\min_{x \in T_y(d_B)} \mathcal{I}(B(x-y), A(x))_1, \\ &\quad \min_{x \in T_y(d_B)} \mathcal{I}(B(x-y), A(x))_2]. \end{aligned}$$

As an example, the interval-valued fuzzy dilation (where the conjunctor $\mathcal{C}_{\min}$ was used) of the original camera image (Fig. 7.10) by the structuring element

$$B = \begin{pmatrix} [0.6, 0.8] & [0.7, 0.9] & [0.6, 0.8] \\ [0.7, 0.9] & \underline{[1, 1]} & [0.7, 0.9] \\ [0.6, 0.8] & [0.7, 0.9] & [0.6, 0.8] \end{pmatrix}, \tag{7.5}$$

(where the underlined element corresponds to the origin) is depicted in Fig. 7.11. It can be seen that the dilation brightens objects in the image. Analogously, an erosion will darken them.

Figure 7.11: Lower bound image (upper), upper bound image (middle) and difference image (lower) of the dilated interval-valued camera image.

7.3.3 Basic Properties of the Interval-valued Fuzzy Morphological Operators

This subsection gives an overview of the basic properties of the interval-valued fuzzy morphological operators: monotonicity, expansivity and restrictivity, interaction with the intersection and union of images and structuring elements, duality, adjointness and idempotence [84]. These properties are mostly analogous to those of the fuzzy morphological operators [29, 93]. However, in some cases stronger conditions are required or less strong results are found. In the following, A, A_1, A_2 and B, B_1, B_2 represent interval-valued fuzzy sets in the universe $\mathbb{R}^n$. A, A_1, A_2 are model for interval-valued images, B, B_1, B_2 are model for interval-valued structuring elements.

Monotonicity

Proposition 7.3.1. *Let $\mathcal{C}_1, \mathcal{C}_2$ be conjunctors and $\mathcal{I}_1, \mathcal{I}_2$ implicators on $\mathcal{L}^I$.*

(i) If $\mathcal{C}_1 \leq_{L^I} \mathcal{C}_2$, then $D^I_{\mathcal{C}_1}(A,B) \subseteq D^I_{\mathcal{C}_2}(A,B)$.

(ii) If $\mathcal{I}_1 \leq_{L^I} \mathcal{I}_2$, then $E^I_{\mathcal{I}_1}(A,B) \subseteq E^I_{\mathcal{I}_2}(A,B)$.

Proof. As an example, we prove (i).
For all $y \in \mathbb{R}^n$

$$\begin{aligned} D^I_{\mathcal{C}_1}(A,B)(y) &= \sup_{x \in T_y(d_B) \cap d_A} \mathcal{C}_1(B(x-y), A(x)) \\ &\leq_{L^I} \sup_{x \in T_y(d_B) \cap d_A} \mathcal{C}_2(B(x-y), A(x)) \\ &= D^I_{\mathcal{C}_2}(A,B)(y) \end{aligned}$$

□

Proposition 7.3.2. *Let $\mathcal{C}$ be a conjunctor and $\mathcal{I}$ be an implicator on $\mathcal{L}^I$. If $A_1 \subseteq A_2$ and $B_1 \subseteq B_2$, then:*

$$\begin{array}{lrcl} \textit{(i)} & D^I_{\mathcal{C}}(A_1,B) & \subseteq & D^I_{\mathcal{C}}(A_2,B), \\ \textit{(ii)} & E^I_{\mathcal{I}}(A_1,B) & \subseteq & E^I_{\mathcal{I}}(A_2,B), \\ \textit{(iii)} & D^I_{\mathcal{C}}(A,B_1) & \subseteq & D^I_{\mathcal{C}}(A,B_2), \\ \textit{(iv)} & E^I_{\mathcal{I}}(A,B_1) & \supseteq & E^I_{\mathcal{I}}(A,B_2). \end{array}$$

Proof. As an example, we prove (i).
For all $y \in \mathbb{R}^n$

$$\begin{aligned} D^I_{\mathcal{C}}(A_1,B)(y) &= \sup_{x \in T_y(d_B) \cap d_{A_1}} \mathcal{C}(B(x-y), A_1(x)) \\ &\leq_{L^I} \sup_{x \in T_y(d_B) \cap d_{A_2}} \mathcal{C}(B(x-y), A_2(x)) \end{aligned}$$

$$= \quad D^I_{\mathcal{C}}(A_2, B)(y)$$

□

The above properties say that if an image is brightened (i.e., when the grey values are increased), then the dilated and eroded images will be brightened as well. On the other hand, if we brighten the structuring element, then also the dilated image will be brightened but the eroded image will be darkened.

For the interval-valued fuzzy opening and closing the monotonicity properties w.r.t. the image follow immediately from those of the dilation and the erosion. However, due to the opposite inclusions for the dilation and erosion in the properties w.r.t. the structuring element, no such properties hold for the opening and closing.

Proposition 7.3.3. *Let $\mathcal{C}$ be a conjunctor and $\mathcal{I}$ be an implicator on $\mathcal{L}^I$. If $A_1 \subseteq A_2$, then:*

$$\begin{array}{lrcl} \textit{(i)} & O^I_{\mathcal{C},\mathcal{I}}(A_1, B) & \subseteq & O^I_{\mathcal{C},\mathcal{I}}(A_2, B), \\ \textit{(ii)} & C^I_{\mathcal{C},\mathcal{I}}(A_1, B) & \subseteq & C^I_{\mathcal{C},\mathcal{I}}(A_2, B). \end{array}$$

Proof. Follows from Proposition 7.3.2. □

Expansivity and Restrictivity

The following proposition shows that, under a very general condition on the structuring element, the interval-valued dilation and erosion are respectivley expansive and restrictive.

Proposition 7.3.4. *Let $\mathcal{C}$ be a semi-norm and $\mathcal{I}$ be a border implicator on $\mathcal{L}^I$. If $B(\mathbf{0}) = 1_{\mathcal{L}^I}$, then:*

$$E^I_{\mathcal{I}}(A, B) \subseteq A \subseteq D^I_{\mathcal{C}}(A, B).$$

Proof. For all $y \in \mathbb{R}^n$

$$\begin{array}{rcl} E^I_{\mathcal{I}}(A, B)(y) & = & \inf\limits_{x \in T_y(d_B)} \mathcal{I}(B(x-y), A(x)) \\ & \leq_{L^I} & \mathcal{I}(B(y-y), A(y)) \\ & = & \mathcal{I}(1_{\mathcal{L}^I}, A(y)) \\ & = & A(y) \end{array}$$

and

$$\begin{array}{rcl} D^I_{\mathcal{C}}(A, B)(y) & = & \sup\limits_{x \in T_y(d_B) \cap d_A} \mathcal{C}(B(x-y), A(x)) \\ & \geq_{L^I} & \mathcal{C}(B(y-y), A(y)) \\ & = & \mathcal{C}(1_{\mathcal{L}^I}, A(y)) \\ & = & A(y) \end{array}$$

□

As a straightforward consequence, the following propostion holds.

Proposition 7.3.5. *Let $\mathcal{C}$ be a semi-norm and $\mathcal{I}$ a border implicator on $\mathcal{L}^I$. If $B(\mathbf{0}) = 1_{\mathcal{L}^I}$, then:*

$$\begin{array}{lllll} \textit{(i)} & D^I_{\mathcal{C}}(A,B) & \supseteq & C^I_{\mathcal{C},\mathcal{I}}(A,B), \\ \textit{(ii)} & D^I_{\mathcal{C}}(A,B) & \supseteq & O^I_{\mathcal{C},\mathcal{I}}(A,-B), \\ \textit{(iii)} & E^I_{\mathcal{I}}(A,B) & \subseteq & O^I_{\mathcal{C},\mathcal{I}}(A,B), \\ \textit{(iv)} & E^I_{\mathcal{I}}(A,B) & \subseteq & C^I_{\mathcal{C},\mathcal{I}}(A,-B). \end{array}$$

Proof. Follows from Proposition 7.3.4 and 7.3.2 as follows:

(i) $C^I_{\mathcal{C},\mathcal{I}}(A,B) = E^I_{\mathcal{I}}(D^I_{\mathcal{C}}(A,B),-B) \subseteq D^I_{\mathcal{C}}(A,B)$.

(ii) $O^I_{\mathcal{C},\mathcal{I}}(A,-B) = D^I_{\mathcal{C}}(E^I_{\mathcal{I}}(A,-B),B) \subseteq D^I_{\mathcal{C}}(A,B)$.

(iii) $O^I_{\mathcal{C},\mathcal{I}}(A,B) = D^I_{\mathcal{C}}(E^I_{\mathcal{I}}(A,B),-B) \supseteq E^I_{\mathcal{I}}(A,B)$.

(iv) $C^I_{\mathcal{C},\mathcal{I}}(A,-B) = E^I_{\mathcal{I}}(D^I_{\mathcal{C}}(A,-B),B) \supseteq E^I_{\mathcal{I}}(A,B)$.

□

Under given conditions, also the interval-valued fuzzy closing and opening are respectively expansive and restrictive.

Proposition 7.3.6. *Let $\mathcal{C}$ be a conjunctor and $\mathcal{I}$ an implicator on $\mathcal{L}^I$.*

(i) If $(\forall (a,b) \in L^I \times L^I)(b \leq_{L^I} \mathcal{I}(a,\mathcal{C}(a,b)))$, then $A \subseteq C^I_{\mathcal{C},\mathcal{I}}(A,B)$.

(ii) If $(\forall (a,b) \in L^I \times L^I)(\mathcal{C}(a,\mathcal{I}(a,b))) \leq_{L^I} b$, then $O^I_{\mathcal{C},\mathcal{I}}(A,B) \subseteq A$.

Proof.

(i) For all $y \in \mathbb{R}^n$

$$\begin{array}{rcl} C^I_{\mathcal{C},\mathcal{I}}(A,B)(y) & = & E^I_{\mathcal{I}}(D^I_{\mathcal{C}}(A,B),-B)(y) \\ & = & \inf\limits_{x \in T_y(-d_B)} \mathcal{I}(B(y-x), \sup\limits_{z \in T_y(d_B) \cap d_A} \mathcal{C}(B(z-x),A(z))) \\ & \geq_{L^I} & \inf\limits_{x \in T_y(-d_B)} \mathcal{I}(B(y-x), \mathcal{C}(B(y-x),A(y))) \\ & \geq_{L^I} & \inf\limits_{x \in T_y(-d_B)} A(y) \\ & = & A(y) \end{array}$$

(ii) Analogously.

□

The conditions on $\mathcal{C}$ and $\mathcal{I}$ will for example be satisfied if $\mathcal{I} = \mathcal{I}_{\mathcal{C}}$ with $\mathcal{C}$ a t-norm on $\mathcal{L}^I$ of which the partial mappings are sup-morphisms (see Proposition 1.5.3 and 1.5.4).

Combining Proposition 7.3.5 and 7.3.6 leads to the following.

Proposition 7.3.7. *Let $\mathcal{C}$ be a conjunctor and $\mathcal{I}$ an implicator on $\mathcal{L}^I$. If $B(\mathbf{0}) = 1_{\mathcal{L}^I}$ and $(\forall (a,b) \in L^I \times L^I)(\mathcal{C}(a,\mathcal{I}(a,b))) \leq_{L^I} b \leq_{L^I} \mathcal{I}(a,\mathcal{C}(a,b)))$, then $E^I_{\mathcal{I}}(A,B) \subseteq O^I_{\mathcal{C},\mathcal{I}}(A,B) \subseteq A \subseteq C^I_{\mathcal{C},\mathcal{I}}(A,B) \subseteq D^I_{\mathcal{C}}(A,B)$.*

Interaction with the Intersection of Images

In this and the following subsections, we study the interaction of the interval-valued morphological operators with the intersection and union of images and structuring elements.

Proposition 7.3.8. *Let $\mathcal{C}$ be a conjunctor and $\mathcal{I}$ an implicator on $\mathcal{L}^I$. It holds that:*

$$\begin{array}{lrcl} \textit{(i)} & D^I_{\mathcal{C}}(A_1 \cap A_2, B) & \subseteq & D^I_{\mathcal{C}}(A_1,B) \cap D^I_{\mathcal{C}}(A_2,B), \\ \textit{(ii)} & E^I_{\mathcal{I}}(A_1 \cap A_2, B) & \subseteq & E^I_{\mathcal{I}}(A_1,B) \cap E^I_{\mathcal{I}}(A_2,B). \end{array}$$

If in (ii) the second partial mappings of $\mathcal{I}$ are meet-morphisms, then it holds that:

$$E^I_{\mathcal{I}}(A_1 \cap A_2, B) = E^I_{\mathcal{I}}(A_1,B) \cap E^I_{\mathcal{I}}(A_2,B).$$

Proof.

(i) From Proposition 7.3.2 (monotonicity w.r.t. the image) and $A_1 \cap A_2 \subseteq A_1$ and $A_1 \cap A_2 \subseteq A_2$, it follows that $D^I_{\mathcal{C}}(A_1 \cap A_2, B) \subseteq D^I_{\mathcal{C}}(A_1,B)$ and $D^I_{\mathcal{C}}(A_1 \cap A_2, B) \subseteq D^I_{\mathcal{C}}(A_2,B)$ and consequently $D^I_{\mathcal{C}}(A_1 \cap A_2, B) \subseteq D^I_{\mathcal{C}}(A_1,B) \cap D^I_{\mathcal{C}}(A_2,B)$.

(ii) For all $y \in \mathbb{R}^n$:

$$\begin{array}{rl} & E^I_{\mathcal{I}}(A_1 \cap A_2, B)(y) \\ = & \inf\limits_{x \in T_y(d_B)} \mathcal{I}(B(x-y), (A_1 \cap A_2)(x)) \\ = & \inf\limits_{x \in T_y(d_B)} \mathcal{I}(B(x-y), \inf(A_1(x), A_2(x))) \\ \leq_{L^I} & \inf\limits_{x \in T_y(d_B)} \inf(\mathcal{I}(B(x-y), A_1(x)), \mathcal{I}(B(x-y), A_2(x))) \\ = & \inf(\inf\limits_{x \in T_y(d_B)} \mathcal{I}(B(x-y), A_1(x)), \inf\limits_{x \in T_y(d_B)} \mathcal{I}(B(x-y), A_2(x))) \\ = & \inf(E^I_{\mathcal{I}}(A_1,B)(y), E^I_{\mathcal{I}}(A_2,B)(y)) \\ = & (E^I_{\mathcal{I}}(A_1,B) \cap E^I_{\mathcal{I}}(A_2,B))(y) \end{array}$$

If the second partial mappings of $\mathcal{I}$ are meet-morphisms, then the third transition becomes an equality.

□

Proposition 7.3.9. *Let $\mathcal{C}$ be a conjunctor and $\mathcal{I}$ an implicator on $\mathcal{L}^I$. It holds that:*

$$\begin{array}{lrcl} \textit{(i)} & C^I_{\mathcal{C},\mathcal{I}}(A_1 \cap A_2, B) & \subseteq & C^I_{\mathcal{C},\mathcal{I}}(A_1,B) \cap C^I_{\mathcal{C},\mathcal{I}}(A_2,B), \\ \textit{(ii)} & O^I_{\mathcal{C},\mathcal{I}}(A_1 \cap A_2, B) & \subseteq & O^I_{\mathcal{C},\mathcal{I}}(A_1,B) \cap O^I_{\mathcal{C},\mathcal{I}}(A_2,B). \end{array}$$

Proof. Follows from Proposition 7.3.8 and 7.3.2 as follows.

(i)

$$\begin{aligned} C^I_{\mathcal{C},\mathcal{I}}(A_1 \cap A_2, B) &= E^I_{\mathcal{I}}(D^I_{\mathcal{C}}(A_1 \cap A_2, B), -B) \\ &\subseteq E^I_{\mathcal{I}}(D^I_{\mathcal{C}}(A_1, B) \cap D^I_{\mathcal{C}}(A_2, B), -B) \\ &\subseteq E^I_{\mathcal{I}}(D^I_{\mathcal{C}}(A_1, B), -B) \cap E^I_{\mathcal{I}}(D^I_{\mathcal{C}}(A_2, B), -B) \\ &= C^I_{\mathcal{C},\mathcal{I}}(A_1, B) \cap C^I_{\mathcal{C},\mathcal{I}}(A_2, B) \end{aligned}$$

(ii) Analogously.

□

The results in Proposition 7.3.8 and 7.3.9 can be extended to the intersection of an arbitrary family.

Proposition 7.3.10. *Let $\mathcal{C}$ be a conjunctor and $\mathcal{I}$ an implicator on $\mathcal{L}^I$. It holds that:*

$$\begin{aligned} &\textit{(i)} \quad D^I_{\mathcal{C}}(\bigcap_{j\in J} A_j, B) \subseteq \bigcap_{j\in J} D^I_{\mathcal{C}}(A_j, B), \\ &\textit{(ii)} \quad E^I_{\mathcal{I}}(\bigcap_{j\in J} A_j, B) \subseteq \bigcap_{j\in J} E^I_{\mathcal{I}}(A_j, B). \end{aligned}$$

If in (ii) the second partial mappings of $\mathcal{I}$ are inf-morphisms, then it holds that:

$$E^I_{\mathcal{I}}(\bigcap_{j\in J} A_j, B) = \bigcap_{j\in J} E^I_{\mathcal{I}}(A_j, B).$$

Proof. Analogous to the proof of Proposition 7.3.8. □

Proposition 7.3.11. *Let $\mathcal{C}$ be a conjunctor and $\mathcal{I}$ an implicator on $\mathcal{L}^I$. It holds that:*

$$\begin{aligned} &\textit{(i)} \quad C^I_{\mathcal{C},\mathcal{I}}(\bigcap_{j\in J} A_j, B) \subseteq \bigcap_{j\in J} C^I_{\mathcal{C},\mathcal{I}}(A_j, B), \\ &\textit{(ii)} \quad O^I_{\mathcal{C},\mathcal{I}}(\bigcap_{j\in J} A_j, B) \subseteq \bigcap_{j\in J} O^I_{\mathcal{C},\mathcal{I}}(A_j, B). \end{aligned}$$

Proof. Analogous to the proof of Proposition 7.3.9. □

The results in Proposition 7.3.8 and 7.3.9 can also be extended to an arbitrary $\mathcal{C}'$-intersection, with $\mathcal{C}'$ a semi-norm.

Proposition 7.3.12. *Let $\mathcal{C}$ and $\mathcal{C}'$ be conjunctors and $\mathcal{I}$ an implicator on $\mathcal{L}^I$.*

1. *(i) If C' is a semi-norm, then*

$$D^I_{\mathcal{C}}(A_1 \cap_{\mathcal{C}'} A_2, B) \subseteq D^I_{\mathcal{C}}(A_1, B) \cap D^I_{\mathcal{C}}(A_2, B).$$

(ii) If $(\forall (u,v,w) \in (L^I)^3)(\mathcal{C}(u, \mathcal{C}'(v,w)) \leq_{L^I} \mathcal{C}'(\mathcal{C}(u,v), \mathcal{C}(u,w)))$, then

$$D^I_{\mathcal{C}}(A_1 \cap_{\mathcal{C}'} A_2, B) \subseteq D^I_{\mathcal{C}}(A_1, B) \cap_{\mathcal{C}'} D^I_{\mathcal{C}}(A_2, B).$$

2. *(i) If C' is a semi-norm, then*

$$E^I_{\mathcal{I}}(A_1 \cap_{\mathcal{C}'} A_2, B) \subseteq E^I_{\mathcal{I}}(A_1, B) \cap E^I_{\mathcal{I}}(A_2, B).$$

(ii) If $(\forall (u,v,w) \in (L^I)^3)(\mathcal{C}'(\mathcal{I}(u,v), \mathcal{I}(u,w)) \leq \mathcal{I}(u, \mathcal{C}'(v,w)))$*, then*

$$E^I_{\mathcal{I}}(A_1, B) \cap_{\mathcal{C}'} E^I_{\mathcal{I}}(A_2, B) \subseteq E^I_{\mathcal{I}}(A_1 \cap_{\mathcal{C}'} A_2, B).$$

Proof.

1. (i) From Lemma 8.1.1, it follows that $A_1 \cap_{\mathcal{C}'} A_2 \subseteq A_1 \cap A_2$. Using Proposition 7.3.2 and 7.3.8 then gives $D^I_{\mathcal{C}}(A_1 \cap_{\mathcal{C}'} A_2, B) \subseteq D^I_{\mathcal{C}}(A_1 \cap A_2, B) \subseteq D^I_{\mathcal{C}}(A_1, B) \cap D^I_{\mathcal{C}}(A_2, B)$.

   (ii) For all $y \in \mathbb{R}^n$:

$$\begin{aligned}
& D^I_{\mathcal{C}}(A_1 \cap_{\mathcal{C}'} A_2, B)(y) \\
= & \sup_{x \in T_y(d_B) \cap d_{A_1 \cap_{\mathcal{C}'} A_2}} \mathcal{C}(B(x-y), (A_1 \cap_{\mathcal{C}'} A_2)(x)) \\
= & \sup_{x \in T_y(d_B) \cap d_{A_1 \cap_{\mathcal{C}'} A_2}} \mathcal{C}(B(x-y), (\mathcal{C}'(A_1(x), A_2(x))) \\
\leq_{L^I} & \sup_{x \in T_y(d_B) \cap d_{A_1 \cap_{\mathcal{C}'} A_2}} \mathcal{C}'(\mathcal{C}(B(x-y), A_1(x)), \mathcal{C}(B(x-y), A_2(x))) \\
\leq_{L^I} & \mathcal{C}'(\sup_{x \in T_y(d_B) \cap d_{A_1}} \mathcal{C}(B(x-y), A_1(x)), \\
& \qquad \sup_{x \in T_y(d_B) \cap d_{A_2}} \mathcal{C}(B(x-y), A_2(x))) \\
= & \mathcal{C}'(D^I_{\mathcal{C}}(A_1, B)(y), D^I_{\mathcal{C}}(A_2, B)(y)) \\
= & (D^I_{\mathcal{C}}(A_1, B) \cap_{\mathcal{C}'} D^I_{\mathcal{C}}(A_2, B))(y)
\end{aligned}$$

   In the fourth transition, Lemma 1.5.1 was used.

2. (i) From Lemma 8.1.1, it follows that $A_1 \cap_{\mathcal{C}'} A_2 \subseteq A_1 \cap A_2$. Using Proposition 7.3.2 and 7.3.8 then gives $E^I_{\mathcal{I}}(A_1 \cap_{\mathcal{C}'} A_2, B) \subseteq E^I_{\mathcal{I}}(A_1 \cap A_2, B) \subseteq E^I_{\mathcal{I}}(A_1, B) \cap E^I_{\mathcal{I}}(A_2, B)$. Remark that if $\mathcal{C}' = \mathcal{C}_{\min}$, i.e., the infimum-operator, which is a meet-morphism, then the equality holds.

   (ii) For all $y \in \mathbb{R}^n$:

$$\begin{aligned}
& E^I_{\mathcal{I}}(A_1 \cap_{\mathcal{C}'} A_2, B)(y) \\
= & \inf_{x \in T_y(d_B)} \mathcal{I}(B(x-y), (A_1 \cap_{\mathcal{C}'} A_2)(x)) \\
= & \inf_{x \in T_y(d_B)} \mathcal{I}(B(x-y), \mathcal{C}'(A_1(x), A_2(x))) \\
\geq_{L^I} & \inf_{x \in T_y(d_B)} \mathcal{C}'(\mathcal{I}(B(x-y), A_1(x)), \mathcal{I}(B(x-y), A_2(x))) \\
\geq_{L^I} & \mathcal{C}'(\inf_{x \in T_y(d_B)} \mathcal{I}(B(x-y), A_1(x)), \inf_{x \in T_y(d_B)} \mathcal{I}(B(x-y), A_2(x))) \\
= & \mathcal{C}'(E^I_{\mathcal{I}}(A_1, B)(y), E^I_{\mathcal{I}}(A_2, B)(y)) \\
= & (E^I_{\mathcal{I}}(A_1, B) \cap_{\mathcal{C}'} E^I_{\mathcal{I}}(A_2, B))(y)
\end{aligned}$$

   In the fourth transition, Lemma 1.5.1 was used.

□

Interaction with the Intersection of Structuring Elements

Proposition 7.3.13. *Let $\mathcal{C}$ be a conjunctor and $\mathcal{I}$ an implicator on $\mathcal{L}^I$. It holds that:*

(i) $D^I_{\mathcal{C}}(A, B_1 \cap B_2) \subseteq D^I_{\mathcal{C}}(A, B_1) \cap D^I_{\mathcal{C}}(A, B_2)$,
(ii) $E^I_{\mathcal{I}}(A, B_1 \cap B_2) \supseteq E^I_{\mathcal{I}}(A, B_1) \cup E^I_{\mathcal{I}}(A, B_2) \supseteq E^I_{\mathcal{I}}(A, B_1) \cap E^I_{\mathcal{I}}(A, B_2)$.

Proof. Analogous to the proof of Proposition 7.3.8 (i). □

As a consequence of the opposite inclusions in the above proposition, no analogous interaction properties w.r.t. structuring element can be found for the interval-valued fuzzy morphological opening and closing.

The result in Proposition 7.3.13 can be extended to the intersection of an arbitrary family.

Proposition 7.3.14. *Let $\mathcal{C}$ be a conjunctor and $\mathcal{I}$ an implicator on $\mathcal{L}^I$. It holds that:*

$$\begin{array}{lll} \textit{(i)} & D^I_{\mathcal{C}}(A, \bigcap\limits_{j\in J} B_j) & \subseteq \bigcap\limits_{j\in J} D^I_{\mathcal{C}}(A, B_j), \\ \textit{(ii)} & E^I_{\mathcal{I}}(A, \bigcap\limits_{j\in J} B_j) & \supseteq \bigcap\limits_{j\in J} E^I_{\mathcal{I}}(A, B_j). \end{array}$$

Proof. Analogous to the proof of Proposition 7.3.13. □

The result in Proposition 7.3.13 can also be extended to an arbitrary $\mathcal{C}'$-intersection, with $\mathcal{C}'$ a semi-norm.

Proposition 7.3.15. *Let $\mathcal{C}$ and $\mathcal{C}'$ be conjunctors and $\mathcal{I}$ an implicator on $\mathcal{L}^I$.*

1. *(i) If C' is a semi-norm, then*

$$D^I_{\mathcal{C}}(A, B_1 \cap_{\mathcal{C}'} B_2) \subseteq D^I_{\mathcal{C}}(A, B_1) \cap D^I_{\mathcal{C}}(A, B_2).$$

(ii) If $(\forall (u,v,w) \in (L^I)^3)(\mathcal{C}(\mathcal{C}'(u,v),w) \leq_{L^I} \mathcal{C}'(\mathcal{C}(u,v),\mathcal{C}(u,w)))$*, then*

$$D^I_{\mathcal{C}}(A, B_1 \cap_{\mathcal{C}'} B_2) \subseteq D^I_{\mathcal{C}}(A, B_1) \cap_{\mathcal{C}'} D^I_{\mathcal{C}}(A, B_2).$$

2. *(i) If C' is a semi-norm, then*

$$E^I_{\mathcal{I}}(A, B_1 \cap_{\mathcal{C}'} B_2) \supseteq E^I_{\mathcal{I}}(A, B_1) \cap E^I_{\mathcal{I}}(A, B_2) \supseteq E^I_{\mathcal{I}}(A, B_1) \cap_{\mathcal{C}'} E^I_{\mathcal{I}}(A, B_2).$$

(ii) If $(\forall (u,v,w) \in (L^I)^3)(\mathcal{C}'(\mathcal{I}(u,v),\mathcal{I}(u,w)) \leq \mathcal{I}(\mathcal{C}'(u,v),w))$*, then*

$$E^I_{\mathcal{I}}(A, B_1) \cap_{\mathcal{C}'} E^I_{\mathcal{I}}(A, B_2) \subseteq E^I_{\mathcal{I}}(A, B_1 \cap_{\mathcal{C}'} B_2).$$

Proof. Analogous to the proof of Proposition 7.3.12. □

Interaction with the Union of Images

Proposition 7.3.16. *Let $\mathcal{C}$ be a conjunctor and $\mathcal{I}$ an implicator on $\mathcal{L}^I$. It holds that:*

$$\begin{array}{lrcl} \textit{(i)} & D^I_{\mathcal{C}}(A_1 \cup A_2, B) & \supseteq & D^I_{\mathcal{C}}(A_1, B) \cup D^I_{\mathcal{C}}(A_2, B), \\ \textit{(ii)} & E^I_{\mathcal{I}}(A_1 \cup A_2, B) & \supseteq & E^I_{\mathcal{I}}(A_1, B) \cup E^I_{\mathcal{I}}(A_2, B). \end{array}$$

If in (i) the second partial mappings of $\mathcal{C}$ are join-morphisms, then it holds that:

$$D^I_{\mathcal{C}}(A_1 \cup A_2, B) = D^I_{\mathcal{C}}(A_1, B) \cup D^I_{\mathcal{C}}(A_2, B).$$

Proof.

(i) Analogous to the proof of Proposition 7.3.8 (ii).

(ii) Analogous to the proof of Proposition 7.3.8 (i).

□

Proposition 7.3.17. *Let $\mathcal{C}$ be a conjunctor and $\mathcal{I}$ an implicator on $\mathcal{L}^I$. It holds that:*

$$\begin{array}{lrcl} \textit{(i)} & C^I_{\mathcal{C},\mathcal{I}}(A_1 \cup A_2, B) & \supseteq & C^I_{\mathcal{C},\mathcal{I}}(A_1, B) \cup C^I_{\mathcal{C},\mathcal{I}}(A_2, B), \\ \textit{(ii)} & O^I_{\mathcal{C},\mathcal{I}}(A_1 \cup A_2, B) & \supseteq & O^I_{\mathcal{C},\mathcal{I}}(A_1, B) \cup O^I_{\mathcal{C},\mathcal{I}}(A_2, B). \end{array}$$

Proof. Analogous to the proof of Proposition 7.3.9. □

The results in Proposition 7.3.16 and 7.3.17 can be extended to the union of an arbitrary family.

Proposition 7.3.18. *Let $\mathcal{C}$ be a conjunctor and $\mathcal{I}$ an implicator on $\mathcal{L}^I$. It holds that:*

$$\begin{array}{lrcl} \textit{(i)} & D^I_{\mathcal{C}}(\bigcup\limits_{j\in J} A_j, B) & \supseteq & \bigcup\limits_{j\in J} D^I_{\mathcal{C}}(A_j, B), \\ \textit{(ii)} & E^I_{\mathcal{I}}(\bigcup\limits_{j\in J} A_j, B) & \supseteq & \bigcup\limits_{j\in J} E^I_{\mathcal{I}}(A_j, B). \end{array}$$

If in (i) the second partial mappings of $\mathcal{C}$ are sup-morphisms, then it holds that:

$$D^I_{\mathcal{C}}(\bigcup_{j\in J} A_j, B) = \bigcup_{j\in J} D^I_{\mathcal{C}}(A_j, B).$$

Proof. Analogous to the proof of Proposition 7.3.16. □

Proposition 7.3.19. *Let $\mathcal{C}$ be a conjunctor and $\mathcal{I}$ an implicator on $\mathcal{L}^I$. It holds that:*

$$\begin{array}{lrcl} \textit{(i)} & C^I_{\mathcal{C},\mathcal{I}}(\bigcup\limits_{j\in J} A_j, B) & \supseteq & \bigcup\limits_{j\in J} C^I_{\mathcal{C},\mathcal{I}}(A_j, B), \\ \textit{(ii)} & O^I_{\mathcal{C},\mathcal{I}}(\bigcup\limits_{j\in J} A_j, B) & \supseteq & \bigcup\limits_{j\in J} O^I_{\mathcal{C},\mathcal{I}}(A_j, B). \end{array}$$

Proof. Analogous to the proof of Proposition 7.3.17. □

The results in Proposition 7.3.16 and 7.3.17 can also be extended to an arbitrary $\mathcal{D}$-union, with $\mathcal{D}$ a semi-conorm.

Proposition 7.3.20. *Let $\mathcal{C}$ be a conjunctor, $\mathcal{D}$ a disjunctor and $\mathcal{I}$ an implicator on $\mathcal{L}^I$.*

1. *(i) If D is a semi-conorm, then*

$$D^I_{\mathcal{C}}(A_1 \cup_{\mathcal{D}} A_2, B) \supseteq D^I_{\mathcal{C}}(A_1, B) \cup D^I_{\mathcal{C}}(A_2, B).$$

(ii) If $(\forall (u,v,w) \in (L^I)^3)(\mathcal{C}(u, \mathcal{D}(v,w)) \leq_{L^I} \mathcal{D}(\mathcal{C}(u,v), \mathcal{C}(u,w)))$, then

$$D^I_{\mathcal{C}}(A_1 \cup_{\mathcal{D}} A_2, B) \subseteq D^I_{\mathcal{C}}(A_1, B) \cup_{\mathcal{D}} D^I_{\mathcal{C}}(A_2, B).$$

2. *(i) If D is a semi-conorm, then*

$$E^I_{\mathcal{I}}(A_1 \cup_{\mathcal{D}} A_2, B) \supseteq E^I_{\mathcal{I}}(A_1, B) \cup E^I_{\mathcal{I}}(A_2, B).$$

(ii) If $(\forall (u,v,w) \in (L^I)^3)(\mathcal{D}(\mathcal{I}(u,v), \mathcal{I}(u,w)) \leq \mathcal{I}(u, \mathcal{D}(v,w)))$, then

$$E^I_{\mathcal{I}}(A_1, B) \cup_{\mathcal{D}} E^I_{\mathcal{I}}(A_2, B) \supseteq E^I_{\mathcal{I}}(A_1 \cup_{\mathcal{D}} A_2, B).$$

Proof. Analogous to the proof of Proposition 7.3.12, where now Lemma 1.5.2 can be used instead of Lemma 1.5.1. □

Interaction with the Union of Structuring Elements

Proposition 7.3.21. *Let $\mathcal{C}$ be a conjunctor and $\mathcal{I}$ an implicator on $\mathcal{L}^I$. It holds that:*

(i) $D^I_{\mathcal{C}}(A, B_1 \cup B_2) \supseteq D^I_{\mathcal{C}}(A, B_1) \cup D^I_{\mathcal{C}}(A, B_2)$,,
(ii) $E^I_{\mathcal{I}}(A, B_1 \cup B_2) \subseteq E^I_{\mathcal{I}}(A, B_1) \cap E^I_{\mathcal{I}}(A, B_2) \subseteq E^I_{\mathcal{I}}(A, B_1) \cup E^I_{\mathcal{I}}(A, B_2)$.

If in (i) the first partial mappings of $\mathcal{C}$ are join-morphisms, then it holds that

$$D^I_{\mathcal{C}}(A, B_1 \cup B_2) = D^I_{\mathcal{C}}(A, B_1) \cup D^I_{\mathcal{C}}(A, B_2).$$

If in (ii) the first partial mappings of $\mathcal{I}$ are dual join-morphisms, then it holds that:

$$E^I_{\mathcal{I}}(A, B_1 \cup B_2) = E^I_{\mathcal{I}}(A, B_1) \cap E^I_{\mathcal{I}}(A, B_2).$$

Proof. Analogous to the proof of Proposition 7.3.8 (ii). □

Proposition 7.3.22. *Let $\mathcal{C}$ be a conjunctor, of which the first partial mappings are join-morphisms, and let $\mathcal{I}$ be an implicator on $\mathcal{L}^I$. It holds that:*

$$O_{\mathcal{C},\mathcal{I}}(A, B_1 \cup B_2) \subseteq O_{\mathcal{C},\mathcal{I}}(A, B_1) \cup O_{\mathcal{C},\mathcal{I}}(A, B_2).$$

If also the first partial mappings of $\mathcal{I}$ are dual join-morphisms, then

$$C_{\mathcal{C},\mathcal{I}}(A, B_1 \cup B_2) \supseteq C_{\mathcal{C},\mathcal{I}}(A, B_1) \cap C_{\mathcal{C},\mathcal{I}}(A, B_2).$$

Proof. Suppose that the first partial mappings of $\mathcal{C}$ are join-morphisms. Using Proposition 7.3.21, 7.3.2 and 7.3.8, we obtain:

$$\begin{aligned}
O_{\mathcal{C},\mathcal{I}}(A, B_1 \cup B_2) &= D^I_{\mathcal{C}}(E^I_{\mathcal{I}}(A, B_1 \cup B_2), -(B_1 \cup B_2)) \\
&= D^I_{\mathcal{C}}(E^I_{\mathcal{I}}(A, B_1 \cup B_2), -B_1 \cup -B_2) \\
&\subseteq D^I_{\mathcal{C}}(E^I_{\mathcal{I}}(A, B_1) \cap E^I_{\mathcal{I}}(A, B_2), -B_1 \cup -B_2) \\
&= D^I_{\mathcal{C}}(E^I_{\mathcal{I}}(A, B_1) \cap E^I_{\mathcal{I}}(A, B_2), -B_1) \\
&\quad \cup D^I_{\mathcal{C}}(E^I_{\mathcal{I}}(A, B_1) \cap E^I_{\mathcal{I}}(A, B_2), -B_2) \\
&\subseteq (D^I_{\mathcal{C}}(E^I_{\mathcal{I}}(A, B_1), -B_1) \cap D^I_{\mathcal{C}}(E^I_{\mathcal{I}}(A, B_2), -B_1)) \\
&\quad \cup (D^I_{\mathcal{C}}(E^I_{\mathcal{I}}(A, B_1), -B_2) \cap D^I_{\mathcal{C}}(E^I_{\mathcal{I}}(A, B_2), -B_2)) \\
&\subseteq D^I_{\mathcal{C}}(E^I_{\mathcal{I}}(A, B_1), -B_1) \cup D^I_{\mathcal{C}}(E^I_{\mathcal{I}}(A, B_2), -B_2) \\
&= O_{\mathcal{C},\mathcal{I}}(A, B_1) \cup O_{\mathcal{C},\mathcal{I}}(A, B_2)
\end{aligned}$$

Suppose now also that the first partial mappings of $\mathcal{I}$ are dual join-morphisms. Using Proposition 7.3.21, 7.3.2 and 7.3.16, we obtain:

$$\begin{aligned}
C_{\mathcal{C},\mathcal{I}}(A, B_1 \cup B_2) &= E^I_{\mathcal{I}}(D^I_{\mathcal{C}}(A, B_1 \cup B_2), -(B_1 \cup B_2)) \\
&= E^I_{\mathcal{I}}(D^I_{\mathcal{C}}(A, B_1 \cup B_2), -B_1 \cup -B_2) \\
&= E^I_{\mathcal{I}}(D^I_{\mathcal{C}}(A, B_1 \cup B_2), -B_1) \cap E^I_{\mathcal{I}}(D^I_{\mathcal{C}}(A, B_1 \cup B_2), -B_2) \\
&= E^I_{\mathcal{I}}(D^I_{\mathcal{C}}(A, B_1) \cup D^I_{\mathcal{C}}(A, B_2), -B_1) \\
&\quad \cap E^I_{\mathcal{I}}(D^I_{\mathcal{C}}(A, B_1) D^I_{\mathcal{C}}(A, B_2), -B_2) \\
&\supseteq (E^I_{\mathcal{I}}(D^I_{\mathcal{C}}(A, B_1), -B_1) \cup E^I_{\mathcal{I}}(D^I_{\mathcal{C}}(A, B_2), -B_1)) \\
&\quad \cap (E^I_{\mathcal{I}}(D^I_{\mathcal{C}}(A, B_1), -B_2) \cup E^I_{\mathcal{I}}(D^I_{\mathcal{C}}(A, B_2), -B_2)) \\
&\supseteq (E^I_{\mathcal{I}}(D^I_{\mathcal{C}}(A, B_1), -B_1) \cap E^I_{\mathcal{I}}(D^I_{\mathcal{C}}(A, B_2), -B_2) \\
&= C_{\mathcal{C},\mathcal{I}}(A, B_1) \cap C_{\mathcal{C},\mathcal{I}}(A, B_2)
\end{aligned}$$

□

The results in Proposition 7.3.21 and 7.3.22 can be extended to the union of an arbitrary family.

Proposition 7.3.23. *Let $\mathcal{C}$ be a conjunctor and $\mathcal{I}$ an implicator on $\mathcal{L}^I$. It holds that:*

$$\begin{array}{lrcl} \textit{(i)} & D^I_{\mathcal{C}}(A, \bigcup\limits_{j\in J} B_j) & \supseteq & \bigcup\limits_{j\in J} D^I_{\mathcal{C}}(A, B_j), \\ \textit{(ii)} & E^I_{\mathcal{I}}(A, \bigcup\limits_{j\in J} B_j) & \subseteq & \bigcap\limits_{j\in J} E^I_{\mathcal{I}}(A, B_j). \end{array}$$

If in (i) the first partial mappings of $\mathcal{C}$ are sup-morphisms, then it holds that

$$D^I_{\mathcal{C}}(A, \bigcup_{j\in J} B_j) = \bigcup_{j\in J} D^I_{\mathcal{C}}(A, B_j).$$

If in (ii) the first partial mappings of $\mathcal{I}$ are dual sup-morphisms, then it holds that:

$$E^I_{\mathcal{I}}(A, \bigcup_{j\in J} B_j) = \bigcap_{j\in J} E^I_{\mathcal{I}}(A, B_j).$$

Proof. Analogous to the proof of Proposition 7.3.8 (ii). □

Proposition 7.3.24. *Let $\mathcal{C}$ be a conjunctor, of which the first partial mappings are sup-morphisms, and let $\mathcal{I}$ be an implicator on $\mathcal{L}^I$. It holds that:*

$$O_{\mathcal{C},\mathcal{I}}(A, \bigcup_{j\in J} B_j) \subseteq \bigcup_{j\in J} O_{\mathcal{C},\mathcal{I}}(A, B_j).$$

If also the first partial mappings of $\mathcal{I}$ are dual sup-morphisms, then

$$C_{\mathcal{C},\mathcal{I}}(A, \bigcup_{j\in J} B_j) \supseteq \bigcap_{j\in J} C_{\mathcal{C},\mathcal{I}}(A, B_j).$$

Proof. Analogous to the proof of Proposition 7.3.22. □

The results in Proposition 7.3.21 and 7.3.22 can also be extended to an arbitrary $\mathcal{D}$-union, with $\mathcal{D}$ a semi-conorm.

Proposition 7.3.25. *Let $\mathcal{C}$ be a conjunctor, $\mathcal{D}$ a disjunctor and $\mathcal{I}$ an implicator on $\mathcal{L}^I$.*

1. *(i) If D is a semi-conorm, then*

$$D^I_{\mathcal{C}}(A, B_1 \cup_{\mathcal{D}} B_2) \supseteq D^I_{\mathcal{C}}(A, B_1) \cup D^I_{\mathcal{C}}(A, B_2).$$

(ii) If $(\forall (u,v,w) \in (L^I)^3)(\mathcal{C}(\mathcal{D}(u,v), w) \leq_{L^I} \mathcal{D}(\mathcal{C}(u,v), \mathcal{C}(u,w)))$, then

$$D^I_{\mathcal{C}}(A, B_1 \cup_{\mathcal{D}} B_2) \subseteq D^I_{\mathcal{C}}(A, B_1) \cup_{\mathcal{D}} D^I_{\mathcal{C}}(A, B_2).$$

2. *If D is a semi-conorm, then*

$$E^I_{\mathcal{I}}(A, B_1 \cup_{\mathcal{D}} B_2) \subseteq E^I_{\mathcal{I}}(A, B_1) \cap E^I_{\mathcal{I}}(A, B_2) \subseteq E^I_{\mathcal{I}}(A, B_1) \cup_{\mathcal{D}} E^I_{\mathcal{I}}(A, B_2).$$

Proof.

1. Analogous to the proof of Proposition 7.3.12 (1.).
2. Since $B_1 \cup_{\mathcal{D}} B_2 \supseteq B_1 \cup B_2$, it follows from Proposition 7.3.2 that

$$E^I_{\mathcal{I}}(A, B_1 \cup_{\mathcal{D}} B_2) \subseteq E^I_{\mathcal{I}}(A, B_1 \cup B_2).$$

Combined with Proposition 7.3.21, we get

$$E^I_{\mathcal{I}}(A, B_1 \cup_{\mathcal{D}} B_2) \subseteq E^I_{\mathcal{I}}(A, B_1) \cap E^I_{\mathcal{I}}(A, B_2).$$

Further,

$$E^I_{\mathcal{I}}(A, B_1) \cap E^I_{\mathcal{I}}(A, B_2) \subseteq E^I_{\mathcal{I}}(A, B_1) \cup E^I_{\mathcal{I}}(A, B_2) \subseteq E^I_{\mathcal{I}}(A, B_1) \cup_{\mathcal{D}} E^I_{\mathcal{I}}(A, B_2).$$

□

Duality

Definition 7.8. *Consider a universe X and two unary operators P and Q on $\mathcal{F}_{\mathcal{L}}(X)$ and an involutive negator $\mathcal{N}$ on $\mathcal{L}$. The operators P and Q are called dual w.r.t. to $\mathcal{N}$ if and only if*

$$P = co_{\mathcal{N}} \circ Q \circ co_{\mathcal{N}}, \text{ i.e., } (\forall A \in \mathcal{F}_{\mathcal{L}}(X))(P(A) = co_{\mathcal{N}}(Q(co_{\mathcal{N}}(A)))).$$

Since $\mathcal{N}$ is involutive then also $Q = co_{\mathcal{N}} \circ P \circ co_{\mathcal{N}}$.

The interval-valued fuzzy dilation and erosion are called dual w.r.t. an involutive negator $\mathcal{N}$ if they are dual for any given structuring element:

Definition 7.9. *The interval-valued fuzzy dilation $D^I_{\mathcal{C}}$ and erosion $E^I_{\mathcal{I}}$ are dual w.r.t. an involutive negator $\mathcal{N}$ if and only if $D^I_{\mathcal{C}}(\cdot, B)$ is dual to $E^I_{\mathcal{I}}(\cdot, B)$ w.r.t. $\mathcal{N}$ for every $B \in \mathcal{F}_{\mathcal{L}^I}(\mathbb{R}^n)$.*

Such duality relation is interesting because it allows us to construct interval-valued dilations from interval-valued erosions, and vice versa. The following proposition however shows that the duality is only guaranteed under a given condition on the used conjunctor and implicator.

Proposition 7.3.26. [130] *Let $\mathcal{C}$ be a conjunctor, $\mathcal{I}$ an implicator and $\mathcal{N}$ a negator on $\mathcal{L}^I$. Then it holds that the interval-valued fuzzy dilation $D^I_{\mathcal{C}}$ is dual to the erosion $E^I_{\mathcal{I}}$ w.r.t. the negator $\mathcal{N}$ if and only if $\mathcal{C} = \mathcal{C}_{\mathcal{I},\mathcal{N}}$ and $\mathcal{I} = \mathcal{I}_{\mathcal{C},\mathcal{N}}$.*

Proof.

$\Leftarrow$: Suppose that $\mathcal{C} = \mathcal{C}_{\mathcal{I},\mathcal{N}}$ and $\mathcal{I} = \mathcal{I}_{\mathcal{C},\mathcal{N}}$. (Since $\mathcal{N}$ is involutive, these two expressions are equivalent as will be shown in the second part of the proof.) It then holds $\forall A, B \in \mathcal{F}_{\mathcal{L}^I}(\mathbb{R}^n)$ and $\forall y \in \mathbb{R}^n$ that:

$$\begin{aligned} D^I_{\mathcal{C}}(A,B)(y) &= \sup_{x\in\mathbb{R}^n} \mathcal{C}(B(x-y), A(x)) \\ &= \sup_{x\in\mathbb{R}^n} \mathcal{N}(\mathcal{I}(B(x-y), \mathcal{N}(A(x)))) \\ &= \mathcal{N}(\inf_{x\in\mathbb{R}^n} \mathcal{I}(B(x-y), \mathcal{N}(A(x)))) \\ &= (co_{\mathcal{N}}(E^I_{\mathcal{I}}(co_{\mathcal{N}}(A), B)))(y) \end{aligned}$$

and

$$\begin{aligned} E^I_{\mathcal{I}}(A,B)(y) &= \inf_{x\in\mathbb{R}^n} \mathcal{I}(B(x-y), A(x)) \\ &= \inf_{x\in\mathbb{R}^n} \mathcal{N}(\mathcal{C}(B(x-y), \mathcal{N}(A(x)))) \\ &= \mathcal{N}(\sup_{x\in\mathbb{R}^n} \mathcal{C}(B(x-y), \mathcal{N}(A(x)))) \\ &= (co_{\mathcal{N}}(D^I_{\mathcal{C}}(co_{\mathcal{N}}(A), B)))(y) \end{aligned}$$

which means that $D^I_{\mathcal{C}}$ and $E^I_{\mathcal{I}}$ are dual w.r.t. the negator $\mathcal{N}$.

$\Rightarrow$: Suppose that $D^I_{\mathcal{C}}$ and $E^I_{\mathcal{I}}$ are dual w.r.t. the involutive negator $\mathcal{N}$. Choose now $A(x) = a$ and $B(x) = b$ for all $x \in \mathbb{R}^n$, with $a, b \in L^I$, i.e., constant mappings. Let y be an arbitrary element of $\mathbb{R}^n$. Then it holds that

$$\begin{aligned} \mathcal{C}(b,a) &= \sup_{x\in\mathbb{R}^n} \mathcal{C}(B(x-y), A(x)) \\ &= D^I_{\mathcal{C}}(A,B)(y) \\ &= (co_{\mathcal{N}}(E^I_{\mathcal{I}}(co_{\mathcal{N}}(A), B)))(y) \\ &= \mathcal{N}(\inf_{x\in\mathbb{R}^n} \mathcal{I}(B(x-y), \mathcal{N}(A(x)))) \\ &= \mathcal{N}(\mathcal{I}(b, \mathcal{N}(a))) \end{aligned}$$

which means that $\mathcal{C} = \mathcal{C}_{\mathcal{I},\mathcal{N}}$. Since $\mathcal{N}$ is involutive, $\forall (a,b) \in (L^I)^2$ the following equivalence holds:

$$\mathcal{C}(b,a) = \mathcal{N}(\mathcal{I}(b, \mathcal{N}(a))) \Leftrightarrow \mathcal{N}(\mathcal{C}(b, \mathcal{N}(a))) = \mathcal{N}(\mathcal{N}(\mathcal{I}(b, \mathcal{N}(\mathcal{N}(a))))) = \mathcal{I}(b,a),$$

which means that $\mathcal{I} = \mathcal{I}_{\mathcal{C},\mathcal{N}}$.

□

Adjointness

Definition 7.10. *Consider a universe X and two unary operators P and Q on $\mathcal{F}_{\mathcal{L}}(X)$. We say that the pair (Q,P) forms an adjunction if and only if*

$$(\forall A_1, A_2 \in \mathcal{F}_{\mathcal{L}}(X))(P(A_1) \subseteq A_2 \Leftrightarrow A_1 \subseteq Q(A_2)).$$

The interval-valued fuzzy dilation $D^I_{\mathcal{C}}$ and erosion $E^I_{\mathcal{I}}$ are called adjoint if they form an adjunction for every given structuring element:

Definition 7.11. *The interval-valued fuzzy dilation $D^I_{\mathcal{C}}$ and erosion $E^I_{\mathcal{I}}$ are called adjoint if and only if the pair $(E^I_{\mathcal{I}}(\cdot, -B), D^I_{\mathcal{C}}(\cdot, B))$ forms an adjunction for every $B \in \mathcal{F}_{\mathcal{L}^I}(\mathbb{R}^n)$.*

The adjointness is however only guaranteed under a given condition on the used conjunctor and implicator as the following proposition shows.

Proposition 7.3.27. [130] *Let $\mathcal{C}$ be a conjunctor and $\mathcal{I}$ an implicator on $\mathcal{L}^I$. The pair $(E^I_{\mathcal{I}}, D^I_{\mathcal{C}})$ forms an adjunction if and only if the pair $(\mathcal{I}, \mathcal{C})$ satisfies the adjunction principle $(\forall (x, y, z) \in (L^I)^3)(\mathcal{C}(z, x) \leq_{L^I} y \Leftrightarrow x \leq_{L^I} \mathcal{I}(z, y))$.*

Proof.

$\Leftarrow$: Suppose that $(\mathcal{I}, \mathcal{C})$ satisfies the adjunction principle:

$$\mathcal{C}(z, x) \leq_{L^I} y \Leftrightarrow x \leq_{L^I} \mathcal{I}(z, y)\ \forall (x, y, z) \in (L^I)^3.$$

Consider arbitrary $A_1, A_2, B \in \mathcal{F}_{\mathcal{L}^I}(\mathbb{R}^n)$, then it holds:

$$\begin{aligned}
D^I_{\mathcal{C}}(A_1, B) \subseteq A_2 &\Leftrightarrow (\forall y \in \mathbb{R}^n)(D^I_{\mathcal{C}}(A_1, B)(y) \leq_{L^I} A_2(y)) \\
&\Leftrightarrow (\forall y \in \mathbb{R}^n)(\sup_{x \in \mathbb{R}^n} \mathcal{C}(B(x - y), A_1(x)) \leq_{L^I} A_2(y)) \\
&\Leftrightarrow (\forall x, y \in \mathbb{R}^n)(\mathcal{C}(B(x - y), A_1(x)) \leq_{L^I} A_2(y)) \\
&\Leftrightarrow (\forall x, y \in \mathbb{R}^n)(A_1(x) \leq_{L^I} \mathcal{I}(B(x - y), A_2(y))) \\
&\Leftrightarrow (\forall x \in \mathbb{R}^n)(A_1(x) \leq_{L^I} \inf_{y \in \mathbb{R}^n} \mathcal{I}(B(x - y), A_2(y))) \\
&\Leftrightarrow (\forall x \in \mathbb{R}^n)(A_1(x) \leq_{L^I} \inf_{y \in \mathbb{R}^n} \mathcal{I}((-B)(y - x), A_2(y))) \\
&\Leftrightarrow (\forall x \in \mathbb{R}^n)(A_1(x) \leq_{L^I} E^I_{\mathcal{I}}(A_2, -B)(x)) \\
&\Leftrightarrow A_1 \subseteq E^I_{\mathcal{I}}(A_2, -B)
\end{aligned}$$

$\Rightarrow$: Suppose that the pair $(E^I_{\mathcal{I}}, D^I_{\mathcal{C}})$ forms an adjunction. Choose now $A_1(x) = a_1$, $A_2(x) = a_2$ and $B(x) = b$ for all $x \in \mathbb{R}^n$, with $a_1, a_2, b \in L^I$, i.e., constant mappings. Let y be an arbitrary element of $\mathbb{R}^n$. Then it holds that

$$\mathcal{C}(b, a_1) = \sup_{x \in \mathbb{R}^n} \mathcal{C}(B(x - y), A_1(x)) = D^I_{\mathcal{C}}(A_1, B)(y),$$

and

$$\begin{aligned}
\mathcal{I}(b, a_2) &= \inf_{x \in \mathbb{R}^n} \mathcal{I}(B(y - x), A_2(x)) \\
&= \inf_{x \in \mathbb{R}^n} \mathcal{I}((-B)(x - y), A_2(x)) \\
&= E^I_{\mathcal{I}}(A_2, -B)(y).
\end{aligned}$$

Thus we have

$$\mathcal{C}(b,a_1) \leq_{L^I} a_2 \Leftrightarrow D^I_{\mathcal{C}}(A_1,B) \subseteq A_2 \Leftrightarrow A_1 \subseteq E^I_{\mathcal{I}}(A_2,-B) \Leftrightarrow a_1 \leq_{L^I} \mathcal{I}(b,a_2).$$

□

A conjunctor $\mathcal{C}$ and an implicator $\mathcal{I}$ on $\mathcal{L}^{\mathcal{I}}$ will for example satisfy the adjunction principle if $\mathcal{C}$ is a t-norm on $\mathcal{L}^{\mathcal{I}}$ of which the partial mappings are sup-morphisms and $\mathcal{I} = \mathcal{I}_{\mathcal{C}}$ [30].

Idempotence

Proposition 7.3.28. *Let $\mathcal{C}$ be a semi-norm and $\mathcal{I}$ a border implicator on $\mathcal{L}^I$. If $B(\mathbf{0}) = 1_{\mathcal{L}^I}$, then it holds that:*

(i) $D^I_{\mathcal{C}}(A,B) \subseteq D^I_{\mathcal{C}}(D^I_{\mathcal{C}}(A,B),B)$,

(ii) $E^I_{\mathcal{I}}(E^I_{\mathcal{I}}(A,B),B) \subseteq E^I_{\mathcal{I}}(A,B)$.

Proof. Follows from Proposition 7.3.4. □

Proposition 7.3.29. *Let $\mathcal{C}$ be a semi-norm on $\mathcal{L}^I$, and let $\mathcal{I}$ be an implicator on $\mathcal{L}^I$ of which the second partial mappings are inf-morphisms. If $B(\mathbf{0}) = 1_{\mathcal{L}^I}$, then it holds that:*

- *If $\mathcal{C}$ and $\mathcal{I}$ satisfy $(\forall (a,b,c) \in (L^I)^3)(\mathcal{I}(a,\mathcal{I}(b,c)) \geq_{L^I} \mathcal{I}(\mathcal{C}(a,b),c)))$, then it holds that*
$$E^I_{\mathcal{I}}(E^I_{\mathcal{I}}(A,B),B) \supseteq E^I_{\mathcal{I}}(A,B).$$
- *If $\mathcal{I}$ is also a border implicator, then*
$$E^I_{\mathcal{I}}(E^I_{\mathcal{I}}(A,B),B) = E^I_{\mathcal{I}}(A,B).$$

Proof. For all $y \in \mathbb{R}^n$

$$\begin{aligned}
E^I_{\mathcal{I}}(E^I_{\mathcal{I}}(A,B),B)(y) &= \inf_{x\in\mathbb{R}^n} \mathcal{I}(B(x-y), \inf_{z\in\mathbb{R}^n} \mathcal{I}(B(z-x),A(z))) \\
&= \inf_{x\in\mathbb{R}^n} \inf_{z\in\mathbb{R}^n} \mathcal{I}(B(x-y),\mathcal{I}(B(z-x),A(z))) \\
&\geq \inf_{z\in\mathbb{R}^n} \inf_{x\in\mathbb{R}^n} \mathcal{I}(\mathcal{C}(B(x-y),B(z-x)),A(z)) \\
&\geq \inf_{z\in\mathbb{R}^n} \mathcal{I}(\sup_{x\in\mathbb{R}^n} \mathcal{C}(B(x-y),B(z-x)),A(z)) \\
&\geq \inf_{z\in\mathbb{R}^n} \mathcal{I}(\mathcal{C}(B(z-y),B(z-z)),A(z)) \\
&= \inf_{z\in\mathbb{R}^n} \mathcal{I}(B(z-y)),A(z)) \\
&= E^I_{\mathcal{I}}(A,B)(y)
\end{aligned}$$

The successive transitions follow respectively from the defintion of the erosion, the second partial mapping of $\mathcal{I}$ being an inf-morphism, the given condition on $\mathcal{I}$ and $\mathcal{C}$, the first partial mapping of $\mathcal{I}$ being decreasing, choosing $x = z$, the fact that $\mathcal{C}$ is a semi-norm and $B(\mathbf{0}) = 1_{\mathcal{L}^I}$ and the definition of the erosion with the symmetry of B.

If $\mathcal{I}$ is a border implicator, then also the reverse inclusion holds due to Proposition 7.3.28. □

The extra conditions on $\mathcal{C}$ and $\mathcal{I}$ in the above proposition are for example satisfied if (Lemma 1.5.5):

- $\mathcal{C}$ is an associative semi-norm on $\mathcal{L}^I$ and $\mathcal{I} = \mathcal{I}_{\mathcal{C},\mathcal{N}}$, where $\mathcal{N}$ is an arbitrary involutive negator on $\mathcal{L}^I$,
- $\mathcal{C}$ is a t-norm on $\mathcal{L}^I$ of which the partial mappings are sup-morphisms and $\mathcal{I} = \mathcal{I}_{\mathcal{C}}$.

Proposition 7.3.30. *Let $\mathcal{C}$ be a conjunctor and $\mathcal{I}$ an implicator on $\mathcal{L}^I$. If $(\forall (a,b) \in (L^I)^2)(\mathcal{C}(a,\mathcal{I}(a,b)) \leq_{L^I} b \leq_{L^I} \mathcal{I}(a,\mathcal{C}(a,b)))$, then it holds that*

(i) $C^I_{\mathcal{C},\mathcal{I}}(C^I_{\mathcal{C},\mathcal{I}}(A,B),B) = C^I_{\mathcal{C},\mathcal{I}}(A,B)$,

(ii) $O^I_{\mathcal{C},\mathcal{I}}(O^I_{\mathcal{C},\mathcal{I}}(A,B),B) = O^I_{\mathcal{C},\mathcal{I}}(A,B)$.

Proof. Under the given conditions, it follows from Proposition 7.3.6 that the interval-valued fuzzy opening is restrictive and the closing is expansive. So, for the opening this means that $O^I_{\mathcal{C},\mathcal{I}}(O^I_{\mathcal{C},\mathcal{I}}(A,B),B) \subseteq O^I_{\mathcal{C},\mathcal{I}}(A,B)$. Further,

$$\begin{aligned} O^I_{\mathcal{C},\mathcal{I}}(O^I_{\mathcal{C},\mathcal{I}}(A,B),B) &= D^I_{\mathcal{C}}(E^I_{\mathcal{I}}(O^I_{\mathcal{C},\mathcal{I}}(A,B),B),-B) \\ &= D^I_{\mathcal{C}}(E^I_{\mathcal{I}}(D^I_{\mathcal{C}}(E^I_{\mathcal{I}}(A,B),-B),B),-B) \\ &= D^I_{\mathcal{C}}(C^I_{\mathcal{C},\mathcal{I}}(E^I_{\mathcal{I}}(A,B),-B),-B) \end{aligned}$$

Since the closing is expansive, it holds that $O^I_{\mathcal{C},\mathcal{I}}(O^I_{\mathcal{C},\mathcal{I}}(A,B),B) \supseteq D^I_{\mathcal{C}}(E^I_{\mathcal{I}}(A,B),-B) = O^I_{\mathcal{C},\mathcal{I}}(A,B)$. □

The condition on $\mathcal{C}$ and $\mathcal{I}$ in the above proposition will for example be satisfied if $\mathcal{C}$ and $\mathcal{I}$ satisfy the adjunction principle. Indeed, in this case, it holds that

$$\mathcal{C}(a,\mathcal{I}(a,b)) \leq_{L^I} b \Leftrightarrow \mathcal{I}(a,b) \geq_{L^I} \mathcal{I}(a,b)$$

and

$$b \leq_{L^I} \mathcal{I}(a,\mathcal{C}(a,b)) \Leftrightarrow \mathcal{C}(a,b) \geq_{L^I} \mathcal{C}(a,b)$$

and both right inequalities are always trivially fulfilled. As mentioned above, the adjunction principle will for example hold if $\mathcal{C}$ is a t-norm on $\mathcal{L}^{\mathcal{I}}$ of which the partial mappings are sup-morphisms and $\mathcal{I} = \mathcal{I}_{\mathcal{C}}$ [30].

7.4 Conclusion

In this chapter, we have given an overview of the evolution from the original binary mathematical morphology for binary images, over greyscale mathematical morphology such as fuzzy mathematical morphology, to interval-valued fuzzy morphology for interval-valued images. The (interval-valued) fuzzy extension is based on the observation that (interval-valued) greyscale imags and (interval-valued) fuzzy sets can be modelled in the same way. As a consequence, binary mathematical morphology can be extended by extending the binary logical framework on which classical set theory is based to the (interval-valued) fuzzy case, as we have shown. The chapter was then ended with an overview of the basic properties of the interval-valued fuzzy morphological operators.

8

Decomposition of Interval-valued Fuzzy Morphological Operators

In this chapter, we investigate the decomposition of the interval-valued fuzzy morphological operators into their $[\alpha_1, \alpha_2]$-cuts [83, 85]. We are interested in the relationships between the $[\alpha_1, \alpha_2]$-cuts of the result of the interval-valued fuzzy dilation, erosion, opening and closing of an interval-valued image by a given interval-valued structuring element and the result of the corresponding binary operators applied on the $[\alpha_1, \alpha_2]$-cuts of those arguments. It will be shown that in some cases, an equality or inclusion (approximation) will be found. For the cases where the equality does not hold, a counterexample is constructed.This is first of all interesting from a theoretical point of view because it provides us a link between interval-valued fuzzy and binary morphology but secondly also because such conversion into binary operators is likely to result in a lower complexity for the calculation or approximation of the $[\alpha_1, \alpha_2]$-cuts. Moreover, the binary dilation and erosion can be further sped up by a decomposition of the structuring element.

The chapter is organized as follows: The decomposition properties for the different $[\alpha_1, \alpha_2]$-cuts of the interval-valued fuzzy morphological dilation, erosion, opening and closing are respectively presented in Section 8.1, 8.2 and 8.3 and this for both the continuous and the discrete case. Additionally, Section 8.4 discusses and illustrates the results. Section 8.5 concludes the chapter.

8.1 Decomposition of the Interval-valued Fuzzy Dilation

Lemma 8.1.1. [57] *If $\mathcal{C}$ is a semi-norm on $\mathcal{L}^I$, then it holds that $\mathcal{C} \leq \mathcal{C}_{\min}$, i.e.:*

$$(\forall (x,y) \in (L^I)^2)(\mathcal{C}(x,y) \leq_{L^I} \mathcal{C}_{\min}(x,y)).$$

Proof. Let $\mathcal{C}$ be a semi-norm on $\mathcal{L}^I$, then it holds for all $(x,y) \in (L^I)^2$ that

- $\mathcal{C}(x,y) \leq_{L^I} \mathcal{C}(x, 1_{\mathcal{L}^I}) = x$,
- $\mathcal{C}(x,y) \leq_{L^I} \mathcal{C}(1_{\mathcal{L}^I}, y) = y$,

from which it follows that $\mathcal{C}(x,y) \leq_{L^I} \mathcal{C}_{\min}(x,y)$. □

Note that lemma 8.1.1 does not necessarily hold if $\mathcal{C}$ is not a semi-norm on $\mathcal{L}^I$.

Example 8.1.2. Let $\mathcal{C}$ be the conjunctor defined as:

$$\mathcal{C}(x,y) = \begin{cases} 0_{\mathcal{L}^I} & \text{if } \inf(x,y) = 0_{\mathcal{L}^I} \\ 1_{\mathcal{L}^I} & \text{else} \end{cases}, \forall (x,y) \in (L^I)^2.$$

One easily verifies that $\mathcal{C}$ is no semi-norm on $\mathcal{L}^I$ (e.g. $\mathcal{C}(1_{\mathcal{L}^I}, [1/4, 1/2]) = 1_{\mathcal{L}^I} \neq [1/4, 1/2]$) and that $\mathcal{C} \not\leq \mathcal{C}_{\min}$ (e.g. $1_{\mathcal{L}^I} = \mathcal{C}(1_{\mathcal{L}^I}, [1/4, 1/2]) >_{L^I} \mathcal{C}_{\min}(1_{\mathcal{L}^I}, [1/4, 1/2]) = [1/4, 1/2]$).

♢

8.1.1 Decomposition by Strict Sub- and Supercuts

Proposition 8.1.3. *Let $A, B \in \mathcal{F}_{\mathcal{L}^I}(\mathbb{R}^n)$, then it holds for respectively all $\alpha_1 \in [0,1[$ and all $\alpha_2 \in [0,1[$ that:*

$$\begin{array}{ll} \textit{(i)} & D^I_{\mathcal{C}_{\min}}(A,B)_{\overline{\alpha_1}} = D(A_{\overline{\alpha_1}}, B_{\overline{\alpha_1}}), \\ \textit{(ii)} & D^I_{\mathcal{C}_{\min}}(A,B)^{\overline{\alpha_2}} = D(A^{\overline{\alpha_2}}, B^{\overline{\alpha_2}}). \end{array}$$

Proof. Let $A, B \in \mathcal{F}_{\mathcal{L}^I}(\mathbb{R}^n)$, and let $\alpha_1, \alpha_2 \in [0,1[$.

(i)

$$\begin{aligned} y \in D^I_{\mathcal{C}_{\min}}(A,B)_{\overline{\alpha_1}} &\Leftrightarrow D^I_{\mathcal{C}_{\min}}(A,B)(y)_1 > \alpha_1 \\ &\Leftrightarrow \sup_{x \in T_y(d_B) \cap d_A} \mathcal{C}_{\min}(B(x-y), A(x))_1 > \alpha_1 \\ &\Leftrightarrow (\exists x \in T_y(d_B) \cap d_A)(\mathcal{C}_{\min}(B(x-y), A(x))_1 > \alpha_1) \\ &\Leftrightarrow (\exists x \in T_y(d_B) \cap d_A)(\min(B_1(x-y), A_1(x)) > \alpha_1) \\ &\Leftrightarrow (\exists x \in T_y(d_B) \cap d_A)(B_1(x-y) > \alpha_1 \text{ and } A_1(x) > \alpha_1) \\ &\Leftrightarrow (\exists x \in T_y(d_B) \cap d_A)(x \in T_y(B_{\overline{\alpha_1}}) \text{ and } x \in A_{\overline{\alpha_1}}) \\ &\Leftrightarrow T_y(B_{\overline{\alpha_1}}) \cap A_{\overline{\alpha_1}} \neq \emptyset \\ &\Leftrightarrow y \in D(A_{\overline{\alpha_1}}, B_{\overline{\alpha_1}}). \end{aligned}$$

This proves that $D^I_{\mathcal{C}_{\min}}(A,B)_{\overline{\alpha_1}} = D(A_{\overline{\alpha_1}}, B_{\overline{\alpha_1}})$.

(ii) Analogous.

□

Proposition 8.1.4. *Let $A, B \in \mathcal{F}_{\mathcal{L}^I}(\mathbb{R}^n)$ and let C be a semi-norm on $\mathcal{L}^I$, then it holds for respectively all $\alpha_1 \in [0,1[$ and all $\alpha_2 \in [0,1[$ that:*

$$\begin{array}{ll} \textit{(i)} & D^I_{\mathcal{C}}(A,B)_{\overline{\alpha_1}} \subseteq D(A_{\overline{\alpha_1}}, B_{\overline{\alpha_1}}), \\ \textit{(ii)} & D^I_{\mathcal{C}}(A,B)^{\overline{\alpha_2}} \subseteq D(A^{\overline{\alpha_2}}, B^{\overline{\alpha_2}}). \end{array}$$

Proof.

(i) The proof is completely analogous to the one from Proposition 8.1.3 (i). We only have that due to lemma 8.1.1

$$\begin{array}{c} (\exists x \in T_y(d_B) \cap d_A)(\mathcal{C}(B(x-y), A(x))_1 > \alpha_1) \\ \Downarrow \\ (\exists x \in T_y(d_B) \cap d_A)(\mathcal{C}_{\min}(B(x-y), A(x))_1 > \alpha_1) \end{array}$$

only holds in one direction for an arbitrary semi-norm on $\mathcal{L}^I$.

(ii) Analogous.

□

The reverse inclusion does not hold in general.

Example 8.1.5. Let $[\alpha_1, \alpha_2] = [1/4, 1/2]$, $\mathcal{C}(r,s) = [r_1 \cdot s_1, r_2 \cdot s_2]$ for all $r, s \in L^I$, $A(x) = [0.3, 0.6]$ for all $x \in [0,1]$, $A(x) = 0_{\mathcal{L}^I}$ for all $x \in \mathbb{R}\backslash[0,1]$, $B(x) = [0.4, 0.7]$ for all $x \in [0,1]$ and $B(x) = 0_{\mathcal{L}^I}$ for all $x \in \mathbb{R}\backslash[0,1]$).

Then on the one hand

$$0 \in D(A_{\overline{0.25}}, B_{\overline{0.25}}) = D(A^{\overline{0.5}}, B^{\overline{0.5}}) = [-1, 1].$$

On the other hand however:

$$\begin{array}{rcl} D^I_{\mathcal{C}}(A,B)(0) & = & \sup\limits_{x \in T_0(d_B) \cap d_A} \mathcal{C}(B(x), A(x)) \\ & = & \sup\limits_{x \in [0,1]} [0.3 \cdot 0.4, 0.6 \cdot 0.7] \\ & = & [0.12, 0.42] \\ & \not\geqslant_{L^I} & [0.25, 0.5], \end{array}$$

and thus $0 \notin D^I_{\mathcal{C}}(A,B)_{\overline{0.25}}$ and $0 \notin D^I_{\mathcal{C}}(A,B)^{\overline{0.5}}$. So, $D^I_{\mathcal{C}}(A,B)_{\overline{0.25}} \not\supseteq D(A_{\overline{0.25}}, B_{\overline{0.25}})$ and $D^I_{\mathcal{C}}(A,B)^{\overline{0.5}} \not\supseteq D(A^{\overline{0.5}}, B^{\overline{0.5}})$.

♢

Further, the following example illustrates that Proposition 8.1.4 is restricted to semi-norms.

Example 8.1.6. Let $\mathcal{C}$ be the conjunctor defined in Example 8.1.2 (which is not a semi-norm). Further, let $A(x) = [1/4, 1/2]$ for all $x \in [0,1]$, $A(x) = 0_{\mathcal{L}^I}$ for all $x \in \mathbb{R}\backslash[0,1]$ and $B(x) = 1_{\mathcal{L}^I}$ for all $x \in [0,1]$, $B(x) = 0_{\mathcal{L}^I}$ for all $x \in \mathbb{R}\backslash[0,1]$. Then for all $y \in D(d_A, d_B) = [-1,1]$ it holds that

$$\begin{aligned} D^I_{\mathcal{C}}(A,B)(y) &= \sup_{x \in T_y(d_B) \cap d_A} \mathcal{C}(B(x-y), A(x)) \\ &= \sup_{x \in T_y(d_B) \cap d_A} \mathcal{C}([1,1],[1/4,1/2]) \\ &= \sup_{x \in T_y(d_B) \cap d_A} [1,1] \\ &= 1_{\mathcal{L}^I}, \end{aligned}$$

and thus $y \in D^I_{\mathcal{C}}(A,B)_{\overline{0.25}}$ and $y \in D^I_{\mathcal{C}}(A,B)^{\overline{0.5}}$. On the other hand, from $A_{\overline{0.25}} = A^{\overline{0.5}} = \emptyset$ it follows that $D(A_{\overline{0.25}}, B_{\overline{0.25}}) = \emptyset$ and $D(A^{\overline{0.5}}, B^{\overline{0.5}}) = \emptyset$, such that $D^I_{\mathcal{C}}(A,B)_{\overline{0.25}} \not\subseteq D(A_{\overline{0.25}}, B_{\overline{0.25}})$ and $D^I_{\mathcal{C}}(A,B)^{\overline{0.5}} \not\subseteq D(A^{\overline{0.5}}, B^{\overline{0.5}})$.

♢

Remark that the decomposition properties for strict sub- and supercuts given above remain valid in the discrete framework.

8.1.2 Decomposition by Strict $[\alpha_1, \alpha_2]$-cuts

Proposition 8.1.7. *Let $A, B \in \mathcal{F}_{\mathcal{L}^I}(\mathbb{R}^n)$, then it holds for all $[\alpha_1, \alpha_2] \in L^I \backslash U_{L^I}$ that:*

$$D^I_{\mathcal{C}_{\min}}(A,B)^{\overline{\alpha_2}}_{\overline{\alpha_1}} \supseteq D(A^{\overline{\alpha_2}}_{\overline{\alpha_1}}, B^{\overline{\alpha_2}}_{\overline{\alpha_1}}).$$

Proof. The proof is analogous to the one from Proposition 8.1.3. Only, now we have that

$$\begin{gathered} \sup_{x \in T_y(d_B) \cap d_A} \mathcal{C}_{\min}(B(x-y), A(x)) \gg_{L^I} [\alpha_1, \alpha_2] \\ \Uparrow \\ (\exists x \in T_y(d_B) \cap d_A)(\mathcal{C}_{\min}(B(x-y), A(x)) \gg_{L^I} [\alpha_1, \alpha_2]) \end{gathered}$$

only holds in one direction. □

The reverse inclusion does not hold in general.

Example 8.1.8. Let $[\alpha_1, \alpha_2] = [0.3, 0.7]$ and let

$$A(x) = \begin{cases} [0.1, 0.8], & x \in [0, 0.5[\\ [0.5, 0.6], & x \in [0.5, 1] \\ 0_{\mathcal{L}^I}, & else \end{cases}$$

and

$$B(x) = \begin{cases} [0.2, 0.9], & x \in [0, 0.5[\\ [0.4, 0.5], & x \in [0.5, 1] \\ 0_{\mathcal{L}^I}, & else \end{cases}.$$

It then holds that

$$\begin{aligned} D^I_{\mathcal{C}}(A,B)(0) &= \sup_{x \in T_0(d_B) \cap d_A} \mathcal{C}_{\min}(B(x), A(x)) \\ &= \sup(\sup_{x \in [0,0.5[} \mathcal{C}_{\min}(B(x), A(x)), \sup_{x \in [0.5,1]} \mathcal{C}_{\min}(B(x), A(x))) \\ &= \sup([\min(0.2, 0.1), \min(0.9, 0.8)], [\min(0.4, 0.5), \min(0.5, 0.6)]) \\ &= \sup([0.1, 0.8)], [0.4, 0.5]) \\ &= [0.4, 0.8], \end{aligned}$$

which means that $0 \in D^I_{\mathcal{C}}(A,B)^{\overline{0.7}}_{\overline{0.3}}$.

On the other hand, since $A^{\overline{0.7}}_{\overline{0.3}} = \emptyset$ it holds that $D(A^{\overline{0.7}}_{\overline{0.3}}, B^{\overline{0.7}}_{\overline{0.3}}) = \emptyset$, which means that $0 \notin D(A^{\overline{0.7}}_{\overline{0.3}}, B^{\overline{0.7}}_{\overline{0.3}})$. As a consequence $D^I_{\mathcal{C}}(A,B)^{\overline{0.7}}_{\overline{0.3}} \not\subseteq D(A^{\overline{0.7}}_{\overline{0.3}}, B^{\overline{0.7}}_{\overline{0.3}})$.

♢

The strict $[\alpha_1, \alpha_2]$-cut of the interval-valued fuzzy dilation based on the conjunctor $\mathcal{C}_{\min}$ can however always be constructed from binary dilations as follows.

Proposition 8.1.9. *Let $A, B \in \mathcal{F}_{\mathcal{L}^I}(\mathbb{R}^n)$, then it holds for all $[\alpha_1, \alpha_2] \in L^I \backslash U_{L^I}$ that:*

$$D^I_{\mathcal{C}_{\min}}(A,B)^{\overline{\alpha_2}}_{\overline{\alpha_1}} = D(A_{\overline{\alpha_1}}, B_{\overline{\alpha_1}}) \cap D(A^{\overline{\alpha_2}}, B^{\overline{\alpha_2}}).$$

Proof. Follows from Proposition 8.1.3 and the fact that $D^I_{\mathcal{C}_{\min}}(A,B)^{\overline{\alpha_2}}_{\overline{\alpha_1}} = D^I_{\mathcal{C}_{\min}}(A,B)_{\overline{\alpha_1}} \cap D^I_{\mathcal{C}_{\min}}(A,B)^{\overline{\alpha_2}}$. □

Due to Lemma 8.1.1, Proposition 8.1.7 is restricted to the semi-norm $\mathcal{C}_{\min}$. For an arbitrary semi-norm $\mathcal{C}$ there is no relation between the strict $[\alpha_1, \alpha_2]$-cuts $D^I_{\mathcal{C}}(A,B)^{\overline{\alpha_2}}_{\overline{\alpha_1}}$ and the binary dilation $D(A^{\overline{\alpha_2}}_{\overline{\alpha_1}}, B^{\overline{\alpha_2}}_{\overline{\alpha_1}})$ as the following example illustrates.

Example 8.1.10. To illustrate that, for an arbitrary semi-norm $\mathcal{C}$, it does not hold in general that $(\forall [\alpha_1, \alpha_2] \in L^I \backslash U_{L^I})(D^I_{\mathcal{C}}(A,B)^{\overline{\alpha_2}}_{\overline{\alpha_1}} \supseteq D(A^{\overline{\alpha_2}}_{\overline{\alpha_1}}, B^{\overline{\alpha_2}}_{\overline{\alpha_1}}))$, Example 8.1.8 can be used again.

For a counterexample of the reverse inclusion we refer to Example 8.1.5, where $0 \in D(A^{\overline{0.5}}_{\overline{0.25}}, B^{\overline{0.5}}_{\overline{0.25}}) = [-1, 1]$ and $D^I_{\mathcal{C}}(A,B)(0) = [0.12, 0.42]$ or thus $0 \notin D^I_{\mathcal{C}}(A,B)^{\overline{0.5}}_{\overline{0.25}}$.

♢

The strict $[\alpha_1, \alpha_2]$-cut of an interval-valued fuzzy dilation based on an arbitrary semi-norm $\mathcal{C}$ can however always be approximated by binary dilations.

Proposition 8.1.11. *Let $A, B \in \mathcal{F}_{\mathcal{L}^I}(\mathbb{R}^n)$, then it holds for all $[\alpha_1, \alpha_2] \in L^I \backslash U_{L^I}$ that:*

$$D^I_{\mathcal{C}}(A,B)^{\overline{\alpha_2}}_{\overline{\alpha_1}} \subseteq D(A_{\overline{\alpha_1}}, B_{\overline{\alpha_1}}) \cap D(A^{\overline{\alpha_2}}, B^{\overline{\alpha_2}}).$$

Proof. Follows from Proposition 8.1.4 and the fact that $D^I_{\mathcal{C}}(A,B)^{\overline{\alpha_2}}_{\overline{\alpha_1}} = D^I_{\mathcal{C}}(A,B)_{\overline{\alpha_1}} \cap D^I_{\mathcal{C}}(A,B)^{\overline{\alpha_2}}$. □

Remark that the decomposition properties for strict $[\alpha_1, \alpha_2]$-cuts given above remain valid in the discrete framework.

8.1.3 Decomposition by Weak Sub- and Supercuts

For an arbitrary semi-norm $\mathcal{C}$, there is no general relation between the weak sub- and supercut $D^I_{\mathcal{C}}(A,B)_{\alpha_1}$ and $D^I_{\mathcal{C}}(A,B)^{\alpha_2}$ and the binary dilations $D(A_{\alpha_1}, B_{\alpha_1})$ and $D(A^{\alpha_2}, B^{\alpha_2})$.

Example 8.1.12. To illustrate that the inclusion $D^I_{\mathcal{C}}(A,B)_{\alpha_1} \subseteq D(A_{\alpha_1}, B_{\alpha_1})$ does not hold in general, we can use Example 8.1.8 again. However, we can now also construct a counterexample based on the fact that for a weak α_1-subcut of an interval-valued fuzzy set A, the inequality $A_1(x) \geq \alpha_1$, that needs to hold for $x \in \mathbb{R}$ to belong to A_{α_1}, is not strict. Let $[\alpha_1, \alpha_2] = [1/4, 1]$, $A(x) = [x/2, x]$ for all $x \in [0,1[$, $A(x) = 0_{\mathcal{L}^I}$ for all $x \in \mathbb{R}\backslash[0,1[$, $B(x) = 1_{\mathcal{L}^I}$ for all $x \in [0,1]$ and $B(x) = 0_{\mathcal{L}^I}$ for all $x \in \mathbb{R}\backslash[0,1]$. Let $\mathcal{C}$ be the conjunctor defined in Example 8.1.5.

It then holds that

$$\begin{aligned} D^I_{\mathcal{C}}(A,B)(0) &= \sup_{x \in T_0(d_B) \cap d_A} \mathcal{C}(B(x), A(x)) \\ &= \sup_{x \in]0,1[} [x/2, x] \\ &= [1/2, 1], \end{aligned}$$

which means that $0 \in D^I_{\mathcal{C}}(A,B)_{0.5}$.

On the other hand, however, since $A_{0.5} = \emptyset$ also $D(A_{0.5}, B_{0.5}) = \emptyset$ and thus $0 \notin D(A_{0.5}, B_{0.5})$. As a consequence $D^I_{\mathcal{C}}(A,B)_{0.5} \not\subseteq D(A_{0.5}, B_{0.5})$. Note that the above example holds for any semi-norm $\mathcal{C}$, since for any semi-norm $\mathcal{C}$ it holds in the example that $\mathcal{C}(B(x), A(x)) = \mathcal{C}(1_{\mathcal{L}^I}, A(x)) = A(x)$ for all $x \in]0,1[$. (An analogous example can be found for weak supercuts. The above results still hold for the weak α_2-supercut where $\alpha_2 = 1$. It then holds that $0 \in D^I_{\mathcal{C}}(A,B)^1$ and $D(A^1, B^1) = \emptyset$.)

In general also $D^I_{\mathcal{C}}(A,B)_{\alpha_1} \not\supseteq D(A_{\alpha_1}, B_{\alpha_1})$. To illustrate this, we can use Example 8.1.5 again (where the strict and weak 0.25-subcuts of A and B coincide). Adapting that example we get that $0 \in D(A_{0.25}, B_{0.25})$ and $0 \notin D^I_{\mathcal{C}}(A,B)_{0.25}$, which leads to $D^I_{\mathcal{C}}(A,B)_{0.25} \not\supseteq D(A_{0.25}, B_{0.25})$. (Analogously for weak supercuts.)

♢

For the semi-norm $\mathcal{C} = \mathcal{C}_{\min}$, the following partial result holds.

Proposition 8.1.13. *Let $A, B \in \mathcal{F}_{\mathcal{L}^I}(\mathbb{R}^n)$, then it holds for respectively all $\alpha_1 \in]0,1]$ and all $\alpha_2 \in]0,1]$ that:*

$$\begin{array}{ll} \textit{(i)} & D^I_{\mathcal{C}_{\min}}(A,B)_{\alpha_1} \supseteq D(A_{\alpha_1}, B_{\alpha_1}), \\ \textit{(ii)} & D^I_{\mathcal{C}_{\min}}(A,B)^{\alpha_2} \supseteq D(A^{\alpha_2}, B^{\alpha_2}). \end{array}$$

Proof. Let $A, B \in \mathcal{F}_{\mathcal{L}^I}(\mathbb{R}^n)$, and let $\alpha_1, \alpha_2 \in]0,1]$.

(i) Analogous to the proof of Proposition 8.1.3. Only, now it holds that:

$$\begin{array}{c} (\exists x \in T_y(d_B) \cap d_A)(\mathcal{C}_{\min}(B(x-y), A(x))_1 \geq \alpha_1) \\ \Downarrow \\ \sup_{x \in T_y(d_B) \cap d_A} \mathcal{C}_{\min}(B(x-y), A(x))_1 \geq \alpha_1. \end{array}$$

(ii) Analogous.

□

To illustrate that the reverse inclusion does not hold, we refer to Example 8.1.12.

Proposition 8.1.13 remains valid in the discrete framework. Moreover, in the discrete framework, the result also holds for arbitrary semi-norms and for $\mathcal{C}_{\min}$ also the reverse inclusion holds.

Proposition 8.1.14. *Let $A, B \in \mathcal{F}_{\mathcal{L}^I_{r,s}}(\mathbb{Z}^n)$, then it holds for respectively all $\alpha_1 \in]0,1] \cap I_r$ and all $\alpha_2 \in]0,1] \cap I_s$ that:*

$$\begin{array}{l} \textit{(i)}\ D^I_{\mathcal{C}_{\min}}(A,B)_{\alpha_1} = D(A_{\alpha_1}, B_{\alpha_1}), \\ \textit{(ii)}\ D^I_{\mathcal{C}_{\min}}(A,B)^{\alpha_2} = D(A^{\alpha_2}, B^{\alpha_2}). \end{array}$$

Proof. Analogous to the proof of Proposition 8.1.13, where now in the discrete case also

$$\begin{array}{c} (\exists x \in T_y(d_B) \cap d_A)(\mathcal{C}_{\min}(B(x-y), A(x))_1 \geq \alpha_1) \\ \Updownarrow \\ \sup_{x \in T_y(d_B) \cap d_A} \mathcal{C}_{\min}(B(x-y), A(x))_1 \geq \alpha_1. \end{array}$$

□

Proposition 8.1.15. *Let $A, B \in \mathcal{F}_{\mathcal{L}^I_{r,s}}(\mathbb{Z}^n)$, then it holds for respectively all $\alpha_1 \in]0,1] \cap I_r$ and all $\alpha_2 \in]0,1] \cap I_s$ that:*

$$\begin{array}{ll} \textit{(i)} & D^I_{\mathcal{C}}(A,B)_{\alpha_1} \subseteq D(A_{\alpha_1}, B_{\alpha_1}), \\ \textit{(ii)} & D^I_{\mathcal{C}}(A,B)^{\alpha_2} \subseteq D(A^{\alpha_2}, B^{\alpha_2}). \end{array}$$

Proof. Analogous to the proof of Proposition 8.1.14, but for an arbitrary semi-norm $\mathcal{C}$, so that

$$\begin{array}{c} D^I_{\mathcal{C}_{\min}}(A,B)(y)_1 \geq \alpha_1 \\ \Uparrow \end{array}$$

$$D^I_{\mathcal{C}}(A,B)(y)_1 \geq \alpha_1$$
$$\Updownarrow$$
$$y \in D^I_{\mathcal{C}}(A,B)_{\alpha_1}.$$

□

8.1.4 Decomposition by Weak $[\alpha_1, \alpha_2]$-cuts

In general, there is no relation between the weak $[\alpha_1, \alpha_2]$-cut $D^I_{\mathcal{C}}(A,B)^{\alpha_2}_{\alpha_1}$ and the binary dilation $D(A^{\alpha_2}_{\alpha_1}, B^{\alpha_2}_{\alpha_1})$ for an arbitrary semi-norm $\mathcal{C}$. To illustrate this, we can use Example 8.1.12 again, where the weak 0.5-supercut and the weak $[0.5, 1]$-cut of A and B coincide and the results remain valid when using the weak $[0.5, 1]$-cut.

For the semi-norm $\mathcal{C} = \mathcal{C}_{\min}$, the following partial result holds.

Proposition 8.1.16. *Let $A, B \in \mathcal{F}_{\mathcal{L}^I}(\mathbb{R}^n)$, then it holds for all $[\alpha_1, \alpha_2] \in L^I \backslash \{0_{\mathcal{L}^I}\}$ that:*

$$D^I_{\mathcal{C}_{\min}}(A,B)^{\alpha_2}_{\alpha_1} \supseteq D(A^{\alpha_2}_{\alpha_1}, B^{\alpha_2}_{\alpha_1}).$$

Proof. Analogous to the proof of Proposition 8.1.7. □

The reverse inclusion $D^I_{\mathcal{C}_{\min}}(A,B)^{\alpha_2}_{\alpha_1} \subseteq D(A^{\alpha_2}_{\alpha_1}, B^{\alpha_2}_{\alpha_1})$ does not hold in general. To illustrate this, we again refer to Example 8.1.12, where using the weak $[0.5, 1]$-cut instead of the weak 0.5-subcut doesn't affect the results.

Remark that the decomposition properties for weak $[\alpha_1, \alpha_2]$-cuts given above remain valid in the discrete framework. Moreover, the weak $[\alpha_1, \alpha_2]$-cut of the discrete interval-valued fuzzy dilation based on the conjunctor $\mathcal{C}_{\min}$ (respectively semi-norm $\mathcal{C}$) can always be constructed from (respectively approximated by) binary dilations as follows.

Proposition 8.1.17. *Let $A, B \in \mathcal{F}_{\mathcal{L}^I_{r,s}}(\mathbb{Z}^n)$, then it holds for all $[\alpha_1, \alpha_2] \in L^I_{r,s} \setminus \{0_{\mathcal{L}^I}\}$ and every semi-norm $\mathcal{C}$ that:*

(i) $D^I_{\mathcal{C}_{\min}}(A,B)^{\alpha_2}_{\alpha_1} = D(A_{\alpha_1}, B_{\alpha_1}) \cap D(A^{\alpha_2}, B^{\alpha_2})$,
(ii) $D^I_{\mathcal{C}}(A,B)^{\alpha_2}_{\alpha_1} \subseteq D(A_{\alpha_1}, B_{\alpha_1}) \cap D(A^{\alpha_2}, B^{\alpha_2})$.

Proof. Follows from the fact that $D^I_{\mathcal{C}}(A,B)^{\alpha_2}_{\alpha_1} = D^I_{\mathcal{C}}(A,B)_{\alpha_1} \cap D^I_{\mathcal{C}}(A,B)^{\alpha_2}$ for every semi-norm $\mathcal{C}$ and from Proposition 8.1.14 and 8.1.15. □

8.1.5 Decomposition by Strict-Weak and Weak-Strict $[\alpha_1, \alpha_2]$-cuts

For an arbitrary semi-norm $\mathcal{C}$, there is no general relation between the strict-weak and weak-strict $[\alpha_1, \alpha_2]$-cuts $D^I_{\mathcal{C}}(A,B)^{\alpha_2}_{\overline{\alpha_1}}$ and $D^I_{\mathcal{C}}(A,B)^{\overline{\alpha_2}}_{\alpha_1}$ and the binary dilations $D(A^{\alpha_2}_{\overline{\alpha_1}}, B^{\alpha_2}_{\overline{\alpha_1}})$ and $D(A^{\overline{\alpha_2}}_{\alpha_1}, B^{\overline{\alpha_2}}_{\alpha_1})$.

To illustrate this, an analogous example as in Example 8.1.12 can be found.

For the semi-norm $\mathcal{C} = \mathcal{C}_{\min}$, the following partial result holds.

Proposition 8.1.18. *Let $A, B \in \mathcal{F}_{\mathcal{L}^I}(\mathbb{R}^n)$. For all $[\alpha_1, \alpha_2] \in L^I \backslash \{1_{\mathcal{L}^I}\}$ and for all $[\alpha_1, \alpha_2] \in L^I \backslash U_{L^I}$ it respectively holds that:*

$$\begin{array}{ll} \textit{(i)} & D^I_{\mathcal{C}_{\min}}(A,B)^{\alpha_2}_{\overline{\alpha_1}} \supseteq D(A^{\alpha_2}_{\overline{\alpha_1}}, B^{\alpha_2}_{\overline{\alpha_1}}), \\ \textit{(ii)} & D^I_{\mathcal{C}_{\min}}(A,B)^{\overline{\alpha_2}}_{\alpha_1} \supseteq D(A^{\overline{\alpha_2}}_{\alpha_1}, B^{\overline{\alpha_2}}_{\alpha_1}). \end{array}$$

Proof. Analogous to the proof of Proposition 8.1.7. □

As can be illustrated analogously as in Example 8.1.12, the reverse inclusion does not hold.

Remark that the decomposition properties for strict-weak and weak-strict $[\alpha_1, \alpha_2]$-cuts given above remain valid in the discrete framework. Moreover, the weak-strict and strict-weak $[\alpha_1, \alpha_2]$-cut of the discrete interval-valued fuzzy dilation based on the conjunctor $\mathcal{C}_{\min}$ (respectively semi-norm $\mathcal{C}$) can always be constructed from (respectively approximated by) binary dilations as follows.

Proposition 8.1.19. *Let $A, B \in \mathcal{F}_{\mathcal{L}^I_{r,s}}(\mathbb{Z}^n)$ and let $\mathcal{C}$ be a semi-norm. For all $[\alpha_1, \alpha_2] \in L^I_{r,s} \setminus U_{L^I}$ it holds that:*

$$\begin{array}{ll} \textit{(i)} & D^I_{\mathcal{C}_{\min}}(A,B)^{\overline{\alpha_2}}_{\alpha_1} = D(A_{\alpha_1}, B_{\alpha_1}) \cap D(A^{\overline{\alpha_2}}, B^{\overline{\alpha_2}}), \\ \textit{(ii)} & D^I_{\mathcal{C}}(A,B)^{\overline{\alpha_2}}_{\alpha_1} \subseteq D(A_{\alpha_1}, B_{\alpha_1}) \cap D(A^{\overline{\alpha_2}}, B^{\overline{\alpha_2}}). \end{array}$$

For all $[\alpha_1, \alpha_2] \in L^I_{r,s} \setminus \{1_{\mathcal{L}^I}\}$ it holds that:

$$\begin{array}{ll} \textit{(i)} & D^I_{\mathcal{C}_{\min}}(A,B)^{\alpha_2}_{\overline{\alpha_1}} = D(A_{\overline{\alpha_1}}, B_{\overline{\alpha_1}}) \cap D(A^{\alpha_2}, B^{\alpha_2}), \\ \textit{(ii)} & D^I_{\mathcal{C}}(A,B)^{\alpha_2}_{\overline{\alpha_1}} \subseteq D(A_{\overline{\alpha_1}}, B_{\overline{\alpha_1}}) \cap D(A^{\alpha_2}, B^{\alpha_2}). \end{array}$$

Proof. Follows from the fact that $D^I_{\mathcal{C}}(A,B)^{\overline{\alpha_2}}_{\alpha_1} = D^I_{\mathcal{C}}(A,B)_{\alpha_1} \cap D^I_{\mathcal{C}}(A,B)^{\overline{\alpha_2}}$ and analogously $D^I_{\mathcal{C}}(A,B)^{\alpha_2}_{\overline{\alpha_1}} = D^I_{\mathcal{C}}(A,B)_{\overline{\alpha_1}} \cap D^I_{\mathcal{C}}(A,B)^{\alpha_2}$ for every semi-norm $\mathcal{C}$ and from Proposition 8.1.3, 8.1.4, 8.1.14 and 8.1.15. □

8.2 Decomposition of the Interval-valued Fuzzy Erosion

Remember that every implicator $\mathcal{I}$ induces a negator $\mathcal{N}_{\mathcal{I}}$ defined by $\mathcal{N}_{\mathcal{I}}(x) = \mathcal{I}(x, 0_{\mathcal{L}^I})$, $\forall x \in L^I$. Based on this induced negator, the class of border implicators can be split into two subclasses.

Definition 8.1. [95] *Let $\mathcal{I}$ be a border implicator on $\mathcal{L}^I$. $\mathcal{I}$ is called an upper border implicator if $\mathcal{N}_{\mathcal{I}} \geq \mathcal{N}_s$; $\mathcal{I}$ is called a lower border implicator if $\mathcal{N}_{\mathcal{I}} \leq \mathcal{N}_s$.*

Lemma 8.2.1. [95] *If $\mathcal{I}$ is an upper border implicator on $\mathcal{L}^I$, then it holds that $\mathcal{I} \geq \mathcal{I}_{EKD}$, i.e.:*

$$(\forall (x,y) \in (L^I)^2)(\mathcal{I}(x,y) \geq_{L^I} \mathcal{I}_{EKD}(x,y) = [\max(1-x_2, y_1), \max(1-x_1, y_2))].$$

Proof. Let $\mathcal{I}$ be an upper border implicator on $\mathcal{L}^I$. For all $(x,y) \in (L^I)^2$ it holds that:

- $\mathcal{I}(x,y) \geq_{L^I} \mathcal{I}(1_{\mathcal{L}^I}, y) = y$,
- $\mathcal{I}(x,y) \geq_{L^I} \mathcal{I}(x, 0_{\mathcal{L}^I}) \geq_{L^I} \mathcal{N}_s(x)$,

from which it follows that $\mathcal{I}(x,y) \geq_{L^I} \mathcal{I}_{EKD}(x,y)$. □

The previous lemma does not necessarily hold if $\mathcal{I}$ is not an upper border implicator. Also, a lower border implicator $\mathcal{I}$ doesn't necessarily satisfy $\mathcal{I} \leq \mathcal{I}_{EKD}$.

Example 8.2.2. Let $\mathcal{I}$ be the implicator defined as:

$$\mathcal{I}(x,y) = \begin{cases} 1_{\mathcal{L}^I} & \text{if } \inf(x,y) = x \\ y & \text{else} \end{cases}, \forall (x,y) \in (L^I)^2.$$

It is easily verified that $\mathcal{I}$ is a border implicator on $\mathcal{L}^I$, with induced negator $\mathcal{N}_{\mathcal{I}}$ given by:

$$\mathcal{N}_{\mathcal{I}}(x) = \mathcal{I}(x, 0_{\mathcal{L}^I}) = \begin{cases} 1_{\mathcal{L}^I} & \text{if } x = 0_{\mathcal{L}^I} \\ 0_{\mathcal{L}^I} & \text{else} \end{cases}, \forall x \in [0,1].$$

From

$$\begin{cases} \mathcal{N}_{\mathcal{I}}(x) = 0_{\mathcal{L}^I} \text{ and } 0_{\mathcal{L}^I} \leq_{L^I} \mathcal{N}_s(x) & x \neq 0_{\mathcal{L}^I}, \\ \mathcal{N}_{\mathcal{I}}(x) = 1_{\mathcal{L}^I} = \mathcal{N}_s(x) & x = 0_{\mathcal{L}^I}, \end{cases}$$

it follows that $\mathcal{N}_{\mathcal{I}} \leq \mathcal{N}_s$ and thus $\mathcal{I}$ is a lower border implicator. Further, since on the one hand e.g. $1_{\mathcal{L}^I} = \mathcal{I}([0.2,0.3],[0.4,0.5]) >_{L^I} \mathcal{I}_{EKD}([0.2,0.3],[0.4,0.5]) = [0.7,0.8]$, and on the other hand $[0.2,0.3] = \mathcal{I}([0.4,0.5],[0.2,0.3]) <_{L^I} \mathcal{I}_{EKD}([0.4,0.5],[0.2,0.3]) = [0.5,0.6]$, it holds that neither $\mathcal{I} \leq \mathcal{I}_{EKD}$, nor $\mathcal{I} \geq \mathcal{I}_{EKD}$.

♢

8.2.1 Decomposition by Weak Sub- and Supercuts

Proposition 8.2.3. *Let $A, B \in \mathcal{F}_{\mathcal{L}^I}(\mathbb{R}^n)$, then it holds for respectively all $\alpha_1 \in]0,1]$ and all $\alpha_2 \in]0,1]$ that:*

$$\begin{array}{ll} \textit{(i)} & E^I_{\mathcal{I}_{EKD}}(A,B)_{\alpha_1} = E(A_{\alpha_1}, B^{\overline{1-\alpha_1}}), \\ \textit{(ii)} & E^I_{\mathcal{I}_{EKD}}(A,B)^{\alpha_2} = E(A^{\alpha_2}, B_{\overline{1-\alpha_2}}). \end{array}$$

Proof. Let $A, B \in \mathcal{F}_{\mathcal{L}^I}(\mathbb{R}^n)$, and let $\alpha_1, \alpha_2 \in]0,1]$.

(i) It holds that:

$$\begin{aligned} y \in E(A_{\alpha_1}, B^{\overline{1-\alpha_1}}) &\Leftrightarrow T_y(B^{\overline{1-\alpha_1}}) \subseteq A_{\alpha_1} \\ &\Leftrightarrow (\forall x \in T_y(d_B))(B_2(x-y) > 1-\alpha_1 \Rightarrow A_1(x) \geq \alpha_1) \\ &\Leftrightarrow (\forall x \in T_y(d_B))(B_2(x-y) \leq 1-\alpha_1 \text{ or } A_1(x) \geq \alpha_1) \\ &\Leftrightarrow (\forall x \in T_y(d_B))(1-B_2(x-y) \geq \alpha_1 \text{ or } A_1(x) \geq \alpha_1) \\ &\Leftrightarrow (\forall x \in T_y(d_B))(\max(1-B_2(x-y), A_1(x)) \geq \alpha_1) \\ &\Leftrightarrow \inf_{x \in T_y(d_B)} \max(1-B_2(x-y), A_1(x)) \geq \alpha_1 \end{aligned}$$

$$\begin{aligned} &\Leftrightarrow \quad \inf_{x \in T_y(d_B)} \mathcal{I}_{EKD}(B(x-y), A(x))_1 \geq \alpha_1 \\ &\Leftrightarrow \quad E^I_{\mathcal{I}_{EKD}}(A,B)_1(y) \geq \alpha_1 \\ &\Leftrightarrow \quad y \in E^I_{\mathcal{I}_{EKD}}(A,B)_{\alpha_1} \end{aligned}$$

Thus $E^I_{\mathcal{I}_{EKD}}(A,B)_{\alpha_1} = E(A_{\alpha_1}, B^{\overline{1-\alpha_1}})$.

(ii) Analogous.

□

Proposition 8.2.4. *Let $A, B \in \mathcal{F}_{\mathcal{L}^I}(\mathbb{R}^n)$ and let $\mathcal{I}$ be an upper border implicator on $\mathcal{L}^I$, then it holds for respectively all $\alpha_1 \in]0,1]$ and all $\alpha_2 \in]0,1]$ that:*

$$\begin{aligned} &\textit{(i)} \quad E^I_{\mathcal{I}}(A,B)_{\alpha_1} \supseteq E(A_{\alpha_1}, B^{\overline{1-\alpha_1}}), \\ &\textit{(ii)} \quad E^I_{\mathcal{I}}(A,B)^{\alpha_2} \supseteq E(A^{\alpha_2}, B_{\overline{1-\alpha_2}}). \end{aligned}$$

Proof.

(i) The proof is completely analogous to the one from Proposition 8.2.3 (i). We only have that due to lemma 8.2.1

$$\begin{aligned} &\inf_{x \in T_y(d_B)} \mathcal{I}_{EKD}(B_2(x-y), A_1(x))_1 \geq \alpha_1 \\ &\Downarrow \\ &\inf_{x \in T_y(d_B)} \mathcal{I}(B_2(x-y), A_1(x))_1 \geq \alpha_1 \end{aligned}$$

only holds in one direction for an arbitrary upper border implicator $\mathcal{I}$ on $\mathcal{L}^I$.

(ii) Analogous.

□

The reverse inclusion does not hold in general.

Example 8.2.5. Let $A(x) = [0.3, 0.5]$ for all $x \in [0,1]$, $B(x) = [0.5, 0.7]$ for all $x \in [0,1]$ and $A(x) = B(x) = 0_{\mathcal{L}^I}$ for all $x \in \mathbb{R}\backslash[0,1]$. Let $\mathcal{I}$ be the following generalisation of the Łukasiewicz implicator: $\mathcal{I}_L(x,y) = [\min(1, 1-x_2+y_1), \min(1, 1-x_1+y_2)]$, $\forall (x,y) \in (L^I)^2$. It can be verified that this implicator is an upper border implicator.

It then holds that

$$\begin{aligned} E^I_{\mathcal{I}_L}(A,B)(0) &= \inf_{x \in T_0(d_B)} \mathcal{I}_L(B(x), A(x)) \\ &= \inf_{x \in [0,1]} \mathcal{I}_L([0.5, 0.7], [0.3, 0.5]) \\ &= [\min(1, 1-0.7+0.3), \min(1, 1-0.5+0.5)] \\ &= [0.6, 1], \end{aligned}$$

and thus $0 \in E^I_{\mathcal{I}_L}(A,B)_{0.4}$ and $0 \in E^I_{\mathcal{I}_L}(A,B)^{0.6}$.

On the other hand, $E(A_{0.4}, B^{\overline{0.6}}) = E(A^{0.6}, B_{\overline{0.4}}) = E(\emptyset,[0,1]) = \emptyset$ and thus $0 \notin E(A_{0.4}, B^{\overline{0.6}})$ and $0 \notin E(A^{0.6}, B_{\overline{0.4}})$, from which it follows that $E^I_{\mathcal{I}}(A,B)_{0.4} \not\subseteq E(A_{0.4}, B^{\overline{0.6}})$ and $E^I_{\mathcal{I}}(A,B)^{0.6} \not\subseteq E(A^{0.6}, B_{\overline{0.4}})$.

♢

Further, Proposition 8.2.4 is also restricted to upper border implicators as the following example shows.

Example 8.2.6. Let $[\alpha_1,\alpha_2] = [0.3, 0.4]$, $A(x) = [0.4, 0.5]$ for all $x \in [0, 0.5]$, $A(x) = [0.2, 0.3]$ for all $x \in]0.5, 1]$, $B(x) = [0.7, 0.8]$ for all $x \in [0, 0.5]$, $B(x) = [0.4, 0.5]$ for all $x \in]0.5, 1]$ and $A(x) = B(x) = 0_{\mathcal{L}^I}$ for all $x \in \mathbb{R}\backslash[0,1]$. Let $\mathcal{I}$ be the lower border implicator from Example 8.2.2 (which is no upper border implicator).

It then holds that

$$\begin{aligned}
E^I_{\mathcal{I}}(A,B)(0) &= \inf_{x\in T_0(d_B)} \mathcal{I}(B(x),A(x)) \\
&= \inf(\inf_{x\in[0,0.5]} \mathcal{I}(B(x),A(x)), \inf_{x\in]0.5,1]} \mathcal{I}(B(x),A(x))) \\
&= \inf(\mathcal{I}([0.7,0.8],[0.4,0.5]), \mathcal{I}([0.4,0.5],[0.2,0.3])) \\
&= \inf([0.4,0.5],[0.2,0.3]) \\
&= [0.2,0.3] \\
&\not\geq_{L^I} [0.3,0.4],
\end{aligned}$$

which means that $0 \notin E^I_{\mathcal{I}}(A,B)_{0.3}$ and $0 \notin E^I_{\mathcal{I}}(A,B)^{0.4}$.

On the other hand, $E(A_{0.3}, B^{\overline{0.7}}) = E(A^{0.4}, B_{\overline{0.6}}) = E([0,0.5],[0,0.5]) = \{0\}$. Consequently $E^I_{\mathcal{I}}(A,B)_{0.3} \not\supseteq E(A_{0.3}, B^{\overline{0.7}})$ and $E^I_{\mathcal{I}}(A,B)^{0.4} \not\supseteq E(A^{0.4}, B_{\overline{0.6}})$.

♢

Remark that the decomposition properties for weak sub- and supercuts given above remain valid in the discrete framework.

8.2.2 Decomposition by Weak $[\alpha_1, \alpha_2]$-cuts

In general, for an arbitrary upper border implicator $\mathcal{I}$, there is no relation between the weak $[\alpha_1,\alpha_2]$-cut $E^I_{\mathcal{I}}(A,B)^{\alpha_2}_{\alpha_1}$ and the binary erosion $E(A^{\alpha_2}_{\alpha_1}, B^{\overline{1-\alpha_1}}_{\overline{1-\alpha_2}})$. This is illustrated in the following example.

Example 8.2.7. To illustrate that the inclusion $E^I_{\mathcal{I}}(A,B)^{\alpha_2}_{\alpha_1} \subseteq E(A^{\alpha_2}_{\alpha_1}, B^{\overline{1-\alpha_1}}_{\overline{1-\alpha_2}})$ does not always hold, we can use Example 8.2.5 again. For $[\alpha_1,\alpha_2] = [0.4, 0.6]$, the weak $[0.4, 0.6]$-cut and the weak 0.4-subcut and 0.6-supercut coincide and the results remain valid for the weak $[0.4, 0.6]$-cut.

In general also $E^I_{\mathcal{I}}(A,B)^{\alpha_2}_{\alpha_1} \not\supseteq E(A^{\alpha_2}_{\alpha_1}, B^{\overline{1-\alpha_1}}_{\overline{1-\alpha_2}})$. Let $\mathcal{I}$ be $\mathcal{I}_{EKD}$, $[\alpha_1,\alpha_2] = [0.3, 0.4]$, $A(x) = [0.4, 0.5]$ for all $x \in [0, 0.5]$ and $A(x) = [0.2, 0.3]$ for all $x \in]0.5, 1]$, $B(x) = [0.7, 0.8]$ for all $x \in [0, 0.5]$ and $B(x) = [0.4, 0.8]$ for all $x \in]0.5, 1]$.

For the binary erosion we find that $E(A^{\alpha_2}_{\alpha_1}, B^{\overline{1-\alpha_1}}_{\overline{1-\alpha_2}}) = E([0, 0.5], [0, 0.5]) = \{0\}$. Further, it also holds that

$$\begin{array}{rcl}
E^I_{\mathcal{I}_{EKD}}(A,B)(0) & = & \inf\limits_{x\in T_0(d_B)} \mathcal{I}_{EKD}(B(x), A(x)) \\
& = & \inf(\inf\limits_{x\in[0,0.5]} \mathcal{I}_{EKD}(B(x), A(x)), \\
& & \inf\limits_{x\in]0.5,1]} \mathcal{I}_{EKD}(B(x), A(x))) \\
& = & \inf(\mathcal{I}_{EKD}([0.7, 0.8], [0.4, 0.5]), \\
& & \mathcal{I}_{EKD}([0.4, 0.8], [0.2, 0.3])) \\
& = & \inf([0.4, 0.5], [0.2, 0.6]) \\
& = & [0.2, 0.5] \\
& \not\geq_{L^I} & [\alpha_1, \alpha_2].
\end{array}$$

As a consequence, $E^I_{\mathcal{I}_{EKD}}(A,B)^{\alpha_2}_{\alpha_1} \not\supseteq E(A^{\alpha_2}_{\alpha_1}, B^{\overline{1-\alpha_1}}_{\overline{1-\alpha_2}})$.

♢

For the upper border implicator $\mathcal{I} = \mathcal{I}_{EKD}$, the following partial result holds.

Proposition 8.2.8. *Let $A, B \in \mathcal{F}_{\mathcal{L}^I}(\mathbb{R}^n)$, then it holds for all $[\alpha_1,\alpha_2] \in L^I \backslash \{0_{\mathcal{L}^I}\}$ that:*

$$E^I_{\mathcal{I}_{EKD}}(A,B)^{\alpha_2}_{\alpha_1} \subseteq E(A^{\alpha_2}_{\alpha_1}, B^{\overline{1-\alpha_1}}_{\overline{1-\alpha_2}}).$$

Proof. Let $A, B \in \mathcal{F}_{\mathcal{L}^I}(\mathbb{R}^n)$ and $[\alpha_1,\alpha_2] \in L^I \backslash \{0_{\mathcal{L}^I}\}$. It holds that:

$$\begin{array}{rcl}
y \in E(A^{\alpha_2}_{\alpha_1}, B^{\overline{1-\alpha_1}}_{\overline{1-\alpha_2}}) & \Leftrightarrow & T_y(B^{\overline{1-\alpha_1}}_{\overline{1-\alpha_2}}) \subseteq A^{\alpha_2}_{\alpha_1} \\
& \Leftrightarrow & (\forall x \in T_y(d_B)) \\
& & ((B_1(x-y) > 1-\alpha_2 \text{ and } B_2(x-y) > 1-\alpha_1) \\
& & \Rightarrow (A_1(x) \geq \alpha_1 \text{ and } A_2(x) \geq \alpha_2)) \\
& \Leftrightarrow & (\forall x \in T_y(d_B)) \\
& & ((B_1(x-y) \leq 1-\alpha_2 \text{ or } B_2(x-y) \leq 1-\alpha_1) \text{ or} \\
& & (A_1(x) \geq \alpha_1 \text{ and } A_2(x) \geq \alpha_2)) \\
& \Leftrightarrow & (\forall x \in T_y(d_B)) \\
& & ((1-B_1(x-y) \geq \alpha_2 \text{ or } 1-B_2(x-y) \geq \alpha_1) \text{ or} \\
& & (A_1(x) \geq \alpha_1 \text{ and } A_2(x) \geq \alpha_2)) \\
& \Leftarrow & (\forall x \in T_y(d_B))
\end{array}$$

$$
\begin{aligned}
& (\max(1 - B_2(x-y), A_1(x)) \geq \alpha_1 \text{ and} \\
& \max(1 - B_1(x-y), A_2(x)) \geq \alpha_2) \\
\Leftrightarrow \quad & (\forall x \in T_y(d_B))(\mathcal{I}_{EKD}(B(x-y), A(x)) \geq_{L^I} [\alpha_1, \alpha_2]) \\
\Leftrightarrow \quad & \inf_{x \in T_y(d_B)} \mathcal{I}_{EKD}(B(x-y), A(x)) \geq_{L^I} [\alpha_1, \alpha_2] \\
\Leftrightarrow \quad & E^I_{\mathcal{I}_{EKD}}(A,B)(y) \geq_{L^I} [\alpha_1, \alpha_2] \\
\Leftrightarrow \quad & y \in E^I_{\mathcal{I}_{EKD}}(A,B)^{\alpha_2}_{\alpha_1}
\end{aligned}
$$

This proves that $E^I_{\mathcal{I}_{EKD}}(A,B)^{\alpha_2}_{\alpha_1} \subseteq E(A^{\alpha_2}_{\alpha_1}, B^{\overline{1-\alpha_1}}_{\overline{1-\alpha_2}})$. □

The reverse inclusion does not hold as illustrated in Example 8.2.7.

The weak $[\alpha_1, \alpha_2]$-cut of the interval-valued fuzzy erosion based on the implicator $\mathcal{I}_{EKD}$ can however always be constructed by binary erosions as follows.

Proposition 8.2.9. *Let $A, B \in \mathcal{F}_{\mathcal{L}^I}(\mathbb{R}^n)$, then it holds for all $[\alpha_1, \alpha_2] \in L^I \backslash \{0_{\mathcal{L}^I}\}$ that:*

$$E^I_{\mathcal{I}_{EKD}}(A,B)^{\alpha_2}_{\alpha_1} = E(A_{\alpha_1}, B^{\overline{1-\alpha_1}}) \cap E(A^{\alpha_2}, B_{\overline{1-\alpha_2}}).$$

Proof. Follows from $E^I_{\mathcal{I}_{EKD}}(A,B)^{\alpha_2}_{\alpha_1} = E^I_{\mathcal{I}_{EKD}}(A,B)_{\alpha_1} \cap E^I_{\mathcal{I}_{EKD}}(A,B)^{\alpha_2}$ and from Proposition 8.2.3. □

Analogously, an interval-valued fuzzy erosion based on an upper border implicator $\mathcal{I}$ can be approximated by binary erosions.

Proposition 8.2.10. *Let $A, B \in \mathcal{F}_{\mathcal{L}^I}(\mathbb{R}^n)$, then it holds for all $[\alpha_1, \alpha_2] \in L^I \backslash \{0_{\mathcal{L}^I}\}$ that:*

$$E^I_{\mathcal{I}}(A,B)^{\alpha_2}_{\alpha_1} \supseteq E(A_{\alpha_1}, B^{\overline{1-\alpha_1}}) \cap E(A^{\alpha_2}, B_{\overline{1-\alpha_2}}).$$

Proof. Follows from the fact that $E^I_{\mathcal{I}}(A,B)^{\alpha_2}_{\alpha_1} = E^I_{\mathcal{I}}(A,B)_{\alpha_1} \cap E^I_{\mathcal{I}}(A,B)^{\alpha_2}$ and from Proposition 8.2.4. □

Remark that the decomposition properties for weak $[\alpha_1, \alpha_2]$-cuts given above remain valid in the discrete framework.

8.2.3 Decomposition by Strict Sub- and Supercuts

In general, there is no relation between the strict sub- and supercuts $E^I_{\mathcal{I}}(A,B)_{\overline{\alpha_1}}$ and $E^I_{\mathcal{I}}(A,B)^{\overline{\alpha_2}}$ and the binary erosions $E(A_{\overline{\alpha_1}}, B^{1-\alpha_1})$ and $E(A^{\overline{\alpha_2}}, B_{1-\alpha_2})$ for an arbitrary upper border implicator $\mathcal{I}$. This is illustrated in the following example.

Example 8.2.11. To show that it does not always hold that $E^I_{\mathcal{I}}(A,B)_{\overline{\alpha_1}} \subseteq E(A_{\overline{\alpha_1}}, B^{1-\alpha_1})$ and $E^I_{\mathcal{I}}(A,B)^{\overline{\alpha_2}} \subseteq E(A^{\overline{\alpha_2}}, B_{1-\alpha_2})$ for an arbitrary upper border implicator $\mathcal{I}$, we can use Example 8.2.5 again, where working with strict sub- and supercuts instead of weak sub- and supercuts does not affect the results.

In general also $E^I_{\mathcal{I}}(A,B)_{\overline{\alpha_1}} \not\supseteq E(A_{\overline{\alpha_1}}, B^{1-\alpha_1})$ and $E^I_{\mathcal{I}}(A,B)^{\overline{\alpha_2}} \not\supseteq E(A^{\overline{\alpha_2}}, B_{1-\alpha_2})$. Let $\mathcal{I}$ be $\mathcal{I}_{EKD}$, $\alpha_1 = 0.5$, $A(x) = [\frac{2-x}{2}, 1]$ for all $x \in]0,1]$, $B(x) = [0.7, 0.8]$ for all $x \in]0,1]$ and $A(x) = B(x) = 0_{\mathcal{L}^I}$ for all $x \in \mathbb{R}\backslash]0,1]$. For the binary erosion we then find that $E(A_{\overline{\alpha_1}}, B^{1-\alpha_1}) = E(]0,1],]0,1]) = \{0\}$. Further, it also holds that

$$\begin{aligned} E^I_{\mathcal{I}_{EKD}}(A,B)(0) &= \inf_{x \in T_0(d_B)} \mathcal{I}_{EKD}(B(x), A(x)) \\ &= \inf_{x \in]0,1]} \mathcal{I}_{EKD}([0.7, 0.8], [\frac{2-x}{2}, 1]) \\ &= \inf_{x \in]0,1]} [\max(1 - 0.8, \frac{2-x}{2}), \max(1 - 0.7, 1)] \\ &= \inf_{x \in]0,1]} [\frac{2-x}{2}, 1] \\ &= [0.5, 1], \end{aligned}$$

which means that $0 \notin E^I_{\mathcal{I}_{EKD}}(A,B)_{\overline{0.5}}$ and $E^I_{\mathcal{I}_{EKD}}(A,B)_{\overline{\alpha_1}} \not\supseteq E(A_{\overline{\alpha_1}}, B^{1-\alpha_1})$.

An analogous example can be found for strict α_2-supercuts.

♢

For the upper border implicator $\mathcal{I} = \mathcal{I}_{EKD}$, the following partial result holds.

Proposition 8.2.12. *For $A, B \in \mathcal{F}_{\mathcal{L}^I}(\mathbb{R}^n)$ it holds for respectively all $\alpha_1 \in [0,1[$ and all $\alpha_2 \in [0,1[$ that:*

(i) $E^I_{\mathcal{I}_{EKD}}(A,B)_{\overline{\alpha_1}} \subseteq E(A_{\overline{\alpha_1}}, B^{1-\alpha_1})$,
(ii) $E^I_{\mathcal{I}_{EKD}}(A,B)^{\overline{\alpha_2}} \subseteq E(A^{\overline{\alpha_2}}, B_{1-\alpha_2})$.

Proof. Let $A, B \in \mathcal{F}_{\mathcal{L}^I}(\mathbb{R}^n)$, and let $\alpha_1, \alpha_2 \in [0,1[$.

(i) Analogous to the proof of Proposition 8.2.3. However, now we only have that for all $y \in \mathbb{R}^n$:

$$\inf_{x \in T_y(d_B)} \max(1 - B_2(x-y), A_1(x)) > \alpha_1$$
$$\Downarrow$$
$$(\forall x \in T_y(d_B))(\max(1 - B_2(x-y), A_1(x)) > \alpha_1)$$

(ii) Analogous.

□

The reverse inclusion does not hold as illustrated in Example 8.2.11.

Proposition 8.2.12 remains valid in the discrete framework. Moreover, in the discrete framework, the result also holds for arbitrary lower border implicators and for $\mathcal{I}_{EKD}$ also the reverse inclusion holds.

Proposition 8.2.13. *For $A, B \in \mathcal{F}_{\mathcal{L}^I_{r,s}}(\mathbb{Z}^n)$ it holds for respectively all $\alpha_1 \in]0,1] \cap I_r$ and all $\alpha_2 \in]0,1] \cap I_s$ that:*

$$\begin{array}{ll} \textit{(i)} & E^I_{\mathcal{I}_{EKD}}(A,B)_{\overline{\alpha_1}} = E(A_{\overline{\alpha_1}}, B^{1-\alpha_1}), \\ \textit{(ii)} & E^I_{\mathcal{I}_{EKD}}(A,B)^{\overline{\alpha_2}} = E(A^{\overline{\alpha_2}}, B_{1-\alpha_2}). \end{array}$$

Proof. Analogous to the proof of Proposition 8.2.12, where now in the discrete case also

$$\begin{array}{c} (\forall x \in T_y(d_B))(\max(1 - B_2(x-y), A_1(x)) > \alpha_1) \\ \Updownarrow \\ \inf\limits_{x \in T_y(d_B)} \max(1 - B_2(x-y), A_1(x)) > \alpha_1. \end{array}$$

□

Proposition 8.2.14. *For $A, B \in \mathcal{F}_{\mathcal{L}^I_{r,s}}(\mathbb{Z}^n)$ it holds for respectively all $\alpha_1 \in]0,1] \cap I_r$ and all $\alpha_2 \in]0,1] \cap I_s$ that:*

$$\begin{array}{ll} \textit{(i)} & E^I_{\mathcal{I}}(A,B)_{\overline{\alpha_1}} \supseteq E(A_{\overline{\alpha_1}}, B^{1-\alpha_1}), \\ \textit{(ii)} & E^I_{\mathcal{I}}(A,B)^{\overline{\alpha_2}} \supseteq E(A^{\overline{\alpha_2}}, B_{1-\alpha_2}). \end{array}$$

Proof. Analogous to the proof of Proposition 8.2.13, but for an arbitrary upper border implicator $\mathcal{I}$, so that

$$\begin{array}{c} E^I_{\mathcal{I}_{EKD}}(A,B)_1(y) > \alpha_1 \\ \Downarrow \\ E^I_{\mathcal{I}}(A,B)_1(y) > \alpha_1 \\ \Updownarrow \\ y \in E^I_{\mathcal{I}}(A,B)_{\overline{\alpha_1}}. \end{array}$$

□

8.2.4 Decomposition by Strict $[\alpha_1, \alpha_2]$-cuts

In general, for an arbitrary upper border implicator $\mathcal{I}$, there is no relation between the strict $[\alpha_1, \alpha_2]$-cut $E^I_{\mathcal{I}}(A,B)^{\overline{\alpha_2}}_{\overline{\alpha_1}}$ and the binary erosion $E(A^{\overline{\alpha_2}}_{\overline{\alpha_1}}, B^{1-\alpha_1}_{1-\alpha_2})$. To illustrate this, we can use Example 8.2.5 and 8.2.7 again, where working with strict $[\alpha_1, \alpha_2]$-cuts instead of respectively weak sub- and supercuts and weak $[\alpha_1, \alpha_2]$-cuts does not effect the results.

For the upper border implicator $\mathcal{I} = \mathcal{I}_{EKD}$, the following partial result holds.

Proposition 8.2.15. *Let $A, B \in \mathcal{F}_{\mathcal{L}^I}(\mathbb{R}^n)$, then it holds for all $[\alpha_1, \alpha_2] \in L^I \backslash U_{L^I}$ that:*

$$E^I_{\mathcal{I}_{EKD}}(A,B)^{\overline{\alpha_2}}_{\overline{\alpha_1}} \subseteq E(A^{\overline{\alpha_2}}_{\overline{\alpha_1}}, B^{1-\alpha_1}_{1-\alpha_2}).$$

Proof. Analogous to the proof of Proposition 8.2.8. Only, now it holds for all $y \in \mathbb{R}^n$ that:

$$\inf_{x \in T_y(d_B)} \mathcal{I}_{EKD}(B(x-y), A(x)) \gg_{L^I} [\alpha_1, \alpha_2])$$
$$\Downarrow$$
$$(\forall x \in T_y(d_B))(\mathcal{I}_{EKD}(B(x-y), A(x)) \gg_{L^I} [\alpha_1, \alpha_2])$$

This however does not change the result. □

To illustrate that the reverse inclusion does not hold, we refer to Example 8.2.7, where using strict $[\alpha_1, \alpha_2]$-cuts instead of the weak $[\alpha_1, \alpha_2]$-cuts does not affect the results.

Remark that the decomposition properties for strict $[\alpha_1, \alpha_2]$-cuts given above remain valid in the discrete framework. Moreover, the strict $[\alpha_1, \alpha_2]$-cut of the discrete interval-valued fuzzy erosion based on the implicator $\mathcal{I}_{EKD}$ (respectively upper border implicator $\mathcal{I}$) can always be constructed from (respectively approximated by) binary erosion as follows.

Proposition 8.2.16. *For $A, B \in \mathcal{F}_{\mathcal{L}^I_{r,s}}(\mathbb{Z}^n)$ it holds for all $[\alpha_1, \alpha_2] \in L^I_{r,s} \setminus U_{L^I}$ and every upper border implicator $\mathcal{I}$ that:*

(i) $E^I_{\mathcal{I}_{EKD}}(A, B)^{\overline{\alpha_2}}_{\overline{\alpha_1}} = E(A_{\overline{\alpha_1}}, B^{1-\alpha_1}) \cap E(A^{\overline{\alpha_2}}, B_{1-\alpha_2})$,
(ii) $E^I_{\mathcal{I}_{EKD}}(A, B)^{\overline{\alpha_2}}_{\overline{\alpha_1}} \supseteq E(A_{\overline{\alpha_1}}, B^{1-\alpha_1}) \cap E(A^{\overline{\alpha_2}}, B_{1-\alpha_2})$.

Proof. Follows from Proposition 8.2.13 and 8.2.14. □

8.2.5 Decomposition by Weak-Strict and Strict-Weak $[\alpha_1, \alpha_2]$-cuts

In general, for an arbitrary upper border implicator $\mathcal{I}$, there is no relation between the weak-strict and the strict-weak $[\alpha_1, \alpha_2]$-cuts $E^I_{\mathcal{I}}(A, B)^{\overline{\alpha_2}}_{\alpha_1}$ and $E^I_{\mathcal{I}}(A, B)^{\alpha_2}_{\overline{\alpha_1}}$ and the respective binary erosions $E(A^{\overline{\alpha_2}}_{\alpha_1}, B^{\overline{1-\alpha_1}}_{1-\alpha_2})$ and $E(A^{\alpha_2}_{\overline{\alpha_1}}, B^{1-\alpha_1}_{\overline{1-\alpha_2}})$ respectively. To illustrate this, we can use Example 8.2.5 and 8.2.7 again, where working with weak-strict and strict-weak $[\alpha_1, \alpha_2]$-cuts instead of respectively weak sub- and supercuts and weak $[\alpha_1, \alpha_2]$-cuts does not effect the results.

For the upper border implicator $\mathcal{I} = \mathcal{I}_{EKD}$, the following partial result holds.

Proposition 8.2.17. *Let $A, B \in \mathcal{F}_{\mathcal{L}^I}(\mathbb{R}^n)$, then it holds for respectively all $[\alpha_1, \alpha_2] \in L^I \setminus U_{L^I}$ and all $[\alpha_1, \alpha_2] \in L^I \setminus \{1_{\mathcal{L}^I}\}$ that:*

(i) $E^I_{\mathcal{I}_{EKD}}(A, B)^{\overline{\alpha_2}}_{\alpha_1} \subseteq E(A^{\overline{\alpha_2}}_{\alpha_1}, B^{\overline{1-\alpha_1}}_{1-\alpha_2})$,
(ii) $E^I_{\mathcal{I}_{EKD}}(A, B)^{\alpha_2}_{\overline{\alpha_1}} \subseteq E(A^{\alpha_2}_{\overline{\alpha_1}}, B^{1-\alpha_1}_{\overline{1-\alpha_2}})$.

Proof.

(i) Analogous to the proof of Proposition 8.2.8. Only, now it holds for all $y \in \mathbb{R}^n$ that:

$$\inf_{x \in T_y(d_B)} \mathcal{I}_{EKD}(B(x-y), A(x))_1 \geq \alpha_1 \text{ and}$$

$$\inf_{x \in T_y(d_B)} \mathcal{I}_{EKD}(B(x-y), A(x))_2 > \alpha_2$$
$$\Downarrow$$
$$(\forall x \in T_y(d_B))(\mathcal{I}_{EKD}(B(x-y), A(x))_1 \geq \alpha_1 \text{ and } \mathcal{I}_{EKD}(B(x-y), A(x))_2 > \alpha_2)$$

This however does not change the result.

(ii) Analogous.

□

To illustrate that the reverse inclusion does not hold, we refer to Example 8.2.7 again, where working with weak-strict or strict-weak $[\alpha_1, \alpha_2]$-cuts instead of weak $[\alpha_1, \alpha_2]$-cuts does not affect the results.

Remark that the decomposition properties for weak-strict and strict-weak $[\alpha_1, \alpha_2]$-cuts given above remain valid in the discrete framework. Moreover, the weak-strict and strict-weak $[\alpha_1, \alpha_2]$-cut of the discrete interval-valued fuzzy erosion based on the implicator $\mathcal{I}_{EKD}$ (respectively upper border implicator $\mathcal{I}$) can always be constructed from (respectively approximated by) binary erosion as follows.

Proposition 8.2.18. *Let $A, B \in \mathcal{F}_{\mathcal{L}^I_{r,s}}(\mathbb{Z}^n)$ and let $\mathcal{I}$ be an upper border implicator. For all $[\alpha_1, \alpha_2] \in L^I_{r,s} \setminus U_{L^I}$ it holds that:*

(i) $E^I_{\mathcal{I}_{EKD}}(A, B)^{\overline{\alpha_2}}_{\alpha_1} = E(A_{\alpha_1}, B^{\overline{1-\alpha_1}}) \cap E(A^{\overline{\alpha_2}}, B_{1-\alpha_2})$,
(ii) $E^I_{\mathcal{I}}(A, B)^{\overline{\alpha_2}}_{\alpha_1} \supseteq E(A_{\alpha_1}, B^{\overline{1-\alpha_1}}) \cap E(A^{\overline{\alpha_2}}, B_{1-\alpha_2})$.

For all $[\alpha_1, \alpha_2] \in L^I_{r,s} \setminus \{1_{\mathcal{L}^I}\}$ it holds that:

(i) $E^I_{\mathcal{I}_{EKD}}(A, B)^{\alpha_2}_{\overline{\alpha_1}} = E(A_{\overline{\alpha_1}}, B^{1-\alpha_1}) \cap E(A^{\alpha_2}, B_{\overline{1-\alpha_2}})$,
(ii) $E^I_{\mathcal{I}}(A, B)^{\alpha_2}_{\overline{\alpha_1}} \supseteq E(A_{\overline{\alpha_1}}, B^{1-\alpha_1}) \cap E(A^{\alpha_2}, B_{\overline{1-\alpha_2}})$.

Proof. Follows from Proposition 8.2.3, 8.2.4, 8.2.13 and 8.2.14. □

8.3 Decomposition of the Interval-valued Fuzzy Closing and Opening

We first prove the following lemma:

Lemma 8.3.1. *Let $A \in \mathcal{F}_{\mathcal{L}^I}(\mathbb{R}^n)$ and let $[\alpha_1, \alpha_2] \in L^I$, then it holds that:*

(i) $\alpha_2 \in]0, 0.5]$ $\Rightarrow$ $A^{\alpha_2} \supseteq A^{\overline{\alpha_2}} \supseteq A_{\overline{1-\alpha_2}}$,
(ii) $\alpha_1 \in [0.5, 1[$ $\Rightarrow$ $A_{\overline{\alpha_1}} \subseteq A^{\overline{1-\alpha_1}} \subseteq A^{1-\alpha_1}$,
(iii) $\alpha_2 \in [0, 0.5[$ $\Rightarrow$ $A^{\overline{\alpha_2}} \supseteq A_{1-\alpha_2}$,
(iv) $\alpha_1 \in]0.5, 1]$ $\Rightarrow$ $A_{\alpha_1} \subseteq A^{\overline{1-\alpha_1}}$.

Proof.

(i) $\alpha_2 \in]0, 0.5]$

$$\begin{aligned} x \in A_{\overline{1-\alpha_2}} &\Leftrightarrow A_1(x) > 1-\alpha_2 \\ &\Rightarrow A_2(x) \geq A_1(x) > 1-\alpha_2 \geq \alpha_2 \text{ (i.e., } x \in A^{\overline{\alpha_2}}) \\ &\Rightarrow A_2(x) \geq \alpha_2 \text{ (i.e. } x \in A^{\alpha_2}) \end{aligned}$$

(ii) $\alpha_1 \in [0.5, 1[$

$$\begin{aligned} x \in A_{\overline{\alpha_1}} &\Leftrightarrow A_1(x) > \alpha_1 \\ &\Rightarrow A_2(x) \geq A_1(x) > \alpha_1 \geq 1-\alpha_1 \text{ (i.e., } x \in A^{\overline{1-\alpha_1}}) \\ &\Rightarrow A_2(x) \geq 1-\alpha_1 \text{ (i.e. } x \in A^{1-\alpha_1}) \end{aligned}$$

(iii) $\alpha_2 \in [0, 0.5[$

$$\begin{aligned} x \in A_{1-\alpha_2} &\Leftrightarrow A_1(x) \geq 1-\alpha_2 \\ &\Rightarrow A_2(x) \geq A_1(x) \geq 1-\alpha_2 > \alpha_2 \text{ (i.e., } x \in A^{\overline{\alpha_2}}) \end{aligned}$$

(iv) $\alpha_1 \in]0.5, 1]$

$$\begin{aligned} x \in A_{\alpha_1} &\Leftrightarrow A_1(x) \geq \alpha_1 \\ &\Rightarrow A_2(x) \geq A_1(x) \geq \alpha_1 > 1-\alpha_1 \text{ (i.e., } x \in A^{\overline{1-\alpha_1}}) \end{aligned}$$

□

8.3.1 Decomposition by Weak Sub- and Supercuts

Proposition 8.3.2. *Let $\mathcal{I}$ be an upper border implicator on $\mathcal{L}^I$ and let $A, B \in \mathcal{F}_{\mathcal{L}^I}(\mathbb{R}^n)$, then it holds for all $\alpha_1 \in]0, 1]$ that:*

$$\begin{aligned} &\textit{(i)} \quad C^I_{\mathcal{C}_{\min},\mathcal{I}}(A,B)_{\alpha_1} \supseteq E(D(A_{\alpha_1}, B_{\alpha_1}), -B^{\overline{1-\alpha_1}}), \\ &\textit{(ii)} \quad O^I_{\mathcal{C}_{\min},\mathcal{I}}(A,B)_{\alpha_1} \supseteq D(E(A_{\alpha_1}, B^{\overline{1-\alpha_1}}), -B_{\alpha_1}), \end{aligned}$$

and for all $\alpha_2 \in]0, 1]$ that:

$$\begin{aligned} &\textit{(iii)} \quad C^I_{\mathcal{C}_{\min},\mathcal{I}}(A,B)^{\alpha_2} \supseteq E(D(A^{\alpha_2}, B^{\alpha_2}), -B_{\overline{1-\alpha_2}}), \\ &\textit{(iv)} \quad O^I_{\mathcal{C}_{\min},\mathcal{I}}(A,B)^{\alpha_2} \supseteq D(E(A^{\alpha_2}, B_{\overline{1-\alpha_2}}), -B^{\alpha_2}). \end{aligned}$$

Proof. As an example we prove (i). Let $\mathcal{I}$ be an upper border implicator on $\mathcal{L}^I$, let $A, B \in \mathcal{F}_{\mathcal{L}^I}(\mathbb{R}^n)$ and let $\alpha_1, \alpha_2 \in]0,1]$. From respectively Proposition 8.2.3, Proposition 8.1.13, and because the binary erosion is increasing in its first argument, we have that:

$$\begin{aligned} C^I_{\mathcal{C}_{\min},\mathcal{I}}(A,B)_{\alpha_1} &= E^I_{\mathcal{I}}(D^I_{\mathcal{C}_{\min}}(A,B), -B)_{\alpha_1} \\ &\supseteq E(D^I_{\mathcal{C}_{\min}}(A,B)_{\alpha_1}, -B^{\overline{1-\alpha_1}}) \\ &\supseteq E(D(A_{\alpha_1}, B_{\alpha_1}), -B^{\overline{1-\alpha_1}}). \end{aligned}$$

(ii), (iii) and (iv) follow analogously from Proposition 8.1.13, Proposition 8.2.3, and because the binary dilation and the binary erosion are increasing in their first argument. □

The previous result allows us to derive, under the restriction of $\alpha_2 \in]0, 0.5]$, a lower bound for the weak α_2-supercut of the interval-valued fuzzy closing and opening in terms of the binary closing and opening.

Proposition 8.3.3. *Let $\mathcal{I}$ be an upper border implicator on $\mathcal{L}^I$ and let $A, B \in \mathcal{F}_{\mathcal{L}^I}(\mathbb{R}^n)$, then it holds for all $\alpha_2 \in]0, 0.5]$ that:*

(i) $C^I_{\mathcal{C}_{\min},\mathcal{I}}(A,B)^{\alpha_2} \supseteq C(A^{\alpha_2}, B^{\alpha_2})$,
(ii) $C^I_{\mathcal{C}_{\min},\mathcal{I}}(A,B)^{\alpha_2} \supseteq C(A^{\alpha_2}, B_{\overline{1-\alpha_2}})$,

and:

(iii) $O^I_{\mathcal{C}_{\min},\mathcal{I}}(A,B)^{\alpha_2} \supseteq O(A^{\alpha_2}, B^{\alpha_2})$,
(iv) $O^I_{\mathcal{C}_{\min},\mathcal{I}}(A,B)^{\alpha_2} \supseteq O(A^{\alpha_2}, B_{\overline{1-\alpha_2}})$.

Proof. As an example, we prove (i). Let $\mathcal{I}$ be an upper border implicator on $\mathcal{L}^I$, let $A, B \in \mathcal{F}_{\mathcal{L}^I}(\mathbb{R}^n)$ and let $\alpha_2 \in]0, 0.5]$. From Proposition 8.3.2, lemma 8.3.1 and the fact that the binary erosion is decreasing in its second argument, it follows that:

$$\begin{aligned} C^I_{\mathcal{C}_{\min},\mathcal{I}}(A,B)^{\alpha_2} &\supseteq E(D(A^{\alpha_2}, B^{\alpha_2}), -B_{\overline{1-\alpha_2}}) \\ &\supseteq E(D(A^{\alpha_2}, B^{\alpha_2}), -B^{\alpha_2}) \\ &= C(A^{\alpha_2}, B^{\alpha_2}). \end{aligned}$$

(ii), (iii) and (iv) follow in an analogous way from Proposition 8.3.2, lemma 8.3.1 and the fact that the binary dilation is increasing in both its arguments and the binary erosion is increasing in its first argument and decreasing in its second argument. □

The above results for weak sub- and supercuts remain valid in the discrete framework. Since we had found a new relationship for the decomposition by weak sub- and supercuts of the interval-valued fuzzy dilation in the discrete framework compared to the continuous framework, also a new relationship can be found for the interval-valued fuzzy closing and opening.

Proposition 8.3.4. *Let $\mathcal{C}$ be a semi-norm on $\mathcal{L}^I_{r,s}$ and $\mathcal{I}$ an upper border implicator on $\mathcal{L}^I_{r,s}$ and let $A, B \in \mathcal{F}_{\mathcal{L}^I_{r,s}}(\mathbb{Z}^n)$, then it holds for all $\alpha_1 \in]0,1] \cap I_r$ that:*

$$
\begin{array}{lrcl}
\textit{(i)} & C^I_{\mathcal{C}_{\min},\mathcal{I}_{EKD}}(A,B)_{\alpha_1} & = & E(D(A_{\alpha_1},B_{\alpha_1}),-B^{\overline{1-\alpha_1}}),\\
\textit{(ii)} & C^I_{\mathcal{C}_{\min},\mathcal{I}}(A,B)_{\alpha_1} & \supseteq & E(D(A_{\alpha_1},B_{\alpha_1}),-B^{\overline{1-\alpha_1}}),\\
\textit{(iii)} & C^I_{\mathcal{C},\mathcal{I}_{EKD}}(A,B)_{\alpha_1} & \subseteq & E(D(A_{\alpha_1},B_{\alpha_1}),-B^{\overline{1-\alpha_1}}),\\
\textit{(iv)} & O^I_{\mathcal{C}_{\min},\mathcal{I}_{EKD}}(A,B)_{\alpha_1} & = & D(E(A_{\alpha_1},B^{\overline{1-\alpha_1}}),-B_{\alpha_1}),\\
\textit{(v)} & O^I_{\mathcal{C}_{\min},\mathcal{I}}(A,B)_{\alpha_1} & \supseteq & D(E(A_{\alpha_1},B^{\overline{1-\alpha_1}}),-B_{\alpha_1}),\\
\textit{(vi)} & O^I_{\mathcal{C},\mathcal{I}_{EKD}}(A,B)_{\alpha_1} & \subseteq & D(E(A_{\alpha_1},B^{\overline{1-\alpha_1}}),-B_{\alpha_1}),
\end{array}
$$

and for all $\alpha_2 \in]0,1] \cap I_s$ *that:*

$$
\begin{array}{lrcl}
\textit{(i)} & C^I_{\mathcal{C}_{\min},\mathcal{I}_{EKD}}(A,B)^{\alpha_2} & = & E(D(A^{\alpha_2},B^{\alpha_2}),-B_{\overline{1-\alpha_2}}),\\
\textit{(ii)} & C^I_{\mathcal{C}_{\min},\mathcal{I}}(A,B)^{\alpha_2} & \supseteq & E(D(A^{\alpha_2},B^{\alpha_2}),-B_{\overline{1-\alpha_2}}),\\
\textit{(iii)} & C^I_{\mathcal{C},\mathcal{I}_{EKD}}(A,B)^{\alpha_2} & \subseteq & E(D(A^{\alpha_2},B^{\alpha_2}),-B_{\overline{1-\alpha_2}}),\\
\textit{(iv)} & O^I_{\mathcal{C}_{\min},\mathcal{I}_{EKD}}(A,B)^{\alpha_2} & = & D(E(A^{\alpha_2},B_{\overline{1-\alpha_2}}),-B^{\alpha_2}),\\
\textit{(v)} & O^I_{\mathcal{C}_{\min},\mathcal{I}}(A,B)^{\alpha_2} & \supseteq & D(E(A^{\alpha_2},B_{\overline{1-\alpha_2}}),-B^{\alpha_2}),\\
\textit{(vi)} & O^I_{\mathcal{C},\mathcal{I}_{EKD}}(A,B)^{\alpha_2} & \subseteq & D(E(A^{\alpha_2},B_{\overline{1-\alpha_2}}),-B^{\alpha_2}).
\end{array}
$$

Proof. Follows in an analogous way as in the proof of Proposition 8.3.2 from Proposition 8.1.14, Proposition 8.1.15, Proposition 8.2.3, Proposition 8.2.4 and the fact that the binary dilation is increasing in its first and second argument and that the binary erosion is increasing in its first argument and decreasing in its second argument. □

The previous result allows us to derive, under the restriction of $\alpha_1 \in]0.5,1] \cap I_r$, an upper bound for the weak subcut of the interval-valued fuzzy closing and opening in terms of the binary closing and opening.

Proposition 8.3.5. *Let* $\mathcal{C}$ *be a semi-norm on* $\mathcal{L}^I_{r,s}$ *and let* $A, B \in \mathcal{F}_{\mathcal{L}^I_{r,s}}(\mathbb{Z}^n)$*, then it holds for all* $\alpha_1 \in]0.5,1] \cap I_r$ *that:*

$$
\begin{array}{lrcl}
\textit{(i)} & C^I_{\mathcal{C}_{\min},\mathcal{I}_{EKD}}(A,B)_{\alpha_1} & \subseteq & C(A_{\alpha_1},B_{\alpha_1}),\\
\textit{(ii)} & C^I_{\mathcal{C}_{\min},\mathcal{I}_{EKD}}(A,B)_{\alpha_1} & \subseteq & C(A_{\alpha_1},B^{\overline{1-\alpha_1}}),\\
\textit{(iii)} & C^I_{\mathcal{C},\mathcal{I}_{EKD}}(A,B)_{\alpha_1} & \subseteq & C(A_{\alpha_1},B_{\alpha_1}),\\
\textit{(iv)} & C^I_{\mathcal{C},\mathcal{I}_{EKD}}(A,B)_{\alpha_1} & \subseteq & C(A_{\alpha_1},B^{\overline{1-\alpha_1}}),\\
\textit{(v)} & O^I_{\mathcal{C}_{\min},\mathcal{I}_{EKD}}(A,B)_{\alpha_1} & \subseteq & O(A_{\alpha_1},B_{\alpha_1}),\\
\textit{(vi)} & O^I_{\mathcal{C}_{\min},\mathcal{I}_{EKD}}(A,B)_{\alpha_1} & \subseteq & O(A_{\alpha_1},B^{\overline{1-\alpha_1}}),\\
\textit{(vii)} & O^I_{\mathcal{C},\mathcal{I}_{EKD}}(A,B)_{\alpha_1} & \subseteq & O(A_{\alpha_1},B_{\alpha_1}),\\
\textit{(viii)} & O^I_{\mathcal{C},\mathcal{I}_{EKD}}(A,B)_{\alpha_1} & \subseteq & O(A_{\alpha_1},B^{\overline{1-\alpha_1}}),
\end{array}
$$

Proof. Follows in an analogous way as in the proof of Proposition 8.3.3 from Proposition 8.3.4 and lemma 8.3.1 and the fact that the binary dilation is increasing in its first and second argument and that the binary erosion is increasing in its first argument and decreasing in its second argument. □

The result also allows us to derive, under the restriction of $\alpha_2 \in]0,0.5] \cap I_s$, a lower bound for the weak supercut of the interval-valued fuzzy closing and opening in terms of the binary closing and opening.

Proposition 8.3.6. *Let $\mathcal{I}$ be an upper border implicator on $\mathcal{L}^I_{r,s}$ and $A, B \in \mathcal{F}_{\mathcal{L}^I_{r,s}}(\mathbb{Z}^n)$, then it holds for all $\alpha_2 \in]0, 0.5] \cap I_s$ that:*

$$
\begin{array}{lrcl}
\textit{(i)} & C^I_{\mathcal{C}_{\min},\mathcal{I}_{EKD}}(A,B)^{\alpha_2} & \supseteq & C(A^{\alpha_2}, B^{\alpha_2}), \\
\textit{(ii)} & C^I_{\mathcal{C}_{\min},\mathcal{I}_{EKD}}(A,B)^{\alpha_2} & \supseteq & C(A^{\alpha_2}, B_{\overline{1-\alpha_2}}), \\
\textit{(iii)} & C^I_{\mathcal{C}_{\min},\mathcal{I}}(A,B)^{\alpha_2} & \supseteq & C(A^{\alpha_2}, B^{\alpha_2}), \\
\textit{(iv)} & C^I_{\mathcal{C}_{\min},\mathcal{I}}(A,B)^{\alpha_2} & \supseteq & C(A^{\alpha_2}, B_{\overline{1-\alpha_2}}), \\
\textit{(v)} & O^I_{\mathcal{C}_{\min},\mathcal{I}_{EKD}}(A,B)^{\alpha_2} & \supseteq & O(A^{\alpha_2}, B^{\alpha_2}), \\
\textit{(vi)} & O^I_{\mathcal{C}_{\min},\mathcal{I}_{EKD}}(A,B)^{\alpha_2} & \supseteq & O(A^{\alpha_2}, B_{\overline{1-\alpha_2}}), \\
\textit{(vii)} & O^I_{\mathcal{C}_{\min},\mathcal{I}}(A,B)^{\alpha_2} & \supseteq & O(A^{\alpha_2}, B^{\alpha_2}), \\
\textit{(viii)} & O^I_{\mathcal{C}_{\min},\mathcal{I}}(A,B)^{\alpha_2} & \supseteq & O(A^{\alpha_2}, B_{\overline{1-\alpha_2}}).
\end{array}
$$

Proof. Follows in an analogous way as in the proof of Proposition 8.3.3 from Proposition 8.3.4 and lemma 8.3.1 and the fact that the binary dilation is increasing in its first and second argument and that the binary erosion is increasing in its first argument and decreasing in its second argument. □

8.3.2 Decomposition by Weak $[\alpha_1, \alpha_2]$-cuts

For the conjunctor $\mathcal{C}_{\min}$ and the implicator $\mathcal{I}_{EKD}$, the weak $[\alpha_1, \alpha_2]$-cuts of the discrete interval-valued fuzzy closing and opening can be obtained as a combination of binary dilations and erosions. For an arbitrary semi-norm $\mathcal{C}$ and an arbitrary upper border implicator $\mathcal{I}$ analogous approximations exist.

Proposition 8.3.7. *Let $\mathcal{C}$ be a semi-norm on $\mathcal{L}^I_{r,s}$ and $\mathcal{I}$ an upper border implicator on $\mathcal{L}^I_{r,s}$ and let $A, B \in \mathcal{F}_{\mathcal{L}^I_{r,s}}(\mathbb{Z}^n)$, then it holds for all $[\alpha_1, \alpha_2] \in L^I_{r,s} \setminus \{0_{\mathcal{L}^I}\}$ that:*

$$
\begin{array}{lrcl}
\textit{(i)} & C^I_{\mathcal{C}_{\min},\mathcal{I}_{EKD}}(A,B)^{\alpha_2}_{\alpha_1} & = & E(D(A_{\alpha_1}, B_{\alpha_1}), -B^{\overline{1-\alpha_1}}) \cap \\
 & & & \quad E(D(A^{\alpha_2}, B^{\alpha_2}), -B_{\overline{1-\alpha_2}}), \\
\textit{(ii)} & C^I_{\mathcal{C}_{\min},\mathcal{I}}(A,B)^{\alpha_2}_{\alpha_1} & \supseteq & E(D(A_{\alpha_1}, B_{\alpha_1}), -B^{\overline{1-\alpha_1}}) \cap \\
 & & & \quad E(D(A^{\alpha_2}, B^{\alpha_2}), -B_{\overline{1-\alpha_2}}), \\
\textit{(iii)} & C^I_{\mathcal{C},\mathcal{I}_{EKD}}(A,B)^{\alpha_2}_{\alpha_1} & \subseteq & E(D(A_{\alpha_1}, B_{\alpha_1}), -B^{\overline{1-\alpha_1}}) \cap \\
 & & & \quad E(D(A^{\alpha_2}, B^{\alpha_2}), -B_{\overline{1-\alpha_2}}), \\
\textit{(iv)} & O^I_{\mathcal{C}_{\min},\mathcal{I}_{EKD}}(A,B)^{\alpha_2}_{\alpha_1} & = & D(E(A_{\alpha_1}, B^{\overline{1-\alpha_1}}), -B_{\alpha_1}) \cap \\
 & & & \quad D(E(A^{\alpha_2}, B_{\overline{1-\alpha_2}}), -B^{\alpha_2}), \\
\textit{(v)} & O^I_{\mathcal{C}_{\min},\mathcal{I}}(A,B)^{\alpha_2}_{\alpha_1} & \supseteq & D(E(A_{\alpha_1}, B^{\overline{1-\alpha_1}}), -B_{\alpha_1}) \cap \\
 & & & \quad D(E(A^{\alpha_2}, B_{\overline{1-\alpha_2}}), -B^{\alpha_2}), \\
\textit{(vi)} & O^I_{\mathcal{C},\mathcal{I}_{EKD}}(A,B)^{\alpha_2}_{\alpha_1} & \subseteq & D(E(A_{\alpha_1}, B^{\overline{1-\alpha_1}}), -B_{\alpha_1}) \cap \\
 & & & \quad D(E(A^{\alpha_2}, B_{\overline{1-\alpha_2}}), -B^{\alpha_2}).
\end{array}
$$

Proof. Follows from Proposition 8.3.4. □

8.3.3 Decomposition by Strict Sub- and Supercuts

Proposition 8.3.8. *Let $\mathcal{C}$ be a semi-norm on $\mathcal{L}^I$ and let $A, B \in \mathcal{F}_{\mathcal{L}^I}(\mathbb{R}^n)$, then it holds for all $\alpha_1 \in [0,1[$ that:*

$$\begin{array}{l} \textit{(i)}\ C^I_{\mathcal{C},\mathcal{I}_{EKD}}(A,B)_{\overline{\alpha_1}} \subseteq E(D(A_{\overline{\alpha_1}}, B_{\overline{\alpha_1}}), -B^{1-\alpha_1}), \\ \textit{(ii)}\ O^I_{\mathcal{C},\mathcal{I}_{EKD}}(A,B)_{\overline{\alpha_1}} \subseteq D(E(A_{\overline{\alpha_1}}, B^{1-\alpha_1}), -B_{\overline{\alpha_1}}), \end{array}$$

and for all $\alpha_2 \in [0,1[$ that:

$$\begin{array}{l} \textit{(iii)}\ C^I_{\mathcal{C},\mathcal{I}_{EKD}}(A,B)^{\overline{\alpha_2}} \subseteq E(D(A^{\overline{\alpha_2}}, B^{\overline{\alpha_2}}), -B_{1-\alpha_2}), \\ \textit{(iv)}\ O^I_{\mathcal{C},\mathcal{I}_{EKD}}(A,B)^{\overline{\alpha_2}} \subseteq D(E(A^{\overline{\alpha_2}}, B_{1-\alpha_2}), -B^{\overline{\alpha_2}}). \end{array}$$

Proof. Follows in an analogous way as in the proof of Proposition 8.3.2 from Proposition 8.2.12 and Proposition 8.1.4 and the fact that the binary dilation is increasing in its first and second argument and that the binary erosion is increasing in its first argument and decreasing in its second argument. □

The previous result allows us to derive, under the restriction of $\alpha_1 \in [0.5,1[$, an upper bound for the strict α_1-subcut of the interval-valued fuzzy closing and opening in terms of the binary closing and opening.

Proposition 8.3.9. *Let $\mathcal{C}$ be a semi-norm on $\mathcal{L}^I$ and let $A, B \in \mathcal{F}_{\mathcal{L}^I}(\mathbb{R}^n)$, then it holds for all $\alpha_1 \in [0.5,1[$ that:*

$$\begin{array}{ll} \textit{(i)} & C^I_{\mathcal{C},\mathcal{I}_{EKD}}(A,B)_{\overline{\alpha_1}} \subseteq C(A_{\overline{\alpha_1}}, B_{\overline{\alpha_1}}), \\ \textit{(ii)} & C^I_{\mathcal{C},\mathcal{I}_{EKD}}(A,B)_{\overline{\alpha_1}} \subseteq C(A_{\overline{\alpha_1}}, B^{1-\alpha_1}), \end{array}$$

and:

$$\begin{array}{ll} \textit{(iii)} & O^I_{\mathcal{C},\mathcal{I}_{EKD}}(A,B)_{\overline{\alpha_1}} \subseteq O(A_{\overline{\alpha_1}}, B_{\overline{\alpha_1}}), \\ \textit{(iv)} & O^I_{\mathcal{C},\mathcal{I}_{EKD}}(A,B)_{\overline{\alpha_1}} \subseteq O(A_{\overline{\alpha_1}}, B^{1-\alpha_1}). \end{array}$$

Proof. Follows in an analogous way as in the proof of Proposition 8.3.3 from Proposition 8.3.8 and lemma 8.3.1 and the fact that the binary dilation is increasing in its first and second argument and that the binary erosion is increasing in its first argument and decreasing in its second argument. □

The above results for strict sub- and supercuts remain valid in the discrete framework. Since we had found a new relationship for the decomposition by strict sub- and supercuts of the interval-valued fuzzy erosion in the discrete framework compared to the continuous framework, also a new relationship can be found for the interval-valued fuzzy closing and opening.

Proposition 8.3.10. *Let $\mathcal{C}$ be a semi-norm on $\mathcal{L}^I_{r,s}$ and $\mathcal{I}$ an upper border implicator on $\mathcal{L}^I_{r,s}$ and let $A, B \in \mathcal{F}_{\mathcal{L}^I_{r,s}}(\mathbb{Z}^n)$, then it holds for all $\alpha_1 \in [0,1[\cap I_r$ that:*

$$
\begin{array}{lrcl}
\textit{(i)} & C^I_{\mathcal{C}_{\min},\mathcal{I}_{EKD}}(A,B)_{\overline{\alpha_1}} & = & E(D(A_{\overline{\alpha_1}},B_{\overline{\alpha_1}}),-B^{1-\alpha_1}),\\
\textit{(ii)} & C^I_{\mathcal{C}_{\min},\mathcal{I}}(A,B)_{\overline{\alpha_1}} & \supseteq & E(D(A_{\overline{\alpha_1}},B_{\overline{\alpha_1}}),-B^{1-\alpha_1}),\\
\textit{(iii)} & C^I_{\mathcal{C},\mathcal{I}_{EKD}}(A,B)_{\overline{\alpha_1}} & \subseteq & E(D(A_{\overline{\alpha_1}},B_{\overline{\alpha_1}}),-B^{1-\alpha_1}),\\
\textit{(iv)} & O^I_{\mathcal{C}_{\min},\mathcal{I}_{EKD}}(A,B)_{\overline{\alpha_1}} & = & D(E(A_{\overline{\alpha_1}},B^{1-\alpha_1}),-B_{\overline{\alpha_1}}),\\
\textit{(v)} & O^I_{\mathcal{C}_{\min},\mathcal{I}}(A,B)_{\overline{\alpha_1}} & \supseteq & D(E(A_{\overline{\alpha_1}},B^{1-\alpha_1}),-B_{\overline{\alpha_1}}),\\
\textit{(vi)} & O^I_{\mathcal{C},\mathcal{I}_{EKD}}(A,B)_{\overline{\alpha_1}} & \subseteq & D(E(A_{\overline{\alpha_1}},B^{1-\alpha_1}),-B_{\overline{\alpha_1}}),
\end{array}
$$

and for all $\alpha_2 \in [0,1[\cap I_s$ *that:*

$$
\begin{array}{lrcl}
\textit{(i)} & C^I_{\mathcal{C}_{\min},\mathcal{I}_{EKD}}(A,B)^{\overline{\alpha_2}} & = & E(D(A^{\overline{\alpha_2}},B^{\overline{\alpha_2}}),-B_{1-\alpha_2}),\\
\textit{(ii)} & C^I_{\mathcal{C}_{\min},\mathcal{I}}(A,B)^{\overline{\alpha_2}} & \supseteq & E(D(A^{\overline{\alpha_2}},B^{\overline{\alpha_2}}),-B_{1-\alpha_2}),\\
\textit{(iii)} & C^I_{\mathcal{C},\mathcal{I}_{EKD}}(A,B)^{\overline{\alpha_2}} & \subseteq & E(D(A^{\overline{\alpha_2}},B^{\overline{\alpha_2}}),-B_{1-\alpha_2}),\\
\textit{(iv)} & O^I_{\mathcal{C}_{\min},\mathcal{I}_{EKD}}(A,B)^{\overline{\alpha_2}} & = & D(E(A^{\overline{\alpha_2}},B_{1-\alpha_2}),-B^{\overline{\alpha_2}}),\\
\textit{(v)} & O^I_{\mathcal{C}_{\min},\mathcal{I}}(A,B)^{\overline{\alpha_2}} & \supseteq & D(E(A^{\overline{\alpha_2}},B_{1-\alpha_2}),-B^{\overline{\alpha_2}}),\\
\textit{(vi)} & O^I_{\mathcal{C},\mathcal{I}_{EKD}}(A,B)^{\overline{\alpha_2}} & \subseteq & D(E(A^{\overline{\alpha_2}},B_{1-\alpha_2}),-B^{\overline{\alpha_2}}).
\end{array}
$$

Proof. Follows in an analogous way as in the proof of Proposition 8.3.2 from Proposition 8.1.3, Proposition 8.1.4, Proposition 8.2.13, Proposition 8.2.14 and the fact that the binary dilation is increasing in its first and second argument and that the binary erosion is increasing in its first argument and decreasing in its second argument. □

The previous result allows us to derive, under the restriction of $\alpha_1 \in [0.5,1[\cap I_r$, an upper bound for the strict subcut of the interval-valued fuzzy closing and opening in terms of the binary closing and opening.

Proposition 8.3.11. *Let* $\mathcal{C}$ *be a semi-norm on* $\mathcal{L}^I_{r,s}$ *and let* $A,B \in \mathcal{F}_{\mathcal{L}^I_{r,s}}(\mathbb{Z}^n)$*, then it holds for all* $\alpha_1 \in [0.5,1[\cap I_r$ *that:*

$$
\begin{array}{lrcl}
\textit{(i)} & C^I_{\mathcal{C}_{\min},\mathcal{I}_{EKD}}(A,B)_{\overline{\alpha_1}} & \subseteq & C(A_{\overline{\alpha_1}},B_{\overline{\alpha_1}}),\\
\textit{(ii)} & C^I_{\mathcal{C}_{\min},\mathcal{I}_{EKD}}(A,B)_{\overline{\alpha_1}} & \subseteq & C(A_{\overline{\alpha_1}},B^{1-\alpha_1}),\\
\textit{(iii)} & C^I_{\mathcal{C},\mathcal{I}_{EKD}}(A,B)_{\overline{\alpha_1}} & \subseteq & C(A_{\overline{\alpha_1}},B_{\overline{\alpha_1}}),\\
\textit{(iv)} & C^I_{\mathcal{C},\mathcal{I}_{EKD}}(A,B)_{\overline{\alpha_1}} & \subseteq & C(A_{\overline{\alpha_1}},B^{1-\alpha_1}),\\
\textit{(v)} & O^I_{\mathcal{C}_{\min},\mathcal{I}_{EKD}}(A,B)_{\overline{\alpha_1}} & \subseteq & O(A_{\overline{\alpha_1}},B_{\overline{\alpha_1}}),\\
\textit{(vi)} & O^I_{\mathcal{C}_{\min},\mathcal{I}_{EKD}}(A,B)_{\overline{\alpha_1}} & \subseteq & O(A_{\overline{\alpha_1}},B^{1-\alpha_1}),\\
\textit{(vii)} & O^I_{\mathcal{C},\mathcal{I}_{EKD}}(A,B)_{\overline{\alpha_1}} & \subseteq & O(A_{\overline{\alpha_1}},B_{\overline{\alpha_1}}),\\
\textit{(viii)} & O^I_{\mathcal{C},\mathcal{I}_{EKD}}(A,B)_{\overline{\alpha_1}} & \subseteq & O(A_{\overline{\alpha_1}},B^{1-\alpha_1}),
\end{array}
$$

Proof. Follows in an analogous way as in the proof of Proposition 8.3.3 from Proposition 8.3.10 and lemma 8.3.1 and the fact that the binary dilation is increasing in its first and second argument and that the binary erosion is increasing in its first argument and decreasing in its second argument. □

The result also allows us to derive, under the restriction of $0 \leq \alpha_2 < 0.5$, a lower bound for the strict supercut of the interval-valued fuzzy closing and opening in terms of the binary closing and opening.

Proposition 8.3.12. *Let $A, B \in \mathcal{F}_{\mathcal{L}^I_{r,s}}(\mathbb{Z}^n)$ and let $\mathcal{I}$ be an upper border implicator on $\mathcal{L}^I_{r,s}$, then it holds for all $\alpha_2 \in [0, 0.5[\cap I_s$ that:*

$$
\begin{array}{lrcl}
\textit{(i)} & C^I_{\mathcal{C}_{\min},\mathcal{I}_{EKD}}(A,B)^{\overline{\alpha_2}} & \supseteq & C(A^{\overline{\alpha_2}}, B^{\overline{\alpha_2}}), \\
\textit{(ii)} & C^I_{\mathcal{C}_{\min},\mathcal{I}_{EKD}}(A,B)^{\overline{\alpha_2}} & \supseteq & C(A^{\overline{\alpha_2}}, B_{1-\alpha_2}), \\
\textit{(iii)} & C^I_{\mathcal{C}_{\min},\mathcal{I}}(A,B)^{\overline{\alpha_2}} & \supseteq & C(A^{\overline{\alpha_2}}, B^{\overline{\alpha_2}}), \\
\textit{(iv)} & C^I_{\mathcal{C}_{\min},\mathcal{I}}(A,B)^{\overline{\alpha_2}} & \supseteq & C(A^{\overline{\alpha_2}}, B_{1-\alpha_2}), \\
\textit{(v)} & O^I_{\mathcal{C}_{\min},\mathcal{I}_{EKD}}(A,B)^{\overline{\alpha_2}} & \supseteq & O(A^{\overline{\alpha_2}}, B^{\overline{\alpha_2}}), \\
\textit{(vi)} & O^I_{\mathcal{C}_{\min},\mathcal{I}_{EKD}}(A,B)^{\overline{\alpha_2}} & \supseteq & O(A^{\overline{\alpha_2}}, B_{1-\alpha_2}), \\
\textit{(vii)} & O^I_{\mathcal{C}_{\min},\mathcal{I}}(A,B)^{\overline{\alpha_2}} & \supseteq & O(A^{\overline{\alpha_2}}, B^{\overline{\alpha_2}}), \\
\textit{(viii)} & O^I_{\mathcal{C}_{\min},\mathcal{I}}(A,B)^{\overline{\alpha_2}} & \supseteq & O(A^{\overline{\alpha_2}}, B_{1-\alpha_2}).
\end{array}
$$

Proof. Follows in an analogous way as in the proof of Proposition 8.3.3 from Proposition 8.3.10 and lemma 8.3.1 and the fact that the binary dilation is increasing in its first and second argument and that the binary erosion is increasing in its first argument and decreasing in its second argument. □

8.3.4 Decomposition by Strict $[\alpha_1, \alpha_2]$-cuts

For the conjunctor $\mathcal{C}_{\min}$ and the implicator $\mathcal{I}_{EKD}$, the strict $[\alpha_1, \alpha_2]$-cuts of the discrete interval-valued fuzzy closing and opening can be found as a combination of binary dilations and erosions. For an arbitrary semi-norm $\mathcal{C}$ and an arbitrary upper border implicator $\mathcal{I}$ analogous approximations exist.

Proposition 8.3.13. *Let $\mathcal{C}$ be a semi-norm on $\mathcal{L}^I_{r,s}$ and $\mathcal{I}$ an upper border implicator on $\mathcal{L}^I_{r,s}$ and let $A, B \in \mathcal{F}_{\mathcal{L}^I_{r,s}}(\mathbb{Z}^n)$, then it holds for all $[\alpha_1, \alpha_2] \in L^I_{r,s} \setminus U_{L^I}$ that:*

$$
\begin{array}{lrcl}
\textit{(i)} & C^I_{\mathcal{C}_{\min},\mathcal{I}_{EKD}}(A,B)^{\overline{\alpha_2}}_{\overline{\alpha_1}} & = & E(D(A_{\overline{\alpha_1}}, B_{\overline{\alpha_1}}), -B^{1-\alpha_1}) \cap \\
 & & & \qquad E(D(A^{\overline{\alpha_2}}, B^{\overline{\alpha_2}}), -B_{1-\alpha_2}), \\
\textit{(ii)} & C^I_{\mathcal{C}_{\min},\mathcal{I}}(A,B)^{\overline{\alpha_2}}_{\overline{\alpha_1}} & \supseteq & E(D(A_{\overline{\alpha_1}}, B_{\overline{\alpha_1}}), -B^{1-\alpha_1}) \cap \\
 & & & \qquad E(D(A^{\overline{\alpha_2}}, B^{\overline{\alpha_2}}), -B_{1-\alpha_2}), \\
\textit{(iii)} & C^I_{\mathcal{C},\mathcal{I}_{EKD}}(A,B)^{\overline{\alpha_2}}_{\overline{\alpha_1}} & \subseteq & E(D(A_{\overline{\alpha_1}}, B_{\overline{\alpha_1}}), -B^{1-\alpha_1}) \cap \\
 & & & \qquad E(D(A^{\overline{\alpha_2}}, B^{\overline{\alpha_2}}), -B_{1-\alpha_2}), \\
\textit{(iv)} & O^I_{\mathcal{C}_{\min},\mathcal{I}_{EKD}}(A,B)^{\overline{\alpha_2}}_{\overline{\alpha_1}} & = & D(E(A_{\overline{\alpha_1}}, B^{1-\alpha_1}), -B_{\overline{\alpha_1}}) \cap \\
 & & & \qquad D(E(A^{\overline{\alpha_2}}, B_{1-\alpha_2}), -B^{\overline{\alpha_2}}), \\
\textit{(v)} & O^I_{\mathcal{C}_{\min},\mathcal{I}}(A,B)^{\overline{\alpha_2}}_{\overline{\alpha_1}} & \supseteq & D(E(A_{\overline{\alpha_1}}, B^{1-\alpha_1}), -B_{\overline{\alpha_1}}) \cap \\
 & & & \qquad D(E(A^{\overline{\alpha_2}}, B_{1-\alpha_2}), -B^{\overline{\alpha_2}}), \\
\textit{(vi)} & O^I_{\mathcal{C},\mathcal{I}_{EKD}}(A,B)^{\overline{\alpha_2}}_{\overline{\alpha_1}} & \subseteq & D(E(A_{\overline{\alpha_1}}, B^{1-\alpha_1}), -B_{\overline{\alpha_1}}) \cap \\
 & & & \qquad D(E(A^{\overline{\alpha_2}}, B_{1-\alpha_2}), -B^{\overline{\alpha_2}}).
\end{array}
$$

Proof. Follows from Proposition 8.3.10. □

8.3.5 Decomposition by Weak-Strict and Strict-Weak $[\alpha_1, \alpha_2]$-cuts

For the conjunctor $\mathcal{C}_{\min}$ and the implicator $\mathcal{I}_{EKD}$, the strict $[\alpha_1, \alpha_2]$-cuts of the discrete interval-valued fuzzy closing and opening can be obtained as a combination of binary dilations and erosions. For an arbitrary semi-norm $\mathcal{C}$ and an arbitrary upper border implicator $\mathcal{I}$ analogous approximations exist.

Proposition 8.3.14. *Let $\mathcal{C}$ be a semi-norm on $\mathcal{L}^I_{r,s}$ and $\mathcal{I}$ an upper border implicator on $\mathcal{L}^I_{r,s}$ and let $A, B \in \mathcal{F}_{\mathcal{L}^I_{r,s}}(\mathbb{Z}^n)$. For all $[\alpha_1, \alpha_2] \in L^I_{r,s} \setminus U_{L^I}$ it holds that:*

(i) $C^I_{\mathcal{C}_{\min},\mathcal{I}_{EKD}}(A,B)^{\overline{\alpha_2}}_{\alpha_1} = E(D(A_{\alpha_1}, B_{\alpha_1}), -B^{\overline{1-\alpha_1}}) \cap E(D(A^{\overline{\alpha_2}}, B^{\overline{\alpha_2}}), -B_{1-\alpha_2}),$

(ii) $C^I_{\mathcal{C}_{\min},\mathcal{I}}(A,B)^{\overline{\alpha_2}}_{\alpha_1} \supseteq E(D(A_{\alpha_1}, B_{\alpha_1}), -B^{\overline{1-\alpha_1}}) \cap E(D(A^{\overline{\alpha_2}}, B^{\overline{\alpha_2}}), -B_{1-\alpha_2}),$

(iii) $C^I_{\mathcal{C},\mathcal{I}_{EKD}}(A,B)^{\overline{\alpha_2}}_{\alpha_1} \subseteq E(D(A_{\alpha_1}, B_{\alpha_1}), -B^{\overline{1-\alpha_1}}) \cap E(D(A^{\overline{\alpha_2}}, B^{\overline{\alpha_2}}), -B_{1-\alpha_2}),$

(iv) $O^I_{\mathcal{C}_{\min},\mathcal{I}_{EKD}}(A,B)^{\overline{\alpha_2}}_{\alpha_1} = D(E(A_{\alpha_1}, B^{\overline{1-\alpha_1}}), -B_{\alpha_1}) \cap D(E(A^{\overline{\alpha_2}}, B_{1-\alpha_2}), -B^{\overline{\alpha_2}}),$

(v) $O^I_{\mathcal{C}_{\min},\mathcal{I}}(A,B)^{\overline{\alpha_2}}_{\alpha_1} \supseteq D(E(A_{\alpha_1}, B^{\overline{1-\alpha_1}}), -B_{\alpha_1}) \cap D(E(A^{\overline{\alpha_2}}, B_{1-\alpha_2}), -B^{\overline{\alpha_2}}),$

(vi) $O^I_{\mathcal{C},\mathcal{I}_{EKD}}(A,B)^{\overline{\alpha_2}}_{\alpha_1} \subseteq D(E(A_{\alpha_1}, B^{\overline{1-\alpha_1}}), -B_{\alpha_1}) \cap D(E(A^{\overline{\alpha_2}}, B_{1-\alpha_2}), -B^{\overline{\alpha_2}}).$

For all $[\alpha_1, \alpha_2] \in L^I_{r,s} \setminus \{1_{\mathcal{L}^I}\}$ it holds that:

(i) $C^I_{\mathcal{C}_{\min},\mathcal{I}_{EKD}}(A,B)^{\alpha_2}_{\overline{\alpha_1}} = E(D(A_{\overline{\alpha_1}}, B_{\overline{\alpha_1}}), -B^{1-\alpha_1}) \cap E(D(A^{\alpha_2}, B^{\alpha_2}), -B_{\overline{1-\alpha_2}}),$

(ii) $C^I_{\mathcal{C}_{\min},\mathcal{I}}(A,B)^{\alpha_2}_{\overline{\alpha_1}} \supseteq E(D(A_{\overline{\alpha_1}}, B_{\overline{\alpha_1}}), -B^{1-\alpha_1}) \cap E(D(A^{\alpha_2}, B^{\alpha_2}), -B_{\overline{1-\alpha_2}}),$

(iii) $C^I_{\mathcal{C},\mathcal{I}_{EKD}}(A,B)^{\alpha_2}_{\overline{\alpha_1}} \subseteq E(D(A_{\overline{\alpha_1}}, B_{\overline{\alpha_1}}), -B^{1-\alpha_1}) \cap E(D(A^{\alpha_2}, B^{\alpha_2}), -B_{\overline{1-\alpha_2}}),$

(iv) $O^I_{\mathcal{C}_{\min},\mathcal{I}_{EKD}}(A,B)^{\alpha_2}_{\overline{\alpha_1}} = D(E(A_{\overline{\alpha_1}}, B^{1-\alpha_1}), -B_{\overline{\alpha_1}}) \cap D(E(A^{\alpha_2}, B_{\overline{1-\alpha_2}}), -B^{\alpha_2}),$

(v) $O^I_{\mathcal{C}_{\min},\mathcal{I}}(A,B)^{\alpha_2}_{\overline{\alpha_1}} \supseteq D(E(A_{\overline{\alpha_1}}, B^{1-\alpha_1}), -B_{\overline{\alpha_1}}) \cap D(E(A^{\alpha_2}, B_{\overline{1-\alpha_2}}), -B^{\alpha_2}),$

(vi) $O^I_{\mathcal{C},\mathcal{I}_{EKD}}(A,B)^{\alpha_2}_{\overline{\alpha_1}} \subseteq D(E(A_{\overline{\alpha_1}}, B^{1-\alpha_1}), -B_{\overline{\alpha_1}}) \cap D(E(A^{\alpha_2}, B_{\overline{1-\alpha_2}}), -B^{\alpha_2}).$

Proof. Follows from Proposition 8.3.4 and 8.3.10. □

8.4 Discussion

The conversion of the $[\alpha_1, \alpha_2]$-cut of an interval-valued fuzzy morphological operator into binary operations on the $[\alpha_1, \alpha_2]$-cuts of the image and structuring element may result in a

reduction of the time needed to compute such $[\alpha_1, \alpha_2]$-cut. For example, in the calculation of the binary dilation of a binary image A by a binary structuring element B, an element $y \in \mathbb{R}^n$ can be considered to belong to this dilation as soon as one element in $T_y(B)$ also belongs to A. The other elements in $T_y(B)$ don't need to be checked anymore. For the calculation of the interval-valued fuzzy dilation, all elements in $T_y(B)$ need to be considered to find the supremum over those elements. Additionally, the binary dilation (respectively erosion) of an image can be further sped up by a decomposition of the structuring element [109, 145], which is especially useful for image processing systems. An analogous reasoning holds for the erosion.

As was shown in the previous sections, we only had equalities for the conjunctor $\mathcal{C}_{\min}$ and the implicator $\mathcal{I}_{EKD}$. For arbitrary semi-norms and upper border implicators only approximations that are not necessarily equalities could be found. As an example, we will illustrate the approximation in Proposition 8.1.17 on the camera image in Fig. 7.10 and the interval-valued structuring element

$$B = \begin{bmatrix} [0.6, 0.8] & [0.7, 0.9] & [0.6, 0.8] \\ [0.7, 0.9] & \underline{[1, 1]} & [0.7, 0.9] \\ [0.6, 0.8] & [0.7, 0.9] & [0.6, 0.8] \end{bmatrix}, \tag{8.1}$$

where the underlined element corresponds to the origin. The lower bound image, the upper bound image and the difference image of the interval-valued fuzzy dilation (based on the conjunctor $\mathcal{C}(x, y) = [\max(0, x_1 + y_1 - 1), \max(0, x_2 + y_2 - 1)], \forall x, y \in \mathbb{Z}^n$) of the camera image by the above structuring element are then given in Fig. 8.1. The weak $[0.4, 0.6]$-cut of this dilation and the binary approximation determined in Proposition 8.1.17 (ii) are finally given in Fig.8.2. We see that we get a rather rough approximation.

8.5 Conclusion

In this chapter we have revealed the relationships between the different $[\alpha_1, \alpha_2]$-cuts of the interval-valued fuzzy morphological operators and the corresponding binary operators both in the general continuous case and the discrete case. In the practical discrete case, the $[\alpha_1, \alpha_2]$-cuts of the interval-valued fuzzy dilation based on the conjunctor $\mathcal{C}_{min}$, the erosion based on the implicator $\mathcal{I}_{EKD}$, and the opening and closing based on those two can always be written in terms of binary operators. For other semi-norms and upper border implicators, we found an approximation in terms of binary operators. The decomposition properties not only provide us an interesting theoretical link between interval-valued fuzzy and binary morphology; they may also be useful to reduce the time needed for the calculation of the $[\alpha_1, \alpha_2]$-cuts of the interval-valued fuzzy morphological operators.

Figure 8.1: Lower bound image (upper), upper bound image (middle) and difference image (lower) of the dilated interval-valued camera image.

Figure 8.2: Weak $[0.4, 0.6]$-cut of the dilated interval-valued camera image (upper) and binary approximation (lower).

9
Construction of Interval-valued Fuzzy Morphological Operators

In the previous chapter, the interval-valued fuzzy morphological operators were decomposed into their $[\alpha_1, \alpha_2]$-cuts and the relationship to the original binary morphological operators was investigated. In this chapter, we tackle the reverse problem [81, 82]: we study the construction of an interval-valued fuzzy set from its $[\alpha_1, \alpha_2]$-cuts or more general from an arbitrary family of nested crisp sets. We search for the conditions under which the $[\alpha_1, \alpha_2]$-cuts coincide with the given crisp sets and illustrate those with examples and counterexamples. The obtained results are then used to extend increasing binary operators to interval-valued fuzzy operators by constructing the result from the applicaion of the binary operator on the $[\alpha_1, \alpha_2]$-cuts of the argument. This allows us to compute the interval-valued fuzzy operators by combining the results of several binary operators or to approximate them by a finite number of binary operators. The construction principle is additionally worked out more in detail for the increasing morphological dilation, which will provide us a nice theoretical link between binary and interval-valued fuzzy mathematical morphology.

In this chapter, we restrict the universe of the interval-valued fuzzy sets to $\mathbb{R}^n$ ($\mathbb{Z}^n$ in the discrete case), corresponding to the image domain of an interval-valued image. Properties that do not specifically concern mathematical morphology will however also hold for a general universe.

The chapter is organized as follows. Section 9.1 studies the construction of the interval-valued fuzzy morphological operators based on weak, strict ,weak-strict and strict-weak $[\alpha_1, \alpha_2]$-cuts in a continuous framework while section 9.2 deals with the construction in a discrete framework. Section 9.3 concludes the chapter.

9.1 Continuous Case

9.1.1 Construction Based on Weak $[\alpha_1, \alpha_2]$-cuts

Introduction

Definition 9.1. *The product of an interval $[\alpha_1, \alpha_2] \in L^I$ and a crisp set $C \in \mathcal{P}(\mathbb{R}^n)$, is defined as the interval-valued fuzzy set $[\alpha_1, \alpha_2]C$ given by:*

$$([\alpha_1, \alpha_2]C)(x) = \begin{cases} [\alpha_1, \alpha_2] & \text{if } x \in C \\ 0_{\mathcal{L}^I} & else \end{cases}, \ \forall x \in \mathbb{R}^n. \tag{9.1}$$

By means of such products, an interval-valued fuzzy set A can be reconstructed from its weak $[\alpha_1, \alpha_2]$-cuts.

Lemma 9.1.1. *Let $A \in \mathcal{F}_{\mathcal{L}^I}(\mathbb{R}^n)$, then it holds that*

$$A = \bigcup_{[\alpha_1,\alpha_2] \in L^I \setminus \{0_{\mathcal{L}^I}\}} [\alpha_1, \alpha_2] A^{\alpha_2}_{\alpha_1},$$

i.e., for all $x \in \mathbb{R}^n$

$$\begin{aligned} A(x) &= \sup_{[\alpha_1,\alpha_2] \in L^I \setminus \{0_{\mathcal{L}^I}\}} ([\alpha_1, \alpha_2] A^{\alpha_2}_{\alpha_1})(x) \\ &= \sup \{[\alpha_1, \alpha_2] \mid [\alpha_1, \alpha_2] \in L^I \setminus \{0_{\mathcal{L}^I}\} \text{ and } x \in A^{\alpha_2}_{\alpha_1}\}. \end{aligned}$$

Proof. For all $x \in \mathbb{R}^n$ and $A \in \mathcal{F}_{\mathcal{L}^I}(\mathbb{R}^n)$, it holds that

$$\begin{aligned} & \Big(\bigcup_{[\alpha_1,\alpha_2] \in L^I \setminus \{0_{\mathcal{L}^I}\}} [\alpha_1, \alpha_2] A^{\alpha_2}_{\alpha_1} \Big)(x) \\ = \ & \sup\{([\alpha_1, \alpha_2] A^{\alpha_2}_{\alpha_1})(x) \mid [\alpha_1, \alpha_2] \in L^I \setminus \{0_{\mathcal{L}^I}\}\} \\ = \ & \sup\{[\alpha_1, \alpha_2] A^{\alpha_2}_{\alpha_1})(x) \mid [\alpha_1, \alpha_2] \in rng(A) \setminus \{0_{\mathcal{L}^I}\}\} \ (rng(A) = \{A(x) \mid x \in \mathbb{R}^n\}) \\ = \ & \sup\{[\alpha_1, \alpha_2] A^{\alpha_2}_{\alpha_1})(x) \mid [\alpha_1, \alpha_2] \in rng(A) \setminus \{0_{\mathcal{L}^I}\} \text{ and } A(x) \geq_{L^I} [\alpha_1, \alpha_2]\} \\ = \ & \sup\{[\alpha_1, \alpha_2] \mid [\alpha_1, \alpha_2] \in rng(A) \setminus \{0_{\mathcal{L}^I}\} \text{ and } A(x) \geq_{L^I} [\alpha_1, \alpha_2]\} \\ = \ & A(x) \end{aligned}$$

□

If we now consider a family $(P_{[\alpha_1,\alpha_2]})_{[\alpha_1,\alpha_2] \in L^I \setminus \{0_{\mathcal{L}^I}\}}$ of crisp subsets of $\mathbb{R}^n$ that is decreasing ($[\alpha_1, \alpha_2] \leq_{L^I} [\alpha_3, \alpha_4] \Rightarrow P_{[\alpha_1,\alpha_2]} \supseteq P_{[\alpha_3,\alpha_4]}$) and we define the interval-valued fuzzy set R in $\mathbb{R}^n$ for all $x \in \mathbb{R}^n$ as

$$R(x) = \sup_{[\alpha_1,\alpha_2] \in L^I \setminus \{0_{\mathcal{L}^I}\}} ([\alpha_1, \alpha_2] P_{[\alpha_1,\alpha_2]})(x) \tag{9.2}$$

$$= \quad \sup\{[\alpha_1,\alpha_2] \mid [\alpha_1,\alpha_2] \in L^I \setminus \{0_{\mathcal{L}^I}\} \text{ and } x \in P_{[\alpha_1,\alpha_2]}\},$$

then we might wonder whether it holds that $(\forall [\alpha_1,\alpha_2] \in L^I \setminus \{0_{\mathcal{L}^I}\})(R^{\alpha_2}_{\alpha_1} = P_{[\alpha_1,\alpha_2]})$. In any case, the following inclusion always holds:

Proposition 9.1.2. *For a decreasing family $(P_{[\alpha_1,\alpha_2]})_{[\alpha_1,\alpha_2]\in L^I\setminus\{0_{\mathcal{L}^I}\}}$ of crisp subsets of $\mathbb{R}^n$ and the interval-valued fuzzy set R defined in (9.2), it holds that:*

$$(\forall [\alpha_1,\alpha_2] \in L^I \setminus \{0_{\mathcal{L}^I}\})(P_{[\alpha_1,\alpha_2]} \subseteq R^{\alpha_2}_{\alpha_1}).$$

Proof. Let $[\beta_1,\beta_2] \in L^I \setminus \{0_{\mathcal{L}^I}\}$ and let $x \in P_{[\beta_1,\beta_2]}$. It then holds that:

$$\begin{array}{rcl} x \in P_{[\beta_1,\beta_2]} & \Leftrightarrow & [\beta_1,\beta_2] \in \{[\alpha_1,\alpha_2] \mid [\alpha_1,\alpha_2] \in L^I \setminus \{0_{\mathcal{L}^I}\} \text{ and } x \in P_{[\alpha_1,\alpha_2]}\} \\ & \Rightarrow & \sup\{[\alpha_1,\alpha_2] \mid [\alpha_1,\alpha_2] \in L^I \setminus \{0_{\mathcal{L}^I}\} \text{ and } x \in P_{[\alpha_1,\alpha_2]}\} \geq_{L^I} [\beta_1,\beta_2] \\ & \Leftrightarrow & R(x) \geq_{L^I} [\beta_1,\beta_2] \\ & \Leftrightarrow & x \in R^{\beta_2}_{\beta_1}. \end{array}$$

As a consequence, $P_{[\beta_1,\beta_2]} \subseteq R^{\beta_2}_{\beta_1}$. □

However, we do not necessarily have an equality.

Example 9.1.3. Let $P_{[\alpha_1,\alpha_2]} =]-1+\alpha_1, 1-\alpha_2[$ for all $[\alpha_1,\alpha_2] \in L^I \setminus \{0_{\mathcal{L}^I}\}$. For $[\beta_1,\beta_2] \ll_{L^I} [\alpha_1,\alpha_2]$ we have that $-1+\beta_1 < -1+\alpha_1 \leq 1-\alpha_2 < 1-\beta_2$ or thus $-1+\alpha_1 \in P_{[\beta_1,\beta_2]}$ and $1-\alpha_2 \in P_{[\beta_1,\beta_2]}$. As a consequence $R(-1+\alpha_1) = \sup\{[\beta_1,\beta_2] | [\beta_1,\beta_2] \in L^I \setminus \{0_{\mathcal{L}^I}\} \text{ and } -1+\alpha_1 \in P_{[\beta_1,\beta_2]}\} = [\alpha_1,\alpha_2]$ and analogously $R(1-\alpha_2) = [\alpha_1,\alpha_2]$, thus $-1+\alpha_1 \in R^{\alpha_2}_{\alpha_1}$ and $1-\alpha_2 \in R^{\alpha_2}_{\alpha_1}$, what means that $R^{\alpha_2}_{\alpha_1} \neq P_{[\alpha_1,\alpha_2]}$.

♢

The reverse inclusion (and thus the equality) only holds under certain conditions. To formulate these conditions, we define the set d_P as

$$d_P = \{x \mid x \in \mathbb{R}^n \text{ and } (\exists [\alpha_1,\alpha_2] \in L^I \setminus \{0_{\mathcal{L}^I}\})(x \in P_{[\alpha_1,\alpha_2]})\}. \tag{9.3}$$

Further, for a fixed point $x \in d_P$, we introduce the set S_x, given by

$$S_x = \{[\alpha_1,\alpha_2] \mid [\alpha_1,\alpha_2] \in L^I \setminus \{0_{\mathcal{L}^I}\} \text{ and } x \in P_{[\alpha_1,\alpha_2]}\}, \tag{9.4}$$

and we denote the supremum of this set by $s_x = [s_{x,1}, s_{x,2}]$:

$$s_x = \sup S_x. \tag{9.5}$$

Remark that $S_x \neq \emptyset$.

The conditions under which the equality holds, are given in the following Proposition:

Proposition 9.1.4. *For a decreasing family $(P_{[\alpha_1,\alpha_2]})_{[\alpha_1,\alpha_2]\in L^I\setminus\{0_{\mathcal{L}^I}\}}$ of crisp subsets of $\mathbb{R}^n$, the interval-valued fuzzy set R defined in (9.2) and the sets d_P and S_x and the supremum s_x of the latter set, respectively defined in expressions (9.3)-(9.5), it holds that:*

$$(\forall[\alpha_1,\alpha_2]\in L^I\setminus\{0_{\mathcal{L}^I}\})(P_{[\alpha_1,\alpha_2]}=R^{\alpha_2}_{\alpha_1})\Leftrightarrow(\forall x\in d_P)(s_x\in S_x).$$

Proof.

- $\Leftarrow$: Follows from the proof of Proposition 9.1.2. Since $s_x(=\sup S_x)\in S_x$ it now also holds that $\sup S_x\geq_{L^I}[\beta_1,\beta_2]\Rightarrow[\beta_1,\beta_2]\in S_x$.
- $\Rightarrow$: Suppose $(\forall[\alpha_1,\alpha_2]\in L^I\setminus\{0_{\mathcal{L}^I}\})(P_{[\alpha_1,\alpha_2]}=R^{\alpha_2}_{\alpha_1})$, or equivalently, $(\forall[\alpha_1,\alpha_2]\in L^I\setminus\{0_{\mathcal{L}^I}\})(x\in P_{[\alpha_1,\alpha_2]}\Leftrightarrow s_x=R(x)\geq_{L^I}[\alpha_1,\alpha_2])$. For all $x\in d_P$, choosing $[\alpha_1,\alpha_2]=s_x=[s_{x,1},s_{x,2}]\in L^I\setminus\{0_{\mathcal{L}^I}\}$ implies $x\in P_{[s_{x,1},s_{x,2}]}$, and thus $s_x\in\{[\alpha_1,\alpha_2]\mid[\alpha_1,\alpha_2]\in L^I\setminus\{0_{\mathcal{L}^I}\}\text{ and }x\in P_{[\alpha_1,\alpha_2]}\}=S_x$.

□

The above condition is however not efficient in practice. Indeed, for a given family $(P_{[\alpha_1,\alpha_2]})_{[\alpha_1,\alpha_2]\in L^I\setminus\{0_{\mathcal{L}^I}\}}$ it would be needed to calculate the set S_x for all $x\in d_P$ and to check whether $s_x\in S_x$. To avoid this work, a necessary condition on the sets $P_{[\alpha_1,\alpha_2]}$ can be used.

Proposition 9.1.5. *For a decreasing family $(P_{[\alpha_1,\alpha_2]})_{[\alpha_1,\alpha_2]\in L^I\setminus\{0_{\mathcal{L}^I}\}}$ of crisp subsets of $\mathbb{R}^n$, the interval-valued fuzzy set R defined in (9.2) and the sets d_P and S_x and the supremum s_x of the latter set, respectively defined in expressions (9.3)-(9.5), it holds that:*

$$(\forall x\in d_P)(s_x\in S_x)\Rightarrow(\forall[\alpha_1,\alpha_2]\in L^I\setminus\{0_{\mathcal{L}^I}\})(P_{[\alpha_1,\alpha_2]}=\bigcap_{[\beta_1,\beta_2]\ll_{L^I}[\alpha_1,\alpha_2]}P_{[\beta_1,\beta_2]}).$$

Proof. Let $[\alpha_1,\alpha_2]\in L^I\setminus\{0_{\mathcal{L}^I}\}$. For all $x\in\bigcap_{[\beta_1,\beta_2]\ll_{L^I}[\alpha_1,\alpha_2]}P_{[\beta_1,\beta_2]}$ it holds that:

$$\begin{aligned}
x\in\bigcap_{[\beta_1,\beta_2]\ll_{L^I}[\alpha_1,\alpha_2]}P_{[\beta_1,\beta_2]} &\Leftrightarrow (\forall[\beta_1,\beta_2]\in L^I\setminus\{0_{\mathcal{L}^I}\})\\
&\quad([\beta_1,\beta_2]\ll_{L^I}[\alpha_1,\alpha_2]\Rightarrow x\in P_{[\beta_1,\beta_2]})\\
&\Leftrightarrow (\forall[\beta_1,\beta_2]\in L^I\setminus\{0_{\mathcal{L}^I}\})([\beta_1,\beta_2]\ll_{L^I}[\alpha_1,\alpha_2]\Rightarrow\\
&\quad[\beta_1,\beta_2]\in\{[\gamma_1,\gamma_2]\in L^I\setminus\{0_{\mathcal{L}^I}\}\mid x\in P_{[\beta_1,\beta_2]}\})\\
&\Leftrightarrow (\forall[\beta_1,\beta_2]\in L^I\setminus\{0_{\mathcal{L}^I}\})([\beta_1,\beta_2]\ll_{L^I}[\alpha_1,\alpha_2]\Rightarrow\\
&\quad(x\in d_P\text{ and }[\beta_1,\beta_2]\in S_x)).
\end{aligned}$$

Since it is given that $s_x\in S_x$, it follows from $[\alpha_1,\alpha_2]\leq_{L^I}s_x$ that $[\alpha_1,\alpha_2]\in S_x$, or thus $x\in P_{[\alpha_1,\alpha_2]}$. As a consequence $\bigcap_{[\beta_1,\beta_2]\ll_{L^I}[\alpha_1,\alpha_2]}P_{[\beta_1,\beta_2]}\subseteq P_{[\alpha_1,\alpha_2]}$.

On the other hand, since the family $(P_{[\alpha_1,\alpha_2]})_{[\alpha_1,\alpha_2]\in L^I\setminus\{0_{\mathcal{L}^I}\}}$ is a decreasing family, we have that $(\forall[\beta_1,\beta_2]\in L^I\setminus\{0_{\mathcal{L}^I}\})([\beta_1,\beta_2]\ll_{L^I}[\alpha_1,\alpha_2]\Rightarrow P_{[\beta_1,\beta_2]}\supseteq P_{[\alpha_1,\alpha_2]})$ and thus $\bigcap_{[\beta_1,\beta_2]\ll_{L^I}[\alpha_1,\alpha_2]} P_{[\beta_1,\beta_2]}\supseteq P_{[\alpha_1,\alpha_2]}$. □

Example 9.1.6. The results in Example 9.1.3 could also have been obtained using the above proposition. Let $[\alpha_1,\alpha_2]\in L^I\setminus\{0_{\mathcal{L}^I}\}$, then it holds that:

$$\begin{aligned}
& (\forall[\beta_1,\beta_2]\in L^I\setminus\{0_{\mathcal{L}^I}\})\\
& ([\beta_1,\beta_2]\ll_{L^I}[\alpha_1,\alpha_2]\Rightarrow -1+\alpha_1<-1+\beta_1 \text{ and } 1-\alpha_2<1-\beta_2)\\
\Rightarrow\ & (\forall[\beta_1,\beta_2]\in L^I\setminus\{0_{\mathcal{L}^I}\})([\beta_1,\beta_2]\ll_{L^I}[\alpha_1,\alpha_2]\Rightarrow\\
& (\forall x\in[-1+\alpha_1,1-\alpha_2])(x\in P_{[\beta_1,\beta_2]}=]-1+\beta_1,1-\beta_2[))\\
\Rightarrow\ & (\forall x\in[-1+\alpha_1,1-\alpha_2])(x\in \bigcap_{[\beta_1,\beta_2]\ll_{L^I}[\alpha_1,\alpha_2]} P_{[\beta_1,\beta_2]}).
\end{aligned}$$

So, e.g. $1-\alpha_2\in \bigcap_{[\beta_1,\beta_2]\ll_{L^I}[\alpha_1,\alpha_2]} P_{[\beta_1,\beta_2]}$, but $1-\alpha_2\notin P_{[\alpha_1,\alpha_2]}$, and thus $P_{[\alpha_1,\alpha_2]}\neq \bigcap_{[\beta_1,\beta_2]\ll_{L^I}[\alpha_1,\alpha_2]} P_{[\beta_1,\beta_2]}$.

♢

The condition in Proposition 9.1.5 is however not a sufficient condition as the following example illustrates.

Example 9.1.7. Let $P_{[\alpha_1,\alpha_2]}=[\frac{\alpha_1+\alpha_2}{2},1]$ for all $[\alpha_1,\alpha_2]\in L^I\setminus\{0_{\mathcal{L}^I}\}$. It holds that $(\forall[\alpha_1,\alpha_2]\in L^I\setminus\{0_{\mathcal{L}^I}\})(P_{[\alpha_1,\alpha_2]}=\bigcap_{[\beta_1,\beta_2]\ll_{L^I}[\alpha_1,\alpha_2]} P_{[\beta_1,\beta_2]})$. However, it does not hold that $(\forall x\in d_P)(s_x\in S_x)$. Consider for example the set $S_{0.5}$. $[0.5,0.5]\in S_{0.5}$ and for all $[\alpha_1,\alpha_2]$, α_1 can not be greater than 0.5 since then $\frac{\alpha_1+\alpha_2}{2}>0.5$. Further also $[0,1]\in S_{0.5}$, so we can conclude that $\sup S_{0.5}=[0.5,1]\notin S_{0.5}$.

As a consequence it does not hold that $P_{[\alpha_1,\alpha_2]}=R^{\alpha_2}_{\alpha_1}$ for all $[\alpha_1,\alpha_2]\in L^I\setminus\{0_{\mathcal{L}^I}\}$. Indeed, $R(0.5)=s_{0.5}=[0.5,1]$ and thus $0.5\in R^1_{0.5}$ at one hand, but on the other hand $0.5\notin P_{[0.5,1]}=[0.75,1]$.

♢

The given condition is not a sufficient condition because is does not necessarily hold that $(\forall[\beta_1,\beta_2]\in L^I\setminus\{0_{\mathcal{L}^I}\})([\beta_1,\beta_2]\ll_{L^I}s_x\Rightarrow[\beta_1,\beta_2]\in S_x))$. In the above example, $s_{0.5}=\sup S_{0.5}=[0.5,1]$. So, e.g. $[0.3,0.8]\ll_{L^I}s_{0.5}$, but $[0.3,0.8]\notin S_{0.5}$ since $0.5\notin P_{[0.3,0.8]}=[0.55,1]$.

Fig. 9.1 gives a graphical representation of four possible sets S_x. In the first three examples, it does not hold that an interval $\beta\ll s_x$ belongs to the set S_x. In these examples, there can be found an $\alpha\in S_x$, for which it holds that if we keep increasing α_1 or α_2, α will no longer belong to S_x at some point, but still $\alpha\ll s_x$. However, if we then keep decreasing the other bound (α_2 or α_1 respectively) at some point α will again belong to the set S_x. If

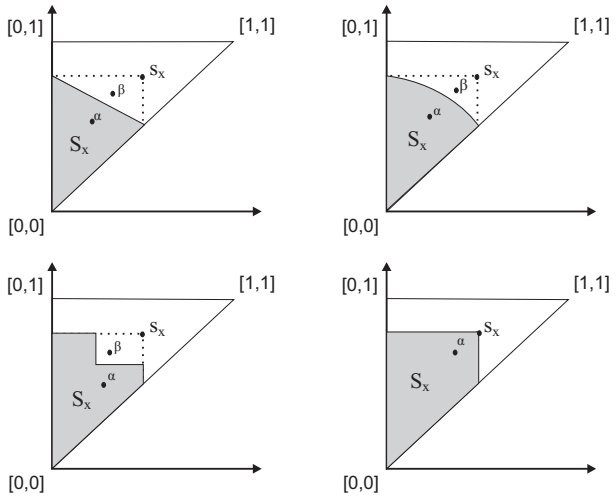

Figure 9.1: A graphical representation of some possible sets S_x.

we want that every interval $\beta \ll s_x$ belongs to S_x, S_x needs to have the form of the fourth example. In that example, for an arbitrary $\alpha \in S_x$, we see that if we keep increasing α_1 or α_2, α will no longer belong to S_x at some point (or reach its maximum possible value). This time however $\alpha \not\ll s_x$ then and decreasing the other bound (α_2 or α_1 respectively) will not result in α belonging to the set S_x again anymore. This special case leads us to the following lemma.

Lemma 9.1.8. *For a decreasing family $(P_{[\alpha_1,\alpha_2]})_{[\alpha_1,\alpha_2]\in L^I\setminus\{0_{\mathcal{L}^I}\}}$ of crisp subsets of $\mathbb{R}^n$, the interval-valued fuzzy set R defined in (9.2) and the sets d_P and S_x and the supremum s_x of the latter set, respectively defined in expressions (9.3)-(9.5), we have that*

$$(\forall x \in d_P)(\forall t \in L^I \setminus \{0_{\mathcal{L}^I}\})(t \ll_{L^I} s_x \Rightarrow t \in S_x)$$
$$\Updownarrow$$
$$[SC] : \Big(\forall [\alpha_1,\alpha_2] \in L^I \setminus \{0_{\mathcal{L}^I}\}\Big)\Big(\forall x \in \mathbb{R}^n\Big)\Big(x \notin P_{[\alpha_1,\alpha_2]} \Rightarrow$$
$$\big((\forall [\beta_1,\beta_2] \in L^I \setminus \{0_{\mathcal{L}^I}\})((\beta_1 < \alpha_1 \text{ and } \beta_2 > \alpha_2) \Rightarrow x \notin P_{[\beta_1,\beta_2]})\big) \text{ or}$$
$$\big((\forall [\beta_1,\beta_2] \in L^I \setminus \{0_{\mathcal{L}^I}\})((\beta_1 > \alpha_1 \text{ and } \beta_2 < \alpha_2) \Rightarrow x \notin P_{[\beta_1,\beta_2]})\big)\Big)$$

Proof.

$\Rightarrow$: Suppose that [SC] would not be true and thus that $\Big(\exists [\alpha_1,\alpha_2] \in L^I \setminus \{0_{\mathcal{L}^I}\}\Big)\Big(\exists x \in \mathbb{R}^n\Big)\Big(x \notin P_{[\alpha_1,\alpha_2]}$ and $\big((\exists [\beta_1,\beta_2] \in L^I \setminus \{0_{\mathcal{L}^I}\})((\beta_1 < \alpha_1$ and $\beta_2 > \alpha_2)$ and $x \in P_{[\beta_1,\beta_2]})\big)$ and $\big((\exists [\gamma_1,\gamma_2] \in L^I \setminus \{0_{\mathcal{L}^I}\})((\gamma_1 > \alpha_1$ and $\gamma_2 < \alpha_2)$ and $x \in$

$P_{[\gamma_1,\gamma_2]})\big)\big)$. This would mean that $s_{x,1} \geq \gamma_1$ and $s_{x,2} \geq \beta_2$. Further, $[\alpha_1,\alpha_2] \ll_{L^I} [\gamma_1,\beta_2] \leq_{L^I} s_x$ and thus $[\alpha_1,\alpha_2] \in S_x$ and $x \in P_{[\alpha_1,\alpha_2]}$ and hence a contradiction.

$\Leftarrow$: Suppose that the condition [SC] is fulfilled. Let $t \in L^I \setminus \{0_{\mathcal{L}^I}\}$, so that $t \ll_{L^I} s_x$. We have to prove that $t \in S_x$.

Suppose that $t \notin S_x$. Since $t \ll_{L^I} s_x$, we have that $t_1 < s_{x,1}$. As a consequence, t_1 is no upperbound for the set of lower bounds of the elements of S_x, which implies that $(\exists y \in]t_1, s_{x,1}])(\exists z \in [y,1])([y,z] \in S_x)$. If $z \geq t_2$ then we would get a contradiction since then $x \in P_{[y,z]} \subseteq P_{[t_1,t_2]}$ and hence $t \in S_x$. So $z < t_2$ and thus $(\exists [y,z] \in L^I \setminus \{0_{\mathcal{L}^I}\})(y > t_1$ and $z < t_2$ and $x \in P_{[y,z]})$.

Analogously, since $t \ll_{L^I} s_x$, we have that $t_2 < s_{x,2}$. As a consequence, t_2 is no upperbound for the set of lower bounds of the elements of S_x, which implies that $(\exists z' \in]t_2, s_{x,2}])(\exists y' \in [0,z'])([y',z'] \in S_x)$. If $y' \geq t_1$ then we would get a contradiction since then $x \in P_{[y',z']} \subseteq P_{[t_1,t_2]}$, i.e., $t \in S_x$. So $y' < t_1$ and thus $(\exists [y',z'] \in L^I \setminus \{0_{\mathcal{L}^I}\})(y' < t_1$ and $z' > t_2$ and $x \in P_{[y',z']})$.

If we combine the above results, then we find that it would hold that $x \notin P_{[t_1,t_2]}$ and $(\exists [y,z] \in L^I \setminus \{0_{\mathcal{L}^I}\})(y > t_1$ and $z < t_2$ and $x \in P_{[y,z]})$ and $(\exists [y',z'] \in L^I \setminus \{0_{\mathcal{L}^I}\})(y' < t_1$ and $z' > t_2$ and $x \in P_{[y',z']})$ and hence a contradiction. So $t \in S_x$.

□

The family defined in Example 9.1.3 fulfils the condition [SC]. More general, a decreasing family $(P_{[\alpha_1,\alpha_2]})_{[\alpha_1,\alpha_2] \in L^I \setminus \{0_{\mathcal{L}^I}\}}$ for which $P_{[\alpha_1,\alpha_2]}$ is an interval with lower bound $f(\alpha_1)$ and upper bound $g(\alpha_2)$, where the functions f and g are respectively increasing and decreasing over $[0,1]$ and $f(\beta_1) \leq g(\beta_2)$ for all $[\beta_1,\beta_2] \in L^I$, is an example of a family that fulfils condition [SC]. An analogous example of a family that fulfils condition [SC] is e.g. the family $(P_{[\alpha_1,\alpha_2]})_{[\alpha_1,\alpha_2] \in L^I \setminus \{0_{\mathcal{L}^I}\}}$ for which $P_{[\alpha_1,\alpha_2]}$ is an interval with lower bound $h(\alpha_2)$ and upper bound $i(\alpha_1)$, where the functions h and i are respectively increasing and decreasing over $[0,1]$ and $h(\beta_2) \leq i(\beta_1)$ for all $[\beta_1,\beta_2] \in L^I$. For families for which [SC] holds, Proposition 9.1.5 is now also a sufficient condition.

Proposition 9.1.9. *For a decreasing family $(P_{[\alpha_1,\alpha_2]})_{[\alpha_1,\alpha_2] \in L^I \setminus \{0_{\mathcal{L}^I}\}}$ of crisp subsets of $\mathbb{R}^n$ that fulfils the condition [SC], the interval-valued fuzzy set R defined in (9.2) and the sets d_P and S_x and the supremum s_x of the latter set, respectively defined in expressions (9.3)-(9.5), it holds that:*

$$(\forall x \in d_P)(s_x \in S_x) \Leftrightarrow (\forall [\alpha_1,\alpha_2] \in L^I \setminus \{0_{\mathcal{L}^I}\})(P_{[\alpha_1,\alpha_2]} = \bigcap_{[\beta_1,\beta_2] \ll_{L^I} [\alpha_1,\alpha_2]} P_{[\beta_1,\beta_2]}).$$

Proof.

$\Rightarrow$: Follows from Proposition 9.1.5.

$\Leftarrow$: Let $x \in d_P$. Since the family $(P_{[\alpha_1,\alpha_2]})_{[\alpha_1,\alpha_2]\in L^I\setminus\{0_{\mathcal{L}^I}\}}$ fulfils condition [SC], we can use Lemma 9.1.8 and obtain successively:

$$\begin{aligned}
& (\forall [\beta_1,\beta_2] \in L^I \setminus \{0_{\mathcal{L}^I}\})([\beta_1,\beta_2] \ll_{L^I} s_x \Rightarrow [\beta_1,\beta_2] \in S_x)) \\
\Leftrightarrow\ & (\forall [\beta_1,\beta_2] \in L^I \setminus \{0_{\mathcal{L}^I}\})([\beta_1,\beta_2] \ll_{L^I} s_x \Rightarrow (x \in P_{[\beta_1,\beta_2]})) \\
\Leftrightarrow\ & x \in \bigcap_{[\beta_1,\beta_2]\ll_{L^I} s_x} P_{[\beta_1,\beta_2]} \\
\Leftrightarrow\ & x \in P_{[s_{x,1},s_{x,2}]} \\
\Leftrightarrow\ & s_x \in S_x = \{[\alpha_1,\alpha_2] \mid [\alpha_1,\alpha_2] \in L^I \setminus \{0_{\mathcal{L}^I}\} \text{ and } x \in P_{[\alpha_1,\alpha_2]}\}.
\end{aligned}$$

□

Remark that if a decreasing family $(P_{[\alpha_1,\alpha_2]})_{[\alpha_1,\alpha_2]\in L^I\setminus\{0_{\mathcal{L}^I}\}}$ does not fulfil condition [SC], then it does not hold that $(\forall [\alpha_1,\alpha_2] \in L^I \setminus \{0_{\mathcal{L}^I}\})(P_{[\alpha_1,\alpha_2]} = R^{\alpha_2}_{\alpha_1})$ anyway. Indeed, due to Lemma 9.1.8 it does not hold that $(\forall x \in d_P)(\forall t \in L^I \setminus \{0_{\mathcal{L}^I}\})(t \ll_{L^I} s_x \Rightarrow t \in S_x)$. As a consequence $(\exists x \in d_P)(\exists t \in L^I \setminus \{0_{\mathcal{L}^I}\})(t \ll_{L^I} s_x$ and $t \notin S_x)$. This implies that $x \notin P_{[t_1,t_2]} \supseteq P_{[s_{x,1},s_{x,2}]}$ or thus $s_x \notin S_x$.

Example 9.1.10. The family $(P_{[\alpha_1,\alpha_2]})_{[\alpha_1,\alpha_2]\in L^I\setminus\{0_{\mathcal{L}^I}\}}$ of crisp subsets of $\mathbb{R}^n$, given by $P_{[\alpha_1,\alpha_2]} = [-1+\alpha_1, 1-\alpha_2]$ for all $[\alpha_1,\alpha_2] \in L^I \setminus \{0_{\mathcal{L}^I}\}$, is an example of a family for which $(\forall [\alpha_1,\alpha_2] \in L^I \setminus \{0_{\mathcal{L}^I}\})(P_{[\alpha_1,\alpha_2]} = R^{\alpha_2}_{\alpha_1})$, with the interval-valued fuzzy set R as defined in (9.2).

♢

The Construction Principle

Based on the results from the introduction of this subsection, we might extend an increasing operator ϕ on $\mathcal{P}(\mathbb{R}^n)$ (i.e., the set of all crisp subsets of $\mathbb{R}^n$) to an operator Φ on $\mathcal{F}_{\mathcal{L}^I}(\mathbb{R}^n)$ as follows:

$$\Phi(A) = \bigcup_{[\alpha_1,\alpha_2]\in L^I\setminus\{0_{\mathcal{L}^I}\}} [\alpha_1,\alpha_2]\phi(A^{\alpha_2}_{\alpha_1}), \text{ for all } A \in \mathcal{F}_{\mathcal{L}^I}(\mathbb{R}^n).$$

Operators having two or more arguments can be extended analogously. We illustrate this for an increasing operator ψ on $\mathcal{P}(\mathbb{R}^n) \times \mathcal{P}(\mathbb{R}^n)$ (like the binary dilation):

$$\Psi(A,B) = \bigcup_{[\alpha_1,\alpha_2]\in L^I\setminus\{0_{\mathcal{L}^I}\}} [\alpha_1,\alpha_2]\psi(A^{\alpha_2}_{\alpha_1}, B^{\alpha_2}_{\alpha_1}), \text{ for all } A,B \in \mathcal{F}_{\mathcal{L}^I}(\mathbb{R}^n).$$

As discussed in the introduction of this subsection, for the operators Φ and Ψ it does not necessarily hold that:

$$\begin{aligned}
&(\forall [\alpha_1,\alpha_2] \in L^I \setminus \{0_{\mathcal{L}^I}\})(\Phi(A)^{\alpha_2}_{\alpha_1} = \phi(A^{\alpha_2}_{\alpha_1})) \\
&(\forall [\alpha_1,\alpha_2] \in L^I \setminus \{0_{\mathcal{L}^I}\})(\Psi(A,B)^{\alpha_2}_{\alpha_1} = \psi(A^{\alpha_2}_{\alpha_1}, B^{\alpha_2}_{\alpha_1})).
\end{aligned}$$

The only binary morphological operator that is increasing, is the binary dilation. We will now extend this operator to interval-valued fuzzy sets by the help of the above introduced construction principle.

Let $A, B \in \mathcal{F}_{\mathcal{L}^I}(\mathbf{R}^n)$. Using the construction principle, we define the extended dilation $\widetilde{D(A,B)}$ of A by B as follows:

$$\widetilde{D(A,B)} = \bigcup_{[\alpha_1,\alpha_2]\in L^I\setminus\{0_{\mathcal{L}^I}\}} [\alpha_1,\alpha_2]D(A^{\alpha_2}_{\alpha_1}, B^{\alpha_2}_{\alpha_1}). \tag{9.6}$$

Proposition 9.1.11. *Let $A, B \in \mathcal{F}_{\mathcal{L}^I}(\mathbb{R}^n)$, then for all $y \in \mathbb{R}^n$ it holds that:*

$$\widetilde{D(A,B)}(y) = \sup_{x\in T_y(d_B)\cap d_A} \mathcal{C}_{\min}(B(x-y), A(x)) = D^I_{\mathcal{C}_{\min}}(A,B)(y).$$

Proof. Let $A, B \in \mathcal{F}_{\mathcal{L}^I}(\mathbb{R}^n)$, and let $y \in \mathbb{R}^n$. From the definition of the binary dilation,

$$D(A^{\alpha_2}_{\alpha_1}, B^{\alpha_2}_{\alpha_1})(y) = \begin{cases} 1 & \text{if } y \in D(A^{\alpha_2}_{\alpha_1}, B^{\alpha_2}_{\alpha_1}) \\ 0 & \text{else} \end{cases},$$

it follows that:

$$\begin{aligned}
\widetilde{D(A,B)}(y) &= \sup_{[\alpha_1,\alpha_2]\in L^I\setminus\{0_{\mathcal{L}^I}\}} ([\alpha_1,\alpha_2]D(A^{\alpha_2}_{\alpha_1}, B^{\alpha_2}_{\alpha_1}))(y) \\
&= \sup\{[\alpha_1,\alpha_2] \mid [\alpha_1,\alpha_2] \in L^I \setminus \{0_{\mathcal{L}^I}\} \text{ and } y \in D(A^{\alpha_2}_{\alpha_1}, B^{\alpha_2}_{\alpha_1})\} \\
&= \sup\{[\alpha_1,\alpha_2] \mid [\alpha_1,\alpha_2] \in L^I \setminus \{0_{\mathcal{L}^I}\} \text{ and } T_y(B^{\alpha_2}_{\alpha_1}) \cap A^{\alpha_2}_{\alpha_1} \neq \emptyset\} \\
&= \sup\{[\alpha_1,\alpha_2] \mid [\alpha_1,\alpha_2] \in L^I \setminus \{0_{\mathcal{L}^I}\} \text{ and } \\
&\qquad (\exists x \in T_y(d_B) \cap d_A)(x \in T_y(B^{\alpha_2}_{\alpha_1}) \text{ and } x \in A^{\alpha_2}_{\alpha_1})\} \\
&= \sup\{[\alpha_1,\alpha_2] \mid [\alpha_1,\alpha_2] \in L^I \setminus \{0_{\mathcal{L}^I}\} \text{ and } (\exists x \in T_y(d_B) \cap d_A) \\
&\qquad ((B_1(x-y) \geq \alpha_1 \text{ and } A_1(x) \geq \alpha_1) \text{ and } \\
&\qquad\qquad (B_2(x-y) \geq \alpha_2 \text{ and } A_2(x) \geq \alpha_2))\} \\
&= \sup\{[\alpha_1,\alpha_2] \mid [\alpha_1,\alpha_2] \in L^I \setminus \{0_{\mathcal{L}^I}\} \text{ and } (\exists x \in T_y(d_B) \cap d_A) \\
&\qquad (\mathcal{C}_{\min}(B(x-y), A(x)) \geq_{L^I} [\alpha_1,\alpha_2])\} \\
&\equiv (*).
\end{aligned}$$

We have to prove that $(*)$ is equal to

$$\sup\{\mathcal{C}_{\min}(B(x-y), A(x)) \mid x \in T_y(d_B) \cap d_A\} \equiv (**).$$

- It holds that:

$$(*) = \sup\{[\alpha_1,\alpha_2] \mid [\alpha_1,\alpha_2] \in L^I \setminus \{0_{\mathcal{L}^I}\} \text{ and } (\exists x \in T_y(d_B) \cap d_A)$$

$$
\begin{aligned}
& & & ([\alpha_1,\alpha_2] \leq_{L^I} \mathcal{C}_{\min}(B(x-y),A(x)))\} \\
& \leq_{L^I} & \sup\{[\alpha_1,\alpha_2] \mid [\alpha_1,\alpha_2] \in L^I \setminus \{0_{\mathcal{L}^I}\} \text{ and} \\
& & & ([\alpha_1,\alpha_2] \leq_{L^I} \sup_{x\in T_y(d_B)\cap d_A} \mathcal{C}_{\min}(B(x-y),A(x)))\} \\
& = & \sup_{x\in T_y(d_B)\cap d_A} & \mathcal{C}_{\min}(B(x-y),A(x))) \\
& = & (**)
\end{aligned}
$$

- On the other hand also $(**) \leq_{L^I} (*)$. If $T_y(d_B) \cap d_A = \emptyset$, then $(**) = 0_{\mathcal{L}^I}$ and thus $(**) \leq_{L^I} (*)$. Otherwise, consider an arbitrary $\epsilon > 0$. Then it holds that:

  $(**)_1 - \epsilon$ is no upper bound for the set of lower bounds of the intervals in the set$\{\mathcal{C}_{\min}(B(x-y),A(x)) \mid x \in T_y(d_B)\cap d_A\}$ and $(**)_2 - \epsilon$ is no upper bound for the set of upper bounds of the intervals in the set $\{\mathcal{C}_{\min}(B(x-y),A(x)) \mid x \in T_y(d_B)\cap d_A\}$

  $\Rightarrow$ $(\exists x \in T_y(d_B)\cap d_A)((**)_1 - \epsilon < \mathcal{C}_{\min}(B(x-y),A(x))_1)$ and $(\exists x' \in T_y(d_B)\cap d_A)((**)_2 - \epsilon < \mathcal{C}_{\min}(B(x'-y),A(x'))_2)$

  $\Rightarrow$ $(**)_1 - \epsilon \in \{\alpha_1 \mid (\exists \alpha_2 \in [\alpha_1,1]$ such that $[\alpha_1,\alpha_2] \in L^I \setminus \{0_{\mathcal{L}^I}\})$ and $(\exists x \in T_y(d_B)\cap d_A)([\alpha_1,\alpha_2] \leq_{L^I} \mathcal{C}_{\min}(B(x-y),A(x)))\}$ and $(**)_2 - \epsilon \in \{\alpha_2 \mid (\exists \alpha_1 \in [0,\alpha_2]$ such that $[\alpha_1,\alpha_2] \in L^I \setminus \{0_{\mathcal{L}^I}\})$ and $(\exists x \in T_y(d_B)\cap d_A)([\alpha_1,\alpha_2] \leq_{L^I} \mathcal{C}_{\min}(B(x-y),A(x)))\}$

  $\Rightarrow$ $(**)_1 - \epsilon \leq \sup\{\alpha_1 \mid (\exists \alpha_2 \in [\alpha_1,1]$ such that $[\alpha_1,\alpha_2] \in L^I \setminus \{0_{\mathcal{L}^I}\})$ and $(\exists x \in T_y(d_B)\cap d_A)([\alpha_1,\alpha_2] \leq_{L^I} \mathcal{C}_{\min}(B(x-y),A(x)))\}$ and $(**)_2 - \epsilon \leq \sup\{\alpha_2 \mid (\exists \alpha_1 \in [0,\alpha_2]$ such that $[\alpha_1,\alpha_2] \in L^I \setminus \{0_{\mathcal{L}^I}\})$ and $(\exists x \in T_y(d_B)\cap d_A)([\alpha_1,\alpha_2] \leq_{L^I} \mathcal{C}_{\min}(B(x-y),A(x)))\}$

  $\Rightarrow$ $[(**)_1 - \epsilon, (**)_2 - \epsilon] \leq_{L^I} \sup\{[\alpha_1,\alpha_2] \in L^I \setminus \{0_{\mathcal{L}^I}\} \mid (\exists x \in T_y(d_B)\cap d_A)([\alpha_1,\alpha_2] \leq_{L^I} \mathcal{C}_{\min}(B(x-y),A(x)))\}$

  Taking $\epsilon \to 0$ gives the result.

□

Since the binary erosion is not increasing in both its arguments, we cannot use the construction principle to extend this morphological operator to an interval-valued fuzzy morphological operator. Such interval-valued fuzzy erosion can however be constructed by duality properties.

Once the interval valued fuzzy dilation $D^I_{\mathcal{C}_{\min}}(A,B)$ has been constructed, also the erosion $E^I_{\mathcal{I}_{EKD}}(A,B)$ can be derived. If we however want a construction of $E^I_{\mathcal{I}_{EKD}}(A,B)$ in terms of binary erosions, the duality can be worked out as:

$$E^I_{\mathcal{I}_{EKD}}(A,B)(y) = (co_{\mathcal{N}_s}(D^I_{\mathcal{C}_{\min}}(co_{\mathcal{N}_s}(A),B)))(y)$$

$$
\begin{aligned}
&= (co_{\mathcal{N}_s}(\bigcup_{[\alpha_1,\alpha_2]\in L^I\setminus\{0_{\mathcal{L}^I}\}} [\alpha_1,\alpha_2]D((co_{\mathcal{N}_s}A)^{\alpha_2}_{\alpha_1}, B^{\alpha_2}_{\alpha_1})))(y)\\
&= \mathcal{N}_s((\bigcup_{[\alpha_1,\alpha_2]\in L^I\setminus\{0_{\mathcal{L}^I}\}} [\alpha_1,\alpha_2]D((co_{\mathcal{N}_s}A)^{\alpha_2}_{\alpha_1}, B^{\alpha_2}_{\alpha_1}))(y))\\
&= \mathcal{N}_s(\sup_{[\alpha_1,\alpha_2]\in L^I\setminus\{0_{\mathcal{L}^I}\}} ([\alpha_1,\alpha_2]D((co_{\mathcal{N}_s}A)^{\alpha_2}_{\alpha_1}, B^{\alpha_2}_{\alpha_1}))(y))\\
&= \mathcal{N}_s(\sup_{[\alpha_1,\alpha_2]\in L^I\setminus\{0_{\mathcal{L}^I}\}} ([\alpha_1,\alpha_2]co(E(co((co_{\mathcal{N}_s}A)^{\alpha_2}_{\alpha_1}), B^{\alpha_2}_{\alpha_1})))(y))
\end{aligned}
$$

The interval-valued fuzzy opening and closing can then be constructed as a combination of the interval-valued fuzzy dilation and erosion.

9.1.2 Construction Based on Strict $[\alpha_1, \alpha_2]$-cuts

Introduction

Analogously as in Subsection 9.1.1, an interval-valued fuzzy set A can also be reconstructed from its strict $[\alpha_1, \alpha_2]$-cuts.

Lemma 9.1.12. *Let $A \in \mathcal{F}_{\mathcal{L}^I}(\mathbb{R}^n)$, then it holds that*

$$A = \bigcup_{[\alpha_1,\alpha_2]\in L^I\setminus U_{L^I}} [\alpha_1,\alpha_2]A^{\overline{\alpha_2}}_{\overline{\alpha_1}},$$

i.e., for all $x \in \mathbb{R}^n$

$$
\begin{aligned}
A(x) &= \sup_{[\alpha_1,\alpha_2]\in L^I\setminus U_{L^I}} ([\alpha_1,\alpha_2]A^{\overline{\alpha_2}}_{\overline{\alpha_1}})(x)\\
&= \sup\{[\alpha_1,\alpha_2] \mid [\alpha_1,\alpha_2] \in L^I \setminus U_{L^I} \text{ and } x \in A^{\overline{\alpha_2}}_{\overline{\alpha_1}}\}.
\end{aligned}
$$

Proof. For all $x \in \mathbb{R}^n$ and $A \in \mathcal{F}_{\mathcal{L}^I}(\mathbb{R}^n)$, it holds that

$$
\begin{aligned}
&(\bigcup_{[\alpha_1,\alpha_2]\in L^I\setminus\{1_{\mathcal{L}^I}\}} [\alpha_1,\alpha_2]A^{\overline{\alpha_2}}_{\overline{\alpha_1}})(x)\\
&= \sup\{([\alpha_1,\alpha_2]A^{\overline{\alpha_2}}_{\overline{\alpha_1}})(x) \mid [\alpha_1,\alpha_2] \in L^I \setminus U_{L^I}\}\\
&= \sup\{([\alpha_1,\alpha_2]A^{\overline{\alpha_2}}_{\overline{\alpha_1}})(x) \mid [\alpha_1,\alpha_2] \in L^I \setminus U_{L^I} \text{ and } A(x) \gg_{L^I} [\alpha_1,\alpha_2]\}\\
&= \sup\{[\alpha_1,\alpha_2] \mid [\alpha_1,\alpha_2] \in L^I \setminus U_{L^I} \text{ and } A(x) \gg_{L^I} [\alpha_1,\alpha_2]\}\\
&= A(x)
\end{aligned}
$$

□

If we now consider a family $(Q_{[\alpha_1,\alpha_2]})_{[\alpha_1,\alpha_2]\in L^I\setminus U_{L^I}}$ of crisp subsets of $\mathbb{R}^n$ that is decreasing ($[\alpha_1,\alpha_2] \leq_{L^I} [\alpha_3,\alpha_4] \Rightarrow Q_{[\alpha_1,\alpha_2]} \supseteq Q_{[\alpha_3,\alpha_4]}$) and we define the interval-valued fuzzy set V in $\mathbb{R}^n$ for all $x \in \mathbb{R}^n$ as

$$\begin{aligned} V(x) &= \sup_{[\alpha_1,\alpha_2]\in L^I\setminus U_{L^I}} ([\alpha_1,\alpha_2]Q_{[\alpha_1,\alpha_2]})(x) \\ &= \sup\{[\alpha_1,\alpha_2] \mid [\alpha_1,\alpha_2] \in L^I \setminus U_{L^I} \text{ and } x \in Q_{[\alpha_1,\alpha_2]}\}, \end{aligned} \tag{9.7}$$

then we might wonder whether it holds that $(\forall [\alpha_1,\alpha_2] \in L^I \setminus U_{L^I})(V_{\overline{\alpha_1}}^{\overline{\alpha_2}} = Q_{[\alpha_1,\alpha_2]})$. In contrast to the case of weak $[\alpha_1,\alpha_2]$-cuts, there is no inclusion that always holds.

Example 9.1.13. Let $Q_{[\alpha_1,\alpha_2]} = [\frac{\alpha_1+\alpha_2}{2}, 1]$ for all $[\alpha_1,\alpha_2] \in L^I \setminus U_{L^I}$. Consider e.g. $x = 0.4$. $x \in Q_{[0.4,0.4]}$ and α_1 can not be greater than 0.4 since then $\frac{\alpha_1+\alpha_2}{2} > 0.4$. Further, $0.4 \in Q_{[0,\alpha_2]}$, for all $\alpha_2 \leq 0.8$. So, $V(0.4) = [0.4, 0.8]$ and thus $0.4 \in V_{\overline{0.3}}^{\overline{0.7}}$ at one hand, but on the other hand $0.4 \notin Q_{[0.3,0.7]} = [0.5, 1]$. As a consequence, it does not hold for all $[\alpha_1,\alpha_2] \in L^I \setminus U_{L^I}$ that $Q_{[\alpha_1,\alpha_2]} \supseteq V_{\overline{\alpha_1}}^{\overline{\alpha_2}}$.

Neither does it hold for all $[\alpha_1,\alpha_2] \in L^I \setminus U_{L^I}$ that $Q_{[\alpha_1,\alpha_2]} \subseteq V_{\overline{\alpha_1}}^{\overline{\alpha_2}}$. For every $[\alpha_1,\alpha_2] \in L^I \setminus U_{L^I}$, we have for $[\beta_1,\beta_2] \ll_{L^I} [\alpha_1,\alpha_2]$ that $\frac{\beta_1+\beta_2}{2} < \frac{\alpha_1+\alpha_2}{2}$ or thus $\frac{\alpha_1+\alpha_2}{2} \in Q_{[\beta_1,\beta_2]}$. As a consequence $V(\frac{\alpha_1+\alpha_2}{2}) = \sup\{[\beta_1,\beta_2] \in L^I \setminus U_{L^I} \mid \frac{\alpha_1+\alpha_2}{2} \in Q_{[\beta_1,\beta_2]}\} = [\alpha_1,\alpha_2]$ or thus $\frac{\alpha_1+\alpha_2}{2} \notin V_{\overline{\alpha_1}}^{\overline{\alpha_2}}$. On the other hand $\frac{\alpha_1+\alpha_2}{2} \in Q_{[\alpha_1,\alpha_2]} = [\frac{\alpha_1+\alpha_2}{2}, 1]$ which means that $V_{\overline{\alpha_1}}^{\overline{\alpha_2}} \not\supseteq Q_{[\alpha_1,\alpha_2]}$.

♢

The equality holds however under certain conditions. To formulate these conditions, we define the set d_Q as

$$d_Q = \{x \mid x \in \mathbb{R}^n \text{ and } (\exists [\alpha_1,\alpha_2] \in L^I \setminus U_{L^I})(x \in Q_{[\alpha_1,\alpha_2]})\}. \tag{9.8}$$

Further, for a fixed point $x \in d_Q$, we introduce the set T_x, given by

$$T_x = \{[\alpha_1,\alpha_2] \mid [\alpha_1,\alpha_2] \in L^I \setminus U_{L^I} \text{ and } x \in Q_{[\alpha_1,\alpha_2]}\}, \tag{9.9}$$

and we denote the supremum of this set by $t_x = [t_{x,1}, t_{x,2}]$:

$$t_x = \sup T_x. \tag{9.10}$$

Remark that $T_x \neq \emptyset$.

The following Proposition gives a necessary condition such that the equality holds:

Proposition 9.1.14. *For a decreasing family $(Q_{[\alpha_1,\alpha_2]})_{[\alpha_1,\alpha_2]\in L^I\setminus U_{L^I}}$ of crisp subsets of $\mathbb{R}^n$, the interval-valued fuzzy set V defined in (9.7) and the sets d_Q and T_x and the supremum t_x of the latter set, respectively defined in expressions (9.8)-(9.10), it holds that:*

$$(\forall [\alpha_1,\alpha_2] \in L^I \setminus U_{L^I})(Q_{[\alpha_1,\alpha_2]} = V_{\overline{\alpha_1}}^{\overline{\alpha_2}}) \Rightarrow (\forall x \in d_Q)(\forall [\beta_1,\beta_2] \in T_x)(t_x \gg_{L^I} [\beta_1,\beta_2]).$$

Proof. Suppose $(\forall [\alpha_1, \alpha_2] \in L^I \setminus U_{L^I}\})(Q_{[\alpha_1,\alpha_2]} = V^{\overline{\alpha_2}}_{\overline{\alpha_1}})$, or equivalently, $(\forall [\alpha_1, \alpha_2] \in L^I \setminus U_{L^I})(x \in Q_{[\alpha_1,\alpha_2]} \Leftrightarrow t_x = V(x) \gg_{L^I} [\alpha_1, \alpha_2])$. It is impossible then that there would exist an $x \in d_Q$, so that there exists a $[\beta_1, \beta_2] \in T_x$ for which $[\beta_1, \beta_2] \not\ll_{L^I} t_x$. Indeed, $[\beta_1, \beta_2] \in T_x$ means that $x \in Q_{[\beta_1,\beta_2]}$, which is equivalent to $t_x \gg_{L^I} [\beta_1, \beta_2]$. □

We would like to mention here that the condition $(\forall x \in d_Q)(\forall [\beta_1, \beta_2] \in T_x)(t_x \gg_{L^I} [\beta_1, \beta_2]) \Rightarrow t_x \notin T_x$ is a necessary and sufficient condition such that $(\forall [\alpha_1, \alpha_2] \in L^I \setminus U_{L^I}\})(Q_{[\alpha_1,\alpha_2]} \subseteq V^{\overline{\alpha_2}}_{\overline{\alpha_1}})$ would hold.

Proposition 9.1.15. *For a decreasing family $(Q_{[\alpha_1,\alpha_2]})_{[\alpha_1,\alpha_2] \in L^I \setminus U_{L^I}}$ of crisp subsets of $\mathbb{R}^n$, the interval-valued fuzzy set V defined in (9.7) and the sets d_Q and T_x and the supremum t_x of the latter set, respectively defined in expressions (9.8)-(9.10), it holds that:*

$$(\forall [\alpha_1, \alpha_2] \in L^I \setminus U_{L^I})(Q_{[\alpha_1,\alpha_2]} \subseteq V^{\overline{\alpha_2}}_{\overline{\alpha_1}}) \Leftrightarrow (\forall x \in d_Q)(\forall [\beta_1, \beta_2] \in T_x)(t_x \gg_{L^I} [\beta_1, \beta_2]).$$

Proof.

$\Leftarrow$: Let $[\alpha_1, \alpha_2] \in L^I \setminus U_{L^I}$ and let $x \in Q_{[\alpha_1,\alpha_2]}$. It then holds that:

$$\begin{aligned}
& x \in Q_{[\alpha_1,\alpha_2]} \\
\Leftrightarrow\ & [\alpha_1, \alpha_2] \in \{[\beta_1, \beta_2] \mid [\beta_1, \beta_2] \in L^I \setminus U_{L^I} \text{ and } x \in Q_{[\beta_1,\beta_2]}\} \\
\Rightarrow\ & \sup\{[\beta_1, \beta_2] \mid [\beta_1, \beta_2] \in L^I \setminus U_{L^I} \text{ and } x \in Q_{[\beta_1,\beta_2]}\} \gg_{L^I} [\alpha_1, \alpha_2] \\
\Leftrightarrow\ & V(x) \gg_{L^I} [\alpha_1, \alpha_2] \\
\Leftrightarrow\ & x \in V^{\overline{\alpha_2}}_{\overline{\alpha_1}}.
\end{aligned}$$

Thus, $Q_{[\alpha_1,\alpha_2]} \subseteq V^{\overline{\alpha_2}}_{\overline{\alpha_1}}$.

$\Rightarrow$: Suppose $(\forall [\alpha_1, \alpha_2] \in L^I \setminus U_{L^I}\})(Q_{[\alpha_1,\alpha_2]} \subseteq V^{\overline{\alpha_2}}_{\overline{\alpha_1}})$, or equivalently, $(\forall [\alpha_1, \alpha_2] \in L^I \setminus U_{L^I})(x \in Q_{[\alpha_1,\alpha_2]} \Rightarrow t_x = V(x) \gg_{L^I} [\alpha_1, \alpha_2])$. It is impossible then that there would exist an $x \in d_Q$, so that there exists a $[\beta_1, \beta_2] \in T_x$ for which $[\beta_1, \beta_2] \not\ll_{L^I} t_x$. Indeed, $[\beta_1, \beta_2] \in T_x$ means that $x \in Q_{[\beta_1,\beta_2]}$, which implies that $t_x \gg_{L^I} [\beta_1, \beta_2]$.

□

The condition in Proposition 9.1.14 is however not a sufficient condition for the equality to hold as the following example illustrates.

Example 9.1.16. Let $Q_{[\alpha_1,\alpha_2]} =]\frac{\alpha_1+\alpha_2}{2}, 1]$ for all $[\alpha_1, \alpha_2] \in L^I \setminus U_{L^I}$. Then $d_Q =]0, 1]$. For $x \in d_Q$, it holds that $[\beta_1, \beta_2] \in T_x \Leftrightarrow x \in]\frac{\beta_1+\beta_2}{2}, 1]$, which is equivalent to $\frac{\beta_1+\beta_2}{2} < x$. So $[\beta_1, \beta_1] \in T_x$ for all $\beta_1 < x$. It is impossible that $\beta_1 \geq x$ for any $[\beta_1, \beta_2] \in T_x$, since then $\frac{\beta_1+\beta_2}{2} \geq x$. So the first component of each element of T_x is less than the first component of the supremum of T_x $(= x)$. Further, also $[0, y] \in T_x$ for all y such that $y < 2x$ and $y < 1$. It is impossible that $\beta_2 \geq 2x$ or $\beta_2 \geq 1$ for any $[\beta_1, \beta_2] \in T_x$, since then respectively $\frac{\beta_1+\beta_2}{2} \geq x$ and $[\beta_1, \beta_2] \notin L^I \setminus U_{L^I}$. So the second component of each

element of T_x is less than the second component of the supremum of T_x ($= \min(2x, 1)$). We conclude that $(\forall x \in d_Q)(\forall [\beta_1, \beta_2] \in T_x)(t_x \gg_{L^I} [\beta_1, \beta_2])$.

It does however not hold that $(\forall [\alpha_1, \alpha_2] \in L^I \setminus U_{L^I})(Q_{[\alpha_1,\alpha_2]} = V_{\overline{\frac{\alpha_2}{\alpha_1}}})$. Consider e.g. $x = 0.4$. $x \in Q_{[\alpha_1,\alpha_1]}$ for all $\alpha_1 < 0.4$ and α_1 can not be greater or equal to 0.4 since then $\frac{\alpha_1+\alpha_2}{2} \geq 0.4$. Further, $0.4 \in Q_{[0,\alpha_2]}$, for all $\alpha_2 < 0.8$. So, $V(0.4) = [0.4, 0.8]$ and thus $0.4 \in V_{\overline{\frac{0.7}{0.3}}}$ at one hand, but on the other hand $0.4 \notin Q_{[0.3,0.7]} =]0.5, 1]$. As a consequence, it does not hold for all $[\alpha_1, \alpha_2] \in L^I \setminus U_{L^I}$ that $Q_{[\alpha_1,\alpha_2]} = V_{\overline{\frac{\alpha_2}{\alpha_1}}}$.

$\diamondsuit$

The given condition is not a sufficient condition because it does not necessarily hold that $(\forall [\beta_1, \beta_2] \in L^I \setminus U_{L^I})([\beta_1, \beta_2] \ll_{L^I} t_x \Rightarrow [\beta_1, \beta_2] \in T_x))$. In the above example, $t_{0.4} = \sup T_{0.4} = [0.4, 0.8]$. So, e.g. $[0.3, 0.7] \ll_{L^I} t_{0.4}$, but $[0.3, 0.7] \notin T_{0.4}$ since $0.4 \notin Q_{[0.3,0.7]} =]0.5, 1]$.

Analogously to Lemma 9.1.8 the property $(\forall [\beta_1, \beta_2] \in L^I \setminus U_{L^I})([\beta_1, \beta_2] \ll_{L^I} t_x \Rightarrow [\beta_1, \beta_2] \in T_x))$ does however hold in the following special case:

Lemma 9.1.17. *For a decreasing family $(Q_{[\alpha_1,\alpha_2]})_{[\alpha_1,\alpha_2] \in L^I \setminus U_{L^I}}$ of crisp subsets of $\mathbb{R}^n$, the interval-valued fuzzy set V defined in (9.7) and the sets d_Q and T_x and the supremum t_x of the latter set, respectively defined in expressions (9.8)-(9.10), we have that*

$$(\forall x \in d_Q)(\forall r \in L^I \setminus U_{L^I})(r \ll_{L^I} t_x \Rightarrow r \in T_x)$$
$$\Updownarrow$$
$$[SC'] : \Big(\forall [\alpha_1, \alpha_2] \in L^I \setminus U_{L^I}\Big)\Big(\forall x \in \mathbb{R}^n\Big)\Big(x \notin Q_{[\alpha_1,\alpha_2]} \Rightarrow$$
$$\big((\forall [\beta_1, \beta_2] \in L^I \setminus U_{L^I})((\beta_1 < \alpha_1 \text{ and } \beta_2 > \alpha_2) \Rightarrow x \notin Q_{[\beta_1,\beta_2]})\big) \text{ or}$$
$$\big((\forall [\beta_1, \beta_2] \in L^I \setminus U_{L^I})((\beta_1 > \alpha_1 \text{ and } \beta_2 < \alpha_2) \Rightarrow x \notin Q_{[\beta_1,\beta_2]})\big)\Big)$$

Proof. Analogous to the proof of Lemma 9.1.8. □

Remark that if a decreasing family $(Q_{[\alpha_1,\alpha_2]})_{[\alpha_1,\alpha_2] \in L^I \setminus U_{L^I}}$ of crisp subsets of $\mathbb{R}^n$ does not satisfy condition [SC'], then it will also not hold that $(\forall [\alpha_1, \alpha_2] \in L^I \setminus U_{L^I})(Q_{[\alpha_1,\alpha_2]} = V_{\overline{\frac{\alpha_2}{\alpha_1}}})$. Indeed, if [SC'] does not hold, then $(\exists [\alpha_1, \alpha_2] \in L^I \setminus U_{L^I})(\exists x \in \mathbb{R}^n)(x \notin Q_{[\alpha_1,\alpha_2]}$ and $(\exists [\beta_1, \beta_2] \in L^I \setminus U_{L^I})(\beta_1 < \alpha_1$ and $\beta_2 > \alpha_2$ and $x \in Q_{[\beta_1,\beta_2]})$ and $(\exists [\gamma_1, \gamma_2] \in L^I \setminus U_{L^I})(\gamma_1 > \alpha_1$ and $\gamma_2 < \alpha_2$ and $x \in Q_{[\gamma_1,\gamma_2]}))$. This would mean that $V_1(x) = t_{x,1} \geq \gamma_1 > \alpha_1$ and $V_2(x) = t_{x,2} \geq \beta_2 > \alpha_2$. As a consequence, $x \in V_{\overline{\frac{\alpha_2}{\alpha_1}}}$ and $x \notin Q_{[\alpha_1,\alpha_2]}$.

In what follows we will therefore concentrate on families for which [SC'] holds.

For a decreasing family $(Q_{[\alpha_1,\alpha_2]})_{[\alpha_1,\alpha_2] \in L^I \setminus U_{L^I}}$ of crisp subsets of $\mathbb{R}^n$ for which condition [SC'] does hold, the necessary condition in Proposition 9.1.14 becomes a sufficient condition.

Proposition 9.1.18. *For a decreasing family $(Q_{[\alpha_1,\alpha_2]})_{[\alpha_1,\alpha_2] \in L^I \setminus U_{L^I}}$ of crisp subsets of $\mathbb{R}^n$ that fulfils condition [SC'], the interval-valued fuzzy set V defined in (9.7) and the sets*

d_Q and T_x and the supremum t_x of the latter set, respectively defined in expressions (9.8)-(9.10), it holds that:

$$(\forall[\alpha_1,\alpha_2] \in L^I \setminus U_{L^I})(Q_{[\alpha_1,\alpha_2]} = V_{\overline{\alpha_1}}^{\overline{\alpha_2}}) \Leftrightarrow (\forall x \in d_Q)(\forall[\beta_1,\beta_2] \in T_x)(t_x \gg_{L^I} [\beta_1,\beta_2]).$$

Proof.

$\Leftarrow$: Since condition [SC'] is fulfilled, Lemma 9.1.17 can be used: $(\forall x \in d_Q)(\forall r \in L^I \setminus U_{L^I})(r \ll_{L^I} t_x \Rightarrow r \in T_x)$. Further, it is given that $(\forall x \in d_Q)(\forall[\beta_1,\beta_2] \in T_x)(t_x \gg_{L^I} [\beta_1,\beta_2])$. Let $[\beta_1,\beta_2] \in L^I \setminus U_{L^I}$ and let $x \in Q_{[\beta_1,\beta_2]}$. We have that:

$$\begin{aligned}
& x \in Q_{[\beta_1,\beta_2]} \\
\Leftrightarrow\ & [\beta_1,\beta_2] \in \{[\alpha_1,\alpha_2] \mid [\alpha_1,\alpha_2] \in L^I \setminus U_{L^I} \text{ and } x \in Q_{[\alpha_1,\alpha_2]}\} \\
\Leftrightarrow\ & \sup\{[\alpha_1,\alpha_2] \mid [\alpha_1,\alpha_2] \in L^I \setminus U_{L^I} \text{ and } x \in Q_{[\alpha_1,\alpha_2]}\} \gg_{L^I} [\beta_1,\beta_2] \\
\Leftrightarrow\ & V(x) \gg_{L^I} [\beta_1,\beta_2] \\
\Leftrightarrow\ & x \in V_{\overline{\beta_1}}^{\overline{\beta_2}}.
\end{aligned}$$

As a consequence, $Q_{[\beta_1,\beta_2]} = V_{\overline{\beta_1}}^{\overline{\beta_2}}$.

$\Rightarrow$: Follows from Proposition 9.1.14.

□

The condition in Proposition 9.1.18 is however not always efficient in practice. For a family $(Q_{[\alpha_1,\alpha_2]})_{[\alpha_1,\alpha_2] \in L^I \setminus U_{L^I}}$ that satisfies condition [SC'], it would be needed to calculate the set T_x for all $x \in d_Q$ and to check whether $t_x \gg_{L^I} [\beta_1,\beta_2]$ for all $[\beta_1,\beta_2] \in T_x$. To facilitate this work, an equivalent condition on the sets $Q_{[\alpha_1,\alpha_2]}$ can be used.

Proposition 9.1.19. *For a decreasing family $(Q_{[\alpha_1,\alpha_2]})_{[\alpha_1,\alpha_2] \in L^I \setminus U_{L^I}}$ of crisp subsets of $\mathbb{R}^n$ that satisfies condition [SC'], the sets d_Q and T_x and the supremum t_x of the latter set, respectively defined in expressions (9.8)-(9.10), it holds that:*

$$\begin{gathered}
(\forall x \in d_Q)(\forall[\beta_1,\beta_2] \in T_x)(t_x \gg_{L^I} [\beta_1,\beta_2]) \\
\Updownarrow \\
(\forall[\alpha_1,\alpha_2] \in L^I \setminus U_{L^I})(Q_{[\alpha_1,\alpha_2]} = \bigcup_{[\beta_1,\beta_2] \gg_{L^I} [\alpha_1,\alpha_2]} Q_{[\beta_1,\beta_2]}).
\end{gathered}$$

Proof.

$\Rightarrow$: Let $[\alpha_1,\alpha_2] \in L^I \setminus U_{L^I}$. For all $x \in Q_{[\alpha_1,\alpha_2]}$ it holds that:

$$\begin{aligned}
& x \in Q_{[\alpha_1,\alpha_2]} \\
\Leftrightarrow\ & [\alpha_1,\alpha_2] \in T_x \\
\Leftrightarrow\ & [\alpha_1,\alpha_2] \ll_{L^I} t_x \\
\Leftrightarrow\ & (\exists[\beta_1,\beta_2] \in L^I \setminus U_{L^I})(t_x \gg_{L^I} [\beta_1,\beta_2] \gg_{L^I} [\alpha_1,\alpha_2])
\end{aligned}$$

$$
\begin{aligned}
&\Leftrightarrow \quad (\exists [\beta_1,\beta_2] \in L^I \setminus U_{L^I})([\beta_1,\beta_2] \gg_{L^I} [\alpha_1,\alpha_2] \text{ and } [\beta_1,\beta_2] \in T_x)\\
&\Leftrightarrow \quad (\exists [\beta_1,\beta_2] \in L^I \setminus U_{L^I})([\beta_1,\beta_2] \gg_{L^I} [\alpha_1,\alpha_2] \text{ and }\\
&\qquad\quad [\beta_1,\beta_2] \in \{[\gamma_1,\gamma_2] \mid [\gamma_1,\gamma_2] \in L^I \setminus U_{L^I} \text{ and } x \in Q_{[\gamma_1,\gamma_2]}\})\\
&\Leftrightarrow \quad (\exists [\beta_1,\beta_2] \in L^I \setminus U_{L^I})([\beta_1,\beta_2] \gg_{L^I} [\alpha_1,\alpha_2] \text{ and } x \in Q_{[\beta_1,\beta_2]})\\
&\Leftrightarrow \quad x \in \bigcup_{[\beta_1,\beta_2] \gg_{L^I} [\alpha_1,\alpha_2]} Q_{[\beta_1,\beta_2]}.
\end{aligned}
$$

$\Leftarrow$: Let $x \in d_Q$. We first prove that $t_x \notin T_x$. Indeed, suppose that $t_x \in T_x$. This would mean that $x \in Q_{[t_{x,1},t_{x,2}]}$. On the other hand, since $t_x = \sup T_x$, it holds that $(\forall [\beta_1,\beta_2])([\beta_1,\beta_2] \gg_{L^I} t_x \Rightarrow x \notin Q_{[\beta_1,\beta_2]})$ or thus $x \notin \bigcup_{[\beta_1,\beta_2] \gg_{L^I} t_x} Q_{[\beta_1,\beta_2]}$ and hence a contradiction. So $t_x \notin T_x$.

We now prove that $(\forall [\beta_1,\beta_2] \in T_x)(t_x \gg_{L^I} [\beta_1,\beta_2])$. Suppose that this would not be true and that there would exist a $[\beta_1,\beta_2] \in T_x$ for which $t_x \not\gg_{L^I} [\beta_1,\beta_2]$. Since $t_x \notin T_x$, this would mean that either $t_{x,1} = \beta_1$ or $t_{x,2} = \beta_2$, but not both.

We consider the case that $t_{x,1} = \beta_1$ and $t_{x,2} > \beta_2$. So $x \in Q_{[t_{x,1},\beta_2]} = Q_{[\beta_1,\beta_2]}$. Since $t_x = \sup T_x$, $(\nexists [\gamma_1,\gamma_2] \in L^I)([\gamma_1,\gamma_2] \gg_{L^I} [t_{x,1},\beta_2]$ and $x \in Q_{[\gamma_1,\gamma_2]})$ or equivalently $x \notin \bigcup_{[\gamma_1,\gamma_2] \gg_{L^I} [t_{x,1},\beta_2]} Q_{[\gamma_1,\gamma_2]}$ and thus $\bigcup_{[\gamma_1,\gamma_2] \gg_{L^I} [t_{x,1},\beta_2]} Q_{[\gamma_1,\gamma_2]} \neq Q_{[t_{x,1},\beta_2]}$, i.e., again a contradiction.

The case $t_{x,2} = \beta_2$ and $t_{x,1} > \beta_1$ leads to a contradiction in an analogous way. We conclude that $(\forall [\beta_1,\beta_2] \in T_x)(t_x \gg_{L^I} [\beta_1,\beta_2])$.

□

Example 9.1.20. The family $(Q_{[\alpha_1,\alpha_2]})_{[\alpha_1,\alpha_2] \in L^I \setminus U_{L^I}}$ of crisp subsets of $\mathbb{R}^n$, given by $Q_{[\alpha_1,\alpha_2]} = [-1+\alpha_1, 1-\alpha_2]$ for all $[\alpha_1,\alpha_2] \in L^I \setminus U_{L^I}$, is an example of a family that satisfies condition [SC'], but for which it does not hold that $(\forall [\alpha_1,\alpha_2] \in L^I \setminus U_{L^I})(Q_{[\alpha_1,\alpha_2]} = V_{\overline{\alpha_1}}^{\overline{\alpha_2}})$, with the interval-valued fuzzy set V as defined in (9.7). Indeed, let $[\alpha_1,\alpha_2] \in L^I \setminus U_{L^I}$, then it holds that $(\forall [\beta_1,\beta_2] \in L^I \setminus U_{L^I})([\beta_1,\beta_2] \gg_{L^I} [\alpha_1,\alpha_2] \Rightarrow -1+\beta_1 > -1+\alpha_1$ and $1-\alpha_2 > 1-\beta_2)$ or thus $(\forall [\beta_1,\beta_2] \in L^I \setminus U_{L^I})([\beta_1,\beta_2] \gg_{L^I} [\alpha_1,\alpha_2] \Rightarrow -1+\alpha_1 \notin Q_{[\beta_1,\beta_2]}$ and $1-\alpha_2 \notin Q_{[\beta_1,\beta_2]})$. On the other hand $-1+\alpha_1 \in Q_{[\alpha_1,\alpha_2]}$ and $1-\alpha_2 \in Q_{[\alpha_1,\alpha_2]}$. So $\bigcup_{[\beta_1,\beta_2] \gg_{L^I} [\alpha_1,\alpha_2]} Q_{[\beta_1,\beta_2]} \neq Q_{[\alpha_1,\alpha_2]}$.

♢

Example 9.1.21. The family $(Q_{[\alpha_1,\alpha_2]})_{[\alpha_1,\alpha_2] \in L^I \setminus U_{L^I}}$ of crisp subsets of $\mathbb{R}^n$, given by $Q_{[\alpha_1,\alpha_2]} =]-1+\alpha_1, 1-\alpha_2[$ for all $[\alpha_1,\alpha_2] \in L^I \setminus U_{L^I}$, is an example of a family for which $(\forall [\alpha_1,\alpha_2] \in L^I \setminus U_{L^I})(Q_{[\alpha_1,\alpha_2]} = V_{\overline{\alpha_1}}^{\overline{\alpha_2}})$, with the interval-valued fuzzy set V as defined in (9.7).

♢

The Construction Principle

Based on the results from the introduction of this subsection and analogous to the construction principle based on weak $[\alpha_1, \alpha_2]$-cuts, we might extend an increasing operator ϕ on $\mathcal{P}(\mathbb{R}^n)$ to an operator Φ on $\mathcal{F}_{\mathcal{L}^I}(\mathbb{R}^n)$ as follows:

$$\Phi(A) = \bigcup_{[\alpha_1,\alpha_2]\in L^I\setminus U_{L^I}} [\alpha_1, \alpha_2]\phi(A^{\overline{\alpha_2}}_{\overline{\alpha_1}}), \text{ for all } A \in \mathcal{F}_{\mathcal{L}^I}(\mathbb{R}^n).$$

Operators having two or more arguments can be extended analogously. We illustrate this for an increasing operator ψ on $\mathcal{P}(\mathbb{R}^n) \times \mathcal{P}(\mathbb{R}^n)$ (like the binary dilation):

$$\Psi(A, B) = \bigcup_{[\alpha_1,\alpha_2]\in L^I\setminus U_{L^I}} [\alpha_1, \alpha_2]\psi(A^{\overline{\alpha_2}}_{\overline{\alpha_1}}, B^{\overline{\alpha_2}}_{\overline{\alpha_1}}), \text{ for all } A, B \in \mathcal{F}_{\mathcal{L}^I}(\mathbb{R}^n).$$

As discussed in the introduction of this subsection, for the operators Φ and Ψ it does not necessarily hold that:

$$(\forall[\alpha_1, \alpha_2] \in L^I \setminus U_{L^I})(\Phi(A)^{\overline{\alpha_2}}_{\overline{\alpha_1}} = \phi(A^{\overline{\alpha_2}}_{\overline{\alpha_1}}))$$
$$(\forall[\alpha_1, \alpha_2] \in L^I \setminus U_{L^I})(\Psi(A, B)^{\overline{\alpha_2}}_{\overline{\alpha_1}} = \psi(A^{\overline{\alpha_2}}_{\overline{\alpha_1}}, B^{\overline{\alpha_2}}_{\overline{\alpha_1}})).$$

We now extend the increasing binary dilation to interval-valued fuzzy sets by the help of the above introduced construction principle as follows:

Let $A, B \in \mathcal{F}_{\mathcal{L}^I}(\mathbf{R}^n)$. The extended dilation $\widetilde{D(A, B)}'$ of A by B is then given by:

$$\widetilde{D(A, B)}' = \bigcup_{[\alpha_1,\alpha_2]\in L^I\setminus U_{L^I}} [\alpha_1, \alpha_2]D(A^{\overline{\alpha_2}}_{\overline{\alpha_1}}, B^{\overline{\alpha_2}}_{\overline{\alpha_1}}). \tag{9.11}$$

Proposition 9.1.22. *Let $A, B \in \mathcal{F}_{\mathcal{L}^I}(\mathbb{R}^n)$, then for all $y \in \mathbb{R}^n$ it holds that:*

$$\widetilde{D(A, B)}'(y) \leq_{L^I} \sup_{x\in T_y(d_B)\cap d_A} \mathcal{C}_{\min}(B(x - y), A(x)) = D^I_{\mathcal{C}_{\min}}(A, B)(y).$$

If $A(x) \gg_{L^I} 0_{\mathcal{L}^I},\ \forall x \in d_A$ and $B(x) \gg_{L^I} 0_{\mathcal{L}^I},\ \forall x \in d_B$, then

$$\widetilde{D(A, B)}'(y) = \sup_{x\in T_y(d_B)\cap d_A} \mathcal{C}_{\min}(B(x - y), A(x)) = D^I_{\mathcal{C}_{\min}}(A, B)(y).$$

Proof. Let $A, B \in \mathcal{F}_{\mathcal{L}^I}(\mathbb{R}^n)$, and let $y \in \mathbb{R}^n$. From the definition of the binary dilation,

$$D(A^{\overline{\alpha_2}}_{\overline{\alpha_1}}, B^{\overline{\alpha_2}}_{\overline{\alpha_1}})(y) = \begin{cases} 1 & \text{if } y \in D(A^{\overline{\alpha_2}}_{\overline{\alpha_1}}, B^{\overline{\alpha_2}}_{\overline{\alpha_1}}) \\ 0 & \text{else} \end{cases},$$

it follows that:

$$\widetilde{D(A, B)}'(y) = \sup_{[\alpha_1,\alpha_2]\in L^I\setminus U_{L^I}} ([\alpha_1, \alpha_2]D(A^{\overline{\alpha_2}}_{\overline{\alpha_1}}, B^{\overline{\alpha_2}}_{\overline{\alpha_1}}))(y)$$

$$
\begin{aligned}
&= \sup\{[\alpha_1,\alpha_2] \mid [\alpha_1,\alpha_2] \in L^I \setminus U_{L^I} \text{ and } y \in D(A^{\overline{\alpha_2}}_{\overline{\alpha_1}}, B^{\overline{\alpha_2}}_{\overline{\alpha_1}})\}\\
&= \sup\{[\alpha_1,\alpha_2] \mid [\alpha_1,\alpha_2] \in L^I \setminus U_{L^I} \text{ and } T_y(B^{\overline{\alpha_2}}_{\overline{\alpha_1}}) \cap A^{\overline{\alpha_2}}_{\overline{\alpha_1}} \neq \emptyset\}\\
&= \sup\{[\alpha_1,\alpha_2] \mid [\alpha_1,\alpha_2] \in L^I \setminus U_{L^I} \text{ and}\\
&\qquad (\exists x \in T_y(d_B) \cap d_A)(x \in T_y(B^{\overline{\alpha_2}}_{\overline{\alpha_1}}) \text{ and } x \in A^{\overline{\alpha_2}}_{\overline{\alpha_1}})\}\\
&= \sup\{[\alpha_1,\alpha_2] \mid [\alpha_1,\alpha_2] \in L^I \setminus U_{L^I} \text{ and } (\exists x \in T_y(d_B) \cap d_A)\\
&\qquad ((B_1(x-y) > \alpha_1 \text{ and } A_1(x) > \alpha_1) \text{ and}\\
&\qquad\quad (B_2(x-y) > \alpha_2 \text{ and } A_2(x) > \alpha_2))\}\\
&= \sup\{[\alpha_1,\alpha_2] \in L^I \setminus U_{L^I} \mid (\exists x \in T_y(d_B) \cap d_A)\\
&\quad (\mathcal{C}_{\min}(B(x-y), A(x)) \gg_{L^I} [\alpha_1,\alpha_2])\}\\
&\equiv (*).
\end{aligned}
$$

We have to prove that $(*)$ is less than or equal to

$$\sup\{\mathcal{C}_{\min}(B(x-y), A(x)) \mid x \in T_y(d_B) \cap d_A\} \equiv (**).$$

It holds that:

$$
\begin{aligned}
(*) \quad &= \quad \sup\{[\alpha_1,\alpha_2] \mid [\alpha_1,\alpha_2] \in L^I \setminus U_{L^I} \text{ and } (\exists x \in T_y(d_B) \cap d_A)\\
&\qquad\qquad ([\alpha_1,\alpha_2] \ll_{L^I} \mathcal{C}_{\min}(B(x-y), A(x)))\}\\
&\leq_{L^I} \quad \sup\{[\alpha_1,\alpha_2] \mid [\alpha_1,\alpha_2] \in L^I \setminus U_{L^I} \text{ and}\\
&\qquad\qquad ([\alpha_1,\alpha_2] \ll_{L^I} \sup_{x \in T_y(d_B) \cap d_A} \mathcal{C}_{\min}(B(x-y), A(x)))\}\\
&= \quad \sup_{x \in T_y(d_B) \cap d_A} \mathcal{C}_{\min}(B(x-y), A(x)))\\
&= \quad (**)
\end{aligned}
$$

If $A(x) \gg_{L^I} 0_{\mathcal{L}^I},\ \forall x \in d_A$ and $B(x) \gg_{L^I} 0_{\mathcal{L}^I},\ \forall x \in d_B$, then also $(**) \leq_{L^I} (*)$, as we will now prove.

If $T_y(d_B) \cap d_A = \emptyset$, then $(**) = 0_{\mathcal{L}^I}$ and thus $(**) \leq_{L^I} (*)$. Otherwise, consider an arbitrary $\epsilon > 0$. It holds that:

$$
\begin{aligned}
&(**)_1 - \epsilon \text{ is no upper bound for the set of lower bounds of the intervals in the set}\\
&\{\mathcal{C}_{\min}(B(x-y), A(x)) \mid x \in T_y(d_B) \cap d_A\} \text{ and } (**)_2 - \epsilon \text{ is no upper bound for}\\
&\text{the set of upper bounds of the intervals in the set } \{\mathcal{C}_{\min}(B(x-y), A(x)) \mid\\
&x \in T_y(d_B) \cap d_A\}\\
\Rightarrow\ &(\exists x \in T_y(d_B) \cap d_A)((**)_1 - \epsilon < \mathcal{C}_{\min}(B(x-y), A(x))_1) \text{ and}\\
&(\exists x' \in T_y(d_B) \cap d_A)((**)_2 - \epsilon < \mathcal{C}_{\min}(B(x'-y), A(x'))_2).
\end{aligned}
$$

For such element x from the first part of the above consequent, for which $(**)_1 - \epsilon < (\mathcal{C}_{\min}(B(x-y), A(x)))_1$, we can choose $\alpha_2 = (**)_1 - \epsilon < (\mathcal{C}_{\min}(B(x-y), A(x)))_1 \leq$

$(\mathcal{C}_{\min}(B(x-y),A(x)))_2$ such that

$$\begin{aligned}(**)_1-\epsilon \quad &\in \quad \{\alpha_1 \mid (\exists \alpha_2 \in [\alpha_1,1[\text{ such that } [\alpha_1,\alpha_2] \in L^I \setminus U_{L^I}) \text{ and}\\ &\qquad (\exists x \in T_y(d_B)\cap d_A)([\alpha_1,\alpha_2] \ll_{L^I} \mathcal{C}_{\min}(B(x-y),A(x)))\}.\end{aligned}$$

Since $A(x) \gg_{L^I} 0_{\mathcal{L}^I},\ \forall x \in d_A$ and $B(x) \gg_{L^I} 0_{\mathcal{L}^I},\ \forall x \in d_B$, for the second part of the consequent, we can choose $\alpha_1 = 0 < (\mathcal{C}_{\min}(B(x'-y),A(x')))_1$, such that

$$\begin{aligned}(**)_2-\epsilon \quad &\in \quad \{\alpha_2 \mid (\exists \alpha_1 \in [0,\alpha_2] \text{ such that } [\alpha_1,\alpha_2] \in L^I \setminus U_{L^I}) \text{ and}\\ &\qquad (\exists x \in T_y(d_B)\cap d_A)([\alpha_1,\alpha_2] \ll_{L^I} \mathcal{C}_{\min}(B(x-y),A(x)))\}\end{aligned}$$

It thus follows that:

$$\begin{aligned}&(**)_1-\epsilon \in \{\alpha_1 \mid (\exists \alpha_2 \in [\alpha_1,1[\text{ such that } [\alpha_1,\alpha_2] \in L^I \setminus U_{L^I}) \text{ and}\\ &(\exists x \in T_y(d_B)\cap d_A)([\alpha_1,\alpha_2] \ll_{L^I} \mathcal{C}_{\min}(B(x-y),A(x)))\} \text{ and}\\ &(**)_2-\epsilon \in \{\alpha_2 \mid (\exists \alpha_1 \in [0,\alpha_2] \text{ such that } [\alpha_1,\alpha_2] \in L^I \setminus U_{L^I}) \text{ and}\\ &(\exists x \in T_y(d_B)\cap d_A)([\alpha_1,\alpha_2] \ll_{L^I} \mathcal{C}_{\min}(B(x-y),A(x)))\}\\ \Rightarrow\ &(**)_1-\epsilon \leq \sup\{\alpha_1 \mid (\exists \alpha_2 \in [\alpha_1,1[\text{ such that } [\alpha_1,\alpha_2] \in L^I \setminus U_{L^I}) \text{ and}\\ &(\exists x \in T_y(d_B)\cap d_A)([\alpha_1,\alpha_2] \ll_{L^I} \mathcal{C}_{\min}(B(x-y),A(x)))\} \text{ and}\\ &(**)_2-\epsilon \leq \sup\{\alpha_2 \mid (\exists \alpha_1 \in [0,\alpha_2] \text{ such that } [\alpha_1,\alpha_2] \in L^I \setminus U_{L^I}) \text{ and}\\ &(\exists x \in T_y(d_B)\cap d_A)([\alpha_1,\alpha_2] \ll_{L^I} \mathcal{C}_{\min}(B(x-y),A(x)))\}\\ \Rightarrow\ &[(**)_1-\epsilon,(**)_2-\epsilon] \leq_{L^I} \sup\{[\alpha_1,\alpha_2] \mid [\alpha_1,\alpha_2] \in L^I \setminus U_{L^I} \text{ and}\\ &(\exists x \in T_y(d_B)\cap d_A)([\alpha_1,\alpha_2] \ll_{L^I} \mathcal{C}_{\min}(B(x-y),A(x)))\} = (*).\end{aligned}$$

Taking $\epsilon \to 0$ gives the result. □

The following example illustrates that if not $A(x) \gg_{L^I} 0_{\mathcal{L}^I},\ \forall x \in d_A$ or not $B(x) \gg_{L^I} 0_{\mathcal{L}^I},\ \forall x \in d_B$, then $(*)$ is not necessarily equal to $(**)$.

Example 9.1.23. Let $A(0) = [0, 0.7]$ and $A(x) = [0.3, 0.5],\ \forall x \in]0, 1]$ and let $B(x) = [0.2, 0.6],\ \forall x \in [0, 0.5]$. Let $y = 0$, then $T_0(d_B) \cap d_A = [0, 0.5]$. $\forall x \in]0, 0.5]$, $\mathcal{C}_{\min}(B(x-0), A(x)) = [0.2, 0.5]$. For $x = 0$, $\mathcal{C}_{\min}(B(0), A(0)) = [0, 0.6]$. Thus $\sup\{\mathcal{C}_{\min}(B(x-y), A(x)) \mid x \in T_y(d_B) \cap d_A\} = \sup\{[0, 0.6], [0.2, 0.5]\} = [0.2, 0.6]$. On the other hand, $(\nexists [\alpha_1, \alpha_2] \in L^I)([\alpha_1, \alpha_2] \ll_{L^I} [0, 0.6])$ and $(\forall [\alpha_1, \alpha_2] \in L^I)([\alpha_1, \alpha_2] \ll_{L^I} [0.2, 0.5] \Rightarrow (\exists x \in T_0(d_B) \cap d_A)([\alpha_1, \alpha_2] \ll_{L^I} \mathcal{C}_{\min}(B(x-y), A(x))))$, from which it follows that $\sup\{[\alpha_1, \alpha_2] \in L^I \mid (\exists x \in T_0(d_B) \cap d_A)([\alpha_1, \alpha_2] \ll_{L^I} \mathcal{C}_{\min}(B(x-y), A(x)))\} = [0.2, 0.5]$.

Remark that if $A(0)$ would have been less than or equal to $[0, 0.5]$, then we would have had an equality.

♢

The construction principle can not be used to extend the binary erosion to an interval-valued fuzzy morphological operator, since it is not increasing in both its arguments. Analogously as for weak $[\alpha_1, \alpha_2]$-cuts, it can however be constructed by duality properties.

$$\begin{aligned}
E^I_{\mathcal{I}_{EKD}}(A,B)(y) &= (co_{\mathcal{N}_s}(D^I_{\mathcal{C}_{\min}}(co_{\mathcal{N}_s}(A),B)))(y) \\
&\leq_{L^I} (co_{\mathcal{N}_s}(\bigcup_{[\alpha_1,\alpha_2]\in L^I\setminus U_{L^I}} [\alpha_1,\alpha_2]D((co_{\mathcal{N}_s}A)^{\overline{\alpha_2}}_{\overline{\alpha_1}}, B^{\overline{\alpha_2}}_{\overline{\alpha_1}})))(y) \\
&= \mathcal{N}_s((\bigcup_{[\alpha_1,\alpha_2]\in L^I\setminus U_{L^I}} [\alpha_1,\alpha_2]D((co_{\mathcal{N}_s}A)^{\overline{\alpha_2}}_{\overline{\alpha_1}}, B^{\overline{\alpha_2}}_{\overline{\alpha_1}}))(y)) \\
&= \mathcal{N}_s(\sup_{[\alpha_1,\alpha_2]\in L^I\setminus U_{L^I}} ([\alpha_1,\alpha_2]D((co_{\mathcal{N}_s}A)^{\overline{\alpha_2}}_{\overline{\alpha_1}}, B^{\overline{\alpha_2}}_{\overline{\alpha_1}}))(y)) \\
&= \mathcal{N}_s(\sup_{[\alpha_1,\alpha_2]\in L^I\setminus U_{L^I}} ([\alpha_1,\alpha_2]co(E(co((co_{\mathcal{N}_s}A)^{\overline{\alpha_2}}_{\overline{\alpha_1}}), B^{\overline{\alpha_2}}_{\overline{\alpha_1}})))(y))
\end{aligned}$$

If $A(x) \gg_{L^I} 0_{\mathcal{L}^I},\ \forall x \in d_A$ and $B(x) \gg_{L^I} 0_{\mathcal{L}^I},\ \forall x \in d_B$, then we have an equality.

The interval-valued fuzzy opening and closing can then be constructed as a combination of the interval-valued fuzzy dilation and erosion.

9.1.3 Construction Based on Weak-Strict and Strict-Weak $[\alpha_1, \alpha_2]$-cuts

Introduction

Analogously as in Subsection 9.1.1and 9.1.2, an interval-valued fuzzy set A can also be reconstructed from its weak-strict and strict-weak $[\alpha_1, \alpha_2]$-cuts.

Lemma 9.1.24. *Let $A \in \mathcal{F}_{\mathcal{L}^I}(\mathbb{R}^n)$, then it holds that*

(i)

$$A = \bigcup_{[\alpha_1,\alpha_2]\in L^I\setminus U_{L^I}} [\alpha_1,\alpha_2]A^{\overline{\alpha_2}}_{\alpha_1},$$

i.e., for all $x \in \mathbb{R}^n$,

$$\begin{aligned}
A(x) &= \sup_{[\alpha_1,\alpha_2]\in L^I\setminus U_{L^I}} ([\alpha_1,\alpha_2]A^{\overline{\alpha_2}}_{\alpha_1})(x) \\
&= \sup\{[\alpha_1,\alpha_2] \mid [\alpha_1,\alpha_2] \in L^I \setminus U_{L^I} \text{ and } x \in A^{\overline{\alpha_2}}_{\alpha_1}\},
\end{aligned}$$

(ii)

$$A = \bigcup_{[\alpha_1,\alpha_2]\in L^I\setminus\{1_{\mathcal{L}^I}\}} [\alpha_1,\alpha_2]A^{\alpha_2}_{\alpha_1},$$

i.e., for all $x \in \mathbb{R}^n$,

$$\begin{aligned} A(x) &= \sup_{[\alpha_1,\alpha_2]\in L^I\setminus\{1_{\mathcal{L}^I}\}} ([\alpha_1,\alpha_2]A^{\alpha_2}_{\alpha_1})(x) \\ &= \sup\{[\alpha_1,\alpha_2] \mid [\alpha_1,\alpha_2] \in L^I \setminus \{1_{\mathcal{L}^I}\} \textit{ and } x \in A^{\alpha_2}_{\alpha_1}\}. \end{aligned}$$

Proof.

(i) For all $x \in \mathbb{R}^n$ and $A \in \mathcal{F}_{\mathcal{L}^I}(\mathbb{R}^n)$, it holds that

$$\begin{aligned} & (\bigcup_{[\alpha_1,\alpha_2]\in L^I\setminus U_{L^I}} [\alpha_1,\alpha_2]A^{\overline{\alpha_2}}_{\alpha_1})(x) \\ = \; & \sup\{([\alpha_1,\alpha_2]A^{\overline{\alpha_2}}_{\alpha_1})(x) \mid [\alpha_1,\alpha_2] \in L^I \setminus U_{L^I}\} \\ = \; & \sup\{([\alpha_1,\alpha_2]A^{\overline{\alpha_2}}_{\alpha_1})(x) \mid [\alpha_1,\alpha_2] \in L^I \setminus U_{L^I} \text{ and} \\ & \qquad\qquad A_1(x) \geq \alpha_1 \text{ and } A_2(x) > \alpha_2\} \\ = \; & \sup\{[\alpha_1,\alpha_2] \mid [\alpha_1,\alpha_2] \in L^I \setminus U_{L^I} \text{ and } A_1(x) \geq \alpha_1 \text{ and } A_2(x) > \alpha_2\} \\ = \; & A(x) \end{aligned}$$

(ii) Analogously.

□

If we now consider families $(M_{[\alpha_1,\alpha_2]})_{[\alpha_1,\alpha_2]\in L^I\setminus U_{L^I}}$ and $(N_{[\alpha_1,\alpha_2]})_{[\alpha_1,\alpha_2]\in L^I\setminus\{1_{\mathcal{L}^I}\}}$ of crisp subsets of $\mathbb{R}^n$ that are decreasing ($[\alpha_1,\alpha_2] \leq_{L^I} [\alpha_3,\alpha_4] \Rightarrow M_{[\alpha_1,\alpha_2]} \supseteq M_{[\alpha_3,\alpha_4]}$ and $[\alpha_1,\alpha_2] \leq_{L^I} [\alpha_3,\alpha_4] \Rightarrow N_{[\alpha_1,\alpha_2]} \supseteq N_{[\alpha_3,\alpha_4]}$) and we define the interval-valued fuzzy sets W and X in $\mathbb{R}^n$ for all $x \in \mathbb{R}^n$ respectively as,

$$\begin{aligned} W(x) &= \sup_{[\alpha_1,\alpha_2]\in L^I\setminus U_{L^I}} ([\alpha_1,\alpha_2]M_{[\alpha_1,\alpha_2]})(x) \\ &= \sup\{[\alpha_1,\alpha_2] \mid [\alpha_1,\alpha_2] \in L^I \setminus U_{L^I} \text{ and } x \in M_{[\alpha_1,\alpha_2]}\}, \end{aligned} \tag{9.12}$$

$$\begin{aligned} X(x) &= \sup_{[\alpha_1,\alpha_2]\in L^I\setminus\{1_{\mathcal{L}^I}\}} ([\alpha_1,\alpha_2]N_{[\alpha_1,\alpha_2]})(x) \\ &= \sup\{[\alpha_1,\alpha_2] \mid [\alpha_1,\alpha_2] \in L^I \setminus \{1_{\mathcal{L}^I}\} \text{ and } x \in N_{[\alpha_1,\alpha_2]}\}, \end{aligned} \tag{9.13}$$

then we might wonder whether it holds that $(\forall[\alpha_1,\alpha_2] \in L^I \setminus U_{L^I})(W^{\overline{\alpha_2}}_{\alpha_1} = M_{[\alpha_1,\alpha_2]})$ and $(\forall[\alpha_1,\alpha_2] \in L^I \setminus \{1_{\mathcal{L}^I}\})(X^{\alpha_2}_{\overline{\alpha_1}} = N_{[\alpha_1,\alpha_2]})$. Similar to the case of strict $[\alpha_1,\alpha_2]$-cuts and in contrast to the case of weak $[\alpha_1,\alpha_2]$-cuts, there is no inclusion that always holds.

Example 9.1.25. Let $M_{[\alpha_1,\alpha_2]} =]-1+\alpha_1, 1-\alpha_2]$ for all $[\alpha_1,\alpha_2] \in L^I \setminus U_{L^I}$. Consider e.g. $x = -0.4$. Then it holds that $(\forall[\beta_1,\beta_2] \in L^I \setminus U_{L^I})((\beta_1 < 0.6 \Rightarrow x \in M_{[\beta_1,\beta_2]})$ and $(\beta_1 \geq 0.6 \Rightarrow x \notin M_{[\beta_1,\beta_2]}))$. So $W(-0.4) = \sup\{[\beta_1,\beta_2] \in L^I \setminus U_{L^I} \mid -0.4 \in M_{[\beta_1,\beta_2]}\} =$

$[0.6, 1]$. As a consequence it holds for example that $-0.4 \notin M_{[0.6,0.6]}$ and $-0.4 \in W_{0.6}^{\overline{0.6}}$ which means that it does not hold for all $[\alpha_1, \alpha_2] \in L^I \setminus U_{L^I}$ that $W_{\alpha_1}^{\overline{\alpha_2}} \subseteq M_{[\alpha_1,\alpha_2]}$.

Neither does it always hold that $W_{\alpha_1}^{\overline{\alpha_2}} \supseteq M_{[\alpha_1,\alpha_2]}$ for all $[\alpha_1, \alpha_2] \in L^I \setminus U_{L^I}$. Consider now e.g. $x = 0.4$. Then it holds that $(\forall [\beta_1, \beta_2] \in L^I \setminus U_{L^I})((\beta_2 \leq 0.6 \Rightarrow x \in M_{[\beta_1,\beta_2]})$ and $(\beta_2 > 0.6 \Rightarrow x \notin M_{[\beta_1,\beta_2]}))$. So $W(0.4) = \sup\{[\beta_1, \beta_2] \in L^I \setminus U_{L^I} \mid 0.4 \in M_{[\beta_1,\beta_2]}\} = [0.6, 0.6]$. As a consequence it holds for example that $0.4 \in M_{[0.6,0.6]}$ and $0.4 \notin W_{0.6}^{\overline{0.6}}$. Analogous examples can be given for strict-weak $[\alpha_1, \alpha_2]$-cuts.

$\diamondsuit$

The equality however holds under certain conditions. To formulate these conditions, we define the sets d_M and d_N as

$$d_M = \{x \mid x \in \mathbb{R}^n \text{ and } (\exists [\alpha_1, \alpha_2] \in L^I \setminus U_{L^I})(x \in M_{[\alpha_1,\alpha_2]})\}. \tag{9.14}$$

$$d_N = \{x \mid x \in \mathbb{R}^n \text{ and } (\exists [\alpha_1, \alpha_2] \in L^I \setminus \{1_{\mathcal{L}^I}\})(x \in N_{[\alpha_1,\alpha_2]})\}. \tag{9.15}$$

Further, for a fixed point $x \in d_M$ (respectively $x \in d_N$), we introduce the set Y_x (respectively Z_x), given by

$$Y_x = \{[\alpha_1, \alpha_2] \mid [\alpha_1, \alpha_2] \in L^I \setminus U_{L^I} \text{ and } x \in M_{[\alpha_1,\alpha_2]}\}, \tag{9.16}$$

$$(\text{respectively } Z_x = \{[\alpha_1, \alpha_2] \mid [\alpha_1, \alpha_2] \in L^I \setminus \{1_{\mathcal{L}^I}\} \text{ and } x \in N_{[\alpha_1,\alpha_2]}\}), \tag{9.17}$$

and we denote the supremum of this set by $y_x = [y_{x,1}, y_{x,2}]$ (respectively $z_x = [z_{x,1}, z_{x,2}]$):

$$y_x = \sup Y_x, \tag{9.18}$$

$$(\text{respectively } z_x = \sup Z_x) \tag{9.19}$$

Remark that $Y_x \neq \emptyset$ and $Z_x \neq \emptyset$.

The following Proposition gives a necessary condition for the equality to hold:

Proposition 9.1.26.

(i) For a decreasing family $(M_{[\alpha_1,\alpha_2]})_{[\alpha_1,\alpha_2] \in L^I \setminus U_{L^I}}$ of crisp subsets of the universe $\mathbb{R}^n$, the interval-valued fuzzy set W defined in (9.12) and the sets d_M and Y_x and the supremum y_x of the latter set, respectively defined in expressions (9.14),(9.16) and (9.18), it holds that:

$$(\forall [\alpha_1, \alpha_2] \in L^I \setminus U_{L^I})(M_{[\alpha_1,\alpha_2]} = W_{\alpha_1}^{\overline{\alpha_2}})$$
$$\Downarrow$$
$$(\forall x \in d_M)(\forall [\beta_1, \beta_2] \in Y_x)(y_{x,1} \geq \beta_1 \text{ and } y_{x,2} > \beta_2).$$

(ii) For a decreasing family $(N_{[\alpha_1,\alpha_2]})_{[\alpha_1,\alpha_2] \in L^I \setminus \{1_{\mathcal{L}^I}\}}$ of crisp subsets of the universe $\mathbb{R}^n$, the interval-valued fuzzy set X defined in (9.13) and the sets d_N and Z_x and the

supremum z_x of the latter set, respectively defined in expressions (9.15),(9.17) and (9.19), it holds that:

$$(\forall[\alpha_1,\alpha_2] \in L^I \setminus \{1_{\mathcal{L}^I}\})(N_{[\alpha_1,\alpha_2]} = X^{\alpha_2}_{\alpha_1})$$
$$\Downarrow$$
$$(\forall x \in d_N)(\forall[\beta_1,\beta_2] \in Z_x)(z_{x,1} > \beta_1 \text{ and } z_{x,2} \geq \beta_2).$$

Proof.

(i) Suppose $(\forall[\alpha_1,\alpha_2] \in L^I \setminus U_{L^I}\})(M_{[\alpha_1,\alpha_2]} = W^{\overline{\alpha_2}}_{\alpha_1})$, or equivalently, $(\forall[\alpha_1,\alpha_2] \in L^I \setminus U_{L^I})(x \in M_{[\alpha_1,\alpha_2]} \Leftrightarrow y_{x,1} = W_1(x) \geq \alpha_1$ and $y_{x,2} = W_2(x) > \alpha_2$. It is impossible then that there would exist an $x \in d_M$, so that there exists a $[\beta_1,\beta_2] \in Y_x$ for which $\beta_1 \not\leq y_{x,1}$ or $\beta_2 \not< y_{x,2}$. Indeed, $[\beta_1,\beta_2] \in Y_x$ means that $x \in M_{[\beta_1,\beta_2]}$, which is equivalent to $y_{x,1} \geq \beta_1$ and $y_{x,2} > \beta_2$.

(ii) Analogously.

□

We would like to mention here that the condition $(\forall x \in d_M)(\forall[\beta_1,\beta_2] \in Y_x)(y_{x,1} \geq \beta_1$ and $y_{x,2} > \beta_2)$ (respectively $(\forall x \in d_N)(\forall[\beta_1,\beta_2] \in Z_x)(z_{x,1} > \beta_1$ and $z_{x,2} \geq \beta_2)$) is a necessary and sufficient condition such that $(\forall[\alpha_1,\alpha_2] \in L^I \setminus U_{L^I})(M_{[\alpha_1,\alpha_2]} \subseteq W^{\overline{\alpha_2}}_{\alpha_1})$ (respectively $(\forall[\alpha_1,\alpha_2] \in L^I \setminus \{1_{\mathcal{L}^I}\})(N_{[\alpha_1,\alpha_2]} \subseteq X^{\alpha_2}_{\alpha_1})$) would hold.

Proposition 9.1.27.

(i) For a decreasing family $(M_{[\alpha_1,\alpha_2]})_{[\alpha_1,\alpha_2]\in L^I\setminus U_{L^I}}$ of crisp subsets of the universe $\mathbb{R}^n$, the interval-valued fuzzy set W defined in (9.12) and the sets d_M and Y_x and the supremum y_x of the latter set, respectively defined in expressions (9.14),(9.16) and (9.18), it holds that:

$$(\forall[\alpha_1,\alpha_2] \in L^I \setminus U_{L^I})(M_{[\alpha_1,\alpha_2]} \subseteq W^{\overline{\alpha_2}}_{\alpha_1})$$
$$\Updownarrow$$
$$(\forall x \in d_M)(\forall[\beta_1,\beta_2] \in Y_x)(y_{x,1} \geq \beta_1 \text{ and } y_{x,2} > \beta_2),$$

(ii) For a decreasing family $(N_{[\alpha_1,\alpha_2]})_{[\alpha_1,\alpha_2]\in L^I\setminus\{1_{\mathcal{L}^I}\}}$ of crisp subsets ofthe universe $\mathbb{R}^n$, the interval-valued fuzzy set X defined in (9.13) and the sets d_N and Z_x and the supremum z_x of the latter set, respectively defined in expressions (9.15),(9.17) and (9.19), it holds that:

$$(\forall[\alpha_1,\alpha_2] \in L^I \setminus \{1_{\mathcal{L}^I}\})(N_{[\alpha_1,\alpha_2]} \subseteq X^{\alpha_2}_{\alpha_1})$$
$$\Updownarrow$$
$$(\forall x \in d_N)(\forall[\beta_1,\beta_2] \in Z_x)(z_{x,1} > \beta_1 \text{ and } z_{x,2} \geq \beta_2).$$

Proof.

(i) $\Leftarrow$: Let $[\alpha_1, \alpha_2] \in L^I \setminus U_{L^I}$ and let $x \in M_{[\alpha_1,\alpha_2]}$. It then holds that:

$$\begin{aligned} & x \in M_{[\alpha_1,\alpha_2]} \\ \Leftrightarrow \quad & [\alpha_1, \alpha_2] \in \{[\beta_1, \beta_2] \mid [\beta_1, \beta_2] \in L^I \setminus U_{L^I} \text{ and } x \in M_{[\beta_1,\beta_2]}\} \\ \Rightarrow \quad & y_{x,1} \geq \alpha_1 \text{ and } y_{x,2} > \alpha_2 \\ \Leftrightarrow \quad & W_1(x) \geq \alpha_1 \text{ and } W_2(x) > \alpha_2 \\ \Leftrightarrow \quad & x \in W_{\alpha_1}^{\overline{\alpha_2}}. \end{aligned}$$

Thus, $M_{[\alpha_1,\alpha_2]} \subseteq W_{\alpha_1}^{\overline{\alpha_2}}$.

$\Rightarrow$: Suppose that $(\forall [\alpha_1, \alpha_2] \in L^I \setminus U_{L^I}\})(M_{[\alpha_1,\alpha_2]} \subseteq W_{\alpha_1}^{\overline{\alpha_2}})$, i.e., $(\forall [\alpha_1, \alpha_2] \in L^I \setminus U_{L^I})(x \in M_{[\alpha_1,\alpha_2]} \Rightarrow W_1(x) = y_{x,1} \geq \alpha_1$ and $W_2(x) = y_{x,2} > \alpha_2)$. It is impossible then that there would exist an $x \in d_M$, so that there exists a $[\beta_1, \beta_2] \in Y_x$ for which $\beta_1 \not\leq y_{x,1}$ or $\beta_2 \not< y_{x,2}$. Indeed, $[\beta_1, \beta_2] \in Y_x$ means that $x \in M_{[\beta_1,\beta_2]}$, which implies that $y_{x,1} \geq \beta_1$ and $y_{x,2} > \beta_2$.

(ii) Analogously.

□

An analogous example to the one in Example 9.1.16 can be used to illustrate that the condition in Proposition 9.1.26 is not sufficient for the equality $M_{[\alpha_1,\alpha_2]} = W_{\alpha_1}^{\overline{\alpha_2}}$ (respectively $N_{[\alpha_1,\alpha_2]} = X_{\overline{\alpha_1}}^{\alpha_2}$) to hold for all $[\alpha_1, \alpha_2] \in L^I \setminus U_{L^I}$ (respectively $L^I \setminus \{1_{\mathcal{L}^I}\}$). The given condition is not a sufficient condition because it does not necessarily hold that $(\forall [\beta_1, \beta_2] \in L^I \setminus U_{L^I})(\beta_1 \leq y_{x,1}$ and $\beta_2 < y_{x,2} \Rightarrow [\beta_1, \beta_2] \in Y_x)$ (and respectively also not that $(\forall [\beta_1, \beta_2] \in L^I \setminus U_{L^I})(\beta_1 < y_{x,1}$ and $\beta_2 \leq y_{x,2} \Rightarrow [\beta_1, \beta_2] \in Z_x)$).

These properties do however hold in the following special case:

Lemma 9.1.28. *For a decreasing family $(M_{[\alpha_1,\alpha_2]})_{[\alpha_1,\alpha_2] \in L^I \setminus U_{L^I}}$ of crisp subsets of $\mathbb{R}^n$, the interval-valued fuzzy set W defined in (9.12) and the sets d_M and Y_x and the supremum y_x of the latter set, respectively defined in expressions (9.14),(9.16) and (9.18), we have that*

$$(\forall x \in d_M)(\forall r \in L^I \setminus U_{L^I})((r_1 \leq y_{x,1} \textit{ and } r_2 < y_{x,2}) \Rightarrow r \in Y_x)$$

$$\Updownarrow$$

$$[SC''a] : \Big(\forall [\alpha_1, \alpha_2] \in L^I \setminus U_{L^I}\Big)\Big(\forall x \in \mathbb{R}^n\Big)\Big(x \notin M_{[\alpha_1,\alpha_2]} \Rightarrow$$

$$\big((\forall [\beta_1, \beta_2] \in L^I \setminus U_{L^I})((\beta_1 < \alpha_1 \textit{ and } \beta_2 > \alpha_2) \Rightarrow x \notin M_{[\beta_1,\beta_2]})\big) \textit{ or}$$

$$\big((\forall [\beta_1, \beta_2] \in L^I \setminus U_{L^I})((\beta_1 > \alpha_1 \textit{ and } \beta_2 < \alpha_2) \Rightarrow x \notin M_{[\beta_1,\beta_2]})\big)\Big)$$

$$\textit{and } (\forall [\alpha_1, \alpha_2] \in L^I \setminus U_{L^I})(\alpha_1 > 0 \Rightarrow (\forall x \in \mathbb{R}^n)(x \in \bigcap_{\beta_1 \in [0,\alpha_1[} M_{[\beta_1,\alpha_2]} \Rightarrow$$

$$(x \in M_{[\alpha_1,\alpha_2]} \textit{ or } (\forall [\beta_1, \beta_2] \in L^I \setminus U_{L^I})(\beta_2 > \alpha_2 \Rightarrow x \notin M_{[\beta_1,\beta_2]}))).$$

Proof.

$\Rightarrow$: Suppose that $\Big(\exists[\alpha_1,\alpha_2] \in L^I \setminus \{0_{\mathcal{L}^I}\}\Big)\Big(\exists x \in \mathbb{R}^n\Big)\Big(x \notin M_{[\alpha_1,\alpha_2]}$ and $\big((\exists[\beta_1,\beta_2] \in L^I \setminus \{0_{\mathcal{L}^I}\})(\beta_1 < \alpha_1$ and $\beta_2 > \alpha_2$ and $x \in M_{[\beta_1,\beta_2]})\big)$ and $\big((\exists[\gamma_1,\gamma_2] \in L^I \setminus \{0_{\mathcal{L}^I}\})$ $((\gamma_1 > \alpha_1$ and $\gamma_2 < \alpha_2)$ and $x \in M_{[\gamma_1,\gamma_2]})\big)\Big)$. This would mean that $s_{x,1} \geq \gamma_1$ and $s_{x,2} \geq \beta_2$. Further, $[\alpha_1,\alpha_2] \ll_{L^I} [\gamma_1,\beta_2] \leq_{L^I} s_x$ and thus $[\alpha_1,\alpha_2] \in S_x$ or $x \in M_{[\alpha_1,\alpha_2]}$, which gives us a contradiction.

Further, suppose that it holds that $(\exists[\alpha_1,\alpha_2] \in L^I \setminus U_{L^I})(\alpha_1 > 0$ and $(\exists x \in \mathbb{R}^n)(x \in \bigcap_{\beta_1 \in [0,\alpha_1[} M_{[\beta_1,\alpha_2]})$ and $x \notin M_{[\alpha_1,\alpha_2]}$ and $(\exists[\beta_1,\beta_2] \in L^I \setminus U_{L^I})(\beta_2 > \alpha_2$ and $x \in M_{[\beta_1,\beta_2]}))$. Since $x \in \bigcap_{\beta_1 \in [0,\alpha_1[} M_{[\beta_1,\alpha_2]}$, it holds that $(\forall \beta_1 \in [0,\alpha_1[)(x \in M_{[\beta_1,\alpha_2]})$, which implies that $y_{x,1} \geq \alpha_1$. Further, since $(\exists[\beta_1,\beta_2] \in L^I \setminus U_{L^I})(\beta_2 > \alpha_2$ and $x \in M_{[\beta_1,\beta_2]})$, it also holds that $y_{x,2} > \alpha_2$. This implies that $[\alpha_1,\alpha_2] \in Y_x$, which contradicts the assumption that $x \notin M_{[\alpha_1,\alpha_2]}$.

$\Leftarrow$: Suppose that the condition [SC"a] is fulfilled. Let $t \in L^I \setminus U_{L^I}$, and let $t_1 \leq y_{x,1}$ and $t_2 < y_{x,2}$. We have to prove that $t \in Y_x$.

Analogous to the proof of Lemma 9.1.8 it can be shown that $(\forall x \in d_M)(\forall r \in L^I \setminus U_{L^I})(r \ll_{L^I} y_x \Rightarrow r \in Y_x)$.

Since $t_2 < y_{x,2}$, t_2 is no upperbound for the set of upper bounds of the elements in Y_x and thus $(\exists s \in]t_2, y_{x,2}])(\exists s' \in [0,s])([s',s] \in Y_x)$.

Suppose that $t_1 = 0$. It then holds that $[t_1,t_2] <_{L^I} [s',s]$, and thus $x \in M_{[s',s]} \subseteq M_{[t_1,t_2]}$ or thus $t \in Y_x$.

Suppose now that $t_1 > 0$. Since $t_2 < y_{x,2}$, it holds that $(\forall r \in [0,t_1[)([r,t_2] \ll_{L^I} y_x)$ or thus $(\forall r \in [0,t_1[)([r,t_2] \in Y_x)$. So $x \in \bigcap_{r \in [0,t_1[} M_{[r,t_2]}$. This implies that $x \in M_{[t_1,t_2]}$ or $(\forall[\beta_1,\beta_2] \in L^I \setminus U_{L^I})(\beta_2 > t_2 \Rightarrow x \notin M_{[\beta_1,t_2]})$. As mentioned above $(\exists s \in]t_2, y_{x,2}])(\exists s' \in [0,s])([s',s] \in Y_x)$ so that we can conclude that $x \in M_{[t_1,t_2]}$, i.e., $t \in Y_x$.

□

Lemma 9.1.29. *For a decreasing family $(N_{[\alpha_1,\alpha_2]})_{[\alpha_1,\alpha_2] \in L^I \setminus \{1_{\mathcal{L}^I}\}}$ of crisp subsets of $\mathbb{R}^n$, the interval-valued fuzzy set X defined in (9.13) and the sets d_N and Z_x and the supremum z_x of the latter set, respectively defined in expressions (9.15),(9.17) and (9.19), we have that*

$$(\forall x \in d_N)(\forall r \in L^I \setminus \{1_{\mathcal{L}^I}\})((r_1 < z_{x,1} \text{ and } r_2 \leq z_{x,2}) \Rightarrow r \in Z_x)$$

$$\Updownarrow$$

$$[SC''b]: \Big(\forall[\alpha_1,\alpha_2] \in L^I \setminus \{1_{\mathcal{L}^I}\}\Big)\Big(\forall x \in \mathbb{R}^n\Big)\Big(x \notin N_{[\alpha_1,\alpha_2]} \Rightarrow$$
$$\big((\forall[\beta_1,\beta_2] \in L^I \setminus \{1_{\mathcal{L}^I}\})((\beta_1 < \alpha_1 \text{ and } \beta_2 > \alpha_2) \Rightarrow x \notin N_{[\beta_1,\beta_2]})\big) \text{ or}$$
$$\big((\forall[\beta_1,\beta_2] \in L^I \setminus \{1_{\mathcal{L}^I}\})((\beta_1 > \alpha_1 \text{ and } \beta_2 < \alpha_2) \Rightarrow x \notin N_{[\beta_1,\beta_2]})\big)\Big)$$

and $(\forall[\alpha_1,\alpha_2] \in L^I \setminus \{1_{\mathcal{L}^I}\})(\alpha_2 > 0 \Rightarrow (\forall x \in \mathbb{R}^n)(x \in \bigcap_{\beta_2 \in [\alpha_1,\alpha_2[} N_{[\alpha_1,\beta_2]} \Rightarrow$

$(x \in N_{[\alpha_1,\alpha_2]}$ *or* $(\forall[\beta_1,\beta_2] \in L^I \setminus \{1_{\mathcal{L}^I}\})(\beta_1 > \alpha_1 \Rightarrow x \notin N_{[\beta_1,\beta_2]})))$.

Proof. Analogous to the proof of Lemma 9.1.28. □

Remark that if a decreasing family $(M_{[\alpha_1,\alpha_2]})_{[\alpha_1,\alpha_2]\in L^I\setminus U_{L^I}}$ of crisp subsets of $\mathbb{R}^n$ does not fulfil [SC"a], then it will also not hold that $(\forall[\alpha_1,\alpha_2] \in L^I \setminus U_{L^I})(M_{[\alpha_1,\alpha_2]} = W_{\alpha_1}^{\overline{\alpha_2}})$. Indeed, condition [SC"a] not being fulfilled, would mean that $(\exists[\alpha_1,\alpha_2] \in L^I \setminus U_{L^I})(\exists x \in \mathbb{R}^n)(x \notin M_{[\alpha_1,\alpha_2]}$ and $(\exists[\beta_1,\beta_2] \in L^I \setminus U_{L^I})(\beta_1 < \alpha_1$ and $\beta_2 > \alpha_2$ and $x \in M_{[\beta_1,\beta_2]})$ and $(\exists[\gamma_1,\gamma_2] \in L^I \setminus U_{L^I})(\gamma_1 > \alpha_1$ and $\gamma_2 < \alpha_2$ and $x \in M_{[\gamma_1,\gamma_2]}))$ or $(\exists[\alpha_1,\alpha_2] \in L^I \setminus U_{L^I})(\alpha_1 > 0$ and $(\exists x \in \mathbb{R}^n)(x \in \bigcap_{\beta_1 \in [0,\alpha_1[} M_{[\beta_1,\alpha_2]}$ and $x \notin M_{[\alpha_1,\alpha_2]}$ and $(\exists[\beta_1,\beta_2] \in L^I \setminus U_{L^I})(\beta_2 > \alpha_2$ and $x \in M_{[\beta_1,\beta_2]}))$. Suppose that $(\exists[\alpha_1,\alpha_2] \in L^I \setminus U_{L^I})(\exists x \in \mathbb{R}^n)(x \notin M_{[\alpha_1,\alpha_2]}$ and $(\exists[\beta_1,\beta_2] \in L^I \setminus U_{L^I})(\beta_1 < \alpha_1$ and $\beta_2 > \alpha_2$ and $x \in M_{[\beta_1,\beta_2]})$ and $(\exists[\gamma_1,\gamma_2] \in L^I \setminus U_{L^I})(\gamma_1 > \alpha_1$ and $\gamma_2 < \alpha_2$ and $x \in M_{[\gamma_1,\gamma_2]}))$. This would mean that $W_1(x) = y_{x,1} \geq \gamma_1 > \alpha_1$ and $W_2(x) = y_{x,2} \geq \beta_2 > \alpha_2$. As a consequence, $x \in W_{\alpha_1}^{\overline{\alpha_2}}$ and $x \notin M_{[\alpha_1,\alpha_2]}$. In the case that $(\exists[\alpha_1,\alpha_2] \in L^I \setminus U_{L^I})(\alpha_1 > 0$ and $(\exists x \in \mathbb{R}^n)(x \in \bigcap_{\beta_1 \in [0,\alpha_1[} M_{[\beta_1,\alpha_2]}$ and $x \notin M_{[\alpha_1,\alpha_2]}$ and $(\exists[\beta_1,\beta_2] \in L^I \setminus U_{L^I})(\beta_2 > \alpha_2$ and $x \in M_{[\beta_1,\beta_2]}))$, we would have that $W_2(x) = y_{x,2} \geq \beta_2 > \alpha_2$ and since $(\forall[\beta_1,\beta_2] \in L^I \setminus U_{L^I})(\beta_1 \in [0,\alpha_1[\Rightarrow x \in M_{[\beta_1,\alpha_2]})$ also $W_1(x) = y_{x,1} \geq \alpha_1$. As a consequence, $x \in W_{\alpha_1}^{\overline{\alpha_2}}$ and $x \notin M_{[\alpha_1,\alpha_2]}$.

An analogous remark holds for a decreasing family $(N_{[\alpha_1,\alpha_2]})_{[\alpha_1,\alpha_2]\in L^I\setminus\{1_{\mathcal{L}^I}\}}$.

In what follows we will therefore concentrate on families for which [SC"a] (respectively [SC"b]) holds. For such families, the necessary condition in Proposition 9.1.26 becomes a sufficient condition.

Proposition 9.1.30.

(i) For a decreasing family $(M_{[\alpha_1,\alpha_2]})_{[\alpha_1,\alpha_2]\in L^I\setminus U_{L^I}}$ *of crisp subsets of* $\mathbb{R}^n$ *that fulfils [SC"a], the interval-valued fuzzy set* W *defined in (9.12) and the sets* d_M *and* Y_x *and the supremum* y_x *of the latter set, respectively defined in expressions (9.14),(9.16) and (9.18), it holds that:*

$$(\forall[\alpha_1,\alpha_2] \in L^I \setminus U_{L^I})(M_{[\alpha_1,\alpha_2]} = W_{\alpha_1}^{\overline{\alpha_2}})$$
$$\Updownarrow$$
$$(\forall x \in d_M)(\forall[\beta_1,\beta_2] \in Y_x)(y_{x,1} \geq \beta_1 \text{ and } y_{x,2} > \beta_2),$$

(ii) For a decreasing family $(N_{[\alpha_1,\alpha_2]})_{[\alpha_1,\alpha_2]\in L^I\setminus\{1_{\mathcal{L}^I}\}}$ *of crisp subsets of* $\mathbb{R}^n$ *that fulfils [SC"b], the interval-valued fuzzy set* X *defined in (9.13) and the sets* d_N *and* Z_x *and the supremum* z_x *of the latter set, respectively defined in expressions (9.15),(9.17) and (9.19), it holds that:*

$$(\forall[\alpha_1,\alpha_2] \in L^I \setminus \{1_{\mathcal{L}^I}\})(N_{[\alpha_1,\alpha_2]} = X_{\overline{\alpha_1}}^{\alpha_2})$$

$$\Updownarrow$$

$$(\forall x \in d_N)(\forall [\beta_1, \beta_2] \in Z_x)(z_{x,1} > \beta_1 \textit{ and } z_{x,2} \geq \beta_2).$$

Proof.

(i) $\Rightarrow$: Follows from Proposition 9.1.26.

$\Leftarrow$: Since condition [SC"a] is satisfied, Lemma 9.1.28 can be used and thus $(\forall x \in d_M)(\forall r \in L^I \setminus U_{L^I})((r_1 \leq y_{x,1} \text{ and } r_2 < y_{x,2}) \Rightarrow r \in Y_x)$. Further, it is given that $(\forall x \in d_M)(\forall [\beta_1, \beta_2] \in Y_x)(y_{x,1} \geq \beta_1 \text{ and } y_{x,2} > \beta_2)$. Let $[\beta_1, \beta_2] \in L^I \setminus U_{L^I}$ and let $x \in M_{[\beta_1,\beta_2]}$. We have that:

$$\begin{aligned}
& x \in M_{[\beta_1,\beta_2]} \\
\Leftrightarrow \quad & [\beta_1, \beta_2] \in \{[\alpha_1, \alpha_2] \mid [\alpha_1, \alpha_2] \in L^I \setminus U_{L^I} \text{ and } x \in M_{[\alpha_1,\alpha_2]}\} \\
\Leftrightarrow \quad & y_{x,1} \geq \beta_1 \text{ and } y_{x,2} > \beta_2 \\
\Leftrightarrow \quad & W_1(x) \geq \beta_1 \text{ and } W_2(x) > \beta_2 \\
\Leftrightarrow \quad & x \in W_{\beta_1}^{\overline{\beta_2}}.
\end{aligned}$$

As a consequence, $M_{[\beta_1,\beta_2]} = W_{\beta_1}^{\overline{\beta_2}}$.

(ii) Analogously.

□

The condition in Proposition 9.1.30 is not always efficient in practice. For a decreasing family $(M_{[\alpha_1,\alpha_2]})_{[\alpha_1,\alpha_2] \in L^I \setminus U_{L^I}}$ (respectively $(N_{[\alpha_1,\alpha_2]})_{[\alpha_1,\alpha_2] \in L^I \setminus \{1_{L^I}\}}$), that satisfies [SC"a] (respectively [SC"b]), it would be needed to calculate the set Y_x (respectively Z_x) for all $x \in d_M$ (respectively d_N) and to check whether $y_{x,1} \geq \beta_1$ and $y_{x,2} > \beta_2$ for all $[\beta_1, \beta_2] \in Y_x$ (respectively $z_{x,1} > \beta_1$ and $z_{x,2} \geq \beta_2$ for all $[\beta_1, \beta_2] \in Z_x$). To avoid this work, an equivalent condition on the sets $M_{[\alpha_1,\alpha_2]}$ (respectively $N_{[\alpha_1,\alpha_2]}$) can be used.

Proposition 9.1.31.

(i) For a decreasing family $(M_{[\alpha_1,\alpha_2]})_{[\alpha_1,\alpha_2] \in L^I \setminus U_{L^I}}$ of crisp subsets of $\mathbb{R}^n$ that fulfills [SC"a], the interval-valued fuzzy set W defined in (9.12) and the sets d_M and Y_x and the supremum y_x of the latter set, respectively defined in expressions (9.14)-(9.18), it holds that:

$$(\forall x \in d_M)(\forall [\beta_1, \beta_2] \in Y_x)(y_{x,1} \geq \beta_1 \textit{ and } y_{x,2} > \beta_2)$$

$$\Updownarrow$$

$$(\forall [\alpha_1, \alpha_2] \in L^I \setminus U_{L^I})(M_{[\alpha_1,\alpha_2]} = \bigcup_{[\beta_1,\beta_2], \beta_1 \geq \alpha_1, \beta_2 > \alpha_2} M_{[\beta_1,\beta_2]}).$$

(ii) For a decreasing family $(N_{[\alpha_1,\alpha_2]})_{[\alpha_1,\alpha_2] \in L^I \setminus \{1_{L^I}\}}$ of crisp subsets of $\mathbb{R}^n$ that fulfills [SC"b], the interval-valued fuzzy set X defined in (9.13) and the sets d_N and Z_x and

the supremum z_x of the latter set, respectively defined in expressions (9.15)-(9.19), it holds that:

$$(\forall x \in d_N)(\forall [\beta_1,\beta_2] \in Z_x)(z_{x,1} > \beta_1 \text{ and } z_{x,2} \geq \beta_2)$$
$$\Updownarrow$$
$$(\forall [\alpha_1,\alpha_2] \in L^I \setminus \{1_{\mathcal{L}^I}\})(N_{[\alpha_1,\alpha_2]} = \bigcup_{[\beta_1,\beta_2],\beta_1>\alpha_1,\beta_2\geq\alpha_2} N_{[\beta_1,\beta_2]}).$$

Proof.

(i) $\Rightarrow$: Let $[\alpha_1,\alpha_2] \in L^I \setminus U_{L^I}$. For all $x \in M_{[\alpha_1,\alpha_2]}$ it holds that:

$$\begin{aligned}
& x \in M_{[\alpha_1,\alpha_2]} \\
\Leftrightarrow\ & [\alpha_1,\alpha_2] \in Y_x \\
\Leftrightarrow\ & y_{x,1} \geq \alpha_1 \text{ and } y_{x,2} > \alpha_2 \\
\Leftrightarrow\ & (\exists [\beta_1,\beta_2] \in L^I \setminus U_{L^I})(\alpha_1 \leq \beta_1 \leq y_{x,1} \text{ and } \alpha_2 < \beta_2 < y_{x,2}) \\
\Leftrightarrow\ & (\exists [\beta_1,\beta_2] \in L^I \setminus U_{L^I})(\alpha_1 \leq \beta_1 \text{ and } \alpha_2 < \beta_2 \text{ and } [\beta_1,\beta_2] \in Y_x) \\
\Leftrightarrow\ & (\exists [\beta_1,\beta_2] \in L^I \setminus U_{L^I})(\alpha_1 \leq \beta_1 \text{ and } \alpha_2 < \beta_2 \text{ and } x \in M_{[\beta_1,\beta_2]}) \\
\Leftrightarrow\ & x \in \bigcup_{[\beta_1,\beta_2],\beta_1\geq\alpha_1,\beta_2>\alpha_2} M_{[\beta_1,\beta_2]}.
\end{aligned}$$

$\Leftarrow$: Let $x \in d_M$. Since $y_x = \sup Y_x$, it holds that $(\forall [\beta_1,\beta_2] \in Y_x)(\beta_1 \leq y_{x,1}$ and $\beta_2 \leq y_{x,2})$.
We now prove that $(\forall [\beta_1,\beta_2] \in Y_x)(\beta_1 \leq y_{x,1}$ and $\beta_2 < y_{x,2})$. Suppose that this would not be true and that there would exist a $[\beta_1,\beta_2] \in Y_x$ for which $\beta_1 \leq y_{x,1}$ and $\beta_2 = y_{x,2}$. So $x \in M_{[\beta_1,y_{x,2}]} = M_{[\beta_1,\beta_2]}$. Since $y_x = \sup Y_x$, $(\nexists [\gamma_1,\gamma_2] \in L^I \setminus U_{L^I})(\gamma_1 \geq \beta_1$ and $\gamma_2 > y_{x,2}$ and $x \in M_{[\gamma_1,\gamma_2]})$ or thus $x \notin \bigcup_{[\gamma_1,\gamma_2],\gamma_1\geq\beta_1,\gamma_2>y_{x,2}} M_{[\gamma_1,\gamma_2]}$. Consequently, $\bigcup_{[\gamma_1,\gamma_2],\gamma_1\geq\beta_1,\gamma_2>y_{x,2}} M_{[\gamma_1,\gamma_2]} \neq M_{[\beta_1,y_{x,2}]}$ and hence a contradiction.
We conclude that $(\forall [\beta_1,\beta_2] \in Y_x)(\beta_1 \leq y_{x,1}$ and $\beta_2 < y_{x,2})$.

(ii) Analogously.

□

Example 9.1.32. The family $(M_{[\alpha_1,\alpha_2]})_{[\alpha_1,\alpha_2]\in L^I\setminus U_{L^I}}$ of crisp subsets of $\mathbb{R}^n$, given by $M_{[\alpha_1,\alpha_2]} = [-1+\alpha_1, 1-\alpha_2]$ for all $[\alpha_1,\alpha_2] \in L^I \setminus U_{L^I}$, is an example of a family that satisfies condition [SC"a], but for which it does not hold that $(\forall [\alpha_1,\alpha_2] \in L^I \setminus U_{L^I})(M_{[\alpha_1,\alpha_2]} = W_{\alpha_1}^{\overline{\alpha_2}})$, with the interval-valued fuzzy set W as defined in (9.12). Indeed, let $[\alpha_1,\alpha_2] \in L^I \setminus U_{L^I}$, then it holds that $(\forall [\beta_1,\beta_2] \in L^I \setminus U_{L^I})(\beta_1 \geq \alpha_1$ and $\beta_2 > \alpha_2 \Rightarrow -1+\alpha_1 \leq -1+\beta_1$ and $1-\beta_2 < 1-\alpha_2)$ or thus $(\forall [\beta_1,\beta_2] \in L^I \setminus U_{L^I})(\beta_1 \geq \alpha_1$ and $\beta_2 > \alpha_2 \Rightarrow 1-\alpha_2 \notin M_{[\beta_1,\beta_2]})$. On the other hand $1-\alpha_2 \in M_{[\alpha_1,\alpha_2]}$. So $\bigcup_{[\beta_1,\beta_2],\beta_1\geq\alpha_1,\beta_2>\alpha_2} M_{[\beta_1,\beta_2]} \neq M_{[\alpha_1,\alpha_2]}$.

An analogous example can be found for strict-weak $[\alpha_1, \alpha_2]$-cuts.

$\diamondsuit$

Example 9.1.33. The family $(M_{[\alpha_1,\alpha_2]})_{[\alpha_1,\alpha_2]\in L^I\setminus U_{L^I}}$ of crisp subsets of $\mathbb{R}^n$, given by $M_{[\alpha_1,\alpha_2]} = [-1+\alpha_1, 1-\alpha_2[$ for all $[\alpha_1,\alpha_2] \in L^I \setminus U_{L^I}$, is an example of a family for which it holds that $(\forall [\alpha_1,\alpha_2] \in L^I \setminus U_{L^I})(M_{[\alpha_1,\alpha_2]} = W^{\overline{\alpha_2}}_{\alpha_1})$, with the interval-valued fuzzy set W as defined in (9.12).

An analogous example can be found for strict-weak $[\alpha_1, \alpha_2]$-cuts.

$\diamondsuit$

The Construction Principle

Based on the results from the introduction of this subsection and analogous to the construction principle based on weak and strict $[\alpha_1, \alpha_2]$-cuts, we might extend an increasing operator ϕ on $\mathcal{P}(\mathbb{R}^n)$ to an operator Φ on $\mathcal{F}_{\mathcal{L}^I}(\mathbb{R}^n)$ in two ways as follows. For all $A \in \mathcal{F}_{\mathcal{L}^I}(\mathbb{R}^n)$,

$$\begin{aligned}\Phi_1(A) &= \bigcup_{[\alpha_1,\alpha_2]\in L^I\setminus U_{L^I}} [\alpha_1,\alpha_2]\phi(A^{\overline{\alpha_2}}_{\alpha_1}),\\ \Phi_2(A) &= \bigcup_{[\alpha_1,\alpha_2]\in L^I\setminus\{1_{\mathcal{L}^I}\}} [\alpha_1,\alpha_2]\phi(A^{\alpha_2}_{\overline{\alpha_1}}).\end{aligned}$$

Operators having two or more arguments can be extended analogously. We illustrate this for an increasing operator ψ on $\mathcal{P}(\mathbb{R}^n)\times\mathcal{P}(\mathbb{R}^n)$ (like the binary dilation). For all $A, B \in \mathcal{F}_{\mathcal{L}^I}(\mathbb{R}^n)$,

$$\begin{aligned}\Psi_1(A,B) &= \bigcup_{[\alpha_1,\alpha_2]\in L^I\setminus U_{L^I}} [\alpha_1,\alpha_2]\psi(A^{\overline{\alpha_2}}_{\alpha_1}, B^{\overline{\alpha_2}}_{\alpha_1})\\ \Psi_2(A,B) &= \bigcup_{[\alpha_1,\alpha_2]\in L^I\setminus\{1_{\mathcal{L}^I}\}} [\alpha_1,\alpha_2]\psi(A^{\alpha_2}_{\overline{\alpha_1}}, B^{\alpha_2}_{\overline{\alpha_1}}).\end{aligned}$$

As discussed in the introduction of this subsection, for the operators Φ and Ψ it does not necessarily hold that:

$$\begin{gathered}(\forall [\alpha_1,\alpha_2] \in L^I \setminus U_{L^I})(\Phi_1(A)^{\overline{\alpha_2}}_{\alpha_1} = \phi(A^{\overline{\alpha_2}}_{\alpha_1}))\\ (\forall [\alpha_1,\alpha_2] \in L^I \setminus U_{L^I})(\Psi_1(A,B)^{\overline{\alpha_2}}_{\alpha_1} = \psi(A^{\overline{\alpha_2}}_{\alpha_1}, B^{\overline{\alpha_2}}_{\alpha_1}))\\ (\forall [\alpha_1,\alpha_2] \in L^I \setminus \{1_{\mathcal{L}^I}\})(\Phi_2(A)^{\alpha_2}_{\overline{\alpha_1}} = \phi(A^{\alpha_2}_{\overline{\alpha_1}}))\\ (\forall [\alpha_1,\alpha_2] \in L^I \setminus \{1_{\mathcal{L}^I}\})(\Psi_2(A,B)^{\alpha_2}_{\overline{\alpha_1}} = \psi(A^{\alpha_2}_{\overline{\alpha_1}}, B^{\alpha_2}_{\overline{\alpha_1}})).\end{gathered}$$

We now extend the increasing binary dilation to interval-valued fuzzy sets using the above introduced construction principle as follows:

Let $A, B \in \mathcal{F}_{\mathcal{L}^I}(\mathbb{R}^n)$. The extended dilations $\widetilde{D(A,B)}''$ and $\widetilde{D(A,B)}'''$ of A by B are then given by:

$$\widetilde{D(A,B)}'' = \bigcup_{[\alpha_1,\alpha_2]\in L^I\setminus U_{L^I}} [\alpha_1,\alpha_2]D(A_{\alpha_1}^{\overline{\alpha_2}}, B_{\alpha_1}^{\overline{\alpha_2}}), \tag{9.20}$$

$$\widetilde{D(A,B)}''' = \bigcup_{[\alpha_1,\alpha_2]\in L^I\setminus \{1_{\mathcal{L}^I}\}} [\alpha_1,\alpha_2]D(A_{\alpha_1}^{\alpha_2}, B_{\alpha_1}^{\alpha_2}). \tag{9.21}$$

Proposition 9.1.34. *Let $A, B \in \mathcal{F}_{\mathcal{L}^I}(\mathbb{R}^n)$, then for all $y \in \mathbb{R}^n$ it holds that:*

(i)

$$\widetilde{D(A,B)}''(y) = \sup_{x\in T_y(d_B)\cap d_A} \mathcal{C}_{\min}(B(x-y), A(x)) = D^I_{\mathcal{C}_{\min}}(A,B)(y).$$

(ii)

$$\widetilde{D(A,B)}'''(y) \leq_{L^I} \sup_{x\in T_y(d_B)\cap d_A} \mathcal{C}_{\min}(B(x-y), A(x)) = D^I_{\mathcal{C}_{\min}}(A,B)(y).$$

If $A(x) \gg_{L^I} 0_{\mathcal{L}^I},\ \forall x \in d_A$ and $B(x) \gg_{L^I} 0_{\mathcal{L}^I},\ \forall x \in d_B$, then

$$\widetilde{D(A,B)}'''(y) = \sup_{x\in T_y(d_B)\cap d_A} \mathcal{C}_{\min}(B(x-y), A(x)) = D^I_{\mathcal{C}_{\min}}(A,B)(y).$$

Proof.

(i) Let $A, B \in \mathcal{F}_{\mathcal{L}^I}(\mathbb{R}^n)$, and let $y \in \mathbb{R}^n$. From the definition of the binary dilation,

$$D(A_{\alpha_1}^{\overline{\alpha_2}}, B_{\alpha_1}^{\overline{\alpha_2}})(y) = \begin{cases} 1 & \text{if } y \in D(A_{\alpha_1}^{\overline{\alpha_2}}, B_{\alpha_1}^{\overline{\alpha_2}}) \\ 0 & \text{else} \end{cases},$$

it follows that:

$$\begin{aligned}
\widetilde{D(A,B)}''(y) &= \sup_{[\alpha_1,\alpha_2]\in L^I\setminus U_{L^I}} ([\alpha_1,\alpha_2]D(A_{\alpha_1}^{\overline{\alpha_2}}, B_{\alpha_1}^{\overline{\alpha_2}}))(y) \\
&= \sup\{[\alpha_1,\alpha_2] \mid [\alpha_1,\alpha_2] \in L^I \setminus U_{L^I} \text{ and } y \in D(A_{\alpha_1}^{\overline{\alpha_2}}, B_{\alpha_1}^{\overline{\alpha_2}})\} \\
&= \sup\{[\alpha_1,\alpha_2] \mid [\alpha_1,\alpha_2] \in L^I \setminus U_{L^I} \text{ and } T_y(B_{\alpha_1}^{\overline{\alpha_2}}) \cap A_{\alpha_1}^{\overline{\alpha_2}} \neq \emptyset\} \\
&= \sup\{[\alpha_1,\alpha_2] \mid [\alpha_1,\alpha_2] \in L^I \setminus U_{L^I} \text{ and } (\exists x \in T_y(d_B) \cap d_A) \\
&\qquad\qquad (x \in T_y(B_{\alpha_1}^{\overline{\alpha_2}}) \text{ and } x \in A_{\alpha_1}^{\overline{\alpha_2}})\} \\
&= \sup\{[\alpha_1,\alpha_2] \mid [\alpha_1,\alpha_2] \in L^I \setminus U_{L^I} \text{ and } (\exists x \in T_y(d_B) \cap d_A) \\
&\qquad\qquad ((B_1(x-y) \geq \alpha_1 \text{and } A_1(x) \geq \alpha_1) \text{ and} \\
&\qquad\qquad\qquad (B_2(x-y) > \alpha_2 \text{ and } A_2(x) > \alpha_2))\}
\end{aligned}$$

$$
\begin{aligned}
&= \sup\{[\alpha_1,\alpha_2] \mid [\alpha_1,\alpha_2] \in L^I \setminus U_{L^I} \text{ and } (\exists x \in T_y(d_B) \cap d_A) \\
&\qquad ((\mathcal{C}_{\min}(B(x-y), A(x)))_1 \geq \alpha_1 \text{ and} \\
&\qquad\qquad (\mathcal{C}_{\min}(B(x-y), A(x)))_2 > \alpha_2])\} \\
&\equiv (*).
\end{aligned}
$$

First, we will prove that $(*)$ is less than or equal to

$$\sup\{\mathcal{C}_{\min}(B(x-y), A(x)) \mid x \in T_y(d_B) \cap d_A\} \equiv (**).$$

It holds that:

$$
\begin{aligned}
(*) \quad &= \quad \sup\{[\alpha_1,\alpha_2] \mid [\alpha_1,\alpha_2] \in L^I \setminus U_{L^I} \text{ and } (\exists x \in T_y(d_B) \cap d_A) \\
&\qquad ((\mathcal{C}_{\min}(B(x-y), A(x)))_1 \geq \alpha_1 \text{ and} \\
&\qquad\qquad (\mathcal{C}_{\min}(B(x-y), A(x)))_2 > \alpha_2])\} \\
&\leq_{L^I} \quad \sup\{[\alpha_1,\alpha_2] \mid [\alpha_1,\alpha_2] \in L^I \setminus U_{L^I} \text{ and} \\
&\qquad\qquad \alpha_1 \leq (\sup_{x \in T_y(d_B) \cap d_A} \mathcal{C}_{\min}(B(x-y), A(x)))_1 \text{ and} \\
&\qquad\qquad\qquad \alpha_2 < (\sup_{x \in T_y(d_B) \cap d_A} \mathcal{C}_{\min}(B(x-y), A(x)))_2\} \\
&= \quad \sup_{x \in T_y(d_B) \cap d_A} \mathcal{C}_{\min}(B(x-y), A(x))) \\
&= \quad (**)
\end{aligned}
$$

It also holds that $(**) \leq_{L^I} (*)$. If $T_y(d_B) \cap d_A = \emptyset$, then $(**) = 0_{\mathcal{L}^I}$ and thus $(**) \leq_{L^I} (*)$. Otherwise, consider an arbitrary $\epsilon > 0$. We have that:

$$
\begin{aligned}
&(**)_1 - \epsilon \text{ is no upper bound for the set of lower bounds of the intervals in} \\
&\text{the set } \{\mathcal{C}_{\min}(B(x-y), A(x)) \mid x \in T_y(d_B) \cap d_A\} \text{and } (**)_2 - \epsilon \text{ is no} \\
&\text{upper bound for the set of upper bounds of the intervals in the set} \\
&\{\mathcal{C}_{\min}(B(x-y), A(x)) \mid x \in T_y(d_B) \cap d_A\} \\
\Rightarrow \quad &(\exists x \in T_y(d_B) \cap d_A)((**)_1 - \epsilon < \mathcal{C}_{\min}(B(x-y), A(x))_1) \text{ and} \\
&(\exists x' \in T_y(d_B) \cap d_A)((**)_2 - \epsilon < \mathcal{C}_{\min}(B(x'-y), A(x'))_2).
\end{aligned}
$$

For such element x from the first part of the above consequent, for which $(**)_1 - \epsilon < \mathcal{C}_{\min}(B(x-y), A(x))_1$, we can choose $\alpha_2 = (**)_1 - \epsilon < (\mathcal{C}_{\min}(B(x-y), A(x)))_1 \leq (\mathcal{C}_{\min}(B(x-y), A(x)))_2$, such that

$$
\begin{aligned}
(**)_1 - \epsilon \in \{\alpha_1 \mid (\exists \alpha_2 \in [\alpha_1, 1[\text{ such that } [\alpha_1,\alpha_2] \in L^I \setminus U_{L^I}) \text{ and} \\
(\exists x \in T_y(d_B) \cap d_A)(\alpha_1 \leq (\mathcal{C}_{\min}(B(x-y), A(x)))_1 \\
\text{and } \alpha_2 < (\mathcal{C}_{\min}(B(x-y), A(x)))_2)\}.
\end{aligned}
$$

For the second part of the consequent, we can choose $\alpha_1 = 0 \leq (\mathcal{C}_{\min}(B(x'-y), A(x')))_1$, such that

$$(**)_2 - \epsilon \in \{\alpha_2 \mid (\exists \alpha_1 \in [0,\alpha_2] \text{ such that } [\alpha_1,\alpha_2] \in L^I \setminus U_{L^I}) \text{ and } (\exists x \in T_y(d_B) \cap d_A)(\alpha_1 \leq (\mathcal{C}_{\min}(B(x-y), A(x)))_1 \text{ and } \alpha_2 < (\mathcal{C}_{\min}(B(x-y), A(x)))_2)\}$$

It thus follows that:

$$\begin{aligned}
& (**)_1 - \epsilon \in \{\alpha_1 \mid (\exists \alpha_2 \in [\alpha_1, 1[)([\alpha_1,\alpha_2] \in L^I \setminus U_{L^I}) \text{ and} \\
& (\exists x \in T_y(d_B) \cap d_A)(\alpha_1 \leq (\mathcal{C}_{\min}(B(x-y), A(x)))_1 \text{ and} \\
& \alpha_2 < (\mathcal{C}_{\min}(B(x-y), A(x)))_2))\} \text{ and} \\
& (**)_2 - \epsilon \in \{\alpha_2 \mid (\exists \alpha_1 \in [0,\alpha_2])([\alpha_1,\alpha_2] \in L^I \setminus U_{L^I}) \text{ and} \\
& (\exists x \in T_y(d_B) \cap d_A)(\alpha_1 \leq (\mathcal{C}_{\min}(B(x-y), A(x)))_1 \text{ and} \\
& \alpha_2 < (\mathcal{C}_{\min}(B(x-y), A(x)))_2))\} \\
\Rightarrow \quad & (**)_1 - \epsilon \leq \sup\{\alpha_1 \mid (\exists \alpha_2 \in [\alpha_1, 1[)([\alpha_1,\alpha_2] \in L^I \setminus U_{L^I}) \text{ and} \\
& (\exists x \in T_y(d_B) \cap d_A)(\alpha_1 \leq (\mathcal{C}_{\min}(B(x-y), A(x)))_1 \text{ and} \\
& \alpha_2 < (\mathcal{C}_{\min}(B(x-y), A(x)))_2))\} \text{ and} \\
& (**)_2 - \epsilon \leq \sup\{\alpha_2 \mid (\exists \alpha_1 \in [0,\alpha_2])([\alpha_1,\alpha_2] \in L^I \setminus U_{L^I}) \text{ and} \\
& (\exists x \in T_y(d_B) \cap d_A)(\alpha_1 \leq (\mathcal{C}_{\min}(B(x-y), A(x)))_1 \text{ and} \\
& \alpha_2 < (\mathcal{C}_{\min}(B(x-y), A(x)))_2))\} \\
\Rightarrow \quad & [(**)_1 - \epsilon, (**)_2 - \epsilon] \leq_{L^I} \sup\{[\alpha_1,\alpha_2] \mid [\alpha_1,\alpha_2] \in L^I \setminus U_{L^I} \text{ and} \\
& (\exists x \in T_y(d_B) \cap d_A)(\alpha_1 \leq (\mathcal{C}_{\min}(B(x-y), A(x)))_1 \text{ and} \\
& \alpha_2 < (\mathcal{C}_{\min}(B(x-y), A(x)))_2)\} = (*).
\end{aligned}$$

Taking $\epsilon \to 0$ gives the result.

(ii) The proof is analogous to the proof of (i). Only now,

$$\begin{aligned}
(**) \equiv \sup\{\mathcal{C}_{\min}(B(x-y), A(x)) \mid x \in T_y(d_B) \cap d_A\} \leq_{L^I} \\
\sup\{[\alpha_1,\alpha_2] \mid [\alpha_1,\alpha_2] \in L^I \setminus \{1_{\mathcal{L}^I}\} \text{ and } (\exists x \in T_y(d_B) \cap d_A) \\
((\mathcal{C}_{\min}(B(x-y), A(x)))_1 > \alpha_1 \text{ and} \\
(\mathcal{C}_{\min}(B(x-y), A(x)))_2 \geq \alpha_2)\} \equiv (*)
\end{aligned}$$

will not always hold, but it is however guaranteed if $A(x) \gg_{L^I} 0_{\mathcal{L}^I}$, $\forall x \in d_A$ and $B(x) \gg_{L^I} 0_{\mathcal{L}^I}$, $\forall x \in d_B$. Then we can always choose $\alpha_1 = 0 < (\mathcal{C}_{\min}(B(x'-y), A(x')))_1$, such that

$$(**)_2 - \epsilon \in \{\alpha_2 \mid (\exists \alpha_1 \in [0,\alpha_2] \text{ such that } [\alpha_1,\alpha_2] \in L^I \setminus \{1_{\mathcal{L}^I}\}) \text{ and}$$

$$(\exists x \in T_y(d_B) \cap d_A)(\alpha_1 < (\mathcal{C}_{\min}(B(x-y), A(x)))_1 \text{ and } \alpha_2 \leq (\mathcal{C}_{\min}(B(x-y), A(x)))_2)\},$$

analogously to the proof of (i).

□

Example 9.1.23 can be used again to illustrate that if not $A(x) \gg_{L^I} 0_{\mathcal{L}^I},\ \forall x \in d_A$ or not $B(x) \gg_{L^I} 0_{\mathcal{L}^I},\ \forall x \in d_B$, then not necessarily

$$\begin{aligned}\sup\{\mathcal{C}_{\min}(B(x-y), A(x)) \mid x \in T_y(d_B) \cap d_A\} \leq_{L^I} \\ \sup\{[\alpha_1, \alpha_2] \in L^I \setminus U_{L^I} \mid (\exists x \in T_y(d_B) \cap d_A) \\ ((\mathcal{C}_{\min}(B(x-y), A(x)))_1 > \alpha_1 \text{ and} \\ (\mathcal{C}_{\min}(B(x-y), A(x)))_2 \geq \alpha_2])\}.\end{aligned}$$

The construction principle can not be used to extend the binary erosion to an interval-valued fuzzy morphological operator, since it is not increasing in both its arguments. Analogously as for weak and strict $[\alpha_1, \alpha_2]$-cuts, it can however be constructed by duality properties.

$$\begin{aligned}E^I_{\mathcal{I}_{EKD}}(A,B)(y) &= (co_{\mathcal{N}_s}(D^I_{\mathcal{C}_{\min}}(co_{\mathcal{N}_s}(A), B)))(y) \\ &= (co_{\mathcal{N}_s}(\bigcup_{[\alpha_1,\alpha_2]\in L^I\setminus U_{L^I}} [\alpha_1,\alpha_2]D((co_{\mathcal{N}_s}A)^{\overline{\alpha_2}}_{\alpha_1}, B^{\overline{\alpha_2}}_{\alpha_1})))(y) \\ &= \mathcal{N}_s((\bigcup_{[\alpha_1,\alpha_2]\in L^I\setminus U_{L^I}} [\alpha_1,\alpha_2]D((co_{\mathcal{N}_s}A)^{\overline{\alpha_2}}_{\alpha_1}, B^{\overline{\alpha_2}}_{\alpha_1}))(y)) \\ &= \mathcal{N}_s(\sup_{[\alpha_1,\alpha_2]\in L^I\setminus U_{L^I}} ([\alpha_1,\alpha_2]D((co_{\mathcal{N}_s}A)^{\overline{\alpha_2}}_{\alpha_1}, B^{\overline{\alpha_2}}_{\alpha_1}))(y)) \\ &= \mathcal{N}_s(\sup_{[\alpha_1,\alpha_2]\in L^I\setminus U_{L^I}} ([\alpha_1,\alpha_2]co(E(co((co_{\mathcal{N}_s}A)^{\overline{\alpha_2}}_{\alpha_1}), B^{\overline{\alpha_2}}_{\alpha_1})))(y))\end{aligned}$$

$$\begin{aligned}E^I_{\mathcal{I}_{EKD}}(A,B)(y) &= (co_{\mathcal{N}_s}(D^I_{\mathcal{C}_{\min}}(co_{\mathcal{N}_s}(A), B)))(y) \\ &\leq_{L^I} (co_{\mathcal{N}_s}(\bigcup_{[\alpha_1,\alpha_2]\in L^I\setminus U_{L^I}} [\alpha_1,\alpha_2]D((co_{\mathcal{N}_s}A)^{\alpha_2}_{\alpha_1}, B^{\alpha_2}_{\alpha_1})))(y) \\ &= \mathcal{N}_s((\bigcup_{[\alpha_1,\alpha_2]\in L^I\setminus U_{L^I}} [\alpha_1,\alpha_2]D((co_{\mathcal{N}_s}A)^{\alpha_2}_{\alpha_1}, B^{\alpha_2}_{\alpha_1}))(y)) \\ &= \mathcal{N}_s(\sup_{[\alpha_1,\alpha_2]\in L^I\setminus U_{L^I}} ([\alpha_1,\alpha_2]D((co_{\mathcal{N}_s}A)^{\alpha_2}_{\alpha_1}, B^{\alpha_2}_{\alpha_1}))(y)) \\ &= \mathcal{N}_s(\sup_{[\alpha_1,\alpha_2]\in L^I\setminus U_{L^I}} ([\alpha_1,\alpha_2]co(E(co((co_{\mathcal{N}_s}A)^{\alpha_2}_{\alpha_1}), B^{\alpha_2}_{\alpha_1})))(y))\end{aligned}$$

If $A(x) \gg_{L^I} 0_{\mathcal{L}^I},\ \forall x \in d_A$ and $B(x) \gg_{L^I} 0_{\mathcal{L}^I},\ \forall x \in d_B$, then the equality holds.

The interval-valued fuzzy opening and closing can then be constructed as a combination of the interval-valued fuzzy dilation and erosion.

9.1.4 Sub- and Supercuts

There is no construction principle based on weak and strict sub- and supercuts, since these sets only give information about the lower or the upper bounds of the intervals on which an interval-valued fuzzy set maps the elements of the universe.

Example 9.1.35. Let $A(x) = [0.3, 0.5]$ for all $x \in [0, 1]$. For example, for $\widetilde{x} = 0.5$, we know that it belongs to A_{α_1} for all $\alpha_1 \in]0, 0.3]$, but this does not give us any information about the upper bound of the interval $A(\widetilde{x}) = [0.3, 0.5]$.

$\diamondsuit$

9.2 Discrete Case

We will now investigate the construction of interval-valued fuzzy morphological operators from the corresponding binary operators in the discrete framework. It will be seen that the characterization of the supremum in the discrete case has as a consequence that some of the difficulties from the continuous case don't arise anymore. Moreover, also some stronger relationships will hold.

9.2.1 Construction Based on Weak $[\alpha_1, \alpha_2]$-cuts

Lemma 9.2.1. *Let $A \in \mathcal{F}_{\mathcal{L}^I_{r,s}}(\mathbb{Z}^n)$, then it holds that $A = \bigcup_{[\alpha_1,\alpha_2] \in L^I_{r,s} \setminus \{0_{\mathcal{L}^I}\}} [\alpha_1, \alpha_2] A^{\alpha_2}_{\alpha_1}$, i.e., $\forall x \in \mathbb{Z}^n$:*

$$\begin{aligned} A(x) &= \sup_{[\alpha_1,\alpha_2] \in L^I_{r,s} \setminus \{0_{\mathcal{L}^I}\}} ([\alpha_1, \alpha_2] A^{\alpha_2}_{\alpha_1})(x) \\ &= \sup \{[\alpha_1, \alpha_2] \mid [\alpha_1, \alpha_2] \in L^I_{r,s} \setminus \{0_{\mathcal{L}^I}\} \text{ and } x \in A^{\alpha_2}_{\alpha_1}\} \\ &= [\max\{\alpha_1 \mid (\exists \alpha_2 \in [\alpha_1, 1] \setminus \{0_{\mathcal{L}^I}\})([\alpha_1, \alpha_2] \in L^I_{r,s} \text{ and } x \in A^{\alpha_2}_{\alpha_1})\}, \\ &\quad \max\{\alpha_2 \mid (\exists \alpha_1 \in [0, \alpha_2])([\alpha_1, \alpha_2] \in L^I_{r,s} \text{ and } x \in A^{\alpha_2}_{\alpha_1})\}]. \end{aligned}$$

Proof. Similar to the proof of Lemma 9.1.1. □

If we now consider a family $(P_{[\alpha_1,\alpha_2]})_{[\alpha_1,\alpha_2] \in L^I_{r,s} \setminus \{0_{\mathcal{L}^I}\}}$ of crisp subsets of $\mathbb{Z}^n$ that is decreasing and we define the interval-valued fuzzy set R in $\mathbb{Z}^n$ for all $x \in \mathbb{Z}^n$ as

$$\begin{aligned} R(x) &= \sup_{[\alpha_1,\alpha_2] \in L^I_{r,s} \setminus \{0_{\mathcal{L}^I}\}} ([\alpha_1, \alpha_2] P_{[\alpha_1,\alpha_2]})(x) \\ &= \sup \{[\alpha_1, \alpha_2] \mid [\alpha_1, \alpha_2] \in L^I_{r,s} \setminus \{0_{\mathcal{L}^I}\} \text{ and } x \in P_{[\alpha_1,\alpha_2]}\}, \end{aligned} \tag{9.22}$$

then we might wonder whether it holds that $(\forall[\alpha_1,\alpha_2] \in L^I_{r,s} \setminus \{0_{\mathcal{L}^I}\})(R^{\alpha_2}_{\alpha_1} = P_{[\alpha_1,\alpha_2]})$. Just as in the continuous case, the following inclusion always holds:

Proposition 9.2.2. *For a decreasing family $(P_{[\alpha_1,\alpha_2]})_{[\alpha_1,\alpha_2]\in L^I_{r,s}\setminus\{0_{\mathcal{L}^I}\}}$ of crisp subsets of $\mathbb{Z}^n$ and the interval-valued fuzzy set R defined in (9.22), it holds that:*

$$(\forall[\alpha_1,\alpha_2] \in L^I \setminus \{0_{\mathcal{L}^I}\})(P_{[\alpha_1,\alpha_2]} \subseteq R^{\alpha_2}_{\alpha_1}).$$

Proof. Analogous to the proof of Proposition 9.1.2. □

The following lemma gives us a condition such that the reverse inclusion would also hold.

Lemma 9.2.3. *For a decreasing family $(P_{[\alpha_1,\alpha_2]})_{[\alpha_1,\alpha_2]\in L^I_{r,s}\setminus\{0_{\mathcal{L}^I}\}}$ of crisp subsets of $\mathbb{Z}^n$, it holds that*

$$\begin{gathered}
(\forall[\alpha_1,\alpha_2] \in L^I_{r,s} \setminus \{0_{\mathcal{L}^I}\})(\forall x \in \mathbb{Z}^n)\\
([\alpha_1,\alpha_2] \in \{[\beta_1,\beta_2] \mid [\beta_1,\beta_2] \in L^I_{r,s} \setminus \{0_{\mathcal{L}^I}\} \text{ and } x \in P_{[\beta_1,\beta_2]}\} \Leftrightarrow\\
\sup\{[\beta_1,\beta_2] \mid [\beta_1,\beta_2] \in L^I_{r,s} \setminus \{0_{\mathcal{L}^I}\} \text{ and } x \in P_{[\beta_1,\beta_2]}\} \geq_{L^I} [\alpha_1,\alpha_2])\\
\Updownarrow\\
[\widetilde{SC}] : \Big(\forall[\alpha_1,\alpha_2] \in L^I_{r,s} \setminus \{0_{\mathcal{L}^I}\}\Big)\Big(\forall x \in \mathbb{Z}^n\Big)\Big(x \notin P_{[\alpha_1,\alpha_2]} \Rightarrow\\
\big((\forall[\beta_1,\beta_2] \in L^I_{r,s} \setminus \{0_{\mathcal{L}^I}\})((\beta_1 < \alpha_1 \text{ and } \beta_2 \geq \alpha_2) \Rightarrow x \notin P_{[\beta_1,\beta_2]})\big) \text{ or}\\
\big((\forall[\beta_1,\beta_2] \in L^I_{r,s} \setminus \{0_{\mathcal{L}^I}\})((\beta_1 \geq \alpha_1 \text{ and } \beta_2 < \alpha_2) \Rightarrow x \notin P_{[\beta_1,\beta_2]})\big)\Big).
\end{gathered}$$

Proof.

$\Rightarrow$: Suppose that it holds that $\Big(\exists[\alpha_1,\alpha_2] \in L^I_{r,s} \setminus \{0_{\mathcal{L}^I}\}\Big)\Big(\exists x \in \mathbb{Z}^n\Big)\Big(x \notin P_{[\alpha_1,\alpha_2]}$ and $\big((\exists[\beta_1,\beta_2] \in L^I_{r,s} \setminus \{0_{\mathcal{L}^I}\})((\beta_1 < \alpha_1$ and $\beta_2 > \alpha_2)$ and $x \in P_{[\beta_1,\beta_2]})\big)$ and $\big((\exists[\gamma_1,\gamma_2] \in L^I_{r,s} \setminus \{0_{\mathcal{L}^I}\})((\gamma_1 > \alpha_1$ and $\gamma_2 < \alpha_2)$ and $x \in P_{[\gamma_1,\gamma_2]})\big)\Big)$. This means that $\sup\{[\beta_1,\beta_2] \mid [\beta_1,\beta_2] \in L^I_{r,s} \setminus \{0_{\mathcal{L}^I}\}$ and $x \in P_{[\beta_1,\beta_2]}\} \geq_{L^I} [\gamma_1,\beta_2]$. Further, then also $[\alpha_1,\alpha_2] \ll_{L^I} [\gamma_1,\beta_2]$ and thus $[\alpha_1,\alpha_2] \in \{[\beta_1,\beta_2] \mid [\beta_1,\beta_2] \in L^I_{r,s} \setminus \{0_{\mathcal{L}^I}\}$ and $x \in P_{[\beta_1,\beta_2]}\}$, what gives us a contradiction.

$\Leftarrow$: Suppose that the condition $[\widetilde{SC}]$ is fulfilled. Let $[\alpha_1,\alpha_2] \in L^I_{r,s} \setminus \{0_{\mathcal{L}^I}\}$. It holds that $(\forall x \in \mathbb{Z}^n)([\alpha_1,\alpha_2] \in \{[\beta_1,\beta_2] \mid [\beta_1,\beta_2] \in L^I_{r,s} \setminus \{0_{\mathcal{L}^I}\}$ and $x \in P_{[\beta_1,\beta_2]}\} \Rightarrow \sup\{[\beta_1,\beta_2] \mid [\beta_1,\beta_2] \in L^I_{r,s} \setminus \{0_{\mathcal{L}^I}\}$ and $x \in P_{[\beta_1,\beta_2]}\} \geq_{L^I} [\alpha_1,\alpha_2])$. We have to prove that also the reverse implication holds.

Suppose that this would not be true, i.e., $(\exists x \in \mathbb{Z}^n)(\sup\{[\beta_1,\beta_2] \mid [\beta_1,\beta_2] \in L^I_{r,s} \setminus \{0_{\mathcal{L}^I}\}$ and $x \in P_{[\beta_1,\beta_2]}\} \geq_{L^I} [\alpha_1,\alpha_2]$ and $[\alpha_1,\alpha_2] \notin \{[\beta_1,\beta_2] \mid [\beta_1,\beta_2] \in L^I_{r,s} \setminus \{0_{\mathcal{L}^I}\}$ and $x \in P_{[\beta_1,\beta_2]}\})$. This would mean that $(\exists y \in [\alpha_1,1])(\exists z \in [y,1])(x \in P_{[y,z]})$. If $z \geq \alpha_2$ then we would get a contradiction since then $x \in P_{[y,z]} \subseteq P_{[\alpha_1,\alpha_2]}$.

So $z < \alpha_2$ and thus $(\exists [y,z] \in L^I_{r,s} \setminus \{0_{\mathcal{L}^I}\})(y \geq \alpha_1$ and $z < \alpha_2$ and $x \in P_{[y,z]})$. Further, also $(\exists z' \in [\alpha_2, 1])(\exists y' \in [0, z'])(x \in P_{[y',z']})$. If $y' \geq \alpha_1$ then we would get a contradiction since then $x \in P_{[y',z']} \subseteq P_{[\alpha_1,\alpha_2]}$. So $y' < \alpha_1$ and thus $(\exists [y', z'] \in L^I_{r,s} \setminus \{0_{\mathcal{L}^I}\})(y' < \alpha_1$ and $z' \geq \alpha_2$ and $x \in P_{[y',z']})$.

If we combine the above results, then we find that it would hold that $x \notin P_{[\alpha_1,\alpha_2]}$ and $(\exists [y,z] \in L^I_{r,s} \setminus \{0_{\mathcal{L}^I}\})(y \geq \alpha_1$ and $z < \alpha_2$ and $x \in P_{[y,z]})$ and $(\exists [y',z'] \in L^I_{r,s} \setminus \{0_{\mathcal{L}^I}\})(y' < \alpha_1$ and $z' \geq \alpha_2$ and $x \in P_{[y',z']})$, what is contradictory to what is given. So $(\forall x \in \mathbb{Z}^n)([\alpha_1,\alpha_2] \in \{[\beta_1,\beta_2] \mid [\beta_1,\beta_2] \in L^I_{r,s} \setminus \{0_{\mathcal{L}^I}\}$ and $x \in P_{[\beta_1,\beta_2]}\} \Leftrightarrow \sup\{[\beta_1,\beta_2] \mid [\beta_1,\beta_2] \in L^I_{r,s} \setminus \{0_{\mathcal{L}^I}\}$ and $x \in P_{[\beta_1,\beta_2]}\} \geq_{L^I} [\alpha_1,\alpha_2])$.

□

The following proposition is a straightforward consequence of the above lemma and Proposition 9.2.2.

Proposition 9.2.4. *For a decreasing family $(P_{[\alpha_1,\alpha_2]})_{[\alpha_1,\alpha_2] \in L^I_{r,s} \setminus \{0_{\mathcal{L}^I}\}}$ of crisp subsets of $\mathbb{Z}^n$ that satisfies [$\widetilde{SC}$] and the interval-valued fuzzy set R defined in (9.22), it holds that:*

$$(\forall [\alpha_1,\alpha_2] \in L^I \setminus \{0_{\mathcal{L}^I}\})(P_{[\alpha_1,\alpha_2]} = R^{\alpha_2}_{\alpha_1}).$$

Proof. Follows from the proof of Proposition 9.2.2 by using Lemma 9.2.3. □

Remark that if the decreasing family $(P_{[\alpha_1,\alpha_2]})_{[\alpha_1,\alpha_2] \in L^I_{r,s} \setminus \{0_{\mathcal{L}^I}\}}$ does not satisfy the condition [$\widetilde{SC}$], it will not hold that $(\forall [\alpha_1,\alpha_2] \in L^I \setminus \{0_{\mathcal{L}^I}\})(P_{[\alpha_1,\alpha_2]} = R^{\alpha_2}_{\alpha_1})$, with the set R as defined in (9.22). Indeed, if [$\widetilde{SC}$] does not hold, then $(\exists [\alpha_1,\alpha_2] \in L^I_{r,s} \setminus \{0_{\mathcal{L}^I}\})(\exists x \in \mathbb{Z}^n)(x \notin P_{[\alpha_1,\alpha_2]}$ and $(\exists [\beta_1,\beta_2] \in L^I_{r,s} \setminus \{0_{\mathcal{L}^I}\})(\beta_1 < \alpha_1$ and $\beta_2 \geq \alpha_2$ and $x \in P_{[\beta_1,\beta_2]})$ and $(\exists [\gamma_1,\gamma_2] \in L^I_{r,s} \setminus \{0_{\mathcal{L}^I}\})(\gamma_1 \geq \alpha_1$ and $\gamma_2 < \alpha_2$ and $x \in P_{[\gamma_1,\gamma_2]}))$. This would mean that $R_1(x) \geq \gamma_1 \geq \alpha_1$ and $R_2(x) \geq \beta_2 \geq \alpha_2$. As a consequence, $x \in R^{\alpha_2}_{\alpha_1}$ and $x \notin P_{[\alpha_1,\alpha_2]}$.

The constructions made in the continuous case can also be performed in the discrete case with the same results. Some remarks need however to be given.

Proposition 9.2.5. *Let $A, B \in \mathcal{F}_{\mathcal{L}^I_{r,s}}(\mathbb{Z}^n)$, then for all $y \in \mathbb{Z}^n$ it holds that:*

$$\widetilde{D(A,B)}(y) = \sup_{x \in T_y(d_B) \cap d_A} \mathcal{C}_{\min}(B(x-y), A(x)) = D^I_{\mathcal{C}_{\min}}(A,B)(y).$$

Proof. The proof is similar to the one of Proposition 9.1.11, where it has to be shown that $(*) = (**)$, with $(*)$ and $(**)$ given by:

$$\begin{aligned}(*) \quad &= \quad \sup\{[\alpha_1,\alpha_2] \mid [\alpha_1,\alpha_2] \in L^I_{r,s} \setminus \{0_{\mathcal{L}^I}\} \text{ and } (\exists x \in T_y(d_B) \cap d_A) \\ &\qquad\qquad (\mathcal{C}_{\min}(B(x-y), A(x)) \geq_{L^I} [\alpha_1,\alpha_2])\}, \\ (**) \quad &= \quad \sup_{x \in T_y(d_B) \cap d_A} \mathcal{C}_{\min}(B(x-y), A(x))).\end{aligned}$$

The proof of $(*) \leq (**)$ is analogous to the proof of Proposition 9.1.11. The proof of $(**) \leq (*)$ however is much simpler in the discrete framework, since we don't have to make use of the characterization of the supremum. If $T_y(d_B) \cap d_A = \emptyset$, then $(**) = 0_{\mathcal{L}^I}$ and thus $(**) \leq_{L^I} (*)$. Otherwise, in the discrete case, it immediately follows from $(**) = \sup_{x \in T_y(d_B) \cap d_A} \mathcal{C}_{\min}(B(x-y), A(x))$ that

$$
\begin{aligned}
& (**)_1 \in \{\alpha_1 \mid (\exists \alpha_2 \in [\alpha_1, 1])([\alpha_1, \alpha_2] \in L^I_{r,s} \setminus \{0_{\mathcal{L}^I}\} \text{ and} \\
& (\exists x \in T_y(d_B) \cap d_A)([\alpha_1, \alpha_2] \leq_{L^I} \mathcal{C}_{\min}(B(x-y), A(x)))\} \text{ and} \\
& (**)_2 \in \{\alpha_2 \mid (\exists \alpha_1 \in [0, \alpha_2])([\alpha_1, \alpha_2] \in L^I_{r,s} \setminus \{0_{\mathcal{L}^I}\} \text{ and} \\
& (\exists x \in T_y(d_B) \cap d_A)([\alpha_1, \alpha_2] \leq_{L^I} \mathcal{C}_{\min}(B(x-y), A(x)))\} \\
\Rightarrow \quad & [(**)_1, (**)_2] \leq_{L^I} \sup\{[[\alpha_1, \alpha_2] \mid [\alpha_1, \alpha_2] \in L^I_{r,s} \setminus \{0_{\mathcal{L}^I}\} \text{ and} \\
& (\exists x \in T_y(d_B) \cap d_A)([\alpha_1, \alpha_2] \leq_{L^I} \mathcal{C}_{\min}(B(x-y), A(x)))\} = (*).
\end{aligned}
$$

□

Analogously to the continuous case we find the following construction of the interval-valued fuzzy erosion $E^I_{\mathcal{I}_{EKD}}$ for all $y \in \mathbb{Z}^n$:

$$
E^I_{\mathcal{I}_{EKD}}(A, B)(y) = \mathcal{N}_s\Big(\sup_{[\alpha_1,\alpha_2] \in L^I_{r,s} \setminus \{0_{\mathcal{L}^I}\}} ([\alpha_1, \alpha_2] co(E(co((co_{\mathcal{N}_s} A)^{\alpha_2}_{\alpha_1}), B^{\alpha_2}_{\alpha_1})))(y)\Big).
$$

The interval-valued fuzzy opening and closing can then be constructed as a combination of the interval-valued fuzzy dilation and erosion.

9.2.2 Construction Based on Strict $[\alpha_1, \alpha_2]$-cuts

Recall that $L^I_{r,s} = \{[\alpha_1, \alpha_2] \mid \alpha_1 \in I_r \text{ and } \alpha_2 \in I_s\}$ (Subsection 7.3.2). We determine the unit e_r (respectively e_s) of the finite chain $I_r = \{0, \frac{1}{r-1}, \ldots, \frac{r-2}{r-1}, 1\}$ (respectively $I_s = \{0, \frac{1}{s-1}, \ldots, \frac{s-2}{s-1}, 1\}$) as $e_r = \frac{1}{r-1}$ (respectively $e_s = \frac{1}{s-1}$). We assume that $e_r = e_s$, which is usually the case in practice [1]. Further, the sum of (respectively difference between) the intervals $[x_1, x_2]$ and $[e_r, e_s]$ is given by $[x_1 + e_r, x_2 + e_s]$ (respectively $[x_1 - e_r, x_2 - e_s]$). The assumption $e_r = e_s$ is needed if we want $[x_1 + e_r, x_2 + e_s]$ and $[x_1 - e_r, x_2 - e_s]$ to be intervals. Additionally, we define the set $G_{r,s}$ by $G_{r,s} = \{[\alpha_1, \alpha_2] \mid (\alpha_1 = -e_r \text{ and } \alpha_2 \in (I_s \setminus \{1\}) \cup \{-e_s\}))\}$. Remark that $G_{r,s} \cap L^I_{r,s} = \emptyset$. Finally, we extend the order relation $\leq_{L^I}$ on $L^I_{r,s}$ to $L^I_{r,s} \cup G_{r,s}$ in a straightforward manner and for this reason, we will use the same notation $\leq_{L^I}$:

$$
x \leq_{L^I} y \Leftrightarrow x_1 \leq y_1 \text{ and } x_2 \leq y_2, \ \forall x, y \in L^I_{r,s} \cup G_{r,s}. \tag{9.23}
$$

[1] On the same device and for the same image, the number of bits used for the storage of a grey value (and consequently the number of allowed grey values) is usually constant and will thus be the same for the grey values that respectively serve as lower and upper upper bound of the intervals

Also the order relation $\ll_{L^I}$ is extended analogously. The infimum and supremum of an arbitrary subset S of $L^I_{r,s} \cup G_{r,s}$ are then respectively given by:

$$\inf S = [\inf_{x\in S} x_1, \inf_{x\in S} x_2] = [\min_{x\in S} x_1, \min_{x\in S} x_2], \tag{9.24}$$

$$\sup S = [\sup_{x\in S} x_1, \sup_{x\in S} x_2] = [\max_{x\in S} x_1, \max_{x\in S} x_2]. \tag{9.25}$$

We can now formulate the following lemma that resembles Lemma 9.1.12, but does differ from it.

Lemma 9.2.6. *Let $A \in \mathcal{F}_{\mathcal{L}^I_{r,s}}(\mathbb{Z}^n)$, then it holds $\forall x \in \mathbb{Z}^n$ that:*

$$A(x) = [\max\{\alpha_1 \mid (\exists \alpha_2 \in [\alpha_1, 1[)([\alpha_1,\alpha_2] \in (L^I_{r,s} \setminus U_{L^I}) \cup G_{r,s} \text{ and } A_1(x) > \alpha_1 \text{ and } A_2(x) > \alpha_2)\}, \max\{\alpha_2 \mid (\exists \alpha_1 \in [0, \alpha_2])([\alpha_1,\alpha_2] \in (L^I_{r,s} \setminus U_{L^I}) \cup G_{r,s} \text{ and } A_1(x) > \alpha_1 \text{ and } A_2(x) > \alpha_2)\}] + [e_r, e_s].$$

Proof.

$$[\max\{\alpha_1 \mid (\exists \alpha_2 \in [\alpha_1, 1[)([\alpha_1,\alpha_2] \in (L^I_{r,s} \setminus U_{L^I}) \cup G_{r,s} \text{ and } A_1(x) > \alpha_1 \text{ and } A_2(x) > \alpha_2)\}, \max\{\alpha_2 \mid (\exists \alpha_1 \in [0, \alpha_2])([\alpha_1,\alpha_2] \in (L^I_{r,s} \setminus U_{L^I}) \cup G_{r,s} \text{ and } A_1(x) > \alpha_1 \text{ and } A_2(x) > \alpha_2)\}] = [A_1(x) - e_r, A_2(x) - e_s] = A(x) - [e_r, e_s].$$

□

As a consequence, we have to take into account the interval $[e_r, e_s]$ also for the construction of interval-valued fuzzy sets. For a decreasing family $(Q_{[\alpha_1,\alpha_2]})_{[\alpha_1,\alpha_2]\in(L^I_{r,s}\setminus U_{L^I})\cup G_{r,s}}$ of crisp subsets of $\mathbb{Z}^n$ and the interval-valued fuzzy set V in $\mathbb{Z}^n$ defined for all $x \in \mathbb{Z}^n$ as

$$V(x) = \sup\{[\alpha_1,\alpha_2] \mid [\alpha_1,\alpha_2] \in (L^I_{r,s}\setminus U_{L^I})\cup G_{r,s} \text{ and } x \in Q_{[\alpha_1,\alpha_2]}\} + [e_r, e_s], \tag{9.26}$$

we might now wonder whether it holds that $(\forall [\alpha_1,\alpha_2] \in L^I_{r,s} \setminus U_{L^I})(V^{\overline{\alpha_2}}_{\overline{\alpha_1}} = Q_{[\alpha_1,\alpha_2]})$. Remark that nonetheless the fact that V is for all $x \in \mathbb{Z}^n$ constructed as the supremum of a set in $(L^I_{r,s} \setminus U_{L^I}) \cup G_{r,s}$, $V(x)$ will always belong $L^I_{r,s}$.

In contrast to the continuous case, the inclusion $Q_{[\beta_1,\beta_2]} \subseteq V^{\overline{\beta_2}}_{\overline{\beta_1}}$ always holds.

Proposition 9.2.7. *For a decreasing family $(Q_{[\alpha_1,\alpha_2]})_{[\alpha_1,\alpha_2]\in(L^I_{r,s}\setminus U_{L^I})\cup G_{r,s}}$ of crisp subsets of $\mathbb{Z}^n$ and the interval-valued fuzzy set V defined in (9.26), it holds that:*

$$(\forall [\alpha_1,\alpha_2] \in L^I_{r,s} \setminus U_{L^I})(Q_{[\alpha_1,\alpha_2]} \subseteq V^{\overline{\alpha_2}}_{\overline{\alpha_1}}).$$

Proof. Let $[\beta_1,\beta_2] \in L^I_{r,s} \setminus U_{L^I}$ and let $x \in Q_{[\beta_1,\beta_2]}$. It then holds that:

$$x \in Q_{[\beta_1,\beta_2]}$$

$$\begin{aligned}
&\Leftrightarrow \quad [\beta_1,\beta_2] \in \{[\alpha_1,\alpha_2] \mid [\alpha_1,\alpha_2] \in (L^I_{r,s} \setminus U_{L^I}) \cup G_{r,s} \text{ and } x \in Q_{[\alpha_1,\alpha_2]}\}\\
&\Rightarrow \quad \sup\{[\alpha_1,\alpha_2] \mid [\alpha_1,\alpha_2] \in (L^I_{r,s} \setminus U_{L^I}) \cup G_{r,s} \text{ and } x \in Q_{[\alpha_1,\alpha_2]}\} + [e_r,e_s]\\
&\qquad\qquad\qquad\qquad\qquad\qquad\qquad\qquad\qquad\qquad \gg_{L^I} [\beta_1,\beta_2]\\
&\Leftrightarrow \quad V(x) \gg_{L^I} [\beta_1,\beta_2]\\
&\Leftrightarrow \quad x \in V^{\overline{\beta_2}}_{\beta_1}.
\end{aligned}$$

As a consequence, $Q_{[\beta_1,\beta_2]} \subseteq V^{\overline{\beta_2}}_{\beta_1}$. □

The following lemma gives us a condition such that the reverse inclusion would also hold.

Lemma 9.2.8. *For a decreasing family $(Q_{[\alpha_1,\alpha_2]})_{[\alpha_1,\alpha_2]\in(L^I_{r,s}\setminus U_{L^I})\cup G_{r,s}}$ of crisp subsets of $\mathbb{Z}^n$, it holds that*

$$\begin{gathered}
(\forall [\alpha_1,\alpha_2] \in (L^I_{r,s} \setminus U_{L^I}) \cup G_{r,s})(\forall x \in \mathbb{Z}^n)\\
([\alpha_1,\alpha_2] \in \{[\beta_1,\beta_2] \mid [\beta_1,\beta_2] \in (L^I_{r,s} \setminus U_{L^I}) \cup G_{r,s} \textit{ and } x \in Q_{[\beta_1,\beta_2]}\} \Leftrightarrow\\
\sup\{[\beta_1,\beta_2] \mid [\beta_1,\beta_2] \in (L^I_{r,s} \setminus U_{L^I}) \cup G_{r,s} \textit{ and } x \in Q_{[\beta_1,\beta_2]}\} \geq_{L^I} [\alpha_1,\alpha_2])\\
\Updownarrow\\
[\widetilde{SC'}] : \Big(\forall [\alpha_1,\alpha_2] \in (L^I_{r,s} \setminus U_{L^I}) \cup G_{r,s}\Big)\Big(\forall x \in \mathbb{Z}^n\Big)\Big(x \notin Q_{[\alpha_1,\alpha_2]} \Rightarrow\\
\big((\forall [\beta_1,\beta_2] \in (L^I_{r,s} \setminus U_{L^I}) \cup G_{r,s})((\beta_1 < \alpha_1 \textit{ and } \beta_2 \geq \alpha_2) \Rightarrow x \notin Q_{[\beta_1,\beta_2]})\big) \textit{ or}\\
\big((\forall [\beta_1,\beta_2] \in (L^I_{r,s} \setminus U_{L^I}) \cup G_{r,s})((\beta_1 \geq \alpha_1 \textit{ and } \beta_2 < \alpha_2) \Rightarrow x \notin Q_{[\beta_1,\overline{\beta_2}]})\big)\Big).
\end{gathered}$$

Proof. Analogous to the proof of Lemma 9.2.3. □

The following proposition is a straightforward consequence of the above lemma and Proposition 9.2.7.

Proposition 9.2.9. *For a decreasing family $(Q_{[\alpha_1,\alpha_2]})_{[\alpha_1,\alpha_2]\in(L^I_{r,s}\setminus U_{L^I})\cup G_{r,s}}$ of crisp subsets of $\mathbb{Z}^n$ that satisfies $[\widetilde{SC'}]$ and the interval-valued fuzzy set V defined in (9.26), it holds that:*

$$(\forall [\alpha_1,\alpha_2] \in L^I_{r,s} \setminus U_{L^I})(Q_{[\alpha_1,\alpha_2]} = V^{\overline{\alpha_2}}_{\overline{\alpha_1}}).$$

Proof. Follows from the proof of Proposition 9.2.7 and Lemma 9.2.8 since, for all $[\beta_1,\beta_2] \in L^I_{r,s} \setminus U_{L^I}$, $\sup\{[\alpha_1,\alpha_2] \mid [\alpha_1,\alpha_2] \in (L^I_{r,s} \setminus U_{L^I}) \cup G_{r,s} \text{ and } x \in Q_{[\alpha_1,\alpha_2]}\} + [e_r,e_s] \gg_{L^I} [\beta_1,\beta_2]$ implies that $\sup\{[\alpha_1,\alpha_2] \mid [\alpha_1,\alpha_2] \in (L^I_{r,s} \setminus U_{L^I}) \cup G_{r,s} \text{ and } x \in Q_{[\alpha_1,\alpha_2]}\} \geq_{L^I} [\beta_1,\beta_2]$ and thus $[\beta_1,\beta_2] \in \{[\alpha_1,\alpha_2] \mid [\alpha_1,\alpha_2] \in (L^I_{r,s} \setminus U_{L^I}) \cup G_{r,s} \text{ and } x \in Q_{[\alpha_1,\alpha_2]}\}$. □

Remark that if a decreasing family $(Q_{[\alpha_1,\alpha_2]})_{[\alpha_1,\alpha_2]\in(L^I_{r,s}\setminus U_{L^I})\cup G_{r,s}}$ of crisp subsets of $\mathbb{Z}^n$ does not fulfil $[\widetilde{SC'}]$, then it will also not hold that $(\forall[\alpha_1,\alpha_2]\in L^I_{r,s}\setminus U_{L^I})(Q_{[\alpha_1,\alpha_2]} = V^{\overline{\alpha_2}}_{\overline{\alpha_1}})$. Indeed, if $[\widetilde{SC'}]$ does not hold, then $(\exists[\alpha_1,\alpha_2]\in(L^I_{r,s}\setminus U_{L^I})\cup G_{r,s})(\exists x\in\mathbb{Z}^n)(x\notin Q_{[\alpha_1,\alpha_2]}$ and $(\exists[\beta_1,\beta_2]\in(L^I_{r,s}\setminus U_{L^I})\cup G_{r,s})(\beta_1<\alpha_1$ and $\beta_2\geq\alpha_2$ and $x\in Q_{[\beta_1,\beta_2]})$ and $(\exists[\gamma_1,\gamma_2]\in(L^I_{r,s}\setminus U_{L^I})\cup G_{r,s})(\gamma_1\geq\alpha_1$ and $\gamma_2<\alpha_2$ and $x\in Q_{[\gamma_1,\gamma_2]}))$. This would mean that $V_1(x)\geq\gamma_1+e_r>\alpha_1$ and $V_2(x)\geq\beta_2+e_s>\alpha_2$. Since $\gamma_2<\alpha_2$ and $\beta_1<\alpha_1$, $[\alpha_1,\alpha_2]\notin G_{r,s}$, but $[\alpha_1,\alpha_2]\in L^I_{r,s}$. As a consequence, $x\in V^{\overline{\alpha_2}}_{\overline{\alpha_1}}$ and $x\notin Q_{[\alpha_1,\alpha_2]}$.

For the construction of the interval-valued fuzzy dilation by strict $[\alpha_1,\alpha_2]$-cuts, we find a stronger result in the discrete case than in the continuous case. We first need to extend the definition of strict $[\alpha_1,\alpha_2]$-cuts from $(L^I_{r,s}\setminus U_{L^I})$ to $(L^I_{r,s}\setminus U_{L^I})\cup G_{r,s}$ as follows. For $A\in\mathcal{F}_{\mathcal{L}^I_{r,s}}(\mathbb{Z}^n)$ and $[\alpha_1,\alpha_2]\in G_{r,s}$,

$$A^{\overline{\alpha_2}}_{\overline{\alpha_1}} = \begin{cases} \mathbb{Z}^n & \alpha_1=-e_r \text{ and } \alpha_2=-e_s \\ A^{\overline{\alpha_2}} & \alpha_1=-e_r \text{ and } \alpha_2\neq -e_s \end{cases}.$$

We define $\widetilde{D(A,B)}'$ for all $x\in\mathbb{Z}^n$ as

$$\widetilde{D(A,B)}'(x) = \sup\{[\alpha_1,\alpha_2] \mid [\alpha_1,\alpha_2]\in(L^I_{r,s}\setminus U_{L^I})\cup G_{r,s} \text{ and } x\in D(A^{\overline{\alpha_2}}_{\overline{\alpha_1}}, B^{\overline{\alpha_2}}_{\overline{\alpha_1}})\} + [e_r,e_s].$$

Remark that $\widetilde{D(A,B)}'(x)\in L^I_{r,s}$ for all $x\in\mathbb{Z}^n$.

The following proposition states that the above constructed dilation $\widetilde{D(A,B)}'$ equals the dilation $D^I_{\mathcal{C}_{\min}}$.

Proposition 9.2.10. *Let $A,B\in\mathcal{F}_{\mathcal{L}^I_{r,s}}(\mathbb{Z}^n)$, then for all $y\in\mathbb{Z}^n$ it holds that:*

$$\widetilde{D(A,B)}'(y) = \sup_{x\in T_y(d_B)\cap d_A} \mathcal{C}_{\min}(B(x-y),A(x)) = D^I_{\mathcal{C}_{\min}}(A,B)(y).$$

Proof. Let $A,B\in\mathcal{F}_{\mathcal{L}^I_{r,s}}(\mathbb{Z}^n)$, and let $y\in\mathbb{Z}^n$. It holds that:

$$\begin{aligned}
\widetilde{D(A,B)}'(y) &= \sup\{[\alpha_1,\alpha_2] \mid [\alpha_1,\alpha_2]\in(L^I_{r,s}\setminus U_{L^I})\cup G_{r,s} \text{ and } \\
&\qquad y\in D(A^{\overline{\alpha_2}}_{\overline{\alpha_1}}, B^{\overline{\alpha_2}}_{\overline{\alpha_1}})\} + [e_r,e_s] \\
&= \sup\{[\alpha_1,\alpha_2] \mid [\alpha_1,\alpha_2]\in(L^I_{r,s}\setminus U_{L^I})\cup G_{r,s} \text{ and } \\
&\qquad T_y(B^{\overline{\alpha_2}}_{\overline{\alpha_1}})\cap A^{\overline{\alpha_2}}_{\overline{\alpha_1}}\neq\emptyset\} + [e_r,e_s] \\
&= \sup\{[\alpha_1,\alpha_2] \mid [\alpha_1,\alpha_2]\in(L^I_{r,s}\setminus U_{L^I})\cup G_{r,s} \text{ and } \\
&\qquad (\exists x\in T_y(d_B)\cap d_A)(x\in T_y(B^{\overline{\alpha_2}}_{\overline{\alpha_1}}) \text{ and } x\in A^{\overline{\alpha_2}}_{\overline{\alpha_1}})\} + [e_r,e_s]
\end{aligned}$$

$$
\begin{aligned}
&= \sup\{[\alpha_1,\alpha_2] \mid [\alpha_1,\alpha_2] \in (L^I_{r,s} \setminus U_{L^I}) \cup G_{r,s} \text{ and} \\
&\qquad (\exists x \in T_y(d_B) \cap d_A)((B_1(x-y) > \alpha_1 \text{ and } A_1(x) > \alpha_1) \text{ and} \\
&\qquad\qquad (B_2(x-y) > \alpha_2 \text{ and } A_2(x) > \alpha_2))\} + [e_r, e_s] \\
&= \sup\{[\alpha_1,\alpha_2] \mid [\alpha_1,\alpha_2] \in (L^I_{r,s} \setminus U_{L^I}) \cup G_{r,s} \text{ and} \\
&\qquad (\exists x \in T_y(d_B) \cap d_A)(\mathcal{C}_{\min}(B(x-y), A(x)) \gg_{L^I} [\alpha_1,\alpha_2])\} \\
&\qquad\qquad + [e_r, e_s] \\
&\equiv (*).
\end{aligned}
$$

We have to prove that $(*)$ is equal to

$$\sup\{\mathcal{C}_{\min}(B(x-y), A(x)) \mid x \in T_y(d_B) \cap d_A\} \equiv (**).$$

It holds that:

$$
\begin{aligned}
(*) \quad &= \quad \sup\{[\alpha_1,\alpha_2] \mid [\alpha_1,\alpha_2] \in (L^I_{r,s} \setminus U_{L^I}) \cup G_{r,s} \text{ and } (\exists x \in T_y(d_B) \cap d_A) \\
&\qquad\qquad ([\alpha_1,\alpha_2] \ll_{L^I} \mathcal{C}_{\min}(B(x-y), A(x)))\} + [e_r, e_s] \\
&\leq_{L^I} \quad \sup\{[\alpha_1,\alpha_2] \mid [\alpha_1,\alpha_2] \in (L^I_{r,s} \setminus U_{L^I}) \cup G_{r,s} \text{ and} \\
&\qquad\qquad ([\alpha_1,\alpha_2] \ll_{L^I} \sup_{x \in T_y(d_B) \cap d_A} \mathcal{C}_{\min}(B(x-y), A(x)))\} + [e_r, e_s] \\
&= \quad (\sup_{x \in T_y(d_B) \cap d_A} \mathcal{C}_{\min}(B(x-y), A(x))) - [e_r, e_s]) + [e_r, e_s] \\
&= \quad (**)
\end{aligned}
$$

The proof of $(**) \leq (*)$ however is much simpler in the discrete framework, since we don't have to make use of the characterization of the supremum. If $T_y(d_B) \cap d_A = \emptyset$, then $(**) = 0_{\mathcal{L}^I}$ and thus $(**) \leq_{L^I} (*)$. Otherwise, in the discrete case, it immediately follows from $(**) = \sup_{x \in T_y(d_B) \cap d_A} \mathcal{C}_{\min}(B(x-y), A(x)))$ that

$$
\begin{aligned}
&(**)_1 \in \{\alpha_1 \mid (\exists \alpha_2 \in [\alpha_1, 1])([\alpha_1,\alpha_2] \in (L^I_{r,s} \setminus U_{L^I}) \cup G_{r,s} \text{ and} \\
&(\exists x \in T_y(d_B) \cap d_A)([\alpha_1,\alpha_2] \leq_{L^I} \mathcal{C}_{\min}(B(x-y), A(x))))\} \text{ and} \\
&(**)_2 \in \{\alpha_2 \mid (\exists \alpha_1 \in [0, \alpha_2])([\alpha_1,\alpha_2] \in (L^I_{r,s} \setminus U_{L^I}) \cup G_{r,s} \text{ and} \\
&(\exists x \in T_y(d_B) \cap d_A)([\alpha_1,\alpha_2] \leq_{L^I} \mathcal{C}_{\min}(B(x-y), A(x))))\} \\
\Rightarrow \quad &(**)_1 \in \{\alpha_1 \mid (\exists \alpha_2 \in [\alpha_1, 1])([\alpha_1,\alpha_2] \in (L^I_{r,s} \setminus U_{L^I}) \cup G_{r,s} \text{ and} \\
&(\exists x \in T_y(d_B) \cap d_A)([\alpha_1,\alpha_2] \ll_{L^I} \mathcal{C}_{\min}(B(x-y), A(x)) + [e_r, e_s]))\} \text{ and} \\
&(**)_2 \in \{\alpha_2 \mid (\exists \alpha_1 \in [0, \alpha_2])([\alpha_1,\alpha_2] \in (L^I_{r,s} \setminus U_{L^I}) \cup G_{r,s} \text{ and} \\
&(\exists x \in T_y(d_B) \cap d_A)([\alpha_1,\alpha_2] \ll_{L^I} \mathcal{C}_{\min}(B(x-y), A(x)) + [e_r, e_s]))\} \\
\Rightarrow \quad &[(**)_1, (**)_2] \leq_{L^I} \sup\{[\alpha_1,\alpha_2] \mid [\alpha_1,\alpha_2] \in (L^I_{r,s} \setminus U_{L^I}) \cup G_{r,s} \text{ and} \\
&(\exists x \in T_y(d_B) \cap d_A)([\alpha_1,\alpha_2] \ll_{L^I} \mathcal{C}_{\min}(B(x-y), A(x)) + [e_r, e_s])\} \\
\Rightarrow \quad &[(**)_1, (**)_2] \leq_{L^I} \sup\{[\alpha_1,\alpha_2] \mid [\alpha_1,\alpha_2] \in (L^I_{r,s} \setminus U_{L^I}) \cup G_{r,s} \text{ and}
\end{aligned}
$$

$$(\exists x \in T_y(d_B) \cap d_A)([\alpha_1, \alpha_2] \ll_{L^I} \mathcal{C}_{\min}(B(x-y), A(x)))\} + [e_r, e_s] = (*).$$

□

Analogously to the continuous case we find the following construction of the interval-valued fuzzy erosion $E^I_{\mathcal{I}_{EKD}}$. For all $y \in \mathbb{Z}^n$,

$$E^I_{\mathcal{I}_{EKD}}(A,B)(y) = \mathcal{N}_s\Big(\sup_{[\alpha_1,\alpha_2]\in(L^I_{r,s}\setminus U_{L^I})\cup G_{r,s}} ([\alpha_1,\alpha_2]co(E(co((co_{\mathcal{N}_s}A)^{\overline{\alpha_2}}_{\overline{\alpha_1}}), B^{\overline{\alpha_2}}_{\overline{\alpha_1}})))(y) + [e_r, e_s]\Big).$$

The interval-valued fuzzy opening and closing can then be constructed as a combination of the interval-valued fuzzy dilation and erosion.

9.2.3 Construction Based on Weak-Strict and Strict-Weak $[\alpha_1, \alpha_2]$-cuts

The following lemma for strict-weak $[\alpha_1, \alpha_2]$-cuts resembles Lemma 9.1.24, but does differ from it. The notation $H_{r,s}$ stands for the set $H_{r,s} = \{[\alpha_1, \alpha_2] \mid \alpha_1 = -e_r \text{ and } \alpha_2 \in I_s\}$. Remark that $H_{r,s} \cap L^I_{r,s} = \emptyset$. We further also extend the order relation $\leq_{L^I}$ on $L^I_{r,s}$ to $H_{r,s} \cup L^I_{r,s}$ in a straightforward manner and for this reason, we will use the same notation $\leq_{L^I}$:

$$x \leq_{L^I} y \Leftrightarrow x_1 \leq y_1 \text{ and } x_2 \leq y_2,\ \forall x, y \in L^I_{r,s} \cup H_{r,s}. \tag{9.27}$$

Also the order relation $\ll_{L^I}$ is extended analogously. The infimum and supremum of an arbitrary subset S of $L^I_{r,s} \cup H_{r,s}$ are then respectively given by:

$$\inf S = [\inf_{x\in S} x_1, \inf_{x\in S} x_2] = [\min_{x\in S} x_1, \min_{x\in S} x_2], \tag{9.28}$$

$$\sup S = [\sup_{x\in S} x_1, \sup_{x\in S} x_2] = [\max_{x\in S} x_1, \max_{x\in S} x_2]. \tag{9.29}$$

Lemma 9.2.11. *Let $A \in \mathcal{F}_{\mathcal{L}^I_{r,s}}(\mathbb{Z}^n)$, then it holds $\forall x \in \mathbb{Z}^n$ that:*

$$A(x) = [\max\{\alpha_1 \mid (\exists \alpha_2 \in I_s)([\alpha_1,\alpha_2] \in (L^I_{r,s} \setminus \{1_{\mathcal{L}^I}\}) \cup H_{r,s} \textit{ and } A_1(x) > \alpha_1 \textit{ and } A_2(x) \geq \alpha_2)\} + e_r, \max\{\alpha_2 \mid (\exists \alpha_1 \in (I_r \setminus \{1\}) \cup \{-e_r\}) ([\alpha_1,\alpha_2] \in (L^I_{r,s} \setminus \{1_{\mathcal{L}^I}\}) \cup H_{r,s} \textit{ and } A_1(x) > \alpha_1 \textit{ and } A_2(x) \geq \alpha_2)\}].$$

Proof.
The result follows from the fact that

$$\max\{\alpha_1 \mid (\exists \alpha_2 \in I_s)([\alpha_1,\alpha_2] \in (L^I_{r,s} \setminus \{1_{\mathcal{L}^I}\}) \cup H_{r,s} \text{ and } A_1(x) > \alpha_1 \text{ and } A_2(x) \geq \alpha_2)\} = A_1(x) - e_r,$$

and

$$\max\{\alpha_2 \mid (\exists \alpha_1 \in (I_r \setminus \{1\}) \cup \{-e_r\})([\alpha_1, \alpha_2] \in (L^I_{r,s} \setminus \{1_{\mathcal{L}^I}\}) \cup H_{r,s} \text{ and } A_1(x) > \alpha_1 \text{ and } A_2(x) \geq \alpha_2)\} = A_2(x).$$

□

For the weak-strict $[\alpha_1, \alpha_2]$-cuts, an analogous result exists if we extend the set $L^I_{r,s}$ to the set $\widetilde{L^I_{r,s}}$, of which the elements don't need to be intervals. Because of the similarity to the set $L^I_{r,s}$, we will nonetheless use the interval notation: $\widetilde{L^I_{r,s}} = \{[\alpha_1, \alpha_2] \mid \alpha_1 \in I_r,\ \alpha_2 \in I_s \cup \{-e_s\} \text{ and } \alpha_2 + e_s \geq \alpha_1\}$. We further also extend the order relation $\leq_{L^I}$ on $L^I_{r,s}$ to $\widetilde{L^I_{r,s}}$ in a straightforward manner and for this reason, we will use the same notation $\leq_{L^I}$:

$$x \leq_{L^I} y \Leftrightarrow x_1 \leq y_1 \text{ and } x_2 \leq y_2,\ \forall x, y \in \widetilde{L^I_{r,s}}. \tag{9.30}$$

Also the order relation $\ll_{L^I}$ is extended analogously. The infimum and supremum of an arbitrary subset S of $L^I_{r,s} \cup H_{r,s}$ are then respectively given by:

$$\inf S = [\inf_{x \in S} x_1, \inf_{x \in S} x_2] = [\min_{x \in S} x_1, \min_{x \in S} x_2], \tag{9.31}$$

$$\sup S = [\sup_{x \in S} x_1, \sup_{x \in S} x_2] = [\max_{x \in S} x_1, \max_{x \in S} x_2]. \tag{9.32}$$

Lemma 9.2.12. *Let $A \in \mathcal{F}_{\mathcal{L}^I_{r,s}}(\mathbb{Z}^n)$, then it holds $\forall x \in \mathbb{Z}^n$ that:*

$$A(x) = [\max\{\alpha_1 \mid (\exists \alpha_2 \in (I_s \setminus \{1\}) \cup \{-e_s\})([\alpha_1, \alpha_2] \in \widetilde{L^I_{r,s}} \setminus U_{L^I} \text{ and } A_1(x) \geq \alpha_1 \text{ and } A_2(x) > \alpha_2)\}, \max\{\alpha_2 \mid (\exists \alpha_1 \in I_r)([\alpha_1, \alpha_2] \in \widetilde{L^I_{r,s}} \setminus U_{L^I} \text{ and } A_1(x) \geq \alpha_1 \text{ and } A_2(x) > \alpha_2))\} + e_s].$$

Proof.
Analogous to the proof of Lemma 9.2.11. □

For given families $(M_{[\alpha_1,\alpha_2]})_{[\alpha_1,\alpha_2] \in (\widetilde{L^I_{r,s}} \setminus U_{L^I})}$ and $(N_{[\alpha_1,\alpha_2]})_{[\alpha_1,\alpha_2] \in (L^I_{r,s} \setminus \{1_{\mathcal{L}^I}\}) \cup H_{r,s}}$ of crisp subsets of $\mathbb{Z}^n$ that are decreasing and the interval-valued fuzzy sets Y and Z in $\mathbb{Z}^n$ respectively defined for all $x \in \mathbb{Z}^n$ as

$$Y(x) = \sup\{[\alpha_1, \alpha_2] \mid [\alpha_1, \alpha_2] \in (\widetilde{L^I_{r,s}} \setminus U_{L^I}) \text{ and } x \in M_{[\alpha_1,\alpha_2]}\} + [0, e_s], \tag{9.33}$$

and

$$Z(x) = \sup\{[\alpha_1, \alpha_2] \mid [\alpha_1, \alpha_2] \in (L^I_{r,s} \setminus \{1_{\mathcal{L}^I}\}) \cup H_{r,s} \text{ and } x \in N_{[\alpha_1,\alpha_2]}\} + [e_r, 0], \tag{9.34}$$

we might now wonder whether it holds that $(\forall [\alpha_1, \alpha_2] \in L^I_{r,s} \setminus U_{L^I})(Y^{\overline{\alpha_2}}_{\alpha_1} = M_{[\alpha_1,\alpha_2]})$, respectively whether it holds that $(\forall [\alpha_1, \alpha_2] \in L^I_{r,s} \setminus \{1_{\mathcal{L}^I}\})(Z^{\alpha_2}_{\overline{\alpha_1}} = N_{[\alpha_1,\alpha_2]})$. Remark

that nonetheless the fact that Y and Z are for all $x \in \mathbb{Z}^n$ constructed as the supremum of a set in $\widetilde{L^I_{r,s}} \setminus U_{L^I}$ and $(L^I_{r,s} \setminus \{1_{\mathcal{L}^I}\}) \cup H_{r,s}$ respectively, $Y(x)$ and $Z(x)$ will always belong $L^I_{r,s}$.

In contrast to the continuous case, the inclusions $M_{[\alpha_1,\alpha_2]} \subseteq Y^{\overline{\alpha_2}}_{\alpha_1}$ and $N_{[\alpha_1,\alpha_2]} \subseteq Z^{\alpha_2}_{\overline{\alpha_1}}$ always hold.

Proposition 9.2.13.

(i) For a decreasing family $(M_{[\alpha_1,\alpha_2]})_{[\alpha_1,\alpha_2]\in(\widetilde{L^I_{r,s}}\setminus U_{L^I})}$ of crisp subsets of $\mathbb{Z}^n$ and the interval-valued fuzzy set Y defined in (9.33), it holds that:

$$(\forall[\alpha_1,\alpha_2] \in L^I_{r,s} \setminus U_{L^I})(M_{[\alpha_1,\alpha_2]} \subseteq Y^{\overline{\alpha_2}}_{\alpha_1}).$$

(ii) For a decreasing family $(N_{[\alpha_1,\alpha_2]})_{[\alpha_1,\alpha_2]\in(L^I_{r,s}\setminus\{1_{\mathcal{L}^I}\})\cup H_{r,s}}$ of crisp subsets of $\mathbb{Z}^n$ and the interval-valued fuzzy set Z defined in (9.34), it holds that:

$$(\forall[\alpha_1,\alpha_2] \in L^I_{r,s} \setminus \{1_{\mathcal{L}^I}\})(N_{[\alpha_1,\alpha_2]} \subseteq Z^{\alpha_2}_{\overline{\alpha_1}}).$$

Proof.

(i) Let $[\beta_1,\beta_2] \in L^I_{r,s} \setminus U_{L^I}$ and let $x \in M_{[\beta_1,\beta_2]}$. It then holds that:

$$\begin{aligned}
& x \in M_{[\beta_1,\beta_2]} \\
\Leftrightarrow\ & [\beta_1,\beta_2] \in \{[\alpha_1,\alpha_2] \mid [\alpha_1,\alpha_2] \in (\widetilde{L^I_{r,s}} \setminus U_{L^I}) \text{ and } x \in M_{[\alpha_1,\alpha_2]}\} \\
\Rightarrow\ & (\sup\{[\alpha_1,\alpha_2] \mid [\alpha_1,\alpha_2] \in (\widetilde{L^I_{r,s}} \setminus U_{L^I}) \text{ and } x \in M_{[\alpha_1,\alpha_2]}\})_1 \geq \beta_1 \text{ and} \\
& (\sup\{[\alpha_1,\alpha_2] \mid [\alpha_1,\alpha_2] \in (\widetilde{L^I_{r,s}} \setminus U_{L^I}) \text{ and } x \in M_{[\alpha_1,\alpha_2]}\})_2 + e_s > \beta_2 \\
\Leftrightarrow\ & Y_1(x) \geq \beta_1 \text{ and } Y_2(x) > \beta_2 \\
\Leftrightarrow\ & x \in Y^{\overline{\beta_2}}_{\beta_1}.
\end{aligned}$$

As a consequence, $M_{[\beta_1,\beta_2]} \subseteq Y^{\overline{\beta_2}}_{\beta_1}$.

(ii) Analogously.

□

The following lemmata give us a condition such that the reverse inclusion would also hold.

Lemma 9.2.14. *For a decreasing family $(M_{[\alpha_1,\alpha_2]})_{[\alpha_1,\alpha_2]\in(\widetilde{L^I_{r,s}}\setminus U_{L^I})}$ of crisp subsets of $\mathbb{Z}^n$, it holds that*

$$\begin{gathered}
(\forall[\alpha_1,\alpha_2] \in (\widetilde{L^I_{r,s}} \setminus U_{L^I}))(\forall x \in \mathbb{Z}^n) \\
([\alpha_1,\alpha_2] \in \{[\beta_1,\beta_2] \mid [\beta_1,\beta_2] \in (\widetilde{L^I_{r,s}} \setminus U_{L^I}) \textit{ and } x \in M_{[\beta_1,\beta_2]}\} \Leftrightarrow \\
\sup\{[\beta_1,\beta_2] \mid [\beta_1,\beta_2] \in (\widetilde{L^I_{r,s}} \setminus U_{L^I}) \textit{ and } x \in M_{[\beta_1,\beta_2]}\} \geq_{L^I} [\alpha_1,\alpha_2])
\end{gathered}$$

$$\Updownarrow$$

$$[\widetilde{SC''a}] : \Big(\forall[\alpha_1,\alpha_2] \in ((\widetilde{L^I_{r,s}} \setminus U_{L^I})\Big)\Big(\forall x \in \mathbb{Z}^n\Big)\Big(x \notin M_{[\alpha_1,\alpha_2]} \Rightarrow$$
$$\big((\forall[\beta_1,\beta_2] \in (\widetilde{L^I_{r,s}} \setminus U_{L^I}))((\beta_1 < \alpha_1 \text{ and } \beta_2 \geq \alpha_2) \Rightarrow x \notin M_{[\beta_1,\beta_2]})\big) \text{ or}$$
$$\big((\forall[\beta_1,\beta_2] \in (\widetilde{L^I_{r,s}} \setminus U_{L^I}))((\beta_1 \geq \alpha_1 \text{ and } \beta_2 < \alpha_2) \Rightarrow x \notin M_{[\beta_1,\beta_2]})\big)\Big).$$

Proof. Analogous to the proof of Lemma 9.2.3. □

Lemma 9.2.15. *For a decreasing family $(N_{[\alpha_1,\alpha_2]})_{[\alpha_1,\alpha_2]\in(L^I_{r,s}\setminus\{1_{\mathcal{L}^I}\})\cup H_{r,s}}$ of crisp subsets of $\mathbb{Z}^n$, it holds that*

$$(\forall[\alpha_1,\alpha_2] \in (L^I_{r,s} \setminus \{1_{\mathcal{L}^I}\}) \cup H_{r,s})(\forall x \in \mathbb{Z}^n)$$
$$([\alpha_1,\alpha_2] \in \{[\beta_1,\beta_2] \mid [\beta_1,\beta_2] \in (L^I_{r,s} \setminus \{1_{\mathcal{L}^I}\}) \cup H_{r,s} \text{ and } x \in N_{[\beta_1,\beta_2]}\} \Leftrightarrow$$
$$\sup\{[\beta_1,\beta_2] \mid [\beta_1,\beta_2] \in (L^I_{r,s} \setminus \{1_{\mathcal{L}^I}\}) \cup H_{r,s} \text{ and } x \in N_{[\beta_1,\beta_2]}\} \geq_{L^I} [\alpha_1,\alpha_2])$$
$$\Updownarrow$$
$$[\widetilde{SC''b}] : \Big(\forall[\alpha_1,\alpha_2] \in (L^I_{r,s} \setminus \{1_{\mathcal{L}^I}\}) \cup H_{r,s}\Big)\Big(\forall x \in \mathbb{Z}^n\Big)\Big(x \notin N_{[\alpha_1,\alpha_2]} \Rightarrow$$
$$\big((\forall[\beta_1,\beta_2] \in (L^I_{r,s} \setminus \{1_{\mathcal{L}^I}\}) \cup H_{r,s})((\beta_1 < \alpha_1 \text{ and } \beta_2 \geq \alpha_2) \Rightarrow x \notin N_{[\beta_1,\beta_2]})\big) \text{ or}$$
$$\big((\forall[\beta_1,\beta_2] \in (L^I_{r,s} \setminus \{1_{\mathcal{L}^I}\}) \cup H_{r,s})((\beta_1 \geq \alpha_1 \text{ and } \beta_2 < \alpha_2) \Rightarrow x \notin N_{[\beta_1,\beta_2]})\big)\Big).$$

Proof. Analogous to the proof of Lemma 9.2.3. □

The following proposition is a straightforward consequence of the above lemmata and Proposition 9.2.13.

Proposition 9.2.16.

(i) For a decreasing family $(M_{[\alpha_1,\alpha_2]})_{[\alpha_1,\alpha_2]\in(\widetilde{L^I_{r,s}}\setminus U_{L^I})}$ of crisp subsets of $\mathbb{Z}^n$ that satisfies $[SC''a]$ and the interval-valued fuzzy set Y defined in (9.33), it holds that:

$$(\forall[\alpha_1,\alpha_2] \in L^I_{r,s} \setminus U_{L^I})(M_{[\alpha_1,\alpha_2]} = Y^{\overline{\alpha_2}}_{\alpha_1}).$$

(ii) For a decreasing family $(N_{[\alpha_1,\alpha_2]})_{[\alpha_1,\alpha_2]\in(L^I_{r,s}\setminus\{1_{\mathcal{L}^I}\})\cup H_{r,s}}$ of crisp subsets of $\mathbb{Z}^n$ that satisfies $[SC''b]$ and the interval-valued fuzzy set Z defined in (9.34), it holds that:

$$(\forall[\alpha_1,\alpha_2] \in L^I_{r,s} \setminus \{1_{\mathcal{L}^I}\})(N_{[\alpha_1,\alpha_2]} = Z^{\alpha_2}_{\overline{\alpha_1}}).$$

Proof.

(i) Follows from the proof of Proposition 9.2.13 and Lemma 9.2.14 since it follows for all $[\beta_1,\beta_2] \in \widetilde{L^I_{r,s}} \setminus U_{L^I}$ from $(\sup\{[\alpha_1,\alpha_2] \mid [\alpha_1,\alpha_2] \in (\widetilde{L^I_{r,s}} \setminus U_{L^I}) \text{ and } x \in M_{[\alpha_1,\alpha_2]}\})_1 \geq \beta_1$ and $(\sup\{[\alpha_1,\alpha_2] \in (\widetilde{L^I_{r,s}} \setminus U_{L^I}) \mid x \in M_{[\alpha_1,\alpha_2]}\})_2 + e_s > \beta_2$

that $\sup\{[\alpha_1,\alpha_2] \mid [\alpha_1,\alpha_2] \in (\widetilde{L^I_{r,s}} \setminus U_{L^I}) \text{ and } x \in M_{[\alpha_1,\alpha_2]}\} \geq_{L^I} [\beta_1,\beta_2]$ and thus $[\beta_1,\beta_2] \in \{[\alpha_1,\alpha_2] \mid [\alpha_1,\alpha_2] \in (\widetilde{L^I_{r,s}} \setminus U_{L^I}) \text{ and } x \in M_{[\alpha_1,\alpha_2]}\}$.

(ii) Follows analogously from the proof of Proposition 9.2.13 and Lemma 9.2.15

□

Remark that if a decreasing family $(M_{[\alpha_1,\alpha_2]})_{[\alpha_1,\alpha_2]\in\widetilde{L^I_{r,s}}\setminus U_{L^I}}$ of crisp subsets of $\mathbb{Z}^n$ does not fulfil $[\widetilde{SC''a}]$, then it will also not hold that $(\forall[\alpha_1,\alpha_2] \in L^I_{r,s} \setminus U_{L^I})(M_{[\alpha_1,\alpha_2]} = Y^{\overline{\alpha_2}}_{\alpha_1})$. Indeed, if $[\widetilde{SC''a}]$ does not hold, then $(\exists[\alpha_1,\alpha_2] \in \widetilde{L^I_{r,s}} \setminus U_{L^I})(\exists x \in \mathbb{Z}^n)(x \notin M_{[\alpha_1,\alpha_2]}$ and $(\exists[\beta_1,\beta_2] \in \widetilde{L^I_{r,s}} \setminus U_{L^I})(\beta_1 < \alpha_1$ and $\beta_2 \geq \alpha_2$ and $x \in M_{[\beta_1,\beta_2]})$ and $(\exists[\gamma_1,\gamma_2] \in \widetilde{L^I_{r,s}} \setminus U_{L^I})(\gamma_1 \geq \alpha_1$ and $\gamma_2 < \alpha_2$ and $x \in M_{[\gamma_1,\gamma_2]}))$. This would mean that $Y_1(x) \geq \gamma_1 \geq \alpha_1$ and $Y_2(x) \geq \beta_2 + e_s > \alpha_2$. Since $\gamma_1 \geq \alpha_1$ and $\gamma_2 < \alpha_2$, it follows that $\alpha_1 \leq \gamma_1 \leq \gamma_2 + e_s \leq \alpha_2$ and thus $[\alpha_1,\alpha_2] \in L^I_{r,s}$. As a consequence, $x \in Y^{\overline{\alpha_2}}_{\alpha_1}$ and $x \notin M_{[\alpha_1,\alpha_2]}$.

An analogous remark holds for strict-weak $[\alpha_1,\alpha_2]$-cuts and condition $[\widetilde{SC''b}]$.

For the construction of the interval-valued fuzzy dilation by weak-strict $[\alpha_1,\alpha_2]$-cuts, we first need to extend the definition of weak-strict $[\alpha_1,\alpha_2]$-cuts from $(L^I_{r,s} \setminus U_{L^I})$ to $(\widetilde{L^I_{r,s}} \setminus U_{L^I})$. For $A \in \mathcal{F}_{\mathcal{L}^I_{r,s}}(\mathbb{Z}^n)$ and $[\alpha_1,\alpha_2] \in \widetilde{L^I_{r,s}} \setminus U_{L^I}$,

$$A^{\overline{\alpha_2}}_{\alpha_1} = \{x \mid x \in \mathbb{Z}^n, A_1(x) \geq \alpha_1 \text{ and } A_2(x) > \alpha_2\}.$$

The dilation $\widetilde{D(A,B)}''$ is then for all $x \in \mathbb{Z}^n$ defined as

$$\widetilde{D(A,B)}''(x) = \sup\{[\alpha_1,\alpha_2] \mid [\alpha_1,\alpha_2] \in (\widetilde{L^I_{r,s}} \setminus U_{L^I}) \text{ and } x \in D(A^{\overline{\alpha_2}}_{\alpha_1}, B^{\overline{\alpha_2}}_{\alpha_1})\} + [0,e_s].$$

For the construction by strict-weak $[\alpha_1,\alpha_2]$-cuts, we need to extend the definition from $(L^I_{r,s} \setminus \{1_{\mathcal{L}^I}\})$ to $(L^I_{r,s} \setminus \{1_{\mathcal{L}^I}\}) \cup H_{r,s}$, as follows. For $A \in \mathcal{F}_{\mathcal{L}^I_{r,s}}(\mathbb{Z}^n)$ and $[\alpha_1,\alpha_2] \in H_{r,s}$,

$$A^{\alpha_2}_{\overline{\alpha_1}} = A^{\alpha_2} = \{x \mid x \in \mathbb{Z}^n \text{ and } A_2(x) \geq \alpha_2\}.$$

We then define $\widetilde{D(A,B)}'''$ for all $x \in \mathbb{Z}^n$ as

$$\widetilde{D(A,B)}'''(x) = \sup\{[\alpha_1,\alpha_2] \mid [\alpha_1,\alpha_2] \in (L^I_{r,s} \setminus \{1_{\mathcal{L}^I}\}) \cup H_{r,s} \text{ and } x \in D(A^{\alpha_2}_{\overline{\alpha_1}}, B^{\alpha_2}_{\overline{\alpha_1}})\} + [e_r,0].$$

Remark that $\widetilde{D(A,B)}''(x) \in L^I_{r,s}$ and $\widetilde{D(A,B)}'''(x) \in L^I_{r,s}$ for all $x \in \mathbb{Z}^n$.

The following proposition states that the above constructed dilations are equal to $D^I_{\mathcal{C}_{\min}}$. Remark that for the strict-weak $[\alpha_1,\alpha_2]$-cuts, this is a stronger result than in the continuous case.

Proposition 9.2.17. *Let $A, B \in \mathcal{F}_{\mathcal{L}^I_{r,s}}(\mathbb{Z}^n)$, then for all $y \in \mathbb{Z}^n$ it holds that:*

(i)

$$\widetilde{D(A,B)}''(y) = \sup_{x \in T_y(d_B) \cap d_A} \mathcal{C}_{\min}(B(x-y), A(x)) = D^I_{\mathcal{C}_{\min}}(A,B)(y).$$

(ii)

$$\widetilde{D(A,B)}'''(y) = \sup_{x \in T_y(d_B) \cap d_A} \mathcal{C}_{\min}(B(x-y), A(x)) = D^I_{\mathcal{C}_{\min}}(A,B)(y).$$

Proof. Analogous to the proof of Proposition 9.2.10. □

Analogously to the continuous case we find the following constructions of the interval-valued fuzzy erosion $E^I_{\mathcal{I}_{EKD}}$. For all $y \in \mathbb{Z}^n$, it holds that

$$E^I_{\mathcal{I}_{EKD}}(A,B)(y) = \mathcal{N}_s\Big(\sup_{[\alpha_1,\alpha_2] \in \widetilde{L^I_{r,s}} \setminus U_{L^I}} ([\alpha_1,\alpha_2] co(E(co((co_{\mathcal{N}_s} A)^{\overline{\alpha_2}}_{\alpha_1}), B^{\overline{\alpha_2}}_{\alpha_1})))(y) + [0, e_s]),$$

and

$$E^I_{\mathcal{I}_{EKD}}(A,B)(y) = \mathcal{N}_s\Big(\sup_{[\alpha_1,\alpha_2] \in (L^I_{r,s} \setminus \{1_{\mathcal{L}^I}\}) \cup H_{r,s}} ([\alpha_1,\alpha_2] co(E(co((co_{\mathcal{N}_s} A)^{\overline{\alpha_2}}_{\alpha_1}), B^{\overline{\alpha_2}}_{\alpha_1})))(y) + [e_r, 0]).$$

The interval-valued fuzzy opening and closing can then be constructed as a combination of the interval-valued fuzzy dilation and erosion.

9.2.4 Sub- and Supercuts

Also in the discrete framework, there is no construction principle based on weak and strict sub- and supercuts, since these sets only give information about the lower or the upper bounds of the intervals on which an interval-valued fuzzy set maps the elements of the universe.

9.3 Conclusion

In this chapter we have studied the construction of increasing interval-valued fuzzy operators from their corresponding binary counterparts in general and more in detail for the morphological operators. This construction was investigated both in the general continuous case and the practical discrete case. In the discrete case, we work with interval-valued fuzzy sets from $\mathcal{F}_{\mathcal{L}^I_{r,s}}(\mathbb{Z}^n)$ instead of $\mathcal{F}_{\mathcal{L}^I}(\mathbb{R}^n)$ since in practice, both the image domain and the range of grey values are sampled due to technical limitations. It was shown that in

both cases the constructed interval-valued fuzzy dilation corresponds to the interval-valued fuzzy dilation $D^I_{\mathcal{C}_{min}}$, that is dual to the erosion $E_{\mathcal{I}_{EKD}}$, which allows us to construct the other basic morphological operators. Further, we found out that the characterization of the supremum in the discrete case has as a consequence that some of the difficulties from the continuous case don't arise anymore. Moreover, also some stronger relationships hold in this practical case.

Conclusion

The contents of this thesis were divided into three main parts. In the first part, an introduction to fuzzy set theory and image processing was given in Chapter 1 and 2 respectively.

After this introduction, we presented several fuzzy logic based video filters in Part II. Chapter 3 and 4 concentrated on removing additive Gaussian noise from greyscale and colour image sequences respectively, while the greyscale and colour filters in respectively Chapter 5 and 6 were developed for the random impulse noise case.

The greyscale filter proposed in Chapter 3 [79, 86] can be seen as a fuzzy logic based improvement of the multiple class averaging filter (MCA) from [146, 149]. Pixels are no longer divided into discrete classes based on their absolute difference in grey value to the central window pixel, but are treated individually by introducing a fuzzy set to represent to which degree this absolute difference is large. Further, the heuristic construction of exponential functions to assign the filtering weights to the neighbourhood pixels is replaced by a more theoretically underbuilt fuzzy logic framework in which fuzzy rules, that correspond to the ideas behind the MCA filter, are used. Such fuzzy rules can easily be extended by including new information as can e.g. be seen in the second colour extension in Chapter 4. Analogously to the MCA filter, the proposed pixel domain filtering framework was extended to the wavelet domain. Contrary to the MCA filter however, we opted for an additional pixel domain time-recursive averaging instead of a filtering of the low-frequency band. The experimental results showed that the proposed pixel domain method outperforms all other compared state-of-the-art pixel domain filters in terms of PSNR and that the wavelet domain extension competes with other state-of-the-art wavelet domain filters of a comparable complexity and outperforms them on sequences obtained by a still camera. The filter is however outperformed by higher complexity methods that use motion compensation or a 3D-transform.

Additionally, in Chapter 4 the filtering framework from Chapter 3 was extended to colour videos. More precisely, we introduced two alternatives [75, 76] for the usually applied filtering of the Y-component of the YUV-transform of the frames with the original greyscale method. In the first proposed filter [75], the variables used in the filtering framework are extended from grey values to colour vectors. In this vector based approach the pixel colours are seen as vectors of which the different components should not be used separately in order to preserve the correlation between the different colour bands. The second proposed approach [76] filters each of the colour bands separately, but to exploit the corre-

lation between the different colour bands, the fuzzy rules in the filtering framework are now extended by incorporating information from the other colour bands. Both approaches are additionally also combined with a refinement of the second subfilter from [119]. From the experimental results, it could be seen that the proposed colour extensions result in a better colour and detail preservation than the YUV approach.

In Chapter 5 two greyscale video filters [77, 74, 80] for the removal of random impulse noise are introduced. Both filters consist of successive noise detection and filtering steps. In this way, details can be better preserved because not all noise needs to be filtered in one drastic denoising step that will inevitably also remove details then. On the other hand, also the remaining noise might be easier to detect if a considerable part of the noise has already been filtered in a previous step. Indeed, more reliable neighbours are available for comparison. In the noise detection steps of the first presented algorithm [80], for each pixel a degree is calculated to which it is considered noisy and all pixels that have a non-zero degree are filtered. In the successive steps of the second proposed method [77, 74], fuzzy rules containing linguistic values are used to determine both a degree to which a pixel is considered noisy and a degree to which it is considered noisefree. Pixels are now filtered if the noisy degree is larger than the noisefree degree. The filtering of detected pixels is performed in a motion compensated way. The motion compensation technique has originally been developed for video compression applications. Although it has already been adopted for the filtering of videos corrupted by additive Gaussian noise, it has not really found its way to impulse noise video filters yet. The correspondence between two pixel blocks in successive frames is usually calculated as the mean absolute distance (MAD) between those blocks. To reduce the influence of noisy impulses on this measure in order to use it in our filters, we have introduced a noise adaptive mean absolute distance. From the experimental results it can be seen that the proposed filters result in a very good trade-off between noise removal and detail preservation. They are further also shown to outperform all other compared state-of-the-art random impulse noise filters.

Analogous to the greyscale methods in Chapter 5, also the random impulse noise colour video filter [78, 73] in Chapter 6 removes the noise step by step to combine a good noise removal to a good detail preservation. Each of the colour bands is filtered separately. However, the fuzzy rules that are used to determine the degrees to which a pixel component is considered noisy and noisefree in each step do now not only require information from a spatio-temporal neighbourhood in the same colour band, but exploit also the extra information that is available from the other colour bands. Pixel components for which the noisy degree is larger than the noisefree degree are filtered. To this, we again applied the noise adaptive block matching technique used in the motion compensation for the filters in the previous chapter. To exploit besides the temporal information also the spatial information available in the sequence as much as possible, we further developed the technique by spreading the search region for corresponding blocks over both the previous and current frame. The experiments show that the proposed method outperforms other state-of-the-art filters both visually and in terms of objective quality measures such as the PSNR and NCD.

The third part of the thesis is more theoretical of nature and deals with interval-valued

fuzzy mathematical morphology.

In Chapter 7, we started with an overview of the evolution from binary mathematical morphology to interval-valued fuzzy mathematical morphology and additionally investigated the basic properties of the interval-valued fuzzy morphological operators [84].

Next, in Chapter 8 we studied the decomposition of the interval-valued fuzzy morphological operators in their $[\alpha_1, \alpha_2]$-cuts [83, 85]. We were interested in the relationship between the $[\alpha_1, \alpha_2]$-cut of the result of such operator applied on an interval-valued image and structuring element and the result of the corresponding binary operator applied on the $[\alpha_1, \alpha_2]$-cut of the image and structuring element. We found that in the practical discrete case, the $[\alpha_1, \alpha_2]$-cuts of the interval-valued fuzzy dilation based on the conjunctor $\mathcal{C}_{min}$, the erosion based on the implicator $\mathcal{I}_{EKD}$, and the opening and closing based on those two can always be written in terms of binary operators. For other semi-norms and upper border implicators, we found an approximation in terms of binary operators. In the continuous case, the relationships are sometimes less strong. If no equality was found, a counterexample was constructed. The decomposition results are first of all interesting from a theoretical point of view since they provide us a link between interval-valued fuzzy mathematical morphology and binary mathematical morphology, but secondly, a conversion into binary operators also reduces the computation time needed for the calculation of such $[\alpha_1, \alpha_2]$-cut.

Finally, in Chapter 9, we also investigated the reverse problem, i.e., the construction of interval-valued morphological operators from the binary ones [81, 82]. Inspired by the construction of an interval-valued fuzzy set from its $[\alpha_1, \alpha_2]$-cuts, we studied the construction of an interval-valued fuzzy set from a general nested family of crisp sets and under which conditions the $[\alpha_1, \alpha_2]$-cuts of the constructed interval-valued fuzzy set corresponds to the crisp sets in the family used for the construction. Using these results, increasing binary operators could be extended to interval-valued fuzzy operators by defining the result of the interval-valued fuzzy operator as the interval-valued fuzzy set that is constructed from the family that arises by applying the binary operator on the $[\alpha_1, \alpha_2]$-cuts of its arguments. This allows us to compute the interval-valued fuzzy operators by combining the results of several binary operators or to approximate them by a finite number of binary operators. Applying the construction principle on the increasing binary morphological dilation, we obtained the interval-valued fuzzy dilation based on the conjunctor $\mathcal{C}_{\min}$, which again provides us a nice theoretical link between interval-valued fuzzy and binary mathematical morphology.

References

[1] ABREU, E., LIGHTSTONE, M., MITRA, S. K., AND ARAKAWA, K. A new efficient approach for the removal of impulse noise from highly corrupted images. *IEEE Transactions on Image Processing 5*, 6 (1996), 1012–1025.

[2] ATANASSOV, K. *Intuitionistic fuzzy sets*. Physica Verlag, Heidelberg, Germany, 1999.

[3] BALSTER, E. J., ZHENG, Y. F., AND EWING, R. L. Feature-based wavelet shrinkage algorithm for image denoising. *IEEE Transactions on Image Processing 14*, 3 (2005), 2024–2039.

[4] BALSTER, E. J., ZHENG, Y. F., AND EWING, R. L. Combined spatial and temporal domain wavelet shrinkage algorithm for video denoising. *IEEE Transactions on Circuits and Systems for Video Technology 16*, 2 (2006), 220–230.

[5] BARRENECHEA, E. *Image processing with interval-valued fuzzy sets - edge detection - contrast*. PhD thesis, Public university of Navarra, Spain, 2005.

[6] BELLERS, E. B., AND DE HAAN, G. *De-interlacing: A Key Technology for Scan Rate Conversion*. Elsevier Science B.V., Sara Burgerhartstraat, Amsterdam, The Netherlands, 2000.

[7] BIRKHOFF, G. *Lattice Theory*, vol. 25 of *AMS colloquium publications*. American Mathematical Society, 1973.

[8] BLOCH, I. Dilation and erosion of spatial bipolar fuzzy sets. In *Proceedings of WILF 2007* (2007), vol. 4578 of *Lecture Notes in Artificial Intelligence*, pp. 385–393.

[9] BLOCH, I. Mathematical morphology on bipolar fuzzy sets. In *Proceedings of ISMM 2007 (International Symposium on Mathematical Morphology)* (2007), pp. 3–4.

[10] BLOCH, I. Duality vs. adjunction for fuzzy mathematical morphology and general form of fuzzy erosions and dilations. *Fuzzy Sets and Systems 160* (2009), 1858–1867.

[11] BLOCH, I., AND MAÎTRE, H. Triangular norms as a tool for constructing fuzzy mathematical morphologies. In *Proceedings of the International Workshop on Mathematical Morphology and its Applications to Signal Processing* (1993), pp. 157–161.

[12] BRITO, A. E., AND KOSHELEVA, O. Interval+image=wavelet: for image processing under interval uncertainty, wavelets are optimal. *Reliable Computing 4*, 4 (1998), 771–783.

[13] CABRERA, S. D., IYER, K., XIANG, G., AND KREINOVICH, V. On inverse halftoning: computational complexity and interval computations. In *Proceedings of CISS 2005 (39th Conference on Information Sciences and Systems)* (The John Hopkins University, 2005). Paper 164.

[14] CAMACHO, J., MORILLAS, S., AND LATORRE, P. Efficient impulse noise suppression based on statistical confidence limits. *Journal of Imaging Science and Technology 50*, 5 (2006), 427–436.

[15] CANDES, E. J., D. L. D. D. L. Y. L. Fast discrete curvelet transforms. *Multiscale Modeling and Simulation 5* (2005), 861–899.

[16] CHALIDABHONGSE, J., AND JAY KUO, C.-C. Fast motion vector estimation using multiresolution-spatio-temporal correlations. *IEEE Transactions on Circuits and Systems for Video Technology 16*, 8 (1997), 993–1007.

[17] CHAN, R. H., HU, C., AND NIKOLOVA, M. An iterative procedure for removing random-valued impulse noise. *IEEE Signal Processing Letters 11*, 12 (2004), 921–924.

[18] CHANG, S. G., B., Y., AND VETTERLI, M. Spatially adaptive wavelet thresholding with context modelling for image denoising. *IEEE Transactions on Image Processing 9* (2000), 1522–1531.

[19] CHATZIS, V., AND PITAS, I. Fuzzy scalar and vector median filters based on fuzzy distances. *IEEE Transactions on Image Processing 8*, 5 (1999), 731–734.

[20] CHEN, T., K., M. K., AND CHEN, L. H. Tri-state median filter for image denoising. *IEEE Transactions on Image Processing 8* (1999), 1834–1838.

[21] CHEONG, H., TOURAPIS, A., LLACH, J., AND BOYCE, J. Adaptive spatio-temporal filtering for video de-noising. In *Proceedings of ICIP 2004 (IEEE International Conference on Image Processing)*, p. 965.

[22] COCCHIA, F., CARRATO, S., AND RAMPONI, G. Design and real-time implementation of a 3-d rational filter for edge preserving smoothing. *IEEE Transactions on Consumer Electronics 43*, 4 (1997), 1291–1300.

[23] COHEN, A., DAUBECHIES, I., AND FEAUVEAU, J. Biorthogonal bases of compactly supported wavelets. *Communications on Pure and Applied Mathematics 45* (1992), 485–560.

[24] COHEN, A., AND KOVACEVIC, J. Wavelets: the mathematical background. In *Proceedings of the IEEE* (2007), vol. 84, pp. 514–522.

[25] DABOV, K., FOI, A., AND EGIAZARIAN, K. Video denoising by sparse 3-d transform-domain collaborative filtering. In *Proceedings of EUSIPCO 2007 (15th European Signal Processing Conference)* (2007).

[26] DAUBECHIES, I. *Ten lectures on wavelets*. SIAM, Philadelphia, 1992.

[27] DAVIS, L., AND ROSENFELD, A. Noise cleaning by iterated local averaging. *IEEE Transactions on Systems, Man and Cybernetics 8* (1978), 705–710.

[28] DE BAETS, B. *Oplossen van vaagrelationele vergelijkingen: een ordetheoretische benadering*. PhD thesis, Ghent University, Belgium, 1995.

[29] DE BAETS, B. Fuzzy morphology: a logical approach. In *Uncertainty Analysis in Engineering and Sciences: Fuzzy Logic, Statistics, and Neural Network Approach*, B. M. Ayyub and M. M. Gupta, Eds. Kluwer Academic Publishers, Boston, 1997, pp. 53–67.

[30] DE COCK, M. *Een grondige studie van linguïstische wijzigers in de vaagverzamelingenleer*. PhD thesis, Ghent University, Belgium, March 2002.

[31] DE WITTE, V., SCHULTE, S., NACHTEGAEL, M., MÉLANGE, T., AND KERRE, E. E. A lattice-based approach to mathematical morphology for greyscale and colour images. In *Computational Intelligence Based on Lattice Theory*, V. G. Kaburlasos and G. X. Ritter, Eds., vol. 67 of *Studies in Computational Intelligence*. Springer-Verlag, Heidelberg, Germany, 2007, pp. 129–148.

[32] DEMIRLI, K., AND DE BAETS, B. A general class of residual operators. In *Proceedings of the seventh IFSA congress* (1997), pp. 271–276.

[33] DENG, T., AND HEIJMANS, H. Grey-scale morphology based on fuzzy logic. *Journal of Mathematical Imaging and Vision 16* (2002), 155–171.

[34] DESCHRIJVER, G., AND CORNELIS, C. Representability in interval-valued fuzzy set theory. *International Journal of Uncertainty, Fuzziness and Knowledge-Based Systems 15*, 3 (2007), 345–361.

[35] DESCHRIJVER, G., AND KERRE, E. E. On the relationship between some extensions of fuzzy set theory. *Fuzzy Sets and Systems 133* (2003), 227–235.

[36] DO, M. N., AND VETTERLI, M. The contourlet transform: an efficient directional multiresolution image representation. *IEEE Transactions on Image Processing 14*, 12 (2005), 2091–2106.

[37] DONOHO, D., AND JOHNSTONE, I. Ideal spatial adaptation by wavelet shrinkage. *Biometrika 8* (1994), 425–455.

[38] EL HASSOUNI, M., CHERIFI, H., AND ABOUTAJDINE, D. Hos-based image sequence noise removal. *IEEE Transactions on Image Processing 15*, 3 (2006), 572–581.

[39] GEORGIOU, P. G., TSAKALIDES, P., AND KYRIAKAKIS, C. Alpha-stable modeling of noise and robust time-delay estimation in the presence of impulsive noise. *IEEE Transactions on neural multimedia 1*, 3 (1999), 291–301.

[40] GOGUEN, J. L-fuzzy sets. *Journal of Mathematical Analysis and Applications 18* (1967), 145–174.

[41] GUO, L., AU, O. C., MA, M., AND LIANG, Z. Temporal video denoising based on multihypothesis motion compensation. *IEEE Transactions on Circuits and Systems for Video Technology 17*, 10 (2007), 1423–1429.

[42] GUO, S. M., LEE, C. S., AND HSU, C. Y. An intelligent image agent based on soft-computing techniques for color image processing. *Expert Systems with Applications 28* (2005), 483–494.

[43] HAMZA, B. A., AND KRIM, H. Image denoising: a nonlinear robust statistical approach. *IEEE Transactions on Signal Processing 49*, 12 (2001), 3045–3053.

[44] HARALICK, R. M., STERNBERG, R. S., AND ZHUANG, X. Image analysis using mathematical morphology. *IEEE Transactions on Pattern Analysis and Machine Intelligence 9*, 4 (1987), 532–550.

[45] HARDIE, R. C., AND BONCELET, C. G. Lum filters: a class of rank-order-based filters for smoothing and sharpening. *IEEE Transactions on Signal Processing 41* (1993), 1061–1076.

[46] HOLSCHNEIDER, M., KRONLAND- MARTINET, R., MORLET, J., AND TCHAMITCHIAN, P. Wavelets, time-frequency methods and phase space. In *Real Time Algorithm for Signal Analysis with the Help of the Wavelet Transform*. Springer-Verlag, Berlin, 1989, pp. 289–297.

[47] HORE, S., QIU, B., AND WU, H. R. Improved vector filtering for color images using fuzzy noise detection. *Optical Engineering 42*, 6 (2003), 1656–1664.

[48] JIN, F., FIEGUTH, P., AND WINGER, L. Wavelet video denoising with regularized multiresolution motion estimation. *EURASIP Journal on Applied Signal Processing 2006*, 1 (2006).

[49] JOHNSTON, J. D. A filter family designed for use in quadrature mirror filter banks. In *Proceedings of ICASSP 1980 (IEEE International Conference on Acoustics, Speech and Signal Processing)* (2007), vol. 1, pp. 291–294.

[50] JOVANOV, L., PIZURICA, A., ZLOKOLICA, V., SCHULTE, S., KERRE, E. E., AND PHILIPS, W. Combined wavelet domain and temporal filtering complient with video codec. In *Proceedings of ICASSP'07 (IEEE International Conference on Acoustics, Speech and Signal Processing)* (2007).

[51] JOVANOV, L., PIZURICA, A., ZLOKOLICA, V., SCHULTE, S., SCHELKENS, P., MUNTEANU, A., KERRE, E. E., AND PHILIPS, W. Combined wavelet-domain and motion-compensated video denoising based on video codec motion estimation methods. *IEEE Transactions on Circuits and Systems for Video Technology 19*, 3 (2009), 417–421.

[52] KARASARIDIS, A., AND SIMONCELLI, E. A filter design technique for steerable pyramid image transforms. In *Proceedings of ICASSP'96 (IEEE International Conference on Acoustics, Speech and Signal Processing)* (1996).

[53] KERRE, E. E. *Fuzzy sets and approximate reasoning*. Xian Jiaotong University Press, 1998.

[54] KERRE, E. E., AND NACHTEGAEL, M. *Fuzzy techniques in image processing*, vol. 52 of *Studies in Fuzziness and soft computing*. Physica-Verlag, Heidelberg, 2000.

[55] KIM, J.-S., AND PARL, H. W. Adaptive 3-d median filtering for restoration of an image sequence corrupted by impulse noise. *Signal Processing: Image Communication 16* (2001), 657–668.

[56] KINGSBURY, N. G. Complex wavelets for shift invariant analysis and filtering of signals. *Journal of Applied and Computational Harmonic Analysis 10*, 3 (2001), 234253.

[57] KLEMENT, E. P., MESIAR, R., AND PAP, E. *Triangular Norms*. Kluwer Academic Publishers, Dordrecht, The Netherlands, 2000.

[58] KO, S. J., AND LEE, Y. H. Center weighted median filters and their applications to image enhancement. *IEEE Transactions on Circuits and Systems 38* (1991), 984–993.

[59] KWAN, H. K. Fuzzy filters for noise reduction in images. In *Fuzzy filters for image processing*, M. Nachtegael, D. Van der Weken, D. Van De Ville, and E. E. Kerre, Eds. Springer, Heidelberg, 2003, pp. 54–71.

[60] LABATE, D., LIM, W., KUTYNIOK, G., AND WEISS, G. Sparse multidimensional representation using shearlets. In *Proceedings of Wavelets XI*, SPIE Proceedings.

[61] LEE, J. S. Digital image smoothing and the sigma filter. *Computer Vision, Graphics, and Image Processing 24* (1983), 255–269.

[62] LIAN, N.-X., ZAGORODNOV, V., AND TAN, Y.-P. Video denoising using vector estimation of wavelet coefficients. In *Proceedings of ISCAS 2006 (IEEE International Symposium on Circuits and Systems)* (2006).

[63] LUKAC, R. Vector order-statistics for impulse detection in noisy color image sequences. In *Proceedings of VIPromCom-2002 (4th EURASIP-IEEE Region 8 International Symposium on Video/Image Processing and Multimedia Communications)* (2002).

[64] LUKAC, R. Adaptive vector median filtering. *Pattern Recognition Letters 24* (2003), 1889–1899.

[65] LUKAC, R. Adaptive color image filtering based on center-weighted vector directional filters. *Multidimensional Systems and Signal Processing 15*, 2 (2004), 169–196.

[66] LUKAC, R., AND MARCHEVSKY, S. Lum smoother with smooth control for noisy image sequences. *EURASIP Journal on Applied Signal Processing 2001*, 2 (2001), 110120.

[67] LUKAC, R., AND PLATANIOTIS, K. N. A taxonomy of color image filtering and enhancement solutions. *Advances in Imaging and Electron Physics 140* (2006), 187–264.

[68] LUKAC, R., PLATANIOTIS, K. N., VENETSANOPOULOS, A. N., AND SMOLKA, B. A statistically-switched adaptive vector median filter. *Journal of Intelligent and Robotic Systems 42*, 4 (2005), 361–391.

[69] MA, Z. H., WU, H. R., AND QIU, B. A robust structure-adaptive hybrid vector filter for color image restoration. *IEEE Transactions on Image Processing 14*, 12 (2005), 1990–2001.

[70] MAHBUBUR RAHMAN, S. M., OMAIR AHMAD, M., AND SWAMY, M. N. S. Video denosing based on inter-frame statistical modeling of wavelet coefficients. *IEEE Transactions on Circuits and Systems for Video Technology 17*, 2 (2007), 187–198.

[71] MALLAT, S. A theory for multiresolution signal decomposition: the wavelet representation. *IEEE Transactions on Pattern Analysis and Machine Intelligence 11*, 7 (1989), 674–693.

[72] MALLAT, S. *A wavelet tour of signal processing (2nd ed.)*. Academic Press, Oval Road, London, 1999.

[73] MÉLANGE, T., NACHTEGAEL, M., AND KERRE, E. E. Fuzzy random impulse noise removal from colour image sequences. *IEEE Transactions on Image Processing*. submitted.

[74] MÉLANGE, T., NACHTEGAEL, M., AND KERRE, E. E. Random impulse noise removal from image sequences based on fuzzy logic. *Journal of Electronic Imaging*. submitted.

[75] MÉLANGE, T., NACHTEGAEL, M., AND KERRE, E. E. A vector based fuzzy filter for colour image sequences. In *Proceedings of IPMU 2008 (12th International Conference on Information Processing and Management of Uncertainty in Knowledge-Based Systems)* (2008).

[76] MÉLANGE, T., NACHTEGAEL, M., AND KERRE, E. E. A fuzzy filter for the removal of gaussian noise in colour image sequences. In *Proceedings of IFSA-EUSFLAT 2009* (2009), pp. 1474–1479.

[77] MÉLANGE, T., NACHTEGAEL, M., AND KERRE, E. E. A fuzzy filter for random impulse noise removal from video. In *Proceedings of NAFIPS 2010 (29th North American Fuzzy Information Processing Society Annual Conference)* (2010). submitted.

[78] MÉLANGE, T., NACHTEGAEL, M., AND KERRE, E. E. A fuzzy filter for the removal of random impulse noise in colour video. In *Proceedings of WCCI 2010 (World Congress on Computational Intelligence)* (2010).

[79] MÉLANGE, T., NACHTEGAEL, M., KERRE, E. E., ZLOKOLICA, V., SCHULTE, S., DE WITTE, V., PIZURICA, A., AND PHILIPS, W. Video denoising by fuzzy motion and detail adaptive averaging. *Journal of Electronic Imaging 17*, 4 (2008), 43005–01 – 43005–19. DOI:10.1117/1.2992065.

[80] MÉLANGE, T., NACHTEGAEL, M., SCHULTE, S., AND KERRE, E. E. A fuzzy filter for the removal of random impulse noise in image sequences. *Image and Vision Computing*. submitted.

[81] MÉLANGE, T., NACHTEGAEL, M., SUSSNER, P., AND KERRE, E. E. On the construction of interval-valued fuzzy morphological operations. *Fuzzy Sets and Systems*. submitted.

[82] MÉLANGE, T., NACHTEGAEL, M., SUSSNER, P., AND KERRE, E. E. Construction of interval-valued fuzzy morphological operators by weak cuts. In *Proceedings of EUROFUSE 2009 (Eurofuse Workshop on Preference Modelling and Decision Analysis)* (2009), pp. 227–232.

[83] MÉLANGE, T., NACHTEGAEL, M., SUSSNER, P., AND KERRE, E. E. Decomposition of interval-valued fuzzy morphological operations by weak $[\alpha_1, \alpha_2]$-cuts. In *Proceedings of IFSA-EUSFLAT 2009* (2009), pp. 67–172.

[84] MÉLANGE, T., NACHTEGAEL, M., SUSSNER, P., AND KERRE, E. E. Basic properties of the interval-valued fuzzy morphological operators. In *Proceedings of WCCI 2010 (World Congress on Computational Intelligence)* (2010).

[85] MÉLANGE, T., NACHTEGAEL, M., SUSSNER, P., AND KERRE, E. E. On the decomposition of interval-valued fuzzy morphological operators. *Journal of Mathematical Imaging and Vision 36*, 4 (2010), 270–290. DOI:10.1007/s10851-009-0185-7.

[86] MÉLANGE, T., ZLOKOLICA, V., SCHULTE, S., DE WITTE, V., NACHTEGAEL, M., PIZURICA, A., KERRE, E. E., AND PHILIPS, W. A new fuzzy motion and detail adaptive video filter. In *Proceedings of ACIVS 2007 (Advanced Concepts for Intelligent Vision Systems)* (2007), vol. 4678 of *Lecture Notes in Computer Science*, pp. 640 – 651.

[87] MEYER, Y. *Wavelets: Algorithms and Applications*. SIAM, Philadelphia, 1993.

[88] MITAIM, S., AND KOSKO, B. Adaptive stochastic resonance in noisy neurons based on mutual information. *IEEE Transactions on Neural Networks 15*, 6 (2004), 1526–1540.

[89] MITCHELL, H., AND MASHKIT, N. Noise smoothing by a fast k-nearest neighbor algorithm. *Signal Processing: Image Communication 4* (1992), 227–232.

[90] MORILLAS, S., GREGORI, V., PERIS-FAJARNS, G., AND LATORRE, P. A fast impulsive noise color image filter using fuzzy metrics. *Real-Time Imaging 11*, 5 (2005).

[91] MORILLAS, S., SCHULTE, S., MÉLANGE, T., KERRE, E. E., AND GREGORI, V. A soft-switching approach to improve visual quality of colour image smoothing filters. In *Proceedings of ACIVS 2007 (Advanced Concepts for Intelligent Vision Systems)* (2007), vol. 4678 of *Lecture Notes in Computer Science*, pp. 254–261.

[92] MORRIS, T. *Computer vision and image processing*. Palgrave Macmillan, 2004.

[93] NACHTEGAEL, M. *Vaagmorfologische en vaaglogische filtertechnieken in beeldverwerking*. PhD thesis, Universiteit Gent, Belgium, 2002.

[94] NACHTEGAEL, M., HEIJMANS, H., VAN DER WEKEN, D., AND KERRE, E. E. Fuzzy adjunctions in mathematical morphology. In *Proceedings of JCIS 2003 (Joint Conference on Information Sciences)* (2003), pp. 202–205.

[95] NACHTEGAEL, M., AND KERRE, E. E. Decomposing and constructing of fuzzy morphological operations over alpha-cuts: continuous and discrete case. *IEEE Transactions on Fuzzy Systems 8*, 5 (2000), 615–626.

[96] NACHTEGAEL, M., AND KERRE, E. E. Connections between binary, gray-scale and fuzzy mathematical morphology. *Fuzzy Sets and Systems 124* (2001), 73–86.

[97] NACHTEGAEL, M., MÉLANGE, T., AND KERRE, E. E. The possibilities of fuzzy logic in image processing. In *Proceedings of PReMI 2007 (Pattern Recognition and Machine Intelligence)* (2007), vol. 4815 of *Lecture Notes in Computer Science*, pp. 198–208.

[98] NACHTEGAEL, M., SCHAEFER, G., MÉLANGE, T., AND KERRE, E. E. Fuzzy image retrieval: a selection of recent advances. In *Proceedings of IPCV 2009 (4th International Conference on Image Processing, Computer Vision and Pattern Recognition)* (2009), vol. II, CSREA Press, pp. 864–869.

[99] NACHTEGAEL, M., SCHULTE, S., DE WITTE, V., MÉLANGE, T., AND KERRE, E. E. Color image retrieval using fuzzy similarity measures and fuzzy partitions. In *Proceedings of ICIP 2007 (14th International Conference on Image Processing)* (San Antonio, United States, 2007).

[100] NACHTEGAEL, M., SCHULTE, S., DE WITTE, V., MÉLANGE, T., AND KERRE, E. E. Image similarity: from fuzzy sets to color image applications. In *Proceedings of VISUAL 2007 (9th International Conference on Visual Information Systems)* (2007), vol. 4781 of *Lecture Notes in Computer Science*, pp. 26–37.

[101] NACHTEGAEL, M., SUSSNER, P., MÉLANGE, T., AND KERRE, E. E. Fuzzy set theory in mathematical morphology: from tool to uncertainty model. *Information Sciences*. accepted.

[102] NACHTEGAEL, M., SUSSNER, P., MÉLANGE, T., AND KERRE, E. E. An interval-valued fuzzy morphological model based on lukasiewicz-operators. In *Proceedings of ACIVS 2008 (Advanced Concepts for Intelligent Vision Systems)* (2008), vol. 5259 of *Lecture Notes in Computer Science*, pp. 601–612.

[103] NACHTEGAEL, M., SUSSNER, P., MÉLANGE, T., AND KERRE, E. E. Modelling numerical and spatial uncertainty in grayscale image capture using fuzzy set theory. In *Proceedings of NASTEC 2008* (2008), pp. 15–22.

[104] NACHTEGAEL, M., SUSSNER, P., MÉLANGE, T., AND KERRE, E. E. Some aspects of interval-valued and intuitionistic fuzzy mathematical morphology. In *Proceedings of IPCV 2008 (International Conference on Image Processing, Computer Vision and Pattern Recognition)* (2008), pp. 538–543.

[105] NACHTEGAEL, M., SUSSNER, P., MÉLANGE, T., AND KERRE, E. E. Fuzzy set theory in mathematical morphology: from tool to uncertainty model. In *Proceedings of WMSCI 2009 (13th World Multi-Conference on Systemics, Cybernetics and Informatics)* (2009), vol. IV, pp. 149–155.

[106] NACHTEGAEL, M., SUSSNER, P., MÉLANGE, T., AND KERRE, E. E. Modelling numerical and spatial uncertainty in grayscale image capture using extended fuzzy set theory. *Journal of Advanced Computational Intelligence and Intelligent Informatics 13*, 5 (2009), 529–536.

[107] NACHTEGAEL, M., SUSSNER, P., MÉLANGE, T., AND KERRE, E. E. Foundations of the interval-valued image model to model and process uncertainty in image capture. In *Proceedings of IWSSIP 2010 (The 17th International Conference on Systems, Signals and Image Processing)* (2010).

[108] PALMA, G., BLOCH, I., AND MULLER, S. Fuzzy connected filters for fuzzy gray scale images. In *Proceedings of IPMU'08 (Information Processing and Management of Uncertainty in Knowledge-Based Systems)* (2008), pp. 667–674.

[109] PARK, H., AND CHIN, R. T. Decomposition of arbitrarily shaped morphological structuring elements. *IEEE Transactions on Pattern Analysis and Machine Intelligence 17*, 1 (1995), 2–15.

[110] PIZURICA, A., ZLOKOLICA, V., AND PHILIPS, W. Noise reduction in video sequences using wavelet-domain and temporal filtering. In *Proceedings of the SPIE conference on Wavelet Applications in Signal and Image Processing* (2003), pp. 48–59.

[111] PO, L. M., AND MA, W. C. A novel four-step search algorithm for fast block motion estimation. *IEEE Transactions on Circuits and Systems for Video Technology 6*, 3 (1996), 313–317.

[112] PONOMARYOV, V., ROSALES-SILVA, A., AND GOLIKOV, V. Adaptive and vector directional processing applied to video colour images. *Electronics Letters 42*, 11 (2006), 623 – 624.

[113] POPOV, A. T. General approach for fuzzy mathematical morphology. In *Proceedings of ISMM 2007 (International Symposium on Mathematical Morphology)* (2007), pp. 39–47.

[114] RAJPOOT, N., YAO, Z., AND WILSON, R. Adaptive wavelet restoration of noisy video sequences. In *Proceedings of ICIP 2004 (International Conference on Image Processing)* (2004), pp. 957–960.

[115] RUSSO, F. Fire operators for image processing. *Fuzzy Sets and Systems 103*, 2 (1999), 265–275.

[116] RUSSO, F. Hybrid neuro-fuzzy filter for impulse noise removal. *Pattern Recognition 32* (1999), 1843–1855.

[117] SAMBUC, R. *Fonctions Φ-floues. Application à l'aide au diagnostic en pathologie thyroidienne*. PhD thesis, Univ. Marseille, France, 1975.

[118] SANGWINE, S. J., AND HORNE, R. E. N. *The Colour Image Processing Handbook*. Chapman&Hall, London, 1998.

[119] SCHULTE, S., DE WITTE, V., AND KERRE, E. E. A fuzzy noise reduction method for color images. *IEEE Transactions on Image Processing 16*, 5 (2007), 1425–1436.

[120] SCHULTE, S., DE WITTE, V., NACHTEGAEL, M., MÉLANGE, T., AND KERRE, E. E. A new fuzzy additive noise reduction method. In *Proceedings of ICIAR 2007 (Image Analysis and Recognition)* (2008), vol. 4633 of *Lecture Notes in Computer Science*, pp. 12–23.

[121] SCHULTE, S., DE WITTE, V., NACHTEGAEL, M., VAN DER WEKEN, D., AND KERRE, E. E. A fuzzy impulse noise detection and reduction method. *IEEE Transactions on Image Processing 15*, 5 (2006), 1153–1162.

[122] SCHULTE, S., DE WITTE, V., NACHTEGAEL, M., VAN DER WEKEN, D., AND KERRE, E. E. Fuzzy random impulse noise reduction method. *Fuzzy Sets and Systems 158* (2007), 270–283.

[123] SCHULTE, S., MORILLAS, S., GREGORI, V., AND KERRE, E. E. A new fuzzy color correlated impulse noise reduction method. *IEEE Transactions on Image Processing 16*, 10 (2007), 2565–2575.

[124] SELESNICK, I. W., AND LI, K. Y. Video denoising using 2d and 3d dual-tree complex wavelet transforms. In *Proceedings of the SPIE conference on Wavelet Applications in Signal and Image Processing* (2003), pp. 607–618.

[125] SENDUR, L., AND SELESNICK, I. W. Bivariate shrinkage functions for wavelet based denoising exploiting interscale dependency. *IEEE Transactions on Image Processing 50*, 11 (2002), 2744–2756.

[126] SERRA, J. *Image Analysis and Mathematical Morphology*. Academic Press, London, 1982.

[127] SERRA, J., AND SOILLE, P. *Mathematical morphology and its applications to image processing*, vol. 2 of *Computational imaging and vision*. Kluwer Academic Publishers, Dordrecht, The Netherlands, 1994.

[128] SHARMA, G. *Digital Color Imaging Handbook*. CRC-Press, London, 2003.

[129] SOILLE, P. Applications of morphological operators. In *Handbook of computor vision and applications*, vol. 3. Academic Press, London, 1999, pp. 283–296.

[130] SUSSNER, P., NACHTEGAEL, M., AND MÉLANGE, T. Interval-valued and intuitionistic fuzzy mathematical morphologies as special cases of L-fuzzy mathematical morphology. *Journal of Mathematical Imaging and Vision*. submitted.

[131] SUSSNER, P., NACHTEGAEL, M., AND MÉLANGE, T. L-fuzzy mathematical morphology: an extension of interval-valued and intuitionistic fuzzy mathematical morphology. In *Proceedings of NAFIPS 2009 (28th North American Fuzzy Information Processing Society Annual Conference)* (2009).

[132] SUSSNER, P., AND VALLE, M. E. Classification of fuzzy mathematical morphologies based on concepts of inclusion measure and duality. *Journal of Mathematical Imaging and Vision 32*, 2 (2008), 139–159.

[133] TEKALP, M. *Digital Video Processing*. Prentice Hall, Inc., 1995.

[134] VETTERLI, M., AND KOVACEVIC, J. *Wavelets and Subband Coding*. Prentice-Hall, 1995.

[135] WANG, G., AND LI, X. The applications of interval-valued fuzzy numbers and interval-distribution numbers. *Fuzzy Sets and Systems 98* (1998), 331–335.

[136] WANG, J. H., LIU, W. J., AND LIN, L. D. An histogram-based fuzzy filter for image restoration. *IEEE Transactions on Systems, Man and Cybernetics, Part B: Cybernetics 32*, 2 (2002), 230–238.

[137] WEBER, S. A general concept of fuzzy connectives, negations and implications based on t-norms and t-conorms. *Fuzzy Sets and Systems 11*, 2 (1983), 115–134.

[138] WIEGAND, T., SULLIVAN, G., BJØ NTEGAARD, G., AND LUTHRA, A. Overview of the h.264/avc video coding standard. *IEEE Transactions on Circuits and Systems for Video Technology 13*, 7 (2003), 560–576.

[139] WINDYGA, P. S. Fast impulsive noise removal. *IEEE Transactions on Image Processing 10*, 1 (2001), 173–179.

[140] XU, H., ZHU, G., PENG, H., AND WANG, D. Adaptive fuzzy switching filter for images corrupted by impulse noise. *Pattern Recognition Letters 25* (2004), 1657–1663.

[141] YIN, H. B., FANG, X. Z., WEI, Z., AND YANG, X. K. An improved motion-compensated 3-d llmmse filter with spatio-temporal adaptive filtering support. *IEEE Transactions on Circuits and Systems for Video Technology 17*, 12 (2007), 1714–1727.

[142] ZADEH, L. Fuzzy sets. *Information and Control 8* (1965), 338–353.

[143] ZHU, C., LIN, X., AND CHAU, L. P. Hexagon-based search pattern for fast block motion estimation. *IEEE Transactions on Circuits and Systems for Video Technology 12*, 5 (2002), 349–355.

[144] ZHU, S., AND MA, K. K. A new diamond search algorithm for fast block-matching motion estimation. *IEEE Transactions on Image Processing 9*, 2 (2000), 287–290.

[145] ZHUANG, X., AND HARALICK, R. Morphological structuring element decomposition. *Computer Vision, Graphics, and Image Processing 35* (1986), 370–382.

[146] ZLOKOLICA, V. *Advanced nonlinear methods for video denoising*. PhD thesis, Ghent University, Belgium, 2006. Chapter 5.

[147] ZLOKOLICA, V. *Advanced nonlinear methods for video denoising*. PhD thesis, Ghent University, Belgium, 2006. Chapter 3, Section 3.

[148] ZLOKOLICA, V., AND PHILIPS, W. Motion-detail adaptive k-nn filter video denoising. `http://telin.ugent.be/~vzlokoli/Report2002vz.pdf`. Report 2002.

[149] ZLOKOLICA, V., PIZURICA, A., AND PHILIPS, W. Video denoising using multiple class averaging with multiresolution. In *Proceedings of the International Workshop VLBV03* (2003), vol. 2849 of *Lecture Notes in Computer Science*, pp. 172–179.

[150] ZLOKOLICA, V., PIZURICA, A., AND PHILIPS, W. Wavelet-domain video denoising based on reliability measures. *IEEE Transactions on Circuits and Systems for Video Technology 16*, 8 (2006), 993–1007.